24th World Mining Congress

MINING IN A WORLD OF INNOVATION

October 18-21, 2016 • Rio de Janeiro /RJ • Brazil

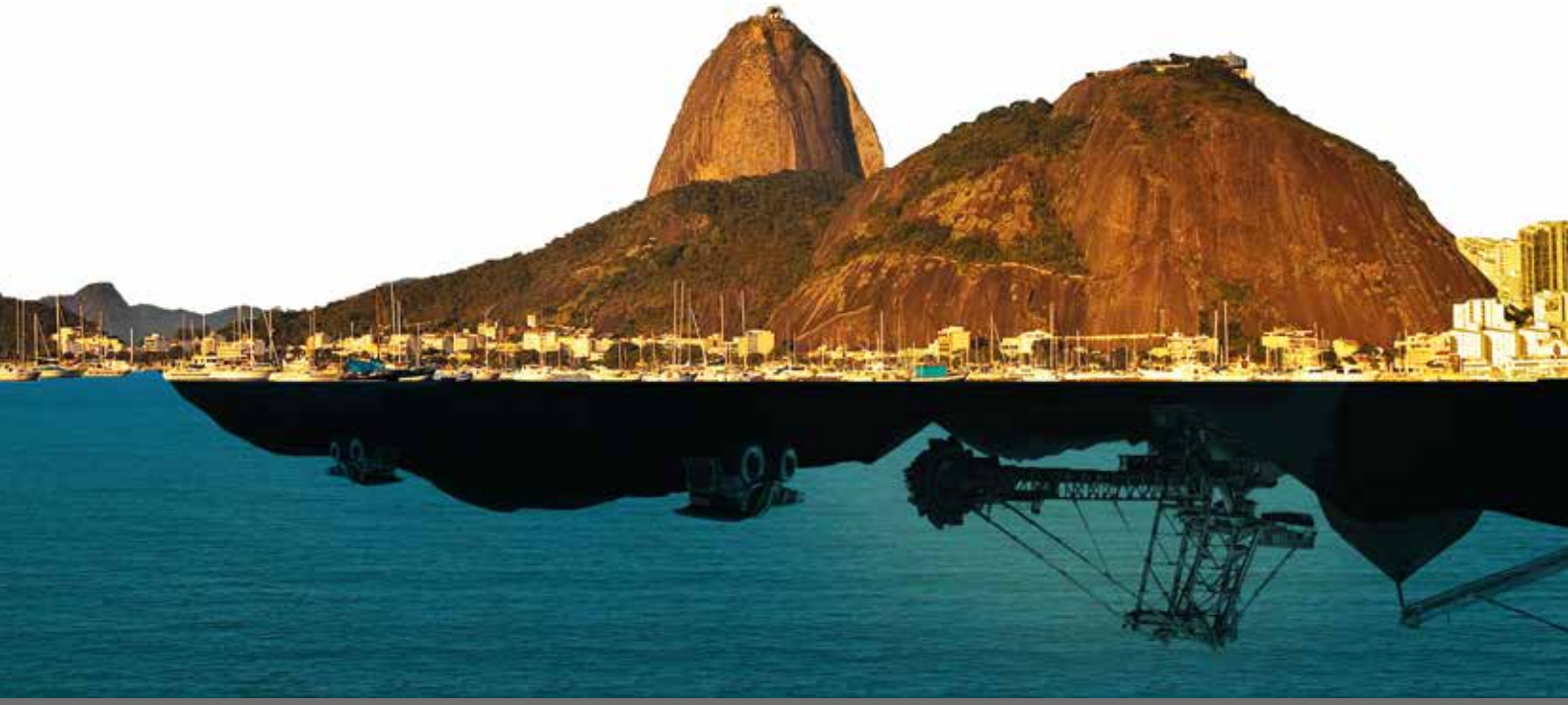

24th World Mining Congress **PROCEEDINGS**

UNDERGROUND MINING

Promotion:

IBRAM
INSTITUTO BRASILEIRO DE MINERAÇÃO
Brazilian Mining Association
Cámara Minera de Brasil

Diamond Sponsorship:

VALE

Votorantim Metais

Gold Sponsorship:

SINFERBASE
Sindicato Nacional da Indústria da Extração do Ferro e Metais Básicos

Silver Sponsorship:

CBMM

Bronze Sponsorship:

AngloAmerican

HYDRO

KINROSS

Special Sponsorship:

ANGLOGOLDASHANTI

Steel Sponsorship:

GERDAU

Special Support:

ANEPAC

GBR
Global Business Reports

MINISTÉRIO DE MINAS E ENERGIA

MINISTÉRIO DA CIÊNCIA, TECNOLOGIA, INOVAÇÕES E COMUNICAÇÕES

BRASIL
GOVERNO FEDERAL

Communication Agency:

Profissionais do Texto
COMUNICAÇÃO CORPORATIVA

Operations Management:

HYRNASTHA
INOVAR

Executive Producer and Marketing:

panda

Commercial Partner – India:

IndusExposium

Commercial Partner – Canada/USA:

AMP

Promotion:

IBRAM
INSTITUTO BRASILEIRO DE MINERAÇÃO
Brazilian Mining Association
Cámara Minera de Brasil

24th World Mining Congress **PROCEEDINGS**

UNDERGROUND MINING

October 18-21, 2016
Rio de Janeiro /RJ • Brazil

IBRAM
INSTITUTO BRASILEIRO DE MINERAÇÃO
Brazilian Mining Association
Câmara Minera de Brasil

IBRAM sede
SHIS QL 12, Conjunto 0 (zero), Casa 04,
Lago Sul – Brasília/DF – CEP: 71.630-205
Phone: +55 (61) 3364-7272 / (61) 3364-7200
ibram@ibram.org.br

IBRAM Minas Gerais
Rua Alagoas, 1270, 10 º andar
Funcionários – Belo Horizonte/MG
CEP: 30130-168
Phone: + 55 (31) 3223-6751
ibram-mg@ibram.org.br

IBRAM Amazônia
Travessa Rui Barbosa, 1536 – B. Nazaré
Belém/PA – CEP: 66035-220
Phone: + 55 (91) 3230-4066
ibramamazonia@ibram.org.br

www.ibram.org.br

https://www.facebook.com/InstitutoBrasileirodeMineracao/

Catalog Card

24th World Mining Congress (24: 2016: Rio de Janeiro, RJ)

24th World Mining Congress PROCEEDINGS – UNDERGROUND MINING / Brazilian Mining Association/Instituto Brasileiro de Mineração (Org). 1ed. - Rio de Janeiro: IBRAM, 2016. e-book

Event held between 18th to 21st October 2016.

Available at: www.wmc2016.org.br and www.ibram.org.br

491 p.

ISBN: 978-85-61993-11-5 e-book

1- Mining. 2- Innovation. 3- Underground Mining. I- Title. II- 24th World Mining Congress. III- Instituto Brasileiro de Mineração.

CDU: 622/5: 502/504

VALE INSTITUTE OF TECHNOLOGY

VALE

Access **www.itv.org** and be part of our team of researchers,
academics, masters' degree and post-graduation students.

Vale Institute of Technology

Created in 2009 with the purpose of stimulating innovation, competitiveness and sustainability in Vale's operations, Vale Institute of Technology (ITV) is a non-profit organization that develops research activities, with emphasis on H2 and H3 horizons as well as training of resources human at post-graduate level. ITV has two locations: one in Belém in the State of Pará, focused on matters related to Sustainable Development, and the other in Ouro Preto, MG, dedicated to Mining and Mineral processing topics.

At the ITV unit in Belém, Vale has been offering a *Master's Degree Program in the Sustainable Use of Natural Resources in Tropical Regions* since 2012. This is a unprecedented initiative in Brazil as it is the first course offered in conjunction with a company from the mineral sector to obtain certification from the Coordination for the Improvement of Higher Education Personnel (Coordenação de Aperfeiçoamento de Pessoal de Nível Superior - Capes), of the Ministry of Education.

In Minas Gerais, ITV launched a pioneering partnership with Universidade Federal de Ouro Preto (UFOP) to structure the *Master's Degree Course in Instrumentation, Control and Mining Process Systems, and Master's Degree Course in Mineral Engineering*. This course has been approved by Capes in 2015 and classes began in 2016. Another innovative partnership that has been being developed is with the ISPT-Instituto Superior Profissional de Tete, Mozambique, consisting in the offer of courses for the Master's Degree Program in Mining at ISPT. These courses are supported financially and operationally by Vale and Capes.

ITV also provides Specialization courses in Mining for Vale's employees and other courses for professional qualification, as well as research activities comprising levels from scientific research to post-doctoral degree.

Luiz Mello

In partnership with Capes, Vale offers academic postdoctoral scholarships for Brazilians and foreigners to researchers who are selected to work at Vale Institute of Technology units, further bringing together the academic community and Vale, expanding the potential generation of innovation and wealth for Vale and Brazil.

Performance Segments

ITV activities are focused across three key segments: Research, Education and Entrepreneurship, following the cycle through which scientific production evolves, creating practical application and generation of concrete benefits for the company. For further information visit: www.itv.org or send an e-mail: info.itv@itv.org.

It is a pleasure for us to participate in the 24th edition of the World Mining Congress - WMC 2016, being held for the first time in Brazil, and we can introduce you to some of the technological, research and innovation solutions in the Mining Sector. It is our commitment to share knowledge, innovation and technology towards the sustainable development of the operations and processes in global mining.

I hope that everyone enjoys the most of the World Mining Congress!

Luiz Mello
CEO of Vale Institute of Technology
Technology and Innovation Executive Manager of Vale

José Fernando Coura

On behalf of the Brazilian Mining Association - IBRAM and its associates, I would like to offer a warm welcome to all the participants of the 24th edition of the World Mining Congress - WMC 2016. This is the first time that the WMC, recognized as one of the most important world mining events, is being held in Brazil. The central theme of this congress is "Mining in a World of Innovation", one of the most current and important issues in the management of mining-sector businesses.

The 24th WMC began to take shape in 2012 when representatives from businesses and entities of the mining sector, as well as the Brazilian government, joined forces to support the country's bid, before the International Organizing Committee, to host the congress (IOC). This was well-deserved, given Brazil is one of the international exponents of mining.

The presentation of the Brazilian bid was made by IBRAM's presidency in conjunction with our Director of Mineral Issues, Marcelo Ribeiro Tunes. It fell to him to deliver the speech underlining the qualities that make IBRAM suitable to organize such an event, of the city of Rio de Janeiro (RJ) to attract and host event participants, and the Brazilian mining industry; factors which proved decisive in convincing the IOC members to choose Brazil as the host of the event in 2016.

With this significant vote of confidence, we are certain that the 2016 WMC will be the stage of an intense diffusion of knowledge, of discussions on the best way forward, and deep analyses of the current and future landscape of the mining industry. Without a doubt, it will also serve as a way to strengthen relationships and enable dialogue between the most diverse actors of the sector's extensive production chain on an international level.

We know that the last few years have been challenging for the mining industry and "innovation" is the key word for new business and the future of the sector itself. The economic environment has altered the rhythm of supply and demand, impacting ore prices and making it more difficult for mining companies to outline their next steps both locally and globally. Nevertheless, this moment offers an opportunity for mining to lay the way for a return to greater productivity in the future.

This is the proposal of the 24th edition of the WMC, amongst others. We also intend to technically and scientifically promote and support cooperation to develop more stages in the sustainable development of operations and processes in the mining sector.

With an optimistic vision of the prospects of the mineral sector, I hope that IBRAM, via this grand event, can awaken the public interest to debate the future of mining and identify innovative actions to further strengthen the mining industry around the world.

We wish everybody an excellent World Mining Congress!

José Fernando Coura
CEO of the Brazilian Mining Institute

Murilo Ferreira

Brazil has a historic vocation for mineral extraction activities, and since the mid-18th century they have practically dominated the dynamics of its economy. Rich in world-class minerals, the country has emerged as one of the leading global players in the mining industry, and it is now the second largest iron ore producer and one of the most significant agents in international trading and exports of this commodity.

The mining industry has become one of the most important pillars of Brazil's development. Despite the decline in iron ore prices and demand in the international markets, especially due to the slowdown in Chinese consumption, and despite the end of the super-cycle, the mining sector has continued to play a key role in maintaining Brazil's balance of trade surplus.

In addition to its positive impacts in the macroeconomic sphere in Brazil, mining has also become a driver of social development, particularly as it has a multiplier effect on other economic activities, contributing to the expansion of various production chains and consequently to the generation of jobs and income. It is noteworthy that in the municipalities where mining companies operate, Human Development Index ratings have been higher than the average figures for their respective states, and much higher than in non-mining municipalities.

In a country like Brazil, whose economic growth, as already mentioned, is strongly dependent upon the expansion of mining activities, the creation of the Brazilian Mining Association, which will turn 40 in December, was essential and absolutely necessary. This is a date to be celebrated, above all because IBRAM has played its role to support and strengthen mining activities with dynamism, efficiency and innovative practices. The sector's companies and organizations can count on a body that assertively and competently represents, coordinates and integrates them, defending their interests and generating conditions conducive to the sustainable development and competitiveness of their businesses.

The holding in Brazil of the 24th edition of the World Mining Congress, organized by an entity of IBRAM's quality, is a milestone and an excellent opportunity for the sector to share ideas, discuss, reflect and find stimuli and feasible ways forward at a time when we need to face the end of the mining super-cycle. The theme of the Congress could not be more appropriate, and I am sure that by its end, promising directions will have been mapped to strengthen the mining industry across the world.

Murilo Ferreira
Chief Executive Officer, Vale S.A.

Professor Jair Carlos Koppe

Mining has been extremely important to the World's economic growth and prosperity for centuries. The mining industry is currently facing an economic and social crises that can impact strongly the mineral production and productivity. In this scenario several challenges must be addressed, among them complex mineral deposits of low grades, water, social and environmental issues as well as declining commodity prices. Considering that the world is changing dramatically in all aspects this is the moment for innovation in mining. The WMC 2016 is under the umbrella of Mining in a World of Innovation in the proper moment. This is a nice opportunity to change our ways in mining technology considering the new evolving technologies such as automation, sensors, cloud computing, data analytics that can increase the mining production and efficiency in the entire value chain. Let's take this moment to spread our experience among academy, industries, practitioners and professionals of the mining sector focusing in the future of a world in constantly innovation.

We would like to thanks all the contributions done by the authors invited speakers and participation of delegates that will make WMC 2016 a very successful meeting. Special thanks to the members of the Scientific Committees that helped in the paper analysis ensuring the quality of the conference.

Welcome to the WMC 2016.

Professor Jair Carlos Koppe
Congress Chairperson

Józef Dubiński

Hermínio Oliveira

The 24th World Mining Congress is one of the most important mining events worldwide and is going to be held in Rio de Janeiro, Brazil, from October 18 to 21, 2016. The premiere of the World Mining Congress took place 58 years ago, in September 1958, in Warsaw, Poland. Currently, the WMC organization gathers 45 mining nations from all over the world.

Each World Mining Congress, which takes place in a different host-nation, is always a great mining occasion for the international community that represents science and industry figures involved in the exploration of mineral assets. We can assert that this congress points to the most significant directions for global mining development and determines priorities for the activities of all institutions related to mineral activity. The same approach is going to be adopted during the 24th World Mining Congress, which is going to concentrate on the theme of "Mining in a World of Innovation". Nowadays, and increasing number of countries hold great knowledge potential on mining. The challenges aforementioned demand mutual cooperation, exchange of technical knowledge and professional experience, as well as assistance to those in need. Personally, I believe that our generation of the world mining society – the heirs of our illustrious ancestors – will follow their accomplishments and guide the organization of the World Mining Congress into a new direction, to assure many more years of effective services to global mining and to the people who have taken part in this challenging activity, yet still necessary for all humankind.

Józef Dubiński
Professor and Doctor of Engineering
Corresponding Member PAS
Chairman of the World Mining Congress International Organizing Committee

HONORARY CHAIRPERSONS

JOSÉ FERNANDO COURA
President-Director of the Brazilian Mining Association (IBRAM)

MURILO FERREIRA
Chief Executive Officer of VALE

SPECIAL HONOUREE

GEOLOGIST MARCELO RIBEIRO TUNES
Director of Mining Affairs at the Brazilian Mining Association (IBRAM)
Former General-Director of the National Department of Mineral Production (DNPM)

CONGRESS CHAIRPERSON

PROFESSOR JAIR CARLOS KOPPE
Federal University of Rio Grande do Sul (UFRGS)

CONGRESS CO-CHAIRS

PROFESSOR EDUARDO BONATES
Federal University of Campina Grande (UFCG)

PROFESSOR ENRIQUE MUNARETTI
Federal University of Rio Grande do Sul (UFRGS)

PROFESSOR GEORGE VALADÃO
Federal University of Minas Gerais (UFMG)

PROFESSOR ISSAMU ENDO
Federal University of Ouro Preto (UFOP)

PROFESSOR LUIS ENRIQUE SÁNCHEZ
University of São Paulo (USP)

CONGRESS TECHNICAL COORDINATION

RINALDO CÉSAR MANCIN
Director of Environmental Affairs at the Brazilian Mining Association (IBRAM)

WORLD MINING CONGRESS CHAIR

M.SC. ENG. JACEK SKIBA
Secretary General of the World Mining Congress

PROF. JÓZEF DUBIŃSKI
World Mining Congress Chairperson and Managing Director of the Central Mining Institute, Katowice, Poland

NATIONAL SCIENTIFIC ADVISORY COMMITTEE

AARÃO DE ANDRADE LIMA – UFCG

ANDRÉ CARLOS SILVA – UFG

ANDRÉ CEZAR ZINGANO – UFRGS

ANTÔNIO EDUARDO CLARK PERES – UFMG

ANTÔNIO PEDRO F. SOUZA – UFCG

CARLOS HOFFMANN SAMPAIO – UFRGS

CARLOS OTÁVIO PETTER – UFRGS

CLÁUDIO LÚCIO L. PINTO – UFMG

DINIZ TAMANTINI RIBEIRO – VALE

EDMO DA CUNHA RODOVALHO – UNIFAL

ENRIQUE MUNARETTI – UFRGS

EUNÍRIO ZANETTI – ITV/VALE

GÉRMAN VINUEZA – ITV/VALE

GEORGIO DI TOMI – USP

IVO ANDRÉ HOMRICH SCHNEIDER – UFRGS

JOÃO FELIPE C. L. COSTA – UFRGS

JOSÉ BAPTISTA OLIVEIRA – UFBA

JOSÉ MARGARIDA DA SILVA – UFOP

JULIO CESAR DE SOUZA – UFPE

LAURINDO DE SALLES LEAL FILHO – ITV/VALE

LINEU AZUAGA AYRES DA SILVA – USP

LUIZ ENRIQUE SÁNCHEZ – USP

MICHEL MELO OLIVEIRA – CEFET/ARAXÁ

MÔNICA CARVALHO – UFPB

PAULO SALVADORETTI – UFRGS

RICARDO CABRAL DE AZEVEDO – USP

ROBERTO CERRINI VILLAS–BÔAS – CETEM
(in memorian)

RODRIGO DE LEMOS PERONI – UFRGS

VLÁDIA CRISTINA SOUZA – UFRGS

WILSON TRIGUEIRO DE SOUZA – UFOP

INTERNATIONAL SCIENTIFIC ADVISORY COMMITTEE

ABANI R. SAMAL, PH.D
University of Utah, US

DR. ANDRE XAVIER
Canadian International Resources and Development Institute (CIRDI), Canada

MR. G.P. KUNDARGI
Chairman-cum-Managing Director, MOIL Limited, India

DR. BISWAJIT SAMANTA
Indian Institute of Technology, India

MR. M. BILGIN KAYNAR
Deputy Chairman Turkish National Committee, Turkey

PROF. DR. CARSTEN DREBENSTEDT
Institut für Bergbau und Spezialtiefbau, Germany

PH.D. DEBORAH J. SHIELDS
Colorado State University, US

PROF. DR. DOMINGO JAVIER CARVAJAL GÓMEZ
Universidad de Huelva, Spain

PROF. ERNEST BAAFI
The University of Wollongong, Australia

PROF. DR. ENG. JAN PALARSKI
Silesian University of Technology, Poland

PROF. DR. ENG. STANISŁAW PRUSEK
Central Mining Institute, Katowice, Poland

DR. FARSHAD RASHIDI-NEJAD
University of New South Wales, Australia

PROF. FERRI HASSANI
Mc Gill University, Canada

PROF. DR. FIDELIS TAWIAH SUORINENI
University of New South Wales, Australia

PROF. GIDEON CHITOMBO
The University of Queensland, Australia

DR. HUA GUO
Queensland Centre for Advanced Technologies
(QCAT), Australia

PROF. HOOMAN ASKARI–NASAB
University of Alberta, Canada

MR.SC. IVAN COTMAN
KAMEN d.d. (Ltd.), Croatiia

PROF. ING. VLADIMÍR SLIVKA
Technical University of Ostrava, Czech Republic

24th World Mining Congress
MINING IN A WORLD OF INNOVATION
October 18-21, 2016 • Rio de Janeiro /RJ • Brazil

Summary

A FIELD INVESTIGATION OF MINING-INDUCED STRATA, GROUNDWATER AND GAS BEHAVIOURS

* Qingdong Qu[1], Hua Guo[1], Clint Todhunter[2], Hamish Kerr[2], Luke Babic[2], and Rohan McGeachie[2]

[1]*The Commonwealth Scientific and Industrial Research Organisation (CSIRO)*
Brisbane, Queensland 4069, Australia
(**Corresponding author: Qingdong.qu@csiro.au*)

[2] *Bulga Underground Operations, Glencore*
Broke, New South Wales 2330, Australia

24th World Mining Congress
MINING IN A WORLD OF INNOVATION
October 18-21, 2016 • Rio de Janeiro /RJ • Brazil

A FIELD INVESTIGATION OF MINING-INDUCED STRATA, GROUNDWATER AND GAS BEHAVIOURS

ABSTRACT

To provide engineering principles and factors for optimal longwall gas drainage design, an integrated field investigation of mining induced strata, groundwater and gas behaviours was carried out at a complex multi-seam underground longwall mine in Australia. Surface deep-hole extensometers and piezometers were installed to continuously monitor the geomechanical and hydrogeological responses. Tracer tests, using sulfur hexafluoride (SF6), were carried out to study goaf gas flow patterns. Gas content before and after mining was measured to determine the gas emission sources and emission levels from various coal seams. The field investigation successfully obtained many insights into the coupled behaviour of strata, groundwater and gas in response to mining, and identified a number of critical factors for gas drainage design such as goaf conditions and sources of gas emissions. The field investigation led to a successful design and implementation of an optimal goaf gas drainage system at the mine.

KEYWORDS

Longwall mining; gas drainage; gas emission; pore pressure; field monitoring

INTRODUCTION

Mining in underground coal mines will induce stress relief and create new fractures in the surrounding strata, which can cause a significant amount of methane gas to be adsorbed in the surrounding gassy coal seams (Karacan, et al. 2011; Guo et al, 2012, 2013, 2015; Qu et al., 2015). If not controlled, the released methane gas will find its way into the active workings of the mine, significantly interfering with coal production efficiency and mining safety. In addition, from an environmental point of view, methane emitted into the atmosphere is a substantial source of fugitive emissions. It is estimated that coal mines represent approximately 8% of the world's anthropogenic methane emissions (Karacan, et al., 2011). By 2020, coal mine methane emissions are projected to increase to as high as 793 Mt CO_2-e (Karacan, et al., 2011), with underground coal mining being the most notable source of fugitive methane emissions.

Optimal gas drainage in modern coal mining not only effectively controls gas emissions to workings but also significantly reduces fugitive emissions. To develop and demonstrate a holistic and optimal approach to planning, design, and operational control for optimal gas drainage, a joint research project entitled "Mine methane capture optimisation and maximisation of emissions abatement" was undertaken in the past three years by the Australian Commonwealth Scientific and Industrial Research Organisation (CSIRO) and the Glencore Bulga Underground Operations. The project was supported by the Australian Government under the auspices of "Coal Mining Abatement Technology Support Package (CMATSP)", and carried out at the Blakefield South mine of the Bulga Underground Operations.

Goaf gas emissions in multi-seam mining conditions are highly complex, and associated with dynamic changes of the goaf properties and environment (Palchick, 2003; Whittles, et al., 2006; Guo et al., 2012; Schatzel, et al., 2012). Design and implementation of an optimal gas drainage system needs to fully recognise this dynamic process as well as the coupled behaviours between mining induced strata, groundwater and gas responses. Therefore, an integrated field investigation was designed and carried out at the mine. Comprehensive and integrated field monitoring and measurements, including strata movement,

coal seam pore pressure changes, gas contents and goaf gas flows, were conducted. This paper presents the key results.

MINE CONDITIONS

The Blakefield South mine of the Bulga Underground Operations is located in the Hunter Valley coalfield in Australia. Mining conditions at the mine are complex and highly gassy. The mine uses a three-gateroad system to access the longwall panels, which are commonly 400 m wide (rib-to-rib) and up to 3.5 km long. Figure 1 shows the mine plan as of September 2013.

The Blakefield seam longwalls (bright yellow lines in Figure 1) are operated underneath old longwall workings (dark yellow lines in Figure 1), which extracted coal from the lower Whybrow coal seam approximately 70-100 m above the current longwalls. The old workings, with a width of about 250 m, did not align with the current longwall panels.

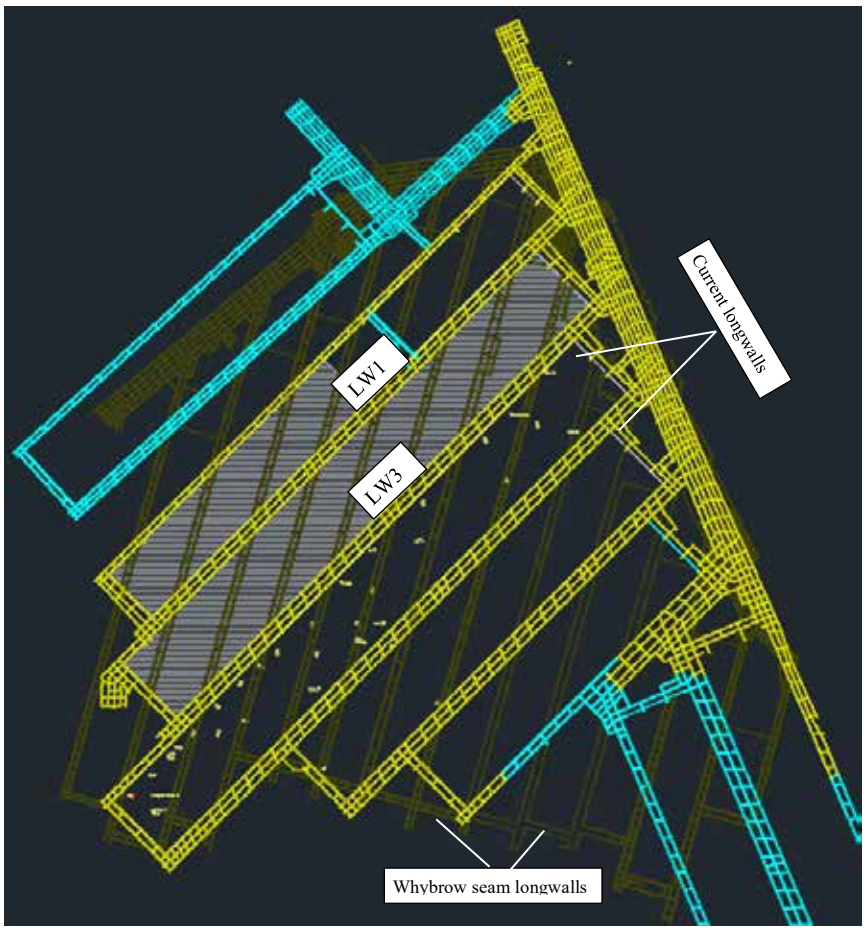

Figure 1 - Mine plan of the Blakefield South mine

The mining seam, Blakefield, comprises four coal plies where the longwall extracts the top three with a cutting height ranging from 2.8 m to 3.4 m. The seam generally dips at 3 degrees, and its depth of cover above the LW1 to LW3 varies between approximately 130 m and 260 m. The mining seam is surrounded by a number of gassy coal seams, including Redbank Creek and Wambo seams in the roof strata and Glen Munro and Woodlands Hill seams in the floor strata. Figure 2 shows a cross section of the Blakefield South mine with the gas content of each coal seam marked. All these surrounding coal seams

were predicted to be significant gas emission sources by the empirical model used at the mine which is expressed as a function between distance of coal seams and the gas release percentage from the coal seams.

Pre-mining gas drainage from the Blakefield seam using surface-to-inseam boreholes have been adopted at the mine to drain gas before development of the longwall gateroads. During mining, surface goaf vertical wells were generally used at LW1 to LW3 to capture gas from the longwall goafs. In addition to these vertical wells, surface directional boreholes were also drilled to intercept the vertical wells at LW1 and LW2 in an attempt to provide a connection of a large gas producing zone (Todhunter, et al., 2012). However, the goaf gas drainage performance at the two longwalls was unsatisfactory, particularly in the initial mining stage over a length of about 400 m.

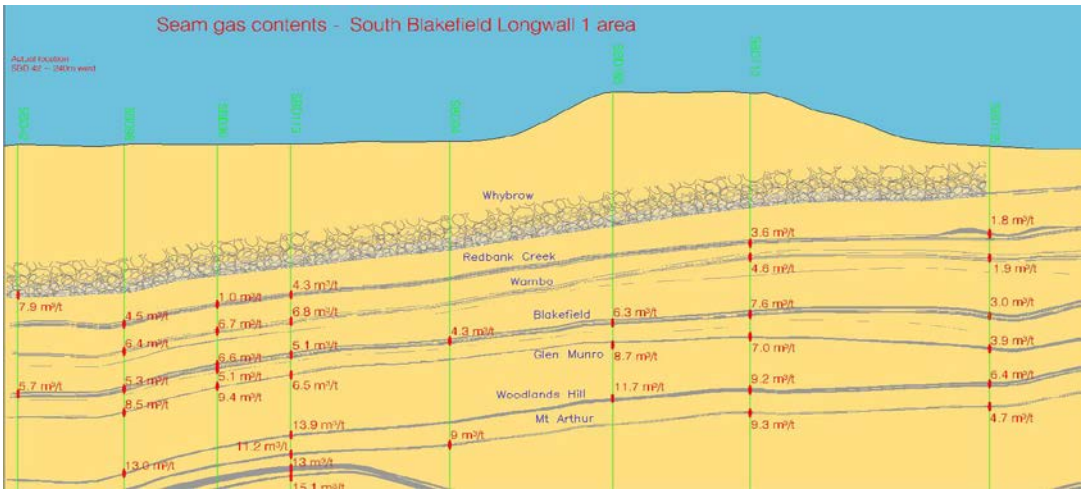

Figure 2 - Cross section of the Blakefield South mine

DESIGN AND IMPLEMENTATION OF THE FIELD INVESTIGATION

Extensive site characterisation of in-situ strata, hydrogeological and gas conditions were carried out before planning of the field investigation. In addition, previous technical and operational data related to gas drainage were collected and reviewed. Based on the results, field monitoring and measurement programs were developed with the key activities located at the middle area of LW3 block in its length. Figure 3 illustrates the key field investigation activities implemented at LW3, which include two surface deep-hole extensometers, a surface deep-hole piezometers into each of the coal seams, gas content measurements before and after mining at three various locations, and release of tracer gases into both the old and the active goafs.

Surface deep-hole multi-anchor extensometers

Two surface extensometers were installed, with one located at 142 m to the longwall panel main gate (MG) edge and the other 123 m to the tail gate (TG) edge. Each extensometer consisted of 11 anchors with most of them placed in the interburden between the Whybrow goaf and the mining seam. A surface data logger system was installed to continuously record the readings at 15 minute intervals.

Surface deep-hole piezometers

The surface piezometer hole was located at LW3 MG chain pillar zone to avoid potential cable shearing from ground movement. A total of eight fibre optic piezometers were installed in this hole into all major coal seams from Redbank Creek to Woodlands Hill, as well as the interburden between the coal seams. The piezometer readings were continuously recorded at 15 minute interval by a surface data logger.

Gas tracing tests

The major tests discussed in this paper involved the injection of sulfur hexafluoride (SF_6) into the Whybrow goafs directly above the LW3 and the Wambo seam through a borehole installed with packers that isolated the injection zone. Gas samples were taken through the mine's tube bundle system from various designated locations in the LW3 goaf, ventilation return, and surface vertical goaf gas drainage wells.

Coal seam gas content measurements before and after LW3 mining

Gas content measurements before and after LW3 mining were carried out at the three different locations across the panel width. When the surface boreholes of the two extensometers (marked E1 and E2 in Figure 3) and the piezometer were drilled, coal cores were taken from various coal seams for pre-mining gas content measurements. After the LW3 mining was completed, another three holes were then drilled near the extensometers and the piezometer for post-mining gas content measurements.

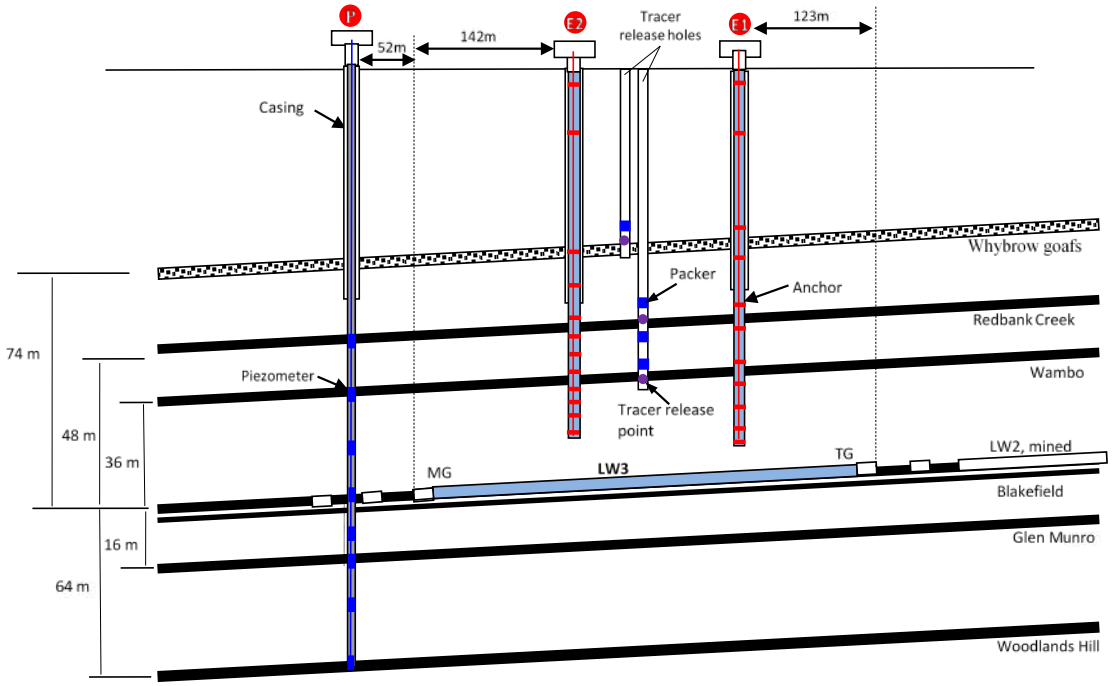

Figure 3 – Field investigation programs shown at a cross-section of the LW3

KEY RESULTS AND ANALYSIS

Overburden caving process and fractures characteristics

Both the extensometers successfully monitored the dynamic movement of the overburden at various levels as the longwall advanced. It is noted that E1 gave more typical results than E2 as the former was located in the mid Whybrow goaf zone while the latter was located on the edge of Whybrow pillar zone. Figure 4 shows the monitored overburden movement by E1, which resulted in a clear understanding of the goaf forming process as well as the characteristics of mining induced strata fractures.

In terms of the upward propagation of strata movement, it can be seen in Figure 4 that the strata layer 11 m above the mining seam started to move at about 12 m inbye of the longwall face, and mining

induced fractures extended up to the Wambo seam and Redbank Creek seam at 27 m and 31 m inbye of the longwall face, respectively. In the mining advance direction, the overburden moved quickly once behind the longwall face and reached the maximum level of delamination at about 60 m inbye, becoming stable in another 60 m of retreat.

Significant strata delaminations were observed in the interburden between the Redbank Creek seam and the working seam (as shown in Figure 4 (b)), indicating a high horizontal permeability was present. In addition, according to the typical conceptual model of overburden deformation (Peng, 2006), strata from 11 m above the working seam up to the Redbank Creek seam can be characterised as within the fractured zone.

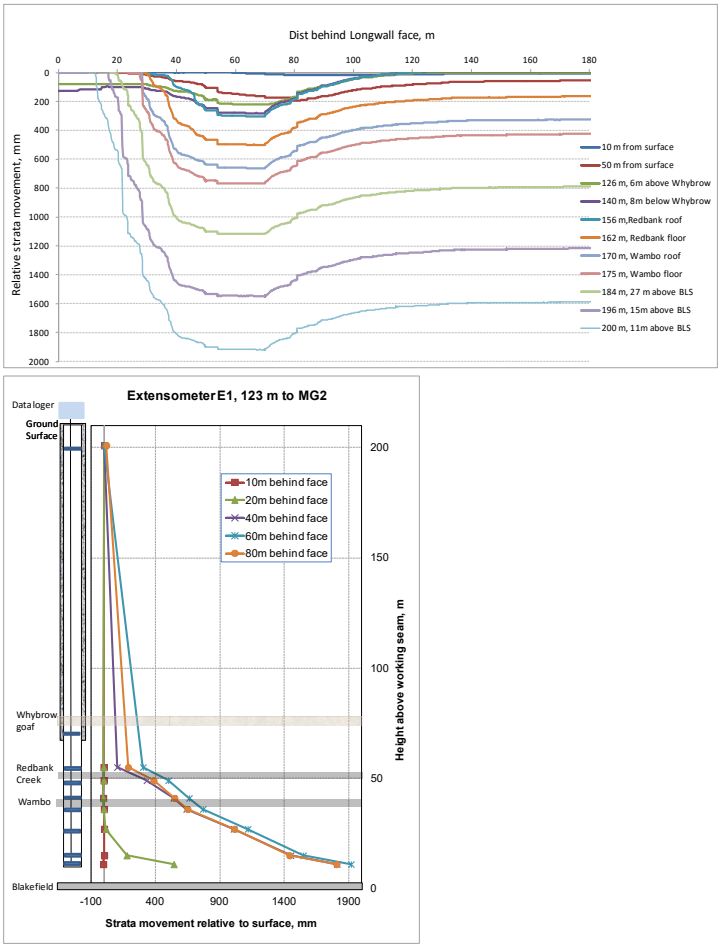

(a) Strata displacement in mining direction (b) strata movement in vertical section

Figure 4 - Monitored overburden movement by extensometer E1

Coal seam pore pressure changes

Figure 5 shows the monitored pore pressure changes in all the major coal seams at the LW3 MG chain pillar zone as the longwall advanced. It can be seen that, of the all seams, Redbank Creek and Wambo in the roof and the lower Blakefield and Glen Munro coal seams in the floor experienced significant depressurisation during mining, indicating gas in these coal seams was released. However, at Woodlands Hill, 65 m below the mining seam, a slight increase in pore pressure was measured.

Pore pressure started to decline as early as 50m outbye of the longwall face, and continued the trend up to 250 m inbye of the longwall face in the case of the Wambo seam. At a location 500 m inbye of the lonwall face, the residue pore pressures in the two overlying coal seams were reduced to as low as 0.2 Mpa, reflecting adsorbed gases in these coal seams would have mostly been released.

In terms of pore pressure changes patterns as the longwall advanced, each coal seams had a different rate and duration of pore pressure reduction, indicating different gas desorption and release characteristics. The Wambo seam, the lower Blakefield seam and the Glen Munro seam showed a relatively high reduction rate, which indicated a high gas desorption and emission rate.

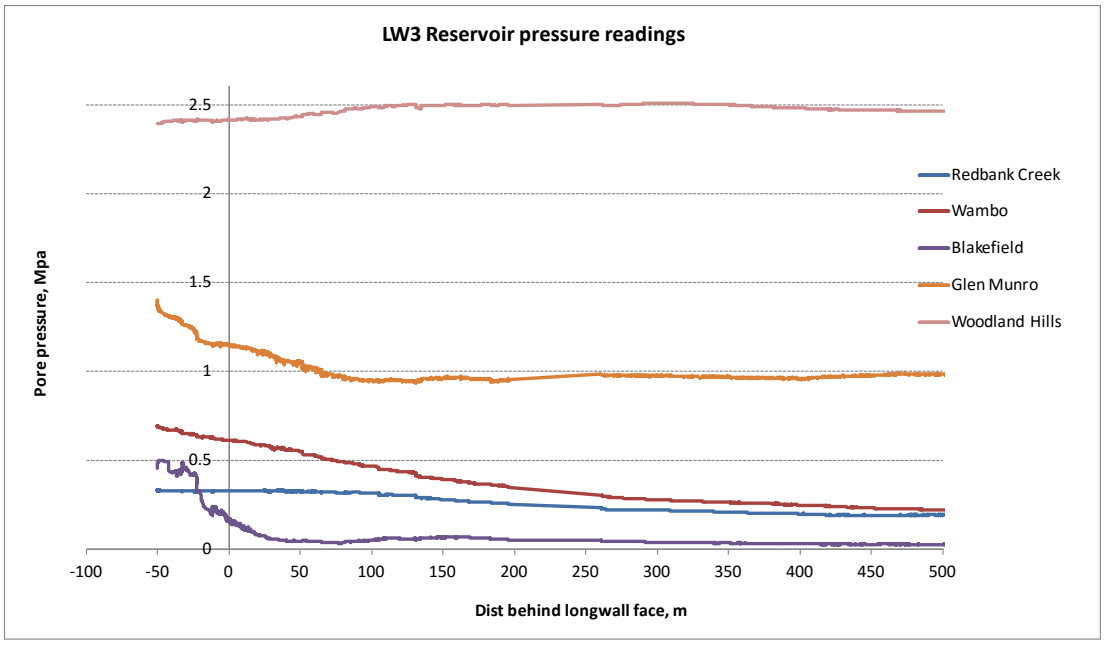

Figure 5 - Coal seam pressure changes as longwall advanced

Gas flow paths and migration patterns

The tracer gas tests were conducted to understand gas flow characteristics and paths between the Whybrow goafs, overburden fractured strata, surrounding coal seams, active goaf, and ventilation return. Figure 6 shows a typical example of the measured tracer gas concentration at a sampling point. From a figure like this, tracer gas flow parameters such as the initial arrival time, the concentration peak time and the concentration change rate can be assessed and compared with that at various sampling locations, and as a result, gas flow velocity and flow directions can be analysed. In addition, with the monitored flow rates of drainage gas and the air in the ventilation return, the effectiveness and mechanisms of goaf gas drainage can be evaluated.

In the test where SF6 was injected into the Whybrow goaf directly above LW3, no SF6 was detected in LW3 active goaf and ventilation return. This suggested that the Whybrow goaf gases actually did not flow down to the active goaf although a significant amount of drainage gas was estimated from the Whybrow goafs. In other words, the Whybrow goaf gases do not contribute to the ventilation gas makes and capturing gas from Whybrow goafs does not actually have an effect on reducing ventilation gas levels. The test also found that almost all operating drainage wells had SF6, indicating a high interconnection or conductivity exists within and across the overlying Whybrow goafs.

In the test where SF6 was injected into the Wambo seam, almost half of injected SF6 was estimated as flowing through the ventilation return. This indicated that, under the drainage of the surface vertical wells, about half of the released Wambo gas flowed into the active goaf.

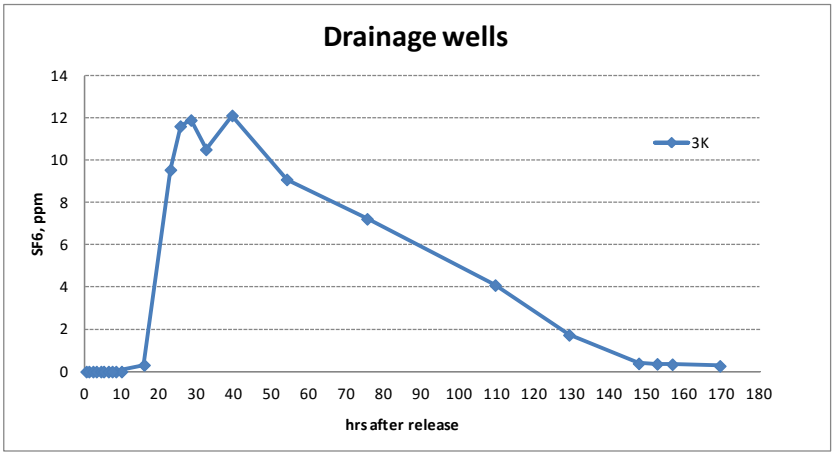

Figure 6 – SF6 concentration variation at a surface goaf gas drainage well

Coal seam gas emissions

Measurements of coal seam gas content before and after longwall extraction can directly identify gas emission sources and evaluate gas release levels from various coal seams during longwall operation. Gas content measurements at different locations can also reveal the emission profile across the longwall panel. Table 1 shows the measured gas contents of various coal seams before and after LW3 excavation at the three measurement locations: two within the goaf and one located in the chain pillar zone.

Table 1- Gas content measurement results before and after the LW3 mining

	MG chain pillar, 52m outside			*Goaf, 142m from MG*			*Goaf, 123m from TG*		
Coal seams	Pre-mining, m3/t	Post-mining, m3/t	Gas released, m^3/t	Pre-mining, m3/t	Post-mining, m3/t	Gas released, m3/t	Pre-mining, m3/t	Post-mining, m3/t	Gas released, m3/t
Redbank Creek	3.6	1.92	**1.68**	2.91	0.86	**2.05**	2.1	1.1	**1**
Wambo	5.99	2.87	**3.12**	3.43	0.74	**2.69**	2.13	1.21	**0.92**
Blakefield	1.19			1.16			1.12		
Lower Blakefield	1.03	1.05	**-0.02**	1.35			1.58		
Glen Munro	6.27	4.02	**2.25**	4.02	1.88	**2.14**	3.7	2.31	**1.39**
Woodlands hill	13.35	13.8	**-0.45**	13.28	12.37	**0.91**	9.99	11.92	**-1.93**

The results clearly show that of the coal seams, Redbank Creek, Wambo, and Glen Munro seams are significant gas emission sources, while the Woodlands Hill seam is not. This is significantly different from the prediction by the Flugge model used at the mine. In addition, the results also indicated that the underlying Glen Munro seam had a high gas content reduction.

As for gas emission patterns across the longwall panel, gas content before mining is different at various locations across the LW3 panel and appears lower at locations closer to the mined LW2. This suggests that the LW2 excavation had an effect on the gas content distribution of the LW3 panel. Gas

content reduction at the MG chain pillar zone reflects that the extent of gas release extends beyond the direct mining region and into the unmined area. For the two measurement locations within the goaf region, residual gas content in the two roof coal seams are quite close, showing their residual conditions are similar.

FACTORS AND CONSIDERATIONS FOR LONGWALL GAS DRAINAGE OPTIMISATION

The results of the field investigation provided a clear understanding of strata, groundwater pressure and gas responses to mining, with a strong correlation between mining induced strata fractures/delamination, pore pressure, gas release from coal seams, and gas migrations in the goaf. In the overburden, where strata fractures/delaminations were created by mining, significant reductions in coal seam pore pressure and gas content were evident. Delamination conditions between the Wambo and the Redbank Creek seams were approximate, as were the residual pore pressure and gas content.

The results of the field investigation also identified a number of key factors for the optimisation of goaf gas drainage design at the Blakefield South mine. It can be concluded that,

- Gas emission sources were the two roof coal seam Wambo and Redbank Creek and the floor seam Glen Munro, whilst the Woodlands Hill seam, situated at 65 m below the working seam, was not.
- Special attention should be given to the Glen Munro seam, where a significant reduction of gas content was seen.
- Capturing gases stored in the Whybrow goafs should be avoided as the gases do not flow down to the active mine workings and therefore contribute to the mine gas emissions.
- Significant delamination occurred from the working seam to the Redbank Creek seam which would likely impact the integrity of surface vertical wells and pose a negative effect on preventing gases from flowing into the ventilation circuit.
- Seam pore pressure monitoring is an effective method to facilitate the assessment of gas emissions from various coal seams.

Based on the above findings, an optimal gas drainage design was developed, which adopted underground horizontal boreholes to replace the surface vertical goaf wells. Such a design not only provides continuous capture of gases from the immediate area of the goaf behind the longwall face but also avoids capturing gases from the Whybrow goafs. In addition, underground horizontal boreholes steering into the floor Glen Munro seam were also designed to preventing gas from flowing up to the goaf.

The design was trialled successfully at the Blakefield South mine. As a result of the trial, a significant reduction in longwall production delays, an increase of gas drainage effectiveness and efficiency, and a remarkable reduction of fugitive emissions were achieved, in comparison to the previous LW3.

CONCLUSIONS

Under the auspices of Australia Government CMATSP project “Mine methane capture optimisation and maximisation of emissions abatement”, a field investigation of mining induced strata, groundwater and gas behaviours was carried out at the Blakefield South mine in Australia. The objective was to provide a fundamental understanding and key factors for the development and demonstration of a holistic and optimal approach to the planning, design, and implementation of optimal mine gas drainage.

Various instruments and methods were used in the field investigation, including surface deep-hole extensometers, surface deep-hole piezometers, tracer tests, and gas content measurement. Many insights into the coupled behaviour of strata, groundwater and gas responses to mining were obtained.

The field investigation successfully identified the three dimensional extent of mining influence, goaf formation process and characteristics, pore pressure changes in the surrounding strata, sources of gas emissions, the profiles of gas emissions across the longwall panel, and effects of the overlying Whybrow goafs. These results have led to an innovative gas drainage design which was trialled successfully at the mine.

ACKNOWLEDGEMENTS

The authors are grateful to Department of Industry and Science, Australian Government for funding this research. The authors would also like to express their sincere gratitude to the management and staff of Glencore Bulga Underground Operations for their significant contributions and CSIRO colleagues who have been involved in this project.

REFERENCES

Karacan, C.Ö., Ruiz F.A., Cotè M., & Phipps, S. (2011). Coal mine methane: A review of capture and utilization practices with benefits to mining safety and to greenhouse gas reduction. *International Journal of Coal Geology* 86, 121–156.

Guo, H., Yuan L., Shen B.T., Qu Q., & Xue J. (2012). Mining-induced strata stress changes, fractures and gas flow dynamics in multi-seam LW mining. *International Journal of Rock Mechanics & Mining Sciences*. 54, 129–139.

Guo, H., Yuan, L., Liang, Y., Qu, Q., Qin, Z., Xue, S., & Xie, J. (2013). Co-extraction of Coal and Methane. In: *Proceedings* of the *23rd World Mining Congress*, Montreal, Canada, 11-15 August 2013. The Canadian Institute of Mining. 14.

Guo, H., Todhunter, C., Qu, Q. and Qin, Z., (2015). Longwall horizontal gas drainage through goaf pressure control. *International Journal of Coal Geology*. 150-151, 276-286.

Palchik, V. (2003). Formation of fractured zones in overburden due to longwall mining. *Environmental Geology* 44, 28–38.

Peng, S.S. (2006). *Longwall Mining (Second Edition)*. West Virginia University.

Qu, Q., Xu, J., Wu, R., Qin, W., & Hu, G. (2015). Three-zone characterisation of coupled strata and gas behaviour in multi-seam mining. *International Journal of Rock Mechanics & Mining Sciences.* 78, 91-98.

Schatzel, S.J., Karacan, C. Ö., Dougherty, H., & Goodman G. V.R. (2012). An analysis of reservoir conditions and responses in longwall panel overburden during mining and its effect on gob gas well performance. *Engineering Geology* 127, 65–74.

Todhunter, C., Crane, I., Foreman, J., Franklin, M., Hill, J., Ferry, J., & Meszaros, G. (2012). Oilfield horizontal drilling technology used to degas an Australian coal mine. World Oil, 103-107.

Whittles, D.N., Lowndes, I.S., Kingman, S.W., Yates, C., & Jobling, S. (2006). Influence of geotechnical factors on gas flow experienced in a UK longwall coal mine panel. *International Journal of Rock Mechanics & Mining Sciences* 43, 369–387.

A METHODOLOGY FOR THE EFFICIENT OPTIMIZATION OF LIFE-OF-MINE SCHEDULES FOR LAMEGO MINE

Paulo Calazans[1], Eduardo Lima[2], Damian Gregory[2], Lorrie Fava[3]

[1]*AngloGold Ashanti*

[2]*Datamine Software*

[3]*MIRARCO, Revolution Mining Software*

24th World Mining Congress
MINING IN A WORLD OF INNOVATION
October 18-21, 2016 • Rio de Janeiro /RJ • Brazil

A METHODOLOGY FOR THE EFFICIENT OPTIMIZATION OF LIFE-OF-MINE SCHEDULES FOR LAMEGO MINE

ABSTRACT

Generating a life-of-mine plan is a complex task that needs to consider various economic, geological, geotechnical, engineering, and mineral processing parameters. It is usually carried out by a team of mining practitioners with expertise in their domains and takes several months to complete. This paper presents the latest developments of a schedule optimization package that maximizes the net present value of a mining operation while honouring precedence, production targets, and resource constraints.

A case study is presented to illustrate the application of the optimization software for a greenfield/brownfield project. In Brazil, the Cuiabá complex located in the state of Minas Gerais, close to the city of Belo Horizonte: includes the Cuiabá and Lamego mines and the Cuiabá and Queiroz plant complexes. The project is based on Lamego mine which is an underground gold deposit consisting of 4 orebodies. A methodology is described for generating mine schedules within hours or days as opposed to weeks or months when carried out using conventional scheduling packages, while identifying a higher net present value for the project. The efforts of the AngloGold Ashanti engineering team deliver high value mine plans quickly and systematically.The method is applied to a case study comparing the results obtained using the conventional scheduling techniques and the optimization software.

KEYWORDS

mine planning, underground mine scheduling, schedule optimization, net present value

INTRODUCTION

AngloGold Ashanti

AngloGold Ashanti is headquartered in Johannesburg, South Africa, and has 19 gold mining operations in nine different countries, as well as several exploration projects. AngloGold´s ore reserves are estimated at 57.5Moz of gold while its mineral resources are estimated at 323.0 Moz. In 2014, the company generated $5.2bn in gold income utilizing $1.21bn of capital expenditure. It corresponds to a production of 4.4Moz of gold.

In the Americas, AngloGold Ashanti has four mining operations as well as an active Greenfield exploration project in Colombia. Three of these four mine operations are in Brazil, one in Goiás state and two in Minas Gerais, the Córrego do Sítio complex and Cuiabá complex, both close to the city of Belo Horizonte. The Cuiabá complex includes the Cuiabá mine which has been in operation for 30 years and a more recently developed underground mine used for this case study: Lamego mine.

The total annual capacity of the complete Cuiabá circuit is 1.7Mt processed at the Cuiabá gold plant which feeds Queiroz hydrometallurgical plant for processing and refining producing also 200,000t of sulphuric acid as a by-product, which is sold commercially on local Brazilian markets. In Figure 1 the general layout of Lamego´s Mine can be seen from an aerial view of the surface infrastructure and a schematic section of the underground development.

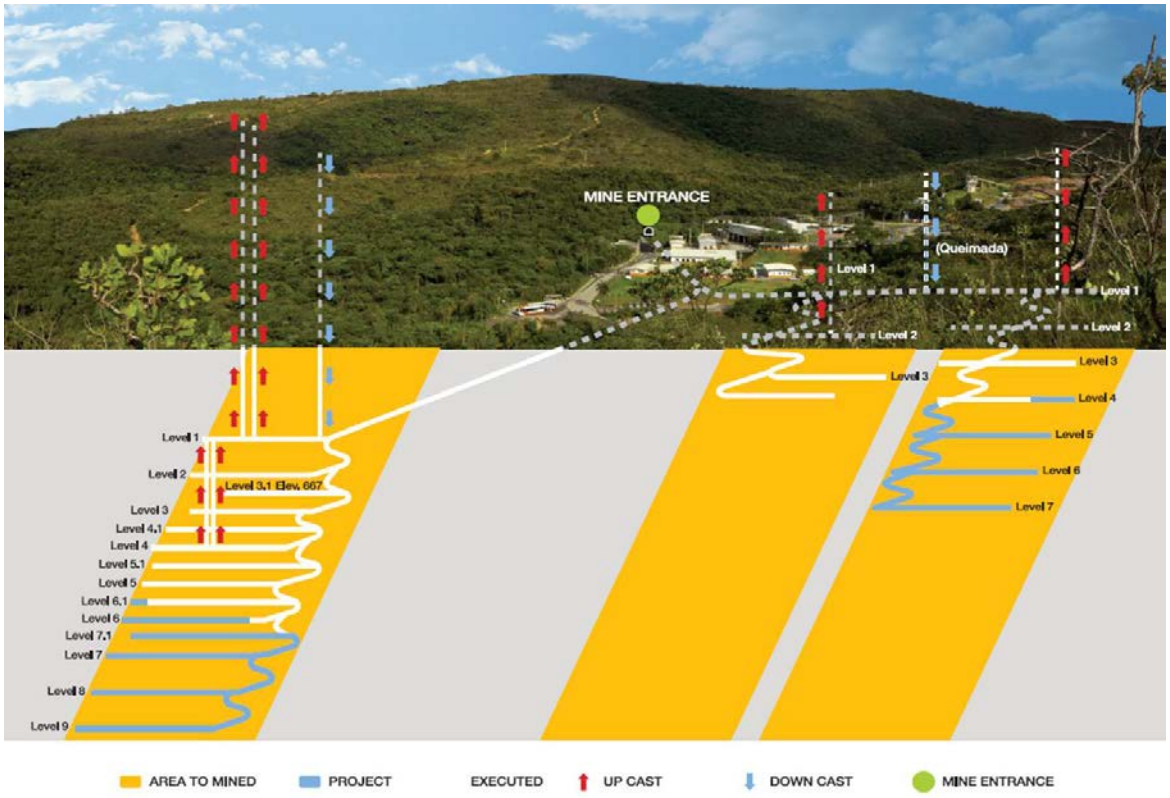

Figure1 - Lamego´s schematic section.

Geology

Lamego´s structure is a regional fold composed of Archean greenstone rocks. The sequence from base to top is metabasalt, banded iron formation BIF, smoky quartz and graphitic schist. The gold mineralisation is hosted mainly in the smoky quartz veins, as free gold, and less on the BIF, related to suphides (Martins et al., 2016). The metabasalt is the core of the fold, being both footwall and hanging wall depending on the limb; the graphitic schists also can be footwall and hanging wall.

Lamego mine is basically composed of 3 main ore bodies. Carruagem orebody is the one that opened the way for the resumption of the Lamego project, the Cabeça de Pedra ore body is located in the hinge region of the large Lamego structure and the Arco da Velha deposit is located on the eastern side of a large fold and extends for 250 m along the strike.

Mining Methods

In Lamego mine there are two different mining methods which were considered: Stope-and-Pillar (Haycocks, 1992), and a variation of Sublevel Stoping (Haycocks & Aelick, 1992). The Stope-and-Pillar mining method can handle variations in the continuity and homogeneity of the ore quality, providing acceptable dilution and good recovery. The advantage of applying this method is that the AngloGold Ashanti team has extensive knowledge of it.

The Stope-and-Pillar method leaves pillars in the stopes that have a large mining area (exceeding 20m span). It allows selectivity, but it has constraints in terms of productivity. The Sublevel Stoping method provides higher productivity and lower operational cost.

Schedule Optimization Tool

The Schedule Optimization Tool, SOT, optimizes the NPV of life-of-mine schedules and has been used by Fava et al. (2013) to generate an optimized life-of-mine schedule of the Leeville underground mining complex (Newmont Mining Corporation). As input, SOT requires a set of development and production tasks (also called activities) representing a mine design. Each excavation, whether access development or stoping, is represented by an activity having properties such as tonnage, metal grade, and mine area. These activities are linked by precedence constraints that represent physical adjacencies between the excavations. A set of required operational resources can be associated with each activity, and constraints can be applied to these resources, either on a mine-wide basis, or more selectively. Finally, a detailed financial model can be specified for the mining project, including operating and capital costs, projected metal prices and the discount rate to be used for the calculation of the NPV.

SOT carries out a search for high-NPV schedules. During this search process, many schedules are generated and the best ones are stored for review by the mine planner. Every schedule generated adheres to all precedence constraints and operational resource constraints, and is evaluated using the selected financial model. SOT uses seeding heuristics to give a good starting point to the search, and an evolutionary algorithm to improve the schedules over many iterations.

CASE STUDY

Data Preparation

A life of mine schedule generated manually using Studio 5D Planner and Enhanced Production Scheduler (EPS) was provided for the purpose of this case study. The schedule contained almost 12,000 activities, the corresponding predecessor and successor dependencies, and numerous fields with properties such as Length, Tonnes, Au content, Description, Orebody, Level, etc. For practical considerations and to ensure the life of mine plan adheres to the mid-term scheduling objectives it was necessary to set the starting day for 65 activities.

Once the scheduling activities are properly linked in EPS there is little or no preparation needed to generate the file to be imported into SOT. For the purpose of this case study two new production fields were calculated – tonnage for each activity and grade for each activity.

Production constraints

Lateral development max 300 m/month

Raise development max 50 m/month

Ore treatment max 480,000 t/year

Total material moved max 650,000 t/year

Costs

Lateral Development 2,722.15 USD/m

Raise Development 44.27 USD/t

Drilling, blasting and transportation for Long Hole stopes ore 38.03 USD/t

Drilling, blasting and transportation for Cut-And-Fill stopes ore 40.75 USD/t

Drilling and blasting of waste 15.01 USD/t

Ore treatment 13.97 USD/t

Capital Investment

Anticipated capital investments for the next 10 years are shown in Table 1.

Table 1 – Projected capital expenditures

Year	USD
2016	8,599,000
2017	3,522,000
2018	3,041,000
2019	3,238,000
2020	2,713,000
2021	1,477,000
2022	1,831,000
2023	1,207,000
2024	274,000
2025	0
2026	0

METHODOLOGY

1. Import Data

Development of a typical SOT project begins with importing the Exchange File created in EPS. In addition to activity duration and precedences, for the purpose of this case study the following EPS fields were imported.

- Tonnes
- Gold grade
- Meters
- Orebody
- Activity Type
- EPS PIN

2. Define Mine Scenario

Operational Resources

The next step is defining the operational resources and resource pools. The following resources were needed:

- Plant – to limit the amount of treated ore
- Jumbo – to limit the lateral development
- Raise – to limit the raise development

This case study did not require investigating different capacity constraints for the operational resources and as a result only one resource pool was created.

Financial Scenario

SOT optimization is driven by NPV. Defining the financial parameters was the next step in the workflow. In addition to Annual Discount Rate, Inflation Rate and Royalty Rate, SOT requires defining product prices. Prices can vary in time and for the purpose of this case study a Gold price in the range between 1,000 and 1,500 USD per troy ounce was used. One financial scenario was used in this case study

Fixed, Point and Sustaining expenditures are also defined at this stage. For the purpose of this case study only Fixed expenditures were used.

Activity Types

Costs per unit length, unit mass, or both were defined for each Activity Type. Where applicable the activity types were associated with the corresponding resources. For example, *Jumbo* resource was assigned to each Sublevel Development and to Primary Development activity types, while *Raise* resource was applied only to Raise activity type.

Mine Scenario

Mining Scenario is a combination of Resource Pool, Financial Scenario, Activity Type, and Plant Recovery. This case study required one Mining Scenario.

3. Parameter Tuning

Select Guidance Heuristic

SOT applies a three stage approach when searching for higher NPV schedules; two stages of parameter tuning are followed by optimization. The first stage uses set of 'guidance' heuristics to compute multiple schedules for the purpose of selecting a heuristic to be used in the optimization process. Twenty schedules were computed for each of the seeding heuristics listed in Table 2. They are ordered as implemented in SOT User Interface.

Table 2 – Guidance Heuristics used in SOT

No	Seeding Heuristic
0	No Guidance
1	Highest Product Grade
2	Highest Product Grade Mine Area
3	Highest Product Weight
4	Highest Product Weight Mine Area
5	Indexed Highest Product Grade Mine Area
6	Indexed Highest Product Weight Mine Area
7	Indexed Least Access by Product Weight Mine Area
8	Indexed Lowest Cost Product Weight Mine Area
9	Least Access by Product Weight Mine Area
10	Lowest Cost Product Weight
11	Lowest Cost Product Weight Mine Area

The Maximum and Average NPV for each of the seeding heuristics are shown in Figure 2. It can be seen that 'Lowest Cost Product Weight Mine Area' heuristic generated schedules with highest average NPV. To protect confidentiality all NPV and Cash Flow values in the following figures and tables have been modified.

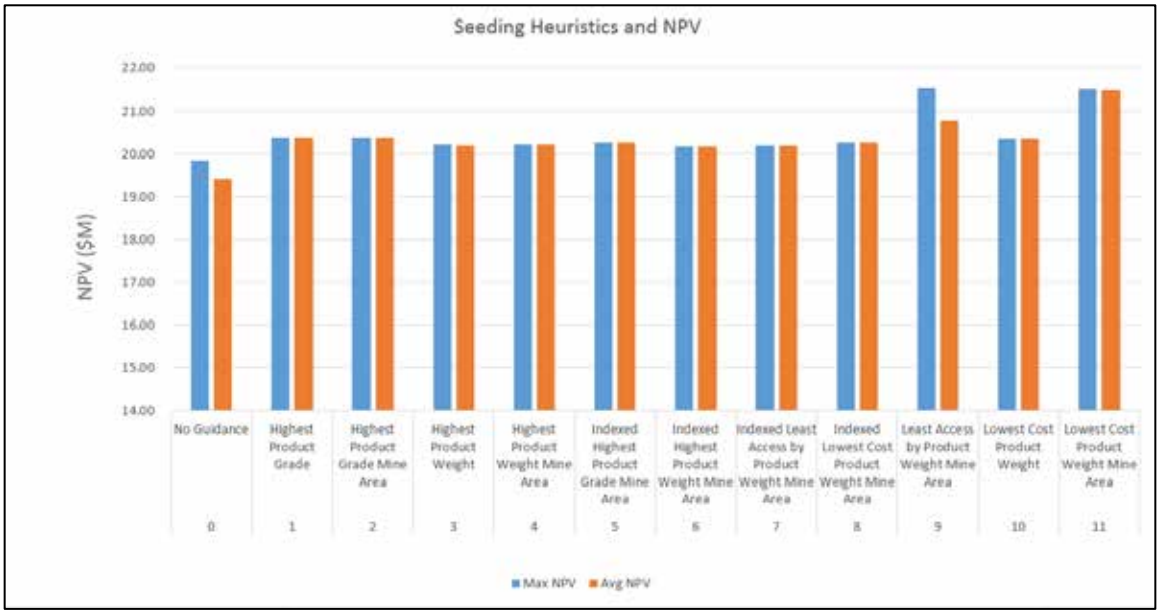

Figure 2 – Comparison of schedules produced with all seeding heuristics

Select Guidance Amount

The scheduling results shown in Figure 2 were computed using 100% guidance. Next, a new set of parameter-tuning runs was executed searching for the most suitable degree of guidance for this case study. Using 'Lowest Cost Product Weight Mine Area' heuristic with 100% guidance there were computed 1,000 new schedules. With the same heuristic additional 3,000 schedules with 90%, 80%, and 70% guidance were computed. Reducing the guidance amount to 90% allowed SOT to deviate from the selected guidance formula for 10% of the stopes, providing more flexibility when generating the schedules. 90% and 80% guidance produced the highest NPV schedules and they were used for the subsequent evolutionary runs.

4. Generate Optimized Schedules

Evolutionary Learning

SOT uses an evolutionary learning mechanism to compute new schedules. The next set of runs were learning runs that used 'Lowest Cost Product Weight Mine Area' heuristic with 90% guidance to generate initial schedules. Within less than 14 hours, the learning run with 100 resets generated 32,070 schedules. Iteration 452 had the maximum NPV of all learning runs. Figure 3 shows graphically the average and maximum NPVs for several iterations of the learning run.

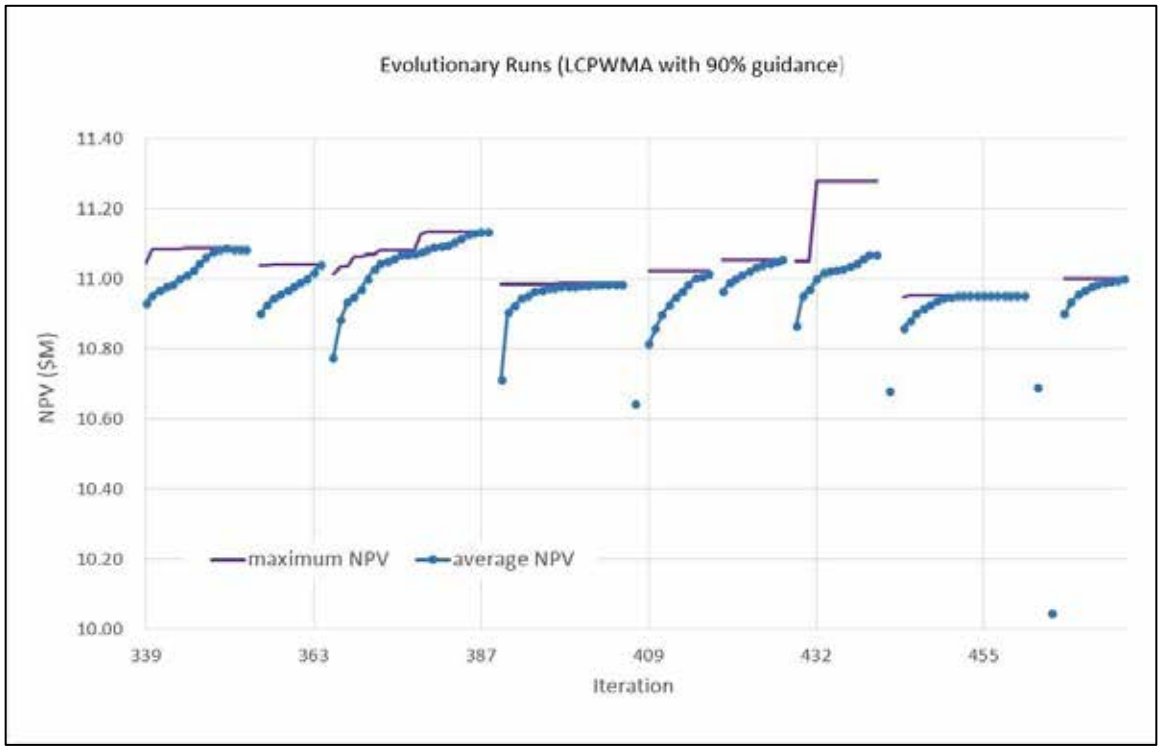

Figure 3 – Evolutionary run for Lowest Cost Product Weight Mine Area heuristic with 90% guidance

Evolutionary run with 'Lowest Cost Product Weight Mine Area' heuristic and 80% guidance was also computed. Within 11 hours the learning run with 100 resets generated 24,134 schedules. Iteration 342 had the maximum NPV that is 2% less compared to evolutionary run with 90% guidance.

Seeded Learning

Use the best solution as a custom heuristic (seed) for further evolutionary learning.

Review the Best Schedules

The best schedules were saved in the SOT database. Their financial and production results were reviewed using the built-in graphing functionalities to ensure all practical constraints were met. The selected schedules were exported from SOT for further analysis and animation in EPS/EPS InTouch.

5. Reference Run

The financial model used by SOT was applied on the baseline schedule created manually in EPS to allow comparison with the schedules generated by SOT. In this run SOT keeps the activity starting date as set in EPS and reports all production, capacity, and financial statistics.

RESULTS

Data preparation, import, and defining SOT inputs took approximately 4 hours. All tuning runs to find the most suitable guidance formula and amount were completed within 5 hours and required 1 hour to set and analyze. The evolutionary run was set within a few minutes and completed in less than 14 hours. Using SOT, the total involvement of the planning engineer was less than 8 hours. Computations were completed in approximately 31 hours. By comparison, the manual schedule was completed in 10 days.

Figures 4, 5, 6 and 7 contain a summary of the production and financial results obtained from SOT and manually. The SOT schedules respected to all production constraints, whereas the manual schedule, for example, inadvertently exceeded the lateral development capacity in year 4, that was limited to 300 m/month, which adds to 3600 m/year.

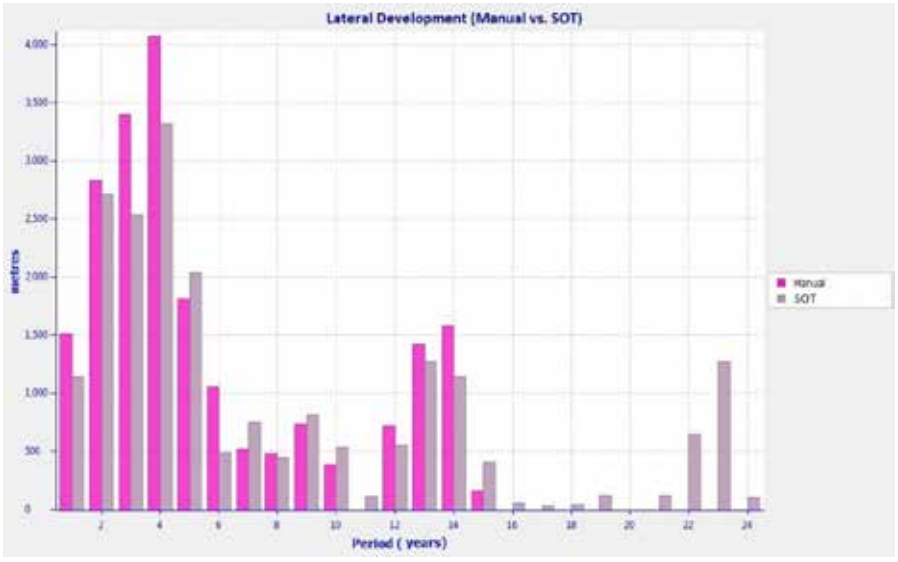

Figure 4 – Annual lateral development (Manual vs. SOT schedules)

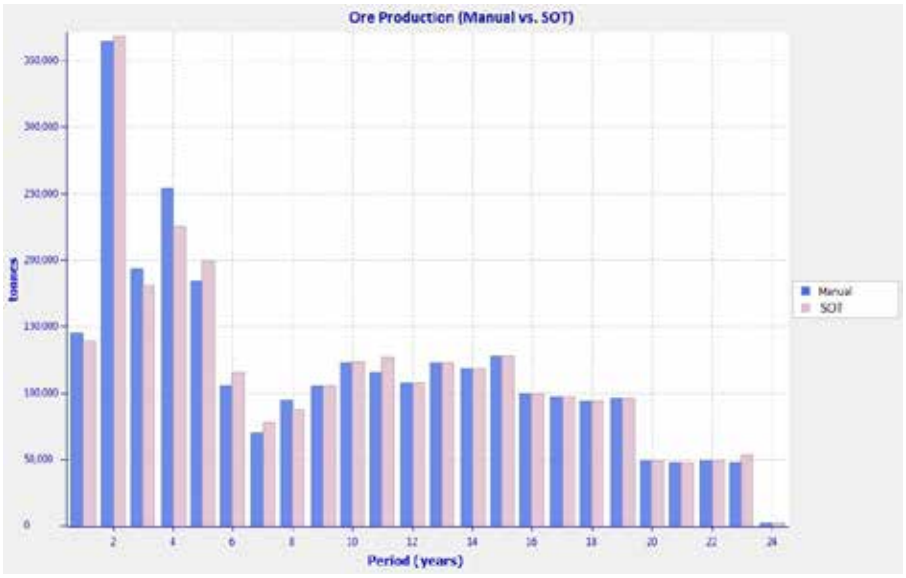

Figure 5 – Annual ore production (Manual vs. SOT schedules)

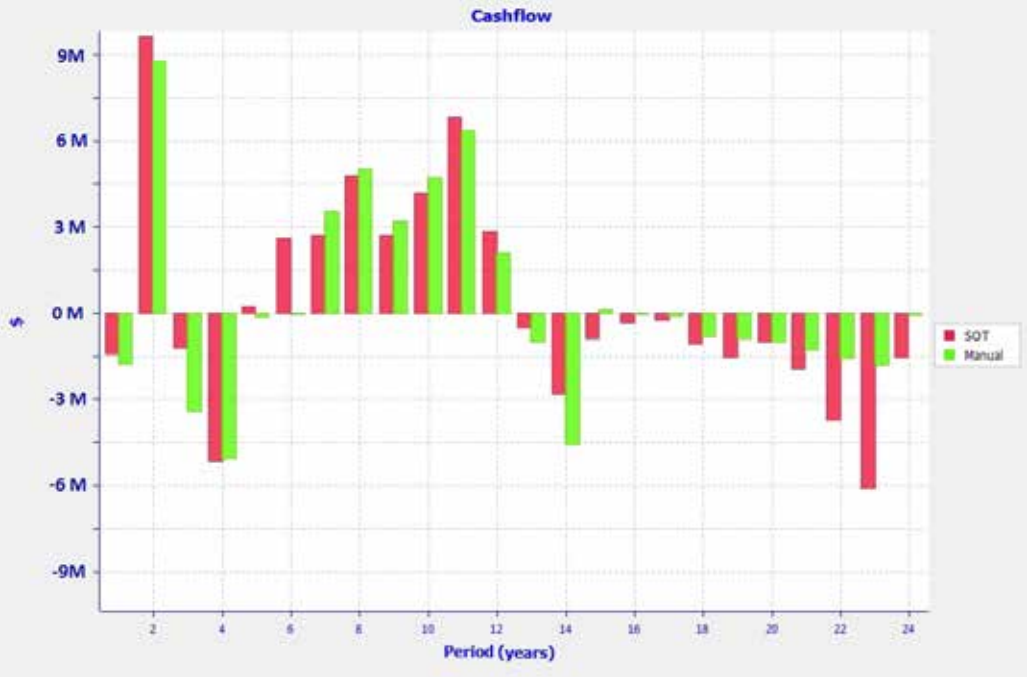

Figure 6 – Annual cash flow (Manual vs. SOT schedules)

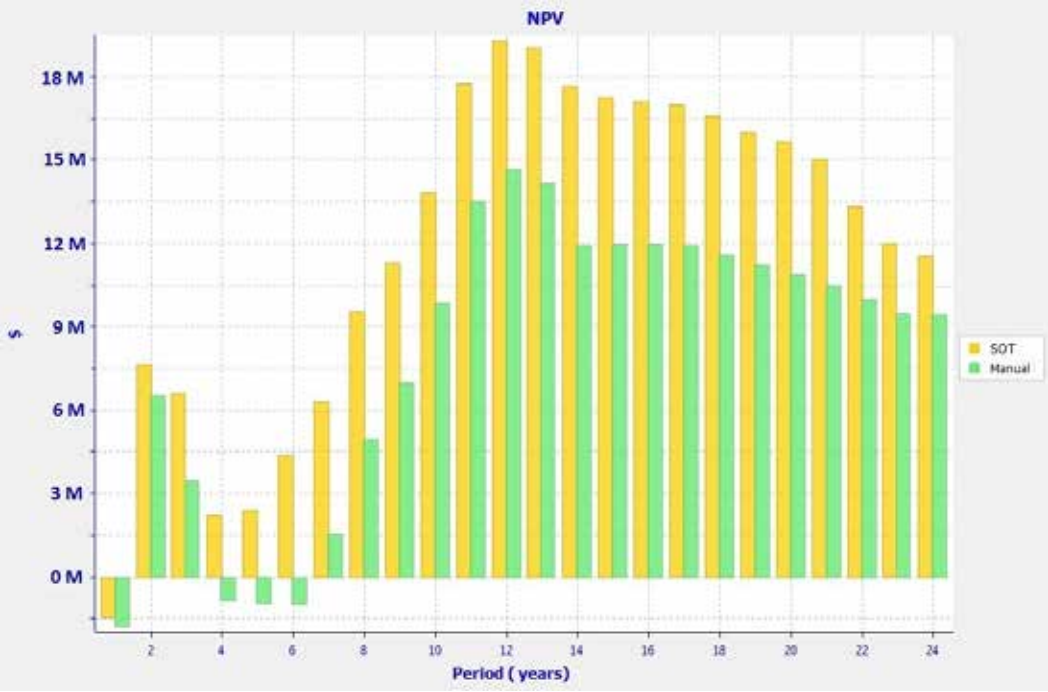

Figure 7 – Cumulative NPV (Manual vs. SOT schedules)

CONCLUSION

With significantly less efforts and within shorter time SOT produced a schedule that adheres to all production constraints and has peak NPV that is 23.8% higher than the manual method. The full mine schedule generated by SOT is 24.7% higher than the manual.

It is possible to conclude from Figure 6 and Figure 7, since both the cash flow and the cumulative NPV decrease in later years, that an optimal solution would end mining operations in year 12. So, why keep mining after year 12?

The pronounced negative cash flows in later years can be attributed to a lack of drilling information to sustain the reserves in the deepest levels of the Carruagem orebody, corresponding to production after Year 12 when the mine starts to mine these areas. From the geological point of view, the orebody outline is continuous in deeper levels and there is a clear perspective to keep mining after year 12, but it should be confirmed be new drilling campaigns.

The outcomes of this study reinforces the need to gather more information for the lower levels of the mine. Also, from a business perspective, it indicates a decision point of whether to assume a risk and project in the deepest levels the potential shown in the upper levels, or to end the operation in year 12.

REFERENCES

Fava, L., Saavedra Rosas, J., Tough, V., and Haarala, P. (2013). Heuristic Optimization of Scheduling Scenarios for Achieving Strategic Mine Planning Targets. 23rd World Mining Congress Aug 11-15, 2013, Montreal, Canada.

Anglo Gold Ashanti Mineral Resource and Ore Reserve Report – December 2015 - Business Unit – Cuiabá – Lamego Lamego Mine Geology / Planning

Hartman H. L. (1992). Stope and pillar mining. In Haycocks C. (Eds.), *SME Mining Engineering Handbook* (2nd ed., pp. 1702-1711) Littleton, Colorado : Society for Mining, Metallurgy, and Exploration, Inc.

Hartman H. L. (1992). Sublevel stoping. In Haycocks C. & Aelick R.C. (Eds.), *SME Mining Engineering Handbook* (2nd ed., pp. 1717-1731) Littleton, Colorado : Society for Mining, Metallurgy, and Exploration, Inc.

Martins, B. S., Lobato, L. M., Rosière, C. A., Hagemann, J. O. S. S., Villanova, F. L. S. P., Silva, R. C. F., Lemos, L. H. A. (2016). The Archean BIF-hosted Lamego gold deposit, Rio das Velhas greenstone belt, Quadrilátero Ferrífero: Evidence for Cambrian structural modification of an Archean orogenic gold deposit. *Ore Geology Reviews, volume 72*, 963-988. doi: 10.1016/j.oregeorev.2015.08.025

A NEW METHOD FOR ANALYSING AND ESTIMATING THE PRODUCTION COSTS USED TO DESIGN UNDERGROUND METALLIFEROUS MINING

*G. Mihaylov

University of Mining and Geology "St. Ivan Rilsky" – 1700 – Sofia, Bulgaria
*(*Corresponding author: mihayg@mgu.bg)*

24th World Mining Congress
MINING IN A WORLD OF INNOVATION
October 18-21, 2016 • Rio de Janeiro /RJ • Brazil

A NEW METHOD FOR ANALYSING AND ESTIMATING THE PRODUCTION COSTS USED TO DESIGN UNDERGROUND METALLIFEROUS MINING

ABSTRACT

This paper aims to present precise calculations in pre-feasibility and feasibility studies since the errors allowed in those computations have serious consequences for the technical and economic indicators of the mine during operation for many years to come. A method has been developed for determining the total mine operating costs. It involves three parts: (1) costs for opening-up and basic development of the ore deposit; (2) costs for the mining technology; (3) structure of the forms for processing and analyzing the results. In the second part special attention is paid to the production costs for stoping. For the purpose, the mining processes are systematized in their logical sequence, some of them being decomposed to operations.

The second part also involves damages caused by ore losses and dilution as an inseparable part of the applied mining technology.

The investigation process is based entirely on the multivariate approach using an original classification of the mining methods which was first presented by the author at 22 WMC – Istanbul. The optimal variant for selecting the mining technology is sought in a multi criteria assessment including material and value indices. This approach allows analytical relationships to be found between the total costs and the geometrical parameters of the stope (basic production unit): stope length, sublevel height (level height, respectively), height of mined-out split, etc.

The procedure proposed for determining the total mine operating costs can find application in designing the mining operations in two mining sites whose practical realization will start in 2016.

KEYWORDS

Mining methods Classification, Production processes Classification, Operating costs structure, Model for a mining technology.

INTRODUCTION

Underground mining is one of the most dynamically developing branches of the mining industry. In practice, 95 percent of today's production processes are mechanised, and the scale of automation exceeds 60 percent. There is an essentially new generation of equipment that is more expensive, with the maintenance costs growing too. The only way to make up for the progressively increasing total costs is *to continuously improve the adopted work organisation*. This means that a coherent system of logically consistent rules should be developed to give content to the concept of Sustainable Organisations. A typical example is the functional dependencies that determine the technical and financial nature of the mining stages. The following stages in the mining process are adopted:

- Capital and mine access development;
- Mining, including:
  - ore and waste development in the block as a main mining unit;
  - production processes;
- Damages arising from ore losses and dilution.

Mining method improvement is the result of the innovation capabilities of a wide range of expertise able to generate and, most importantly, implement new ideas. Ultimately, this is a project whose positive evaluation depends on its place in space called Standards of Excellence. The selection of the best option requires sufficient objective criteria, which essentially fall into two groups: value and natural criteria. The complexity of the task requires *a multi-criteria evaluation*. Its components can

give content to the concept of evaluation complexity where a set of indicators is formed and corresponds to points in the n-dimensional Euclidean space.

The successful selection of the actual mining method is preceded by detailed exploration. Natural settings are exceptionally diverse and cannot be properly interpreted without statistical methods and a probability approach to risk assessment in the decision-making process. The best option is defined after three groups of constraining parameters have been introduced:

- rock mechanics;
- exchange metal prices;
- available funding /investment/ to implement the project.

This paper attempts to outline the general costs when selecting the best mining method by considering the above three mining stages.

MINING METHOD-RELATED COSTS

Mine access development

The block development costs are estimated using the main block geometric dimensions:

- Block length, L_{BL}
- Level height, H_{ET};
- Sub-level height (in case the block is divided into sub-levels), h_{PE};

Each mine development has a length L, a section S, and the volume will obviously be $V = L \times S$. The selected approach is based on the principle that each development is identifiable by a unique code. In this specific case, this is achieved by introducing three indices *i, j, k,* where $i = \overline{1, M}$ is the serial number of the mining method under study; M is the total number of mining methods (M=38). It is based on the classification prepared by the author (Mihaylov,2011). According to this classification, the mining methods can be classified using the class - group - sub-group - option scheme; $j = \overline{1, N}$ characterises the type of working. In this case N=4 since four types of workings are considered: horizontal developments (j=1), declines (j=2), vertical openings (j=3), and stopes (j=4). The serial number of each development type is characterised by the index $k = \overline{1, P}$. The maximum number of developments in each type is algorithmically capped at P=10. Some are ore developments, whereas others are waste rock developments. This requires the use of a forth index in the analysis of value criteria $l = \overline{1, Q}$ where Q is the total number of options. In this specific case, Q=2, i.e. where l=1, these are ore developments and where l=2, these are waste rock developments. Then, if C is the value for $1 m^3$, then the following equation will be valid:

$$CENA_{jkl} = V_{jkl} \times C_{jl} \tag{1}$$

Here, the valid rule is: if l=1, then $C_{j1} \neq 0$ and $C_{j2}=0$ and vice versa: if l=2, then $C_{j2} \neq 0$, $C_{j1}=0$.

Then the total value for all developments whose total number is k for the i mining method of j type will be $\sum_{k=1}^{P} \sum_{l=1}^{Q} CENA_{kl}$, and the sum of all developments for i the mining method of j type will be

$$SUMC_{ij} = \sum_{j=1}^{N} \sum_{k=1}^{P} \sum_{l=1}^{Q} CENA_{ijkl} . \tag{2}$$

The costs need to be classified in groups due to the specific nature of horizontal developments, declines, vertical openings, and stopes. For instance, the following sum should be used for the i mining method: $SUMC_{i1} + SUMC_{i2} + SUMC_{i3} + SUMC_{i4}$, i.e.

$$SUMPR_i = \sum_{j=1}^{N} SUMC_{ij} \quad (3)$$

In this case $SUMPR_i$ is the first value criteria derived by using this methodology. The total length $SUML_i$ and the total volume $SUMV_i$ can be estimated by analogy for all developments for the i mining method

$$SUML_i = \sum_{j=1}^{N}\sum_{k=1}^{P} L_{ijk} \; ; \quad (4\text{ a})$$

$$SUMV_i = \sum_{j=1}^{N}\sum_{k=1}^{P} V_{ijk} \quad (4\text{ b})$$

These indicators depend on the structure of the i mining method under consideration. To become objective evaluation criteria, they need to be referred to the total contained reserves in the block ZBL_i As an exception, the contained reserves can be viewed as a constant, i.e. ZBL_i = const. Thus, there are three evaluation criteria for the set of options. One is a value criterion used to determine the costs of development of 1t of reserves CPR_i .

$$CPR_i = \frac{SUMPR_i}{ZBL_i}, \quad \text{USD/t} \quad (5)$$

The other two are natural criteria: a linear factor $KLPR_i$ and a volume factor $KOPR_i$ for the developments:

$$KLPR_i = \frac{1000 SUML_i}{ZBL_i}, \quad \text{m/1000t} \quad (6\text{ a})$$

$$KOPR_i = \frac{1000 SUMV_i}{ZBL_i}, \quad \text{m}^3\text{/1000t} \quad (6\text{ b})$$

The estimation procedure for CPR_i , $KLPR_i$, $KOPR_i$ is valid for all mining methods included in the set $i = \overline{1, M}$. It is not valid where a method i is inapplicable due to natural, technical or economic constraining conditions.

Mining unit operating costs

The systematic study of the production processes as a logical sequence have resulted in a consistent classification. It forms the basis of the approach used to analyse the operating costs applicable to the block as a main mining unit. Table 1 shows the classification of the production processes.

The two indices in Table 1 correspond to the ore breakup operations. The three indices allow for two possible methods of gravity flow. Loading, haulage and gravity flow should be viewed as elements of a “three-element process”. The process behaviour varies since haulage may precede or follow loading in different case scenarios. Where the mining scheme includes gravity flow, the structure of the bottom of the mining unit must be taken into consideration.

The types of cost incurred in the processes can be classified in a similar manner to the production processes. This classification is shown in Table 2. The principle used to estimate the mine operating costs is as follows: Each production process A_a is conducted at the relevant cost B_b. Based on Tables 1 and 2 a solid [C_{ab}] can be produced where $a = \overline{1, D}$ and $b = \overline{1, E}$, where D=7, a E=3.

Table 1 – Classification of the production processes

No	Production process	Symbol
1.	Breaking up of ore	A_1
	- drilling	A_{11}
	- charging	A_{12}
	- blasting	A_{13}
2.	Loading	A_2
3.	Haulage	A_3
	incl. – Gravity flow	A_{31}
	• in contact with caved rock	A_{311}
	• in open stopes	A_{312}
4.	Ground support	A_4
5.	Rock stress control	A_5
6.	Ventilation	A_6
7.	Supporting and auxiliary processes	A_7

Table 2 – Classification of the types of cost incurred in the production processes

No	Cost type	Symbol
1.	Equipment depreciation and repair costs	B_1
2.	Labour costs incl. wages and salaries, social contributions	B_2
3.	Consumables and electrical power	B_3

The actual implementation of the approach is unthinkable without further breakdown of costs. Table 3 shows this cost breakdown, thus providing specific details required for the additional analysis.

The variable nature of the three groups of costs in Table 3 shows that further analysis will require a uniform measurement system.

The introduction of the term “specific costs” in USD/t is most appropriate. This reduction, however, depends directly on at least three groups of organisational factors:

Group I: Number of working days per year;
Number of work shifts per 24 hrs;
Time between repairs;

Group II: Selection of a method to estimate equipment productivity;
Possible combination of production processes;
Cycle times;
Ventilation organisation after blasting;

Group III: Methodological basis for estimating consumable and electrical power costs;
Preparation of standards regulating consumable and electrical power costs based on direct and indirect methods.

Table 3 – Breakdown of cost required for the additional analysis

Operating cost structure		Symbol
1.	Equipment depreciation and repair	B_1
1.1	Depreciation allowance	AMORT
1.2	Overhaul	REMONT1
1.3	Repair	REMONT2
Total depreciation allowance, USD/annum		SUMAMOR
2.	Labour costs	B_2
2.1	Wages and salaries	ZAPLATA
2.2	Social contributions	NACHISL
2.3	Benefits	DOBAVB
2.4	Corporate social responsibility	COSORE
Total labour costs, USD/shift		SUMZAPL
3.	Consumables and electrical power	B_3
3.1	Consumables	MATER
3.2	Electrical power	ENER
3.3	Fuel and lubricants	GORSM
3.4	Spare parts	REZER
3.5	External services	USLUGI
Total costs incurred in consumables and power, USD/t		SUMMER

The three groups of factors are a key element in the operating cost analysis. Cost optimisation will require the accumulation and examination of a significant amount of data, particularly regarding the output of the block as a main mining unit. It depends on the cycle times and possible combination of production processes, respectively. The high mobility of contemporary equipment allows for a single piece of equipment to operate in more than one mining unit. The time this equipment is in operation increases. However, the metreage and tonnage of development need to be greater. The specific costs can be estimated by applying some transformations and using the specific nature of the three groups of factors:

- depreciation and repair, *SUMAMSP*;
- salaries, social contributions and benefits, *SUMZASP*;
- consumables and electrical power, *SUMMER*.

Thus, the total operating costs can be estimated for a certain production process

$$SUMPRP = SUMAMSP + SUMZASP + SUMMER, \quad \text{USD/t} \tag{7}$$

Using Tables 1 and 2, the total costs for all production processes will be

$$ALLSUM = \sum_{a=1}^{D}\sum_{b=1}^{E} SUMPRP_{ab}, \quad \text{USD/t} \tag{8a}$$

Cost analysis on a process by process basis should be carried out for all mining methods. According to the adopted classification of mining methods (Mihaylov,2011), the set $i = \overline{1,M}$ determines the total number of methods under consideration. In this case M=38. This should finally write as follows:

$$ALLSUM_i = \sum_{a=1}^{D}\sum_{b=1}^{E} SUMPRP_{abi}, \quad \text{USD/t} \tag{8b}$$

In order to simplify the algorithm, the production processes include operations A_{11}, A_{12}, A_{13} and gravity flow A_{31} and related alternatives A_{311} and A_{312} (Table 1). Thus, the index *D* is assigned 11, with the resultant array of numbers being $MAC = D \times E \times M = 11 \times 3 \times 38 = 1254$ which

characterises the costs on a process by process basis for all mining methods included in the classification.

ASSESSMENT OF DAMAGES ARISING FROM LOSS AND DILUTION

Each mining method is characterised by some losses and dilution. The related damages have far-reaching economic implications that can compromise a technique implemented through state-of-the-art mining equipment. Therefore, an important task in selecting the best method is to systematically examine the nature of losses and dilution and their possible control. The papers of M.I.Agoshkov (Agoshkov et al, 1966) and V.R.Imenitov (Imenitov, 1984) are used as a basis for the methodological approach to the analysis of damages from losses and dilution.

Assessment of loss damages

The procedure used consists of the following steps:

Step 1 Assessment of damages arising from the loss of 1t of economic reserves *SHTZA*. This value is estimated as the sum of the costs *SUMR1* plus the sale proceeds *DPECH.* On the other hand, *SUMR1* includes the costs incurred in:

- exploration, *DGPR*;
- depreciation allowance for capital stripping, *DAMOR*;
- ore breaking up as per Table 1 – A_1(A_{11}, A_{12}, A_{13}).

Step 2 Assessment of loss damages referred to 1t of extractable reserves, *SHTUZA.* This parameter is directly affected by mining losses typical of every mining method, AE_i ($i = \overline{1,M}$ according to the classification of mining techniques (Mihaylov,2011). There is a functional dependency *ETA = 1 – AE* where *ETA* is the recovery. In this case the damages arising from the losses as referred to 1t of extractable reserves will be

$$SHTUZA_i = \frac{ETA_i \times SHTZA_i}{1 - ETA_i}, \quad \text{USD/t} \tag{9}$$

It should be emphasised here that only the operating losses AE_i are taken into account. The total mining losses will be subjected to another analysis relating to the selection of capital development method.

Assessment of dilution damages

The procedure does not differ from that set out in 3.1. It consists of the following steps:

Step 1 Assessment of damages arising from mixing of ore and 1t of rock waste *SHTOB*. This parameter is estimated as a sum of the following figures:

- cost of transport of 1t of ore to the processing facilities, *RAZTR;*
- cost of processing of 1t of ore at the processing facilities, *RAZPROF*;
- loss of metal (contained commodity in waste), *DUOTP*.

Step 2 Estimation of the tonnage of rock mixed with 1t of extractable reserves, *XSKALA.* This parameter depends on the contained commodity in the solid *AM* and the actually extracted ore *AF*. In this case it is a zero-dimensional parameter.

Step 3 Assessment of the economic damage from dilution assigned to 1t of extractable reserves, *SHTUOB*. *SHTUOB* is obviously in direct ratio to *XSKALA*. On the other hand, XSKALA is determined by the dilution *B*, where $B = \frac{AM - AF}{AM}$. Every mining method is characterised by varying tonnages of actually mined ore AF_i at AM=const where $i = \overline{1,M}$ is the serial number

according to the classification of mining methods (Mihaylov,2011). Therefore, the dilution factors *B* and the grades in the actually mined ore *AF* coincide. Then

$$SHTUOB_i = XSKALA_i \times SHTOB_i, \quad \text{USD/t} \tag{10}$$

Similarly to *ETA*, the analysis of dilution damages uses an ore grade variation factor: RO = 1-B. This allows the ore tonnage factor *KKOL* to be found in the expression

$$KKOL = \frac{ETA}{RO} = \frac{1-AE}{1-B} \tag{11}$$

Depending on operating losses *AE* and dilution *B* the factor *KKOL* is circa 1, including KKOL=1, where AE=B.

GENERAL MODEL FOR A MINING METHOD

The scope of application of a mining method (mining technique) is defined within a certain range of natural setting variation. On the other hand, the mining method is defined by actual geometric dimensions of the block as a main mining unit. There are functional dependencies between the mining unit dimensions and the efficiency evaluation indicators. Just like at the planning stage, their assessment at the reconstruction and modernisation stage is one of the key steps of the innovation process.

By adding up the development costs CPR_i , operating costs $ALLSUM_i$ and damages arising out of losses $SHTUZA_i$ and dilution $SHTUOB_i$ an important value indicator can be produced

$$CFULL_i = CPR_i + ALLSUM_i + SHTUZA_i + SHTUOB_i, \quad \text{USD/t} \tag{12}$$

The index i corresponds to the serial number of the method under consideration in the classification of mining methods represented by the set $i = \overline{1,M}$ where M is the total number of the methods (in this case M=38).

This approach shows a significant potential in the attempt to find the optimal geometric parameters, for instance the block length L_{BL}, the level height H_{ET} and the sub-level height h_{PE}, respectively, the layer height h_{SL}, etc. Generally, the target function is as follows:

$$CFULL = f_1(L_{BL}, h_{PE}) \rightarrow \min; \text{ or} \tag{13a}$$

$$CFULL = f_2(H_{ET}, L_{BL}) \rightarrow \min. \tag{13b}$$

The problem can be expanded by introducing variables relating to natural settings: thickness of ore vein (ore body) W, dip α, commodity grade *AM*, etc.

Following the steps of $CFULL_i$ assessment, it can be concluded that there is an analogy between the principles of management of complex production systems and those of mining methods, i.e.:

- There is an identical structure of information flows characterising the input and output parameters;
- The factors affecting the management effectiveness can be classified in two groups: manageable and unmanageable.

The most essential difference in mining method management as compared to all other production systems is the role and significance of unmanageable factors. They form the constraining conditions as to the method applicability, for instance dip α, orebody thickness *W*, commodity grade *AM*, etc.

The structure of the manageable factors is such that they can improve the mine site environment at the expense of the innovation processes. The wider range of manageable factors is related mainly to the block output, stability of the construction units of the mining method, air conditioning, the size of the low-grade portion, etc.

Taking into consideration the specifics of the mining techniques, i.e. compulsory processing of the run-of-mine ore at the processing plant, the index called LEVEL OF SUCCESSFUL DECISION (LSD) is produced.

$$LSD = CFULL + RPROF\,, \quad \text{USD/t} \tag{14a}$$

Where *RPROF* are the costs of processing run-of-mine ore at the processing plant, USD/t. Then the expression for *LSD* will finally read as follows:

$$LSD = CPR_i + ALLSUM_i + SHTUZA_i + SHTUOB_i + RPROF_i\,, \quad \text{USD/t} \tag{14b}$$

Figure 1 shows the path used to get LSD_i for the mining method *i*. Thus, having presented the overall procedure, the main purpose can be formulated as follows: *To find such a combination of manageable parameters* $\beta_1, \beta_2, \ldots \beta_m$ *which, in the presence of preliminary (input) parameters* $\alpha_1, \alpha_2, \ldots \alpha_n$ *and taking into account the unknowns* $x_1, x_2, \ldots x_k$, *will guarantee a maximum of the target function LSD*. The expanded function *LSD* will read as follows:

$$LSD = F(\alpha_1, \alpha_2, \ldots, \alpha_m, \beta_1, \beta_2, \ldots, \beta_n, x_1, x_2, \ldots, x_k) \rightarrow \max \tag{14c}$$

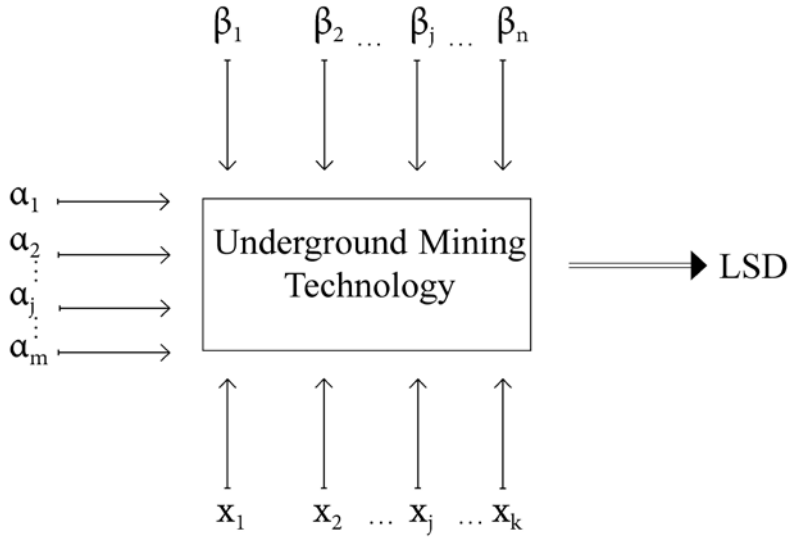

Figure 1 – The path used to get LSD for the mining method

Figure 2 shows the block diagram for *LSD* implementation. Table 4 shows the most common parameters used to determine the *LSD* for underground mine operations. The structure of the three groups of indicators is open, i.e. new ones can be added to each group depending on the specifics of the site under study. The implementation of the algorithm used to find the maximum value of the *LSD* function requires the parallel application of both principal approaches in the decision-making theory. The inductive approach is employed in data accumulation relating to preliminary (input) α_i and manageable β_j parameters. The deductive approach is used where the actual project implementation shows stable *LSD* levels within a sufficiently long period. Then the effect of the individual groups of factors is examined with a view to determining those which are of greatest relative influence.

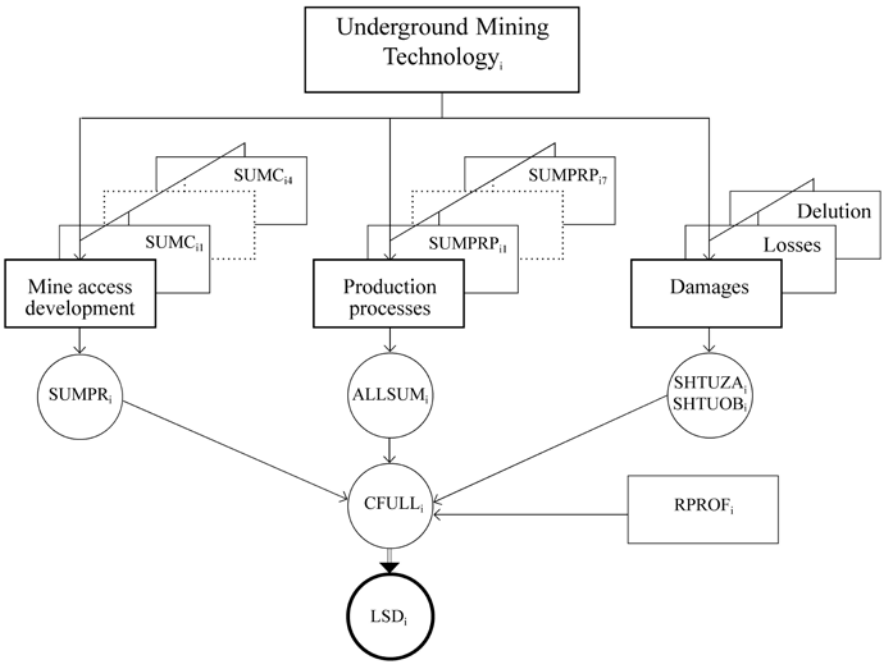

Figure 2 – Block-diagram for LSD implementation

Table 4 – The most common parameters used to determine the LSD

No	Group of parameters	Description	Symbol
1	Preliminary (input) parameters α_i $i=\overline{1,m}$	Reserves (resources) within the contour of the orefield.	α_1
		Orefield size (if the deposit requires orefield division).	α_2
		Mine output	α_3
		Mill-head grade	α_4
2	Manageable parameters β_j $j=\overline{1,n}$	Ore and wall rock stability	β_1
		Losses	β_2
		Dilution	β_3
		Specific power consumption, kWh/t	β_4
		Monthly output referred to 1 kW, t/kW	β_5
3	Unknown parameters x_l $l=\overline{1,k}$	Orebody thickness	x_1
		Dip	x_2
		Commodity content	x_3
		Exchange metal price	x_4
		Mining depth	x_5

CONCLUSION

The high variability of settings precludes the selection of only one mining method for a specific site. On the other hand, the geometric parameters of the mining unit also vary and this is largely due to the shape and size of the orebodies and the equipment selected to carry out the production processes. To solve such type of multivariant problems, the costs (planned and actually incurred) are of paramount importance. In this specific case, these are the development and operating costs. The damages arising from losses and dilution are added as they vary from one mining method to another. The variety of the input data requires a certain unifying code. It can be found by using three classifications based on various indicators.

The first classification is that of the mining techniques. It comprises a set of *M* mining methods.

The second classification is that of development types (four in total).

The third classification is that of the production processes in the block as a main mining unit (seven in total).

A considerable dataset is accumulated and needs to be systematised. For instance, each group of operating costs consists of three elements: equipment depreciation and repair costs; labour costs; consumables and electrical power costs. The selection of an optimum method is based on a certain number of criteria systematised in two sections: value and natural criteria. Thus, the basis required for mining method modelling is formed. The information flows including input parameters, manageable parameters and unknown parameters have been systematised for this purpose. All of them are open to additional ones. A possible way to evaluate the efficiency of each options is the indicator used here that allows for the level of successful decision (*LSD*). The most difficult task is to find a solution to the target function *LSD*. Apparently the number of unknowns exceeds the number of equations. Thus, the solution is sought by introducing appropriate input and constraining conditions using the principles of the inductive and deductive approach.

REFERENCES

Mihaylov, G. (2011) Technological and Geomechanical Logistics for Underground ore Mining. 22nd World Mining Congress & Expo. Volume II , pp.493-499, 11 – 16 September, Istanbul, Turkey.

Агошков, М.И., Г.М.Малахов. (1966) Подземная разработка рудных месторождений. Недра, Москва, p. 664. (in Russian).

Именитов, В.Р. (1984) Процессы подземных горных работ при разработке рудных месторождений. Недра, Москва, p.504. (in Russian).

AN INVESTIGATION INTO EFFECT OF MINE TAILING PARTICLE SIZE IN THE STRENGTH EVOULUTION OF CEMENTED MINE BACK FILL

M. Kermani, F.P. Hassani

McGill University, Mining Engineering Department,
Montreal, QC. Canada H3A 2A7

24th World Mining Congress
MINING IN A WORLD OF INNOVATION
October 18-21, 2016 • Rio de Janeiro /RJ • Brazil

AN INVESTIGATION INTO EFFECT OF MINE TAILING PARTICLE SIZE IN THE STRENGTH EVOULUTION OF CEMENTED MINE BACK FILL

M. Kermani[1], F.P. Hassani[1,*]

Mining Engineering Department, McGill University
Montreal, Quebec, Canada

ABSTRACT

In this paper, the effect of particle size of tailings and binder concentration on the mechanical and rheological properties of cemented mine backfill were investigated by conducting a series of laboratory experiments. Different mine backfill samples were prepared and tested. Large numbers of samples with various mixture designs were cast and cured over 56 days. The mechanical properties of samples were investigated using uniaxial compression test (UCS), and the results were compared with those of reference samples made. The test results indicated that the tailing particle size has a great effect on the uniaxial compressive strength, (UCS) and rheological properties of backfill. The rheology analysis revealed that the modification of particle size of tailings particle can modify the rheological properties of mine backfill. Finally, the study showed that the use of slag/cement binder can enhance the uniaxial compressive strength of samples.

KEY WORDS

Cemented backfill; UCS; rheology; Tailing Particle Size; Paste Backfill

INTRODUCTION

The process of filling the void created by underground mining activities with waste materials is defined as mine backfilling. Mine backfill has become an integral part of underground mining methods all around the world. Mine backfilling is primarily used to increase ore extraction, increase ground mine stabilization, and deposit waste materials. The increase of demand for minerals and increase of the depth of mining operations are the main challenges facing the mining industries. These challenges require to apply innovative methods that can meet the mining operation requirements in an environmentally friendly manner. At the same time, consistently increasing environmental standards and mine closure regulations require innovative approaches in mine waste disposal technology.

Cemented paste backfill (CPB) basically consists of tailings, binder and water. Tailings is the main part of mine backfill material and its physical properties can defined the ultimate mechanical properties of place backfill. Tailings particle size has a crucial role in mine backfill engineering. The effect of tailings particle size on the mechanical properties of placed backfill has been investigated by many authors (Aref et al., 1989; M. Benzaazoua et al., 2002; Kesimal et al., 2004) and the results of their investigations indicate that the fineness and density of tailings have important effects on the compressive strength, water/binder ratio, and microstructure of cemented backfill (Fall, Benzaazoua, & Ouellet, 2005). Furthermore, it was shown that tailings particle size essentially affects the shear strength, settlement, compaction and hydraulic conductivity of mine backfill (Benzaazoua, Fall et al. 2004; Ouellet, Bussiere, Aubertin, & Benzaazoua, 2007; Kermani et al. 2009 and 2010). Another investigation carried out by Kesimal et al. (2004) indicated that decreasing the amount of fine particles in tailings can increase the uniaxial compressive strength of cemented backfill due to the improvement in the gradation of tailings (Kesimal, Yilmaz et al. 2004).

1. Materials

1.1. Tailings

Tailings are waste materials produced in ore processing plants. The materials consist primarily of finely ground host rock. The physicochemical properties of tailings have a significant effect on the mechanical performance of mine backfill (Benzaazoua, Fall et al. 2004, Kesimal, Yilmaz et al. 2004). In this research, two tailings with different particle size distribution were used to investigate the effect of particle size on the mechanical and rheological properties of cemented paste backfill (CPB). Both tailing samples were delivered from a mines located in Ontario, Canada. The mineralogical content of the tailings generally consists of quartz, albite and slight quantity of calcite, muscovite, pyrrhotite, chalcopyrite, anorthite, and chlorite. The particle size distribution of the tailings was determined by using the laser diffraction methods (ASTM, 1996). The result is presented and compared with the average size of 11 mine tailings from

*Corresponding author. Tel.: +1 514 398 8060. E-mail: ferri.hassani@mcgill.ca; ferrihassani@hotmail.com

the provinces of Quebec and Ontario, reported by Ouellet et al. (2007) in Fig. 1 as well as Table 1 and it was observed that the tailing was courser than the average size of 11 mine tailings.

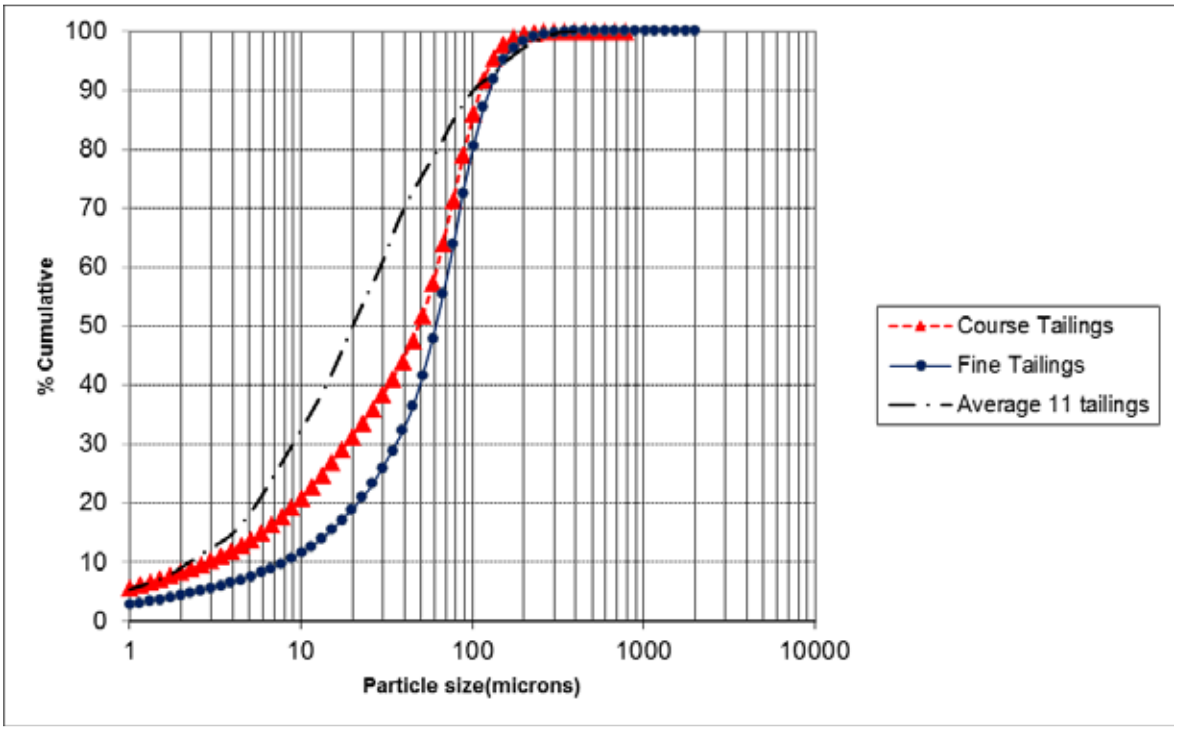

Fig. 1. Particle size distributions of tailings and average size of 11 mine tailings. (please provide the source file of this figure for re-production)

Table 1. Physical properties of the tailings.

Material	D_{10} (µm)	D_{50} (µm)	D_{60} (µm)	D_{90} (µm)	C_u	C_c	Specific gravity, G_s
Tailings used in this study	4.1	82.1	52.4	116.5	28.4	2.39	2.85
11 mine tailings reported by Ouellet et al. (2008)	2.2	20	29	102	13.2	1.24	Not available

D_{10} = particle diameter size that 10% of the sample particles are finer than
D_{30} = particle diameter size that 30% of the sample particles are finer than
D_{60} = particle diameter size that 60% of the sample particles are finer than
D_{90} = particle diameter size that 90% of the sample particles are finer than
$C_u = D_{60}/D_{10}$ = coefficient of uniformity
$C_c = (D_{30})^2/(D_{60} \times D_{10})$ = coefficient curvature

1.2. Binder

Binders are mainly used to increase the mechanical stability of fill materials. The most expensive part of mine backfill is the binders, and the cost of binder used in backfill could represent up to 75% of backfill costs (Hassani and Archibald 1998). Normal Portland cement, fly ash and blast furnace slag have been mainly used for mine backfill. In this research, two different binder were used:

i. a combination of 90% blast furnace slag and 10% Portland cement (90Slag/10Cement),
ii. Portland cement both provided by Lafarge Canada, were used.

These binders are generally used in different mines in Ontario, Canada. The densities of the slag and Portland cement used were 2.89 g/cm^3 and 3.07 g/cm^3, respectively. The Blaine specific surface areas of the slag and Portland cement

were 5998 cm^2/g and 3710 cm^2/g, respectively. The chemical compositions of the blast furnace slag and Portland cement are shown in Table 2.

Table 2. Chemical composition of the Portland cement and blast furnace slag provided by Lafarge.

Chemical composition	Blast furnace slag (wt%)	Portland cement (wt%)
CaO	37.129	61.13
SiO_2	36.127	19.39
Al_2O_3	10.385	4.61
MgO	13.246	3.3
SO_3	3.362	2.27
Fe_2O_3	0.668	2.01
Na_2O	0.424	2.03
K_2O	0.489	0.71

1.3. Sample preparation and curing

In order to investigate the effect of tailing particle size on the UCS evolution of CPB, 108 cylinders of backfill specimens with 16 different mixtures were prepared. The samples were made with stilled water. Two different binder agents used for preparing the samples namely Portland cement and a combination of 90% blast furnace slag and 10% type 10 Portland cement. The yield stress of samples was kept constant at 250 pa as is practiced in the mine in Canada. Moreover four extra batches (CT7, CT8, CT9 and CT10) were prepared at yield stress of 100 and 500 pa to investigate the effect of yield stress on the mechanical strength of cemented backfill. Sample mixtures were prepared in small batches in a 5-L stainless steel bowl. The mixtures were mixed for 5 min. A mixer was used to mix the ingredients. Cylindrical, polyvinyl moulds 10 cm deep and 5 cm in diameter were used to cast the mixtures. Those specimens were then cured in a curing chamber where the relative humidity was kept constant at (90±2)% and the temperature was adjusted to (25±1) °C. The specimens then were tested at 7 d, 14 d, 28 d and 56 d. Table 3 shows the mixture characteristics and symbolization corresponding to CPB samples.

Table 3. Binder mixtures characteristics of backfill samples.

Sample No.	Course Tailings (wt%)	Fine Tailings (wt%)	Slag Cement (wt%)	Portland cement (wt%)	CPB Yield Stress (Pa)
CT1/3C	97	0	0	3	250
CT2/6C	94	0	0	6	250
CT3/9C	91	0	0	9	250
CT4/3SC	97	0	3	0	250
CT5/6SC	94	0	6	0	250
CT6/9SC	91	0	9	0	250
FT1/3C	0	97	0	3	250
FT2/6C	0	94	0	6	250

FT3/9C	0	91	0	9	250
FT4/3SC	0	97	3	0	250
FT5/6SC	0	94	6	0	250
FT6/9SC	0	91	9	0	250
FT7/6C	94	0.5	6	0	100
FT8/6C	94	0.5	6	0	500
FT9/6SC	94	0.5	6	0	100
FT10/6SC	94	0.5	6	0	500

2. Experimental setup

2.1.Rheological Characterisation

In order to measure the rheological properties of the materials a desktop shear vane rheometer was used. Table 4 shows the rheometer specification used in this research. Initially, two 3-Kg representative samples were carefully selected and prepared from Course Tailings (CT) and Fine Tailings (FT). Then, the 3 Kg-tailing samples mixed with 6% of cement by total dry weight of the sample. Water was added to the mixture in order to make a thick paste. The samples were sheared with the rheometer and the yield stress and solid concentration were measured. A small amount of water was added to the mixture and the test repeated till the yields shear stress dropped below 70. The result is presented in Figure 2.

Table 4: Rheometer Specification

Rheometer	Viscometer 550
Vane	FL 100
Vane Diameter (mm)	22
Vane Height (mm)	16
Rotation Rate (deg/min)	75
Rotation Rate (1/s)	0.02182
Rate of Shear (mm/s)	0.24
Room Temperature (°C)	22

Figure 2: The effect of tailing particle size and solid concentration on yield stress

2.2.Unconfined compressive strength (UCS) tests

The mechanical strength of the cured specimens was measured. The test was conducted with a "Wykeham Farrance 100 kN" pressure equipped with a 50 kN load cell by conducting uniaxial compression tests (ASTM, 2006). A linear variable displacement transducer (LVDT) sensor was used to obtain the samples' vertical deformation rate (strain). Samples were taken out from the humidity room just prior to conducting the unconfined compressive strength test. A data acquisition board and a computer setup were used to record and display the data. On a given curing day for each mixture, three samples underwent the unconfined compression testing and the average value of the three results was recorded as the overall result of the UCS test.

3.Results and discussion

3.1. Effect of binder concentration on the backfill strength

In order to investigate the effect of binder concentration on the samples, the binder dosage was changed from 3 wt% to 9 wt% (in 3% increments). Figure 3 and Figure 4 show the result of the UCS tests obtained from the specimens tested at 7 d, 14 d and 28 d of curing. As expected, the UCS values increased with increasing curing time (due to the hydration of normal Portland cement and blast furnace slag). The results show that for a given curing time, the UCS values increase by increasing the amount of binder concentration (wt%). Furthermore, Figure 3 also shows that the acquisition of mechanical strengths for samples prepared with slag/cement binder are more rapid than the CPB samples prepared with Portland cement which could be beneficial due to the fact that mining cycle could be reduced and consequently mining operation would be more efficient. The diagrams also show that the UCS values of specimens made with slag/cement binder are higher than those of specimens made with the same amount of cement concentration. It can be concluded that the using slag/cement binder can increase the mechanical strength of fill materials. Furthermore, backfill strength can rapidly reach to the required UCS of 1 MPa reported as minimum strength requirement for a cemented backfill in a typical underground mining operation.

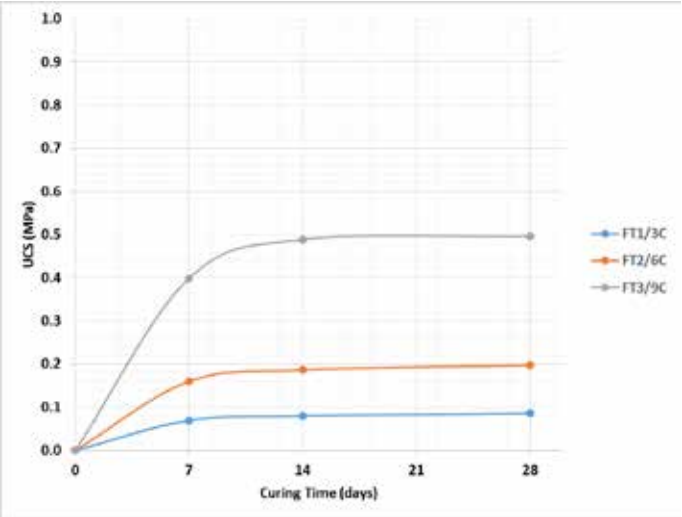

Figure 3: Effect of binder dosage on the uniaxial compressive strength (UCS) of CPB prepared with FT (fine tailings)

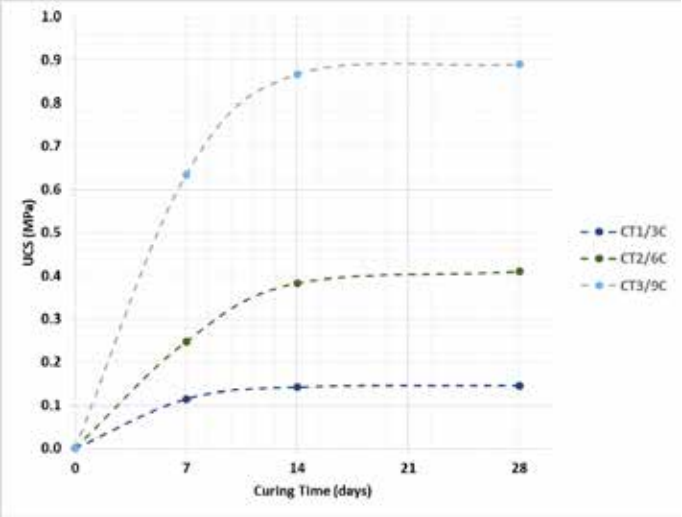

Figure 4: Effect of binder dosage on the uniaxial compressive strength (UCS) of CPB prepared with CT (course tailings)

3.2. Effect of tailing particle size on the backfill strength

In order to investigate the effect of tailing particle size on the uniaxial compressive strength, the result of UCS test of the CPB samples prepared with Fine tailings (FT) and Course Tailings(CT) with different binder concentrations are presented in Figure 5. It can be observed that the samples prepared with fine tailings has lower mechanical strength in comparison to the samples prepared with course tailings. It could be due to the higher surface area of fine particles in comparison to course tailings. Therefore, elevated amount of binder is required to cover the higher surface area of fine particles of tailings. It can also observed that the UCS evolution of CPB samples prepared with course tailings is more rapid than the samples prepared with fine tailings.

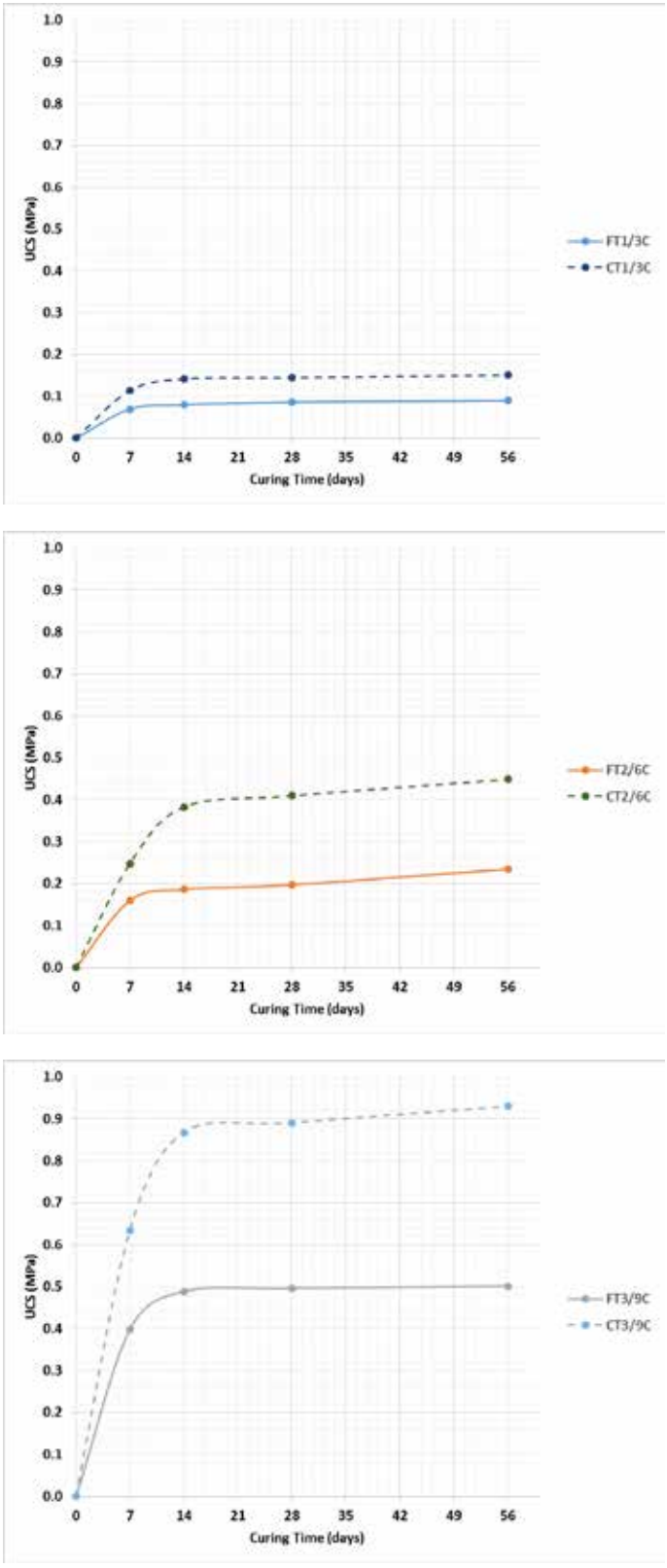

Fig. 5. Effect of tailing particle size on the uniaxial compressive strength (UCS) of CPB

4.3. Effect of CPB solid concentration and yield stress on the backfill strength

The UCS test results of CPB samples prepared with Portland cement and 90Slag/10Cement binder at various yield stress are shown in Figure 6 and Figure 7 respectively. The UCS values of CPB samples increase with the increase of curing time due to hydration of binder agents. Additionally, the UCS values of CPB samples increase with the increase of yield stress. This expected behaviour can be due to the reduction of the water to binder ratio. In fact, by reducing the water to binder ratio, the total porosity is decreased and therefore, the density and the strength of the material are increased.

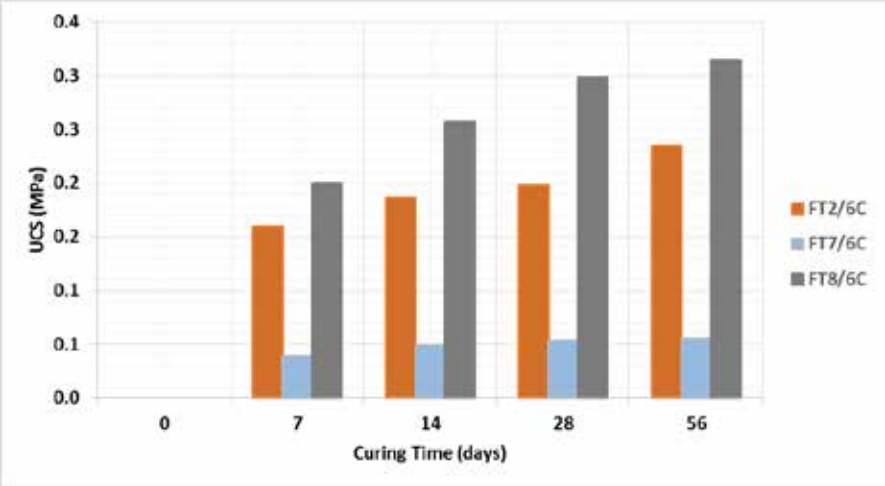

Figure 6: The effect of yield stress and solid concentration on the UCS of CPB prepared with FT (fine tailings) (a)

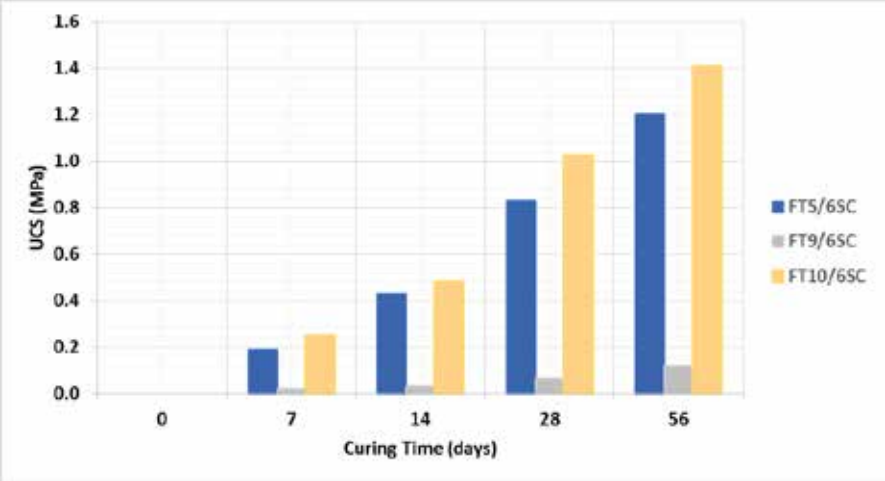

Figure 7: The effect of solid concentration on the UCS of CPB prepared with FT (fine tailings)

5. Conclusions

The effect of particle size of tailings and binder dosage as well as different binders on the mechanical properties of CPB is presented in this paper. The investigation confirmed that CPB specimens produced by the addition of 90Slag/10Cement have higher mechanical strength in comparison to CPB specimens made with Portland cement. Therefore the use of 90Slag/10Cement binder agent can contribute to better underground stabilization and mine safety. Moreover, the research also shows that the particle size of tailings has great effect on the UCS of the samples. The results demonstrated that strength development of CPB prepared with course tailings is more rapid than CPB specimens prepared with fine tailings. It was also demonstrated that binder dosage and binder types strongly influences the UCS evolution of CPB samples. Furthermore it was demonstrated that the yield stress of CPB can be mainly changed by the particle size of tailings.

In conclusion, the mechanical properties and rheological properties of CPB can be changed by changing particle size distribution of tailings which can influence the mining operation cost and mining cycle time. Therefore there is a possibility to increase and improve the mining production with the alteration of tailings particle size.

Acknowledgments

The authors acknowledge the financial support given by NSERC. The authors are also grateful for the help and contribution of other graduate and undergraduate students at McGill and Concordia Universities.

References

Aref, K., Hassani, F. P., & Churcher, D. A. (1989, October 20-5). *A study on liquefaction potential of paste backfill.* Paper presented at the Fourth International Symposium on Mining with Backfill Innovations in Mining Backfill Technology, Montreal, Canada.

Belem, T., et al. (2001). The effect of microstructural evolution on the physical properties of paste backfill. Tailings and Mine Waste 01.

Benzaazoua, M., Belem, T., & Bussiere, B. (2002). Chemical factors that influence the performance of mine sulphidic paste backfill. *Cement and Concrete Research, 32*.

Benzaazoua, M., et al. (2004). "A Contribution to Understanding the Hardening Process of Cemented Paste Backfill." Minerals Engineering **17**(2): 141-152.

Benzaazoua, M., Fall, M., & Belem, T. (2004). A Contribution to Understanding the Hardening Process of Cemented Paste Backfill. *Minerals Engineering, 17*(2), 141-152.

Fall, M., Benzaazoua, M., & Ouellet, S. (2005a). Experimental characterization of the influence of tailings fineness and density on the quality of cemented paste backfill. [doi: DOI: 10.1016/j.mineng.2004.05.012]. *Minerals Engineering, 18*(1), 41-44.

Brakebusch, F. W. (1994). "Basics of paste backfill systems." Mining Engineering **46**: 1175-1178.

Hassani, F. and J. F. Archibald (1998). Mine Backfill 1998. Montreal, Canadian Institute of Mining, Metallurgy and Petroleum.

Kermani, M., et al. (2010). An investigation into the mechanical properties of Gelfill and hydraulic backfill in various curing temperatures. Proceeding of the 12th International Symposium on Environmental Issues and Waste Management in Energy and Mineral Production, Prague, Czech Republic.

Kermani, M., et al. (2009). The effect of sodium silicate concentration and pulp density on the strength of Gelfill. Proceeding of the 18th International Symposium on Mine Planning and Equipment Section, Banff, Canada.

Kesimal, A., et al. (2004). "Evaluation of paste backfill mixtures consisting of sulphide-rich mill tailings and varying cement contents." Cement and Concrete Research **34**(10): 1817-1822.

Mitchell, R. J. and B. C. Wong (1982). "Behaviour of cemented tailings sands." Canadian Geotechnical Journal: 289-295.

Ouellet, S., et al. (2007). "Characterization of cemented paste backfill pore structure using SEM and IA analysis." Bull Eng Geol Environ(April).

AN OVERVIEW ON THE USE OF COAL COMBUSTION RESIDUES IN ACTIVE AND ABANDONED COAL MINES

***Jan Palarski[1] and Franciszek Plewa[1]**

[1] Silesian University of Technology, Faculty of Mining and Geology, Akademicka 2A, 44-100 Gliwice, Poland

*(*Corresponding author: jan.palarski@polsl.pl)*

24th World Mining Congress
MINING IN A WORLD OF INNOVATION
October 18-21, 2016 • Rio de Janeiro /RJ • Brazil

AN OVERVIEW ON THE USE OF COAL COMBUSTION RESIDUES IN ACTIVE AND ABANDONED COAL MINES

Abstract

Coal mining operations create a variety of environmental impacts involving e.g. surface subsidence, emission of gases and water pollution. Current Polish underground coal mining expands into increasing depths. The use of conventional coal extraction methods - room and pillar and longwall with caving - is becoming increasingly difficult. Control of the roof by caving has numerous technical advantages and does not generate additional costs, which in case of traditional hydraulic backfill can easily make the mining operations unprofitable. However, presence of caving zones generates many problems related to the stability of the rock mass and mine subsidence, mine water inflow, spontaneous coal ignition, methane hazard etc., which are generally considered as environmental and safety issues. The coal mining is modifying existing methods and testing innovative technologies. Filling (grouting) of caving zone is an important component of modern underground mining operations. This method serves a number of functions in underground coal mines and offers many environmental benefits. What is more, filling of voids in caving does not interfere with mining production and does not involve significant additional costs. This paper will discuss different components of an effective longwall production and filling process of caving area.

In Silesia, mining activities have been carried out for hundreds of years. The mining operations have produced underground cavities that can be filled by different materials such as crushed waste rock, sand, tailing and coal combustion by-products. Beneficial use of tailing and fly ash for coal mine reclamation occurs in varying degrees across Silesia. In various locations, fly ash slurry has been injected into underground abandoned coal mine workings to provide structural support for subsidence reduction. In this paper, a review of the used technologies and main environmental issues will be presented.

Introduction

Hard coal, mined in Silesia Region as well as in the eastern part of Poland, is a key national resource. In Polish underground coal industry, modern mining technologies have been successfully tested and used in the last 50 years. More than 95% of the coal produced underground is extracted by different longwall mining methods (Figure 1). Unfortunately, coal mining, preparation, transport and use has environmental consequences.

A major part of the Silesia Coal Region in Poland is undermined. Surface subsidence due to the loss of subsurface support after the removal of coal has resulted in a vast amount of damage to properties and infrastructures. In addition waste and saline water from coal mines are significant environmental problems. Polish coal industry uses backfilling in operating mines and in abandoned underground mine workings for the purposes of either reduction of such damages or disposal of waste materials. In Poland, the filling of the voids created by underground coal mining operations is probably as old as coal mining itself in the Silesia Region.

Currently, most of Polish coal mines successfully adopts new technologies of filling of voids in caving. Due to financial restrictions most of backfill operations have been stopped, however many mines are equipped with the hydraulic backfill infrastructure. This infrastructure, mainly pipelines networks, can be easily applied for transportation of fine-grained mixtures used for voids filling in caving. The mixture preparation plants are relatively simple and often only some parts of unused backfill preparation plants (water and material tanks, railway bridges etc.) are used. Due to hard economic conditions of coal production, the adopted solutions for the goaf filling must be robust, not generate significant investment and operational costs, and not interfere with the main production cycle.

Application of filling of voids results in improved control of spontaneous coal combustions, better ventilation conditions, and creates opportunity for disposal significant volumes of saline mine waters. In specific conditions the technology of filling of caving is even able to reduce mine subsidence. However, as explained in this paper, it is difficult to meet condition required to achieve the significant subsidence reduction. Observations in the mines show that the main obstacle in wide and complex use of this technology is limited availability of fly ashes from hard coal combustion, which are the practically only useful solid component in fill mixtures. The low availability of these by-products from power industry results in inconsistent application of voids filling, leads to limited efficiency and below expectation results.

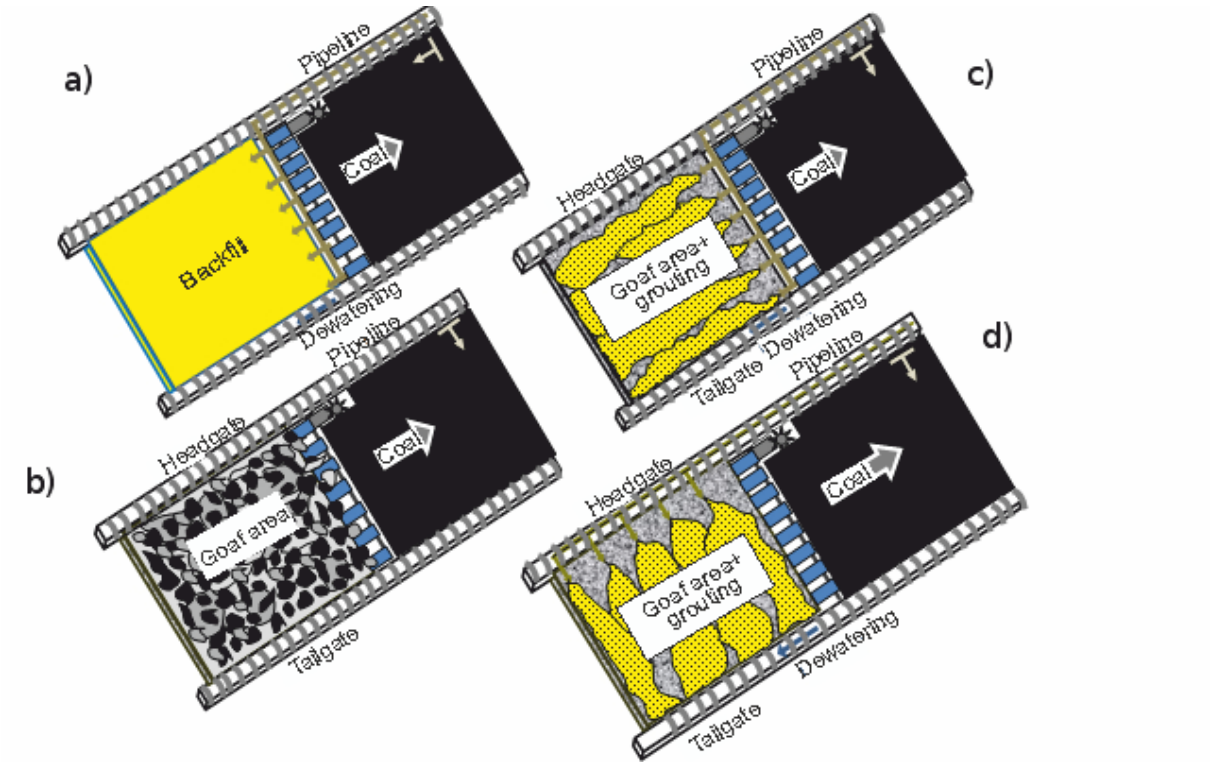

Figure 1 – Longwall methods used in Polish underground coal mines; a) longwall with backfill, b) longwall with caving, c,d) longwall with goaf grouting – 2 methods *(*Palarski, J 2013)

Formation of the caving and hazards during mining

Polish coal mines produce round 72 million tons of coal per annum (year 2015), from which 91% come from longwall with caving, 4% from longwall with traditional backfill, while the remaining 5% comes from room and pillar and development workings in the coal seams. Mining with caving is the most environmentally unfriendly type of mine operations.

When an underground coal seam is extracted over a wide area, the immediate roof will collapse (Figure 2). Formation and shape of the caving depends on the geological structure of the overlying strata. In Silesia Coal Mining Region, the caving zone created by coal extraction is highly fragmented, and extends upwards two to ten times the thickness of the mined seam. Above this zone is a fractured zone characterized by mining-induced fractures. Rock displacements are propagated further to the ground surface forming an overlapping zone - so-called bending zone. The caving area immediately behind a longwall face becomes often a reservoir for methane as the permeability of the overlying and underlying strata increases. Additionally, in worked-out area (caving zone), coal can be left from the extracted seam or from other overlying or underlying coal seams. Spontaneous combustion of coal losses in caving zone poses significant safety, environmental and economic problems in mining operations. In Polish coal mines, fill slurry injection into the gob zone is a newer approach, and is used to avoid the hazards associated with rock mass deformation, gas accumulation and spontaneous combustion.

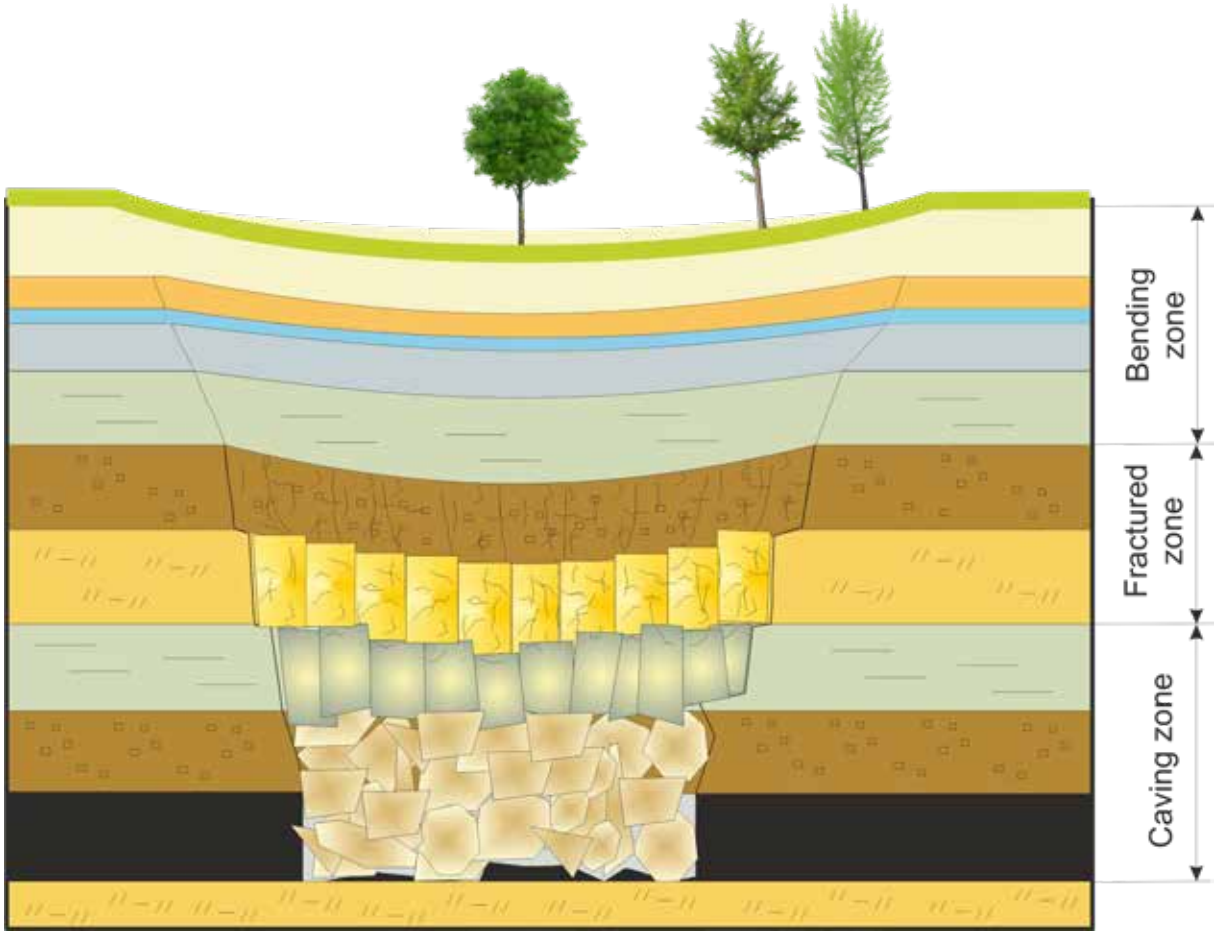

Figure 2 - Fractured zones evolution over caving as a result of longwall mining of coal

The gob absorption of fill slurry

Directly after extraction of some amount of coal from a longwall, the total volume of void being created is equal to the volume of extraction. In later stages of caving and fracturing processes, this volume is distributed between large voids in caving, voids of all fractures and also the volume of surface subsidence. Therefore, the volume of extraction clearly represents the theoretical maximal absorption (accumulation, filling) of slurry. A roof fall rocks absorb a fill mixture or part of it; part of water flows out. Practically the absorption of caving area is limited in the first place due to presence of caved rocks in the space available for gravitational filling as well as due to many other conditions, like geometry of the longwall panel, continuity of the voids, migration properties of fill mixtures and so on. Because direct observation of the state of caving filling is impossible, absorption of voids was analysed statistically. Data under analysis were taken from 65 longwalls in Polish coal mines, where caving filling was adopted. The selected results from filling (grouting) of voids in Polish coal mines are presented in Figure 3.

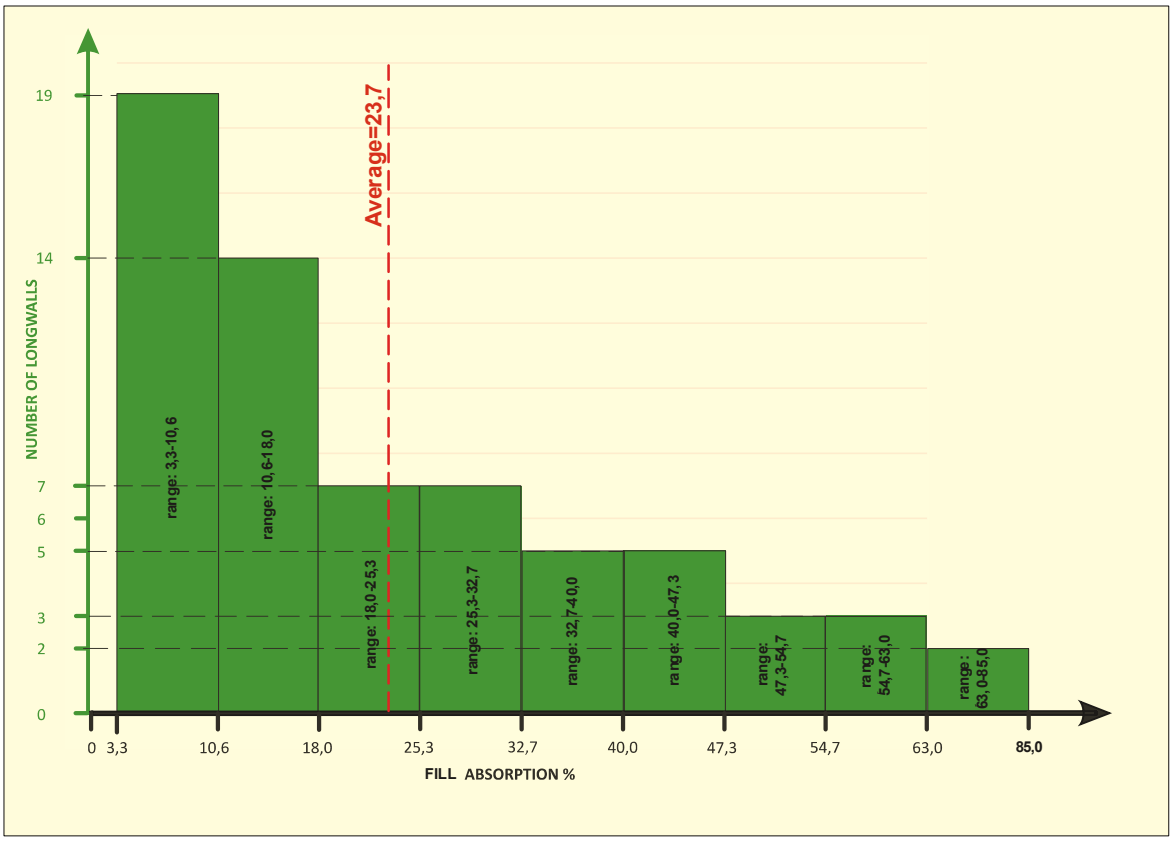

Figure 3 – Fill absorption in different longwalls

The absorption values (fill accumulated in caving) for the considered longwalls ranged from 3% to 85%. Presented results do not specify the type of fill mixture used in each case nor any other data related to specific local conditions of the considered longwalls. Results of this analysis demonstrate that the overall level of filling is relatively low. The absorption for 32 of the analysed longwalls was smaller than 20%. It means that the amount of introduced fill mixture could only create a thin isolation layer along the isolation dam in the tailgate of the longwall panel. Such level of filling allows to achieve nothing more than an improved ventilation and reduction of fire hazard, due to elimination of air penetration into the caving. Influence on roof subsidence and reduction of the fractured zone evolution may be achieved only in the cases where intensive process of voids filling were conducted, with a level of filling higher than 40%.

Technological aspects of filling of voids in caving

Technological limitations and economic factors of backfill motivate the search for new fill methods for coal mines. One of them is the longwall method with grouting of roof fall rocks (Figures 1 and 4). Increasing surrounding pressure against waste disposal, particularly the fine waste on the surface, and concern about mining damage, have resulted in an increase in the popularity of using fly ash, tailings and binding agent mixtures as compaction slurry (grout) for roof fall rocks in gob areas of longwalls.

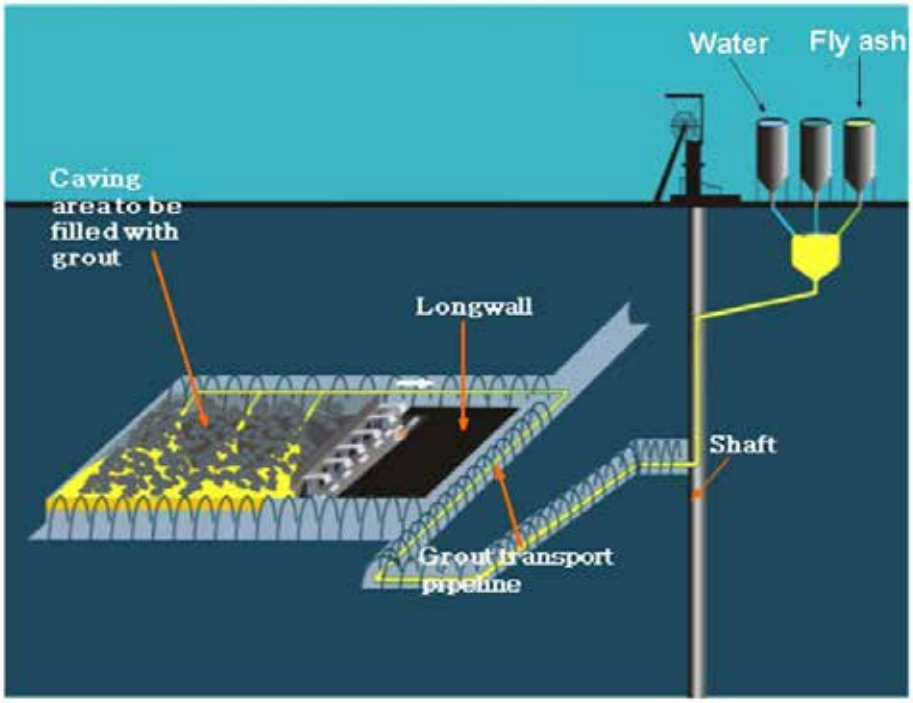

Figure 4 – Schematic view of fill infrastructure and longwall

The grouting method for roof fall rocks is based on a longwall with caving. The grouting method does not need to keep open the room behind the longwall support, in comparison with other backfill methods. This technology allows separate extraction from the filling process. The injection of a slurry is carried out through pipes in two ways (Figures 1 and 4):

- the grouting pipes are drawn behind the support line and reach unconsolidated cave rocks up to 15 m away from the line (Figure 1c),
- the pipes are left in a mined–out area or they are placed in a bore hole drilled to the gob from a headgate (Figure 1d).

Application of voids filling in caving is able to reduce numerous problems related to mining operations, but generally it is not able to reduce significantly the fracturing process in the rock mass above mining operations. It has been noted that the grouting of fall rocks contributes to a reduction of surface damage by up one half (maximum) when compared to the standard caving method. The traditional backfill decreases the parameters of surface deformation by about 70-80%. From the other side, simplicity of this technology and low costs (both capital and operational) encourage the mining industry to apply filling of voids as a cheap method.

Additionally, coal spontaneous combustion and ventilation problems are reduced by using this technology. In thick seams, by filling of caved rocks in the upper slice, a new artificial roof is created for the next slice. For successful grouting of caved rocks, the best productivity and lowest cost of production is achieved for cases where:

- seams or slices have dips of 5–10° and thicknesses from 2.0–2.5 m;
- roof strata has good rock fragmentation and regular caving, and
- longwall conditions: face length (width) 200–250 m, working up-dip and grouting from the face pipeline.

Selection of fill slurry

To improve the safety, environmental performance and economics of coal mining operations, fill mixtures (grout) are produced from various waste materials. To ensure the maximum safety of the filled caving area, the challenge is to use a slurry that is able to tightly fill the free spaces and stabilize the goaf without being affected by potential long-term strength loss due to chemical weathering.

The mechanical and rheological properties of fill slurry depend on mineralogical, physical and chemical properties of the waste materials, binder types, and their proportions. The important parameters for determining the suitability of placed fill are the compressibility, strength, binding time and strength loss during and after curing periods due to chemical weathering caused by the presence of aggressive mine water (chlorides, sulphates and others). A wide range of other physical properties of fine-grained mixtures undergo testing procedures, as it

is defined by Polish standard PN-G/11011:1998: "Materials for stabilised backfill and grouting of cavings – requirements and test procedures". The standard requirements can be divided into three groups:

1. Properties affecting flow regime changes in a transport pipeline – density, slump, rheological parameters of the slurry;
2. Factors influencing the fill placement process –draining, stiffening time, set time;
3. Properties of already stabilised fill material – compressive strength, wetting resistance, compressibility, and permeability.

Table 1 presents typical range of values of the most important parameters of mixtures used in different mining technologies. The high mechanical properties shown in Table 1 for stabilised mixtures can be achieved with use of coal combustion by-products (fly ash) and/or with addition of binders, like commonly used Portland cement. Filling of caving does not require specific parameters of mixture of fine grained solids and water in comparison with other underground technologies like stabilised backfill, construction of backfill plugs and packs etc. The draining might relatively high due to absorption of excessive water by the rocks. Relatively poor mechanical properties of solidified fill together with high water content allow to use mixtures with slump flow values between 210 and 250 mm. High slump flow is required to achieve long distance migration range, which in this application is much important than supporting properties of the final fill material. Generally, the concentration of mixtures for filling of caving is between 20% and 50%. This means, for example, that a longwall caving with volume of 500 000 m^3 creates an opportunity to dispose more than 100 000 m^3 of saline water, which makes significant environmental benefit from the application of caving filling.

Table 1 - Criteria for the use of finely grained mixtures (<0,5 mm) in underground mining technologies

Parameter	Slump flow R [mm]	Set time C_t [days]	End of binding T_k [days]	Compressive strength R_c [MPa]	Wetting resis-tance R_{28} [%]	Draining w_n [%]	Comp-ressibi-lity S [%]	Perme-ability K [m/s]
Stabilised backfill (C <75%)	160 -180	< 1	< 2	0.5 after 7 days	< 20	< 7	< 15	$< 10^{-7}$
Filling of cavings (C<60%)	210 - 250	n/a	< 28	0.1 after 28 days	< 80	< 14	n/a	$< 10^{-7}$ (10^{-9})
Filling of abandoned workings	160 - 210	< 7	< 14	0.5 after 28 days	< 20	< 7	n/a	n/a
Construction of backfill packs and plugs	160 - 180	< 2	< 2	0.5 after 7 days	< 20	< 7	< 5	$< 10^{-7}$
Liquidation of shafts – insulating plugs	160 - 180	< 2	< 3	0.5 after 7 days	< 10	< 7	< 5	$< 10^{-9}$
Liquidation of shafts – fill of the column	160 - 180	n/a	< 28	0.1 after 28 days	< 80	< 7	n/a	n/a
Grouting of loose or porous rocks	160 - 210	n/a	< 14	0.5 after 28 days	< 20	< 7	< 7	$< 10^{-7}$

Preparation of fill slurry

Fill slurry preparation plants can be arranged in many ways, to accommodate specific requirements, depending on the number of components, ways of their delivery, operational flow rate, and other factors. The main components of a fill slurry preparation plant are presented in Figure 5. A fill slurry preparation plant shall contain at least:

- vehicles discharge utilities
- tanks and silos for all solid and liquid components
- conveyors and feeders for transportation of components from tanks to mixer
- an ample water supply
- mixer
- electronic control system.

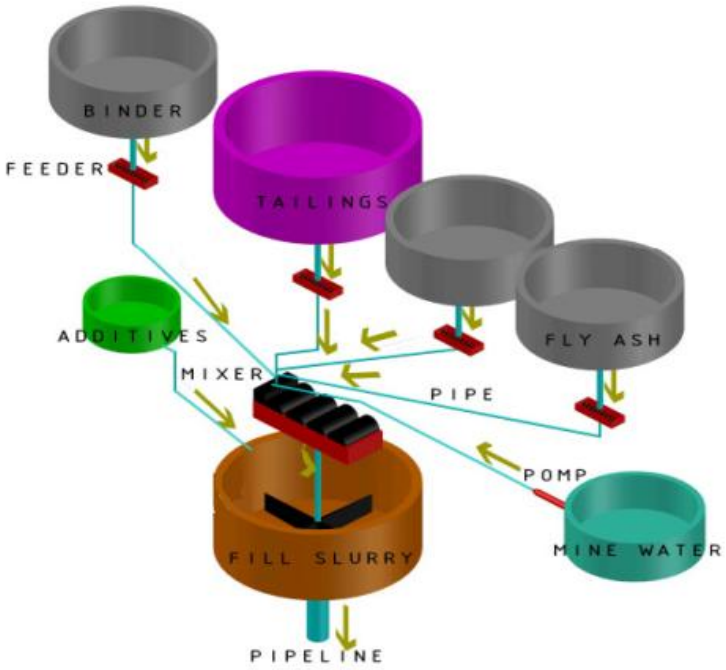

Figure 5 – Schematic diagram illustrating the fill slurry preparation plant (Palarski, J 2013)

Tanks for fly ash and other components must have at least a volume required for a single operation cycle (generally one shift). The water supply must be enough to produce the required amount of slurry and to

Figure 6 - Discharge of fly ash and storage tank

clean the mixer and pipelines at the end of an operation cycle. Slurry tanks are necessary when the capacity of the mixing system is lower than the expected injection capacity. They can also be used as retention tanks in the case of irregularities in the injection flow rate. As already mentioned, Polish coal mines use mainly gravitational transport of slurries. In mine with large and complicated infrastructure, fill mixture can be transported by gravity to an underground pump tank and from the tank a pump is used to lift the slurry to the filling void. Such a solution reduces operational costs of grouting operations, but limits the ability to control slurry parameters and fill efficiency. Coal mines are often equipped with specialized slurry preparation plants, where all fly ash reloading and transport operations do not harm the environment. Fly ash is delivered by tank wagons or trucks and pneumatically discharged into storage tanks (Figure 6). All processes are controlled and monitored from a main control room.

Backfilling of abandoned underground workings

Mining in abandoned coal mines in Silesia was carried out in at least several seams at depths of between 50m to 1,200m. The abandoned mines contain huge volumes of unfilled workings, often flooded or gas filled and also contain considerable quantities of coal in pillars and the surrounding strata. All these closed underground coal mines are subject to some risk of spontaneous combustion of unmined coal.

In the Silesia coal mining region in the period between 1993-2015 it was necessary to fill or seal a length of about 5500km of mine workings and 120 km of shafts. The filling of mine workings during closure processes allowed mines to reduce the possibilities of subsidence, surface damage, gas movement, underground fires and sudden inrushes of mine water, thereby opening up under-mined areas for further beneficial use. Not all the openings can be reached from other underground workings, so there is a need to drill bore-holes from the surface to fill the voids (Figure 7 and 8).

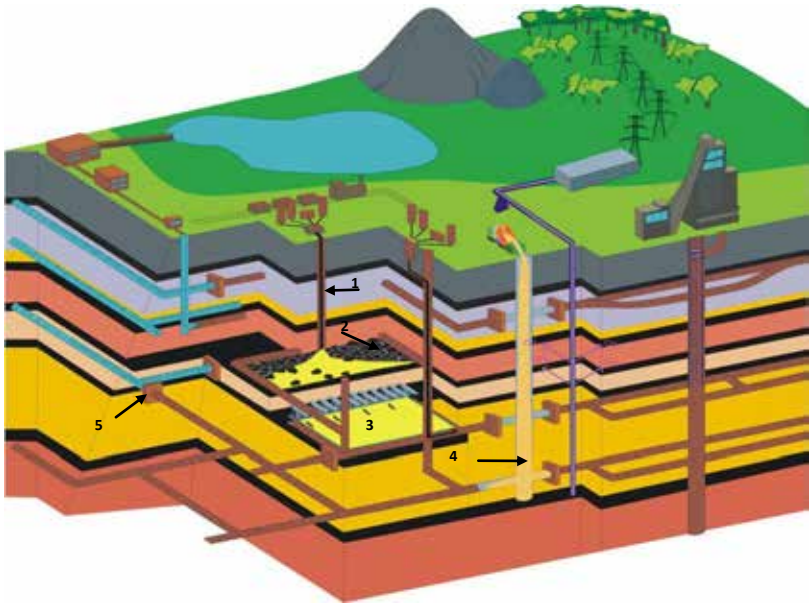

Fig. 7 - Closure process of mine
1 – borehole; 2 – caving area; 3 – longwall with backfill; 4 – shaft filling; 5 – seal.

The holes are situated to get the best filling of the voids and to avoid sudden inrushes of water. Void filling is executed through bore-holes of 120 and 200mm diameter, by the following methods:

- pneumatic transport of dry fly-ash with capacities up to 30t/h, at a pressure of about 0.25 MPa;
- pneumatic transport of fly-ash moistened with water at the outlet at quantities up to 20 l/minute;
- supply by gravity or by pump the water-ash mixture or a mixture of ash (up to 70% of the dry mass), tailing (up to 25%), cement (up to 10%), and calcium chloride (2%) and water; the concentration of the mixture sets each time according to the state and conditions of void filling (mixture concentration < 75% by mass).

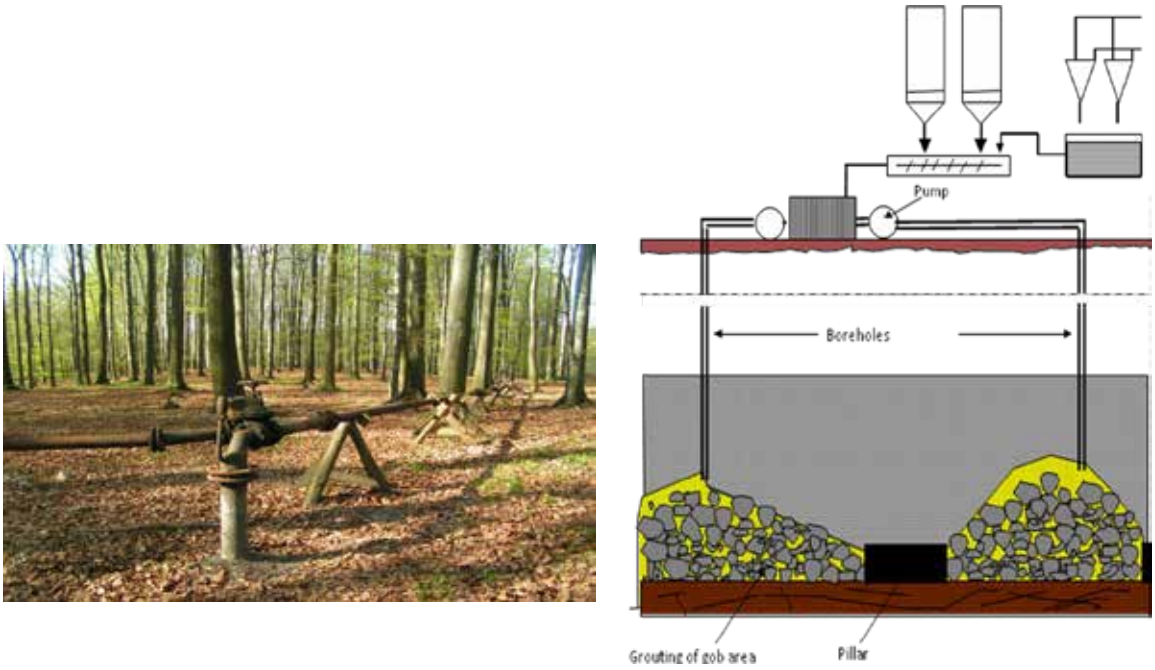

Figure 8 - The filling of mine workings through bore-holes

The last solution is the most effective and it has been frequently used in Polish collieries. The tightness of the fill of underground voids is controlled by TV cameras inserted through the bore-hole down on the line or by geophysical techniques.

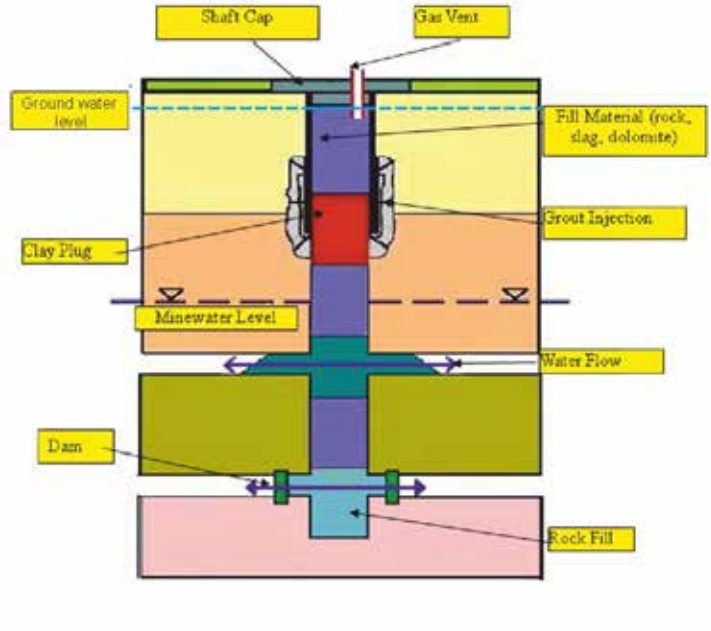

Figure 9 – Shaft filling

The abandoned shafts are filled or left without any filling due to water pumping. Before filling the shaft, all equipment such as guides, cables, ropes, pipes or ladders must be removed, and the shaft insets must be prepared for constructing the stoppings and fill dams, causing the caving zones or creating the plugs from the material used for filling the shafts. Hard core in the form of broken rock is recommended for shaft inset locations and sumps. The remaining part of the shaft can be filled with mining wastes as well as with demolition materials (crushed brick, concrete etc.). When water or gas flows into the shaft it is necessary to prepare clay seals; their

thickness and depth depend on geological conditions around the shaft, the technical state of its support, and on the material used for its filling and seal construction (Figure 9).

Conclusions

Filing of caving is widely applied among Polish coal mines. Most of the mines have unused backfill infrastructure, which can be easily adopted for the purposes of caving filling. The main reason for use of this technology is for reduction of spontaneous ignition of coal residues in caving, which can exclude a longwall for long time from operation. Utilisation of large volumes of saline waters is also important benefit of filling of voids. If a range of criteria are met, filling of voids in caving could have significant influence on subsidence reduction and surface protection. Research and development in the field of filling should be concentrated on finding other materials, which are able to replace fly ashes.

References

Palarski, J 2013 'Environmentally friendly mining technologies in Polish coal mining industries' in the Proceedings of 23 rd WMC – Canada, Montreal, Quebec, August 11th - 15th.

Palarski, J, Plewa F, Strozik G 2014 'Filling of voids in coal longwall mining with caving – technical, environmental, and safety aspects' in the Proceedings of MINEFILL 2014 – Australia, Perth

.

ASSESSMENT OF VIBRATION ATTENUATION, FREQUENCY SPECTRA AND STRUCTURAL RESPONSE CAUSED DUE TO BLASTING IN MINES

*P. K. Singh[1]

[1]Director
CSIR- Central Institute of Mining and Fuel Research
Dhanbad, India 826015
*(*Corresponding author: pradeep.cimfr@gmail.com)*

24th World Mining Congress
MINING IN A WORLD OF INNOVATION
October 18-21, 2016 • Rio de Janeiro /RJ • Brazil

ASSESSMENT OF VIBRATION ATTENUATION, FREQUENCY SPECTRA AND STRUCTURAL RESPONSE CAUSED DUE TO BLASTING IN MINES

ABSTRACT

Ground vibrations arising from rock blasting is one of the fundamental problems in the mining industry and its prediction and controls play an important role in the minimization of environmental complaints. Therefore, based on 1305 measured blast vibration events from 320 blasts recorded at 17 mines which includes ten open pit mines viz. three from coal, three from iron ore, one from limestone, one from manganese, one from chromite and one from lead-zinc and rest 7 mines from underground sector viz. two lead-zinc mines and five coal mines. A best site-specific propagation law by considering recorded peak particle velocity, distance and maximum charge per delay, was established and analysed with a comparative approach. Furthermore an attenuation relation developed for 16 different rock zones to study the role of each zone in the attenuation characteristics of blast induced ground vibration and air overpressure/noise. Frequency spectrum analyses of each event were also performed to assess the risk of resonance occurrence in the building. The responses of the structures in the close proximity of the mining area were recorded and natural frequency of 40 houses/buildings was determined. The behaviour of frequency with different strata were also analysed comparatively. As the ground vibration amplitude (PPV), ground vibration duration and ground vibration frequency are the principal three factors causing damage to any structure, a thorough investigation was comprehended to assess the extent of damage potentiality for these three factors. In this paper detailed analyses of the recorded vibration data from 16 mines have been analysed and recommendation has been given with reference to the open pit and underground mines of different categories.

KEYWORDS

Ground vibration, Vibration attenuation, Frequency spectra, Structure response, Air over-pressure

INTRODUCTION

Explosives are a major source of energy required for breakage and fragmentation of rocks. Although significant developments have taken place in explosive technology, the science of explosive energy utilization has not made much progress. Only a small fraction of the total energy (≈15 %) is utilized for actual breakage and displacement of rock mass (Hagan, 1973). This is due to the lack of understanding of the actual breakage mechanisms which are complicated in nature and vary widely depending upon a host of parameters and also the short lived interaction between blasts induced transient forces and rock mass. Rock blasting involves a series of interrelated phenomena e.g. detonation process within the explosive, the transfer of explosive energy from explosion products to the surrounding rock medium and the later action of this explosive energy (Lang, 1983). Each of these phases, or rock blasting in general, is influenced by a number of variables, which can be grouped into the following categories:

1. Explosive parameters
2. Blast design parameters
3. Rock parameters

The first two are controllable whereas the third is uncontrollable as they are dictated by nature. It is essential to know the effect of these parameters on blasting for efficient utilization of explosive energy in a given rock mass. The ultimate aim of any blasting investigation, therefore, should be to predict the degree of fragmentation and displacement produced by an explosive in a given set of rock conditions. Important parameters of an explosive are strength, velocity of detonation, density, water resistance, detonation pressure and sensitivity. Explosives having high bulk strength and detonation velocity perform better in strong massive rocks as they produce high borehole pressures. Excessive borehole pressure causes unnecessary crushing in soft and porous rocks. Density, degree of fineness and compaction of explosives, control the detonation velocity and energy release. Explosives like emulsions and water-gels produce high strain energy and low gas energy. They perform better in

stronger formations. Explosives with more gas energy are suitable in situations where more displacement is desired. Water resistance is another important property. Performance of ANFO decreases in watery holes due to desensitization and creates nitrogen oxide fumes indicating incomplete detonation. Gelled products such as gelatinized slurries perform better in such situations.

A judicious selection of blast design parameters such as burden, spacing, bench height, stemming, sub-drilling, delay timing, initiation sequence and decoupling, is essential for an efficient blast. Smaller burdens and spacing increase drilling costs whereas high values cause vibration problems. Most blasting situations need sub-drilling. But at the same time excessive sub-drilling results in floor damage and ground vibrations. Excessive stemming causes under loading of holes and vice versa. In the same manner other variables like bench height, blasthole diameter and its inclination, priming and delay time also influence blasting considerably. All these parameters should be properly chosen so that they are compatible with a given explosive and rock mass conditions.

Rock characteristics often vary greatly from place to place in a mine or from one end to another of a single face. Hence, blast design parameters and explosives need to be selected based on rock mass properties, e.g. strength, density, porosity, longitudinal wave velocity, impedance, stress-strain behaviour and structural discontinuities.

Blasting, in many cases is the best and cheapest method of rock breakage, although only 15 to 30 % of explosive energy is utilized in fragmentation (Hagan, 1979; Jimeno et al., 1995). The vibration energy that travels beyond the zone of rock breakage is wasted and can cause damage to surface structures and annoyance to the residents in the vicinity of the mines (Siskind et al., 1980). The undesirable known side effects of detonation of explosives are vibration, noise/air over-pressure, flyrock, dust and fumes (Singh et al., 1996).Ground vibrations are more important as compared to other unwanted outputs, because of the involvement of the public residing in the vicinity of mining sites and regulating agencies. Also with the emphasis shifting towards environment friendly activities, the field of ground vibrations has become important. Furthermore, if the frequency of ground vibrations is within the natural frequency range of the structure, it may lead to more damage due to the resonance effect (Singh et al., 1997). Therefore, prediction of ground vibrations are very important to reduce potentialdamage due to blasting. Peak particle velocity (PPV) is the most popular form to predict ground vibration as it is directly proportional to the strain induced in the ground during vibration (Dauetas et al., 1993; Athanasopoulous and Pelekis, 2000).

The heterogeneity of the rock mass and the complexity of local geology, often makes the prediction of peak particle velocity a difficult task. In recent years, several empirical relations to predict PPVs have been developed by different researchers based on data obtained from different mines (Duvall et al., 1963; Langefors and Kihlstrom, 1963; Ambraseys and Hendron, 1968; Dowding, 1971; Ghosh and Daemen, 1983; Kahriman, 2002; Kuzu, 2008; Cardu et al., 2015). Most of these models are based on the two parameters:

1. Maximum explosive weight per delay
2. Distance from the blasting site to measuring point

Presently, several researchers focusing on application of artificial intelligence techniques such as artificial neural networks (ANNs) in prediction modelling for ground vibrations (Singh and Singh, 2005; Sawmliana et al., 2007; Iphar et al., 2008; Khandelwal and Singh, 2009; Mohamed, 2009; Amnieh, 2012; Bakhshandeh and Bahadori, 2014). Peak particle velocity in combination with frequency of ground vibration have been globally used in practice for assessment of blast-induced damage to structures, for example, USBM (United States Bureau of Mines), DGMS (Directorate General of Mines Safety, India). One can observe from these standards that low frequencies have higher damage potential than high frequencies.

Since vibration is felt in most of the blasting cases, the reaction to this sensation is due to curiosity, concern, and even fear. Human response has been investigated by many researchers (Goldman, 1948; Whiffin and Leonard, 1971; Chang, 1973; Atherton, et al., 1976; Siskind et al., 1980, Singh et al., 2004). This is a highly subjective phenomenon; that is, the response is a mixture of physiological and psychological factors individual to each person. It is impossible to establish a vibration level where nobody will complain. There are always some persons in a population who will complain no matter how small the disturbance is. Several researchers (Power, 1966, Nicholls et al., 1971; Roy, et al. 2005) recognised that the duration of the vibration was critical. Most evident was that a higher level could be tolerated if the blast event was short. Singh et al. (2004) concluded based on the

extensive field study that the blast event duration of 20 seconds long with low frequency wave at large distances (5.5 km) resulted into numerous complaints.

In this paper, a comparative assessment of all the blasting parameters weather it is controllable or uncontrollable have been accomplished by analysing the data gathered from 17 different mines including 10 opencast and 7 underground mines in India.

BRIEF DISCRIPTION OF EXPERIMENTAL SITES

This paper deals with the extensive study conducted on three opencast coal mines of Northern Coalfields Limited, One open-pit Lead-zinc mine of Hindustan Zinc Limited, five opencast mines of Tata Steel Limited including three iron ore mine, one chromite and one manganese mine, one limestone mine of Satna Cement Works, two underground Lead Zinc mine of Hindustan Zinc Limited, five underground coal mines including two of Eastern Coalfields Limited, one of South Eastern Coalfields Limited and two of Mahanadi Coalfields Limited.

Jayant, Dudhichua and Nigahi projects of Northern Coalfields Limited are located in the Singrauli Coalfields. The rocks are of Gondwana formation having coal bearings of Barakars within it. Three coal seams viz. Purewa top, Purewa bottom and Turra are being mined. The thickness of Purewa top, Purewa bottom and Turra seams are 5-9 m, 9-12 m and 13-19 m respectively. The thickness of partings between Purewa bottom and Purewa top seams is 17-32 m, whereas between Turra and Purewa bottom seams it is 52-59 m. The overburden above Purewa top seam is 12-95 m. The mineable coal reserves are 349 and 492 million tonne respectively. The average stripping ratio is 2.6 m^3 of overburden per tonne of coal. The dip of the coal seam is 10-30 in northerly direction. Both the mines produce about 10 million tonne of coal and about 30 million cubic meters of overburden.

Rampur-Agucha mine is the India's largest Lead-Zinc opencast mine of M/s Hindustan Zinc Limited. The mine had the initial reserves of 96.0 million tonnes of Pb-Zn composite sulphide ore containing 13.54% of Zn & 1.97% of Pb.The rocks of the area form a part of Mangalwar complex of Bhilwara geological cycle (3.2-2.5 billion years) belonging to Archean age and comprising of magmatites, gneiss, graphite mica schist, pegmatites and impure marbles.General strike of the orebody is N50oE and dipping at 60-70oSE. Both hanging wall and footwall contacts of the mineralisation are sheer contacts. The ore body is hosted by graphite mica sillimanite gneiss in lens shaped doubly plunging synform with strike length of 1550 m and width varying from a few meters in the NE to 100 m in the central and SW section. The average width of ore body is 58 m over a strike length of 1550 m.

Joda East, Noamundi, and Katamati Iron Mines are captive mechanised open-pit mine of Tata Steel Limited in Jharkhand state of India. Iron ores of this region occur in the Iron ore series of Upper Dharwar age. The principal rocks found within the area are quartzitic sandstone, shales and cherty quartzites both banded and unbanded. Sometimes colloidal quartzites contain bands of Haematite and are recognised as Banded Haematite Jaspars (BHJ). Shales in this area are often silicified iron ore deposits and these are mainly confined to the top portions of the series. The rocks show a general strike NNE-SSW direction with a westerly dip.

The Sukinda Chromite Mine of Tata Steel Limited is located in Jajpur district of Orissa state. The Sukinda ultramafic complex is part of the metamorphosed Pre-Cambrian of Peninsular India. A thick (1m-12m) mantle of soil and laterite overlies the majority of the Sukinda ultramafic field, with outcrops being scarce, i.e. less than 10% of the total surface area. Pyroxenite band is occurring at the southern part of the lease area in between lumpy and friable ore bands.

Joda West Manganese Mines of M/s Tata Steel Limited is situated in the district of Keonjhar of Odisha state. The lease area falls in survey of India Topo Sheet No. 73 G/5& 73 F/8 between latitude N 21°58′00″ to N 22°02′00″ and longitude E 85°23′00″ to E 85°26′00″. The area has an undulating topography with highest and lowest elevation being around 650 m and 500 m respectively. Sona River is the main perennial river flowing in this area. The rock formation of the area belongs to the iron ore group of upper Dharwar age. Manganese ore deposits are associated with Shales, Laterite, Chert and Quartzite of Iron ore Group. It is distributed within the Horse shoe shaped synclinorium, plunging towards NNE over-folded towards SW. The manganese ore occurs as tabular lenses and as irregular veins in the country rock. It also occurs in the form of float and nodular masses.

The Sagmania Limestone Mines of M/s Satna Cement Works are situated at about 10 km North-East of Satna railway station. The limestone deposit in the mine belongs to the Vindhyan upper Group and is Upper Vindhyan in age. The mining lease area lies between longtitude 80°51′56″ & 80°55′28″ and Latitude 24°37′9″ & 24°40′5″. The general topography of the area is without any remarkable relief and forms more or less flat terrain with a general dip of approximately 3° to 5° towards south between S10oW and S5°E. The main lithological formations, which have been encountered in the area, are Bhander Limestone and Sirbu Shale in patches at places.

The Kayad Lead-Zinc mine of Hindustan Zinc Limited is located on the eastern fringe of Kayad village near Ajmer city (about 9 km). The deposit lies between latitude N26º31'30" and longitude E74º41' and 74º42'. There are three lenses – the Main lens, K1A lens and S1 lens. The main host rock is Quartz mica schist with some mineralization also occurring in calc silicate. Main lens has been dissected at many places by pegmatite. The lenses lie parallel to the axial plane foliation/ cleavage/ fracture of the fold system or shear fractures governed by the lithological variations. The main lens ranges in average width from 5 m in steeper portions to about 40 m in the flat lying portion. Maximum strike of the main lens is 900 m at the depth of approx. 250 m from the surface. It shows a general reducing trend in depth. This lens shows swelling and pinching nature probably because of superimposition of different phases of folding. The total Reserves and Resources of the Mine is 11.4 Million tonnes with 10.61 % Zn, 1.61 % Pb and 33 ppm Ag.

SindesarKhurd mine is located 6 km north of RajpuraDariba Mine in Rajsamand district of Rajasthan state of India. The latitude and longitude of the Sindesar block are 24°59′N to 25°01′N and 74°09′E to 74°10′E. The block comprises an assemblage of medium to high grade metamorphic equivalents of orthoquartzites, carbonates and carbonaceous facies rocks flanked by meta-argillites belonging to Bhilwara Super group of Archaean age. The oldest rock in the region is Banded Gneissic Complex of Mangalwar Group. The deposit is located in the central part of the eastern limb of Synformal fold and is concealed at a depth of 100m. The strike direction of ore body is N10-15E with a strike length of about 400 m. The dip of the ore body is 400 -600 towards N80W.

Kalidaspur Project of Satgram Area Eastern Coalfields Limited is located in the district of Bankura on the Southern part of river Damodar at about 17 km from Raniganj Railway Station. The lease hold area of the project is 934.20 hectares. The project area is made up of two sub-blocks viz. Kalidaspur and Kalikapur. It has a triangular shape with apex formed by duke and Damodarriver to the North-West. Damodarriver running North-West and South-East forms the Eastern boundary. Southern boundary is formed by a major fault between Kalikapur and Ardhagram in Kalikapur and in outcrop of the Kalidaspur block.

Pinoura underground mine of South Eastern Coalfields Limited is located in the Pinoura Block of Johilla Coalfields in Umaria District of Madhya Pradesh. The Latitude and Longitude of the geological block are N23°20′13″ to 23°21′45″ and E80°54′30″ to 80°56′50″. The total area of the mine boundary is 440 hectares. The lease area of the Pinoura mine is 526 hectares. The entire block is covered by soil and below the soil cover is NE part Supra Barkar formation and the remaining area is occupied by Lameta beds. The depth of cover varies from 104 m to 137 m. There are 5 nos. of faults varying with 3 m to 150 m down throw and one no. F-10 is 50 m up throw. There are 6 seams present in the block namely Johilla top, Johilla bottom, L1-A, L1-B, L1-C and LII. Out of six seams only 2 seams are workable i.e. JB and L1-B. Johilla Bottom seam is workable in patches, which can be approached from L1-B seam. L1-B seam is main workable seam and study was conducted in this seam.

Orient Mine No. 3 of Orient Area, Mahanadi Coalfields Limited, is situated in Jharsuguda District of Orissa State. The geology of the mine confirms to the geology of Ibriver Coalfields. The property lies between the latitudes 20°21′ and 23°0′ and longitudes 82°10′ and 84°0′. The Ib Coalfields constitutes a semi-circular half basin with the open end towards west. The structural trends are compatible with the form of the metamorphic sedimentary contact. The present working panel of the mine is in Lajkura seam IV, which is being developed by Bord and Pillar method of mining. The strike in Lajkura seam is generally along S 700 with dip around 1 in 10. The thickness of the seam is 2.5 m. There is a major up-throw fault of 90 m on the North-East side of the mine. The depth of cover of the present working ofLajkura Seam IV is about 103 m and it varies from 103 m to 109 m.

Hingir Rampur colliery of Hingir Rampur, Mahanadi Coalfields Limited is situated in Jharsuguda District of Orissa State. The area is free from major fault. In this area, outcrop of seven coal seams have been found viz. Hingir Rampur seam I, II, III, IV, V, Lajkura top &Lajkura bottom. HR seam I & IV are being depillared and HR seam V is partially developed by Bord and Pillar method

of working. The dip of HR seam IV is S84030'W and gradient is 1 in 20. For the study point of view the blast was conducted at only 46 m depth all though the actual depth of working face is more than 100 m.

INSTRUMENTATION AND MEASUREMENT TECHNIQUES

The ground vibrations produced by blasting were monitored by deploying 5-8 seismographs for each blast at various locations. The seismographs deployed for monitoring purpose were namely BlastMate III, MiniMate, MiniMate Blaster and MiniMate plus. All the seismographs have tri-axial transducers for vibration recording and microphone for noise/air over-pressure recording. The response of structures was monitored by eight channel seismographs with geophone placed on the structures and on the ground near their foundations.

EXPERIMENTAL DETAILS

The experimental blasts and data were collected from seventeen mines including ten opencast and seven underground mines. To assess the nature of blast induced ground vibration, the nature of frequency and the response of structures in different strata and rock, opencast mines of coal, limestone, Iron, Lead –zinc, Chromite and Manganese were selected whereas coal and Lead-zinc mines were selected in underground category. Altogether, 1305 ground vibration data (724 from opencast and 581 from underground blast) were recorded from 313 blasts (including 138 opencast blasts and 175 underground blasts). The blastholes were initiated by Nonel tubes, Electronic detonators as well as detonating cords. Extended seismic arrays were used to identify the vibration characteristics at near-field and far-field. The blast design parameters experimented in opencast and underground mines during the study are summarised in Table 1 and Table 2 respectively.

Table 1. Summarised details of blast design parameters experimented at Open pit mines.

Name of the Mine	No. of blasts	Hole depth [m]	No. of holes	Bur-den [m]	Spac-ing [m]	Q_{total} [kg]	Q_{max} [kg]	Distance range (m)	Range of PPV (mm/s)	Range of frequency (Hz)
Nigahi Project, Coal India Limited	11	42.5 - 49.5	61 - 124	9.25 - 10	12 -13	188185 - 403487	6170 - 13016	700 - 8550	0.683 – 41.2	3.7 - 23
Jayant Project, Coal India Limited	23	9 - 42.5	14 - 104	8.5 - 10.5	10.5 - 12.5	5049 - 133985	460 - 4768	900 - 6000	0.886 - 18.5	3.13 - 19
Dudhichua Project, Coal India Limited	10	18.5 - 56	21 - 80	8 - 10.5	10 - 13	58905 - 194180	3200 - 26490	920 - 7400	1.09 – 27.6	3.19 - 13.2
Rampura Agucha Mine, Hindustan Zinc Limited	15	4.2 – 12.2	34 - 230	2.75 - 4.2	1.2 -6	700 - 40708	84 - 498	300 - 1600	0.539 – 7.47	8.38 - 126
Sukinda Chromite Mine, Tata Steel Limited	17	2.5 - 13	13 - 119	3 - 4.5	4 - 6	133 - 10228	17 - 900	40 – 954	0.413 – 17.5	2.75 - 80.8
Joda West Manganese Mine, Tata Steel Limited	16	2.5 -10	7 - 78	2 - 3	2 - 3.5	125 - 2475	8.3- 95	100 - 639	0.622 – 9.78	3 – 24.8
Joda East Iron Mine, Tata Steel Limited	15	5.5 - 12	27 - 135	3-4.2	3.2-5	1830 - 8620	80 - 340	100 - 1240	0.683 – 9.6	2.63 - 11.4
Noamundi Iron Mine, Tata Steel Limited	7	5.4 - 12.5	25 - 155	2.3 - 4.4	3.3 -5	3980 - 17381	90- 280	80 - 1240	0.699 – 25.6	3 - 27.1
Katamati Iron Mine, Tata Steel Limited	6	6 – 11.3	30 - 100	3.5 - 4.2	4.2 - 4.8	4519 - 12515	110 - 453	140 - 1000	0.568 – 7.06	3.25 – 15.6
Sagmania Limestone Mines, Satna (SCW)	18	5.5 – 9.5	10 - 43	3 - 4	4 - 5	82 - 2106	21 - 156	50 – 500	1.03 – 36.2	13.5 – 98.3

Table 2. Summarised details of blast design parameters experimented at underground mines.

Name of the Mine	No. of blasts	No of holes	No. of PPV data recorded	Q_{Total} (kg)	Q_{max} (kg)	Depth of cover (m)	PPV (mm/s)	Frequency (Hz)
Kalidaspur Colliery, Coal India Limited	44	3 - 32	115	1.11-10.2	1.11-10.2	55-80	0.321 -10	20.6-165
Narsamunda Colliery, Coal India Limited	11	10-16	44	5.18-5.55	1.85	24-190	0.29-5.23	26.2-78
Pinoura colliery, Coal India Limited	52	13	140	7.2	2.22	104-137	0.151 -5.68	20.3-190
Orient Mine No. 3, Coal India Limited	16	12-14	62	5.5-6.6	2.22	103-109	0.19-1.14	25.1-219
Hingir Rampur Colliery, Coal India Limited	6	14	30	7.0	2.22	46	1.43-4.17	22-114
Kayad Mine, Hindustan Zinc Limited	34	26-90	123	58-325	1.9-12.5	80 - 250	0.381 -40.3	30-231
Sindesar Khurd Mine, Hindustan Zinc Limited	12	4-10	73	101.6 - 522.7	25.4-75	107 - 200	0.811 -16.2	13.8-196

MONITORING OF GROUND VIBRATIONS

Seismographs having eight as well as four channels provided with two/one tri-axial transducer(s) for monitoring of vibration (in mm/s) were used. The blast vibrations were recorded at standard samples rate of 1024 samples per second for the blast conducted at more than 200 m whereas sample rate of 4096 per second were used when blasts were conducted in close proximity to the monitoring point. The recorded peak particle velocities varied widely depending upon the distance to the monitoring locations from the blasting face and the amount of explosives detonated in the blast round. It varied between 0.151 and 40.3 mm/s in case of underground mines whereas for opencast it varied between 0.413 and 36.2 mm/s.

As expected, the vibration amplitudes and frequencies are affected by increasing distance, depth below the surface and geology. Decrease of vibration amplitude with distance on the surface has been well documented in numerous studies (Singh et al., 1997; Singh, 2002; Singh and Roy, 2010). Lewandowski et al. (2009) postulated that an area with abnormal geology would behave differently than its surroundings when exposed to blast vibration. The geometric spreading as the strongest effect whereas other loss mechanisms such as absorption, dispersion and reflection from existing geological discontinuities influence the vibration amplitude and frequencies significantly (Stavropoulov, 2014).

OPENCAST BLAST RESULTS AND ANALYSES

Altogether 724 blast vibration data were recorded from 145 blasts conducted at 10 different opencast mines. The vibrations were recorded in terms of peak particle velocity (PPV) in mm/s and frequency in Hz. The recorded magnitudes of vibrations (PPVs) at their respective scaled distances are plotted separately for all the mines to predict the ground vibration level and vibration attenuation characteristics were determined with the help of the regression plot. The maximum vibration recorded in the study was 36.2 mm/s from the blast conducted at Sagmania Limestone mine with explosive weight per delay of 105 kg and total explosive weight detonated in the blast round was 1,050 kg. The associated dominant frequency was 27 Hz. Blast vibration monitoring station was at a distance of 50 m. Non-electric detonators were used as initiation system. Attempts were made to record the vibration at the roof of the structures in the periphery of the mine to estimate the natural frequency.

Dominant frequencies recorded from open pit blasting conducted at 10 different opencast mines are plotted together and are presented in figure 1. It is evident that high frequency vibration data were recorded mostly at near-fields from the limestone bed. Most of the frequencies recorded from coal, manganese, iron and chromite mines were of low frequency i.e. less than 25 Hz. However, there was a common trend that the frequency get lowered with distances and it emphasized that the dominancy of the upper layer of the strata on the recorded frequency.

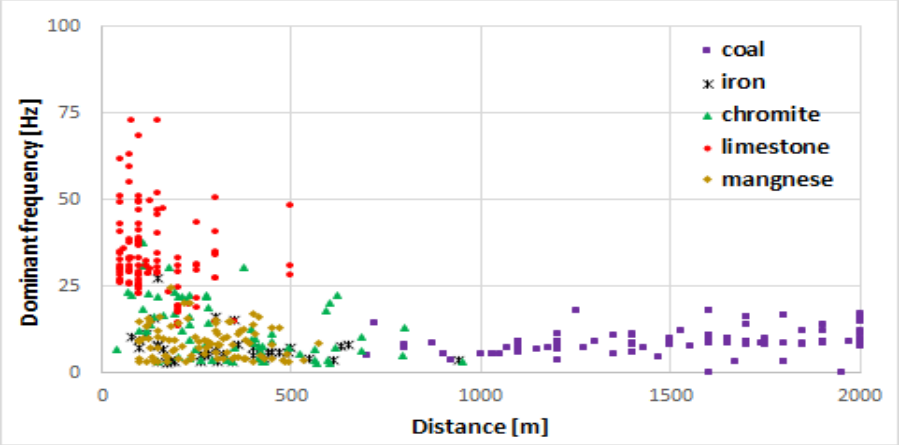

Figure 1. Plot of dominant frequencies of blast waves recorded at various locations in the periphery of the mines opted for study.

Regression analyses of vibration data were performed to derive the propagation equations separately for the each mine and a comparative analysis was made to evaluate the attenuation characteristics (Figure 2, 3, 4 & 5). The USBM predictor model has been used for blast vibration predictor equation. The scaled distance concept is used for blast vibration prediction and is defined as the actual distance (R) of the vibration measuring point from blasting face divided by square root of the maximum explosives weight per delay (Q_{max}).

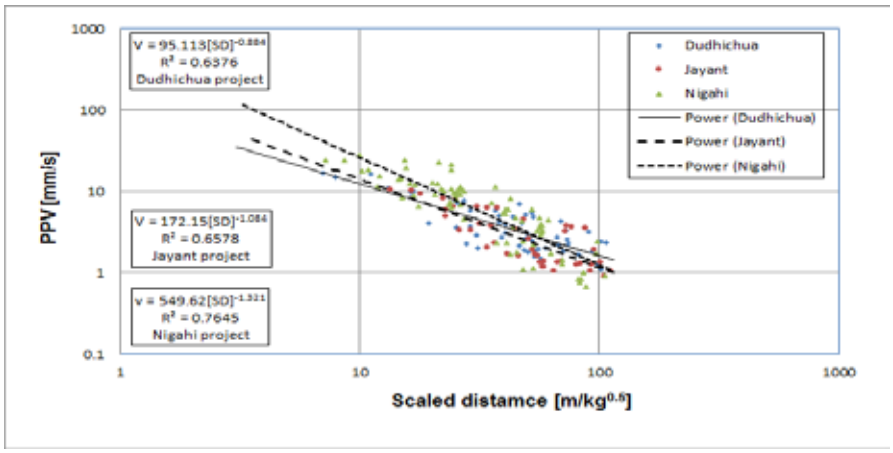

Figure 2. Propagation plot of vibration data with their respective scaled distances for opencast coal mines of Northern Coalfields Limited.

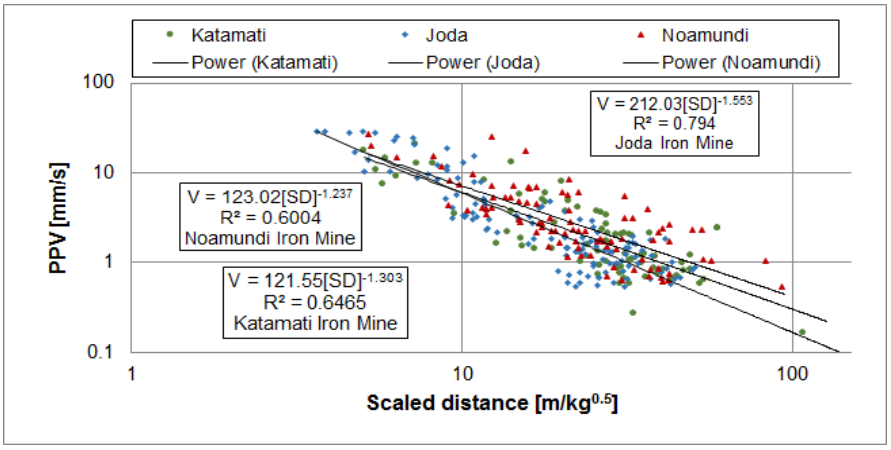

Figure 3. Propagation plot of vibration data with their respective scaled distances for iron ore mines of Tata Steel Limited.

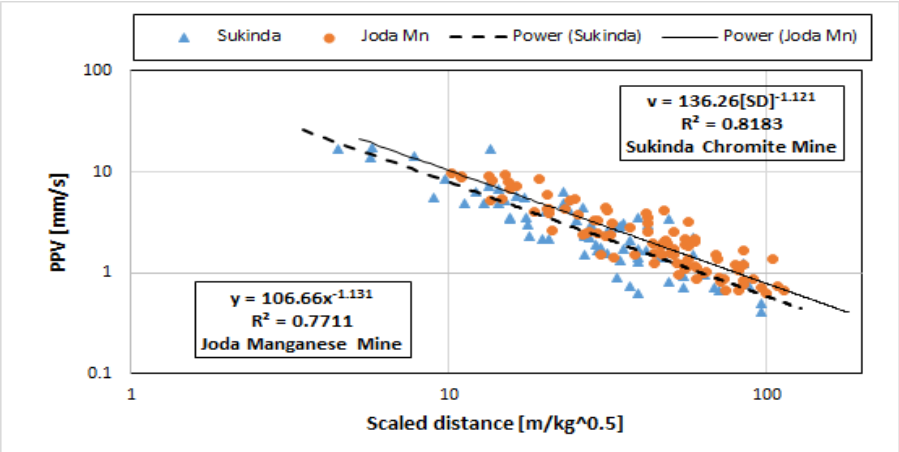

Figure 4. Propagation plot of vibration data with their respective scaled distances for Joda West Manganese mine and Sukinda Chromite Mine of Tata Steel Limited.

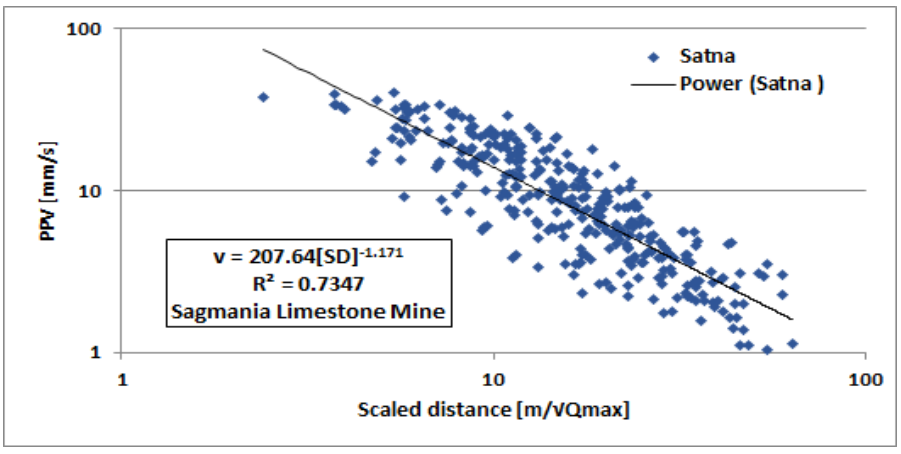

Figure 5. Propagation plot of vibration data with their respective scaled distances for Sagmania Limestone Mine of Satna Cement Works.

UNDERGROUND BLAST RESULTS AND ANALYSES

The study was conducted at seven underground mines including five coal and two lead-Zinc mines. A total of 175 blasts were conducted and attempts were made to record 581 ground vibration

data. The no of blastholes detonated during the study varied from 3 to 90. The total explosive weight detonated was in the range of 1.11 to 522.7 kg. The blast induced ground vibration recorded were in the range of 0.29 to 40.3 mm/s. The dominant frequency of the blast vibrations varied between 13.8 and 231 Hz. The plot of peak particle velocities with their respective dominant peak frequencies for all five underground coal mine is presented in Figure 6. A propagation plot of vibration data with their respect to scaled distances is presented in Figure 7.

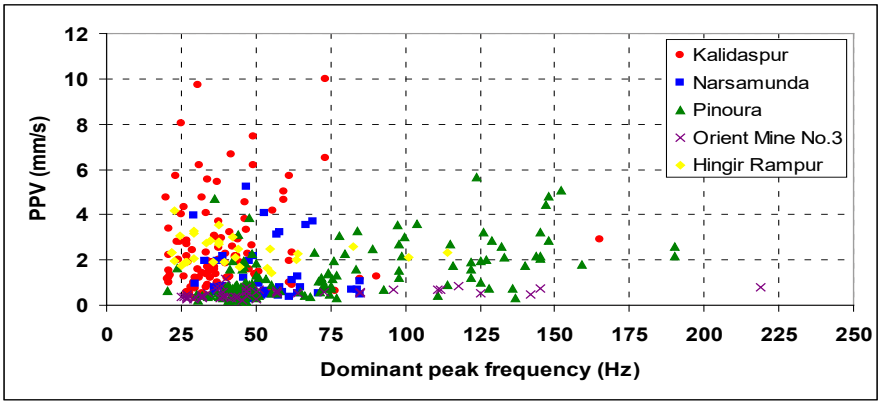

Figure 6. Plot of peak particle velocities with associated dominant peak frequencies.

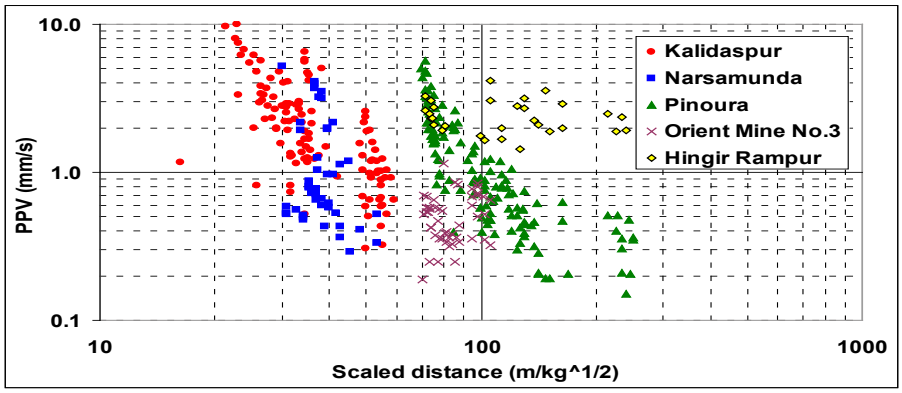

Figure 7. Propagation plot of vibration data with their respective scaled distances.

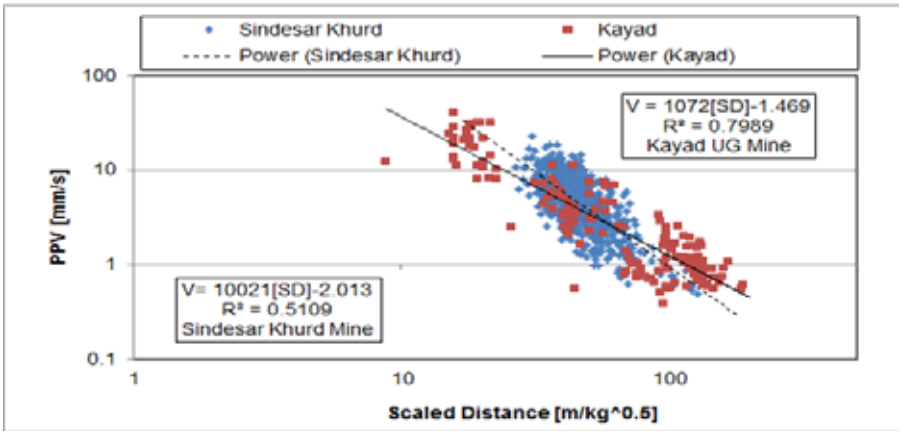

Figure 8. Propagation plot of vibration data with their respective scaled distances for Lead-Zinc mines of Sindesar Khurd and Kayad underground project.

DETERMINATION OF NATURAL FREQUENCY OF STRUCTURES

The ground motions resulting from blast induced seismic waves are transmitted to the structure upside through the foundation, resulting into the vibration of the structure. The dynamic property of any structure includes its natural frequency and damping ratio. The influence of frequency on the structure's dynamic response includes two aspects. One is the frequency of blasting waves (external cause) and the other is the fundamental frequency of the structure (internal cause). The structures do not respond immediately to blast vibrations when the frequency of waves is much greater than the fundamental frequency of the structure. The attenuation of blast vibration waves with high frequency is very rapid. On the contrary, for the in-putting blast waves with low frequency, the whole structure vibrates because the half-wave length is longer than the characteristic dimension of the structure. Especially when the magnitude of primary frequency of blast waves is very close to the fundamental frequency of the structure, the structure produces the resonance and causes the whole structure to vibrate more seriously.

The study included monitoring the amplitudes of vibration simultaneously on the ground surface near the foundation of the structure and at various levels in the structures such as roof/floor levels, mid-wall, corner wall etc. For this purpose the transducers of 8-channel seismographs were used. Some of the reinforced concrete structure is shown in photograph 1 whose responses to blast vibrations were recorded. The recorded blast wave signals on the ground and on the structure at one of the structure reinforced concrete structure is shown in Figure 9. The vibration recorded near the foundation of the house (Tran, Vert, Long) and on the structure (Tran 2, Vert 2, Long 2). The recorded persistence of vibration was less than one seconds. The maximum amplification occurred at resonance frequency because of low differential responses and is shown in figure 10. The computational process involved in determination of natural frequency of the structure is shown in Figure 11.

Similar exercises were carried out to monitor the response of various structures in the periphery of the mines. Amplification factor was determined directly from the vibration time histories. Maximum vibrations in the structures were documented. Ground particle vibration velocities and frequencies were then picked off the records at corresponding moments of time or immediately preceding the time of the peak structure vibrations. The maximum amplification of vibration in the structures was observed at the roof level at all the experimental sites. The natural frequencies of the structures in the periphery of the experimental sites were determined in order to design safe blasts during further investigation. The details of some of the structures studied with their response to vibrations and their fundamental frequencies are presented in Table 3 & 4. Natural frequency of structures/houses recorded in the periphery of different open pit and underground mines are depicted in figure 12.

Photograph 1. Monitoring of response of reinforced concrete structure to blast induced vibration.

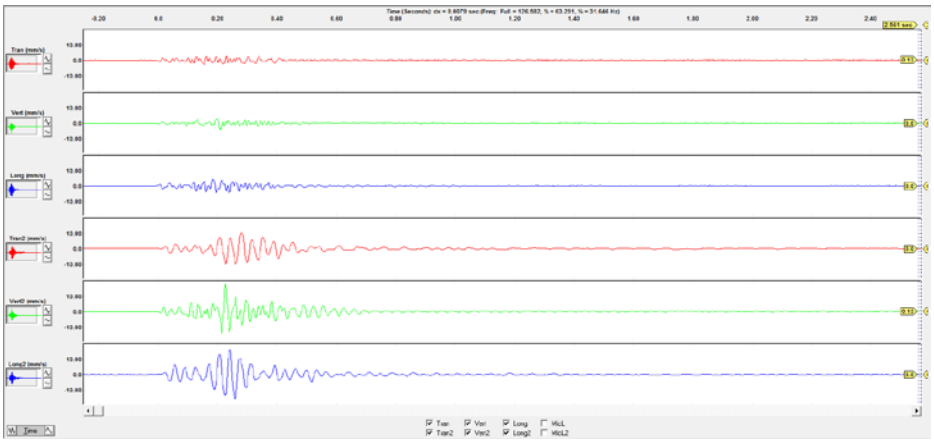

Figure 9. Blast wave signature recorded at reinforced concrete structure (at 300 m) foundation and on the structure from the blast conducted at Sagmania Limestone Mine.

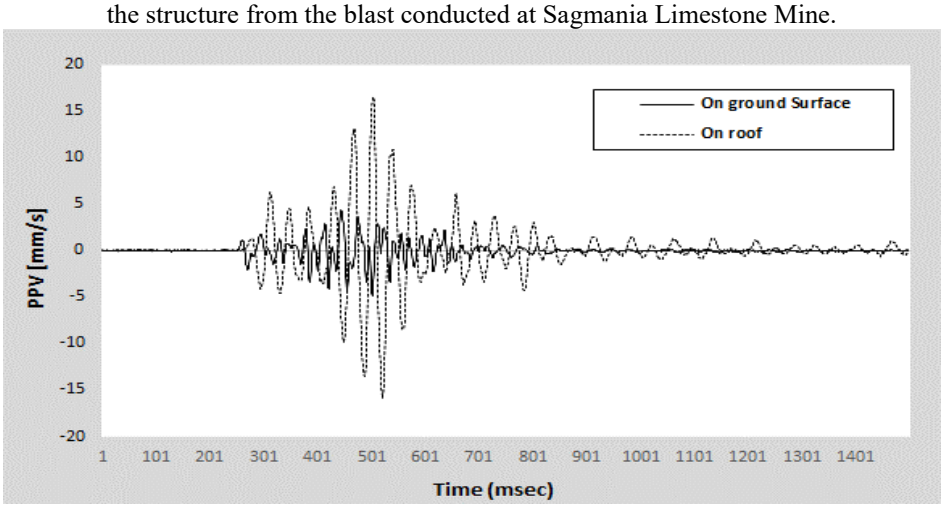

Figure 10. Peak structure response and forcing ground vibration at reinforced concrete structure due to blasting.

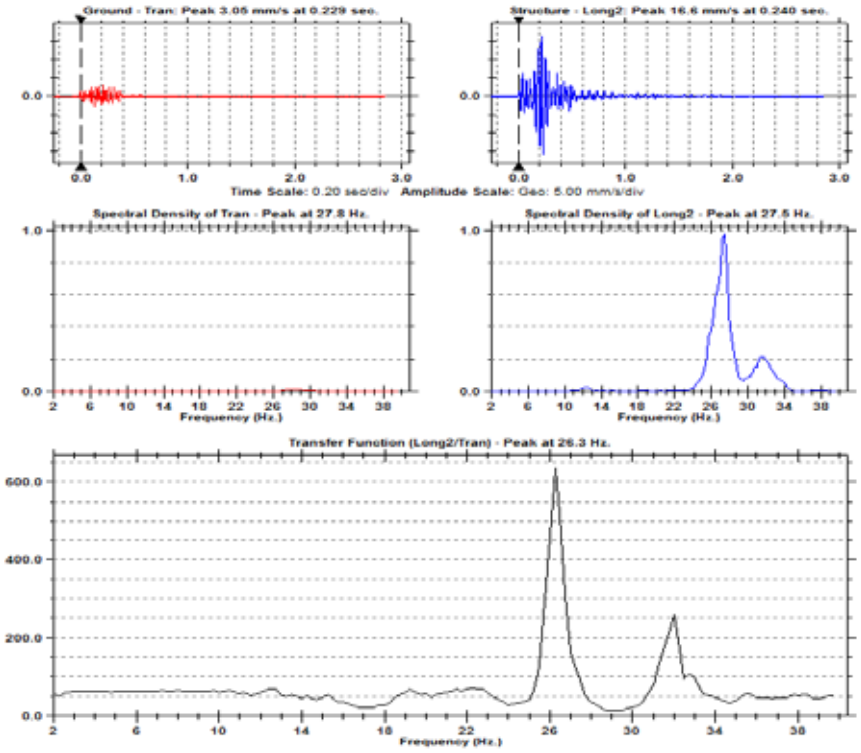

Figure 11. Processing of blast wave signature recorded at reinforced concrete structure for determination of natural frequency of the house.

Table 3. Details of the structures response determined in the periphery of the opencast mines.

Name of the Mine	No. of structure responses measured	Range of Natural frequency	Range of Amplification in PPV
Rampura Agucha Mine, HZL	3	7.63 – 12.9	1.55 – 3.25
Jayant Project, NCL	3	3.5 – 8.75	1.27 – 4.45
Nigahi Project, NCL	5	6.25 – 9.88	1.22 – 6.22
Dudhichua projects, NCL	2	3.25 – 6.88	1.43 – 5.09
Sukinda Chromite Mine, TSL	2	7.5 – 12.9	1.5 – 2.7
Joda West Manganese Mine, TSL	2	8.25 – 13.0	1.4 – 2.0
Sagmania Limestone mine, SCW	3	10.8 – 15.0	1.08 – 2.82
	20 nos.	3.25-15.0	1.08-6.22

Table 4. Details of the structure response determined in the proximity of underground mines.

Name of the Mine	No. of structure responses measured	Range of Natural frequency	Reduction in PPV (%)
Sindesar Khurd Mine, HZL	10	10.3 – 14.0	16.3 – 49.8
Kayad Underground Mine, HZL	2	14.0 – 15.9	37.3 – 38.2
Kalidaspur Colliery, ECL	1	10.0 – 11.8	40 – 55
Narsamunda Colliery, ECL	1	10.5	16
Orient Mine No. 3, MCL	3	7.0 – 7.75	4 – 44
Pinoura Colliery, SECL	3	6.75 – 8.3	12 – 38.8
	20 nos.	6.75-15.9	4-55

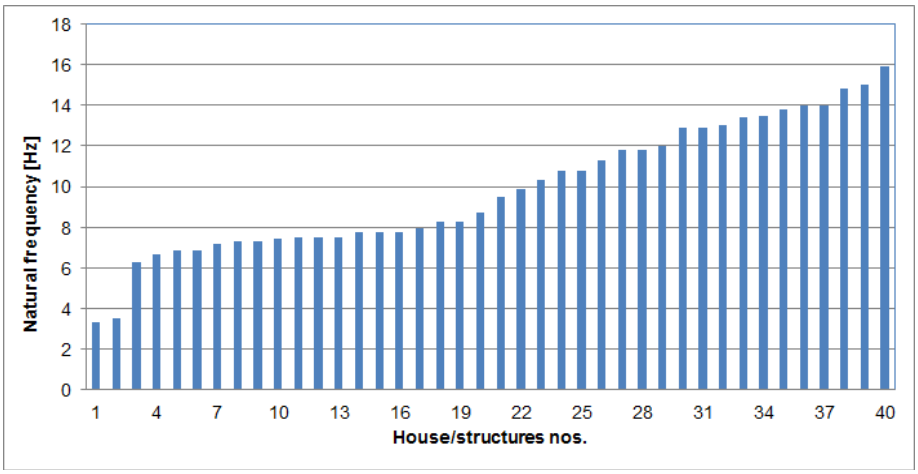

Figure 12. Natural frequency of structures/houses recorded in the periphery of different open pit and underground mines.

DISCUSSION ON STRUCTURAL RESPONSE AND DYNAMIC AMPLIFICATION

The measured responses of residential and other structures are critical indicator of troublesome ground vibrations. Essentially, cracking from blast vibrations occurs when excessive stresses and strains are produced within the planes of the walls or between walls at the corners. Above-ground portions of structures tend to amplify horizontal ground motion, with the degree of response dependent on the vibration frequency, natural frequency and damping characteristic of the structure. The natural frequencies of 20 structures in the periphery of the opencast mines and 20 structures in the proximity of the underground mines were recorded. The highest amplification factor of 6.22 was monitored at Panjreh Bhawan building at Singrauli Coalfields area of Northern Coalfields limited. The amplification factor of 1.22 to 6.22 were recorded which corresponds to excitation frequencies within 3.3-9.88 Hz. The natural frequencies of the structures in the periphery of the opencast mines ranged between 3.25 and 15.0 Hz whereas in the proximity of underground mines it varied between 6.75 and 15.9 Hz. In case of underground mine blasting, the reduction in vibration up to 55% on the roof of the structures were found (maximum height of structures 3.2m). The recorded principal frequencies of the blast waves were mostly in the excitation frequencies of the structures and thus, were the reasons for higher amplitude of vibration in the structures. The maximum heights of structures were up to 14 m. The peak structure response and the incoming ground vibrations waveforms are superimposed for absolute and differential responses analyses. The maximum amplifications occurred at resonance frequency (Figures 11) because of low differential responses. The frequencies below resonance did not show amplifications because there were no relative displacement and hence, no appreciable strain.

DISCUSSION ON THE PERSISTENCE OF VIBRATION IN THE STRUCTURES

Ground vibration duration is an equally important parameter in considering structural response. Using the swing analogy, we can easily make a swing go higher without pushing it harder, by simply pushing it again. The more times we push the swing the higher it will go. Longer ground vibrations continue to shake the house causing greater amplitude of structural response. Complete avoidance of superposition and amplification of the vibrations in a larger blast is impossible to achieve because the duration of the vibration is always considerably larger than the effective delays used between the charges in smaller blasts (Singh et al, 2003 & Valdivia et. al 2003). It was observed that persistence of vibration in the structures was more than 12 seconds due to dragline blasts (Figure 13) whereas in case of underground mine blasts it was less than 2 seconds (Figure 14). Amplifications of upto 6.22 times were recorded for opencast blasts. Such blast events were unacceptable to the resident, although no damage was recorded in the structures. The seismologists in earthquake engineering typically used acceleration levels to quantify damage potentials. These may be of moderate and even lower levels than found in blasting. However, their low frequencies produce large particle velocities and enormous displacements. Richter (1958) stated that 0.1 g acceleration at 1 Hz is ordinarily considered damaging in earthquake seismology. The corresponding particle velocity and displacement are 156.21 mm/s and 24.89 mm respectively, assuming simple harmonic motion. The same

acceleration at 20 Hz will only produce 7.82 mm/s of particle velocity and 0.06 mm of displacement. Richter also observed that the damage potential of a given vibration is dependent on its duration, with 0.1 g at 1 Hz likely not to produce damage for events for a few seconds, but very serious of earthquake-type events of 25 to 30 sec.

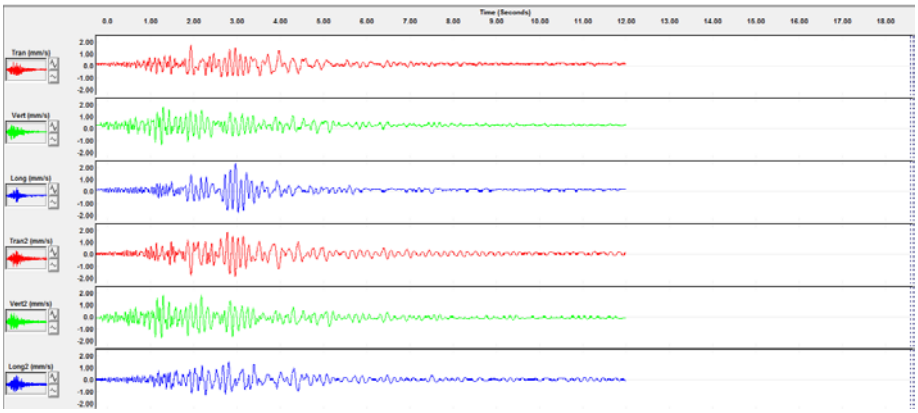

Figure 13. Blast wave signature recorded at reinforced concrete structure (at a distance of 5.2 km) due to open pit blasting at Jayant project of Coal India Limited.

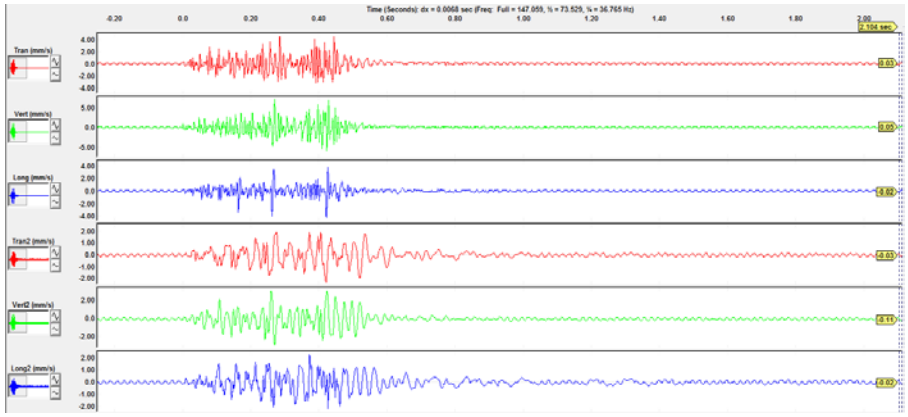

Figure 14. Blast wave signature recorded at reinforced concrete structure (at a distance of 280 m) from the underground blasting at Sindesar Khurd Mine of Hinduastan Zinc Limited

CONCLUSIONS

In most of the open pit blasts the frequency of blast vibration recorded is less than 25 Hz whereas in case of underground blasts it is opposite i.e. more than 25 Hz. These low frequencies are due to the low-velocity surface layer (top soil) and long vibration monitoring locations. The Fast Fourier Transform (FFT) analyses of recorded data from open pit blasts revealed that the maximum concentration of vibration energy was in the range of 3.7-24.8 Hz whereas in case of underground blasts it is in between 26.2 and 78 Hz. The structures studies were having fundamental frequencies in between 3.25-15.0 Hz in case of open pit whereas 6.75-15.9 Hz for underground case. The incoming vibration has frequency in the range of fundamental frequency of the structures, resonance occurred and the resultant amplitude of vibration on the structure got amplified. This is the reason why the structures at higher floors vibrated with higher amplitude of vibration than that of ground.

It is concluded that if a structure is exposed to ground vibrations near its fundamental frequency, the structure will amplify the vibration. Ground vibrations below the fundamental frequency of the structure will cause the structure to vibrate at least as much as the ground. However, if

the frequency of the ground vibration is 40% higher than the fundamental frequency of the structure, the structure will vibrate less than the ground.

The amplifications of vibration in the structures were more than five folds depending upon the height of the structures, its fundamental frequencies and also the frequencies of in-coming vibration. The persistence of vibrations were up to 12 seconds in the structures at far-off distances due to open pit blasting whereas in case of underground blasting the maximum persistence is up to 2 seconds. The long persistence of vibration in the structures at far-off distances was of great concern. It is recommended that the blast should be designed in such a way that its total duration should not be more than 1500 ms in environmentally sensitive areas. It has been also observed that the timing of delay intervals between two detonations had no influence on the frequency content of the vibrations. Geology was the controlling factor for predominate frequencies of vibration in this study.

The regression analysis revealed that the fastest attenuation of blast vibration in case of open pit blasting comes from the Iron mine whereas in case of underground mines fastest attenuation was observed in Sindesar Khurd Pb-Zn Mine.

REFERENCE

Hagan TN. Rock breakage by explosives. *Proceedings Nat. Symp. Rock Fragmentation*, Adelaide, pp1-17.

Lang LC. A brief analysis of Livingstons cratering theory, *SweDeFo report DS*: 1983; 1.

Hagan TN. Rock breakage by explosives. *Acta Astronaut* 1979; 6(3): 329-340.

Jimeno EL, Jimeno CL, Carcedo A. Drilling and Blasting of rocks. CRC Press, 1995.

Siskind, D. E., Stagg, M. S., Kopp, J. W. and Dowding, C. H., 1980. Structure Response and Damage Produced by airblast from Surface Mine Blasting. U. S. Bureau of Mines, RI 8485, 111 p.

Singh PK, Vogt W, Singh RB and Singh DP, 1996. Blasting side effects - investigations in an opencast coal mine in India. *Int. Journal of Surface Mining Reclamation and Environment*, Netherlands, Vol. 10, pp. 155-159.

Singh PK, Vogt W, Singh RB, Singh MM, Singh DP. Response of surface structures to rock blasting. Mineral Res Eng 1997, 6(04): 185-194.

Dauetas AA, Denisyuk II, Kuzmenko AA, Vorobev VD. Seismic effects of blasting in rock (vol. 103). CRC Press, 1993.

Athanasopoulos GA, Pelekis PC. Ground vibrations from sheetpile driving in urban environment: measurements, analysis and effects on building and occupants. Soil Dyn Earthq Eng 2000, 19(5): 371-387.

Duvall WI, Johnson, CF, Meyer, AVC. Vibrations from blasting at lowa limestone quarries. USBM RI 6270, 1963.

Langefors U, Kihlstrom B. the modern technique of rock blasting. Wiley, New York, 1963.

Ambraseys NR, Hendron AJ. Dynamic behaviour of rock masses: rock mechanics in engineering practices. Wiley, London, 1968.

Dowding CH. Response of buildings to ground vibrations resulting from construction blasting (Doctoral dissertation, University of Illonois at Urbana-Champaign), 1971.

Ghosh A, Daemen JK. A simple new blast vibration predictor. Proc. 24th US Symp. Rock Mechanics, Texas, USA; 1983, p. 151-161.

Kahriman A. Analysis of ground vibrations caused by bench blasting at Can open-pit lignite mine in Turkey. Environ Geol 2002, 41(6):653-661.

Kuzu C. The importance of site-specific characters in prediction models for blast-induced ground vibrations. Soil Dyn Earthq Eng 2008, 28(5): 405-414.

Cardu M, Mucci A, Uyar G. Investigating the effects of bench geometry and delay times on the blast induced vibrations in an open-pit quarry. GEAM 2015, 1: 45-56.

Singh TN, Singh V. An intelligent approach to prediction and control ground vibration in mines. Geotech Geol Eng 2005, 23(3): 249-262.

Sawmliana C, Roy PP, Singh RK, Singh TN. Blast induced air overpressure and its prediction using artificial neural network. Mining Techn 2007, 116(2): 41-48.

Iphar M, Yavuz M, Ak H. Prediction of ground vibrations resulting from the blasting operations in an open-pit mine by adaptive neuro-fuzzy inference system. Environ Geol 2008, 56(1): 97-107.

Khandelwal M, Singh TN. Prediction of blast-induced ground vibration using artificial neural network. Int. J Rock Mech Min Sci 2009, 46(7): 1214-1222.

Mohamed MT. Artificial neural network for prediction and control of blasting vibrations in Assiut (Egypt) limestone quarry. Int J Rock Mech Min Sci 2009, 46(2): 426-431.

Amnieh HB, Siamaki A, Soltani S. Design of blasting pattern in proportion to the peak particle velocity (PPV) Artificial Neural Network. Safety Sci. 2012, 50(9): 1913-1916.

Amnieh HB, Bahadori M. Safe vibrations of spilling basin explosions at “Gotvand Olya Dam” Using Artificial Neural Network. Arch Min Sci 2014, 59(4): 1087-1096.

Goldman DE. A Review of Subjective Responses of Vibrating Motion of the Human Body in the Frequency Range, 1 to 70 Cycles per Second. *Naval Medical Res. Inst.* Proj. NM 004001, Rept. 1, March 16, 1948, 17 p.

Whiffin AC, Leonard DR, 1971. A survey of traffic induced vibrations. *Road Res. Lab., Dept. Environment,* Crow Thorne, Berkshire, England, Rept. RRL. LR 418, 58 p.

Chang F. 1973. Human Response to Motions in Tall Buildings. *Proc. ASCE*, Vol. 99, No. 2, June 1973, pp 1259-1272.

Atherton GH, Polensek A, Corder SE. Human Response to Walking and Impact Vibration of Wood Floors. *Forest Production Journal*, 1976, 26(10): 40-47.

Singh PK, Singh RB, Prakash AJ. Study on effect of delay timing, total charge and direction of initiation on blast induced vibration. *Unpublished report of Ministry of Coal*, Government of India, 2004, 142 p.

Power DV. A survey of complaints of seismic related damage to surface structures – Salmon Event. *Bull. Seis. Soc. Am*., 1966, 56(6): 1413-1428.

Nicholls, HR, Johnson CF, Duvall WI. Blasting vibrations and their effects of structures. *United State Bureau of Mines, RI 656*, 1971, p 105.

Roy MP, Sirveiya AK, Singh PK. Low frequency long duration blast vibrations and their effect on residential structures. *Proc. 31st Ann. Conf. on Explosives and Blasting Technique,* Int. Soc. of Explosives Engineers, Orlando, USA, 2005, pp. 101-112.

Singh PK. Blast vibration damage to underground coal mines from adjacent open-pit blasting. Int J Rock Mech Min Sci. 2002; 39(8)959–973.

Singh PK, Roy MP. Damage to surface structures due to blast vibration. Int J Rock Mech Min Sci. 2010; 47(6): 949–961.

Lewandowski T, Richards L, Hamson L, Merchant M, Spargo A. The Impact of geological fractures on level of ground vibrations. In: Proceedings of the 9th International Symposium on Rock Fragmentation and Blasting (Fragblast 9); Granada, Spain: September13–17, 2009:535–543.

Stavropoulou M. Discontinuity frequency and block volume distribution in rock masses. Int J Roc Mech Min Sci. 2014; 65: 62-74.

Singh PK, Roy MP, Singh RK, Sirveiya AK. 2003. Impact of blast design and initiation sequence on blast vibration. *Proceedings of National Seminar on Explosives and Blasting, DGMS*, Dhanbad, India, pp 118-126.

Valdivia, C., Vega, M., Scherpenisse, C. R., and Adamson, W. R., 2003. Vibration simulation method to control stability in the Northeast corner of Escondida Mine. *International Journal of Rock fragmentation by blasting, FRAGBLAST*, Vol. 7, No. 2, pp. 63-78.

Richter, C. F., 1958. Elementary Seismology. *W. H. Freeman and Co., SanFrancisco, USA*, 768 pp.

BLAST DESIGN AND VIBRATION CONTROL AT LEAD-ZINC UNDERGROUND MINES UNDERNEATH DENSLEY POPULATED AREA

*M. P. Roy[1], Ranjit K Paswan[1] and P. K. Singh[1], L. S. Shekhawat[2]

[1]*CSIR- Central Institute of Mining and Fuel Research*
Dhanbad, India 826015
*(*Corresponding author: mproy14@yahoo.com)*

[2]*Hindustan Zinc Limited, Udaipur, India 313004*

24th World Mining Congress
MINING IN A WORLD OF INNOVATION
October 18-21, 2016 • Rio de Janeiro /RJ • Brazil

BLAST DESIGN AND VIBRATION CONTROL AT LEAD-ZINC UNDERGROUND MINES UNDERNEATH DENSLEY POPULATED AREA

ABSTRACT

Blast induced ground vibrations have been a constant problem for the mining and construction industries. The population near the mining area and the regulatory agencies responsible for setting safety and environmental standards are always a threat and the safety of the nearby dwellers are always a concern. Questions frequently come up about blast vibration effects and specifically about whether vibrations can or could have caused any damage in homes and other structures. The answer depends primarily on vibration levels, frequencies and persistence of vibration and to a lesser degree on site and structure specific factors.

This paper is based on the problems faced at two lead-zinc underground mines of Hindustan Zinc Limited as the mining operations are actively being done underneath a densely populated area. One site is Kayad underground mine where mining is being carried out by sublevel open stoping method at an vertical depth of 100 m to 390 m. The Kayad village is only 100 m horizontally away from the underground mining areas. Hence, blast induced ground vibration is one of the major issues for the resident of Kayad village. The study involves the optimization of blast design parameters at slot raise and ring hole blast to control blast induced vibration within safe limits while ensuring improved production, productivity with greater safety. The impact of 110 slot raise blasts and 52 ring hole blasts were conducted and 405 vibration data were monitored in the village at different locations. Extensive experiments were performed and blast induced vibrations were controlled in the village. The deck blasting i.e. up to four explosives decks were used in a blast hole and the explosives charges were separated by delay detonators which helped in controlling the vibration in the village.

The second mining site with similar problem was at Sindesar Khurd Mine where mining is being operated just below the Sindesar Khurd village at a depth from 75 m to 360 m. All available technical knowledge is being incorporated to improve the blasting practices at Sindesar Khurd underground lead-zinc mine. Altogether, 347 ground vibration data from 82 blasts were collected in the adjoining village. Initially, the blasts were performed with100 kg of emulsion cartridge explosives distributed in 4 holes and were detonated with explosives weight per delay of 25 kg. Subsequently, the maximum explosives fired with electronic delay detonator was 1000 kg and the explosives weight per delay was also enhanced to 75 kg which contributed in speedy recovery of mineral to meet the demand. The vibration data recorded in the village were less than 10 mm/s. Electronic detonators and non-electric detonators (NONELs) were used at both the mines and a comparative study has also been performed for both the initiation systems.

KEYWORDS

Ground vibration, Slot raise blast, Ring hole blast, Initiation systems, Velocity of detonation

INTRODUCTION

Blast induced ground vibrations are one of the most undesirable outcome of blasting practices in mining engineering and are complex phenomena controlled by many variables. It involves the interaction between three dominant aspects: the geology of the rock mass; the geometry of the exposed surfaces and the boreholes; and the explosives and initiation sequence. The rapid release of energy is used to fragment and move rock from its geological setting and make the broken rock available for excavation, transport and further, mechanical comminution. The chemical energy of the explosives used in blasting does not all do useful work – some of it is converted to seismic energy (ground vibrations), acoustic energy (noise or airblast), and heat (Singh & Vogt 1998). A blast produces fine material of limited utility, unwanted gasses and air-borne dust. At some level all of the results of a blast have an economic effect to the mining, quarrying or construction project. Little and Van Rooyen (1988) produced a useful summary of a blast which they describe as the “explosives-rock mass interaction.”

The rock mass inputs are a function of the geological setting of the ore body. The explosives characteristics are chosen by the blasting engineer based on the rock mass properties and the desired blasting objectives. The blast design implements the explosives and initiation sequence given the geology and the available geometry (blasthole diameter, blasthole length, number and length of decks etc.) to focus

the available energy on the blasting objectives. Blasting engineer needs to have confidence in the outcome of their blast design. The primary blast outputs may be identified visually by a casual observer at the drawpoint (loading point) i.e. from a safe position. These are fragmented rock, the disposition and location of that fragmented rock, environmental outputs including ground vibration. Although due to practical difficulty, the inspection is only possible in face blast only, rather in the ring blast area in underground operations. While such observations are needed and important is the feedback to the blaster for each blast, it is essential to have quantitative information to ensure that a rigorous process of blast control and improvement occurs. The challenge is formidable given the violent release of energy in a blast and the engineering properties of the rock being broken and moved.

Harries (1988) gives a non-exhaustive list of over fifty variables involved in managing a blast and opines that while some of the variables may be controlled "this leaves an uncomfortably large number of variables whose effect on blasting and subsequent operations has to be assessed."

The major concern in underground metal mine blasting is the ground vibration reaching to the houses of the nearby population. The real cause of complaints by people about blasting is related to structural response due to ground vibrations and air overpressures. All blast vibration complaints are due to how much complainant's houses shake, not how much the ground shakes. The three factors of ground vibrations that determine the degree of shaking are ground vibration amplitude (peak particle velocity; PPV), its duration and its frequency (Singh et al., 2008). Human beings notice and react to vibration at levels much lower than the levels established as structural damage thresholds (Singh and Roy, 2010). Previous studies on human response to transient vibrations have established that human tolerance to vibration decreases the longer the vibration continues.

Vibrations can be generated by natural events or man-made activities. Natural events include earthquakes, volcanoes, and lightning strikes. Man-made activities include machinery vibrations, vibrations generated by trains, planes, automobiles, rock blasting, etc,. The amount and type of vibrations that reach a site are dependent on the amount of energy released at the source, the energy travel pathways from the source to the site, the distance from the source to the site, and the characteristics of the of site. Small events like vibrating machinery result in vibrations that travel only a short distance before they dissipate. Large events like earthquakes may be felt in larger area. There is significant discrepancy between the expected vibration amplitudes in terms of specific vibration energy released and that actually measured in the stope blasts under investigation, keeping all other conditions constant (Mohanty et al., 2013). The mining industry needs realistic design levels and also practical techniques to safe guard the structures in their periphery. At the same time, mines safety control agencies responsible for blasting and explosives need reasonable, appropriate and technologically established and supportable blast vibration damage criteria on which to base their regulations (Lal et al., 2012). Finally, neighbours around the mining operations require really protection of their property and health. Last but not the least, the mining operations should not be stopped only due to apprehension of the damage to the structures/buildings.

The mining industry needs realistic design levels and also practical techniques to safe guard the structures in their periphery. At the same time, mines safety control agencies responsible for blasting and explosives need reasonable, appropriate and technologically established and supportable blast vibration damage criteria on which to base their regulations. Finally, neighbours around the mining operations require really protection of their property and health. Last but not the least the mining operations should not be stopped only due to apprehension of the damage to the structures/buildings.

This paper investigates the issue of ground vibration complaints at Kayad village and Sindesar Khurd village due to blasting at kayad and Sindesar Khurd underground mine respectively and its plausible solutions. Attempts were performed through systematic steps by changing blast designs viz; amount of explosives in a round or in a delay, position and timing of deck, firing sequence, hole diameter and length and by means of various initiation systems in order to get desired blast results.

DETAILS OF EXPERIMENTAL SITE

Kayad underground mine

Kayad underground mine is a Lead-Zinc mine of Hindustan Zinc Limited. The mine is located at Kayad village in Ajmer district of Rajasthan state in India. The mine is located on the eastern fringe of Kayad village. The deposit lies between latitude N26º31'30" and longitude E74º41' and 74º42'. The Kayad village is 9 km NNE of Ajmer city and is well connected by tar road

There are three lenses – the Main lens, K1A lens and S1 lens. The main host rock is Quartz mica schist with some mineralization also occurring in calc silicate. Main lens has been dissected at many places by pegmatite. The lenses lie parallel to the axial plane foliation/ cleavage/ fracture of the fold system or shear fractures governed by the lithological variations. The main lens has been explored to variable depths and maximum up to 50 mRL while K1A and S1 goes up to 350 mRL. The main lens ranges in average width from 5 m in steeper portions to about 40 m in the flat lying portion. Maximum strike of the main lens is 900 m at the depth of approx 250 m from the surface. It shows a general reducing trend in depth. This lens shows swelling and pinching nature probably because of superimposition of different phases of folding. The total reserves and resources of the mine are 11.4 Million tonnes with 10.61 % Zn, 1.61 % Pb and 33 ppm Ag.

Sindesar khurd underground mine

Sindesar Khurd Mine (SKM) is an underground Lead-Zinc operation of Hindustan Zinc Limited with designed ore production capacity of 2 million tonne per annum. This mine is located at Sindesar Khurd village in Rajsamand district of Rajasthan state in India. The mine is trackless operation using 50 tonne LPDTs &17tonne LHDs and mechanized development techniques. In the uppermost block of mine, blasthole open stoping method is practiced with rib pillars but in the subsequent lower blocks mining will be done by sublevel stoping method with post filling in primary-secondary sequence. The mine is a dry mine with minimal encounter of water.

The whole area is covered with 20-30m thick alluvium. The deposit comprises an assemblage of medium to high grade metamorphic equivalents of ortho-quartzites, carbonates and carbonaceous facies flanked by meta-argillites of pre-Cambrian, pre- Aravalli age. The structural imprints of the rocks suggest at least four stages of deformation giving rise to a doubly plunging synform (or basin) with its axis trending N-S to approximately NE, with a steep dip towards east. The rock types generally encountered are Calc-Biotite Schists, Calc-Quartzite/Siliceous Dolomites, Graphite Mica Schists, Calc-Silicate bearing Dolomites and Quartzite veins. The Calc-silicate bearing Dolomitic lens, present within the Mica Schist-Chert horizon, forms the principal host rock for the sphalerite-galena mineralisation. The Carboniferous Schist forms the subordinate host in terms of grade. The strike of orebody is north south &length around 2.3km with westerly dipping with 50^0-65^0 dip. The ore body is concealed at 120m depth from surface.

The ground at Sindesar Khurd Mine falls in good ground conditions with the RMR of 70. Stopes of 75-85m height and width varying from 15-50m have been mined out successfully. There are presently 4 sets of joints. General topography level is around 530mRL and the ore body is concealed below 120m depth from surface. Orebody is explored from surface up to the depth of 1200m and still the orebody is open. The mine is divided into several blocks of which 425mRL-315mRL and 290mRL-215mRL blocks with sublevels at 400mRL, 375mRL & 350mRL and 265mRL & 240mRL respectively are under production and 195-160mRL block is under development. The Satellite view of Sindesar Khurd and Kayad underground Mine adjacent to the Sindesar Khurd and Kayad village is shown in figure 1.

Figure 1. Satellite view of Sindesar Khurd and Kayad underground Mine adjacent to the Sindesar Khurd and Kayad village respectively.

EXISTING BLAST VIBRATION STANDARDS

Different countries have set their own standards on the basis of their extensive field investigations carried out in their mines for several years. There is a plethora of standards available world-over based on various aspects of ground vibrations e.g. amplitude, peak particle velocity, frequency, acceleration, etc. These parameters are used either as a single criterion or in combination; sometimes frequency is combined with amplitude and velocity. Peak particle velocity has been traditionally used in practice for the measurement of blast damage to structures.

United States Bureau of Mine (USBM) published RI 8507 in 1980 and recommended blasting level criteria which set a peak particle limit based upon predominant frequency of the seismic wave. A further review of limits imposed, raise question about how relatively small limits, such as 0.25 inch/s can be technically justified. Several researchers stated that no engineering study or research justified such limits. But when such restrictive levels are imposed, they are more of a political limits intended to reduce or eliminate public complaints. The obvious intent of regulations is to reduce public annoyance and the corresponding complaints. The effectiveness of such arbitrary limits in reducing complaints is highly suspect, but their economic impact can be substantial. Criteria applied, as law should be based upon solid research conducted by a well-recognized and accepted authority.

Good legislation will set limits that balance the costs and benefits to all stakeholders, based upon standards grounded in good science and justice. An overview of few vibration standards implemented by various counties is given in following Tables 1-5.

Table 1. Australian standards (Ca-23-1967) *(Just and Chitombo, 1987)*.

Type of structures	Maximum values
Historical building and monuments and buildings of special value	0.2 mm displacement for frequencies less than 15 Hz
Houses and low rise residential buildings, commercial buildings not included below	19 mm/s resultant ppv for frequencies greater than 15 Hz
Commercial buildings and industrial buildings or structures of reinforced concrete or steel construction	0.2 mm maximum displacement corresponds to 12.5 mm/s ppv at 10 Hz and 6.25 mm/s at 5 Hz

Table 2. USA standard after *Siskind et al.* (1980).

Type of structures	Peak particle velocity (mm/s)	
	Frequency (<40 Hz)	Frequency (>40 Hz)
Modern homes, dry wall interior	18.75	50
Older homes, plaster on wood lath construction	12.5	50

Table 3. German standard *After German DIN4150* (1986).

Type of structures	Peak particle velocity (mm/s) at foundation		
	<10 Hz	10-50 Hz	50-100 Hz
Offices and industrial premises	20	20-40	40-50
Domestic houses and similar constructions	5	5-15	15-20
Buildings that do not come under the above because of their sensitivity to vibration	3	3-8	8-10

Table 4. USSR standard.

Type of structures	Allowable PPV (mm/s)	
	Repeated	One fold
Hospitals	8	30
Large panel residential buildings and children's institutions	15	30
Residential and public buildings of all types except large panels, office and industrial buildings having deformations, boiler rooms and high brick chimneys	30	60
Office and industrial buildings, high reinforced concrete pipes, railway and water tunnels, traffic flyovers	60	120
Single storey skeleton type industrial buildings, metal and block reinforced concrete structures, soil slopes which are part of primary structures, primary mine openings (service life upto 10 years) pit bottoms, main entries, drifts	120	240

Table 5. Permissible peak particle velocity (PPV) in mm/s at the foundation level of structures in mining area *(DGMS circular 7 of 1997).*

	Dominant excitation frequency, Hz		
	< 8 Hz	8-25 Hz	> 25 Hz
(A) Buildings/structures not belong to the owner			
1. Domestic houses/structures (Kuchcha, brick & cement)	5	10	15
2. Industrial buildings	10	20	25
3. Objects of historical importance and sensitive structures	2	5	10
(B) Buildings belonging to owner with limited span of life			
1. Domestic houses/structures	10	15	25
2. Industrial buildings	15	25	50

BLASTING DETAILS AND MONITORING OF VIBRATION

Blast vibration monitoring was carried out at 3 to 4 locations in Kayad village. The number of holes detonated in a blast round for slot raise and ring blasting varied from 2 to 13. The total explosives weight detonated in blast around varied from 70 to 310 kg. The maximum explosives weight per delay varied between 4.1 and 18.75 kg. The diameters of the blast holes were 76 mm.

The blast vibration generated due to slot raise and ring blasts have been taken for analyses. In all the cases the monitoring of blast vibration were performed for vertical depth of 30 m to 185 m and horizontal distance up to 300 m from the vertically above point from the underground blasting face. Recorded blast vibration data were in the range of 2.34 to 14.6 mm/s.

Recorded blast vibration data were analyzed at a regular interval. The vibration data recorded from the production blasts (slot raise and ring) have been taken for analyses and generalized prediction equation has been established and is given as equations 1.

$$v = 1244.1 \times \left(\frac{R}{\sqrt{Q_{max}}} \right)^{-1.51} \quad \text{(Equation 1)}$$

Correlation co-efficient = 89.2 %

Where, v = Peak particle velocity (mm/s); R = Distance between vibration monitoring point and blasting face and Q_{max} = Maximum explosive weight per delay (kg)

Extensive blast vibration monitoring was carried out in Sindesar Khurd village. Blast vibration generated from 82 ring blasts has been taken for analyses out of which 38 blasts were performed by electronic delay detonators and rest 44 blasts were performed by nonel initiation system. The number of holes detonated in a blast round varied from 2 to 16. The total explosives weight detonated in blast around varied from 82 to 792 kg. The maximum explosives weight per delay varied between 17 and 75 kg. The diameters of the blast holes for rings were of 89 mm & 115 mm. The numbers of deck between explosives were sometimes 1 and sometimes 2 of 1.8 to 2 m depending on the size of the blast.

Four to five seismographs were deployed to record the vibrations for each blast at various locations. The locations of the seismographs for three sites were fixed for all the blast vibration monitoring. Rest two locations were varying as per the complaint from the resident of the houses. The depth of cover of the monitoring locations varied between 100 and 198 m. The blast monitoring locations were at 99 m at the village boundary and up to 456 m in the village. The radial distances between the blasting locations and monitoring points were from 142 to 467 m. Recorded blast vibration were in the range of 2.34 to 14.6 mm/s.

Recorded blast vibration data were analyzed at an regular interval. In this paper only important 82 blasts have been considered for analyses. Based on the recorded blast vibration data predictor equation has been established. The established equation for the mine is:

$$v = 9714.8 \times \left(\frac{R}{\sqrt{Q_{max}}} \right)^{-2.007} \quad \text{(Equation 2)}$$

Correlation co-efficient = 71.6 %

The above equation has been used to compute the predicted level of vibration at various locations in the village and accordingly the explosives weight per delay were practiced. The recorded dominant peak frequencies of vibration were in the range of 26-249 Hz (Figure 2) whereas the most common range was 54 to 129 Hz. Hence, the safe limit of ground vibration (PPV) for the safety of houses and other structures of Sindesar Khurd village has been taken as 15 mm/s as per Indian Standard (Table 5).

The recorded frequencies of vibrations at Kayad underground mine were in the range of 30.1-246 Hz. The Fast Fourier Transform (FFT) analyses of vibration data obtained shows that the concentrations of vibration energy were in the range of 50-150 Hz. At Sindesar Khurd village the recorded dominant peak frequencies of vibration were in the range of 26-249 Hz whereas the most common range was 54 to 129 Hz. Hence, the safe level of vibration for both the mines has been taken as 15 mm/s for the safety of houses/structures as per DGMS standard (Table 5). The plot of recorded dominant peak frequency of vibration at Kayad village and Sindesar Khurd village with respective radial distance from the blasting sites is presented in Figure 2. The regression plot of blast vibration data for both the mines is presented in Figure 3.

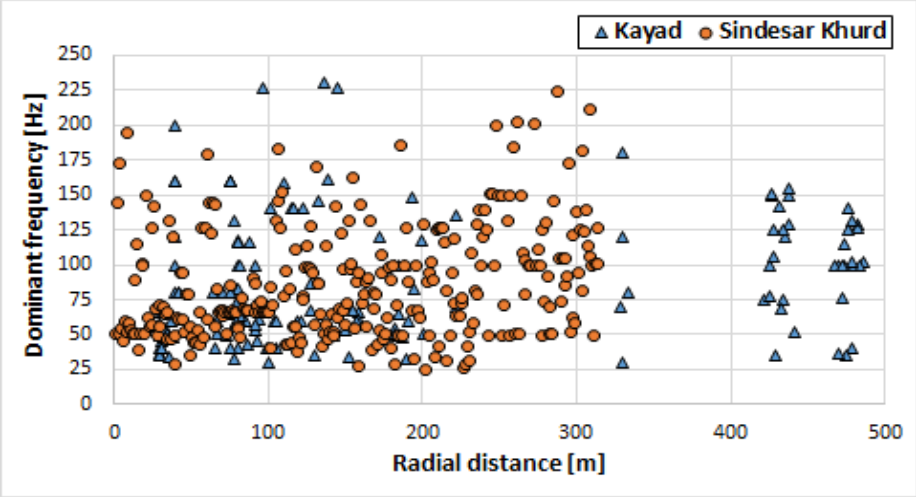

Figure 2. The plot of recorded dominant peak frequency of vibration at Kayad village and Sindesar Khurd village with respective radial distance.

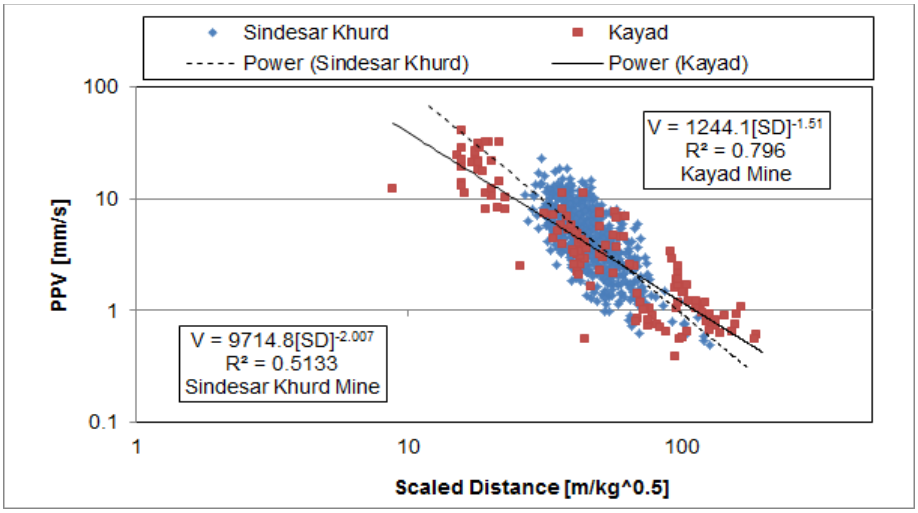

Figure 3. Propagation plot of vibration data with their respective scaled distances for Lead-Zinc mines of Sindesar Khurd and Kayad underground project.

OPTIMISATION OF BLAST DESIGN PARAMETERES

Kayad underground mine

Experimental blasts were conducted at Kayad underground mine with different blast design to optimise blast design parameters and to control ground vibration at lowest possible levels. The delay interval provided between all the holes were modified in view of the recorded magnitude of vibration in the village. The slot raise blasts commenced after sufficient development blasts were performed in north and south decline faces. The numbers of holes and deck charging were modified to get desired pull from the slot raise blast. The maximum pull of 2.7 m was recorded in a few blasts. Although the explosives loaded in slot holes were 1.9 to 2.2 kg. The number of blast holes varied between 3 and 14 depending upon the condition of blast holes. The total explosives in a blast round varied between 16 and 172 kg. The initial design of slot raise blasting is presented in Figure 4.

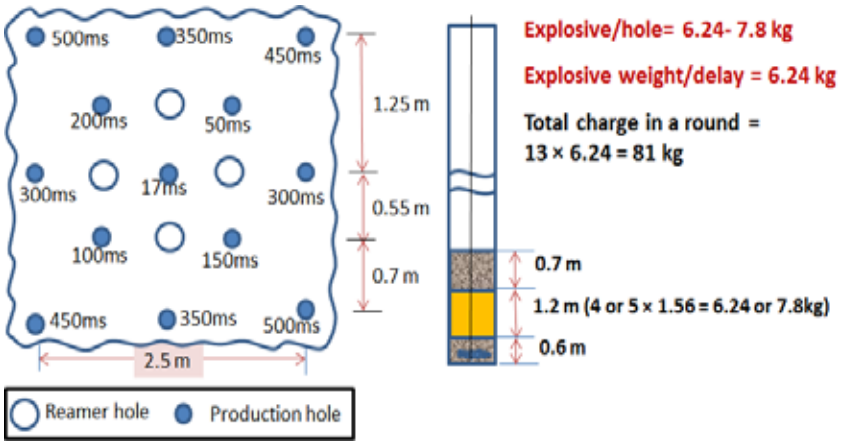

Figure 4. Initially recommended design for slot raise blast at Kayad underground mine.

The ring blasts were ultimately planned after sufficient opening of the stope by slot raise blasting. Initially, the ring blasting started with emulsion cartridge explosives of 150 kg distributed in 5 blast holes and were detonated keeping the explosive weight per delay of 25 kg. Subsequently, the blasts were optimized in successive trial blasts in order to improve productivity and also to maintain the vibration level within 15 mm/s. View of the blast holes and its connection with electronic delay detonators is presented in Figure 5. The number of blast holes detonated in case of ring blasting varied from 2 to 7. The total explosives detonated in a blasting round were in the range of 64 to 340 kg and explosives weight per delay was 10.92 - 17.16 kg. The layout of the seven blast holes is depicted in Figure 6. In this case a few blast holes were decked up to 4 places with the help of electronic delay detonators.

Figure 5. View of the blast holes and their connections with electronic delay detonators.

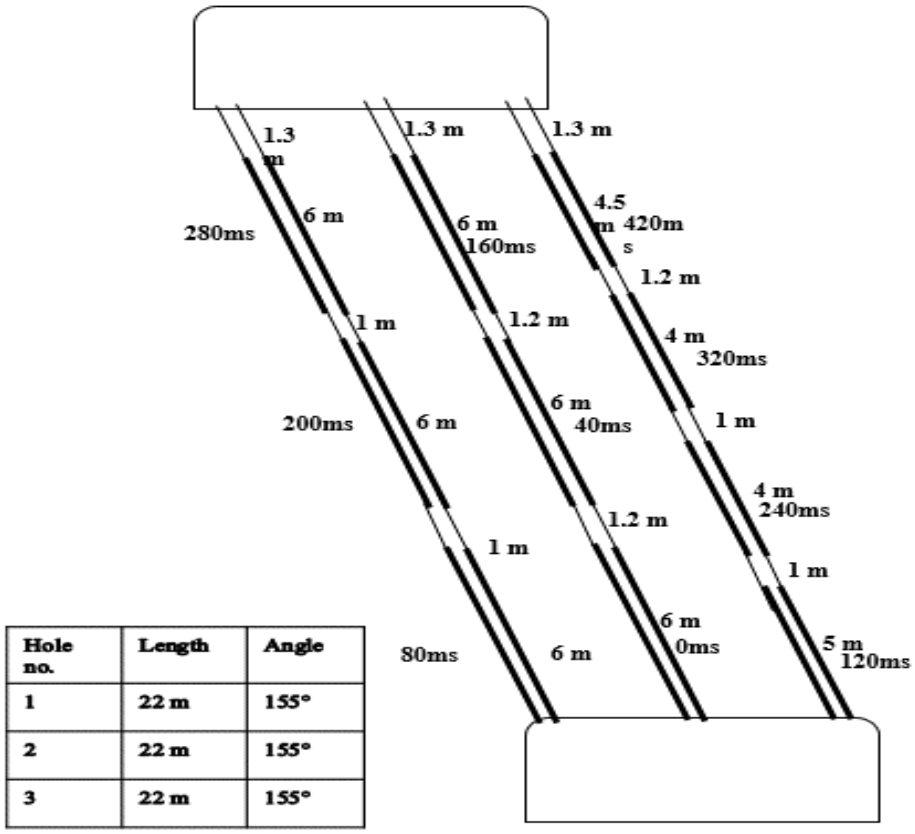

Hole no.	Length	Angle
1	22 m	155°
2	22 m	155°
3	22 m	155°

Figure 6. The typical layout of the three blast holes implemented at Kayad underground mine.

The main parameter involved in the blast vibration phenomena has been be summarized by Aldas & Bilgin 2002 and are; the explosive rock intraction, blast induced wave transmission property of a rock unit (i.e. waves traveling along specific layers), distance between blast location and mesurment point, geology of the propagation media such that fault bedding planes etc. and also the geology at the measurement point.

Blast waveform analyses were carried out to get the optimal interval between the blast holes and beween the exploives decks within the blast holes with the help of seed waveform and linear suprimposition of waves techniques. It has been found that the delay interval of 20 ms to 80 ms, the increase at an interval of 20 ms is found optimal in case of deck charging while the minimum delay of 40 ms to maximum of 80 ms is to be provided between the two successive blast holes. Figure 7 depicts the typical blast wave signature recorded at S1 stope blasting conducted at 325 mRL by optimised delay intervals between the blastholes and between the decks at Kayad village.

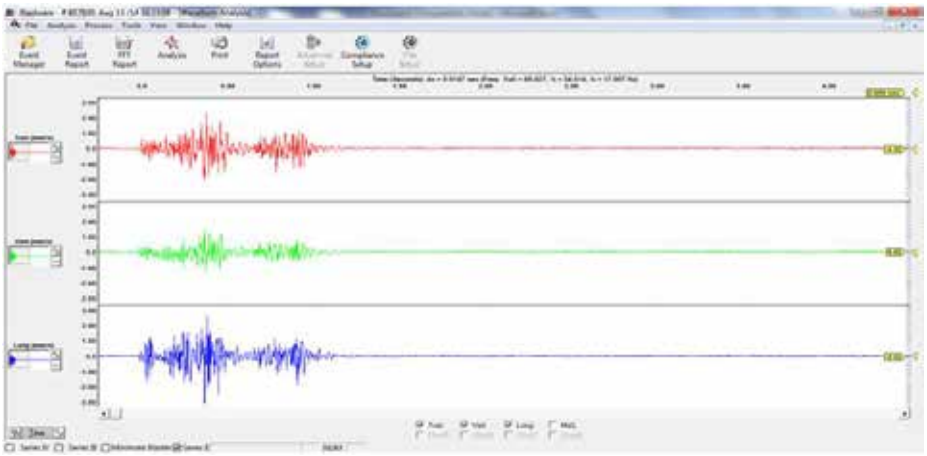

Figure 7. Blast wave signature recorded at Kayad village due to production blast at S1-325 mRL.

Furthermore, two methodologies were adopted for providing decks and its detonations. The first one is by detonating hole one by one i.e. from bottom deck to top deck at an interval of 20 ms up to 4 decks for all the blast holes and the second methodology by taking two explosives decks first (bottom slice) and latter on two explosives decks (top slice). The stem deck materials between the slices were withhold by using drill cutting material anchored to bolted wooden piece. This concept was used to eliminate the damage of the top deck explosives column due to detonation of bottom deck explosive column. These two methods of placement of decks were experimented in few blasts at Stope using electronic delay detonators and the results were encouraging in both the conditions but latter method showed much better results. These concepts have been presented in Figure 8. In a few blasts, sympathetic detonation was also one of the reasons of excessive blast vibration levels in the village. The sympathetic detonation was documented with the help of VOD signature of explosive traces at number of testing. Subsequently, the deck length was standardised which was in the range of 15-20 times of drill hole diameter. Thirty production blasts were conducted during the study period at 325 mRL, 350 mRL and at 375 m RL for different stope.

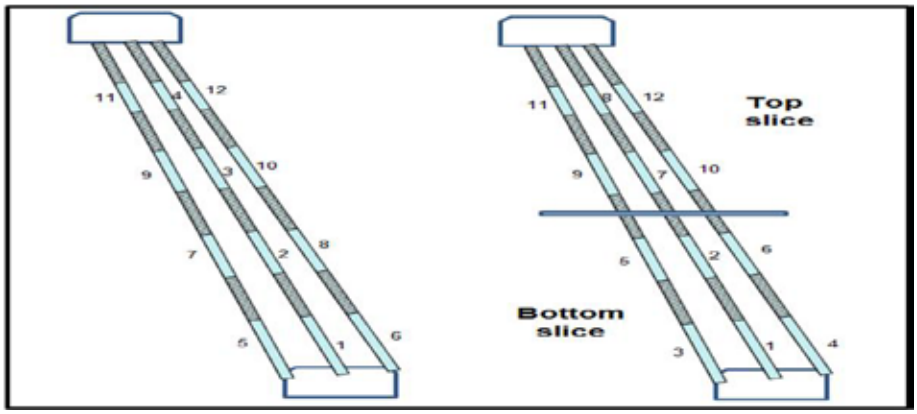

Figure 8. Detonation of the ring blast holes by detonating holes one by one and by taking bottom slice first and top slice afterwards.

The in-the-hole continuous velocity of detonation of emulsion explosives was also recorded for 4 holes of Ring (R-1) at 325mRL of S-1 Stope. Out of 4 holes 3 holes were deck charged. The amount of explosives detonated in 1st hole was 26 kg (15.6 kg + 10.5 kg) whereas in 2nd hole and 3rd hole it was 44 kg (15.6 kg + 10.5 kg + 10.5 kg+ 7.5 kg) and 41 kg (15.6 kg + 10.5 kg + 7.5 kg + 7.5 kg) respectively. The delay timing provided in 1st hole, 2nd hole and 3rd holes were 0/20ms, 40/60/100/120ms and

80/100/140/160ms. The recorded in-the-hole VOD of explosives of 1st hole and 2nd hole were in the range of 4846-5260 m/s and are presented in Figure 9 and Figure 10.

Figure 9. In-the-hole VOD trace of super power 80 cartridge emulsion explosive.

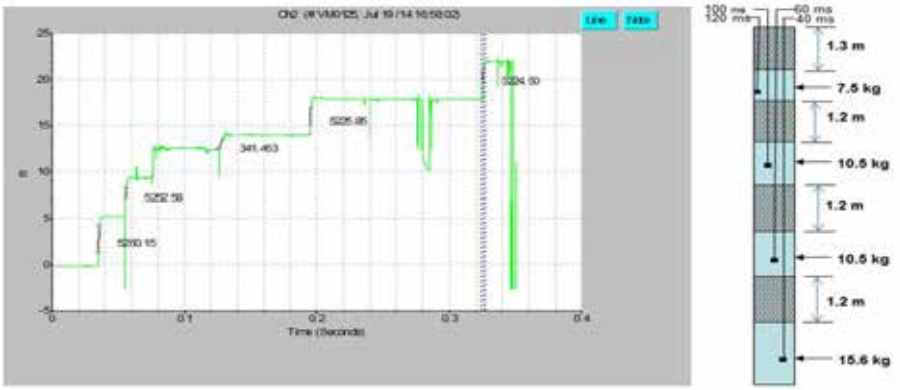

Figure 10. In-the-hole VOD trace of super power 80 cartridge emulsion explosive in deck charged holes.

Sindesar khurd mine

Based on the analysis of the recorded data due to implementation of various blast design parameters and recorded vibration data, it was recorded that whenever the scattering in nonel tubes were more than 10 % excessive vibration were recorded. Hence, nonel detonators having scattering percentage within 10% are only utilized in ring blasting. The delay intervals were selected in such a manner which will not overlap considering the scattering percentage of ±10%.

Two signature blasts (single hole blast) were conducted at 400mRL and 350mRL to optimise the delay interval between the holes and in the deck for reduction of vibration level in the village.

Signature blast analyses were carried out for the blast conducted at 350mRL-BH-5/HW/R-5 and at 400mRL- BH-5/FW/R-2. Figures 11 depict the blast wave signature recorded at Sindesar village due to signature blasts.

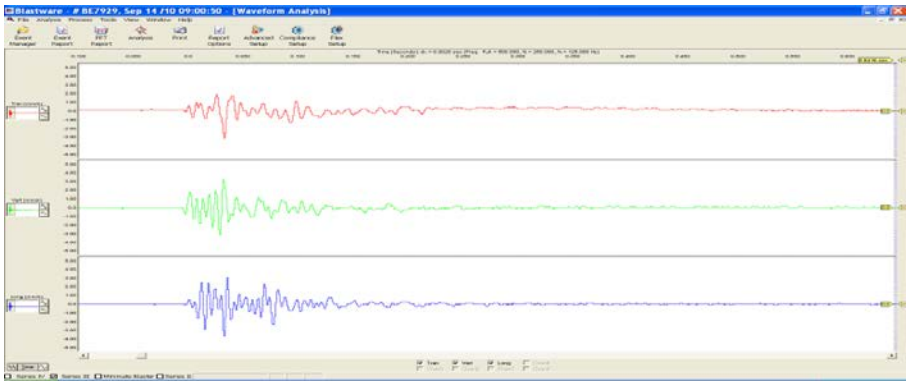

Figure 11. Blast wave signature recorded at Sindesar Khurd village due to the single hole blast conducted at 350mRL-BH-5/HW/R-5.

The implemented delay interval between the holes are 37ms and 56ms whereas the delay intervals between decks is 15ms for the blast conducted at 350mRL, whereas for the blast conducted at 400mRL, the delay interval between the holes are 29ms and 52ms whereas the delay interval between decks is 15ms.

A few blasts were taken with electronic delay detonators to eliminate the chances of scattering in delay timing in those blasts where explosives of more than550 kg were detonated in a blasting round. Additional sub level interval was also planned to be reduced in further stope to 25m from 50m. Blasthole diameter was also reduced from 102 mm & 89 mm from 115 mm in production rings in order to obviate excessive charge density in a particular hole.

In few blasts, sympathetic detonation was also one of the reasons of excessive blast vibration levels in the village (Figure 12 and 13). It has been verified with the help of VOD of explosives trace. Subsequently, the deck length was standardized which was in the range of 12-17D, where D is the hole diameter. In case of nonel, it is very difficult to maintain the delay interval of 17or 25ms between the decks in all the blast holes due to non-availability of suitable nonel detonators in the Indian market. Electronic detonators are being used in deck blasting to get desired fragmentation and obviate excessive generation of vibration.

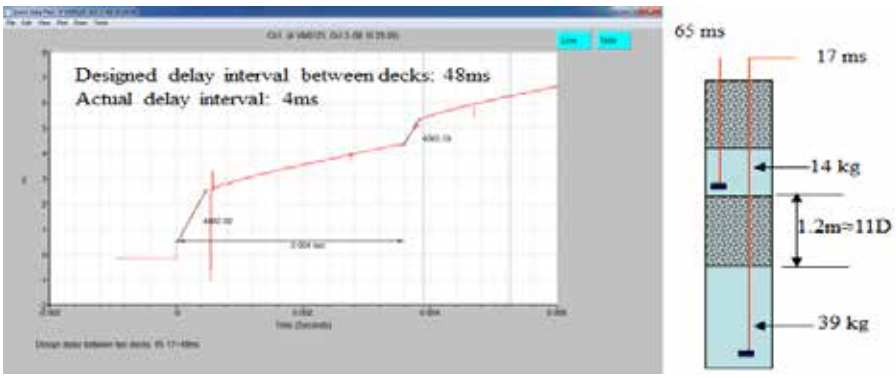

Figure 12. In-the-hole VOD trace showing sympathetic detonation of upper deck due to bottom deck blasting (Deck size=1.2m i.e.11D).

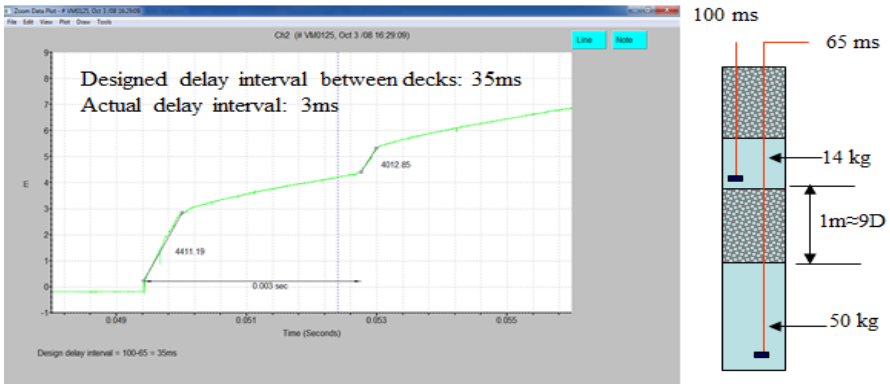

Figure 13. In-the-hole VOD trace showing sympathetic detonation of upper deck due to bottom deck blasting (Deck size=1.0m i.e. 9D).

In case of deck blasting, two methodologies were adopted, taking hole one by one (bottom deck & top deck fired with 15ms delay interval) or taking bottom slices first and then top slices. The deck materials between the holes were withheld by using plastic tag anchored to bolted rod. This concept was used to eliminate the damage of the top deck explosives column due to detonation of bottom explosive. These two ways placement of deck were experimented in few blasts at 350m-BH-5/FW/R-5, R-8 & R-9using electronic delay detonators and the results were encouraging in both the conditions but latter condition showed better results. Slot designs for the stopes are depicted in Figure 14. Figure 15 depicts the ring hole design for stopes of different levels.

Using this concept, the maximum explosives fired with electronic delay detonator was 642 kg and was detonated with the explosives weight per delay of 56 kg. The vibration data recorded in the village by detonation of these two blasts were lower in comparison to those recorded in earlier using the same quantity of explosives in nonel initiation system.

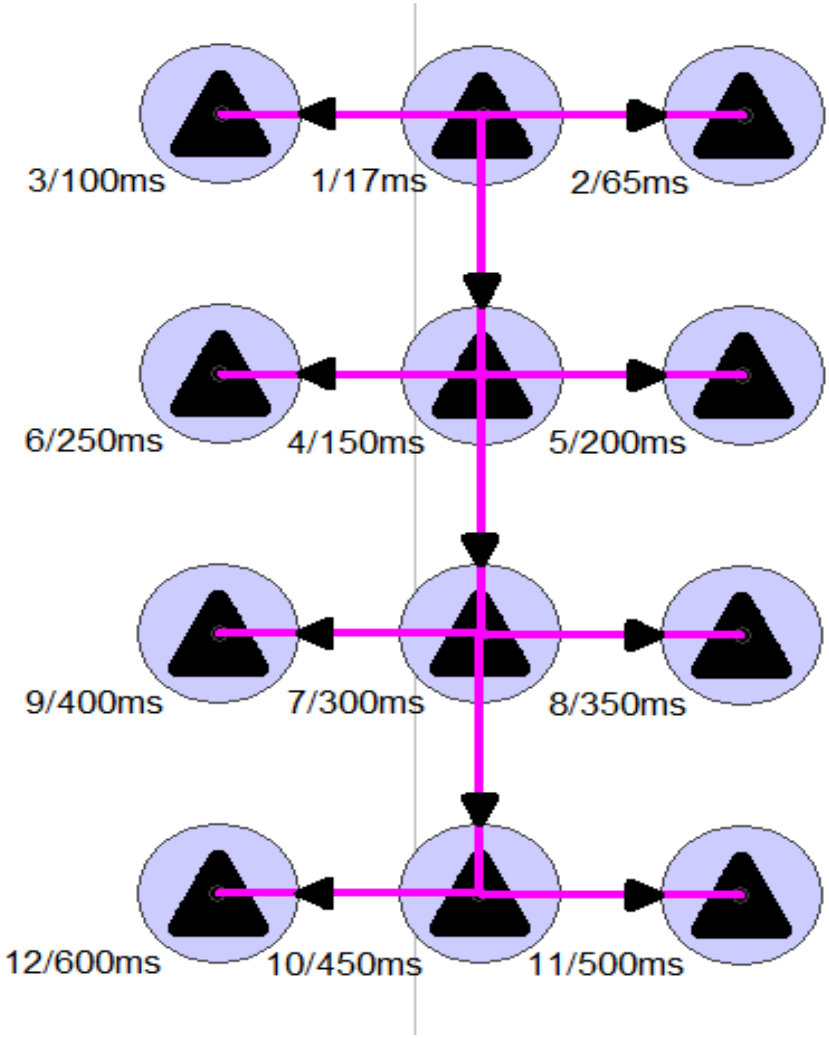

Delay No.	Explosives (kg)	Delay timings [ms]	Blast design parameters
1.	50	17ms	No. of holes: 12
2.	50	65ms	
3.	50	100ms	Hole diameter: 165 mm
4.	50	150ms	
5.	50	200ms	Explosives: Emulsion cartridge
6.	50	250ms	
7.	50	300ms	Total explosives to be used: 600 kg
8.	50	350ms	
9.	50	400ms	Maximum charge per delay: 50 kg
10.	50	450ms	
11.	50	500ms	Initiation system – Nonel delay detonator
12.	50	600ms	

Figure 14. Recommended Slot design for the stopes of different levels.

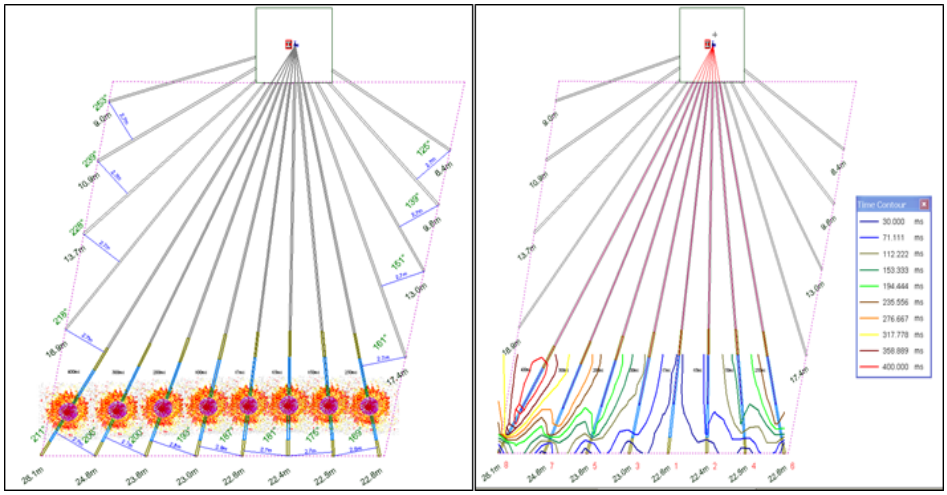

Length of the holes (m)	Explosives weight (kg)	Delay timings of Nonel detonator [ms]	Delay timings of electronic delay detonator [ms]	Blast design parameters
26.1	58.5	500ms	400ms	No. of holes: 8 No. of explosives deck: 8 Hole diameter: 115 mm Toe burden: 2.6 m Explosives: Emulsion cartridge Total Explosive to be used: 425 kg Maximum charge per delay: 58.5 kg Initiation system: Nonel delay detonators or Electronic delay detonators
24.8	55.5	400ms	300ms	
23.6	55.5	300ms	220ms	
23.0	50	200ms	140ms	
22.6	50	100ms	60ms	
22.4	50	17ms	0	
22.5	50	65ms	40ms	
22.8	55.5	150ms	100ms	

Figure 15. Recommended Ring design for the stopes of different levels.

Further blasts were conducted for two rings together (partially) with electronic delay detonators for distributed charge concentration and to increase the size of the blast to meet the targeted production of the mine, but it is always not feasible because of site constraints. Such types of seven blasts were conducted at R-8 & R-9 rings of BH-4, BH-5 and N-1Stopes at 400m RL (Table 6). The delay arrangements were set in both the rings in a way that the blast wave signatures of both the rings are not producing constructive impacts. Figure 17 depicts the recorded blastwave signature at village due to the blast conducted at 400mRL-BH-5/R-8& R-9 Ring which shows that the blast waves of both the rings are independently recorded.

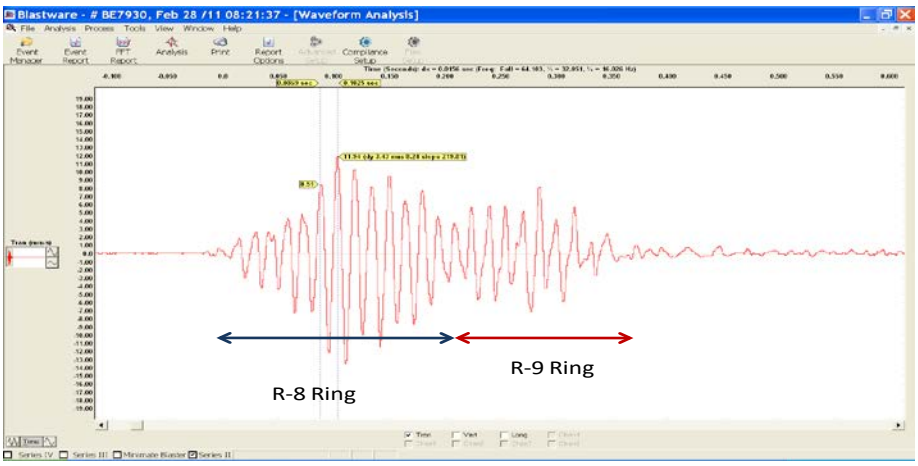

Figure 17. Blastwave signature recorded at village due to the blast conducted at 400mRL-BH-5/R-8& R-9 Ring.

Table 6. Details of blast design parameters and recorded PPV when two rings were blasted together at BH-5, BH-4 and N-1 400mRL and 350m RL.

Location of blast	Ring no.	Delay timing [ms]	Total explo-sives weight [kg]	Explosives weight/ delay [kg]	Recorded PPV range value [mm/s]
BH-5 stope Hang wall 400mRL	R-8 (6 holes)	0, 15, 30, 45, 60 & 75	604	50	4.88-6.24
	R-9 (9 holes)	90, 105, 120, 135, 150, 165, 180, 195 & 210			
BH-5 stope Hang wall 400mRL	R-8 (6 holes)	0, 15, 30, 45, 60 & 75	649	50	3.05-9.02
	R-9 (8 holes)	90, 105, 120, 135, 150, 165, 180 &195			
N-1 stope Hang wall 400mRL	R-8 (11 holes)	0, 15, 30, 45, 60, 75, 90, 105, 120, 135, 150,	698	50	6.65-9.71
	R-9 (9 holes)	165/180, 195 210, 225, 240, 255, 270, 285 &300			
BH-5 stope Foot wall 400mRL	R-8 (8 holes)	0, 15/105, 30, 45, 60/120, 135, 150 &165	716	50	4.6-9.8
	R-9 (5 holes)	210/270, 225, 240, 255 &285			
BH-5 stope Hang wall 400mRL	R-8 (5 holes)	0, 15/75, 30, 45 & 60	577	50	5.97-7.10
	R-9 (11 holes)	90/195, 105/210, 120, 135, 150, 165, 180/270, 225, 240, 255 &270			
BH-5 stope Foot wall 400mRL	R-8 (10 holes)	0/90, 15, 45, 60, 75, 105, 120, 135/180, 150 &165/195	708	50	3.22-10.4
	R-9 (7 holes)	210, 225, 240, 255, 270, 285 & 300			
BH-4 stope Foot wall 400mRL	R-8 (12 holes)	0, 15/165, 30, 45/150, 60, 75, 90, 105/135, 120, 180, 195, &210/225	736	56	5.7-10.1
	R-9 (6 holes)	270, 285, 300, 315, 330 & 345			

CONCLUSIONS

Kayad underground mine is successfully producing the minerals in close proximity to the inhabitant area by adopting state of the art blasting practices as discussed in the text. The blast vibration recorded in the village are well within the acceptable limits and there is no complain from the residents. The development face blast with delay intervals of 25 ms between the holes for 5 centre holes resulted into generation of lower levels of vibration. The use of delay intervals of 200 ms to 300 ms between two successive cut holes gave excellent blast results. It was also recorded that the electronic initiation system generated lower level of vibration than those produced by Nonel initiation system. The recorded reduction

in the vibration levels due to initiation of blast holes by electronic delay detonators was up to 12.5 % than those blast holes which were initiated with shock tube initiation system.

The delay interval between the holes of 40ms and 80ms at ring hole blasts and detonated with delay interval between decks of 20ms to 80 ms resulted into reduced levels of vibration. The recorded vibration data in the structures shows that there is reduction in the level of vibration as the height of the structures increases. The recorded vibration data are of the high frequency and caused reduction in the level of vibration in the structures. The concept of taking bottom slice first and then the top slice gave desired results. The results were very encouraging and recorded vibration data in the village and achieved fragmentation was acceptable by the villagers as well as by the mine management. Accordingly, blasts with 340 kg of emulsion explosives were performed and the recorded vibration levels in the village were below 8 mm/s. The concept of taking 4 explosives decks in a hole was successfully implemented and it was also confirmed by the VOD trace of the recorded data that all the decks were detonated independently.

Sindesar Khurd Mine is continuously working on blast design to keep vibration within acceptable limits in nearby village and to achieve optimum fragmentation.

The delay interval between the holes of 37ms and 56ms and detonation with delay interval between decks of 15ms for the blast conducted at 350mRL yielded excellent fragmentation and reduced level of vibration. The blast conducted at 400mRL with delay interval between the holes of 29ms and 52ms and detonated with delay interval between decks of 15ms also gave desired blast results. The delay intervals between the two rings were provided in such a manner that the higher depth rings should be blasted first.

The concept of taking two ring together and another technique of taking bottom slice first and then the top slice (after deck ore body) was very much beneficial. The results were very encouraging and recorded vibration data in the village and achieved fragmentation was acceptable. Big size blast of 792 kg was performed and the recorded vibration levels were below 10 mm/s. Further, it has been also planned to take blasts with 900 to 1100 kg in those stopes which are at far-off distances from the village.

ACKNOWLEDGEMENT

The authors express their gratitude to Director, CSIR-Central Institute of Mining and Fuel Research, Dhanbad, India for his encouragement and support during the field study. The authors are also thankful to the mine personnel of Kayad Mine and Sindesar Khurd Mine for providing necessary facilities during the course of this investigation. The opinions are those of the authors and not necessarily the organizations to whom they belong.

REFERENCE

Singh PK, Vogt W. Ground vibration: Prediction for safe and efficient blasting. *International Journal of ERZMETALL, GDMB publication*, Germany, 1998, 51(10): 677-684.

Little TN, Van Rooyen F. The Current State of the Art of Grade Control Blasting in the Eastern Goldfields, in *Proceedings of the Aus. IMM Explosives in Mining Workshop* 1988, pp 87-95 (The Australian Institute of Mining and Metallurgy: Melbourne).

Harries G, Beattie T. The Underwater Testing of Explosives and Blasting, *Explosives in mining Workshop* 1988, pp 9 (The Australian Institute of Mining and metallurgy: Melbourne).

Singh PK, Mohanty B, Roy MP. Low frequency vibrations produced by coal mine blasting and their impact on structures. *International Journal of Blasting and Fragmentation*, USA, 2008, 2(1): pp 71-89.

Singh PK, Roy MP. Damage to surface structures due to blast vibration. *International Journal of Rock Mechanics and Mining Sciences*, 2010, 47(6):949-961.

Mohanty B, Zwaan D, Malek F. Diagnostics of production blasts in a deep underground mine. *Engineering and Mining Journal*, 2013, 214(8): 52

Lal AK, Daripa M, Kumar A, Chittora V, Roy MP, Singh PK. Blast optimization at Sindesar Khurd underground mine to improve productivity with reduced level of vibration, in *Proceedings 10th International Symposium on Rock Fragmentation by Blasting 2012,* pp 231-240 New Delhi, India,

DGMS (Tech) S&T 1997. *Subject: Damage of the Structures due to Blast Induced Ground Vibration in the Mining Areas*. Circular No 7, pp 317-322.

DIN, 1999. *Structural Vibration – Effects of Vibration on Structures in Deutsche Norm*, 4150-3 pp-4.

CHALLENGES OF MINES RESCUE IN EXPANDING MINE OPERATIONS

J. K. Armstrong[1] and C. Feyerabend[2]

[1]*Dräger Safety Canada Limited*
2425 Skymark Ave.
Mississauga, Ontario L4W 4Y6, Canada

[2]*Dräger Safety AG & Co. KGaA*
Revalstrasse 1
23560 Lübeck, Germany

24th World Mining Congress
MINING IN A WORLD OF INNOVATION
October 18-21, 2016 • Rio de Janeiro /RJ • Brazil

CHALLENGES OF MINES RESCUE IN EXPANDING MINE OPERATIONS

ABSTRACT

As mines are constantly growing and expanding so do the challenges for emergency response teams. They have to keep up with the pace that is set by current and future production techniques.
Although mines have now reached depths of several kilometers and their dimensions and complexity are of an entire city, mines rescue still must be able to reach the most remote areas within the mine in a swift and safe manner. The duration of breathing apparatus and physical human capabilities are natural limitations. Therefore alternative methods have to be explored to extend the time under oxygen for mine rescue teams without putting additional stress on the team members. To address this global trend, Dräger, Goldcorp and Paus have partnered together to develop a mine rescue vehicle that allows mines rescue teams to travel for an extended period of time in a contaminated atmosphere without the use of their breathing apparatus, thus extending the range of their mission. By application of current available techniques the safe expansion of production in a mine can be ensured by giving mines rescue teams the capabilities to respond to accidents in a safer and faster way.

KEYWORDS

Mine Rescue, First Response, Mine Escape, Emergency Preparedness and Response, Deep Mining

INTRODUCTION

With the easily accessible resources getting fewer there is a global trend to search for higher ore grades underground and or continually expanding mines underground to extend the life time. While in some areas this trend has just begun in other countries the mines are reaching depths or horizontal dimensions that pose extreme challenges. (Codelco, 2016)
These include safety relevant topics, such as rock stability, heat and seismicity, but also more basic issues such as distances to the working face, which can become crucial considering the cost to develop a new shaft or decline. To overcome this, there is a is a growing interest in collaboration to drive the development and support of deeper mines and tackle the complexity of underground mining by collaboration between various stakeholders. This is evidenced by the fact that several industry and research groups and networks have formed, e.g. the I2mine project in Europe or the Ultra-Deep Mining Network by the Centre for Excellence in Mining Innovation in Canada. Due to commodity pricing and the trend towards renewable energy metal/non-metal mining will be the driving force behind this development.

MAIN TEXT

An emergency situation only amplifies the challenges as outlined above. Especially in the event of ventilation failure or a fire the increasing air temperature and levels of hazardous gases are major risks that need to be accounted for in any mine emergency plan.
One of the main restrictions to consider is the oxygen time of the closed-circuit breathing apparatus (CCBA) as currently used by mine rescue teams around the globe. Within this time the distance to the incident or location, the assigned task and the time back needs to be covered. With increasing depth or expansion, the distances to overcome become larger thus reducing the already limited operational time. Current state-of-the art are CCBAs are rated at 4hrs. While in theory longer duration sets would be possible

these would require more bulk and weight thus significantly increasing the strain on the team members. Already today the full duration of CCBA is rarely utilized due to several limiting factors.
A safety buffer is usually utilized in that the twice the time used on the ingoing trip should be allowed for returning to the fresh air base to allow for unforeseen events on the way back. (Wokplace Safety North, 2011) In addition several mine rescue organizations have imposed time restrictions for the usage of CCBA related to the hazards of heat stress. (Wokplace Safety North, 2014) Also in the event of reduced visibility through smoke the time required to overcome the distances will be increased by reducing the speed at which people or machinery can move.
The German regulations for escape distances with self-rescue devices derived from numerous tests and incidents may be used as an indicator to illustrate these effects. It shows that even in the event of using a light escape set the distances that can be covered are significantly decreased in higher temperatures, on inclines and declines and considering poor visibility. According to the tables the walking distances have to be reduced by up to 30-50% for each of these factors. Emphasis is put on the fact that if these conditions are combined with longer distances, individual assessment of distances will be necessary. (Bresser, Fuchs, Hermülheim, Langer, Ollesch, Junker, 2007) This certainly holds true for the use of much heavier equipment such as a CCBA-set and carrying full emergency gear.

All these factors combined can easily create scenarios where even with traditional motorized transport mine rescue teams are reaching the limits of covering the complete mine while still having sufficient time left to fulfill their mission in an efficient manner.

This outlines the need for 3 elements in future mine rescue scenarios for deeper and expanding mines:

1. Mine rescue teams need to get to an incident site faster
2. Emergency personnel needs to be protected along the way without having to utilize precious oxygen time of the CCBA in order to be well rested and have sufficient time buffer to fulfill the tasks at hand
3. Safe evacuation of team member and/or mine personnel and egress is a basic requirement however becomes increasingly more important and complex the longer the distance to cover.

To assist mines to tackle these tasks within the Mine Emergency Plan there currently already are a number of concepts available. Portable shelters may be moved along and provide refuge for the miners for a defined time, thus taking time pressure off the mine rescue team. Permanent rooms at strategic locations may serve as a collection point for workers which can help in shortening the period for allocation of missing personnel as well as serve as an extension of the fresh air base.
A concept to actually avoid lengthy mine rescue missions is an emergency plan utilizing equipment known as the First Response and Emergency Escape Kit (FREEK). In this scenario especially trained personnel in the mine can access a FREEK station equipped with self-contained breathing apparatus and turnout gear to swiftly fight a smaller fire before it can turn into a bigger incident. In case this cannot achieved the team can pull back to the FREEK station, top off the SCBA cylinders and start the evacuation to a point of safety.
However these solutions have their limitations in that they do not help the mine rescue team get to the incident once a situation requires the immediate response by the team.

For this reason the Canadian mining company Goldcorp explored the options to overcome the hazard scenarios out of their own risk assessment for its deep mining operations. Even with a comparatively modest depth of 1.2 kilometers with a horizontal expansion of 12 kilometers from the ramp access at the mine operation Musselwhite in Canada the time needed to reach the remotest point in the mine with good visibility would have already accounted for 45 minutes. In a traditional vehicle the CCBA would have to be donned and considering the time back only little time would have been left until the time to return. Considering the heat stress limitation as above and poor visibility, basically no further expansion would be possible.

To address this scenario a concept was developed in which an encapsulated vehicle would be used in order to reach a scene without utilizing the CCBA of the rescue team with capabilities to drive in

poor visibility, toxic gas and being rugged enough to survive the mining environment. Together with PAUS, a mining vehicle manufacturer and Dräger, a leading supplier of medical and safety technology this concept was refined and put into reality in the development of the MRV 9000 mine rescue vehicle which has since been subject to evaluation testing under realistic conditions at the Mine Emergency Response Drill of the American Mine Safety and Health Administration (MSHA) in Missouri. (Heuer, 2016)

To suit the requirements of the mine rescue teams a vehicle chassis was chosen that fit the demands regarding size, ruggedness, load capability and climbing power to carry out missions in critical situations with difficult ground conditions. The vehicle was combined with a cassette for transporting rescue personnel and possible patients or persons to be evacuated. Including the drivers cabin it provides space for 6 persons from the rescue staff and two patients, with the possibility to place an additional patient on a stretcher in the cassette. Both the cabin and the cassette are equipped with an air purging system that is independent from the ambient air. The system allows the mine rescue team to access the incident site without using their CCBA set, carrying out their mission and then reentering the vehicle and again purging the vehicle from hazardous substances to egress the mine without the need to use the breathing apparatus. The breathing air system of the vehicle is designed for a mission scenario with an operating time of five hours with a recharge and turnaround time of 45 minutes to be ready for the next mission. Additional monitoring systems, such as gas monitoring and thermal imaging systems can be deployed to allow better assessment of the ventilation of the surrounding atmosphere as well as ensuring maneuverability in situations with low visibility. Also an air conditioning system is integrated to help reduce the heat stress. With these elements the vehicle addresses all three elements as outlined above, getting the rescue personnel to the incident swift, safely and rested to maximize the utilization of the breathing apparatus for the actual task and enabling egress and evacuation of personnel from remote locations in a protected manner.

Of course there are limitations to the use of the concept. It might be necessary to be adapted to specifics of the mine where possible, especially height and size requirements need to be considered to ensure a wide operational coverage, sufficient oxygen is necessary for the use of the combustion engine and it is limited to non-coal mines due to restrictions in the ex-protection. Also the proper integration into the emergency plan and training of all involved staff is a crucial element to make the whole concept work in an actual incident.

CONCLUSIONS

The paper shows that deep and expanding mines pose extreme challenges for mine rescue teams and thus can limit the safe operation of a mine due to the limits of existing emergency plans. However, through close cooperation of various stakeholders utilizing various sources of expertise from mine operators, suppliers and other institutions tools can be developed that give mine operators options they can pick from to create a coherent safety concept to answer the individual challenges of their mine operation.

REFERENCES

Bresser, G., Fuchs, E., Hermülheim, W., Langer, G., Ollesch, E.,& Junker, M. (2007). *Handbuch für das Grubenrettungswesen im Steinkohlenbergbau.* Essen, Germany: VGE Verlag GmbH.

Codelco (2016) *División El Teniente.* Retrieved from Codelco website https://www.codelco.com/elteniente.

Heuer, S. (2016). Underground Pit Stop. *Mining Report Glückauf, 152(2), 100-104.*

Workplace Safety North (2011). *Handbook of Training in Mine Rescue and Recovery Operations* (2011 ed.). North Bay, ON: Author.

Workplace Safety North (2014). *Mine Rescue Heat Stress Report. Ontario.* Retrieved from Workplace Safety North website: https://www.workplacesafetynorth.ca/sites/default/files/resources/Mine_Rescue_Heat_Stress_Report_2014.pdf.

CHARACTERIZATION OF THE CEMENTED BACKFILL FOR AGUILAR MINE

*M. A. Zeni and A. Zingano
FEDERAL UNIVERSITY OF RIO GRANDE DO SUL
Av. Paulo Gama, 110
Porto Alegre – Rio Grande do Sul, Brazil
*(*Corresponding author: marilia.a.zeni@gmail.com)*

24th World Mining Congress
MINING IN A WORLD OF INNOVATION
October 18-21, 2016 • Rio de Janeiro /RJ • Brazil

CHARACTERIZATION OF THE CEMENTED BACKFILL FOR AGUILAR MINE

ABSTRACT

Maximum extraction of an orebody is becoming crucial to make mining projects viable due to the continuous reduction of mineral resources, and the high cost involved in the construction of a mining structure. Therefore, in addition to the choice of the mining method, it is valuable to use additional recovery methods, such as pillar recovery. The aim of this study is to define a methodology to characterize the backfilling (cemented backfill) used in empty chambers that allows the subsequent recovery of adjacent pillars. The characterization of the backfill consists in determining its compressive strength required to a fill to resist the stresses involved in the pillar recovery process, as well as developing an optimal grain-size distribution for the aggregates, and finding the cement-water ratio needed to reach the desired strength. The methodology developed to obtain the new characterization is comprised of several steps which include field work and laboratory tests. Firstly, the cement content parameters and the grain size of the aggregates (already used at the filling manufacturing plant), as well as their corresponding strength, were obtained through analyses in the field work. Then, theoretical calculations of the cement content and optimal granulometric distribution were done based on the uniaxial compressive strength that has been found to resist the geomechanical requests from the bedrock. Then later, this theoretical characterization was tested using backfill specimens, followed by execution of compression tests. During the first stage of this methodology, it has been found a high proportion of clay particle size in the aggregates, which were affecting the strength results obtained from the characterization initially used. From this point, we decided to build the optimal granulometric curve without this fraction. The uniaxial compressive strength calculated as 2.69 MPa was obtained from the long-term planning that determines the full recovery of the existing pillars in the mine. Thus, the entire area to be mined was considered as a single block. Finally, the cement content has been found out as 4% by weight, which together with the optimal grain size results is able to achieve the expected strength values. In order to effectively fulfill the mine's production planning over the next years of its lifespan, the fill should ensure the mine local geomechanical stability at open stopes level, with vertical walls of stable backfill, and also global stability at the contacts between levels and access stopes. This will only be accomplished if the new characterization method is correctly applied.

KEYWORDS

Backfill, pillar recovery, grain-size distribution, uniaxial compressive strength

INTRODUCTION

Several underground mining methods make use of temporary or permanent pillars as part of the mine support. Among them are the room and pillars methods, longhole, and sublevel stoping (Society for Mining, Metallurgy, and Exploration, Inc. [SME] 2011). The usage of pillars in these methods aims to control the movements in the host rock within the region of influence of the mine.

A good pillar design must take a minimum size to reduce the amount of ore left behind on the pillars while complying with the safety requirements established in the project, and it must also consider other factors like, the strength properties and geological structures of the rock mass.

However, when the economic value of the ore left on the pillars is high (due its market price, its tonnage, or its mineral content, or when the mining yield from the orebody is low compared to its potential, due to its low self-sustainability), change the mining method and/or pillar recovery must be considered in order to recover the resources of the deposit, but the compromising safety requirements still taken into account. The backfilling is an artificial support method, which it will allow to recover the natural support structures left behind that it is got economic available ore content. Also, filling methods are applied when the host rock is soft or weak, and don't have self-support for long term.

Among the artificial support methods to maximize the orebody recovery, the backfilling method must be highlighted. It consists of filling with waste material the empty space caused by the excavations where it has been mined. Generally this waste material comes from the mine itself or from nearby areas. The backfill can act superficially, locally or in the whole mine structure, and it depends on the mining methods, type of rock mass deformation, and the mechanical properties of its composition (Brady e Brown, 2005).

The aim of this study is to make a new characterization of the cemented backfill be used in the stopes of a polymetallic mine, thus allowing the subsequent recovery of adjacent pillars, in order to comply with the safety, operational, and financial requirements.

This work was developed in Aguilar mine, which belongs to Glencore International AG, which extracts and produces zinc, lead and silver in the province of Jujuy – Argentina. The Aguilar mine operates with a mining method known as Transverse Stoping. The stopes were designed to have adjacent pillars, and it is mined according to the demand (considering its content and tonnage), and also observing the geomechanical criteria for sequencing, thus avoiding the risk of collapses.

The Aguilar underground mine is currently composed of two distinct sections: a section called "*Capa A*" which has three sectors named as 15, 18 and Sub-18, and another section called "*Pique Inferior*". The section that is targeted in this study is Capa A.

The total monthly production from Capa A is approximately 5,900 m³ of ore, while the monthly production of cemented backfill for Capa A is approximately 5,500 m³. It makes clear that this mine produces more empty spaces than it can fill, leaving a large portion of empty chambers in this section, which in the long term has caused large landslides and sectors in unstable conditions.

The backfill plant of Capa A section (Betonmac S.A.) was built in 2012, and its production capacity is 220 m³/day (considering two shifts of ten hours each). It has automatic or manual operation and requires three workers in the plant and two workers in the control of aggregates.

The process of backfill production starts by sieving the aggregates, where two grids are fed with waste from one of the mine dumps, selecting the fraction between 1½" and 3½" to be used on the backfill plant. Then, the sorted material is transported through the mine's shaft for about 300 m underground to the backfill plant, which is located at level 13 in the Capa A section. The material is then sent by conveyor to the mixing drum, where an automatic balance controls the amount of material to be added for each batch.

At the same time, bags are filled up with 1,000 kg of cement from two bins located at the surface, and then they are transported by trolleys to the Capa A's entry (equivalent to level zero). From there, a loader carries the cement bags to level 13 where the backfill plant is placed. The loader is able to carry three bags in each cycle. On the level 13, there is a small stock of cement bags. A hoist moves the bags to a smaller bin, which has a pipeline to the balance that adds the exact amount of cement to the mixture. In addition to cement and aggregates, water is added in a certain proportion, and after approximately 1.5 min inside the drum, the backfill is ready to use. It is then poured through the transport shaft to lower levels.

EXPERIMENTAL

The methodology for the backfill characterization used in Aguilar mine takes into account field survey and subsequent analysis of the laboratory tests. First, the dosage of water and cement used in the backfill was identified by visiting the backfill plant, questioning the personnel in charge of the plant, and monitoring the production process. Afterwards, aggregates used for the backfill production were collected on different days and used to obtain the granulometric curve.

The aggregates sampling was done in five random days, from August to October 2015, taking the samples directly from the conveyor belt. Then, a granulometric analysis was performed by sieving the sampled material, using the following mesh sizes: 88.90 mm, 50.80 mm, 12.70 mm, 6.35 mm, 4.76 mm, 0.60 mm. The mesh sizes were chosen based on the sieves available in the laboratory. All sorted material was weighed on an analytical balance, and based on these values, the grain-size distribution curves were plotted for each sample. To determine the clay content in the aggregates, four samples were submitted to the laboratory of chemical analysis where the clay fraction was separated with a #200 sieve (0.074 mm), following the Argentine standards of geotechnical studies (CIRSOC 401, 2006).

The backfill specimens used in the compression tests were made at the mine during the filling operation of the stopes. The material was sampled directly from the loader's bucket before being disposed into the chamber. Then, four specimens were prepared, and they were tested after 7, 14, 21, and 28 days. The mean for the compression tests results was taken for each curing time, i.e., the average strength for 7, 14, 21, and 28 days. In addition, the information previously collected in the field allowed to observe the causes for the results obtained in the laboratory.

The uniaxial compressive strength required for the section Capa A was calculated using the Mitchell's stability method (Mitchell, 1983), through Equation 1.

$$UCS = (F * B * \gamma_b) / (1 + B/H) \quad (1)$$

where *UCS* is the uniaxial compressive strength, *F* is the safety factor, γ_b is the bulk density of the aggregates, *B* is the block width, and *H* is the block height. We consider the whole section as a single block because the pillar recovery project goes through the entire Capa A section, i. e., at the end of the mine, the whole section will be backfilled. The dimensions of this section were obtained using the AutoCAD software.

In order to obtain the optimal granulometric curve for the backfill in the Capa A section, a field investigation was first performed to determine the maximum particle size present in the aggregates. This information was compared with the granulometric tests made in the first stage of the research. From this data, the granulometric curve was constructed using the Equation 2 (Potvin et al., 2005).

$$P = 100\ (d/d_{max})^{0.5} \quad (2)$$

where *d* is the particle size in mm, d_{max} is the maximum particle size also in mm, and *P* is the percentage of aggregates smaller than *d*.

The particle size values used for the calculation were the same as the sieves' opening sizes used in the granulometric tests in the first stage, in order to be able to later perform the same granulometric test, and confirm the granulometric curve.

The cement content was determined using the Equation 3 (Canadian Rockburst Research Program, CRRP, 1995).

$$UCS = 27\ (c/n)^{1.57} \quad (3)$$

where *UCS* is the unconfined compressive strength, *c* is the cement content, and *n* is the porosity of the aggregates, obtained from Potvin et al. (2005).

The last research stage was to confirm in laboratory if the new theoretically calculated characteristics of the backfill would meet the calculated values for compression strength. For this step, aggregates were collected from the backfill plant and sorted according to the mesh sizes of 88.90 mm, 50.80 mm, 12.70 mm, 6.35 mm, 4.76 mm, 0.60 mm. To these, another sieve of 74µm (# 200) was added in order to remove the clay fraction from the aggregates.

The decision to remove the clay fraction was taken after a visual inspection of the aggregates, since this fraction could be affecting the quality of the backfill, and consequently, its strength. Having the aggregates sorted out and the optimal granulometric curve ready, 40 backfill specimens were prepared according to ASTM C 31/C 31M Standard (*Standard Practice for Making and Curing Concrete Test Specimens in the Field*). The specimens have 30 cm in height and 15 cm in diameter.

After reaching the predefined curing time, the specimens received a header (a graphite-sulfur mixture was melted and poured into a mold where the specimens were positioned). This header was necessary to provide a flat and parallel base for the cylinders. After about two minutes, the header was solidified and the specimens were ready for testing. The compression test was carried out in a hydraulic press (Cosacon) of 100 kN capacity, without load control. The maximum applied force (when the specimen breaks) was showed in an analog gauge and registered in a spreadsheet. Figure 1 shows a specimen inside the hydraulic press ready for the compression test.

RESULTS

In the field work, it has been identified that the cement content in the backfill is 5% and that the water/cement ratio currently applied is 1:1. Both the amount of cement and the amount of water are quite reasonable and commonly used in other mines, according to Potvin et al. (2005). Although the water/cement ratio is not that the theory recommends, it should be 0.8:1. It is not an inconvenience, since this ratio is commonly used, achieving reasonable strength values.

Figure 1 - Backfill specimen ready for testing in the hydraulic press

After sieving and weighing the sampled aggregates at the backfill plant, the granulometric curves were plotted (Figure 2). It can be noticed that a greater variability in the grain size occurs in the portion smaller than 50 mm, although some of the curves do not show this trend.

Afterwards, a visual inspection on the aggregate material indicated that it could has a large clay content. So it was decided to test the clay content in the samples, resulting in an average of clay content of 1.82% by weight, which is fairly representative, taking into account that the cement amount in the backfill is low. The clay present in the aggregates prevents the formation of the cement film that joins the particles, which reduces the backfill strength (Potvin et al., 2005). Therefore, the clay content must be removed from the aggregate material by washing process the aggregate.

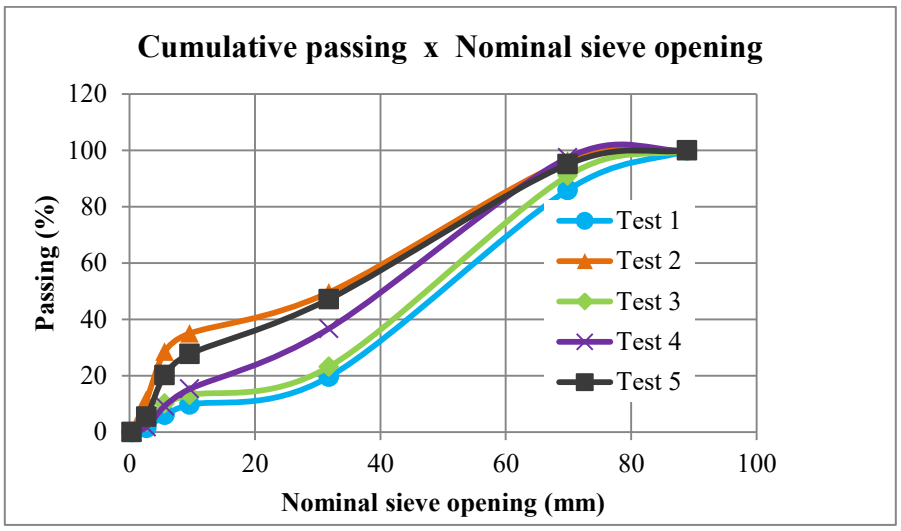

Figure 2 - Granulometric curves for the aggregates utilized in the backfill

A total of 92 backfill specimens, containing 5% of cement, water/cement ratio of 1:1, and variable granulometry according to the curves showed in Figure 2, were prepared and tested between May and September 2015. The average strength results for different curing times are shown in Table 1.

Table 1 - Average results of compression tests for different curing times

	7 days	14 days	21 days	28 days
Average strength (MPa)	1.42	1.36	1.60	1.85

The average strength results are not so low, but due to the high variability in the particle sizes, several specimens broke even before they were tested, which represents a low-quality fill. The variance for the 28 days of curing time is 8.74, confirming the high variability of the results, since a standard deviation of 2.96 is a large spread in the strength results, as well as the coefficient of variation (160%) also demonstrates the high heterogeneity of the results at 28 days.

Figure 3 shows the scatter plot of compressive strength against curing time, for all specimens. 20 out of 92 specimens could not be tested because they broke after demolding or during transportation.

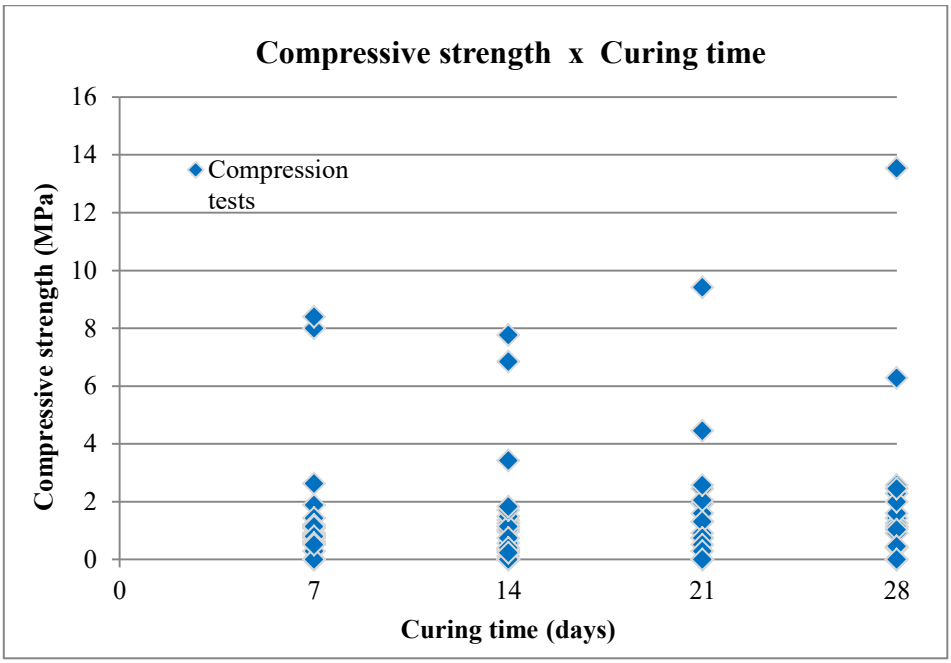

Figure 3 – Scatter plot of the compressive strength against curing time

The required strength for the backfill was calculated using the following parameters: block width, B = 330 m; block height, H = 220 m; bulk density, γ_b = 1.6 t/m³; safety factor, F = 1.3. The bulk density was provided by the company and the safety factor is the usual value adopted in the project. Using these parameters in the Equation 1, the required compressive strength is 274.56 t/m² or 2.69 MPa. This result indicates that the backfill characterization needs improvements since the strength for the backfill currently produced is 1.85 MPa. This is a significant difference, and this material probably would not provide the stability required for operation.

The optimal granulometry for the backfill aggregates produced in Aguilar mine is presented in Table 2, and the respective optimal size distribution curve is shown in Figure 4.

Table 2 - Optimal granulometry for the backfill aggregates

Opening size (mm)		Nominal size	Passing
mesh (–)	mesh (+)	(mm)	(%)
-	88.90	88.90	100.0
88.90	50.80	69.85	75.6
50.80	12.70	31.75	37.8
12.70	6.35	9.53	26.7
6.35	4.76	5.56	23.1
4.76	0.60	2.68	8.2
0.60	0.074	0.33	2.9

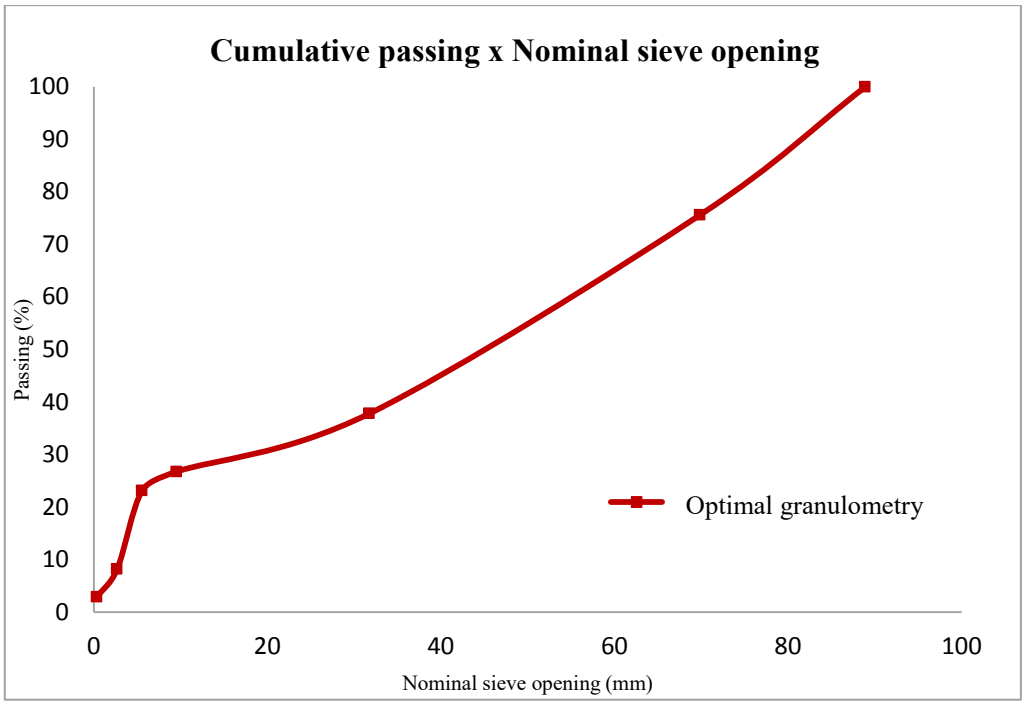

Figure 4 - Optimal granulometric curve for the backfill aggregates

Comparing the granulometric curves obtained in the first stage of this study (Figure 2) and the optimal granulometric curve (Figure 4), it is clear that besides the aggregate not having a constant size distribution, they are also not close to the optimal curve theoretically determined.

Using the Equation 3, and considering a porosity n = 0.22, the cement content required to reach the compressive strength of 2.69 MPa is 4% by weight. At the same time, the clay material size was washed from aggregate.

Finally, 40 specimens were made with the new characterization, and the average results for the compression tests are presented in Table 3. For the samples with 28 days, the results' variance is 0.06, which represents a great uniformity in the strength values, which is also reflected by the standard deviation (0.25) and in the coefficient of variation (9.19%). Therefore, the strength and granulometry obtained using 4% of cement content are quite satisfactory.

Table 3 - Average results for the compression tests for different curing times

	7 days	14 days	21 days	28 days
Average strength (MPa)	1.03	1.50	2.24	2.72

Figure 5 shows the scatter plot of compressive strength against curing time for all specimens with the new characterization. A lower dispersion for each curing time is now evident, which could be expected due to the variance result.

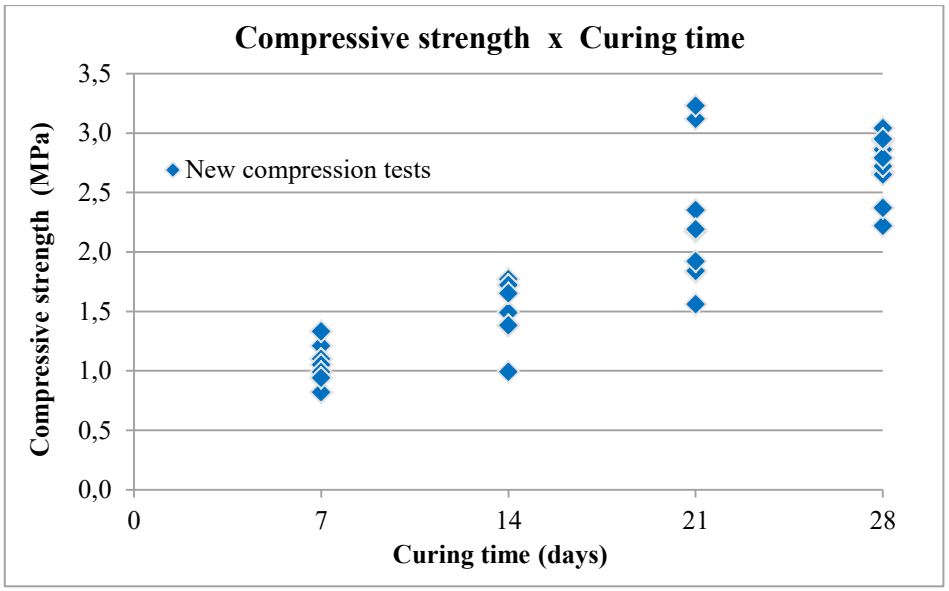

Figure 5 - Scatter plot of the compressive strength against curing time using the new characterization

CONCLUSIONS

It is evident that the current characterization of the backfill produced in Aguilar mine is not in accordance with the strength requirements. It occurs because there is no adequate granulometric control of the aggregates used in the backfill. The proportion of clay in the aggregates is quite high (1.82% on average), and even if the cement content is increased, this problem is not fixed. The only way to improve these results is primarily removing the clay fraction from the aggregates to allow the cement to properly adhere to them, and also controlling their size distribution to be as close as possible to the optimal granulometric curve.

The maximum strength of the backfill currently produced in Aguilar is 1.85 MPa (28 days of curing time and using 5% of cement content). Reducing the cement content to 4%, removing the clay fraction and controlling the grain size distribution according to the optimal granulometric curve, made possible to achieve 2.72 MPa of compressive strength, as verified in the compression tests with the backfill specimens.

As explained above, to make possible the recovery of all pillars, the minimum backfill strength should be 2.69 MPa, so the grain size control is urgent because the backfill currently produced do not comply with the geomechanical requests in the mine.

The methodology presented in this study was developed specially to improve the results obtained for the backfill, striving for geomechanical stability of the mine, which is closely related to the operational security, and also for the best use of the orebody. The same methodology should be applied when changing the room sizes and/or mine, doing a new determination of the required backfill strength.

This study will continue with the backfill implementation, and *in-situ* monitoring of the loads on the rock pillars, in order to measure the stress variation in the pillars during the filling and recovery operations. With this monitoring, it will be possible to simulate the pillars' behavior elsewhere in the mine, favoring the mine planning.

REFERENCES

Association for Testing Materials (2003). ASTM C 31/C 31M: *Standard Practice for Making and Curing Concrete Test Specimens in the Field*. Pennsylvania, USA.

Brady, B. H. G., & Brown, E. T (2005). *Rock Mechanics for Underground Mining*. (3rd ed.). USA: Springer Science.

Camiro Mining Division (1995). *Canadian Rockburst Research Program*. Mining Research Directorate, Canada.

Hamrin, H. (2001). Underground mining methods and applications. *Underground Mining Methods: Engineering Fundamentals and International Case Studies*. Society for Mining, Metallurgy and Exploration: Littleton, Colorado.

Mitchell, R. J. (1983). *Earth Structures Engineering*. (1st ed.). Winchester, USA: Allen Unwin Inc.

Potvin Y., Thomas E. & Fourie A. (2005). *Handbook on Mine Fill* (1st ed.). Australian Centre of Geomechanics, WA, Australia.

Quesnel, W. J. F., Deruiter, H., & Pervik, A. (1989). *The Assessment of Cemented Rock Fill for Regional and Local Support in a Rockburst Environment*. Proceedings of the 4th International Symposium on Mining with Backfill, Montreal, October 1989, pp.217-224.

Research Center of National Security Regulations for Civil Works CIRSOC 401 (2006). *Argentine Regulations Geotechnical Studies* (1st ed.). Argentina

Society for Mining, Metallurgy, and Exploration Inc. (2011). *SME Mining Engineering Handbook.* (3rd ed.). USA.

COAL DUST EXPLOSION CONTROL IN POLISH INDUSTRY

K.Cybulski
[1]*Assist. Prof. Ph.D.Eng, Central Mining Institute (GIG), Poland, 40-166 Katowice, Pl. Gwarkow 1, tel.: +48 323246603, +48 323246501, kcybulski@gig.eu*

24th World Mining Congress
MINING IN A WORLD OF INNOVATION
October 18-21, 2016 • Rio de Janeiro /RJ • Brazil

COAL DUST EXPLOSION CONTROL IN POLISH INDUSTRY

ABSTRACT

Coal dust explosions still remain one of the major hazard in Polish industry. In comparison with other hazards they occur rarely, but for that reason their actual hazardous impact is often underestimated. Coal dust explosions still result in catastrophic events that often carry with fatalities. Contrary to what is generally believed coal dust explosion hazard exists not only in mining industry but also in its other branches, e.g. power and cement plants, thermal power stations etc. In Polish industry coal dusts are the most common dusts that pose explosion hazard.
In the paper methods of evaluation and control of coal dust explosion hazard are describe, separately in coal mining and other branches of the industry. The evaluation consists in an assessment of ignition and explosion parameters that defines ignition susceptibility of a dust cloud and consequences of a potential explosion. They form the basis of explosion risk assessment.
After a short description of ignition indices and explosion parameters defined in international standards the paper reviews explosive properties of Polish coal dusts formed both from hard and brown coals. Then the apparatus designed to assess the parameters is described, starting from small, laboratory scale through an intermediate, semi-industrial scale up to the large scale directly related to industrial conditions.
In European low, the Directive 94/9/EC, the approach to explosion control is summarized in so-called *principles of integrated explosion safety*:

- above all, if possible, prevent the formation of explosive atmospheres,
- where explosive atmospheres may still appear, prevent its ignition,
- should an explosion nevertheless may occur, halt it immediately and/or limit the range of explosion flames and explosion pressures to a sufficient level of safety.

At Experimental Mine *Barbara* of Central Mining Institute the assessment of explosion and ignition parameters has been carried out for over half a century. Currently, the laboratory at EM *Barbara* has the equipment for the assessment of all parameters that characterize ignitibility and explosibility of industrial dusts, defined in European Standards. EM *Barbara* also has numerous large scale facilities, from 1 m^3 vessels, through 5 m^3 vessel up to 136 m^3 silo, surface experimental gallery and underground experimental entries.
Also included in the paper are examples of catastrophic coal dust explosions that occurred in the last years in Poland.
The paper also presents procedures aimed to mitigate underground coal dust explosions with the use of protection zones and barriers. According to Polish standards those procedures are obligatory in Polish mines.

KEYWORDS

Safety, dust explosion, industrial hazard,

INTRODUCTION

Dust hazards, i.e. the coal dust explosion hazard and the impact of dusts harmful to health are the basic hazards occurring in coal mining. The coal dust explosion hazard identification requires detailed data and the knowledge on the causes of such hazard both in the quantitative and qualitative aspects.

BASIC INFORMATION

Coal dust in quantities that enable a coal dust explosion is present in hard coal mines in virtually every heading. The hard coal mines dustiness is really high.

Adding the coal dust explosions to mine gases explosions significantly increases the threat and may affect the entire mine. The coal dust that may explode is the fine dust that passes through a 1 mm mesh.

Explosive coal dust is dust containing above 10% of volatiles (Vb), i.e. gases and vapors released from the coal in the process of devolatilization. The Vb value criterion became the basis for dividing the coal beds according to the hazard level. According to valid mining rules and regulations, coal dust explosion hazard exists where coal in a coal bed features Vb > 12%.

In the case of coal beds not explosion-prone (Vb < 12%) no safety means against coal dust explosion are undertaken. Three conditions occurring simultaneously are necessary to initiate the coal dust explosion:

- The first one is the coal dust itself as the fuel of the explosion. In the underground mining conditions this fuel is the dangerous mining dust deposits within the heading area in which the coal dust content is at the edge of the detonating ability.
- The second factor is the aerodynamic factor, i.e. a certain phenomenon of dynamic character that generates a pressure wave. The wave propagation in the heading lifts up subsequent layers of settled dust and creates a combustible cloud of dust and air.
- The third factor is the ignition source; once occurred within the cloud area it is able to ignite it.

The coal dust explosion limits define the range where the coal dust scuffed up into the air creates an explosive mixture. The limits range from 45 to 1000 g/m3. The strongest explosions occur at 300 - 500 g/m3.

It is assumed that the minimum ignition temperature of a coal dust cloud in the case of Polish coals is 823 K (550°C). This refers to the temperature initiating the explosion of a scuffed up dust cloud. This threshold varies, depending on the coal type. It is worth to note that the threshold is rather low – lower than the selfignition temperature of methane. It is also worth mentioning that lowest detected minimum ignition temperature for Polish coals is 783 K (510°C). The higher the carbonification, the higher the temperature.

The coal dust explosion initiator is understood as a factor directly triggering the explosion. To make the dust explosion possible the dust must be scuffed up into the air and form a cloud. If the cloud with concentration within the explosion limits will be affected by a thermal factor of appropriate, high temperature, the coal dust will explode.

Basic factors having impact on the coal dust explosion propagation are the coal dust explosiveness, the coal dust volatility content, the coal dust granularity, the coal dust explosion limit, the ignition source, dispersion conditions, dustiness degree and distribution of the coal dust within the heading, presence of methane in the air, the dimensions and location of the heading.

Basic parameters of the coal dust explosion:

- Explosiveness threshold: 50 to 1000 g/m^3,
- Strongest explosions at concentrations: 300 to 500 g/m^3,
- Minimum ignition temperature of the primary cloud: 500 to 600 ^{0}C,
- The explosion flame temperature: 1000 to 1200 ^{0}C,
- Minimal oxygen concentration in the air: from 16.5 %,
- Minimum ignition energy of coal dust: 200 to 3000 mJ,
- The explosion flame velocity: 30 to 200 m/s – weak explosions,
  200 to 700 m/s – medium explosions,
  700 to 1000 m/s – strong explosions,
  > 1000 m/s – violent explosions.
- Pressure rise in heading: 1 bar (3 to 5 bars),
- CO content in the atmosphere: from 3 % (over 10 %).

Factors that are the most frequent ignition sources of the coal dust explosion are explosions of methane, sparking of rocks, explosives, detonating fuse, firing a few fuses at the same time, electric arc, open source of light, explosions of fire gases.

Specification of the coal dust explosion consequences:

- Explosion fire: burning of people, fires, generation of huge amounts of CO;
- Explosion blast victims suffering from impact and pressure, falling of heading roof, devastation of roof supports, damage of machinery and heading equipment.
-

An example of gas composition in a testing gallery 1 sec after explosion:

- O_2 - 1.0 % (min 0.1 %),
- CO_2 - 9.5 % (max 15 %),
- CO - 9.0 % (max 10.8 %),
- H_2 - 5.5 %,
- CH_4 - 2.4 %.
-

Defense lines against coal dust explosion.

The first line of defense is based on the rule: no coal dust - no coal dust explosion threat. All attempts within this formula aim at limiting coal dust development and in case of its occurrence at removing it or disabling its ability to be dispersed.

The second line of defense is based on elimination of ignition sources of the explosion by:

- Control of the thermal factors (ignition sources) able to ignite the coal dust and initiate the explosion,
- Making the dust slow-burning.

The third line of defense is a mitigation of coal dust explosion development.

In order to prevent the coal dust explosion propagation, stone dusting and water sprinkling actions are undertaken. The zones of the headings where the dusting and sprinkling is done, the size of which is specified in the mining rules and regulations, are called safeguard zones. The quality of these safeguard zones decides whether the explosion sequence will be limited or even impossible to occur.

According to the rules valid in Poland the mining dust is considered safe as long as it contains:

- At least 70% of non-flammable solid parts in non-methane zones,
- At least 80% of non-flammable solid parts in methane zones,
- Fading water disabling the dust transport and disabling its dispersibility.

Unfortunately sometimes happens that it is either very difficult or even impossible in the mining conditions to maintain the appropriate, determined by rules and regulations, content of non-flammable particles or water within the entire safeguard zone. In some cases these regulations are simply neglected. The last line of defense are the stone dust barriers built in order to limit the explosion range, i.e. slow it down and thus reduce the range of the disaster.

Four basic lines of defense against the coal dust explosion, integrated into a system assuring the safety of the miners at work, are based on the following actions:

- Limiting the possibility of coal dust development, its removal and control of its dispersibility to prevent the development of a combustible mixture,
- Control of the explosion initiation by limiting the possibility of ignition sources able to ignite the primary cloud,

- Mitigation of the development of the coal dust explosion,
- Limiting the range of the explosion.

The basic rule within the system is to implement the next line of defense in case the previous one failed. The basic lines of defense are supplemented by supportive ones:

- Monitoring the coal dust explosion hazard,
- Rules and regulations concerning the issue of the hazard control,
- R&D studies on control of dust explosion hazard.

The coal dust explosion risk assessment.

The coal dust explosion risk assessment is a multi-stage process covering:

- Risk analysis determined by:
  - Classification of the action areas (collecting information necessary to assess the risk),
  - Hazard identification (based on experience and knowledge already possessed),
  - Risk estimation by assuming the probability of the hazard occurrence and the degree of its consequences.
- Determination of the acceptability of the risk with respect to the valid legal rules and regulations and other mandatory standardized requirements.

The basic goals of the risk assessment are the following:

- Checking whether the hazard has been identified and if the risk related is known,
- Demonstration that the risk analysis has been carried out and appropriate preventive means have been implemented,
- Careful selection of appropriate tools for work stands, materials and determination of appropriate work organization,
- Determination of priorities to be respected in actions aimed at eliminating or limiting the risk,
- Providing constant improvement in work safety.

Coal dust explosion hazard depends on ignition and explosion properties of the particular dust involved. For different coal dusts those properties may change significantly. To gain better knowledge on explosive properties of a dust, tests with dust of interest are carried out in experimental facilities of different scales.

For many years at Experimental Mine Barbara of Central Mining Institute tests of explosive properties of dusts are carried out in the equipment of various scales, from laboratory scale through semi-industrial up to full industrial scale. In that time a large database of ignition and explosion properties has been gathered, including the properties of coal dusts.

In spite of the large effort put into an assessment of explosive properties of coal dusts the demand for new data does not decrease. Although the mine regulations and standards does not rely on ignition and explosion properties described by a set of parameters to the same extent as in other industries a better insight into explosive properties of coal dusts is useful when dealing with dust explosion hazards in coal mines. For different coal dusts their explosive properties may differ significantly. Furthermore, different dusts from the same origin, the same coal, may have different explosive properties because of differences in granularity, moisture and impurity content etc. For tests of explosive properties of dusts a wide variety of equipment is used, beginning from the small, laboratory scale through an intermediate, semi-industrial scale up to the large scale directly related to industrial conditions.

For many years at Experimental Mine Barbara of Central Mining Institute an assessment of explosive properties of industrial dusts, including coal dusts, has been carried out by use of apparatus of different scale.

Laboratory scale tests

In international standards the explosive properties of dusts are described by a set of explosion indices and ignition parameters. The standards also define the apparatus and provide procedures to assess the parameters. Among the parameters those of most widely used are:

- Maximum explosion pressure p_{max},
- Constant K_{St},
- Minimum ignition energy of a dust cloud *MIE*,
- Minimum ignition temperature of a dust cloud T_{CL},
- Minimum ignition temperature of a dust layer $T_{5\ mm}$.

Photo 1. Standard 20-l sphere – the equipment for the assessment dust explosion properties

Photo 2. The equipment for the assessment of minimum ignition temperature of a dust cloud

EM Barbara have a full set of apparatus designated in the European Standards for an assessment of explosion indices and ignition parameters of industrial dusts. The equipment is intensively used in everyday work to evaluate dust explosion hazard. Photo 1 and 2 present examples of the apparatus. The standard 20-l sphere (Fig. x) is used to assess maximum explosion pressure pmax, maximum rate of pressure rise (dp/dt)max together with KSt, lower explosion limit LEL and limiting oxygen concentration LOC. In Fig. x the equipment utilized to assess minimum ignition temperature of a dust cloud is shown.

Explosibility of Polish coal dusts

Many tests of dusts derived from Polish coals, both hard colas and brown coals have been carried out at EM Barbara with use of the equipment mentioned in the previous section. Data presented in Table 1 summarize those results.

Table 1. Tests of dusts derived from Polish coals

Parameter	Hard coal dusts	Brown coal dusts
Maximum explosion pressure $\mathbf{p_{max}}$, bar	6.0 – 9.1	6.7 – 9.3
$\mathbf{K_{st\ max}}$, m·bar/s	28 – 135	98 – 202
Ignition temperature of a dust cloud $\mathbf{T_{CL}}$, °C	420 – 560	370 – 410
Ignition temperature of a dust layer $\mathbf{T_{5\ mm}}$, °C	250 – 400> 400	240 – 300
Minimum ignition temperature of a dust cloud **MIE**, mJ	65 < MIE < 7400 MIE > 7400	3 < MIE <100

Both ignition and explosive properties of Polish hard coal dusts demonstrate a great diversity. The properties depends not only on a sort of the coal, its origin, but also on features of the particular dust, such as granularity, moisture content etc. Generally, the properties can be summarize by giving the range of values a particular parameter falls within.

The values of maximum explosion pressure are in the range from a few bars up to about 9 bar. Basically, for all Polish hard coal dusts KSt max value is smaller than 200 m·bar/s. Their ignitibility, expressed

by minimum ignition energy MIT, minimum ignition temperature of a dust cloud TCL and a dust layer T5 mm, also falls within a relatively wide range.

As hard coal dusts are explosible dusts met in Polish industry most often EM Barbara has introduced for them an additional classification. The dusts are divided into three groups: weakly explosible dusts with Kst max ≤ 70 m·bar/s, moderately explosible with Kst max between 71 and 110 m·bar/s, and strongly explosible having larger Kst max than 110 m·bar/s. The classification has only demonstrative nature.

Polish brown coal dusts are generally easier to ignite and theirs explosions are more violent. This is particularly so when the dusts are dried up and their moisture content drops to about 10%. Natural moisture content of Polish brown coals is usually in the range 40-50%.

Intermediate scale tests

Explosion tests in laboratory scale, thou relatively easy to carry out should be regarded as an approximation of dusts behavior in real industrial condition. The limitations of laboratory scale apparatus, particularly the standard 20-l sphere, are well recognized and widely discussed. To improve the approximation the equipment of larger volumes is used. In semi-industrial scale, for the tests the standard 1 m3 vessel is utilized. The vessel at Experimental Mine Barbara meets the requirements of Standards both European (EN 14034-1, 2011&EN 14034-2, 2011) and in the United States (ASTM E 1226-05, 2005) as well as international (ISO 6184/1, 1985). Photo 3.

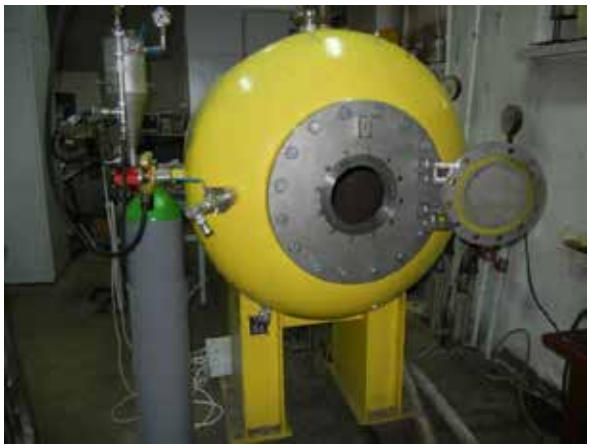

Photo 3. Standard 1 m^3 vessel – the equipment for the assessment of explosion parameters of dusts

Photo 4. Dust explosion in 5 m^3 vessel used to test explosive properties of dusts, gases and vapors

Another equipment of that scale is 5 m^3 vessel (Photo 4). The vessel is equipped with the dispersion system that allows generation of fairly uniform dust clouds of desired parameters – concentration, turbulence intensity. Because of its less compact geometry, L/D ratio over 2, the vessel, among other applications, can serve to study cooling effect of the walls. The results obtained in the vessel are very useful for adjustment/calibration of numerical model of dust explosion.

To the vessel's outlet sections of pipes, each approximately 5 m long, with the diameter of 500 mm can be attached, forming a duct that will guide the explosion out from the chamber. The duct sections are mounted on mobile supports allowing flexible configuration of an experiment.

The scope of experiments possible to carry out in the vessel is not limited to dust explosion. In fact in recent years many test of gas explosions, including methane and other hydrocarbons as well as vapor explosions have been performed in the vessel.

Large scale facilities

The large scale facility at EM Barbara, both surface and underground, are well known and have been described in many papers. The underground experimental facility consists of several entries among which the most important are the 400 m and 200 m entries. Both entries are equipped with measuring panels deployed along the entries walls. Depending on particular needs the panels allow installation of different measuring equipment. Because of its geometry, the facility also allows experiments in interconnected workings with different points of explosion initiation. The entries can be used to perform strong dust/gas explosions or when the explosion behavior in complex geometry is investigated. Very strong dust explosion were performed in the underground facility, including large scale detonation in dust-air mixtures.

The surface experimental gallery has served for over 3500 tests of dust and hybrid mixture explosions. The gallery is a 100 m long pipe, 2 m in diameter. The pipe is closed at one end and opened at the opposite. Every 10 m, starting from the closed end, an access to the gallery wall exists allowing installation of different measuring equipment. Most often the explosion is initiated by primary explosion at the closed end. Than the explosion in dust/gas-air mixture propagates toward the open end.

Whenever an easy access of numerous measuring equipment to the working area and a visual observation of explosion final development is sought the gallery is the facility of choice. On the other hand, because of its limited strength, only weak explosions, with overpressure up to app. 1 bar, can be performed in there.

Photo 5. Grain silo of the volume 136 m^3

Photo 6. Dust explosion in the grain silo

The silo of the volume 136 m3 recently raised at the experimental site of EM Barbara is our newest large scale facility. Because of its limited strength the silo is used to investigate large scale, relatively weak dust explosions. It is planned however to reinforce the silo walls and particularly its roof to enable performance of stronger dust explosions. Photo 5 and 6.

Information on accident in the Dolna Odra Power Plant

Dolna Odra Power Station is a coal-fired power station at Nowe Czarnowo near Gryfino in West Pomeranian Voivodeship, Poland. It consists of 8 units with total electric power of 1,772 MW, which went in service between 1974 and 1977. Since 1993, Dolna Odra has gone through modernization process. In 2008 the power plant generated 5.9TWh of electricity and 2.2TWh in first half of 2009.

On January 24th 2010, due to a dust explosion in the Power Plant a significant part of a plant's coal supply system has been damaged. Key generation facilities of the plant have not been destroyed and generation units remain operational. Coal supply system, however partially damaged, allows supply of fuel to boilers. Due to the accident one employee was killed and three others were injured.

At the moment of incident four of eight units were in operation. In order to minimize potential danger resulting from the accident, it was decided to temporarily shut down all units. Two units were relaunched after short time.

Photo 7. The Dolna Odra Pover Plant, the course of explosion

Photo 8. The Dolna Odra Pover Plant after explosion

One of the transfer buildings after the dust explosion

In the explosion both hard coal and biomass dust were involved. The explosion was initiated in the area of the mill No. 5 of the unit No. 7. The explosion ran along the galleries on the level 19.5 m and 22 m then propagated down the inclined galleries A and C under the transfer buildings of the lines 1 and 3. The explosion caused practically complete destruction of the buildings. (Photo 7, 8)

The danger of coal dust explosion is one of most significant natural threat occurring in hard coal mines. The coal dust explosion in hard coal mines is perceived as a mining disaster the extent of which is strictly related to the range of the explosion. Stone dust barriers are used to slow down the already developed coal dust explosion. They are used to actually limit the range and extent of the disaster.

In Poland, vast surveys concerning the effectiveness of such stone dust barriers, have been carried out in the Experimental Mine "Barbara" of the Central Mining Institute. As a result of these surveys the stone dust barriers have been developed and implemented in Polish coal mines. These barriers are the Experimental Mine "Barbara" type consisting of wooden shelves. The construction of the barrier shelves includes the base (rack) placed on scantlings and supports on which a platform of loose boards of 35 or 50 cm length is placed. On such shelves the stone dust is piled in the form of a cone. In the case of a powerful explosion the base is being raised together with the platform.

Photo 9. Stone dust barrier

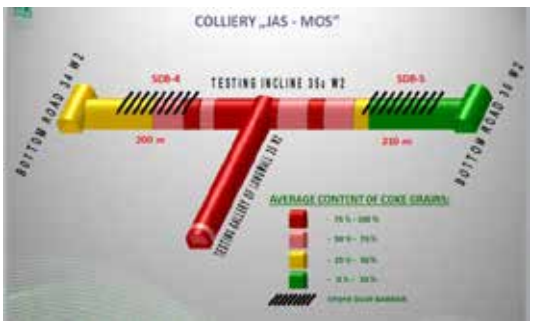

Fig. 1. Jas-Mos colliery – the range of explosion. (SDB- stone dust barrier)

During this process the stone dust is lifted together with the boards and dissipated by the explosion throughout the excavation. In case of less powerful explosions the blast first lifts up the boards of the platform

and then overturns them. It is worth mentioning that such barriers, in each case of coal dust explosions in Polish coal mines, proved to effectively stop the spreading explosions Fig 1.

However, the experience gained during tens of years point out that there are a number of obstacles connected with using the anti explosion stone dust barriers. The most important one is the time consuming preparation of this construction.

The solution which seems to be able to eliminate some of these obstacles is the use of containers (tanks) or bags with the stone dust placed on the barrier platforms. Furthermore this solution would determine the direction of future surveys concerning the universality of the anti explosion barriers in their construction both in the case of stone dust barriers as well as water dams where, depending of the circumstances and conditions of the excavation and the valid rules and regulations concerning safety matters in the coal mine, the containers could be filled either with water or stone dust.

Such solutions lead to conclusions that the stone dust barriers using either tanks or containers could eliminate a number of difficulties connected with maintaining "classic" stone dust barriers, however the possibility of implementing them in the mining industry still depends on the results regarding their efficiency in reality.

Results of the last research

Apart from constructional requirements, areas of application of and safety matters, the stone dust barriers must meet strict requirements of effective slowing down all kinds of explosions that may occur in a coal mine.

The effectiveness of the barrier is determined as the minimal amount of the stone dust per 1m2 of the excavation cross section capable of reliable explosion stopping. The effectiveness of the anti explosion stone dust barriers depends mainly on:

- The time of their activation i.e. the time gap between the moment when the blast reaches and activates the barrier (dissipation of the stone dust within the excavation) and the moment when the flame reaches the barrier,
- The state of dissipation (concentration) of the stone dust and the size (the length) of the stone dust cloud at the moment of the flame "arrival",
- The position of the stone dust with regards to the barrier zone at the moment of the flame arrival,
- The content of the incombustible material in the stone dust cloud,
- The location of the barrier within the excavation,
- The violence of the explosion including the initial energy.

It is the power of the explosion that actually determines the effectiveness of the stone dust barriers – its violence and extreme circumstances (e.g. very violent explosions versus very mild and explosions featuring sudden changes in the speed (with sudden accelerations). Mild explosions of the coal dust most frequently occur in dry excavations and feature low dynamic blast values which decide upon the appropriate activation of the barrier. According to the rules of using barriers in general, the stone dust barriers have been foreseen to be used in the case of dry environments in the excavations. This is why during the surveys the emphasis was put on mild coal dust explosions.

The main objective of the survey was to determine the basic parameters characterizing the effectiveness of the stone dust barriers with the use of tanks in slowing down the coal dust explosions what was done in real conditions in an experimental heading at 400 m in the Experimental Mine "Barbara" followed by assessment of the effectiveness of the barriers based on the results of the carried out experiments.

Test stand

The Experimental Mine "Barbara" of the Central Mining Institute has an experimental test site located 46 meters below the ground surface consisting of a network of underground experimental headings equipped with systems measuring the parameters of explosions enabling monitoring the coal dust and gas explosions and carrying out strength tests of the anti explosion barriers in real conditions.

The tests of the closed type anti explosion stone dust barriers effectiveness in slowing down the coal dust explosions were carried out on a 400 m long horizontal section of the experimental underground heading at 46 m underground.

Method of the research

The effectiveness of the anti explosion barriers in the process of slowing down the coal dust explosion was determined exposing the tested barriers to the pressure wave and the flame of the coal dust explosion. For initiating the explosion the primary explosion of a methane air mixture of 9.5% CH_4 stoichiometrical concentration was used. (Photo 10)

The methane air mixture was prepared at the end of the experimental heading behind a paper membrane (a methane chamber) and initiated using a mortar placed in the front part of the heading using explosive powder.

The size of the methane chamber determines the power of the initiation. Directly behind the methane chamber develops the so called dust zone. In the test the coal dust containing ca 40% volatiles, less that 4 % temporary water. The content of incombustible solid particles and fractions below 0.075 mm equals 5% and ranges from 38 % to 65 % respectively.

It has been assumed that the tests of the a.m. barriers would be carried out in conditions analogical to those in which the "classic" anti explosion stone dust barriers had been tested, while respecting the mining rules and regulations concerning the construction and location of such barriers in the excavations.

Due to the purpose of the research (determining the effectiveness of the barrier using a minimal amount of the stone dust) the total amount of the stone dust placed on the barrier as calculated per $1m^2$ of the excavation cross section in the place (Q) of the barrier location was smaller than the requirements of the regulations (at least 200kg of stone dust per $1m^2$ of the excavation in the case of non methane zones and at least 400 kg of stone dust per $1m^2$ of the excavation in the case of methane zones).

The measuring system

Every time, while carrying out the tests with the use of a set of sensors distributed along the experimental heading, dynamic monitoring and recording of the basic parameters, necessary to determine the effectiveness of the barriers i.e. the barrier reaction time and the static pressure, the range and the location of the head of the flame on the path between the closed end of the heading, where the explosion had been initiated and the place of the barrier location and within the area directly behind the barrier were performed. (Photo 11)

The signals from the sensors, once amplified directly in the control station, are transmitted to the underground relay station and from there to the computer data processing station on the surface.

Photo 10. Methane mixture preparation chamber

Photo 11. The measuring sensors

Technical characteristics of the stone dust barriers with containers

The stone dust anti explosion barrier with containers consists of a wooden platform (identical as in the case of "regular" stone dust barriers) on which sets of tanks filled with stone dust are placed.

The tanks may be filled with the stone dust either before being placed on the platform or afterwards. The tanks are put on the platform in a line depending on the size of the excavation (the length of the platform) at a regular distance between each other ranging between a few up to a dozen or so cm. the tanks are put on the platform in such a way that the longer side of the tank is perpendicular to the excavation axis.

The tested stone dust barrier with the tanks placed in an experimental heading at 400 m. is presented in Photo 12, 13.

Photo 12. Stone dust barrier with tanks placed in an experimental heading at 400 m. before explosion

Photo 13. Stone dust barrier with tanks placed in an experimental heading at 400 m. after explosion

The specification of technical parameters and the effectiveness of barriers is presented in Table 2, and the specification of explosion parameters is presented in Table 3. The diagrams of the course of explosions are presented in figure 2, 3, 4.

Table 2. Specification of technical parameters and the effectiveness of barriers

Number of experiment	Ignition	Dust zone	Barrier parameters									Stone dust concentration			Range of flame
			Location of barrier	Length of barrier	Number of shelves	Number of bags		Amount of stone dust				Q	Q_v	Q_1	
						barrier	shelf	barrier	shelf		bag				
	m^3	kg/m^3	mb	m	number	number	number	kg	kg	kg/mb	kg	kg/m^2	kg/m^3	kg/m^2	mb
1	50	0,300	71-90	19	15	105	7	630	42	14,0	6	84	4,4	5,6	> 160
2	50	0,250	101-122	21	8	24	3	960	120	40	40	128	6,1	16	120 -140
3	50	0,200													> 160

Table 3. Specification of explosion parameters

Length of gallery [m] / Number of experiment	Barrier activating time [s] / Velocity of flame [m/s] / Explosion pressure [kPa]								Average velocity [m/s]
	40	60	80	100	120	140	160	180	
1	0,654	0,865	1,093	-	1,501	1,539	1,679	-	168
	61	95	87	-	98	526	143	-	
	77	78	79	68	65	-	-	-	
2	0,570	0,758	0,896	1,053	1,512	-	-	-	105,6
	106,4	144,9	127,4	43,6	-	-	-	-	
	-	73	75	110	77	52	-	-	
3	0,539	0,758	0,936	1,165	1,355	1,824	2,569	-	77,6
	91,3	112,4	87,3	105,3	42,6	26,8	-	-	
	-	51	57	79	70	56	-	-	

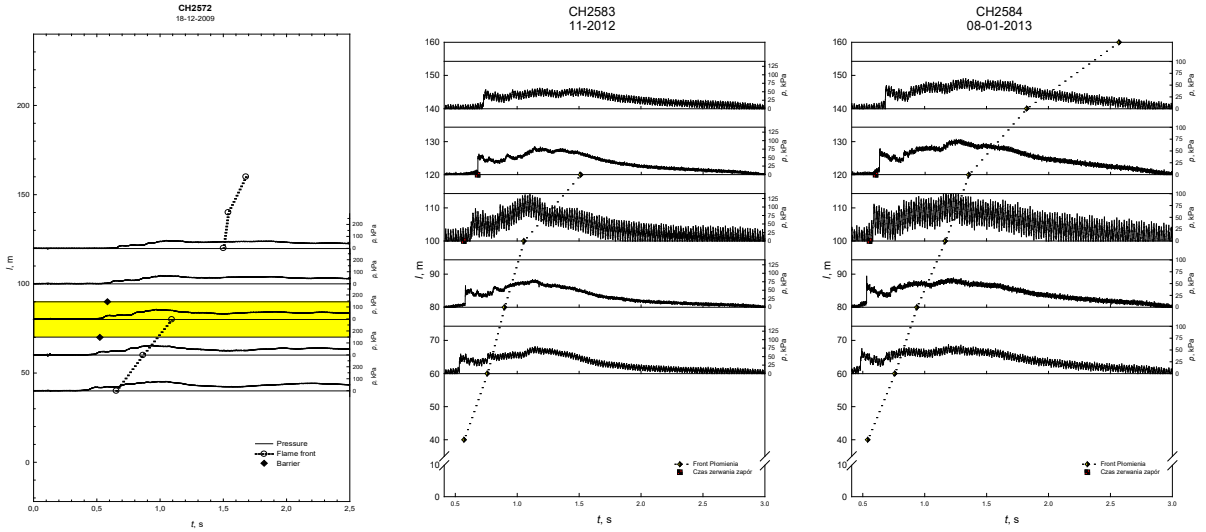

Figure 2,3,4. Wave diagram of explosion resistance test

The technical characteristics of the anti explosion closed type stone dust barriers constructed of four-chamber stone dust bags

The anti explosion closed type stone dust barriers consist of stone dust bags. Hanging the dust bags in their destination location is done by wrapping the upper part of the bag with the stone dust a few times around a metal bar (the carrying set), which ends are fixed in a rigid way to the lining elements on opposite sidewalls of the excavation. The bags are filled with stone dust on the excavation floor before being hung. The upper part of the bag, wrapped around the bar, tightens itself due to gravitation under the weight of the stone dust. This ensures stable and durable hanging. The effectiveness of the four chamber stone dust bags anti explosion barriers in the process of slowing down the coal dust explosion was determined exposing the tested barriers to the pressure wave and the flame of the coal dust explosion. For initiating the “main” explosion the primary explosion of a methane air mixture of 9.0% CH4 stoichiometrical concentration was used (Photo 14, 15).

Photo14. Stone dust barrier with bags placed in an experimental heading at 400 m. before explosion

Photo 15. Stone dust barrier with bags placed in an experimental heading at 400 m. after explosion

The purpose of the survey was to determine the effectiveness of stone dust barriers constructed with the use of four-chamber dust bags in slowing down the coal dust explosion spread. The survey was carried out according to the following parameters:

- Initiation – explosion of a methane air mixture of 50 m^3 capacity,
- Number of stone dust bags hung on a single shelf (the carrying set) – 7 pcs,
- Amount of stone dust placed on the barrier – 120 kg per 1 m^2 of the 400 m experimental heading,
- Distance between the shelves (carrying sets) – 1 m.

The specification of technical parameters and the effectiveness of the tested anti explosion barriers is presented in Table 4, and the specification of explosion parameters is presented in Table 5. The diagrams of the course of explosions are presented in figure 5,6.

Table 4. Specification of technical parameters and the effectiveness of barriers

Number of experiment	Ignition	Dust zone	Barrier parameters									Stone dust concentration			Range of flame
			Location of barrier	Length of barrier	Number of shelves	Number of bags		Amount of stone dust				Q	Q_v	Q_1	
						barrier	shelf	barrier	shelf		bag				
	m^3	kg/m^3	mb	m	number	number	number	kg	kg	kg/mb	kg	kg/m^2	kg/m^3	kg/m^2	mb
4	50	0.180	70 - 89	19	19	150	18x8	900	18x48	18x16	6	120	6,7	18x6,4	80 – 100
5							1x6		1x36	1x12				1x4,8	> 140

Table 5. Specification of explosion parameters

Length of gallery [m] / Number of experiment	Barrier activating time [s] / Velocity of flame [m/s] / Explosion pressure [kPa]								Average velocity [m/s]
	40	60	80	100	120	140	160	180	
4	0.474	0.701	0.955	-	-	-	-		83.7
	84.4	88.1	78.7	-	-	-	-	-	
	-	155,6	90,5	107,9	80,7	-	-	-	
5	0.700	1.020	1.270	1.550	1.740	2.020	-		74.6
	57.1	62.5	80.0	71.4	105.3	71.4	-	-	
	-	53,1	36,0	46,6	37,3	-	-	-	

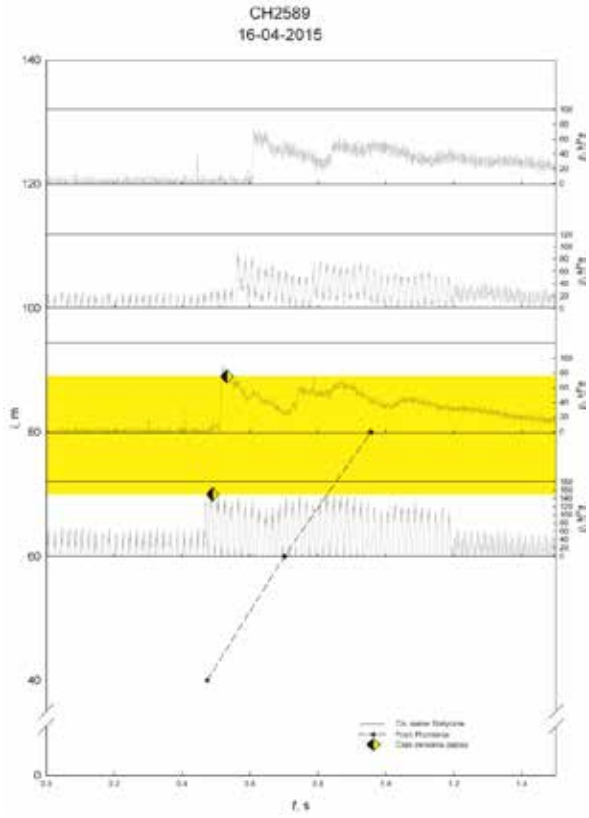

Figure 5. Wave diagram of explosion resistance test

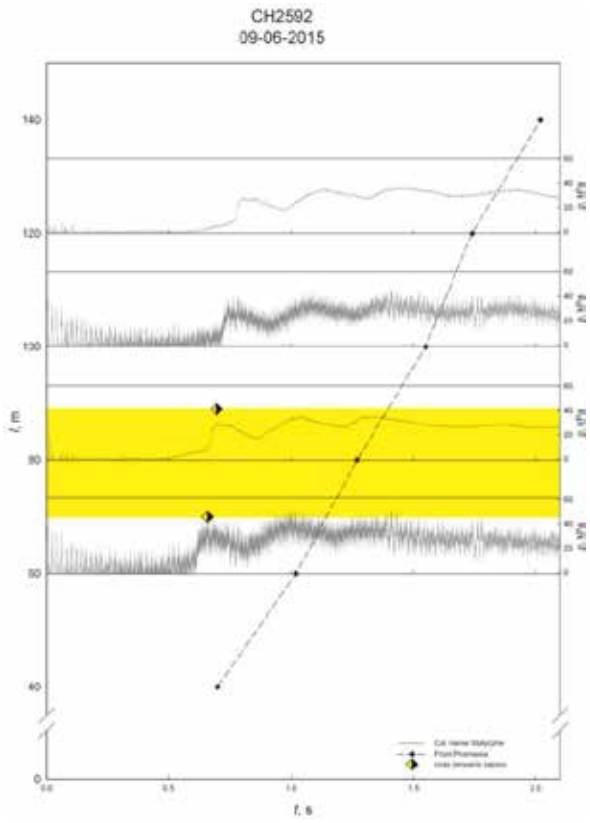

Figure 6. Wave diagram of explosion resistance test

CONCLUSIONS

1. The purpose of the survey was to determine the effectiveness of various types of anti explosion dust barriers i.e. their capability of extinguishing the coal dust explosion flame.
2. The tested anti explosion barriers feature good effectiveness in slowing down major (strong) coal dust explosions, however insufficient in the case of minor (weak) explosions under conditions in which the survey was being carried out.
3. For many years at Experimental Mine Barbara of Central Mining Institute tests of explosive properties of dusts are carried out in the equipment of various scales, from laboratory scale through semi-industrial up to full industrial scale. In that time a large database of ignition and explosion properties of dusts has been built. The tests carried out in laboratory equipment have provided an input to the database – coal dust ignition and explosion parameters of Polish hard and brown coals.
4. Wherever safety issues are crucial, the large scale experiments are still a source of invaluable and irreplaceable information on industrial hazards.

REFERENCES

Bartknecht, W. (1989). Dust Explosions: Course, Prevention, Protection. Springer-Verlag, Berlin.

Eckhoff, R.K. (2003). Dust explosions in the process industries. Third edition. Gulf Professional Publishing, Amsterdam.

Cybulski K., Dyduch Z. (2015) Explosive properties of dusts tests in facilities of different size. Sudbury.

Cybulski K., Dyduch Z. (2015) Suppression of coal dust explosions with passive barriers of different type. Sudbury.

COST ESTIMATION IN COAL MINING: THE EVOLUTION OF QUICK EVALUATION METHODS

J. Gavronski*, C. Petter, and B. Escobar[1], R. D'Arrigo[2]

Universidade Federal do Rio Grande do Sul[1]
Av. Bento Gonçalves 9500
Porto Alegre, Brazil 91501-970
*(Corresponding Author: *Jgavronski@gmail.com)*

Departamento de Engenharia de Minas e Programa de Pós-Graduação em Engenharia de Minas, Metalúrgica e de Materiais[2]
Av. Bento Gonçalves, 9500
Setor 4 - Prédio 74 - Sala 211
Porto Alegre, Brazil 91501-970

24th World Mining Congress
MINING IN A WORLD OF INNOVATION
October 18-21, 2016 • Rio de Janeiro /RJ • Brazil

COST ESTIMATION IN COAL MINING: THE EVOLUTION OF QUICK EVALUATION METHODS

ABSTRACT

New developments in mining involve many uncertainties from reserve estimation, technological characterization of the ore, and local, economic, and political factors. Such developments rely on large amounts of resources and have long maturation periods. These factors highlight the necessity to periodically reassess projects throughout each phase of their operation from a technical and economic point of view. The decision to start the investment or continue investing time and resources in a mine needs to be revised in light of new information that will be aggregated throughout the course of its development. For such revision to be possible, especially in the earliest stages of the project there is the need to use quick evaluation methods which, although less accurate, may confirm the whether or not to continue more demanding studies and project implementation. The paper presents and discusses the method termed "Quick Evaluations", and discusses in a special way the use of techniques originally proposed by O'Hara and Stebbins in coal projects.

KEYWORDS

Mineral Evaluations, Coal Mining, Parametric Method

INTRODUCTION

The first feasibility studies for a given mining project are initiated after an evaluation of mineral reserves generates interest. The purpose of such studies is to determine whether further geologic investigation, mine planning, metallurgical studies and other studies will recompense their investment.

As these studies are only preliminary, many characteristics within them lack sufficient details to safely define the mine layout, process flowchart, final product quality, and many other important aspects for the development of the project. Therefore, these factors rely on the experience and skill of the engineers and qualified persons which perform the study.

Many proposals for classification systems or project planning exist. Their authors, in general, propose an expected level of accuracy of the cost estimates calculated during every step. The models (Reynolds and Frew), presented below, exemplify two different project phase classification systems or studies.

Reynolds (1990) proposes the following project classification phases or studies during the related engineering development levels with the indicated precision in investment values:

Table 1 - Accuracy of mining studies during different phases (Reynolds, 1990)

Project Phase	% Engineering Concluded	Precision (%)
Conceptual	0	± 50
Pre-Feasability	0 – 30	25 – 30
Feasability	30 +	10 – 15
Detailed Study	60	± 5

Note that by Reynolds' proposition the term "conceptual" corresponds to a phase which is very preliminary to the project, where practically speaking no proper engineering studies exist and the calculated costs reflect only the order of magnitude expected. By the term "engineering", Reynolds' implies the dimensions or scale, although preliminary, of the facilities or equipment required for the project.

The same term "conceptual", as defined by Frew (presented in 1990), corresponds to a more advanced stage of evaluation, providing therefore values, expectedly, more accurate.

Table 2 – Description of different mining estimates (Frew, 1990)

Type of Estimate	Description	Precision (%)
Indicative	Based on imperical data from other projects	± 30
Preliminary	Based on conceptual projects and price/cost estimations	± 20
Workable	Based on flowcharts, sizes of known equipment, and arrangements and estimated prices for equipment and materials	± 10
Definitive	Based on constructive engineering drawings and final price	± 5

QUICK EVALUATIONS

For assessments at the initial stage, most authors propose empirical rules, sometimes called "rules of thumb" with the rule of six-tenths being the most used, as described by Mular (1978) as in Equation 1:

$$\text{Cost 1/Cost 2} = (\text{Capacity 1/Capacity 2})^{0,6} \quad (1)$$

This simple rule compares the investment that should be analyzed for a stipulated production capacity, with another known and existing investment of similar operation and physical and political environment, stating that: the relationship between costs (investments) is proportional to the 0.6 power of capacity ratio.

Many other "rules of thumb" have been proposed, many of which are applicable for only one specific type of mineral (Metal, Coal, Gold, etc.).

To assist in this initial phase of the project there are several published papers based on empirical formulas from actual operational statistics, mostly in the form of tables, graphs or formulas for the purpose of establishing purchasing values and operating costs for equipment, facilities and services, as well as the costs for design and planning of equipment and facilities. Normally, these papers define the acquisition and operating costs according to predetermined type and size of equipment or facilities quickly. Such definitions are termed "quick evaluations" within the technical literature.

The "Comparison Method" proposed by Stebbins and Schumacher (SME 2011) is based on comparison of similar projects with adjustments to balance differences. To facilitate understanding, within this article are presented tables and graphs that provide indications for acquisition values, operating costs, equipment sizing, facilities and services. The background information includes: listing of operations, supplies

and equipment, deposit information, and proposed development. A good example, for reference, is the "Mine and Mill Equipment Costs - An Estimator's Guide, Western Mine Engineering Inc" (2015). The background information is combined with labor costs, productivity, supply costs, and equipment prices (Stebbins, 2011). Accuracy of the method depends on the basis of the information available from published works, empirical formulas, and statistics of actual operations.

In the other hand, the so-called "Parametric Methods" estimate derived costs through generalized algorithms. Most present the following relationship: "Cost = x (parameter)y". The variable "parameter" can represent many design characteristics (length, mass, etc.), and most often represents a production rate.

The variables x and y are values derived from known data of statistical evaluations or estimated from field operations. Examples of this methodology may be found in the U. S. Bureau of Mining Cost Estimating System (CES USBM 1987) and the O'Hara Model (1980).

The publication of the USGS (Circular 9298 Simplified Cost Models For Prefeasibility Mineral Evaluations) contains: models for well drilling, models of underground mines, models for milling, cost equations for access roads, power lines, tailings dams and also adjustment factors to the variation in transport distances for open pit models and variation in depth of mining to underground models.

Another known parametric method, the O'Hara model, proposes costs derived from general parameterization algorithms. Using this method, T. Alan O'Hara in 1980 developed mathematical models to estimate mining costs. From O'Hara's formulas MAFMO software - Modele d'Analyse Financière sur Micro-Ordinateur was developed at the Centre of GEOTECHNIQUE et d'Exploitation du Sous-sol of the Ecole Nationale Superieure des Mines de Paris, which effected estimates of CAPEX and OPEX in addition to financial risk analysis. Currently, a group of researchers from the Federal University of Rio Grande do Sul is developing software called MAFMINE which is based on MAFMO and the O'Hara formulations with adjustments made to capture modern mining technology costs.

THE MAFMINE SOFTWARE

Development of MAFMINE software involved the use of a computer model known as client-server. Clements (2003) client-server is a computational model which separates clients and server which are interconnected usually using a computer network. Each instance of a client can send data requests to the connected server and wait for an answer. In turn, the server can accept these requests, process them and return the result to the client.

In the case of the software MAFMINE, the server is running one or more programs that share their resources with customers. The client does not share their resources, but requests the contents of a server or service function. Clients therefore initiate communication sessions with the server which waits for incoming requests. All data are stored on the server, which typically has much higher safety controls that most customers. Servers can better control access and resources to ensure that only clients with the appropriate permissions can access and change data.

Some features present in MAFMINE software:

- Investment Cost Estimation
- Operating Cost Estimation
- Export of Data for Risk Analysis (in the implementation phase)
- Save project settings
- Change of base year and country estimates
- Print report data
- Model Customization for different users (in the implementation phase)

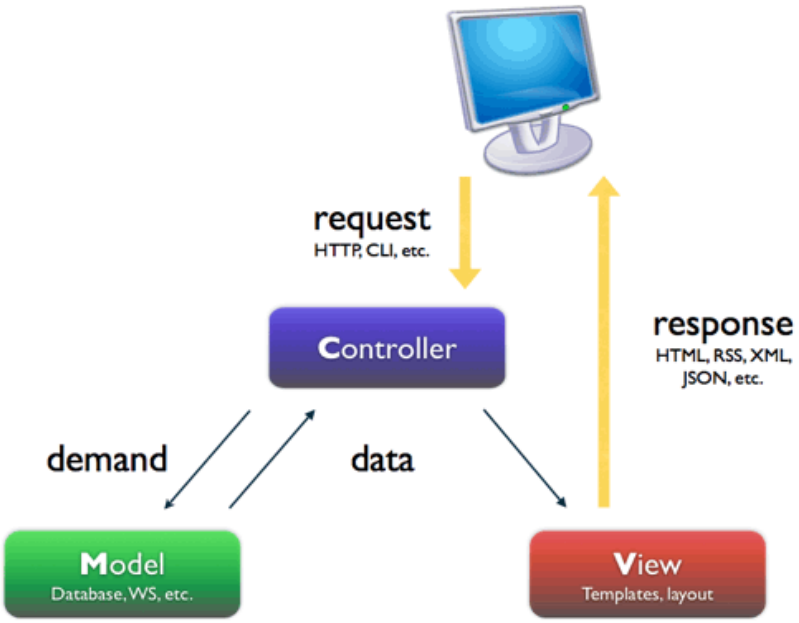

Figure 1 – Operating Software Architecture of MAFMINE

RESULTS AND DISCUSSION

Below are shown the results obtained with the O'Hara model through the MAFMINE software. The results are compared in two distinct situations both in terms of mineralization and in mining technique. In the first operation (CASE 1), the conceptual study of an open pit copper mine (performed by a consulting firm) is tested by comparing the CAPEX between the consultant and MAFMINE. Then (CASE 2) compares the OPEX from MAFMINE to the result obtained by applying Stebbins methodology (SHERPA) and the actual OPEX from an underground coal mine. Both Cases 1 and 2 are focused on operations in Brazil.

CASE 1

- Daily ore production: 12,000 t
- Daily waste production: 48,000 t
- Initial stripping: 12,126 Mt, 80% w / o use of explosives and 20% w / use of explosives
- Ground conditions of beneficiation plant: flat with less than 3 m of earthmoving.
- Ground support of building foundations: resistant soil with low humidity
- Climatic characteristics: tropical
- Processing plant capacity: 10,224 t / day
- Work Index - Wi = 16
- Electricity: high voltage provided by the existing system located 50 km away
- Water availability: it was assumed that the water supply sources are rare. The new water intake (not recycled) will be located 20 km from the plant.

Table 3 – Values proposed by case 1 investment consulting firm (Carriconde, 2010)

ITEM	CHARACTERISTICS	VALUE (USD)
Mining Equipment		59.185.860
Initial Stripping	4.575.000 m³	10.982.000

Crushing Circuit		18.093.636
Grinding Circuit		19.467.865
Flotation Circuit		6.391.176
Thickening and Filtration		6.452.010
Substation	15000 KVA	3.000.000
HV Line	50 km	2.750.000
Water Catchment	10.000 m³ / dia a 20 km	10.000.000
Water Tank	50.000 m³	700.000
Pumps	600 m³/h	2.676.000
Tailings Dam	(initial dam)	1.500.000
Land Acquisition	120 hectares	600.000
Laboratory		600.000
Auxiliary Buildings		1.800.000
Machinery and Tools (workshops)		900.000
Shipping/Transport	(balances, scales, chargers, etc)	1.200.000
Environmental Studies		350.000
Project (implementation/deployment)		17.483.826
Contingency	10 %	16.413.237
TOTAL INVESTMENT		180.545.610

Table 4, below, shows the results of the MAFMINE estimation. The overall results obtained by the application are very similar to those obtained by the conceptual study. The total value of investments made by MAFMINE exceeds the conceptual study by 10.85%.

Table 4 – Report generated by MAFMINE

Investment Costs	M U$ (2008)
Open Pit Mine	
Land Preparation	1,54
Pre Stripping	24,85
Equipment	402,303
Maintenance Facilities	117,637
Viability Studies	49,587
Project Supervision and Provisional Costs	70,539
Pre-production	39,188
Total	94,315
Beneficiation Plant	
Land Preparation	18,448
Foundations	107,299
Crushing facilities, Storage and Transfer	134,126
Buildings	89,416
Grinding Equipment and Stockpiling of Fines	246,554
Concentration Unit	57,791
Thickening and Filtration Unit	14,903
Concentrate Storage Unit	0,9738
Sedimentation basins	23,844

Viability studies	58,049
Project Supervision	78,165
Pre-production	43,425
Total	88,176
Infrastructure	
Electricity	72,948
Water Tanks	52,168
Auxiliary services	27,698
Access routes	21,913
Staff Accommodations	0,2
Total	17,673
Total Investment	200,164

Some individual values suffer a bit more difference, such as pre-stripping and mining equipment. These are items that should be investigated in the model. As the model becomes old, items such as electricity and pumping can also be updated for greater precision in the results.

CASE 2

Year – 2013
Underground Coal Mine
Method- Room and Pillar
Country – Brazil/Santa Catarina State/ Criciúma City

Table 5 – Case 2 value comparison, Stebbins, MAFMINE, and Actual

Mining Method	Project	Production ROM (t/year)	Actual OPEX (US$ 2013)	Stebbins (US$ 2011)	MAFMINE (US$ 2012)
Room and Pillar	Verdinho	1,047,568	19,74	20,18	19,80

CONCLUSION

Although the results are less accurate than those obtained with a conventional design, the so-called "Quick Evaluations" are less accurate but easier and applied faster. They require little information but when combined with experience can provide good results. In addition, the results can be evaluated and adjusted with each compilation by documenting all assumptions and calculations of the sources of the estimated costs.

Reliability is proportional to the quality of information available on the specific nature of the orebody. Reliability also increases with the level of effort involved in evaluating the information. The more there is information available to be evaluated, the greater the reliability of the estimated costs. So cost estimation constitutes an interactive process design and assessment throughout the mining project's development process.

At this point it should be noted that reliable results can only be achieved with good understanding of the specific characteristics of the deposit and diligent work.

REFERENCES

Carriconde, M.C., (2010) *Verificação Da Aplicabilidade Do Programa Mafmo Como Ferramenta Auxiliar Na Estimativa De Custos Para Desenvolvimento De Estudos De Viabilidade Econômica Em Projetos Conceituais*

Clements, P. (2003) *Documenting Software Architectures: Views and Beyond* (pp. 13-15). Boston, MA

Darling, P. (2011). Mining: Ancient, Modern and Beyond. In: Darling, P. SME Mining Engineering Handbook (pp. 3-10)

D'arrigo, R. F. et al. (2011). *Estimativa Preliminar de Custos de Captial e Operacional de uma Mina de Carvão a Céu aberto Atraves do Modelo de O´Hara*. III Congresso Brasileiro de Carvão Mineral. Gramado, RS

Gentry, D. W. (1979) *Mine valuation: technical overview*. AIME.

Hustrulid, W., Kuchta, M. (1995) *Open Pit Mine Planning & Design*. A.A. Balkema. Rotterdam

Infomine USA., (2009) *Mine and Mill Equipment Costs: An Estimator's Guide*. Spokane, WA

Mular, A. L., (1982) *Mining and Mineral Processing Equipment Costs and Preliminary Capital Cost Estimates*. Canadian Institute od Mining and Metallurgy. Ottawa,

Nagle, A. J., (1988) *Aide a l'Estimation des Paramètres Economiques d'un Projet Minier dans les Etudes de Prefaisabilité*.

O'Hara, T. A., (1980) *Quick guides to the evaluation of ore bodies*.

O'Hara, T.A., Suboleski, S.C., (1992) *Cost and Cost Estimation*, Chapter 6.3: SME Mining Engineering Handbook ,2ª Ed., Vol. 1.

Parkinson, E.A., Mullar, A.L., (1972) *Mineral Processing Equipment Costs and Preliminary Capital Cost Estimations*, Canadian Institute of Mining and Metallurgy,

CURRENTLY USED TECHNOLOGY OF SHAFT SINKING IN POLISH COPPER MINES – ANALYSIS OF WEAK POINTS, AND POSSIBILITY TO IMPROVEMENTS

*S.Fabich, S.Świtoń and M.Rajczakowska

KGHM Cuprum Research and Development Centre Ltd.
Sikorskiego 2-8 Street
53-659 Wroclaw, Poland
*(*Corresponding author: sswiton@cuprum.wroc.pl)*

24th World Mining Congress
MINING IN A WORLD OF INNOVATION
October 18-21, 2016 • Rio de Janeiro /RJ • Brazil

CURRENTLY USED TECHNOLOGY OF SHAFT SINKING IN POLISH COPPER MINES – ANALYSIS OF WEAK POINTS, AND POSSIBILITY TO IMPROVEMENTS

ABSTRACT

Currently the copper ore extraction in Poland is done only in the Foresudetic Monocline area. Due to the nature of copper ore deposits (pseudo-stratified type of the deposit) the current model of ore extraction is based on using vertical shafts. Currently, a 1250 m deep shaft sinking process with 650 m deep freezing zone, would require about five years duration. Due to the technology of shaft sinking currently used in the Foresudetic Monocline area, where the deposit extends from 1200 m to 1700 m, revenues from extracted copper ore will be delayed. To improve this process in 2015 CuBR - governmental project was launched. The main objective of this is to develop innovative method of the deep ore deposits access. Currently first phase is finalized. In this paper the result of this task is presented. The goal of this part of the project was to analyze all the technological elements which are on the critical path of the shaft sinking in currently used technology. Indication of the consequences of partial or total elimination of some of them, alternative solutions, which guarantee full functionality and security, will also be provided.

KEYWORDS

Mine shafts, Shaft sinking, Foresudetic Monocline

INTRODUCTION

The copper ore extraction in Poland is done only in the Foresudetic Monocline area (LGOM area exploited by KGHM Polska Miedź S.A.). The nature of this deposit is causing the necessity for developing of vertical shafts. Currently shaft sinking process require about five years duration. To achieve the targeted copper production, it is necessary to open new parts of the deposit. Besides foreign assets of the KGHM, the biggest prospects for exploitation in Poland are the new parts of the orebody in the Foresudetic Monocline.

Taking the above into consideration, it is required to develop shaft sinking technology to allow opening the deposit as fast as possible. This will result in the implementation of new technologies for shaft sinking that provide the shortest time schedule and lowest cost. Ultimately, it is assumed that in the case of the Foresudetic Monocline deposit at a depth of 1300 m, the whole process of development will last no longer than three years.

Polish government with KGHM cooperation launched research and development project to achieve above results. This is so called CuBR program. This paper presents the results of first stage, that was developed within I-MORE project done within this programme. The assumption has been made that this project will be covered with two types of actions:

- The first action is based on experience gained during current technology of shaft sinking usage. Analysis of all technological and organizational solutions that are currently available will be used. This will indicate the elements that have the greatest impact on the achievable performance. Then modifications of this technology will be made to achieve the primary objective of this project, which is shortening the duration of shaft sinking to 3 years. Those modifications will result with some changes of technical solutions for the lining as well as equipment at the surface and inside the shaft during sinking. This part is presented in this paper.
- The second action is to find a new way of gaining access to the orebody. Review is based on experience from other technologies used in different countries. This will be done with emphasis on geological and mining conditions. These technologies will be subjected to a detailed technical,

economical and risks analysis. That will allow assessing whether those methods are applicable to open deep copper ore deposits in Poland.

GEOLOGICAL CONDITIONS

Polish copper mines are located in specific structure of rock mass as well as in difficult hydro-geological environment. Rock strength is also an issue. Up to the 380 meters depth there are Cenozoic loose (soil) and cohesive rock mostly saturated with water (quartz sands, gravel and clay, with intrusions of lignite – a few meters thickness). Maximum water pressure at the bottom of this layer is around 3.6 MPa. Due to mentioned limitations before start of shaft sinking process rock mass is frozen. Mentioned limitations are also the reason why cast-iron tubbing lining (40 to 110 mm thick) with concrete backfilling (60 cm thick) has to be used.

Below the Cenozoic rocks up to the depth of 980 m Mesozoic rocks are deposited. Those rocks are represented only by lower Triassic – Bunter (consisting Rhaetian middle and lower mottled sandstone). Triassic rocks are very differentiated hydro-geologically. Rhaetian rocks (up to 20 meters thick) consisting marlstone, anhydrite, and limestone. Those rocks have various strength (between 20 and 190 MPa). Quality (RQD) of rhaetian rocks is between 40 and 80% (Piestrzynski, 2008).

Sandstones of middle mottled sandstone (Bunter) are also very differentiated. Mostly their structure consists quartz sandstones with clay and clayish-carbonate binder heavily cleaved. Strength of those rocks is between 17 and 85 MPa. The wet strength (when rock is saturated with water) of those rocks decrease significantly, and sometimes in many cases rock simply fell into pieces. Quality of the rock is very low (RQD=45%-80%). Due to hydro-geological and geological reasons Rhaetian rocks are frozen before the shaft sinking, and the lining of those rocks contains cast-iron tubings with 120 to 140 mm thickness, with additional concrete backfilling (60 – 75 cm) (Piestrzynski, 2008).

Sandstones of lower mottled sandstone (Bunter) are represented by sandstones with clay, clayish-carbonate and carbonate binder. Strength of those rocks is much higher (70 – 130 MPa) than strength of middle mottled sandstones. Quality is good (RQD = 50 to 100 %). Those sandstones are mainly unsaturated with water. Shafts in those rocks are sunken without any special preparation of the rocks – concrete linen with the thickness between 60 and 75 cm (Piestrzynski, 2008).

Below the Mesozoic rocks Permian rocks (P24 Aller, P23 Leine, P22 Strassfurt, P21 Werra) are located.

In the area where shaft`s sump is located red sandstone (Rotliegend) rocks are deposited. Strength of those rocks is between 15 and 45 MPa. Those rocks are very fragile for saturation (when the rock is saturated with water, strength drops significantly). RQD is between 90% and 99%. Shafts are sunken without any special treatment of the rocks with concrete lining (75 cm thick).

TECHNICAL SOLUTIONS USED FOR SHAFTS SINKING IN POLISH COPPER MINES

The technology that is currently used in LGOM area is fully dependent on the way of rock mass treatment in conjunction with type of lining used in a specific part of the shaft. In general there are three types of technologies that are used for shaft sinking. In frozen rock mass up to 380 m below the surface (Cenosoic rocks, rhaetian and middle Buntsadndstein) the technology based on mechanical miner is used. Below this depth drilling and blasting method is introduced. In both cases (in frozen rock mass) tubing lining is used, due to its waterproof parameters. In the rock mass that is not frozen drilling and blasting technology is used with lining made of concrete. Generally speaking two main technologies may be described:

a) Technology I – sinking of the shaft with tubbing linen in frozen rock mass,

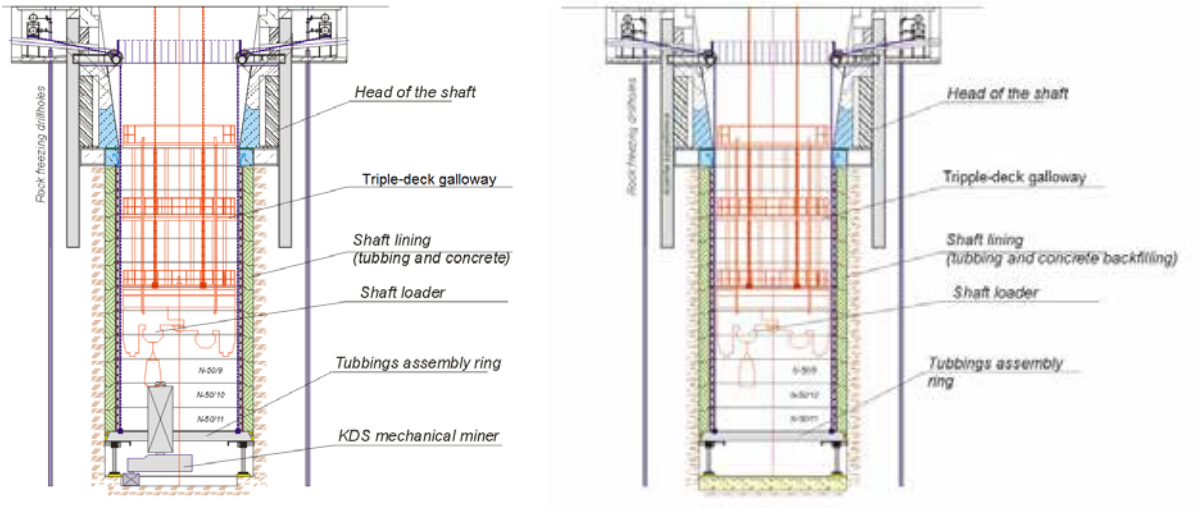

Figure 1 – Equipment of the shaft in Technology Ia (sinking of the shaft in frozen soils) and Ib (sinking of the shaft in frozen rocks)

b) Technology II – sinking of the shaft with concrete linen, below the frozen rock mass

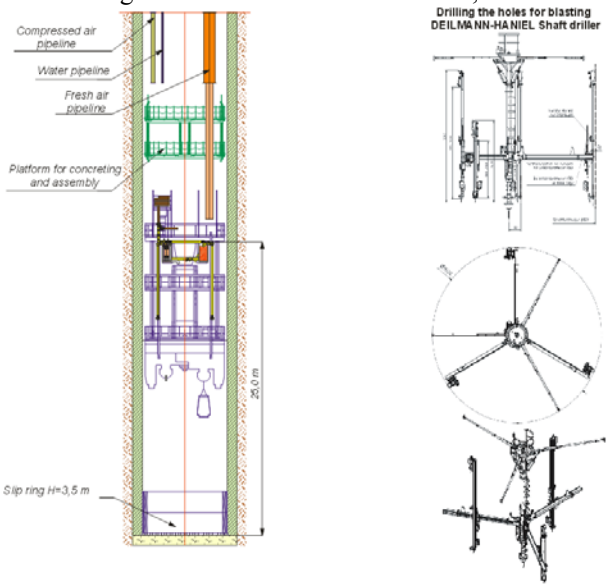

Figure 2 – Equipment of the shaft in Technology II (sinking below the frozen rock mass)

Both technologies require similar equipment inside the shaft (fig. 1 and 2). Tubbing ring assembly (technology I) is done with assembly ring, which is carried by three ropes connected to winches located at the top of the shaft. Assembly ring is expanded at the bottom of the shaft by hydraulic actuator.

In the area of frozen loose rock mass (Cenozoic rocks) mentioned assembly ring is additionally equipped with mechanical miner. When the top of frozen cohesive rock mass is reached mechanical miner is detached, and platform for blasting is mounted in its place. Further deepening of the shaft (with tubing lining) is conducted using a blasting method.

When the floor of frozen zone is reached the type of lining is changing, from now concrete type of lining is used (and in some special places that are vulnerable reinforced concrete is used). As a consequence of such approach the technology of shaft sinking has to be changed (technology II), what

results with some changes in sinking stage equipment. Assembly ring for the tubings is detached and in its place steel formwork is attached.

In both technologies all tasks are done from triple deck sinking stage (fig. 3). Loading of the blasted material is done by shaft mucker (fig. 3), which is attached under the third deck of the stage. In this method drilling is done with pneumatic drillers and Deilmann-Haniel shaft driller.

Figure 3 – Mechanical miner (left) and shaft mucker (right)

Technology I

This type of technology is used for frozen soils (Ia) and frozen rocks (Ib). In the soils the diameter of the shaft opening is equal 9.22 m (in soils), and in rocks it is 9.3 m (the dimension of the opening is strictly connected with the thickness of the lining). The difference in the diameter is due to different type of rock extraction method that is used in both cases. Equipment that is used during the frozen rock mass excavation needs more space in the shaft. Process starts with drilling the shaft bottom with mechanical miner (frozen soils with uniaxial compressive strength up to 20 MPa). When the shaft bottom is drilled up to necessary deepness, then the material is loaded into the buckets with shaft mucker. When the shaft bottom is prepared, and relatively flat, then the assembly ring for tubings is lowered down, and located at the shaft bottom. Afterwards it is used to assembly tubings into a ring. When the ring is mounted, then the hydraulic actuator is expanding to lift the assembled ring and connect it with the one from previous technological cycle with bolts. In the last phase of this cycle the concrete backfill is pumped behind the tubings. In this technology whole cycle lasts 24 hours (9 hours for drilling frozen soils with mechanical miner, and transportation the material to the surface included) (Fabich and oth., 2010).

Each cycle in technology Ib (in cohesive frozen rocks with drilling and blasting method) starts with cleaning the bottom of the shaft, and then drilling the blast holes is performed. In this technology the diameter of the opening is equal 9.3 m (dependent on the shaft lining thickness). When the blasting is completed, the extraction of the material from the shaft bottom is done with shaft mucker. The material is transported to the surface with buckets. When the shaft bottom is levelled then the assembly ring for tubings is lowered down and tidily fastened at the shaft bottom. When the tubing ring is assembled, then is lifted to connect it with the one mounted in previous technological cycle. Afterwards the concrete backfilling is pumped behind the tubing ring. Full cycle lasts 36 hours, while average time needed for drilling the drill holes for blasting, blasting itself, and transporting the material to the surface lasts 21 hours. (Drilling and blasting lasts about 8 hours) (Fabich and oth., 2010).

Technology II

When the frozen rock mass bottom is reached, the type of the lining is changed. There is no necessity to use waterproof lining in unsaturated with water rock mass. The change of the lining type is connected with necessity of different technology usage. In this technology tasks that are carried out contain drilling and blasting for one concrete segment assembly (3.5 m). The diameter of the opening is strictly dependent on the shaft lining thickness (for example for lining 0.6 m it is 8.7 m). In the first phase of this cycle the blast holes are drilled for depth ranging from 3.2 to 3.6 m. Then the blasting is performed.

Afterwards the extraction from the shaft bottom is done with shaft mucker. When the bottom of the shaft is cleaned, then the formwork (slip ring) is mounted. The height of this ring is 3.5 m. When everything is stabilised and tidily fastened, then the concrete is pumped behind the formwork. The thickness of this lining is usually 0.6 m. In some parts of the shaft reinforced concrete is used. It is done especially at connection between the shaft and the development levels of the mine (inlets). Typical cycle in this technology lasts about 56.8 hours (drilling and blasting, transporting the material to the surface lasts 43 hours, drilling and blasting lasts 13.3 hours) (Fabich and oth., 2010).

ANALYSIS OF TECHNOLOGICAL SOLUTIONS IN REGARDS OF SHAFT SINKING CRITICAL PATH

The analysis of the sinking process technological solutions, to select the most relevant in regards of its duration, was performed in two stages. In the first one, typical schedule of shaft sinking was developed. It was based on the experience gained during previous shaft sinking. In the second stage, technological processes that are influencing overall sinking period duration were separated from the schedule.

Typical schedule for shaft sinking

In the first stage typical schedule for shaft sinking was developed. This was based on example on shaft that has been sunken in December 2013. Total duration of this shaft sinking was 1989 days. Shaft depth was 1219 m, so the average, the daily progress of the sinking was 0.61 m/d.

Technological solutions with the highest influence on shaft sinking

Activities that have the biggest influence onto shaft sinking process were divided into two main subgroups:

- Directly related to the sinking progress (shaft sinking using different technologies). This subgroup includes following shaft items:
  - excavations;
  - shaft lining
  - concrete curbs;
  - shaft stations (with lining);
  - shaft bottom.
- Indirectly related to the sinking progress. This subgroup includes following items:
  - assembly and disassembly of the equipment in the shaft,
  - drilling boreholes,
  - installation of elements of the drainage system,
  - building a temporary reinforcement, etc.).

Full analysis of those activities indicates that the technological operations directly related to directly to the sinking progress occupy about 66% of the total sinking time. Other activities related indirectly with shaft sinking that must be implemented to provide safe operation and to meet all quality standards that were introduced within technical documentation of the shaft sinking engineering, occupy a total of about 34% of the total time spent on shaft sinking (Fabich and oth., 2013).

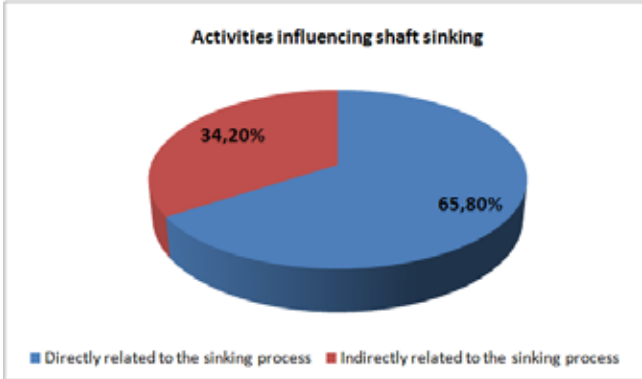

Figure 4 Activities influencing shaft sinking

Further analysis of all activities related to the shaft sinking process (both direct and indirect) shows that the activities connected with shaft sinking with usage of technology I (with tubing lining and both KDS-2 mechanical miner and drill and blast method) are influencing total shaft sinking duration mostly – it takes approximately 31.5% of that time. This duration is strictly connected with the length of the shaft that is done with this technology (almost 55% of total shaft length). The second technological activity in terms of its duration (almost 15.4% of the total time) is the grouting of tubing lining. This operation is not affecting shaft sinking process directly; nevertheless it is required to deliver proper connection between shaft lining and the rock mass and in the end is required to provide safe operation of the shaft in the future and to reduce its maintenance. Assuming that there is a very close relationship between the construction on the column tubing and it's grouting, both activities occupy a 47% of the total shaft sinking time.

Other activities that are significant in terms of its duration are:

a) activities directly affecting sinking rate:
   - Shaft sinking with concrete lining – 10.2%;
   - Shaft sinking in rock salt – 9.2%;
   - Shaft stations performing – 7.4%.

b) activities indirectly affecting sinking rate:
   - Assembly and disassembly of shaft equipment (collar steel, working stage, service stage, mechanical miner, tubing assembly ring, shaft form) – 6.5%;
   - Test boreholes drilling – 4.1%;
   - Installation of temporary sinking equipment in the shaft – 3.0%.

Figure 5 All activities related to the sinking process

Further analyses of the schedule were focused on detailed tasks in each particular subgroup of the activities (directly and indirectly related to the shaft sinking process).

In the subgroup of activities directly related to the shaft sinking, the one with the highest impact on the sinking duration was shaft sinking with mechanical miner (technology Ia). This activity took 23% out of total time of activities directly related to shaft sinking. The second one in terms of its duration was shaft sinking with tubing lining with drill and blast method (technology Ib). It took 20% of those activities total duration. In general shaft sinking in frozen zone is the longest operation out of all directlu related to shaft sinking, and it takes about 43%.

With an assumption that the zone below the frozen rock mass does not require pre-grouting, the third in terms of its influence onto the sinking duration is technology II.1 (sinking with concrete lining). This activity lasts about 15.4% of the total time for activities in this subgroup. Together with concrete curbs (technological foot) and technological niches, which are located within concrete lining, those operations cover more than 22% of the total time for subgroup I (directly related to shaft sinking) activities.

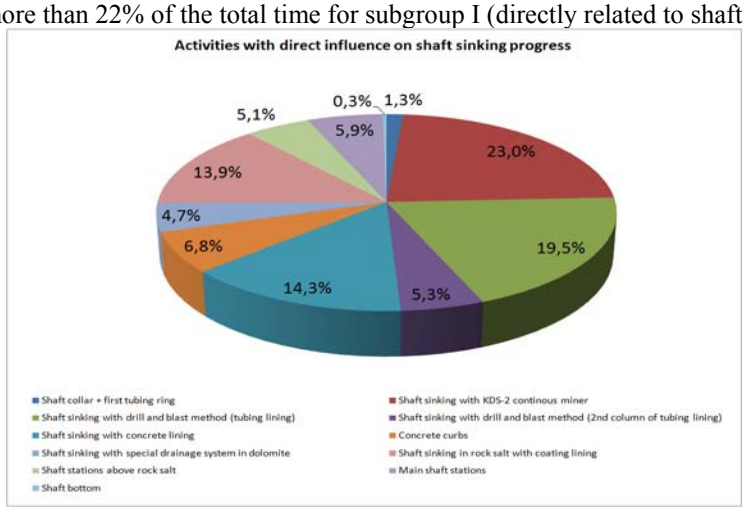

Figure 6 Activities with direct influence on shaft sinking progress

In the subgroup II (activities indirectly related to shaft sinking) activity that has the biggest influence is the grouting of the tubings. Both stages (II and III) of grouting occupy more than 45% of total working time provided for activities directly related to the progress of shaft sinking. The second in terms of its duration is drilling of test boreholes. This activity takes almost 12% of the time in the subgroup II. Other operations, mainly assembly and disassembly of the shaft equipment, as well as temporary shaft equipment for sinking installation here are of marginal importance.

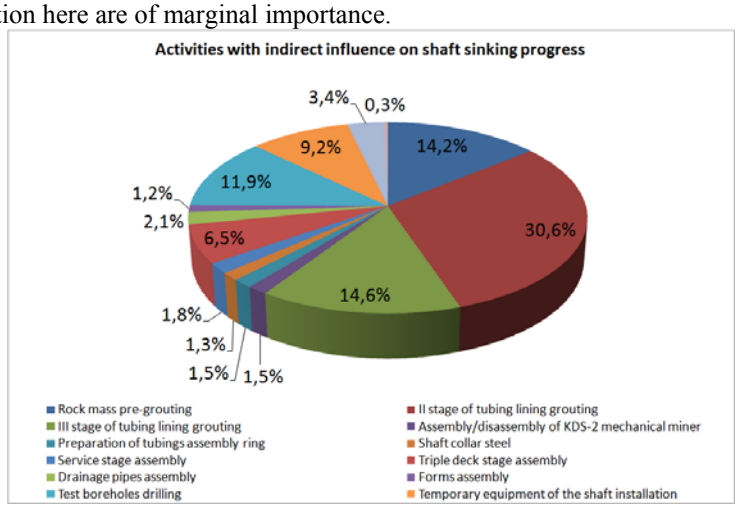

Figure 7 Activities with indirect influence on shaft sinking progress

OPTIMIZATION OF CURRENTLY USED SHAFT SINKING TECHNOLOGY

Current technology of shaft sinking in LGOM was designed for specific hydro-geological conditions. This technology was developed more than 40 years ago.

According to safety of the shaft sinking this technology is proven, and assure full security of processes. Obstacles that show up during the process are triggered by variety of hydro-geological conditions, and relatively low identification of local hydro-dynamical conditions, even though brand new technologies are used to recognise it. Nevertheless, additional methods of rock mass recognition during the shaft sinking (long-hole drilling from the bottom of the shaft) are very efficient, and allow making good decisions to fulfil all safety requirements. It has to be remembered that technologies shown in this paper epitomizes some shortcomings – mainly about the efficiency of drilling in cohesive rocks (time is really an issue in this method).

Main obstacle in gaining correct progress times is connection between the bottom of the shaft and need of lining assembly (necessity of settling down the assembly ring for tubings as well as hydraulically extended slip ring (formwork) for concrete lining at the bottom of the shaft). Another obstacle is the necessity of using the drilling and blasting method in cohesive rocks (which has the biggest influence for efficiency). Cycle times that are achieved in technology Ia with KDS-2 mechanical miner in comparison with technology Ib with drilling and blasting method of rock extraction are almost 12 hours shorter. It is quite significant difference and it is caused only by the method of rock extraction. Taking into consideration depth of cohesive frozen rock (more than 360 m) in currently sunken shaft as well as in the shafts that will be sunken in the near future, it can be assumed that currently used technology will allow shortening the process for about 120 days. The main goal is to achieve 1.5 m/day progress of shaft sinking in cohesive frozen rock mass. It may be achieved by introducing mechanical rock extraction (similar to the one that is currently used for non-cohesive frozen rock). It has to be suited for geological conditions of LGOM area (rocks with strength up to 100 MPa).

Following items have been identified for possible optimization in technology I.1:

c) modernization of the mechanical miner;
d) modifications of tubing assembly ring;
e) hanging tubing assembly ring on DYWIDAGs rather than positioning it on a shaft bottom;
f) optimisation of organizational items (combining periodic technical check of the continuous miner, with concreting of the space behind the tubings);

Introducing those items into the process will allow to gain 7.25 h per cycle. Base on this the sinking rate should be around 1.78 m/day (0.47 m/day more than in current technology).

Following items have been identified for possible optimization in technology I.2:

g) the introduction of mechanical mining in frozen hard rock using the modified mechanical miner;
h) modifications of the assembly ring;

Introducing those items into the process will allow to reduce cycle time to 26 hours. Base on this the sinking rate should be around 1.64 m/day (0.62 m/day more than in current technology).

Technology II brings up similar problems. Recalculating current shaft sinking progress (56.8 hours/3.5 meters of shaft) for the 1.5 meters long segment (just to make it comparable with technology I) cycle time lasts 24.3 hours, with almost 18.4 hours needed for drilling, blasting, and transporting the material to the surface. It gives almost 5.7 hours for drilling and blasting. Introducing mechanical rock extraction in this technology would also cause decreasing in rock extraction time from 18.4 hours to 12.7 hours, and also decrease overall cycle time (1.5 m segment) to 18.6 hours. After recalculation to 3.5 meter segment (real one) cycle time will last 43.4 hours. Taking into consideration that average length of shafts sunken in technology II is about 300 – 600 m, such a change will decrease the whole sinking time for additional 50 – 100 days (Fabich and oth., 2010).

Following items have been identified for possible optimization in technology II:

i) new form construction with new way of attachment under the stage;
j) construction of a new working stage, to allow performing concrete works from central deck.

Introducing those items into the process will allow reducing the sinking rate to 2.0 m/day (0.69 m/day more than in current technology).

Among the processes indirectly linked to the progress shaft sinking the greatest effect will be achieved by optimizing following items:

- optimisation of test boreholes drilling, that will include following items:
  - the parallel use of two drilling rigs;
  - increasing the length of the boreholes;
  - changing the way of the coring drilling, with emphasis on the application of the wireline drilling;
  - elimination of core drilling in unsaturated layers;

  With all those optimisations it is possible to achieve 33% at activities duration.
- reduction of tubing grouting;
  - improvement of tubings horizontal flanges sealing, due to modification of the traditional sealing method (with lead), with new addition of polyethylene gasket;
  - limitation of tubing grouting phase II scope only by concrete plugs (instead of both concrete and cementing plugs);
  - parallel grouting with two sets of pumps;

  With all those optimisations it is possible to achieve 39% at activities duration.
- Parallel process of temporary shaft equipping while sinking (with accordance to safety regulations).
  - equipping of the shaft in a prolonged series (from ~ 80 to ~ 120 m);
  - adjusting the length of the individual shaft equipment elements to the technological solutions of shaft sinking;
  - Use quick couplers in terms of connecting both pipelines and shaft brackets;

  With all those optimisations it is possible to achieve 67% at activities duration.

Activities that are related directly and indirectly to the shaft sinking process, are repetitive in a technological cycles. It should therefore strive to shorten the duration of a particular technological cycle, by analyzing each activity falling within the scope of that cycle. Reducing the total time of one cycle, in conjunction with the number of executed cycles will cause reduction of overall shaft sinking process.

In general, efforts should be made to ensure that above activities implemented under each of these processes should translate into increase of their productivity, which can be met by reducing the duration of the individual steps that make up these processes. The proper course of action, giving the greatest effect is the parallel performance of some activities.

SUMMARY

To summarize the current state of knowledge which is derived from the experience of many generations of engineers and technicians that were dealing with polish copper mines shafts sinking it has to be stated that currently used technology guarantees safety during shaft sinking. This is extremely important due to more and more difficult geological conditions that are appearing within new shafts (greater depth, as the mines go deeper).

The weakness of the currently used technology is the duration of shaft sinking. It allows sinking 1220 m deep shaft in about 1990 days, giving a mean sinking progress ratio of 0.61 m/day.

According to the analysis that was made, it is possible to accelerate that process, with using a current technology. However, this may be achieved by reducing the duration of some technological activities. Among all analyzed activities those with biggest influence on shaft sinking process are:

a) Activities directly related to shaft sinking:
   - Shaft sinking with tubing lining (frozen): - 31.5%;
   - Shaft sinking with concrete lining - 10.2%;
   - Shaft sinking in rock salt - 9.2%;
   - Shaft stations - 7.4%;

b) Activities indirectly related to shaft sinking:
   - tubing lining grouting (II and III phase) - 15.4%;
   - assembly and disassembly of the equipment in the shaft - 6.5%;
   - test boreholes drilling - 4.1%;

- temporary sinking equipment installation - 3.0%.

The analysis of all activities that are performed during shaft sinking has shown that more than 34 percent of total sinking duration is connected with activities indirectly related to shaft sinking process.

Currently highest sinking rate (1.31 m/day) is achieved with the technology used for shaft sinking in frozen soft rock mass with usage of mechanical miner. This rate is also observed below the frozen rock mass where drill and blast method of sinking is used. In case of shaft sinking in frozen hard rock the rate is about 1 m/d. This difference is caused by extended time of drilling and blasting regimes in compare with lack of those with mechanical miner. In dolomite where special drainage is used, the sinking rate is about 0.55 m/day. It is caused by serial system of works. First sinking with initial bolt lining is done, then special drainage system is installed, and finally permanent concrete lining is applied. The lowest sinking rate in the shaft is observed within the shaft stations. This has a value of 0.18 m/day. This is natural, as stations are developed horizontally, not vertically.

Tubing lining grouting has the highest duration among indirect activities of shaft sinking. Average rate of this process is about 2.1 tubing ring per day.

Installation of temporary shaft steel is carried out with an average progress of about 18.4 m/day, and the progress of test boreholes drilling is a little over 20 m/day.

Company that currently is the primary contractor of shafts sinking in polish copper mines has experienced, trained staff, basic technologies and the most suitable equipment to perform the tasks arising from the changes in the currently applied technology. The most important of these changes are:

- modification of work organization, with emphasis on the introduction of parallelism with regard to safe conditions for their conduct;
- maximization of time usage effectiveness;
- modification of sinking bucket – increase its capacity to $5m^3$;
- modification of buckets loading process – usage of 2 loaders (muckers), and three or four buckets (two of them are loaded at the shaft bottom);
- modernization of continuous miner to be able to use is in hard frozen rock;
- drilling blast holes with modular jumbo (triple or quadruple);
- used technology bolting shaft walls in parallel with rock loading after blasting;
- changes in working platform – adjustment the number of decks, connecting with shaft form to allow parallel execution of some processes;
- changes in shaft form design – form height, its installation method, its bottom sealing, its suspension, its cooperation with Dywidag bolts;
- changes in tubings assembly ring – ensuring full cooperation of assembly ring with modernized mechanical miner and Dywidag bolts as well as its integration with working platform decks.

Mentioned modifications of currently used technology will allow shortening duration of the activities related to shaft sinking for about 22%. Thus, for example, the use of these solutions in previous shaft would allow for shorten it's sinking for about 440 days (~ 14.4 months).

REFERENCES

Fabich S. and others. (2013) *Post-completion SW-4 shaft documentation"* (not published), Wroclaw.
Walewski J. (1965) *Rules for mines design. Part V. Designing of shafts (in Polish).*
Fabich S. and others (2010), *Technical design of SW-4 shaft sinking* (in Polish) (not published)
Piestrzyński A. and others (2008), *KGHM Monography, second edition* (in Polish)

DESIGNING OF LONGWALLS WITH HIGH OUTPUT CAPACITY IN THE VERY GASSY HARD COAL SEAMS

E.Krause[1], J.Skiba[2]

[1]*Assist. Prof. Ph.D.Eng, Central Mining Institute (GIG), Poland, 40-166 Katowice, Pl. Gwarkow 1, tel.: +48 323246603, +48 323246501, (*Corresponding author: ekrause@gig.eu)*

[2]*Ph.D.Eng , Central Mining Institute (GIG), Poland, 40-166 Katowice, Pl. Gwarkow 1, tel.: +48 323246603,*

24th World Mining Congress
MINING IN A WORLD OF INNOVATION
October 18-21, 2016 • Rio de Janeiro /RJ • Brazil

DESIGNING OF LONGWALLS WITH HIGH OUTPUT CAPACITY IN THE VERY GASSY HARD COAL SEAMS

ABSTRACT

Exploitation of the coal seams in Polish hard coal mines, in the conditions of: increasing with exploitation depth methane content of deposits, growing output capacity - results in continuously higher methane emissions into the exploitation workings.

Increased methane emissions into the environment of the longwalls, in the conditions of growing coal output capacity, require calculation of several versions of methane emissions' forecasts, at the stage of designing coal exploitation for such a variable parameters like: length of the longwall and its average daily exploitation progress. The calculated values of forecasted methane emissions into environment of the longwall, together with analysis of ventilation potential and technique of methane drainage to be applied will constitute basis for determining output capacity of the longwall.

Besides, designing of highly concentrated coal output in the very gassy coal seams is also heavily connected with adjustment of proper method and parameters of longwall ventilation as well as scope of methane prevention in order to provide safety work conditions for the miners.

KEYWORDS

Exploitation of the coal seams, longwall, coal output efficiency, methane emissions, ventilation, methane drainage

INTRODUCTION

Exploitation of the hard coal from the increasing depth, in the coal seams with growing methane content and with continuously higher output capacity substantially resulted in higher methane emissions - mainly into the exploitation workings of the longwalls. Increase of output capacity, which can be clearly seen in Polish hard coal mines in the last two decades was the result of successive increase of the longwalls' length and implementation of highly efficient coal shearers. In the longwalls located in the highly gassy deposit, increase of absolute methane-bearing capacity of the longwalls in the conditions of applied active prophylactics, based on the ventilation and drainage was very often too high - forcing limitations in output capacities of the longwalls.

The results of the research conducted by Central Mining Institute of Katowice confirmed, that in the conditions of increased output capacity in the gassy coal seams share of methane released to the gob zone of the longwalls as a result of degassing the overlying and underlying seams is increasing when comparing with total methane released into the environment of the longwall. Influence of the coal output capacity on the development of methane hazard in the longwalls located in the gassy coal seams was discussed in the following papers: [7], [9], [4] i [2].

Designing of highly concentrated coal exploitation in the longwalls located in heavy gassy deposit should be preceded by forecasting of methane release volume, analysis of ventilation capacity and drainage effectiveness – finishing with determination of coal output capacity of the longwall only then [3], [5] i [6].

The source of methane release into the environment of the longwall during coal exploitation are:

- exploited coal seam,
- underlying and overlying coal seams, which are under exploitation release caused by operated longwall having released their desorptive methane resources.
- post-exploitation gobs from previous exploitations, conducted with the environment of exploited coal seam.

The underlying and overlying seams under exploitation release of the longwall, their methane content and distance from the exploited seam have impact on the volume of released methane resources migrating into the environment of the longwalls' gobs.

Volume of the underlying and overlying seams released by conducted exploitation depends on the length and inclination of the longwall and its exploitation progress. Depth of the longwall and its inclination have direct impact on the range of degassing and size of degassing zone cross-section.

The ranges of the underlying and overlying coal seams' degassing for the longwall's length L_s from the interval 0-400 m and its inclination α in the range 0°-50° are shown on the nomogram – figure 1. Determination of the exploitation release based on the length of the longwall and its inclination angle allows to identify underlying and overlying coal seams being under degasification range, as well as those which should be considered when forecasting methane release into the environment of the longwall [8].

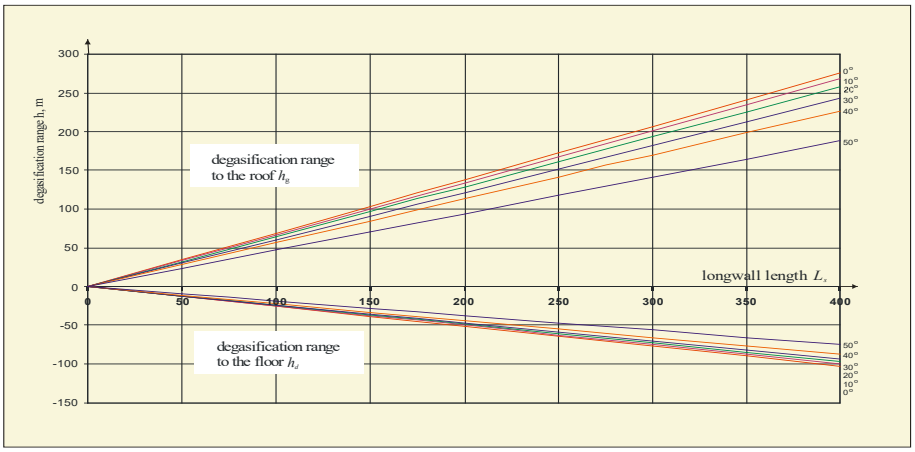

Fig. 1. Range of degassing the overlying and underlying seams according to the length of the longwall and its inclination angle [8]

Length of the longwall has the biggest impact on the volume of the released deposit over and under the exploited coal panel and in consequence on the volume of released methane to the environment of the longwall's gob. The empirical interrelations enabling to calculate ranges of the releases: h_g and h_d according to the parameters L_s and α were shown in the paper [11]. Increase of the output capacity due to the increase of the longwall length, substantially affects quantity of the methane release into its environment.

Together with the increase of the longwall length from L_1 to L_2 (fig.2) there is an increase of cross section through the desorption zone and in consequence volume of increased deposit increase over and under exploited coal panel. Increasing the longwall length from L_1 to L_2 results in the increase of the cross section through the deposit, what has direct impact on the volume of the deposit being degasified adjacent to the longwall and on the volume of released methane. For the longwall length L_1 the exploitation release reaches up to the overlying seams p_1, p_2 and p_3, however for the length L_2 range of the release reaches up to the seams p_1, p_2, p_3, p_4 and p_5.

For the longwall length L_1 the exploitation release reaches (degasify) underlying seam n_1 and when increasing longwall length up to L_2 it reaches seams n_1 and n_2.

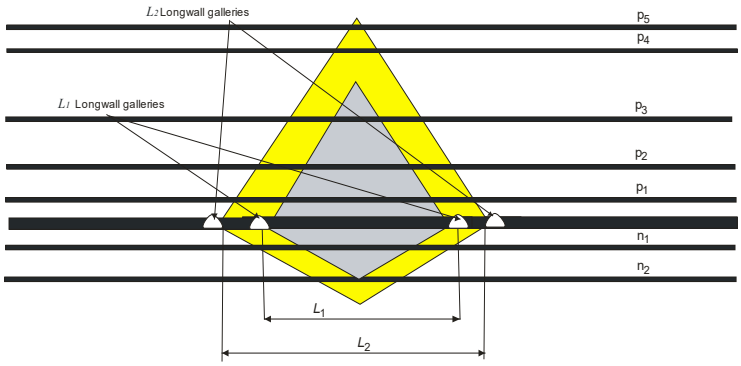

Fig. 2. Vertical cross section through the desorption zone of the longwalls with the lengths: L_1 and L_2: p_1, p_2, p_3, p_4 and p_5– overlying seams, n_1 and n_2 – underlying seams [2]

It can be concluded, that length of the longwall has substantial impact on the volume of released methane being consequence of degasification of the overlying and underlying coal seams.

The results of the forecasting calculations conducted for the designed longwalls with two lengths of 200 m and 300 m, i.e. longer by 50% in the same conditions confirm almost twofold increase of forecasted absolute methane-bearing capacity i.e. by almost 100%.

FACTORS HAVING IMPACT ON THE ACCURACY OF METHANE RELEASE INTO ENVIRONMENT OF DESIGNED LONGWALLS' FORECASTS CALCULATIONS.

In the conditions of growing output capacity, in the very gassy coal seams, precisely elaborated forecast has impact not only on the safety exploitation conditions but also on the designed output capacity of the longwall.

Each of applied methane release into environment of designed longwall forecasting methods should be based on the parameters obtained during precise recognition of geological and gassy conditions in the surrounding strata of designed exploitation. Forecasts of methane release into environment of the longwall are often connected with certain miscalculations resulting from not very proper input data assumptions, in specific concerning thickness of underlying and overlying coal seams and their methane contents.

Determination of methane content distribution both: in the exploited coal seam as well as in the underlying and overlying coal seams has substantial impact on the results of forecasts of methane release into environment of the longwall calculations. Methane content values in the exploited coal seam are identified based on the tests conducted during development works contouring the coal panel plot.

In the conditions of high mining speed of heavy gassy coal seam the issue of longwall's output capacity depends on its methane content and mining speed of the shearer. Designing of the longwall's coal output capacity with high output capacity should include mean methane content distribution along the coal panel length, duration of one shearer's cut and ventilation capacity of the longwall.

Forecasting of methane emissions from the exploited coal seam's coal is getting even more important in the conditions of high output longwalls. Calculation of the methane release during coal exploitation forecast must be based on the precise methane content of the exploited coal seam recognition in the plot of the exploitation length of the coal panel.

Methane content distribution in the plot of designed coal panel

During development works of the workings surrounding coal panel plot, in the distances of every 200 m or smaller, according to binding mining law regulations, the coal seam methane content sampling tests are being conducted and its results are recorded on the coal seam maps.

According to elaborated forecasting of methane release into the longwall environment algorithm the mean methane content in the individual cross sections of the coal panel length as well as its distribution along coal panel length are being determined [8].

In the coal seam, where the coal exploitation is being planned boarder coordinates of the coal panel plot are electronically introduced into the grid of contractual coordinates' system, where the axis of abscissae is in accordance with the direction of longwall mining (along with coal panel length), and axis of ordinates is in accordance with the direction of longwall mining. On the plotted workings the results of methane content measurements are being recorded, in order draw methane content isolines. Coal panel length is being divided into plots with the lengths of 100 m or smaller. For each plot, the axis crossing the cross section in its middle is being determined. It is being used to calculate mean methane content for individual cross sections. It is calculated as an arithmetic mean for the coal panel 50m length sections. Following interrelation is being used :

$$M_{mean} = \frac{\sum_{i=0}^{i=n} \frac{(M_i + M_{i+50})50}{2}}{L_s} + \frac{\frac{(M_n + M_k)k}{2}}{L_s}, \ \mathrm{m^3/T_{daf}} \qquad (1)$$

where:

M_i – methane content on the cross section line in the point of i–division of the longwall length, m^3/T_{daf};

M_{i+50} – methane content on the cross section line in the division point $i+50$, m^3/T_{daf}; etc.;

M_k - methane content on the cross section line in the point k crossing with the longwall side working if k<50 m, m^3/T_{daf};

$k = L_s - 50 \cdot n$ – length of final section of the longwall, m;
n – number of 50-m sections dividing longwall;
i – another 50 – m section of the longwall length;
L_s – longwall length, m
Method of mean methane content calculation in the single cross section is shown on fig. 3. As a result one can get horizontal distribution of exploited coal seam methane content along the length of coal panel.

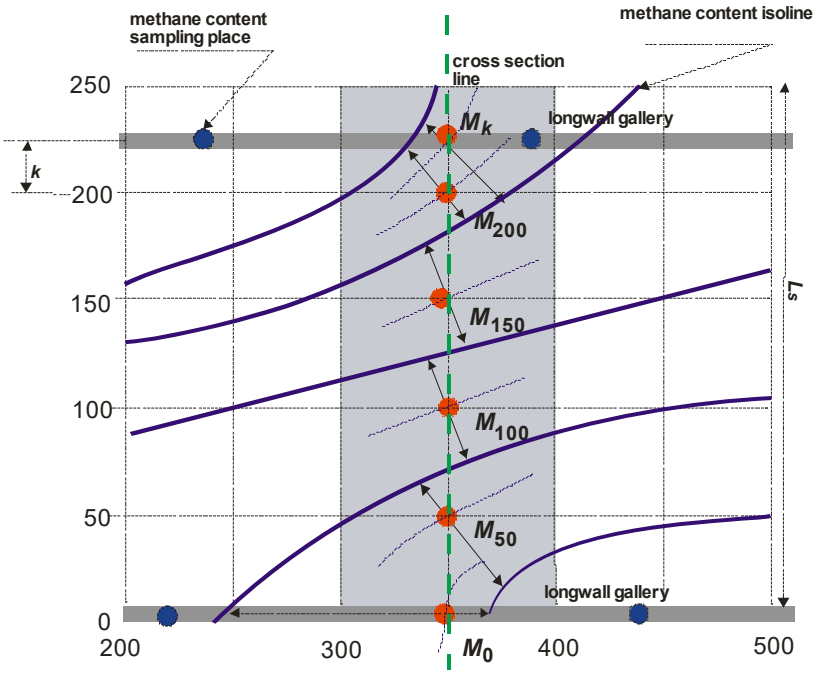

Fig. 3. Determination of mean methane content $M_{śr}$ for single cross section: L_s – length of the longwall, k – length of final section of the longwall [8]

An example of prepared mean methane content distribution M_{mean} on designed coal panel length is shown on fig. 4. At the beginning of 450 m coal panel length mean longwall methane content M_{mean} in the following cross sections is between 3.850 - 4.560 m^3CH_4/T_{daf}. In the further part there is gradual drop of the mean methane content of the coal seam down to 0.450 m^3CH_4/T_{daf}.

In the conditions of conducting coal exploitation with the transverse system to the rise beginning of coal panels' exploitation starts in the heavy gassy seam and then gradually decreases together with the progress of exploitation, which can be seen on fig. 4. Change of the seam's methane content can also occur along length of the coal seam. In the high capacity of coal output distribution of methane content is getting even more important when forecasting methane release.

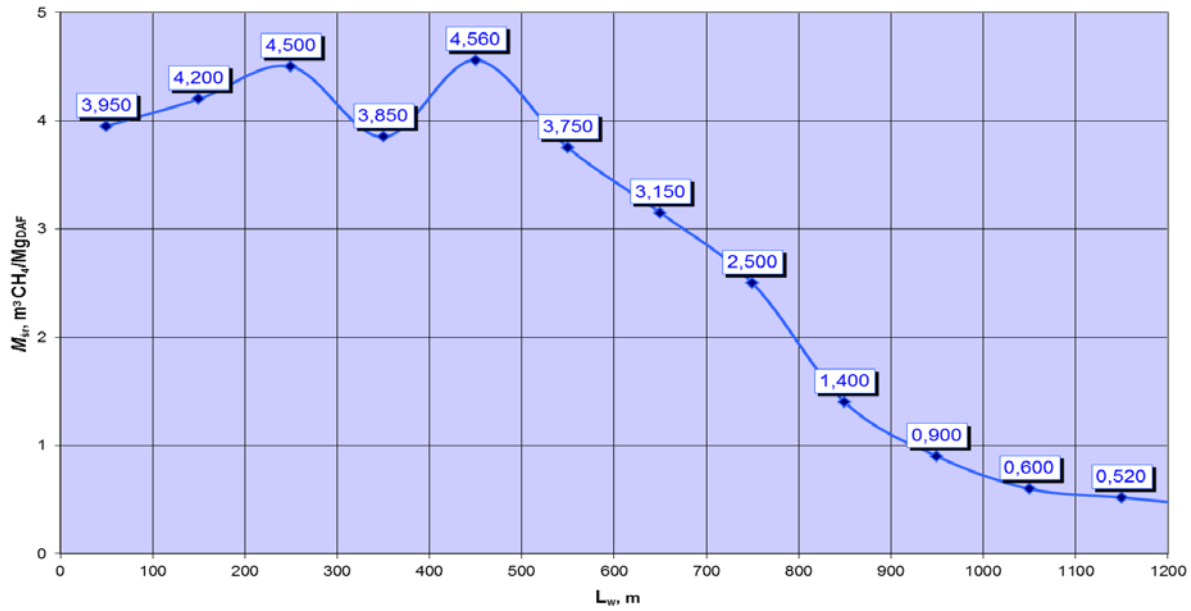

Fig. 4. An example of mean methane content distribution M_{mean} along designed coal panel length L_w

Forecasting of methane release from the exploited coal seam by coal shearer

Values of mined coal methane content in the beginning of exploited coal panel are lower than those determined by the primary methane content M_o sampling tests performed during development works of the galleries surrounding the coal panel plot, and in consequence also lower than distribution of mean methane content M_{mean} along the designed coal panel length (fig. 4).

The research enabling to estimate methane content of the coal seam mined by the shearer are based on the several tests performed in the coal seams with the methane content varying from 2.5 to 8.0 m^3CH_4/T_{daf}. The samples were collected from the longwall face as well as from the following distances ahead of it: 1, 2, 3, 6 and 12 m and then their methane content was determined.

Based on the analysis of the exploited coal seams' methane content tests results ahead of the face [4] the exploited by the shearer coal seam degasification function η_s depending on the primary methane content M_o was determined. M_o was determined during developing works of the longwall galleries. Estimated value of η_s can be described by the following formula

$$\eta_s = 8.354 \cdot M_o^{0.67} \qquad (2)$$

Changes of degasification coefficient η_s of the exploited coal seam before and after coal exploitation depending on the primary methane content M_o are shown by the continuous line on fig. 5.
Dashed line shows total interrelation between the degasification coefficient of the exploited coal seam η from its primary methane content M_o and can be expressed by the following formula

$$\eta = 18.355 \cdot M_o^{0.504} \qquad (3)$$

Above interrelation is based on the methodology concerning methane release into the environment of the longwalls elaborated in the Experimental Mine „Barbara" [1].
The course of the function described by formula (2), continuous line on fig. 5, enables determination of coal degasification coefficient η_s depending on primary methane content M_o „in situ" of the exploited coal seam.

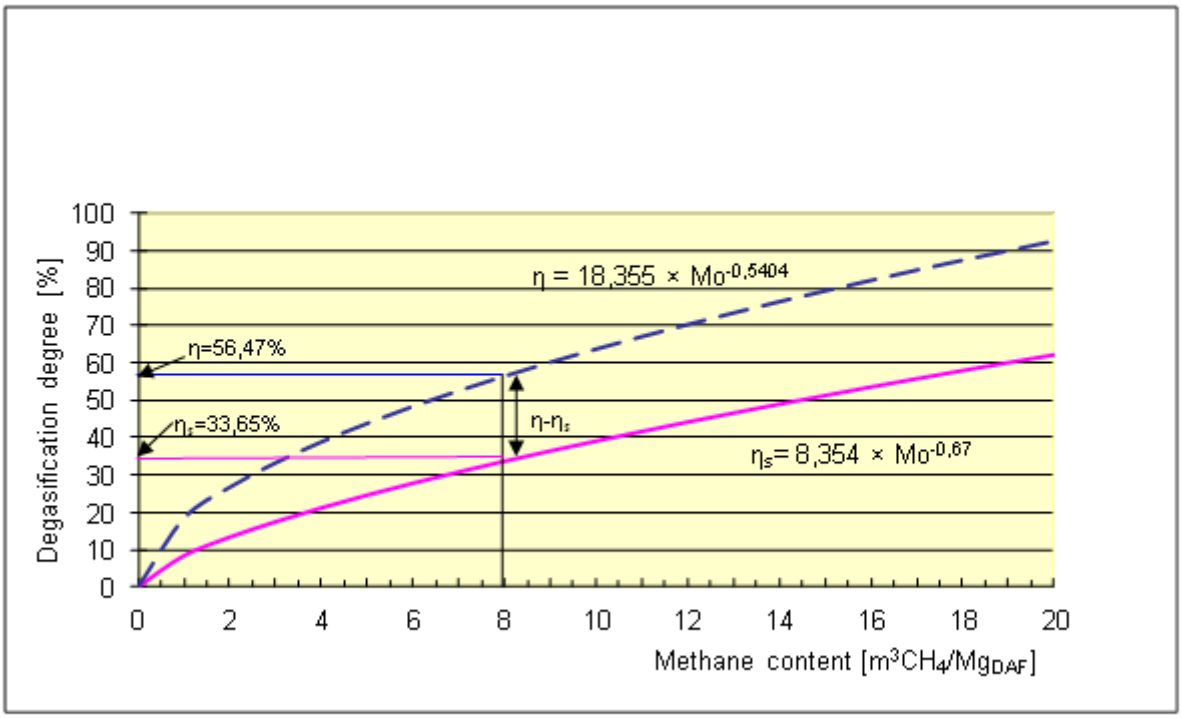

Fig. 5. Degasification coefficient of exploited coal seam mined by the shearer depending on its primary methane content M_o [4]

Having considered function interrelations according to the formulas (2) and (3), it must be stated that, forecasted methane volume released into the environment of the longwall from every single tone of exploited coal can be described as product of $\eta \cdot M_o$, however volume of methane directly released into the longwall when mining by shearer is product of $\eta_s \cdot M_o$. Elaborated interrelation, described by the formula 4, increased accuracy of calculation the forecasted methane release into the environment of the longwall, when mining by the shearer depending on the primary methane content M_o of exploited coal seam.

Considering above, formula (2) should be applied for the calculations of the methane release into the longwall working forecasting, when mining by the coal shearer. On Fig. 5 for determined primary methane content M_o of exploited coal seam, which was 8 m^3CH_4/T_{daf} certain values of degasification coefficient η and η_s i.e. : 56.47% and 33.65% were referred to. Accuracy of methane release to the environment of the longwall during coal extraction forecasts should consider dependence of degasification coefficient based on formula 2.

Forecasted volume of methane released during coal shearer mining should be calculated according to the following formula:

$$V_{CH_4} = \frac{L_s \, m_e \, \gamma \, z \, M_o \, \eta_s}{100 \, t} \qquad (4)$$

where:
L_s – longwall length, m;
m_e – high of exploited longwall, m;
γ - coal thickness, T/m^3;
z – shearer's coal cut, m;
M_o – methane content of exploited coal seam, m^3CH_4/T_{daf};
t – duration of single shearer's cut cycle, min;
however η_s coefficient of exploited coal seam degasification – according to formula (2).

Table below contains results of methane release to the environment of the longwalls forecasts during coal mining. It was assumed, that designed longwall has L_s = 250 m, high m_e = 3 m, and shearer cut z = 0.8 m in the coal seam with primary methane content M_o of 8 m^3CH_4/T_{daf}. The calculations were performed for three cut

duration cycles i.e. : 80 min, 100 min and 120 min. Value η_s was calculated using formula (2), however forecasting of methane release to the environment of the longwall when mining was calculated according to the formula (4).

Forecasts of methane release to the environment of longwall when mining by shearer	
Duration of cutting cycle,	Forecasted methane release to the longwall when mining by shearer (according to formula 4)
80 min	V_{CH_4} = 26.25 m^{3}CH$_4$/min
100 min	V_{CH_4} = 21.00 m^{3}CH$_4$/min
120 min	V_{CH_4} = 17.50 m^{3}CH$_4$/min

Forecasted volumes of released methane were confirmed by underground tests for different shearer cutting cycles' durations verifying to some extend function interrelation of degasification coefficient η_s (formula 2).

In order to conclude it must me stated that partial degasification of the exploited coal seam ahead of the longwall face $\Delta\eta=\eta-\eta_s$ due to the increase of gas permeability of the seam, as well as fracture flow of methane from that seam in the roof strata, in the zone covering „active volume" of rock strata [10], contribute to the decreasing of methane content of exploited coal seam, and consequently to decreasing methane emissions during mining operations. Estimated function of exploited coal seam mined by shearer degasification degree related to its methane content M_o (formula 2), allows for increasing accuracy of conducted calculations forecasted methane release into the longwall environment, what in the conditions of growing output capacity is significant for determination of admissible, safe coal output volume.

Highly efficient coal shearers can be characterized by high cutting speed, what makes the cutting cycle duration shorter. When increasing operating speed of the shearer automatically the coal output capacity is being increased, including volume of methane released during mining to the environment of the longwall what was shown in above table.

Calculated, forecasted volumes of released methane to the environment of the longwall during mining shown in the table allow for calculation of necessary volume of the air to be delivered to the longwall in order not to overcome admissible methane contents of 2% at the output of the longwall.

Assuming coefficient of not stable methane emission during mining process, which can be 1.55 for 3 duration cycles it was calculated the following:

- t = 80 min and V_{CH_4} = 26.25 m^{3}CH$_4$/min, required air flow Q = 2,038 m^3/min;
- t = 100 min and V_{CH_4} = 21.00 m^{3}CH$_4$/min, required air flow Q = 1,617 m^3/min;
- t = 120 min and V_{CH_4} = 17.50 m^{3}CH$_4$/min, required air flow Q = 1,356 m^3/min;

When decreasing duration of shearer's one cut from 120 min down to 80 min, the essential air flow in the longwall must be increased from 1,356 m^3/min up to 2,038 m^3/min. Such a significant increase of the air flow in the longwall, in order to achieve planned output capacity, is very often limited by ventilation capacity of the longwall area.

It must be concluded, that achieving high capacity of coal output in the very gassy coal seams is very often limited by lack of sufficient ventilation capacity.

It is not only methane released from the exploited coal seam, which can be the factor limiting output capacity of the longwall. Significant share in decreasing planned coal output capacity can be also played by methane released from the overlying and underlying seams.

Methane content distribution in the underlying and overlying coal seams

In the overlying and underlying coal seams, which occur within the exploitation release range, dispersed methane content data are most often known, and can be referred to the seams where the development works were performed.

Not very numerous determined methane contents in the underlying and overlying coal seams can be the subject for differences between forecasted and real methane release data.

Method of forecasted methane release to the environment of the longwalls elaborated in Central Mining Institute of Katowice [8] assumes detailed calculation for each individual coal seam or layer and for each determined cross section in the plot of designed coal panel exploitation.

Trends in methane content changes depend on the differences between their determined values in some coal seams and distances between them. It was assumed, that primary methane content of the coal seams is linear function of the depth of occurrence. It is mostly referring to the methane content growing with the depth. It does not mean however that the methane content can always increase with the depth as it also happens that it decreases.

Methane content values of underlying and overlying seams the exploited coal seam are calculated based on the changes of the gradient with the depth by 1 meter.

The methane content gradient is calculated based on the following formula:

$$g_w = \frac{M_d - M_g}{l_k}, \text{ m}^3/\text{T}_{daf}/\text{m} \tag{5}$$

where:

T - primary methane content of the overlying coal seam, m^3/T_{daf},

M_d - primary methane content of the underlying coal seam, m^3/T_{daf},

l_k - distance between the seams determined based on the difference between their spot heights, m.

Positive value of the gradient means that methane content increases with the depth, negative – that it decreases.

Primary methane content of each intermediate seam is being calculated according to the formula (6):

$$M_i = g_w \cdot \left(c_g - c_i\right), \text{ m}^3/\text{T}_{daf} \tag{6}$$

where c_i- spot height of the intermediate seam floor, m

c_g- spot height of the overlying seam, m

Such an attitude allows to calculate approximate values of methane content in the underlying and overlying seams located within the exploitation release range of the longwall.

An example of simulative primary methane content distribution in the strata is shown on figure 6.

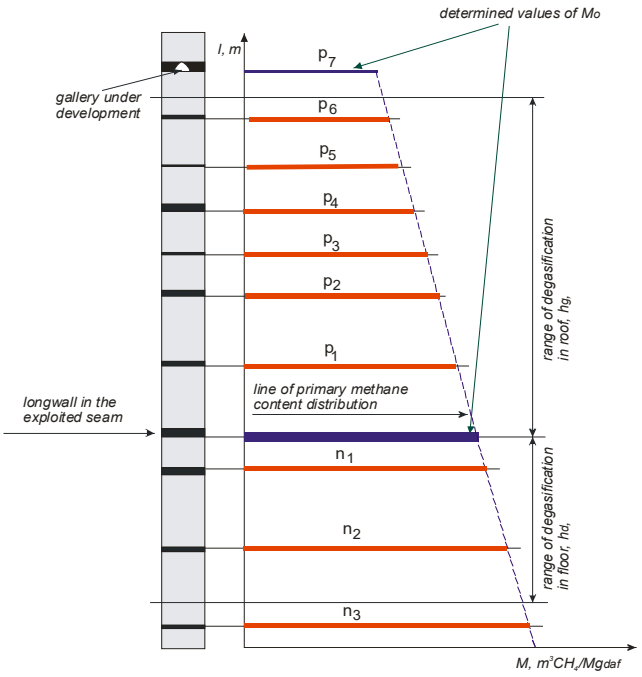

Fig. 6. Simulative vertical methane content distribution M of the seams within the relaxation and degasification zone caused by the longwall: l – distance , p_1 – p_7 – overlying seams, n_1 i n_3 – underlying seams, range of degasifying: h_d – in the floor and h_g – in the roof , M_o – determined primary methane content [8]

Knowledge of degasification degree of underlying and overlying seams in the surrounding of designed longwall function interrelations enables to calculate desorptive methane resources released into environment of longwall's gob.

Degasification degree of the coal seams in the surrounding of designed longwall

Distance of underlying and overlying coal seams from the exploited seam and its methane content have direct impact on the degree of relaxed seam degasification.

Degasification degree of individual overlying coal seams η_{podb} can be determined by general equation:

$$\eta_{podb} = A \cdot e^{B \cdot l_u}, \% \quad (7)$$

where:

A, B - coefficients characteristic for specific conditions,

e - cardinal number.

l_u - assumed distance of the overlying seam from exploited seam calculated based on the formula:

$$l_u = \frac{l}{m_e \cdot \alpha} \quad (8)$$

where l means real distance from the exploited seam, m_e means seam's exploitation thickness (thickness of exploited layer) a α is the coefficient dependent on the gobs' filling method and reaches following values:

- for the exploitation with roof falling - α = 1,
- for the exploitation with dry backfilling α = 0.3 ÷ 0.5,
- for the flushing with deads α = 0.2 ÷ 0.4,
- for the flushing with sand α = 0.05 ÷ 0.15.

For the conditions of Polish coal mines it is assumed that for the overlying coal seams: A=67.71, B= -0.04 [8].

Degasification degree of overlying coal seams can be also determined using coal seams' degasifying curve elaborated in Experimental Mine "Barbara" GIG and shown on fig. 7.

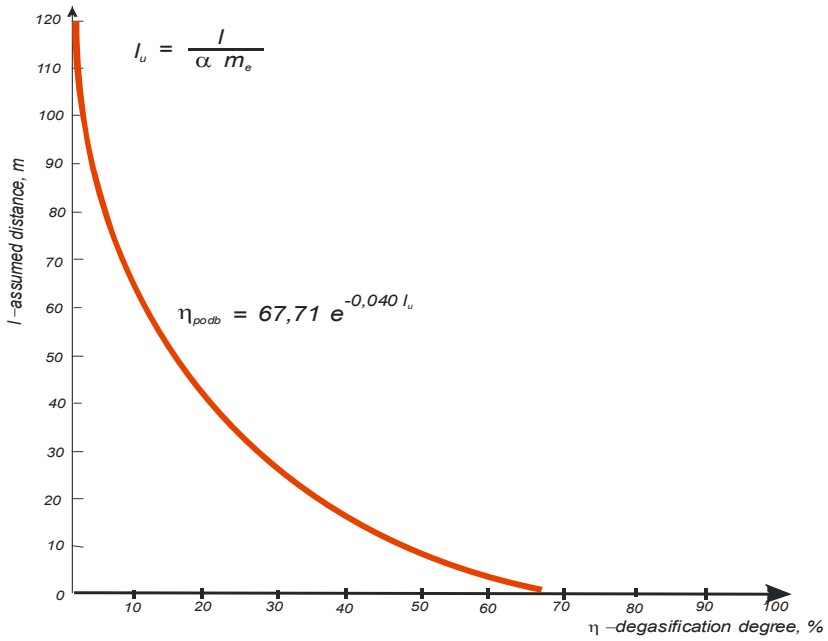

Fig. 7. Coal seams' degasifying curve of the overlying seams and coal layers η_{podb} elaborated in Experimental Mine "Barbara" GIG [1]

Degasification degree of overlying coal seams depend on mainly depends on real distance from the exploited seam and from the thickness of the exploited seam.

In order to increase accuracy of forecasted method with regard to overlying seams, based on the analysis of the research conducted in Experimental Mine "Barbara" GIG, following function was elaborated according to the formula (9):

$$\eta_{nadb} = 75.981\ e^{-0.027\ l} - 4.799 \qquad (9)$$

where l – real distance of the overlying seam from the exploited-one.

Degasification degree of the overlying seams is shown on fig. 8.

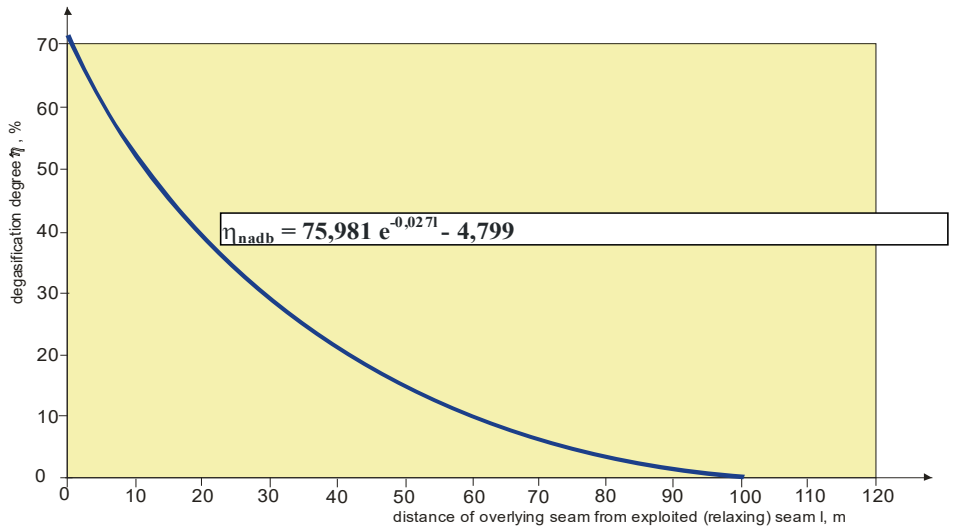

Rys. 8. Coal seams' degasifying curve of the underlying seams η_{nadb} depending on the distance from the exploited seam l [3]

Degasification degree function of the underlying seams, according to the formula (9) increased accuracy of presently used forecasting method [8].

Knowledge of degasification degree of underlying and overlying seams has direct impact on the methane emission value during coal panel exploitation. Accuracy of the methane release forecasts along the length of the coal panel depends properly estimated function interrelations concerning degasification degree of the exploited coal seam as well as underlying and overlying seams in its surrounding.

FORECAST OF METHANE RELEASE INTO THE ENVIRONEMNT OF DESIGNED LONGWALL

Methane release is the process consisting in releasing its desorptive resources from the surrounding strata of the longwall. Kinetics of methane release depends on the longwalls' parameters and its progress as well as on related damage, relaxation and degasification of surrounding deposit, which cause desorption of methane from the coal seams.

In the process of methane release there are following regularities:

- methane from mined coal of exploited coal seam is being released when mining by coal shearer and during coal transportation,
- methane from the longwall cheek is being released within 24 hours (maximum) after its opening by the shearer's cut and has direct impact on degasification of the coal from the longwall cheek,
- methane from the coal seams as well as overlying and underlying layers is being released during relatively long time, and its intensiveness depends on the parameters of the longwall, methane content of the surrounding deposit, from the distance of exploited coal seam and it decreases in the time function.

Forecasting of methane release into the environment of the longwall consists in calculation of absolute methane-bearing capacity i.e. volume of released methane during exploitation in the time unit.

The calculation algorithm of the forecast considers methane release depending on the daily longwall progress. Total methane release is the whole of methane release from the exploited coal seam and from the overlying and underlying coal seams and layers.

Forecasting of methane release volume along the coal panel length, for the mean methane content distribution (fig.4), when assuming longwall progress: 1- 10 m/day, every 0.5 m/day, is shown on fig. 9.

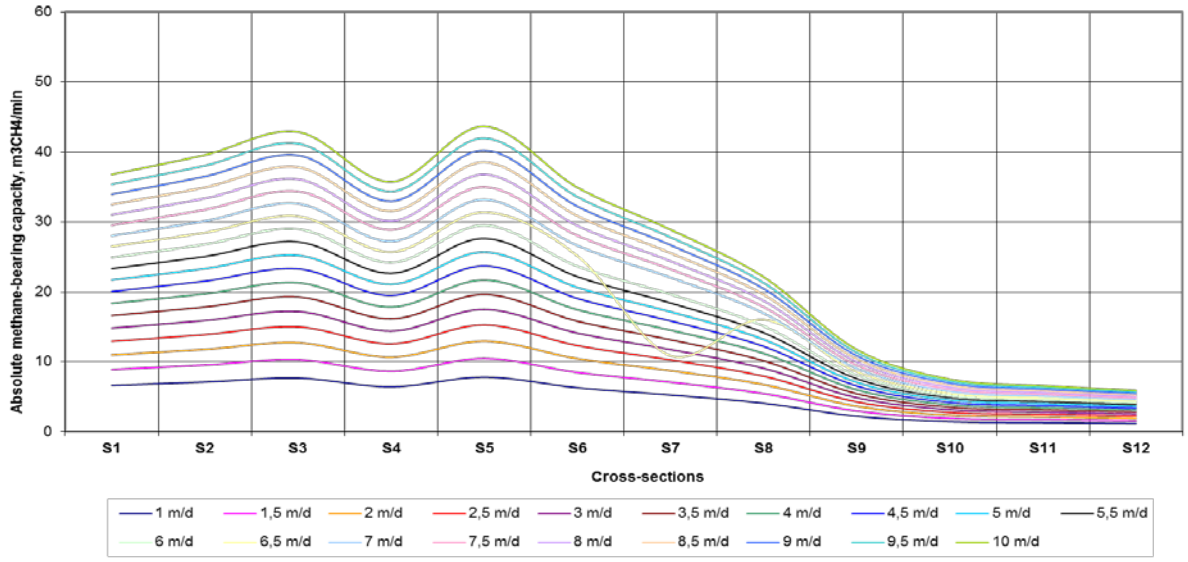

Fig. 9. Graphical interpretation of forecasted absolute methane-bearing capacity of the coal panel 1: $\dot{V}_M$ – absolute methane-bearing capacity, S1–S12 – cross sections.

Dynamic forecast of absolute methane-bearing capacity of the longwalls allows for determination od methane release along designed length of the coal panel in the conditions of different coal output capacity. The

results of the forecasts enable selection of proper ventilation system of the longwall and appropriate methane hazard prophylactics, including methane drainage. Knowledge of methane hazard level at the stage of designing coal panels' exploitation constitutes basement for determination of safe output limit from the longwall in the conditions of different coal output capacity.

CONCLUSIONS

1. Increasing methane content of the coal seams with their depth and growing longwalls' coal output capacity in the last two decades had direct impact on increased methane release into the environment of exploited coal panels (longwalls).
1. Dynamic method of methane content forecasting allows to very precisely calculate values of methane release depending: on longwall progress, methane resources in the exploited coal seam as well as in the underlying and overlying seams along coal panel length.
2. Forecasting method of methane release into the environment of longwalls in its assumptions takes into consideration methane content distribution in the exploited coal seam as well as in the overlying and underlying seams including their degasification degree, what has direct impact on the accuracy of the forecasting.
3. Forecasting of methane volume released into the environment of the longwall working when mining by shearer, at the stage of designing the exploitation allows to calculate admissible, safe output capacity according to safety regulations.
4. Improving applied methods of forecasting methane release into the environment of the longwall in the conditions of increased output capacity allows for: proper designing longwall ventilation conditions as well as selecting correct methane prophylactics in order to provide safe exploitation conditions.

REFERENCE

[1] Kozłowski B. (1972): Forecasting of methane hazard in the hard coal mines. Katowice, Wyd. „Śląsk"
[2] Krause E.: Factors developing increase of methane hazard in the longwalls with high output capacity. Przegląd Górniczy nr 9/2005, s.19-25.
[3] Krause E.(2009): Evaluation and methane hazard fighting in the hard coal mines. Prace Naukowe GIG Nr 878
[4] Krause E. (2009): Forecasting of methane release into the longwalls' environment when mining by shearer. Przegląd Górniczy nr 3-4
[5] Krause E. (2009): Degasification degree of the underlying coal seams within the range of exploitation release. XVI Międzynarodowa Konferencja Naukowo – Techniczna „Górnicze Zagrożenia Naturalne 2009" nt. „Technika wiertnicza i strzałowa a zagrożenia górnicze", Targanice k. Żywca
[6] Krause E, Cybulski K., Qu Xianchao (2011): Impact of methane release forecasts accuracy on the safety work conditions in the environment of the longwalls, 2011 China International Forum on Coal Mine Gas Control & Safety Engineering, Hefei, Anhui Province, Chiny
[7] Krause E., Łukowicz K. (1999): Forecasts of absolute methane bearing capacity for the longwalls with high output capacity. Konferencja GIG nt. „Najnowsze osiągnięcia w zakresie przewietrzania kopalń oraz zwalczanie zagrożeń pożarowych, gazowych i klimatycznych. Katowice – Szczyrk
[8] Krause E., Łukowicz K. (2000): Dynamic forecast of absolute methane-bearing capacity of the longwalls. (poradnik techniczny). Instrukcja nr 14. Katowice, GIG
[9] Cybulski K. , Krause E., Łukowicz K. (1999): Impact of the output capacity on the methane hazard development in the longwall workings. 1 Szkoła Aerologii Górniczej. Kraków AGH.
[10] Drzewiecki J.: Longwalls' methane content versus exploitation progress. Archiwum Górnictwa nr 49/2004.
[11] Pawiński J. Roszkowski J. Strzemiński J.(1995): Ventilation of the coal mines. Katowice, Śląskie Wyd. Techn. .

DETERMINING THE OPTIMAL SOLUTION FOR THE EXECUTION OF UNDERGROUND MINING CONSTRUCTIONS, GIVEN THE GEOLOGICAL AND MINING CONDITIONS

*N. Dobritoiu and I.S. Mangu

University of Petrosani
20 Universitatii Street
Petrosani, Romania
(**Corresponding author: dobritoiun_2001@yahoo.com*)

24th World Mining Congress
MINING IN A WORLD OF INNOVATION
October 18-21, 2016 • Rio de Janeiro /RJ • Brazil

DETERMINING THE OPTIMAL SOLUTION FOR THE EXECUTION OF UNDERGROUND MINING CONSTRUCTIONS, GIVEN THE GEOLOGICAL AND MINING CONDITIONS

ABSTRACT

The modern methods used in designing underground mining constructions are using graph structure-based models. The graph structure-based models contain: the environmental conditions of the area where an underground mining construction is to be built and the technological elements involved in the process of building an underground mining construction. The usage of the graph-structure model in mining design creates a great number of options for the construction process. Therefore, these options ought to be evaluated and based on a decision criterion, so that an optimal choice can be made.

KEYWORDS

Matrix of connections, graph, critical path, mining work, optimum solution, natural conditions.

GENERAL IDEAS

To build an underground mining construction one can choose from among various digging methods at their disposal. The selection of the digging method is done taking into consideration the geological and mining conditions of the types of rock from the digging site.

Having chosen the digging method, one can select the type of technological means corresponding to the selected method.

The dynamics of the environmental changes that will affect the geological and mining conditions of a mining construction will result in the altering of the digging methods and the technologies selected for those methods.

Selecting the best digging method and the corresponding technological means can be done using the graph structure models. Due to the high number of digging methods and various technologies, the use of graph structure methods is required for adequate selection.

The graph structure models allow us to determine the geological and mining conditions of the rock layers where the mining construction will be located.

The usage of graph structure methods in the design of mining constructions when the geological and mining conditions are known results in a high number of design solutions.

From the high number of options generated using the conditions-solutions connection matrix, a large number can be set aside because of the exiting incompatibilities between the nodes of the non-adjacent columns of the conditions-solutions graph.

Quantifying every admissible variant of solution by using a system of indicators and knowing an optimization criterion, one can determine the optimal solution for building an underground mining construction when the environmental conditions are given.

MODEL OF GENERATION, EVALUATION AND ESTABLISHMENT OF AN OPTIMAL VARIANT OF ACTION FOR CAPITALIZATION OF DEPOSITS

General ideas regarding the classification of the information used for the graphs design

The information used to design the building of an underground mining construction can be classified using the following criteria [10, 11]:

1. The classification of information according to the nature of the state variables

Any complex system can be characterized by a determined number of parameters which, at a certain moment, take on different values and define a certain state of the system, hence, they are also called state variables. Variables of state describe the system from two points of view: a qualitative and a quantitative one. Depending on the described domain, variables of state can be grouped in: category variables, continuous variables and discrete variables.

The *category variables* represent that group of variables of state which describe the complex system from a qualitative point of view, for example: the nature of the face rocks, the type of coal, the rate of methane emanation, the type of support in a face, the type of underground transport, etc.

The *continuous variables* represent that group of state variables which describe the complex system from a quantitative point of view (mass, volume, length and time). Continuous state variables can get any value within a given interval, for example: the thickness of the seam, the length of the working face, the length of a borehole, etc.

The d*iscrete variables* describe the quantitative side of the system discretely, i.e. the number of items, elements or number of component parts. Discrete variables can get only certain values within a given interval without going through intermediate values, for example: the number of seams, the number of face advances, the number of support units, the number of workers needed on a work site, etc.

2. The classification of the variables according to the time dependent variation

Modifications in time of the value of one or several continuous or discrete variables lead to the modification of the state of the complex system from a quantitative point of view only. Any complex system is known to evolve in the course of time, to change both qualitatively and quantitatively. The evolutions in time of the variables describing the state of a complex system can be: dynamic, quasi-static and static.

Dynamic variables of state are those variables which in the course of a period of time change continuously, so they are functions of time. The trajectories of these variables are not constant throughout the time interval being analysed.

Quasi-static variables of state are those variables which in the course of a period of time undergo only changes of a discrete nature. The trajectories of these variables look like a stepped graph throughout the period of time under consideration.

Static variables of state are those variables of state which in the course of a period of time remain constant. The trajectories of these variables are constant throughout the period of time under consideration.

3. The classification of variables of state according to their relation to the decision-maker

Throughout the existence of a certain complex system, changes are brought about frequently or periodically with a view to modifying its state qualitatively as well as quantitatively, depending on the purpose. There are variables of state that can or cannot be modified using man's intervention. Thus, variables of state can accordingly be grouped in: stimulus variables and response variables.

Stimuli variables represent the multitude of the variables of state that cannot be modified by the human intervention, for example: the number of strata, the nature of the rocks from the stope, the depth of the deposit, etc.

Response variables represent the multitude of the variables of state that can be modified by human intervention, for example: the number of drills being used simultaneously for drilling holes in the stope, the work force needed on the work site, etc.

4. Variables that can indicate the result

The purpose of the management of any system is to transform the multitude of stimuli, S, into admissible responses, R. Any operator that can turn objective stimuli into responses is called a determiner. The determiner is the man or group of people that transform stimuli S into responses R using certain rules. The transformation stimuli-responses: $S \rightarrow M \rightarrow R$ is expected to result in the most effective transformation. The variables characterizing the results depend on the S and R set and are called result indicators.

The database required to design the conditions graph

The information required to determine the graph structure model that is to be used for the design of the conditions where the underground mining construction is being built can be systematized and classified in the following groups [9]:

1. the group of information of static and category stimuli includes [9]:
- the relief on the surface of the deposit where the underground mining construction is to be built;
- the type of depth of the deposit;
- the type of rocks from the strata covered by the underground mining construction etc.

2. the group of information of static and continuous stimuli includes [9]:
- the mean value of the depth of the stratum where the underground mining construction is to be built;
- the flow of the accumulation of underground water, etc.

3. the group of information of static and discrete stimuli includes [9]:
- the number of reserve units that form the rock bed where the underground mining construction is situated;
- the number of tectonic accidents of the same type in the underground strata where the mining construction is to be built etc.

4. the group of information of dynamic and category stimuli includes [9]:
- the category of variation of the ground stability per deposit direction and deposit slope;
- the category of variation of the tectonic accidents per deposit direction and deposit slope, etc.

5. the group of information of dynamic and continuous stimuli includes [9]:
- the variation of the absolute water flow of water bearing sheets located in the roof of the deposit;
- the variation of the water pressure in a water bearing sheet located in the rock bed;
- the variation of the absolute volume of mine gases emanation in the deposit and in the rock bed etc.

6. the group of information of dynamic and discrete stimuli includes [9]:
- the variation of the number of accidents of the same type per deposit direction and deposit slope;
- the variation of the number of water deposits per deposit inclination and deposit slope etc.

The database required to design the solutions graph [9]

The "Reactions categories" type of information is required to design the graph structure model used to generate solutions for the building of underground mining constructions. For example:
- the digging method and the exploitation options;
- the method used to cut the rocks from the rock bed;
- the method used to partially ventilate the work site;
- the method used to supply the work site;
- the method of using temporary means and the temporary consolidation of the galleries resulted after the cutting of the rocks from the work site;
- the method used to temporarily reinforce the walls of the underground mining construction;
- the method of definitive consolidation of the underground mining construction;
- the method used in the underground mine development.

GRAPHICAL-ANALYTICAL MODEL USED TO GENERATE THE METHOD, OPTIONS OF DIGGING AND TECHNOLOGICAL MEANS TO EXECUTE AN UNDERGROUND MINING CONSTRUCTION [1, 3, 4, 11, 12]

Presentation of the graphical-analytical model used to generate the digging conditions of an underground mining site

The site of the underground mining building can be represented through a descriptive model that contains: the series of rock strata, the tectonics of the ground, the gas dynamics of the ground, the hydrogeology of the ground.

The description of the rocks formation includes the description of the following data: the nature and type of rocks, the physical, mechanical and chemical characteristics of each type of rock, the geometrical parameters of the rock formation, the mineralogical and petro-graphical description of the rock

formation, the dynamic of the gases in the rock formations and the hydro-dynamics of the ground, the occurrence of tectonic accidents, etc.

Once we have the descriptive model of the ground where the underground mining workings are to be dug, we can attempt to transpose it into a graphical-analytical model.

In order to transpose the data presented in the descriptive model into a graph structure model, these data have to be systematized according to the aforementioned presentation (2).

Once the systematization of the data from the descriptive model has been done, the next step is the plotting of the graph of conditions.

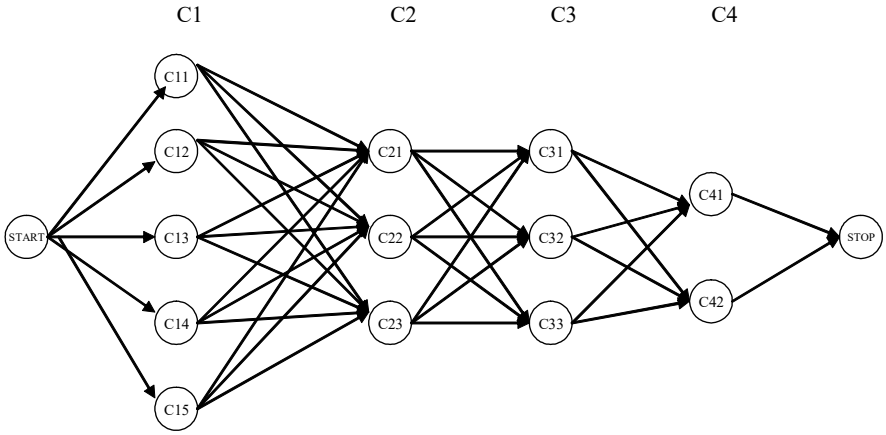

Figure 1 - Graph example

This graph enables the generation of a high number of conditions under which the underground mining construction can be dug.

A graph represents a graphical construction created from columns of nodes linked with left-to-right oriented arcs (figure 1).

A column of nodes represents the values of a parameter that is used to describe the natural conditions under which the mining construction is being built. The number of columns of nodes in the graph is equal to the number of parameters used to describe the natural environment where the mining construction is being dug.

A column of nodes represents the values of a parameter that is used to describe the natural conditions under which the mining working is dug. The number of columns of nodes in the graph is equal to the number of parameters used for describing the natural environment in which the mining working is being dug.

The order of the columns of nodes is based on the degree of relationship of the data, while the order of nodes in the column depends on the values taken on by the parameter attached to that column.

The graph begins with a single node column which represents the starting node of the graph called ”START” and it also ends in a single node column called ”STOP”.

The arcs of a graph link the nodes belonging to two adjoining columns. The order of linking is from left to right. These arcs can take the following values:

- "1" when there is a relationship between the two nodes, i.e. the nodes are compatible;
- "0" when there is no relationship between the two nodes, i.e. the nodes are incompatible. (e.g.: in the nodes column type of rocks in the deposit, for the node “foliated marl” and the adjoining node, “the values of the coefficient of abrasiveness of the types of rocks situated at the underground mining construction site”, have the following values: high abrasiveness, medium abrasiveness, decreased abrasiveness and no abrasiveness. We notice that there is no compatibility between the “foliated marl” node and the nodes from the adjoining column, with the following values: high abrasiveness, medium abrasiveness, decreased abrasiveness and no abrasiveness).

Remarks

1. All the arcs having their origin in the ”START” node and their destination in the ”STOP” node have the value ”1”.

2. The ”START” and ”STOP” nodes are compatible with nodes in the graph, as a result of the graph construction.

The graph representation of the parameters describing a massif through which a mining working is dug solves only the compatibility between adjacent nodes. Under the circumstances, the number of conditions that would be generated by this graphical construction is:

$$N_d = \prod_{i=1}^{n} n_i$$

where: i=1, 2, 3, , n –represents the number of columns in the graph;

n_i – represents the number of nodes in the column “i”.

For the graph in figure 1 $N_d = 1 \cdot 5 \cdot 3 \cdot 3 \cdot 2 \cdot 1 = 90$ paths can be generated.

Obviously, not all the paths generated by the graph in fig. 1 are admissible.

In order to determine the number of paths admitted, one will have to solve the compatibility of the nodes in a column with all the nodes belonging to the non-adjacent column. This is not possible using the model with a graph structure. However, the problem can be solved by means of the connection or contingence matrix which represents the transposition of the graph structure model to analytical form.

The connection matrix representing the analytical transposition of the graph structure model in figure 1 is presented in figure 2.

Nr. crt.	Specifica-tions	Parameter values	C_1					C_2			C_3			C_4		C_5
			c_{11}	c_{12}	c_{13}	c_{14}	c_{15}	c_{21}	c_{22}	c_{23}	c_{31}	c_{32}	c_{33}	c_{41}	c_{42}	c_{51}
C_0		c_{01}	1	1	1	1	1	1	1	1	1	1	1	1	1	1
C1		c_{11}						1	1	1	1	1	0	1	0	1
		c_{12}						1	1	1	0	1	1	0	0	1
		c_{13}						1	1	1	1	0	1	1	1	1
		c_{14}						1	1	1	1	1	1	0	1	1
		c_{15}						1	1	1	0	1	1	1	0	1
C2		c_{21}									1	1	1	1	0	1
		c_{22}									1	1	1	0	1	1
		c_{23}									1	1	1	1	0	1
C3		c_{31}												1	1	1
		c_{32}												1	1	1
		c_{33}												1	1	1
C4		c_{41}														1
		c_{42}														1

Figure 2 - The connection matrix

Remark. *The data necessary to draw the graph (fig. 1) and the connection matrix (fig. 2) are taken at random.* The connection matrix is composed of two modules:

- the first module of the matrix represents the connection module resulting from the analytical transposition of the graph structure model and it is the dark part in the matrix;
- the second module of the matrix is ”the module of the added matrix” and it solves the compatibility of the nodes from non-adjacent columns.

The graphical-analytical model for generating technological solutions and technological options for executing underground mining construction

Given the group of methods for digging an underground mining site and the sets of operations of the digging process, we identify for each set of operations all the types of (simple and complex) mining equipment, installations, devices, tools and we create a list with all this data.

For each group of mining equipment on the list, we identify all the types of equipment belonging to each group. Also, for each type of equipment we identify the existing typo-dimensions.

Having the list of equipment with all the data about a group of equipment, the types of equipment and the typo-dimensions of each piece of equipment, we will draw the “solution graph”.

The "solution graph" is identical with the graph in figure 1.

In order to solve the problem of the compatibility of the nodes belonging to the non-adjacent columns, we can use the connection matrix. Under these circumstances, the compatibility between two nodes belonging to adjacent and non-adjacent columns results in a technological coupling which can be used in the digging operations. The information required to determine the compatibilities between the nodes of the adjacent and non-adjacent columns can be found in technical books showing descriptions of the technical-economic characteristics and of the natural conditions in which this equipment can work. These compatibilities are determined by the specialists in this field.

The graph of solutions and the way in which it has been plotted generate solutions to technologies and technological options. In order for these technologies to be applicable, i.e. to be admitted, the connection matrix is used. The way of generating and determining the admissible solutions is identical with the one used for generating the digging conditions for an underground mining site.

The model with the graph structure for generating a technology or technological variants for digging underground mining workings when the natural conditions under which they are executed are known

Given the two graph structure models for generating the conditions of execution of an underground mining construction, as well as the technologies and the technological options for the digging of a mining work, the following question arises: how does one use the two types of models with a graph structure to determine the technology and the technological option for the digging of an underground mining site, given the natural conditions of the digging?

The answer to this question is: the two graphs are combined into one, generating a new graph called "the conditions-solutions graph". However, this new graph cannot be used to solve the aforementioned problem. To be able to use it to determine technologies or technological options given the natural conditions of the underground mining construction, we also need the connection matrix resulting from the analytical transposition of the "conditions-solutions" graph. The new matrix solves the connection between the "conditions" and "solutions" graphs. This connection is created by completing the matrix with the module "added matrix". This connection is solved using the module "added matrix", also called the "connecting module" i.e. it connects the "condition matrix" to the "solution matrix" and it is situated on the right of the modules of the condition matrix, figure 3.

Nr. crt	Specifications	Parameter Values	Columns of condition matrix	Columns of Solution matrix	Sf
C0					
		Lines of condition matrix	CONDITION MATRIX	MODULE OF CONNECTION BETWEEN CONDITION MATRIX AND SOLUTION MATRIX	
		Lines of solution matrix		SOLUTION MATRIX	

Figure 3 - The connections conditions-solutions matrix

Remarks

1. The data used to draw the solutions graph and its matrix of connections belong to "Responses" type according to the "the nature of variables (or the values they can take on)" criterion used for the classification of data.

2. The type of data corresponding to the "variation in time" and "relation to the decision-maker" criteria is the same as in the case of the construction of the conditions graph.

EXAMPLE [1, 3, 4, 10, 11, 12]

For this example, we have used information from the "Indicative of estimate and costs per unit of work articles for underground mining constructions, C. M. 1982", Romania [13].

Due to the complexity of the conditions-solutions graph, we will not describe it here. Nevertheless, we will describe the analytical transposition of the graph into a table, "the conditions-solutions matrix", appendix 1. Depending on the conditions under which the underground mining construction is to be built, we have identified a way to determine the method and the optimal technology to be used for the building of the underground mining construction.

In order to determine the best options of building the underground mining construction, we will use the cost per unit building criterion. For certain situations, to determine the best solution to build the underground mining construction, we can use various simple and complex optimization criteria.

From the connections matrix presented in appendix 1, we select the set of conditions for the building of the underground mining construction, i.e. the natural conditions set corresponding to 0101 code. The segments of this code correspond to:

- first 01 segment – the type of the rocks from the mining site;
- second 01 segment – the value of the type of rock – hard rocks.

Creating the conditions-solutions matrix corresponding to the set of determined conditions

To create the conditions-solutions matrix corresponding to the determined set of conditions (see appendix 2), we need to follow these steps:

- step 1. In appendix 1, we identify the line containing the 0101 code. We follow the line to the right and delete all columns that contain the "0" value in the cells corresponding to this line,
- step 2. We focus on the line containing the 0001 variable. From the columns that belong to the 01 variable, we delete all the lines that are part of the set of conditions that describe the rock bed where the underground mining construction is located.
- step 3. We identify the column "variable code segment" and we go down vertically until we reach the 02 variable lines. We delete all the lines matching to the columns deleted from the group of columns corresponding to the 02 variable. We do the same for all the variables.

Remark

- the set of columns that correspond to the STOP variable has one value. This value appears only in that set of columns;
- the group of lines corresponding to the START variable has one value. This value appears only in that set of lines;
- the nodes corresponding to the START and STOP artificial variables are compatible with every node of the graph.

The matrix presented in appendix 2 was graphically converted into a graph and can be seen in appendix 3.

The number of solutions generated by the graph in appendix 3 can be obtained using the relation:

$$N=\prod_{1}^{n} n_i = 1\cdot 1\cdot 6\cdot 1\cdot 1\cdot 3\cdot 1\cdot 2\cdot 1\cdot 2\cdot 3\cdot 3\cdot 1 = 648 \text{ paths}$$

where n_i represents the number of nodes from the graph presented in appendix 3.

From the maximum number of solutions that can be generated using the graph from appendix 3, only a small number of them are admissible solutions.

In order to eliminate the impossible solutions, we use the analysis for the compatibility of the nodes with the non-adjacent columns for every path generated by the matrix presented in appendix 2.

Identifying the optimal solution for the building of the underground mining construction

Let us consider the problem of identifying the optimal solution for the building of an underground mining construction under a certain set of conditions.

In order to determine the best option to build an underground mining construction, given the set of conditions, we must determine the values of the cost per unit function for every node in the graph. These values are based on the given set of conditions and the values from every node.

In appendix 3, for every node that belongs to the columns of nodes that form the solutions graph, you can find attached the values of the costs per unit (for column 2 – 12 we have attached random values for the costs per unit, depending on the given set of conditions).

We notice that for the column of nodes "12" ("STOP"), the value of the 01 node is equal to the value of the costs per unit, i.e. 0.

There are situations when, for a set of given conditions, there is no compatibility between the nodes of two adjoining columns. In order to build a graph for the given conditions, we use a false node for the column that has no compatibilities with the nodes of the adjoining column. This node will have the value of the costs per unit function, 0. The false node will be compatible with all the nodes in the graph.

Remark. The best solution for building an underground mining construction can also be determined using another type of evaluation of the execution options (time, productivity, production, etc.).

The values of the evaluation partial functions for each of the nodes of the columns that describe the solutions matrix will be completed in the modules of the section belonging to the solutions matrix and the compatibilities matrix (see the matrix presented in appendix 4).

As we have seen, two adjoining columns form a module in the connections matrix. Example: the group of lines of variable 10 and the group of columns of variable 11 combine into a module composed of three lines and three columns (see figure 3).

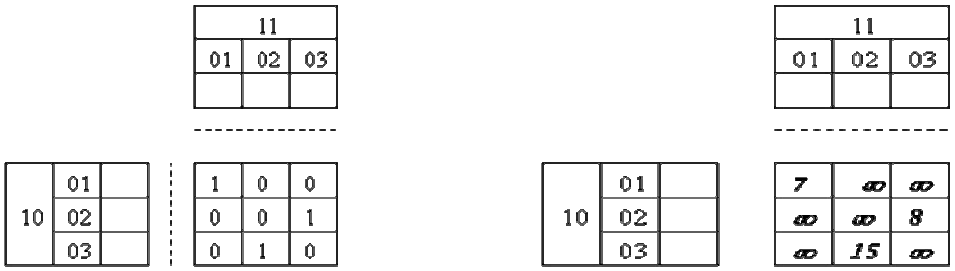

Figure 4

a. The module presented in appendix 2 b. The module presented in appendix 4

We fill in the cells of the 10-11 modules from appendix 5 following these steps:

- in the cells of the figure 3 module, with 0 value, we add ∞ (see the module in figure 3.b);
- in the cells from figure 3.a., with 1 value, we add the values corresponding to the nodes from column 11 of the graph presented in appendix 3 (see figure 3.b).

Remark. If all the cells from the module presented in figure 3.a had the 1 value, then in the 1101 column we would add only the value 7, in the column 1102 – the value 15, and in the column 1103 – the value 8.

For the matrix in appendix 4, we add, horizontally, the following types of columns:

- a column to separate the compatibility matrix and the rest of the columns;
- a column for each variable;
- a column for "critical path value".

Then, after line 1201, we will add, horizontally, a line which will contain the "value of the critical path".

The algorithm used to determine the optimal solution [3, 4, 5]

Given the matrix presented in appendix 5 and the graph in appendix 4, we can determine the critical path. The critical path can have minimum and maximum values. These values are determined by the functions used to evaluate the solutions generated by the type of matrix presented in appendix 5.

The algorithm used here is taken from the critical path analysis (CPA) and is combined with a test of compatibility between the nodes of the columns non-adjacent that describe an option of building a mining construction.

The algorithm used to determine the best solution using an evaluation function consists of the following situations:

- *situation 1*. We identify the first column of nodes that belongs to the conditions matrix – in our example 0101 (in the given case, the conditions matrix is represented by one group of values and this group contains one column). We move down on the 0101 column until we reach the 0101 line. We add the 0 value in the cell resulted from the intersection of the 0101 line and the "critical path value" column. In the cells of the columns 00 and 01 we add the path that has the 01, 01 values.

- *situation 2.* We identify the first group of columns that belong to the 02 solutions matrix. We move down on column 0203 until we reach the 0101 line, where we see the 13 value. When we encounter the 13 value, we add the value from the cell resulted from the intersection of the 0101 line and the "critical path value" column, 13+0=13. We follow the same procedure for all the columns of the 02 variable: 0204 column, 16+0=16. We add the result in the cell generated at the intersection of the "critical path value" column and the 0204 line. We follow these steps until we go through all the columns from the first group of columns of the solutions matrix.

At the same time with adding the values in the "critical path value", we add the path 01 from the line 0101 in the 0203 – 0208 lines, in the cell from the 00 columns. For the 02 column, we add to these lines the 03, 04, 05, 06, 07, 08 codes.

Example: For the group of lines described by the 02 variable, we have the following nodes:

0203 – with the codes sequence: 01, 01, 03

0204 – with the codes sequence: 01, 01, 04

0208 – with the codes sequence: 01, 01, 08

- *situation 3*. We move to the right of the first group of columns of the solutions matrix and we identify the group of columns for the 03 variable. Then we move down on the first column of this group of columns until we meet the 0 value. We add 13 to 0. We move down until we meet the 0204 line, where we reach the ∞ value. We add 16 to the values we find on the same line corresponding to the last column. We continue until we reach the last line that belong to the 02 variable and we get the following set of values: (13.∞, 14, ∞, 14, ∞). From this set of values we select the minimum value, 13. We add this value in the 0302 cell, the "critical path value" column.

We check the compatibility of the nodes that form the critical path. The critical path is given by the values: 0001, 0101, 0203, to which we add the 0302 value. This verification can be done following the next steps:

- we move down on column 0302 and we check the compatibility between node 0101 and node 0302. It results compatibility. In this situation we fill in the critical path on line 0302, in the area of the added columns. We also add value 13 in the cell "03 - critical path value".

These two stages are to be repeated for the 04, 05, 06, 07, 08, 09. Therefore, we get the values in the corresponding lines and columns.

- *situation 4.* This refers to the general situation. We follow the next steps:

  - step 1. We move down on column 1001 until we reach line 0902. To value 15 we add the 43 value, from the same line, in the "critical path value" column. We get value 58. We continue to move down until we reach the 0903 line, until we reach value 15. We add to it value 38, from the same line in the last column. We get value 53. From the set of values (58, 53), we select the minimum value, 53.

  - step 2. We check the compatibilities of the existing non-adjacent nodes that belong to the path corresponding to the minimum value, 53. This is the road given by the 0903 line. The line 0903 contains of: 0001, 0101, 0203, 0302, 0406, 0502, 0601, 0702, 0802, 0902, to which we add the code of the 1001 column.

We repeat these two steps and for columns 1002, 1003. We get the values from the columns that have been added.

In the cell resulted from the intersection of column 10, that belongs to the group of added columns, and the "critical path value" line, we add the minimum value that results from the set of values from the group of lines of variable 10, i.e. (53, 50, 51), the minimum value is 50 and it corresponds to line

1002. The path described by the 1002 line is a minimum path. The 50 value is added to the cell resulted from the intersection of the "critical path value" line and column 10.

We continue in the same manner for the group of columns of variable 11, thus getting the values from the group of lines that belong to variable 11. The minimum path from the group of lines that belong to variable 11 is given by line 1103, (0001, 0101, 0203, 0302, 0406, 0502, 0601, 0702, 0802, 0902, 1002, 1103) and it has the 58 value.

When we reach the last column of nodes, i.e. column no. 12, we use the same steps as in situation 3. Thus, we get the set of values (60, 66, 58) and we determine the minimum value, which is 58. This value corresponds to the accepted path that belongs to line 1103. Both the accepted path (0001, 0101, 0203, 0302, 0406, 0502, 0601, 0702, 0802, 0902, 1002, 1102) that belongs to line 1103, and the minimum value 58 will be written down in line 1201. We will add the code of line 1201 to the path that has been written down. This accepted path is the shortest road described by the graph in appendix 4 and generated by matrix 5. Its value is 58 monetary units.

CONCLUSIONS

The model with graph structure:

- allows us to synthesize the description of the environmental conditions of a rock bed where an underground mining construction is to be built;
- allows us to synthesize the elements of the solutions used to build an underground mining construction;
- connects the environmental conditions elements and the components of the solutions used to build an underground mining construction;
- allows us to quickly update the data with the new pieces of information that appear in the conditions group and in the "Categories reactions" group;
- allows us to determine the optimal solution to build an underground construction, given the environmental conditions;
- needs a small amount of time to determine the optimal solution.

The model presented can be applied in a software application.

References

[1] Burceacov, A.C., Proiectirovanie Şaht, Izdatelstva Nedra, Moskva, 1989 (in Russian).

[2] Dogaru, Metode noi în proiectare. Elemente de grafică 3D, Editura Ştiinţifică şi Enciclopedică, Bucureşti, 1988 (in Romanian).

[3] Dobriţoiu, N., The use of the graphical-analytical models to determine the methods and the technologies of execution of the underground mining works when the set of natural conditions of digging are known, Proc. of the International Conf. on Energy and Environment Technologies and Equipment (EEETE '10), Univ. Politehnica, Bucharest, Romania, April 20-22, 2010. Published by WSEAS Press, www.wseas.org

[4] Dobriţoiu, N., How to generate and evaluate the optimal method for the capitalization of a deposit of available mineral substances, 22nd *WORLD MINING CONGRESS* 11-16 Sept. 2011 Istanbul.

[5] Dobriţoiu, N., Cercetări în vederea structurării şi integrării informaţiilor geologico-miniere şi topografice într-un sistem CPAC (Cercetarea şi Proiectarea Asistate de Calculator) pentru zăcământul de cărbune Valea Jiului. Teză Doctorat, Universitatea din Petroşani, 1998 (in Romanian).

[6] Kagramanian, A., Modelirovanie i upravlenie gornorudnimi predpriiatiiami, Editura Nedra, Moskva, 1989 (in Russian).

[7] Murgu, M., Evaluarea geologică şi industrială a zăcămintelor minerale, Editura Tehnică, Bucureşti, 1986 (in Romanian).

[8] Nabradov, I. P., Principiile de construire a modelelor economico- matematice ale minelor în funcţiune, Ugoli, nr.12/1984 (in Romanian).

[9] Popa, A. (coord.), Manualul inginerului de mine, vol. I, II, III, IV, V, Editura Tehnică, Bucureşti, 1984-1989 (in Romanian).

[10] Rozniacenko, S. S., Modelarea matematică în industria minieră, Editura Nedra, Moscova, 1981 (in Romanian).

[11] Simionescu, A., Modelarea matematică în proiectarea minelor, Litografia I.M.P., Petroşani, 1980 (in Romanian).

[12] Ţoi, C., Matematiceskie Osnovs Automatizirovannoi Sistems Proiectirovania Şaht, Alma-Ata, 1979 (in Russian).

[13] *** Indicatoarele de norme de deviz şi preţuri unitare de deviz pe articole de lucrări pentru construcţii miniere şi montaje în subteran C.M. 1982 (in Romanian).

Annex no. 1

The graph conditions-solutions for generating technologies and technological variants for digging a horizontal mining working

code of variabe	Name of variable	Name of element variable	code of elem. vari.	01					02								03		04						05							06		07					08		09		10			11			12
				01	*02*	03	04	05	01	02	03	04	05	06	07	08	01	02	01	02	03	04	05	06	01	02	03	04	05	06	07	01	02	01	02	03	04	05	01	02	01	02	03	01	02	03	01
00				/	/	1	1	1	1	1	1	1	1	1	1	1	1	1	1	1	1	1	1	1	1	1	1	1	1	1	1	1	1	1	1	1	1	1	1	1	1	1	1	1	1	1	1	1	1
01	Type of roks and the values	extra-hard rocks	*01*						0	0	1	1	1	1	1	1	0	0	0	0	0	0	0	1	1	1	1	0	0	0	0	1	0	0	1	0	0	1	0	1	0	1	1	1	1	1	1	1	1	1
		very hard rocks	*02*						0	0	1	1	1	1	1	1	0	0	0	0	0	0	0	1	1	1	1	0	0	0	0	1	0	0	1	0	1	0	0	1	0	1	1	1	1	1	1	1	1	1
		hard rocks	*03*						1	1	1	1	1	1	1	1	0	0	1	1	1	1	1	0	1	1	1	1	1	1	1	1	1	1	1	1	1	1	0	1	1	1	1	1	1	1	1	1	1	1
		semi-hard rocks	*04*						1	1	1	1	1	1	1	1	1	1	1	1	1	1	1	0	0	0	1	1	1	1	1	0	1	1	1	1	1	0	1	0	1	0	1	1	1	1	1	1	1	1
		soft rocks	*05*						1	1	1	1	1	1	1	1	1	1	1	1	1	1	1	0	0	0	0	1	1	1	1	0	1	1	1	1	1	0	1	0	1	0	1	1	1	1	1	1	1	1
02	Method of executing the profile of the mining workings and temporary suport seting with the values	cutting the profile by means of a drifting machine and temporary support setting	*01*														1	0	1	1	1	1	1	0	0	0	0	1	1	1	1	1	0	0	0	0	1	1	1	1	1	1	1	1	1	1	1	1
		cutting the profile by means of a drifting machine without temporary support setting	*02*														0	1	0	0	0	0	0	1	1	1	1	0	0	0	0	1	0	1	1	1	1	0	1	1	1	1	1	1	1	1	1	1
		cutting the profile by drilling-blasting, hand loading and temporary support setting	*03*														1	0	1	1	1	1	1	1	0	1	0	1	1	1	1	1	0	1	0	1	0	0	0	1	1	1	1	1	1	1	1	1
		cutting the profile by drilling-blasting, hand loading without temporary support setting	*04*														0	1	0	0	0	0	0	1	1	1	1	0	0	0	0	1	0	1	1	1	1	0	1	1	1	1	1	1	1	1	1	1
		cutting the profile by drilling-blasting, pneumatic mechanical loading and temporary support setting	*05*														1	0	1	1	1	1	1	0	0	0	0	1	1	1	1	1	0	0	0	0	1	1	1	1	1	1	1	1	1	1	1	1
		cutting the profile by drilling-blasting, pneumatic mechanical loading without temporary support setting	*06*														0	1	0	0	0	0	0	1	1	1	1	0	0	0	0	1	0	1	1	1	1	0	1	1	1	1	1	1	1	1	1	1
		cutting the profile by drilling-blasting, electrical mechanical loading and temporary support setting	*07*														1	0	1	1	1	1	1	0	0	0	0	1	1	1	1	1	0	0	0	0	1	1	1	1	1	1	1	1	1	1	1	1
		cutting the profile by drilling-blasting, electrical mechanical loading without temporary support setting	*08*														0	1	0	0	0	0	0	1	1	1	1	0	0	0	0	1	0	1	1	1	1	0	1	1	1	1	1	1	1	1	1	1
03	Dismantling temporar	with dismantling temporary support	*01*																1	1	1	1	1	1	0	0	0	1	1	1	1	0	1	0	0	0	0	1	1	1	1	1	1	1	1	1	1	1
		without dismantling temporary support	*02*																0	0	0	0	0	1	1	1	1	0	0	0	0	1	0	1	1	1	1	0	1	1	1	1	1	1	1	1	1	1
04	Setting shutterings and skeleton ribs with the values	setting fir squared timber shuttering for brick and concrete masonery	*01*																						0	0	0	1	1	1	1	0	1	0	0	0	0	1	1	1	1	1	1	1	1	1	1	1
		setting fir squared timber shuttering for brick and concrete masonery	*02*																						0	0	0	1	1	1	1	0	1	0	0	0	0	1	1	1	1	1	1	1	1	1	1	1
		setting steel shuttering for concrete work	*03*																						0	0	0	1	1	1	1	0	1	0	0	0	0	1	1	1	1	1	1	1	1	1	1	1
		setting panel shuttering for concrete work and brick masonry	*04*																						0	0	0	1	1	1	1	0	1	0	0	0	0	1	1	1	1	1	1	1	1	1	1	1
		setting plank and fir board shuttering for concrete work and masonery	*05*																						0	0	0	1	1	1	1	0	1	0	0	0	0	1	1	1	1	1	1	1	1	1	1	1
		without setting shutterings and skeleton ribs	*06*																						1	1	1	0	0	0	0	1	0	1	1	1	1	0	1	1	1	1	1	1	1	1	1	1
05	Type of permanent support with or withant shuttering with the values	support by guniting	*01*																													1	0	0	0	0	0	1	0	1	0	1	1	1	1	1	1	1	1
		wooden support	*02*																													1	0	1	1	1	1	1	1	1	1	1	1	1	1	1	1	1	1
		support by ring	*03*																													1	0	1	1	1	1	0	1	1	1	1	1	1	1	1	1	1	1
		support by precast concrete-block walling and shuttering	*04*																													1	1	0	0	0	0	1	1	1	1	0	1	1	1	1	1	1	1
		support by concrete cast in position and shuttering	*05*																													1	1	0	0	0	0	1	1	1	1	0	1	1	1	1	1	1	1
		support by concrete cast in position, floor concreting and shuttering	*06*																													1	1	0	0	0	0	1	1	1	1	0	1	1	1	1	1	1	1
		support by precast concrete-block walling, floor included and shuttering	*07*																													1	1	0	0	0	0	1	1	1	1	0	1	1	1	1	1	1	1
06	Dismantling shutterinds …	without dismantling shutterings and skeleton ribs	*01*																															1	1	1	1	0	1	1	1	1	1	1	1	1	1	1	1
		with the dismantling of shuttering and skeleton ribs	*02*																															0	0	0	0	1	1	1	1	0	1	1	1	1	1	1	1
07	Type of lagging used with the values	cover board lagging	*01*																																				1	1	1	1	1	1	1	1	1	1	1	1
		steel-mesh lagging	*02*																																				1	1	1	1	1	1	1	1	1	1	1	1
		oak or fir plank lagging	*03*																																				1	1	1	1	1	1	1	1	1	1	1	1
		steel lagging (IUMP type)	*04*																																				1	1	1	1	1	1	1	1	1	1	1	1
		without lagging	*05*																																				1	1	1	0	1	1	1	1	1	1	1	1
08	Type of floor with the values	cover board lagging	*01*																																						1	1	1	1	1	1	1	1	1	1	1	1
		steel-mesh lagging	*02*																																						1	1	1	1	1	1	1	1	1	1	1	1
09	Type of dewatering channel with	concrete channel	*01*																																								1	1	1	1	1	1	1	1	1	1
		unsustenable channel	*02*																																								1	1	1	1	1	1	1	1	1	1
		without channel	*03*																																								1	1	1	1	1	1	1	1	1	1
10	Type of transport used in the values	with mine locomotive	*01*																																													1	0	0	1
		conveyor belt transportation	*02*																																													0	0	1	1
		conveyor belt transportation and locomotive	*03*																																													0	1	0	1
11	Type of mining workings furnishing	mine railway and planking furnishing	*01*																																															1
		mine railway and conveyor belt furnishing	*02*																																															1
		belt conveyor furnishing	*03*																																															1

Reduced matrix

Code of variables	Name of variable	Name of element variable "I"	*cod elem. varia. i*	***00***	***01***	***02***						***03***	***04***	***05***			***06***	***07***		***08***	***09***		***10***			***11***			***12***
				01	01	03	04	05	06	07	08	02	06	01	02	03	01	02	05	02	02	03	01	02	03	01	02	03	01
00			*01*		***1***	1	1	1	1	1	1	1	1	1	1	1	1	1	1	1	1	1	1	1	1	1	1	1	1
01	Type of roks and the values	extra-hard rocks	*01*			***1***	***1***	***1***	***1***	***1***	***1***	1	1	1	1	1	1	1	1	1	1	1	1	1	1	1	1	1	1
02	Method of executing the profile of the mining workings and temporary suport seting with the values	cutting the profile by drilling-blasting, hand loading and temporary support setting	03									***1***	1	0	1	0	1	1	0	1	1	1	1	1	1	1	1	1	1
		cutting the profile by drilling-blasting, hand loading without temporary support setting	*04*									***0***	1	1	1	1	1	1	0	1	1	1	1	1	1	1	1	1	1
		cutting the profile by drilling-blasting, pneumatic mechanical loading and temporary support setting	*05*									***1***	0	0	0	0	1	0	1	1	1	1	1	1	1	1	1	1	1
		cutting the profile by drilling-blasting, pneumatic mechanical loading without temporary support setting	*06*									***0***	1	1	1	1	1	1	0	1	1	1	1	1	1	1	1	1	1
		cutting the profile by drilling-blasting, electrical mechanical loading and temporary support setting	*07*									***1***	0	0	0	0	1	1	0	1	1	1	1	1	1	1	1	1	1
		cutting the profile by drilling-blasting, electrical mechanical loading without temporary support setting	*08*									***0***	1	1	1	1	1	1	0	1	1	1	1	1	1	1	1	1	1
03	Dismantling temporar	without dismantling temporary support	*02*										***1***	1	1	1	1	1	0	1	1	1	1	1	1	1	1	1	1
04	Setting shutterings and skeleton ribs with the values	without setting shutterings and skeleton ribs	*06*											***1***	***1***	***1***	1	1	0	1	1	1	1	1	1	1	1	1	1
05	Type of permanent support with or withant shuttering with the values	support by guniting	*01*														***1***	0	1	1	1	1	1	1	1	1	1	1	1
		wooden support	*02*														***1***	1	1	1	1	1	1	1	1	1	1	1	1
		support by ring	*03*														***1***	1	0	1	1	1	1	1	1	1	1	1	1
06	Dismantling shutterinds …	without dismantling shutterings and skeleton ribs	*01*															***1***	***0***	1	1	1	1	1	1	1	1	1	1
07	Type of lagging used with the values	steel-mesh lagging	*02*																	***1***	1	1	1	1	1	1	1	1	1
		without lagging	*05*																	***1***	0	1	1	1	1	1	1	1	1
08	Type of floor with the values	steel-mesh lagging	*02*																		***1***	***1***	1	1	1	1	1	1	1
09	Type of dewatering channel with	unsustenable channel	*02*																				***1***	***1***	***1***	1	1	1	1
		without channel	*03*																				***1***	***1***	***1***	1	1	1	1
10	Type of transport used in the values	with mine locomotive	*01*																							***1***	***0***	***0***	1
		conveyor belt transportation	*02*																							***0***	***0***	***1***	1
		conveyor belt transportation and locomotive	*03*																							***0***	***1***	***0***	1
11	Type of mining workings furnishing	mine railway and planking furnishing	*01*																										***1***
		mine railway and conveyor belt furnishing	*02*																										***1***
		belt conveyor furnishing	*03*																										***1***

Annex no. 3

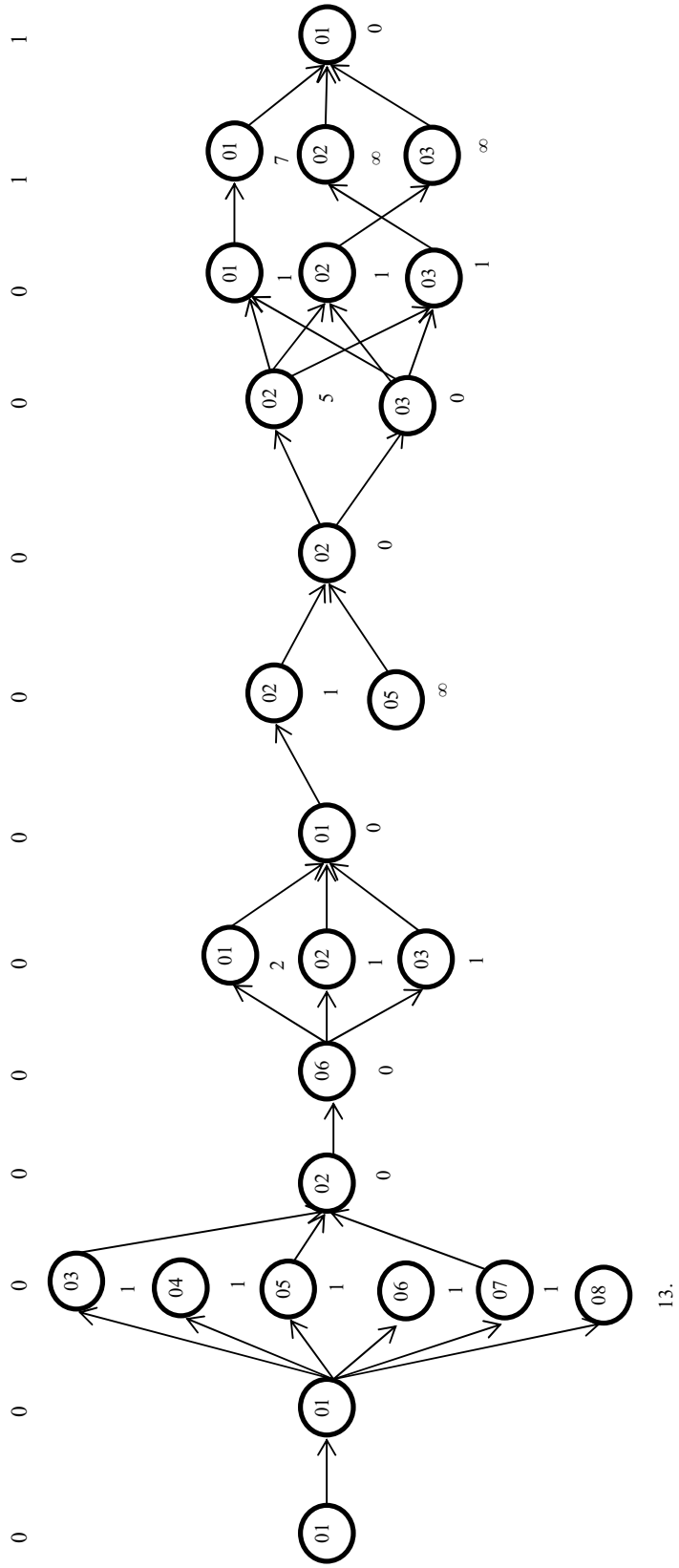

13.

Code of variable	Code of elem. variable, i	00	01	02						03	04	05			06	07		08	09		10			11			12		00	01	02	03	04	05	06	07	08	09	10	11	12	Critical path value
		01	01	03	04	05	06	07	08	02	06	01	02	03	01	02	05	02	02	03	01	02	03	01	02	03	01																
00	***01***		***0***	1	1	1	1	1	1	1	1	1	1	1	1	1	1	1	1	1	1	1	1	1	1	1	1		01														***0***
01	***01***			***13***	***16***	***14***	***15***	***14***	***13,5***	1	1	1	1	1	1	1	1	1	1	1	1	1	1	1	1	1	1		01	01													***0***
02	03									***0***	1	0	1	0	1	1	0	1	1	1	1	1	1	1	1	1	1		01	01	03												***13***
	04									***∞***	1	1	1	1	1	1	0	1	1	1	1	1	1	1	1	1	1		01	01	04												***16***
	05									***0***	0	0	0	0	1	0	1	1	1	1	1	1	1	1	1	1	1		01	01	05												***14***
	06									***∞***	1	1	1	1	1	1	0	1	1	1	1	1	1	1	1	1	1		01	01	06												***15***
	07									***0***	0	0	0	0	1	1	0	1	1	1	1	1	1	1	1	1	1		01	01	07												***14***
	08									***∞***	1	1	1	1	1	1	0	1	1	1	1	1	1	1	1	1	1		01	01	08												***13.5***
03	***02***										***0***	1	1	1	1	1	0	1	1	1	1	1	1	1	1	1	1		01	01	03	02											***13***
04	***06***											***20***	***15***	***18***	1	1	0	1	1	1	1	1	1	1	1	1	1		01	01	03	02	06										***13***
05	***01***														***0***	0	1	1	1	1	1	1	1	1	1	1	1		01	01	03	02	06	01									***33***
	02														***0***	1	1	1	1	1	1	1	1	1	1	1	1		01	01	03	02	06	02									***28***
	03														***0***	1	0	1	1	1	1	1	1	1	1	1	1		01	01	03	02	06	03									***31***
06	***01***															***10***	***∞***	1	1	1	1	1	1	1	1	1	1		01	01	03	02	06	02	01								***28***
07	***02***																	***0***	1	1	1	1	1	1	1	1	1		01	01	03	02	06	02	01	02							***38***
	05																	***0***	0	1	1	1	1	1	1	1	1																	***∞***
08	***02***																		***5***	***0***	1	1	1	1	1	1	1		01	01	03	02	06	02	01	02	02						***38***
09	***02***																				***15***	***12***	***13***	1	1	1	1		01	01	03	02	06	02	01	02	02	02					***43***
	03																				***15***	***12***	***13***	1	1	1	1		01	01	03	02	06	02	01	02	02	03					***38***
10	***01***																							***7***	***∞***	***∞***	1		01	01	03	02	06	02	01	02	02	03	01				***53***
	02																							***∞***	***∞***	***8***	1		01	01	03	02	06	02	01	02	02	03	02				***50***
	03																							***∞***	***15***	***∞***	1		01	01	03	02	06	02	01	02	02	03	03				***51***
11	***01***																										***0***		01	01	03	02	06	02	01	02	02	03	01	***01***			***60***
	02																										***0***		01	01	03	02	06	02	01	02	02	03	03	***02***			***66***
	03																										***0***		01	01	03	02	06	02	01	02	02	03	02	***03***			***58***
12	***01***																												01	01	03	02	06	02	01	02	02	03	02	***03***	01		***58***
Value critical path																													0	0	13	13	13	28	28	38	38	38	50	58	58		

DRAINAGE OF PROCESSING RESIDUALS FROM POTASH MINING FOR THE APPLICATION AS BACKFILL

*F. Schreiter, H. Mischo
Institute for Mining and Special Civil Engineering, TU Bergakademie Freiberg
Fuchsmuehlenweg 9
09599 Freiberg, Germany
*(*Corresponding author: falk.schreiter@mabb.tu-freiberg.de)*

24th World Mining Congress
MINING IN A WORLD OF INNOVATION
October 18-21, 2016 • Rio de Janeiro /RJ • Brazil

DRAINAGE OF PROCESSING RESIDUALS FROM POTASH MINING FOR THE APPLICATION AS BACKFILL

ABSTRACT

The requirements for environmental protection are continuously growing, especially for mining activities. One way to minimize the visible impact of underground mining activities is the reduction of waste rock material disposal. The most ecologic way for minimizing the volume of waste rock disposal is to use these as backfill. Using waste rock for backfill not only reduces the size of waste dumps, but it contributes to the stabilization of excavated parts of the deposit. Particularly in room and pillar mining systems, it might be possible to minimize the dimensions of the needed pillars and thus increase the excavation grade of the deposit. Especially in room and pillar shaped potash mines, backfill has not only to become a rigid body that will rapidly absorb the convergence forces. It also has to be inert to the salt minerals in the mine. Processing residuals from flotation and hot solving process normally contain fluids in a range from 7 to 10 percent. These fluids contained in the backfill material are normally unsaturated in $MgCl_2$ and by the way able to solve $MgCl_2$ based rocks like carnallitit. At different mining sites carnallitit is underlying the mined sylvinite and by the way responsible for the stability of the pillars. To guarantee the stability of the mine cavities, the free flow of $MgCl_2$ unsaturated fluid from the backfill masses into the mine has to be prevented as much as possible. To determine the amount and the duration time of the dewatering process, a technical experiment with different types of processing residuals has been developed.

The processing residuals are installed in tubes (diameter 30 cm height 6 m). On the bottom of every tube, a drainage system is discharging the drained fluid to a trapping system on a balance. The complete installation is encapsulated. The balances are connected with a data logging system that is saving periodically the values of the weight of the tread out fluids. Thus this research installation allows the securing of the applicability of processing residual as backfill masses.

KEYWORDS

Backfill material, processing residuals, potash, fluids

PROBLEM STATEMENT AND INTRODUCTION

Degradation of economically minable deposits, combined with increasing requirements in environmental protection, are bringing changes in mining standards of modern mining operations in industrialized countries. The primary goals for the mining industry are to increase the exploitation rates of the deposits and minimize the environmental impact; more specifically to minimize the processing residuals to be dumped.
Classical room and pillar mining methods used in flat angular bedded sedimentary deposits (for example potash) become more inefficient in terms of extraction rate with respect to the increasing depth and more difficult mining conditions (Rauche 2015). This is caused by need of increase the pillar dimensions with increasing the depth for geomechanical reasons. To address this problem, backfilling of the mined areas could take place for supporting the cavities. The material used as backfill has to certain to lot boundary conditions. In this article two of these conditions are assessed on site. The first one is the sufficient availability, the second one is to guarantee that the backfill material will not react with the hostrock or the deposit itself. In general a sufficient availability is complied with processing residuals on site. Backfill operation using this material is also reducing the amount of the dumped material. Based on the mainly used processing technologies in German potash mining, the material is containing different amounts of process liquors. These liquors are usually saturated in NaCl, but not in other chlorides. Thus, it is essentially to know the amount of the draining fluid of a backfilled body to prevent solving processes potentially in the bottom where highly soluble minerals are located.

There exist established test procedures and guidelines for the determination of fluid content and the fluid retention capacity of soil material. Guidelines for determination of Fluid content of soils as for example DIN 18121 and DIN ISO 11465 can be widely adapted to test procedures with the salt grit like processing residuals.

The retention capacity for soil can be tested in accordance to DIN EN ISO 11274 and DIN EN ISO 11275 . Furthermore there are different articles dealing with water retention characteristics and capability of soils, their prediction and mathematical estimation (for example (Gupta und Larson 1979; Aubertin et al. 2003; Maidment 1993; Rawls et al. 1991; Stewart 1991)). These assumptions can not be transferred to salt processing residuals because of their specific grain size distributions (more or less monodisperse), their sur-

face properties of the grains and also of the special properties of the contained fluids (saturated brine) and their behavior which is very different from the behavior of water.
For this reasons it had been decided to develop and execute a new big scale test procedure to verify the fluid retention capability of processing residuals used as backfill under in situ approximated conditions
Beside simulations and small scale laboratory experiments, the best way for assessing the properties of the backfill body is to measure the drainage in a big scale experiment. Composition, implementation and results of this experiment are illustrated in this article. The sequence of the steps performed while the tests had been done is shown in Fig. 1.

Fig. 1 scematic overview about the testing process

SETTING

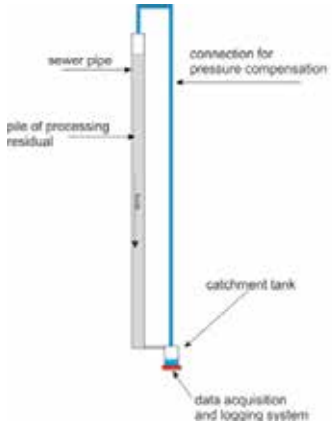

Figure 2 sketch of the test installation

The experiment is displayed in Fig. 1 and was built up in the laboratory of the Department for Mining and Special Civil Engineering.
It consists of three vertical tubes with a diameter of approximately 300 mm and a height of 6 m (Fig. 2). Sealed commercially sewer pipes were used for the pipes.
For installation and filling up of the tubes, a temporary scaffold had been structured. On the bottom the tubes are sealed with concrete. The top of the concrete forms a funnel to a drainage tube with a valve (Fig. 5), going outside the backfill column.
The surface of the concrete is sealed with a bituminous painting and is covered with a fiber mat and a layer of gravel Fig. 4), this constitutes as a filter that will prevent the backfill material from running out of the pipe and enables at the same time the fluid drainage.

Figure 3 - overall view of the experiment

Figure 5 -setup of the filter – inner drainage system

Figure 6 - setup of the outer drainage system

Figure 4 - catchment tank

The fluids are collected in a 40 l holding catchment tank, located on a self-logging electronic scale (Fig. 6). The top of the catchment tank is further connected to another tube on the top of the sewer pipes to ensure the possibility of pressure equalization in the complete system avoiding influences of atmospheric air (see Fig. 7). In this way, a completely closed system is generated preventing any influence from the ambient air. The log of the measured values is

captured by a computer which is connected to the scale. There are used three scales in total with three computers, one for each of the sewer pipes filled with material.

INSTALLATION OF THE MATERIALS TO BE TESTED AND STARTING OF THE TEST SEQUENCE

The tests have been commenced immediately after the delivery of the material, while the samples have been taken approximately 24 hours before the installation. This reflects a typical set up and scheduling of operation on a mine site.

To avoid mistakes and false readings in measurement, like potential fluid traps in the drainage system, an amount of 1.5 l of saturated salt brine was filled in the drainage system before the material was filled in.

The installation of the material to be tested was done in three sections per material type in a pipe. Every one of these sections had a height of around two meters. The material was filled in buckets of approximately 10 l of content and was lifted up from the ground to the installation height using a pulley. The material was tilted with gravitation in to the pipe (Fig. 8). After the insertion of three buckets the material was compressed using a 3 kg weighting mass, with around the diameter of the pipe simulating the load of an LHD in a real backfill operation. The built in process was stopped after accomplishing a material height of around 6 meters as reflecting typical backfill situation in German potash mines. Finally every pipe was sealed with a socket plug.

All in all, there were three parallel tests with different backfill materials constructed. Sample 1 was a mixture of processing residuals of two production lines with a ratio of 70 % of residual 1 and 30 % of residual 2. Sample 2 consisted of 100 % of residual 1 and sample 3 of 100 % of residual 2 from the processing line

Fig. 7 top of the experimental arrangement in height of 6 meters

Fig. 8 Installation of the material

of a German potash mine. Altogether, there was a mass of 604 kg of mixture of residuals, 546 kg of residual 1 and 590 kg of residual 2 built in.

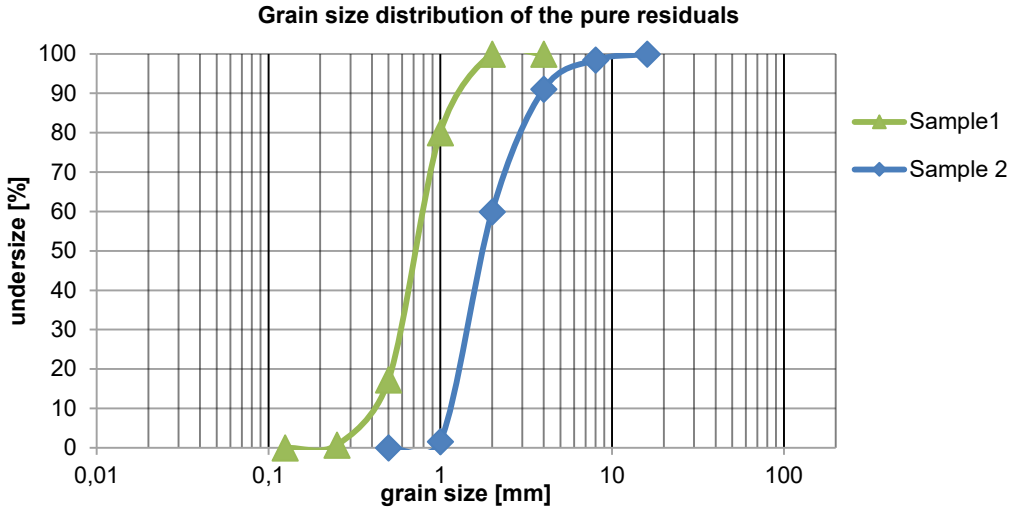

Figure 9 -Grain size distribution of Sample 1 and Sample 2

After completing the installation, the valves on the bottom of the piles were opened and the experiment started. At the beginning of the experiment, the data from the scales were logged every 10 minutes. After the fast drainage at the beginning of the experiment was lapsed, the interval of logging was increased to 30 minutes.

RESULTS

Already during the installation process, obvious differences in the characteristics of the tested material had been determined. The occurring fact of different grain size distributions in the materials was already known. Both sample 2 and 3, can be called monodisperse distributed. The grain size distribution of both tested pure residuals is shown in Fig. 9

The calculated grain size distribution of the mixture of the examined processing residuals is represented additionally in Fig. 10. Comparing both samples, the obviously wider spread grain size distribution of the mixture is visible. Using the same procedure for material installation, the grain size distribution has an effect on the attainable installation density. Installing the pure residuals, an installation density of approx. 1.3 t/m³ was obtainable, while the mixed material reached a density of 1.4 t/m³ at the same installation process.

In addition to the differences on the grain sizes, a clear difference in the moisture contained in the materials could be detected. Subjectively Sample 2 showed the highest content of moisture, objectively it is the material with the lowest content of fluids. The shown effect of high fluid visibility may be based on the relatively coarse and similar sized grain structure which is not able to retain the fluids with adhesive forces inside the grain matrix.

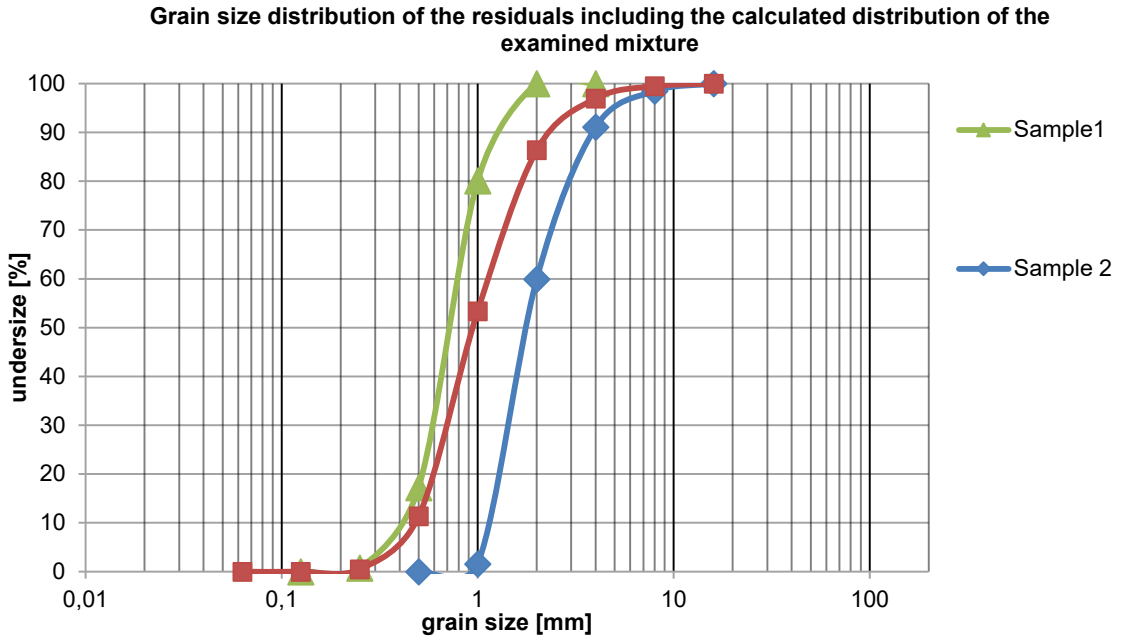

Figure 10 - Grain size distribution of Sample 1 and Sample 2 including a calculated distribution of the mixture of 70 % of sample 1 and 30 % of sample 2

The installed sample 1 is objectively the material with the highest amount of fluids within the matrix. During the installation processes, subjectively the material 1 appears to be significantly drier. This can be explained by the wider spread grain size spectrum and the enlarged surface per volume unit, which is able to capture the free fluids.

The tests started after the completion of the material installation by start logging the data and opening the drainage valves. The masses (in kg) of the drained fluids during the experiment were logged and are shown in Fig. 10.

One possible interpretation of the graphs on Fig. 10, showing the drained fluids confirms the formerly described misimpression of the fluid content of the different materials by its visual appearances. The fast and permanent heavy drainage from the material at Sample 2 on the first days of the experiment can be explained with the low retention capacity based on the grain size distribution range of the material.
The drainage of the residual mixture also shows a rapid initiation and a continuing strong fluid flow analogical to material 2. The graph for this sample in Fig. 10 is flattening abruptly after a testing period of only 4.5 days. After that (unexpected early) date no further drainage of the material could be determined. Therefore a validation of the test setup by reviewing the weighing and logging systems was done as well as a test of the permeability of the drainage system. Since no failure could be detected in the checks, the stopping of drainage had been explained with retention capacity of tested material.

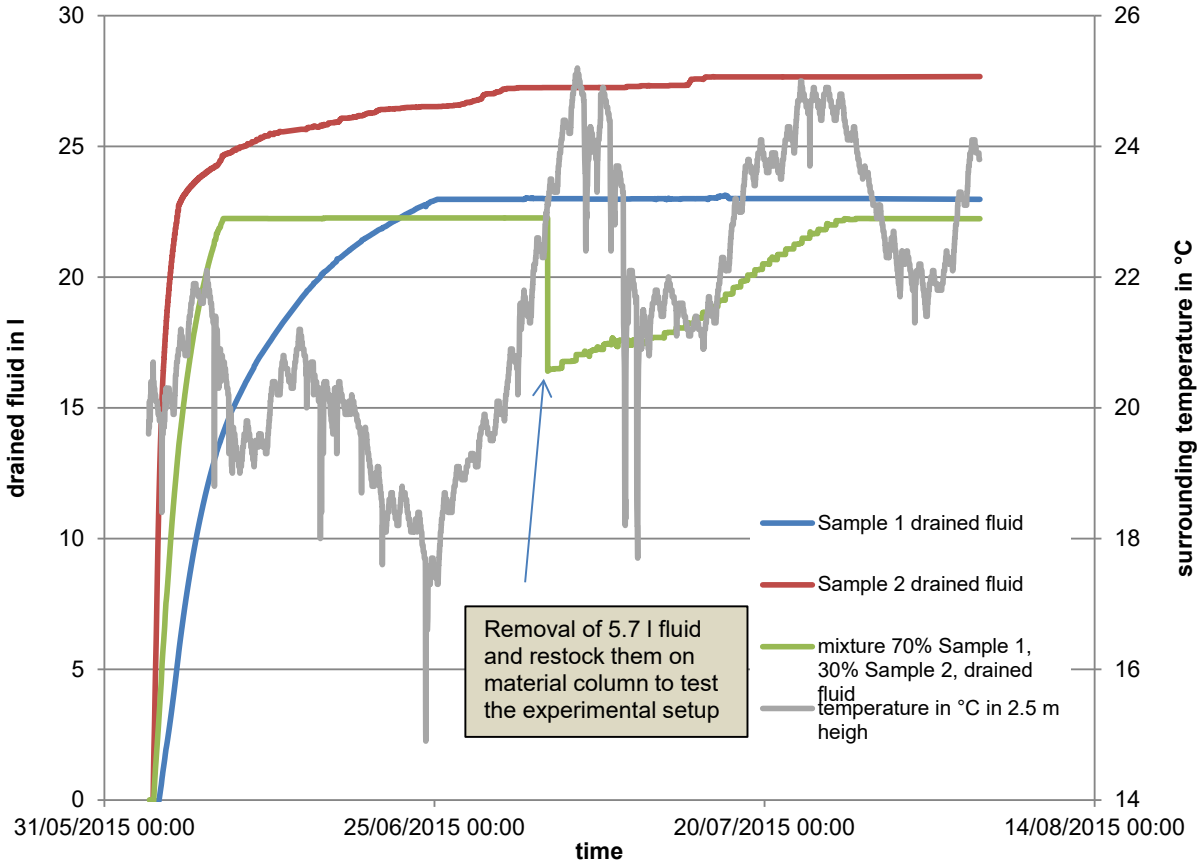

Figure 11 - Mass of the time dependent drained fluids from the residuals. The grey line shows the temperature in the laboratory during the experiment.

Table 1- measured humidity in the samples taken at end of experiment

sample number	mix	Sample 1	Sample 2
6	1.70	0.32	0.37
5	2.56	-	0.30
4	2.48	0.60	0.54
3	2.85	0.94	0.77
2	3.16	1.04	0.39
1	4.18	2.71	0.60

As expected, the drainage of material 1 ran long lasting and more continuously. This behavior can be explained with the grain size distribution of the material. The monodisperse fine granular material has large specific surface and relatively small grain interstices. These interstices can adhesively hold a large amount of fluids. Furthermore, the resistance of the material for the drainage is significantly larger than for Sample 2. At the end of the tests, several material samples were taken from the residual columns in a vertical distance of one meter. With these samples the determination of distribution of humidity in the pillar have been conducted.

The evaluation of data analysis is showing a significant decrease of moisture with upward position in pillar. The respective data are illustrated in Table 1. The samples were taken approximately in the middle of the column. The number of each Sample in Table 1 is approximately the respective height of the pillar in meters.

The result of decreasing humidity with increasing height of the pillar can be explained with evaporation processes and capillary effects on the surface of the testing pillar (the system is closed, humidity cannot evaporate), everything will be trapped in the catchment tank). Furthermore it was assumed that due to the increasing downward pressure, the ability of the material to store fluids in the grain interstices (getting smaller → more adhesive forces) is also increasing.

INTERPRETATION

The trend of the graphs in Fig. 10 are showing esp. for the monodisperse distributed Sample 1 and also for the bi-disperse mixture of sample 1 and sample 2 a rapid drainage of contained fluids already after a short time of initialization. The intensity of drainage was smoothly decreasing and stopped abruptly. In the case of Sample 3, with a ratio of 70 % Sample 1 and 30 % Sample 2, this stop entered already around 7 days after start of the experiment. At this time 22.2 l of fluid had drained out of the material. Afterwards, only very small amounts of fluids had drained but are not visible in the graphs in Fig. 10.

Based on the material data determined at the test, the remained humidity in residual had been identified. Therefore a value of 2.52 % was calculated for Sample 3. This calculated value differs a bit from the mean of the material samples taken in the column after the end of the experiment. The mean of these six samples had a value of 2.82 %. The difference of these two values can be explained by using complete different methodic ways for determination. The mean humidity determined by examination of after-test samples for sample 1 is 1,12 % and for sample 2 is 0,5%. The measured humidities for sample 3 and sample 1 represented in Table 1 are generaly showing a decreasing of the value with increasing sampling position. Sample 2 is showing an exception with the highest amounts of humidity in sample 3 at the middle of the column. This fact can be explained with inhomogeneous grain size distributions in the material column (caused by inhomogeneous sample material) and the relation of the measurement error to the contained value.

CONCLUSIONS

The processing residuals of a potash mine are not able to keep their contained fluids stable over a medium term timespan. Using these materials for backfill, the contained fluids will drain rapidly within only a few days out of the backfill matrix, thus posing a significant risk of solution processes of underlying salt structures. This method can only be recommended at sites where no processes caused by the contained fluids are to be expected.

Using such materials on sites where the free fluids contain typically NaCl saturated, they may dissolve soluble materials in the bottom or wall of an adit. Therefore the use of this type of material has to be avoided for safety reasons. The use of the moisty residuals for backfill at such places will not be feasible without drying the material with technical processes to a humidity of +/- 1 %. Drying the material could be done through an evaporation process which needs a huge amount of energy in order to vaporize the contained water.

For this reason at sites where slightly soluble minerals occur in the bottom or bottom near area, an economical use of residual materials from wet potash treatment methods is consequently not permittable.

REFERENCES

DIN 18121-2:2012-02, Soil, investigation and testing - Watercontent - Part 2: Determination by rapid methods.

DIN ISO 11465:1996-12, Soil quality - Determination of dry matter and water content on a mass basis - Gravimetric method (ISO 11465:1993).

2014: DIN EN ISO 11274:2014, Soil quality - Determination of the water retention characteristics - Laboratory methods (ISO 11274:1998 + Cor. 1:2009).

2014: Soil quality - Determination of unsaturated hydraulic conductivity and water-retention characteristic - Wind's evaporation method (ISO 11275:2004); German version EN ISO 11275:2014.

Aubertin, M.; M Mbonimpa, M.; B Bussière, B.; R P Chapuis, R.P. (2003): A model to predict the water retention curve from basic geotechnical properties. In: *Canadian Geotechnical Journal* 40 (6), S. 1104–1122. DOI: 10.1139/t03-054.

Gupta, S. C.; Larson, W. E. (1979): Estimating soil water retention characteristics from particle size distribution, organic matter percent, and bulk density. In: *Water Resources Research* 15 (6), S. 1633–1635. DOI: 10.1029/WR015i006p01633.

Maidment, David R. (1993): Handbook of hydrology. New York: McGraw-Hill.

Rauche, Henry (2015): Die Kaliindustrie im 21. Jahrhundert. Stand der Technik bei der Rohstoffgewinnung und der Rohstoffaufbereitung sowie bei der Entsorgung der dabei anfallenden Rückstände. 1. Aufl. 2015 (SpringerLink : Bücher).

Rawls, W. J.; Gish, T. J.; Brakensiek, D. L. (1991): Estimating Soil Water Retention from Soil Physical Properties and Characteristics. In: B. A. Stewart (Hg.): Advances in Soil Science. New York, NY: Springer New York, S. 213–234. Online verfügbar unter http://dx.doi.org/10.1007/978-1-4612-3144-8_5.

Stewart, B. A. (Hg.) (1991): Advances in Soil Science. New York, NY: Springer New York.

EFFECT OF PARTICLE SIZE ON WEAR IN MINE BACKFILL DISTRIBUTION SYSTEMS DETERMINED USING A ROTARY TEST AND IN-SITU TESTING

K.J. Creber and *M.F. Kermani and M. McGuinness and F.P. Hassani

McGill University
3450 University Street
Montreal, Canada H3A 0E8
*(*Corresponding author: mehrdad.fadaeikermani@mail.mcgill.ca)*

24th World Mining Congress
MINING IN A WORLD OF INNOVATION
October 18-21, 2016 • Rio de Janeiro /RJ • Brazil

EFFECT OF PARTICLE SIZE ON WEAR IN MINE BACKFILL DISTRIBUTION SYSTEMS DETERMINED USING A ROTARY TEST AND IN-SITU TESTING

ABSTRACT

Mine backfill is transported hydraulically from the surface to stope through a pipeline system, creating significant wear in some mines and minimal wear in others. Wear rate prediction of mine backfill distribution systems is beneficial for improved safety and operational performance of underground mines. In this study, wear rate measurements are performed on a rotary wear test apparatus that consists of a pipe spool filled with mine backfill materials and rotated around its centreline axis. Relative wear rates are established between different ratios of two mine backfill materials, tailings and sand. It is found that higher wear rates are the result of larger particle size distributions.

KEYWORDS

Backfill, distribution, system, pipeline, wear, rate, test, prediction

INTRODUCTION

Mine backfilling is the practice of filling cavities created by underground mining. Slurry fill and paste fill are two methods classified as hydraulic mine backfill. Hydraulic mine backfill essentially consists of inert materials (tailings or waste rock), water and different cementitious materials such as Portland cement and blast furnace slag. The fill materials are usually prepared on the surface and transported underground through a series of pipelines and/or boreholes to fill the excavated underground cavities created by mining activities by using a pumping system and/or gravitational force. The transportation of hydraulic mine backfill causes wear in the mine backfill distribution system, which presents significant challenges for the mining industry. In general, wear in the pipeline is caused by the properties of both the fill itself and of its flow behaviour through the distribution system.

In this paper, the effect of particle size distribution of inert tailings and sand materials used at a Canadian zinc mine, on the wear rate were investigated by conducting a low stress wear test. The test was developed to estimate the wear rate in mine backfill distribution pipelines. The prediction of a wear rate could help the mining industry to predict when the backfill pipeline has worn too thin and be able to change the pipeline in advance of failure. Furthermore, this research aimed to study the interaction among mine backfill properties and pipe wear.

Pipelines used in mine backfill systems are susceptible to erosive-corrosive conditions that can cause significant problems due to wear and the thinning of pipeline walls. McGuinness and Cooke identify the problems associated with the thinning of pipeline walls, creating undesirable safety and operational concerns due to potential injury of personal that can occur due to pipeline failure, as well as the changing mechanical energy balance and hydraulic profile of the distribution system, which can lead to slack flow, free fall, and severe localized wear (McGuinness & Cooke, 2011).

Pipeline wear is not a new problem and engineers have been working to understand its fundamental behaviours for decades. In 1975, much work had been done in the field of slurry pipeline wear and summarized well by Truscott (Truscott, 1975). The effects of particle hardness, size, shape, mixture concentration and density, corrosive conditions, pipeline material properties, and flow properties were identified and studied to some degree.

Many factors have an influence on pipeline wear and are suggested to include (1) solid phase of slurry: size, shape, sharpness, density, harness, concentration, toughness, (2) liquid phase of slurry: viscosity, density, (3) pipeline properties: composition, hardness, elongation, resilience, orientation, density, (4) pipeline flow regime: velocity, pressure (Steward & Spearing, 1992a). Different wear tests can be used to focus on evaluating one or more of these factors.

Wear Testing

Wear tests are designed to test specific modes of wear that are being experienced in application. Different wear tests have their own advantages and limitations. Mine backfill distribution systems suffer predominantly from abrasion wear due to its high solids concentration (Hewitt, Allard, & Radziszewski, 2009). Abrasive wear can erode a surface through two mechanisms: (1) deformation (impact) wear, and (2) cutting (sliding) wear. There is also low and high stress wear, in addition to chemical corrosion effects, and synergistic effects between erosion and corrosion (Budinski, 2007).

In the low stress wear regime, it is believed that chemical effects will play a dominant role in the wear and the properties of the aggregate will play a secondary role in the wear rate (López, Congote, Cano, Toro, & Tschiptschin, 2005).

The synergistic effects between erosion and corrosion were reported by Postlethwaite et al. and they suggested two mechanisms for this phenomena: (1) solid particles remove the passive film that would prevent further corrosion in a purely liquid system, and (2) the mechanical forces responsible for deformation and cutting wear also produce an increase in anodic dissolution rate of the metal material (Postlethwaite, Tinkler, & Hawrylak, 1972).

Slurry transportation through pipelines is used across many industries and in many applications, thus leading to a greater depth of research into low pulp density slurry wear than high pulp density paste wear. Experimental techniques to evaluate wear resistance and characterize wear mechanisms is exhaustive. However, the final conclusions of many studies only present a comparative analysis of the relative wear resistance of various pipeline materials (Boothroyde & Jacobs, 1977; Hocke & Wilkinson, 1978).

Different wear tests have been used to measure pipeline wear. Some authors have chosen to use a full flow loop wear test where slurry or paste is circulated through a recirculating pipeline loop using a pump (Cooke, 1996). With this test, pipeline conditions in the field are very well recreated, however it is an expensive solution to wear testing and requires significant physical space to operate.

To reduce physical space requirements, Cooke built a scale model recirculating loop test with 50 mm nominal diameter pipes in additional to the full scale 125 mm nominal diameter recirculating loop (Cooke, 1996). Scaling laws were then developed using the results of the full size and scale model tests. Steward and Spearing did experimental tests with a recirculating loop test, using mine tailings for backfill applications (Steward & Spearing, 1992b). The internal diameter of the pipeline varied from 26.2 mm to 74.1 mm. They tested the effect of slurry density, slurry velocity, and pipeline diameter on the wear rate. Empirical correlations were created for each parameter tested. It was found that there is a decrease in pipeline wear with increasing density due to the decreased mean free path (Steward & Spearing, 1992c). Higher concentrations reduce the distance a particle can travel before contacting another particle, which reduce its velocity, energy, and ability to cause pipeline wear.

Various ASTM standard tests have been developed and successfully used for slurry erosion applications as well as minefill distribution system wear such as ASTM G75-15 *Standard Test Method for Determination of Slurry Abrasivity (Miller Number) and Slurry Abrasion Response of Materials (SAR Number)*, ASTM G105-02(2007) *Standard Test Method for Conducting Wet Sand/Rubber Wheel Abrasion Tests* and ASTM G119-09 *Standard Guide for Determining Synergism Between Wear and Corrosion.*

The majority of previous research using wear tests to investigate slurry wear in pipelines has been done at low solids concentrations, because that is how most slurry is transported. However, this does not reflect the properties of backfill, which is transported at high solids concentrations.

Boothroyde and Jacobs had suggested the construction of a wear simulation rig and a method that they described as "…to rotate a straight pipe sample, half filled with slurry, about an axis through its centreline." (Boothroyde & Jacobs, 1977) In this research, a rotary test similar to the one suggested by Boothroyde and Jacobs is used to evaluate the pipe wear rate.

This test method allows the use of all minefill components, including large gravel found in some minefill aggregates. A high concentration of solids can be tested, reflecting the reality of hydraulic backfill. This test also allows the use of a pipeline material in its original form, without any machining or modifications to the material and potentially its properties.

METHOD

Equipment

To perform the rotary test, an apparatus was constructed to provide a spinning motion to the pipe spools and is illustrated in Figure 1. It consists of a series of rollers spaced evenly apart, which allow the pipe spools to sit between two adjacent rollers. The rollers spin under power of an electric motor and a series of sprockets and chain, which transfer their motion to the pipe spools.

Figure 1 - Diagram of the roller machine

In order to seal the backfill materials inside the pipe spools and avoid material leakage, a system of parts were assembled that apply pressure to a lubricated o-ring that is in contact with the spool edge, as illustrated in Figure 2.

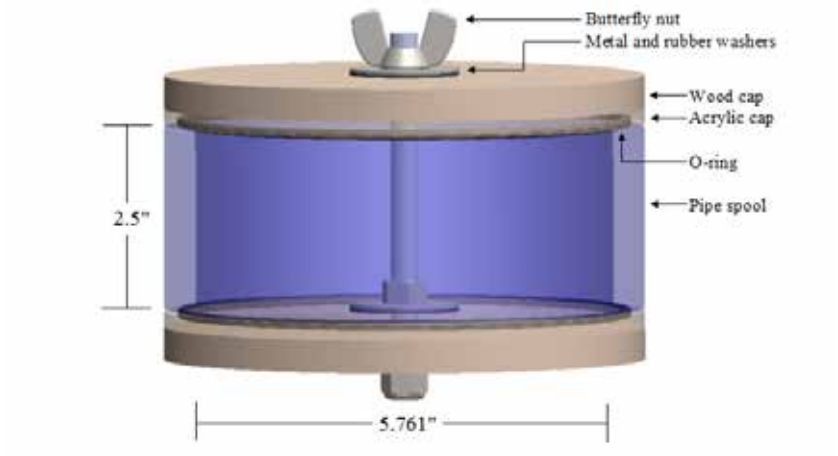

Figure 2 - Diagram of a pipe spool with end caps

Through preliminary testing, some test parameters were identified and specified as constant parameters, summarized in Table 1.

Table 1 - Constant test parameters

Spool Internal Diameter	≈ 5.761”
Spool Length	2.5”
Spool Rotational Speed	40 RPM
Mass of Dry Material	500 g
Mass % Solids	75%
Cycle Length	≈ 4 days
Test Length	36 days

- Typical slurry fill is 60-75% solids by weight and paste fills are 75-88% solids by weight. By choosing 75% solids by weight, a median value for both types of mine backfill was used.

- The cycle length of four days between each time the material is emptied from the spool and refilled was determined by analyzing the results of several particle size distributions. A four day cycle time was deemed acceptable to preserve the original size characteristics of the aggregates.

- A total test length of 36 days was chosen after inspecting graphs of thickness loss over time and realizing linear relations in a reasonable amount of time, with enough data to mitigate any initial effects in the first couple cycles where there may be inconsistent layers of pipe material because of corrosion.

Sample Preparation

Upon receiving a shipment of mine backfill material (sand and tailings) from the mine, each sample was first fully homogenized by mixing in a concrete mixer. Material characterization (particle size distribution, specific gravity, mineralogy, pH, moisture content) of the mine backfill material was then performed on each homogenized sample.

Test Procedure

For any given test, three identical trials were performed with three separate spools and cap assemblies. Based on the moisture content of the sample material(s), a given mass of wet material(s) and

process water were added to the spool to achieve a pulp density of 75% solids by weight. Once all components of the backfill were added to the spool, the top cap was placed onto the spool and sufficient pressure to seal in the mine backfill mixture was applied with a wing nut.

The spool was then placed onto the rotary machine, which rotates the spool at a rate of 40 rpm. Four days were allowed to pass, with continuous rotation of the pipe spools on the roller machine. After four days of rolling, the pipe spools were removed, and the mine backfill mixture inside was removed and discarded. The spools were extensively cleaned, then dried by placing in an oven at 175°C for one hour. After the spools were removed from the oven, they were allowed to cool for about a half hour prior to taking their dry mass. The difference between initial and final spool mass was calculated and recorded, which is considered as the spool wear.

This concludes the procedure for one cycle of the test. This procedure was then repeated in its entirety for nine cycles of four days each, until the total test length achieved 36 days.

MATERIALS

Pipe Material

The spools are sections of an API 5L X52 pipeline and its properties are listed in Table 2 and Table 3. Canadian mines commonly use API 5L X52 and API 5L X42 pipes in their mine backfill distribution systems. For these tests, API 5L X52 pipes were chosen as it is used at the mine in this study. The tests are all performed on 6" nominal diameter, schedule 80 pipes. The internal diameter of a new pipe from the manufacturer is specified at 5.761". However, a relatively large tolerance in wall thickness of +15%, -12.5% does exist.

Table 2 - Chemical properties of spool material

Chemical Composition, %											
C	**Si**	**Mn**	**P**	**S**	**Cu**	**Ni**	**Cr**	**Mo**	**V**	**Nb**	**Ti**
0.06	0.17	1.03	0.015	0.001	0.02	0.01	0.02	TR	0.001	0.032	0.001

Table 3 - Mechanical properties of spool material

Tensile Tests			Hardness, HRB	Specific Gravity
Tensile Strength (psi)	**Yield Strength (psi)**	**Elongation (%)**		
76430	70630	31	87	7.86

Abrasive Materials

In this paper, all mine backfill materials, including sand, tailings, and process water were taken from a zinc mine in Canada. No binder materials were used in this study. Five different mixtures were prepared, using different ratios of tailings and sand. Table 4 shows the characteristics corresponding to these mixtures, as well as the mean of 11 other mine tailings, for reference.

Table 4 - Physical properties of abrasive material mixtures

Material Ratios	D_{10} (µm)	D_{20} (µm)	D_{30} (µm)	D_{50} (µm)	D_{60} (µm)	D_{90} (µm)	C_u	C_c	Specific gravity
100% Tailings	3.4	7.8	11.6	22.9	34.9	102.6	10.1	1.1	2.86
100% Sand	149.0	189.9	232.8	328.7	424.4	2443.6	2.8	0.9	2.69
75T / 25S	5.0	10.2	15.8	41.5	60.8	424.4	12.1	0.8	2.82
50T / 50S	7.5	15.5	33.5	136.7	198.9	917.9	26.5	0.8	2.78
25T / 75S	14.7	51.8	144.2	246.9	298.7	1551.8	20.3	4.7	2.73

Mean of 11 mine tailings (Ouellet, Bussière, Aubertin, & Benzaazoua, 2007)	2.2	5.3	9	20	29	100	13.2	1.27	Not available

D_{10} = particle diameter size that 10% of the sample particles are finer than
D_{30} = particle diameter size that 30% of the sample particles are finer than
D_{60} = particle diameter size that 60% of the sample particles are finer than
D_{90} = particle diameter size that 90% of the sample particles are finer than
$C_u = D_{60}/D_{10}$ = coefficient of uniformity
$C_c = (D_{30})^2/(D_{60} \times D_{10})$ = coefficient curvature

The mineralogy of the tailings and sand materials were tested using x-ray fluorescence and the results are presented in Table 5.

Table 5 - Mineralogy of tailings and sand materials

Chemical Composition	Tailings (wt%)	Sand (wt%)
SiO_2	54.79	69.69
Al_2O_3	18.64	12.03
Fe_2O_3	6.75	2.31
CaO	5.67	7.56
K_2O	3.46	2.11
Na_2O	3.32	3.89
MgO	3.26	1.70
SO_3	2.83	0

Process Water

The pH of the process water used in testing was measured due to its potential effects on corrosion and the synergistic erosion-corrosion process that can significantly increase wear rates. In addition, the pH of slurry mixtures, using process water and sand or tailings were measured using guidelines outlined in ASTM D4972-01(2007) *Standard Test Method for pH of Soils*. The results of these tests are summarized in Table 6.

Table 6 - pH of process water and slurry mixtures

Sample	pH
Water	7.48
Tailings	8.17
Sand	8.00

RESULTS

A pipe wall thickness loss (t_{loss}) is calculated from the measured mass loss (m_{loss}), using the density of the metal pipe material (ρ_{pipe}), its internal diameter (D_{old}) and length (ℓ),

$$V_{loss} = \frac{m_{loss}}{\rho_{pipe}} \tag{1}$$

$$D_{new} = \sqrt{\left(\frac{4}{\pi \ell}\right) V_{loss} + D_{old}^2} \tag{2}$$

$$t_{loss} = \frac{D_{new} - D_{old}}{2} \quad (3)$$

Shown in Figure 3 to Figure 7 are the time history plots of spool wall thinning over the course of the 36 day testing period.

A linear trend is fit to the data. No attempt was made to fit the linear trend through the origin where there was zero thickness loss at zero test time. The first cycle of four days is also ignored in the linear trend calculations as it is not representative of the overall trend in some tests.

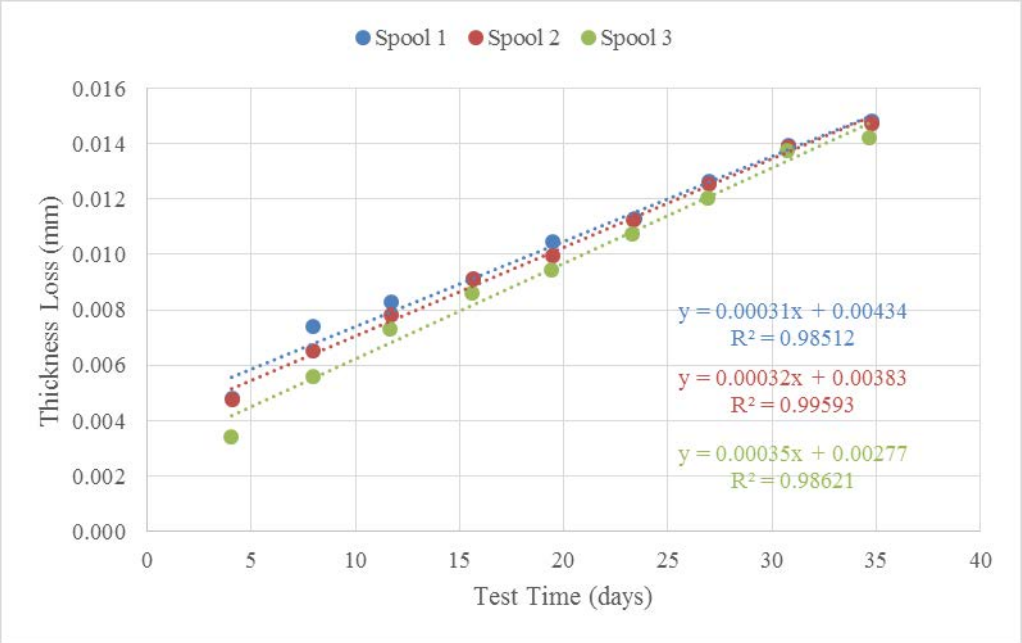

Figure 3 - Time history of test (100% tailings)

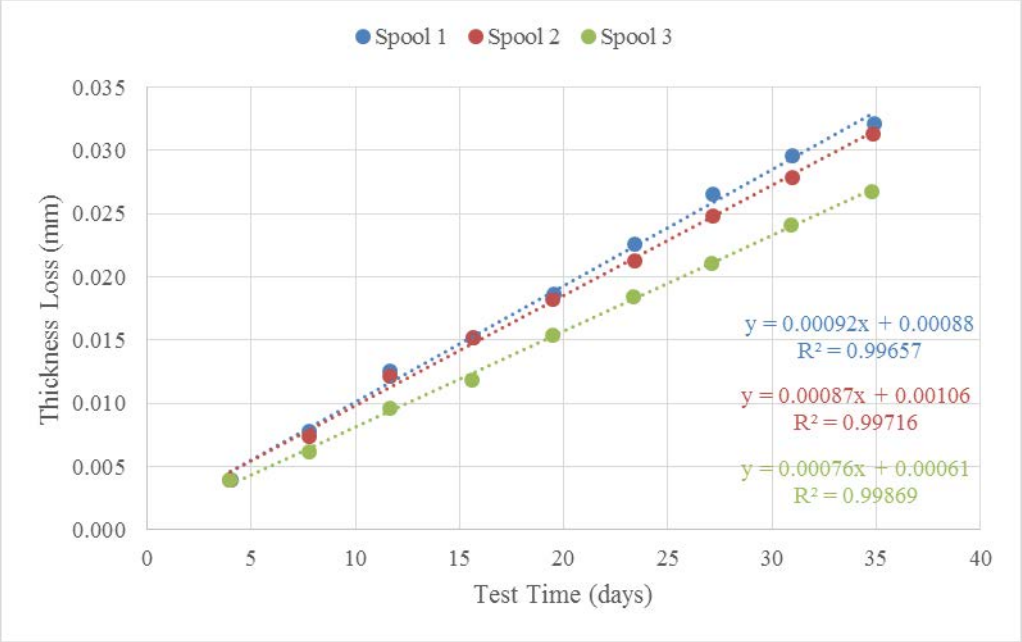

Figure 4 - Time history of test (75% tailings / 25% sand)

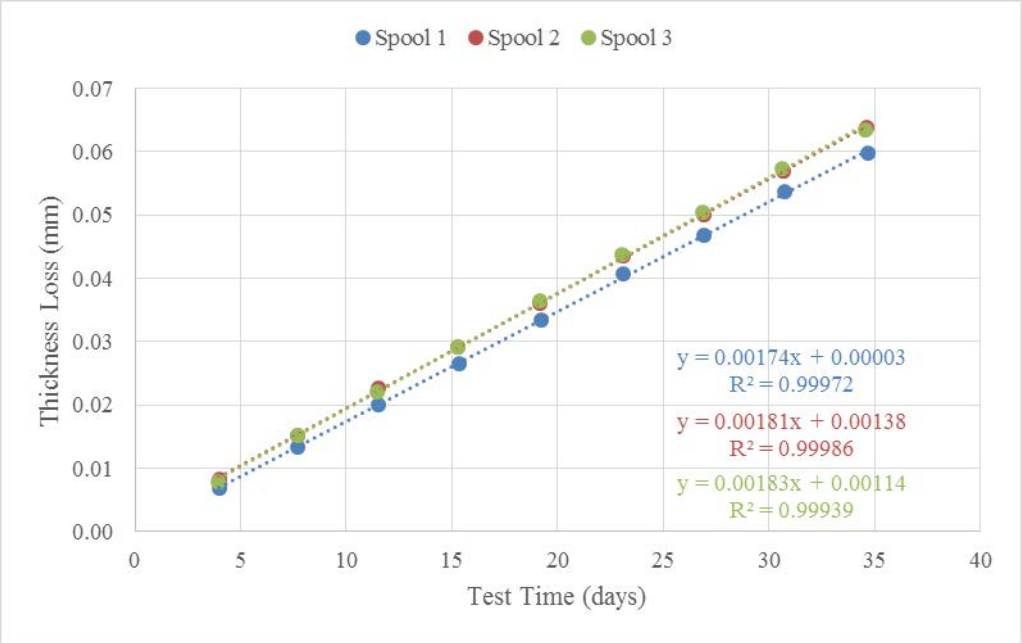

Figure 5 - Time history of test (50% tailings / 50% sand)

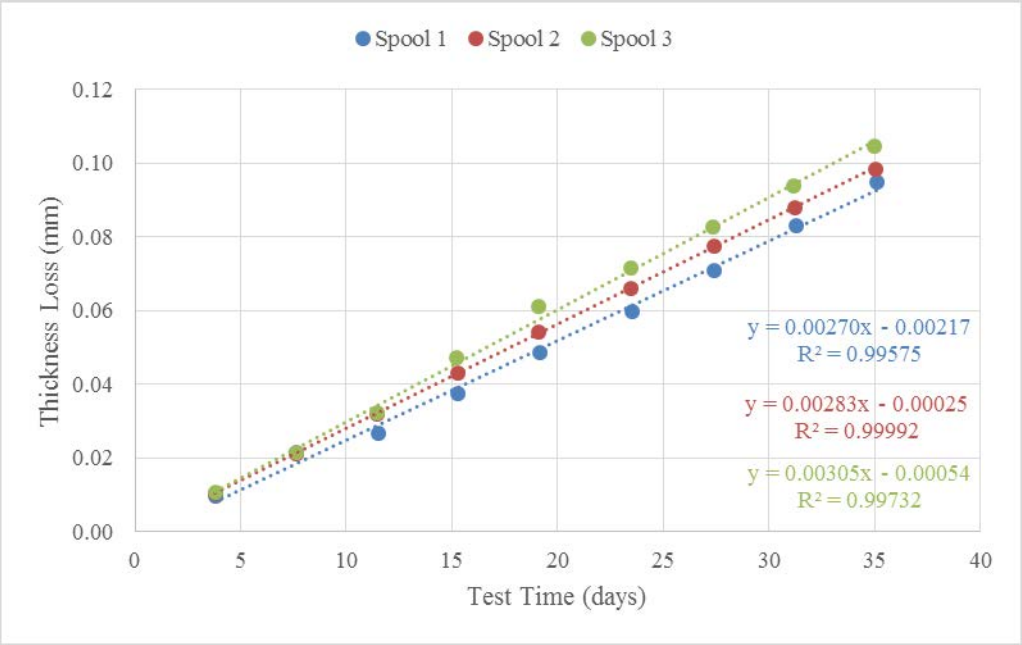

Figure 6 - Time history of test (25% tailings / 75% sand)

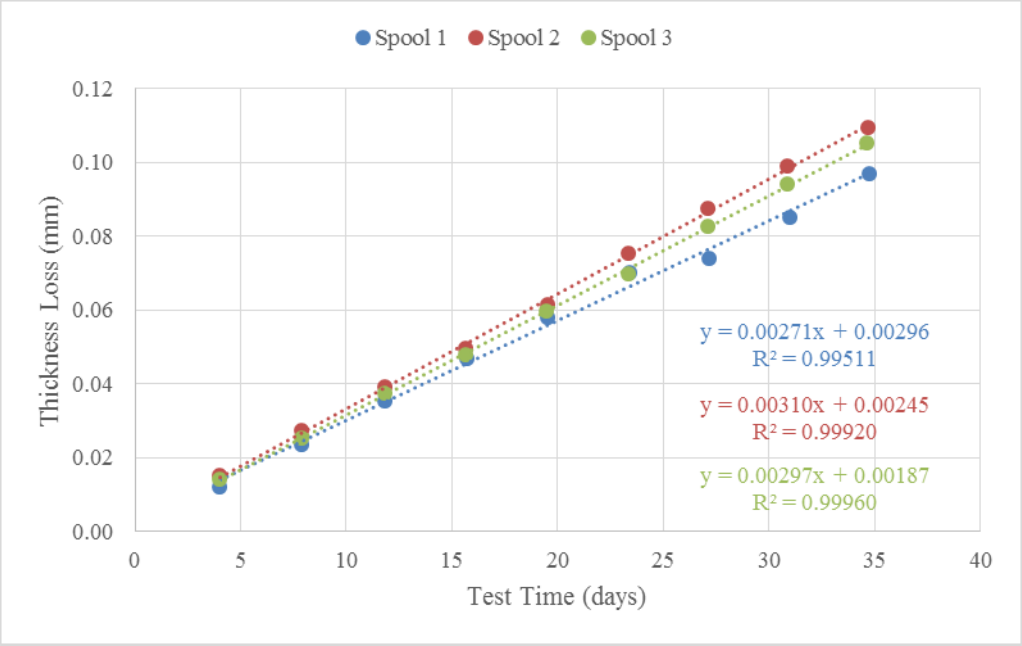

Figure 7 - Time history of test (100% sand)

DISCUSSION

The wear rates calculated from the results of the rotary wear test are compiled in Table 7 and presented graphically in Figure 8. The wear rate is quoted in mm/day, which represents a pipe wall thickness loss, calculated based on a measured mass loss.

Table 7 - Summary of results

	Wear Rate (mm/day)				
	100% Tailings	**75% Tailings 25% Sand**	**50% Tailings 50% Sand**	**25% Tailings 75% Sand**	**100% Sand**
Spool 1	0.00031	0.00092	0.00174	0.00270	0.00271
Spool 2	0.00032	0.00087	0.00181	0.00283	0.00310
Spool 3	0.00035	0.00076	0.00183	0.00305	0.00297
Average	0.00033	0.00085	0.00179	0.00286	0.00293
St. Dev.	0.00002	0.00008	0.00005	0.00018	0.00020

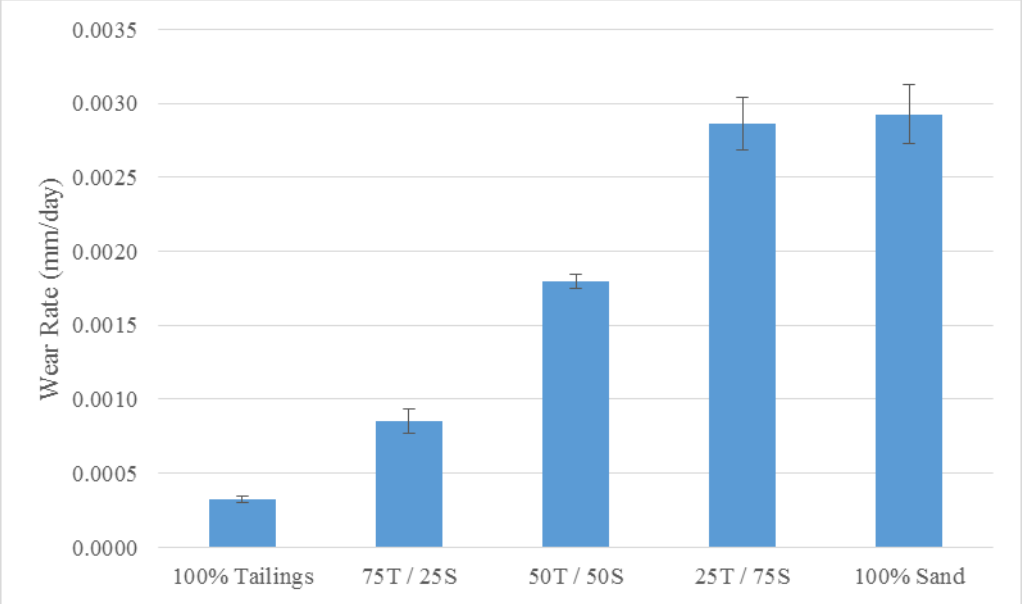

Figure 8 - Summary of results

It is found that average wear rates are between 0.00033 mm/day and 0.00293 mm/day. The wear rate increases as the particle size of the abrasive materials increases, due to an increasing concentration of sand and decreasing concentration of tailings. Thus, the results of this research are in agreement with the research conducted by other investigations (Desale, Gandhi, & Jain, 2009; Truscott, 1975). There is little difference between 25T/75S and 100% sand, suggesting that a substantial amount of fine tailings material must be added to a backfill mixture to realize a decrease in pipeline wear.

The tailings and sand materials used in this study have similar mineralogy, both composed primarily of quartz. Thus, the mineralogy of the materials is not affecting the wear rate results as significantly as the particle size difference seems to be.

At the Canadian zinc mine in this study, where typical backfill recipes are 50T/50S or 45T/55S, the authors of this paper measured the wear rate of the mine backfill distribution system pipelines using an ultrasonic thickness gauge over a two year period from 2013 to 2015. An average wear rate between three different levels in the mine was found to be 0.09 mm/100k tonnes of paste that has flowed through the pipe. Comparing the results of this wear test, with in-situ wear rate data, a correlation can be made.

$$Wear\ rate_{in-situ}\left[\frac{\text{mm}}{\text{100k tonnes}}\right] = K \times Wear\ rate_{laboratory}\left[\frac{\text{mm}}{\text{day}}\right] \quad (4)$$

Using the rotary wear test results from the laboratory, for the 50T/50S mix, and the average in-situ wear rate, the correlation parameter (K) can be solved:

$$K = Wear\ rate_{in-situ}\left[\frac{\text{mm}}{\text{100k tonnes}}\right] \Big/ Wear\ rate_{laboratory}\left[\frac{\text{mm}}{\text{day}}\right] \quad (5)$$

$$= \frac{0.09\ \text{mm/100k tonnes}}{0.00179\ \text{mm/day}}$$

$$K = 50.3\ \frac{\text{day}}{\text{100k tonnes}}$$

Further investigation must be done to conclude if the correlation parameter is global or can only be applied to the mine in this study.

The rotary test accounts for the solid phase of the slurry, liquid phase of the slurry, and pipeline properties. It does not account for the pipeline flow regime, including velocity, which is known to be a major factor is slurry pipeline wear. This test assumes a constant velocity between all tests to isolate the other parameters.

Although theoretically the mine backfill mixture is spinning inside of the rotary test spools at 0.3 m/s, its cohesive properties may be significantly reducing this speed. The degree to which the velocity of the backfill mixture is affected inside the spool will vary as its aggregate components change. With the solids percentage held constant, among various aggregate mixtures of different particle sizes, the flowability of each mixture will change. It could be due to this fact that more wear is occurring with larger particle size, as the mixture has more flowability and thus more relative motion against the spool wall.

One drawback of the test is that no external pressures are applied to the abrasive backfill material, against the pipe wall, as is the case in pressurized backfill distribution systems. This is a low stress wear test.

The effect of corrosion was not specifically measured in this test. It was assumed that the majority of wear was due to abrasion. We do not believe corrosion is a major contributing factor because the backfill mixtures are only slightly basic. This should be investigated further to confirm.

CONCLUSION

The effect of different ratios of mine backfill material on the mine backfill pipe wear, simulated in a laboratory test, is presented in this paper. The investigation confirmed that the particle size distribution of the backfill material has a great impact on pipeline wear. The results demonstrate that the wear rate increases with the increase of overall particle size of the backfill mixture. It was also shown that while the rotary test can be effectively used to measure the wear rate, this test faces some limitations which need to be considered.

Preliminary analysis shows that wear rate results from the laboratory rotary test, when quoted in mm/day, can be scaled by a factor of 50.3 to estimate in-situ wear rates, when quoted in mm/100k tonnes of paste.

ACKNOWLEDGEMENTS

The authors acknowledge the financial support given by NSERC for the mine backfill distribution system wear study. The authors are also grateful for the help and support of Glencore, Vale, Barrick, Lake Shore Gold, IAMGOLD and HudBay Minerals. The help and contribution of other graduate and undergraduate students at McGill University must also be recognized. The authors thank Glencore for the donation of the roller machine for the wear study.

REFERENCES

Boothroyde, J., & Jacobs, B. E. A. (1977). *Pipe wear testing 1976-1977*. BHRA Fluid Engineering.

Budinski, K. G. (2007). *Guide to Friction, Wear, and Erosion Testing*: ASTM International.

Cooke, R. (1996). Pipeline material evaluation for the mina grande hydrohoist system. *Hydrotransport 13*.

Desale, G. R., Gandhi, B. K., & Jain, S. C. (2009). Particle size effects on the slurry erosion of aluminium alloy (AA 6063). *Wear, 266*(11-12), 1066-1071. doi:10.1016/j.wear.2009.01.002

Hewitt, D., Allard, S., & Radziszewski, P. (2009). Pipe lining abrasion testing for paste backfill operations. *Minerals Engineering, 22*(12), 1088-1090. doi:10.1016/j.mineng.2009.03.010

Hocke, H., & Wilkinson, H. N. (1978). Testing Abrasion Resistance of Slurry Pipeline Materials. *Tribology International, 11*(5), 289-294. doi:Doi 10.1016/0301-679x(78)90060-9

López, D., Congote, J. P., Cano, J. R., Toro, A., & Tschiptschin, A. P. (2005). Effect of particle velocity and impact angle on the corrosion–erosion of AISI 304 and AISI 420 stainless steels. *Wear, 259*(1-6), 118-124. doi:10.1016/j.wear.2005.02.032

McGuinness, M., & Cooke, R. (2011). *Pipeline wear and the hydraulic performance of pastefill distribution systems: the Kidd Mine experience*. Paper presented at the Minefill 2011, 10th International Symposium on Mining with Backfill.

Ouellet, S., Bussière, B., Aubertin, M., & Benzaazoua, M. (2007). Microstructural evolution of cemented paste backfill: Mercury intrusion porosimetery test results. *Cement and Concrete Research, 37*, 1654–1665.

Postlethwaite, J., Tinkler, E. B., & Hawrylak, M. (1972). *Corrosion studies in slurry pipelines*. Paper presented at the Hydrotransport 2.

Steward, N. R., & Spearing, A. J. S. (1992a). Combating pipeline wear - an advancing technology. *Journal of the South African Institute of Mining and Metallurgy, 92*(6), 149-157.

Steward, N. R., & Spearing, A. J. S. (1992b). The performance of backfill pipelines. *Journal of the South African Institute of Mining and Metallurgy, 92*(1), 27-34.

Steward, N. R., & Spearing, A. J. S. (1992c). *Wear of backfill pipelines in South African gold mines*. Paper presented at the International Conference in Bulk Materials Handling and Transportation, Wollongong, Australia.

Truscott, G. F. (1975). *A literature survey on wear of pipelines*. BHRA Fluid Engineering.

ESTIMATION OF INFLUENCE OF MINING-TECHNICAL AND ORGANIZATIONAL CONDITIONS ON EFFICIENCY OF EXPLOITATION OF TRUCKS IN OPEN-PITS

Sabitov Agibay R., Galiyev Seitgali Zh., Samenov Galymzhan K.

JSC "ERG Research Engineering Center"
01000 Kazakhstan, Astana, Kabanbay Batyr st.30A, 302
*(*Corresponding author:seitgaligaliyev@mail.ru)*

24th World Mining Congress
MINING IN A WORLD OF INNOVATION
October 18-21, 2016 • Rio de Janeiro /RJ • Brazil

ESTIMATION OF INFLUENCE OF MINING-TECHNICAL AND ORGANIZATIONAL CONDITIONS ON EFFICIENCY OF EXPLOITATION OF TRUCKS IN OPEN-PITS

ABSTRACT

In the article analyses the joint exploitation of Hitachi EH-3500 ACII and BelAZ-75131 quarry trucks in the conditions of Kachar Open-Pit are carried out. The works of technological auto transport of Kachar Open-Pit straitened on the mining-technical and mining-geometrical parameters of condition on speed terms in combination of trucks of BelAZ and Hitachi result in inhibition and decline of efficiency of high-performance of Hitachi trucks. Speed losses are provided by narrow transport verges constricted by the grounds of turn at changing of directions of motion in a career, speed limitations, overload of trucks and different powerful potential of trucks, on models, by organization of transport from lower horizons by single-sideband roads with two-sided motion. In the conditions of megascopic time of voyage of trucks there is a decline of work time of excavators on loading, that along with mark factors results in the decline of prime price of mining and transport works on the whole.

The geometrical analysis of motorway showed that slopes on conventions are not everywhere self-possessed in accordance with a leading slope, that does not exceed 80‰in practice. There are areas, exceeding a slope in 100 ‰ higher. That negatively affects on efficiency of work of a transport equipment, because not all trucks are identically effective on the semi-steep and horizontal areas of route.

The primary purpose of the conducted practical research was optimization of the modes and external of a mining-transport complex of Kachar career. For achievement of the set aim in hired the methodical providing of analysis, estimation, optimization, planning and planning of mining-transport complexes of quarries of corporate CAS of management was used by the geotechnological complex (ACSM GC "Djetygara") and her module of logical and statistical imitation of truck and excavator systems of quarries the Informative programmatic-methodical complex "Cebadan-Auto".

Estimation of mining-transport possibilities of the trucks-excavator system of the Kachar career was produced on the actual plan of mining works for the end of 2014. The account of mining-and-geological and mining and technical factors came true by the task of actual or planned position of mining works in quarry space, quality and physical and mechanical descriptions of extractive mining rock on the loading points.

On the preliminary results of modelling of work of truck-excavator complex for the effective use of technological auto transport of Kachar quarry by the specialists of the "Research engineering center ERG" is offered in an ore-rocky zone maximally to eliminate crossing of trucks of different types, namely to divide front of works of present park of trucks: the Hitachi EH 3500 ACII trucks work in an ore-rocky zone only; for the removal of the loose stripping the BelAZ-75131 trucks are used only.

The results of modelling show that during separate exploitation of trucks the Hitachi EH-3500 trucks has better indexes. When compared to a base variant the middle technical speed of movement increases on 12-28 %, the specific expense of fuel diminishes on 12-24 %, expenses on a mining-transport complex diminish on 8-16 %, specific current expenses diminish on 8-17 %. Meanwhile possible to get an annual economic effect 7 884 500 $.

KEYWORDS

Mining-transport complex, Open-Pit, transport, dispatching, optimization, planning, simulation modelling, economic.

MODERN STATE OF MINING-TRANSPORT WORKS

One of the largest enterprises in Kazakhstan and CIS at the market of iron-ore raw material is JSC “Sokolov-Sarbay mining and processing company (SSGPO). It includs Sokolov, Sarbay, Kachar and Kurdjunkul quarries. Kachar administratiom conducts the development of iron deposit by the open method. Presently the Kachar quarry has a depth about 422 m (project depth on the end of working off - 750 м).

The Kachar quarry is developing dynamically and attained the project power in 15 million ton of ore in a year on the first turn project. In 2008 year, by order of JSC "SSGPO" by the institute "Giproruda" the project of reconstruction of the Kachar quarry was executed with engaging off the South area of the deposit. The annual capacity on ore of the incorporated quarry is defined by the project on the level of 23 million ton, including 18 million ton - in the Northern area and 5 million ton - in the Southern. South area of the deposit set to explore by the single quarry space with a basic quarry with the use of the existent systems of extraction and transportation.

Annual capacity of the Kachar quarry on 2014 year was 14 960 thousandы tones on an iron-stone at middle maintenance of iron of 32,75% and 47 425 thousand м3 on stripping.

During the last decade on the Kachar quarry the park of shovel and transport equipment was revived. The 7 high-performance hydraulic power-shovels are purchased, including Hitachi EX 5500T-6, EX 3600T-6, Terex RH 170-B, and also more than 20 power-shovels of the Russian producers, two pneumatic-heel loaders of CAT-993K for work in breast faces. In the quarry the trucks of BelAZ-75131 are exploited by a carrying capacity of 130 t (13 units) and Hitachi EX 3500 by the carrying capacity of 168 t (21 units).

Planned annual capacity of motor transport of the Kachar quarry for the 2015 year 14 mln.t. on iron-ore at middle maintenance of iron 32,64% and 51 mln.t on a stripping. A general volume on rock mass accounts 65 mln.t.

Table 1 - Planned volumes of extraction on horizons of quarry on a motor transport

Horizon	Ore		Stripping		Rock mass	
	T.t.	T.m^3	T.t.	T.m^3	T.t.	T.m^3
+30	300,0	97,0	6223,0	2821,0	6523,0	2918,0
+15	0	0	4572,0	1816,0	4572,0	1816,0
+/- 0	0	0	4779,0	1838,0	4779,0	1838,0
-15	205,0	72,7	4342,0	1670,0	4547,0	1742,7
-30	374,4	130,0	4420,0	1700,0	4794,4	1830,0
-45	244,0	85,9	3701,0	1423,0	3945,0	1508,9
-60	282,0	97,8	3869,0	1488,0	4151,0	1585,8
-75	207,0	71,0	3881,0	1493,0	4088,0	1564,0
-90	415,0	141,5	3588,0	1380,0	4003,0	1521,5
-105	532,8	181,5	2980,0	1146,0	3512,8	1327,5
-120	577,1	194,2	2723,0	1048,0	3300,1	1242,2
-135	512,1	178,9	2423,0	932,0	2935,1	1110,9
-150	945,2	322,2	2018,0	776,0	2963,2	1098,2
-165	1076,4	340,9	658,0	253,0	1734,4	593,9
-180	1638,0	515,7	278,0	107,0	1916,0	622,7
-195	1976,0	601,8	109,0	42,0	2085,0	643,8
-210	1571,0	466,7	242,0	93,0	1813,0	559,7
-225	1245,0	375,2	143,0	55,0	1388,0	430,2
-240	869,0	250,1	0	0	869,0	250,1
-255	1030,0	303,0	39,0	15,0	1069,0	318,0
	14000,0	**4426,1**	**50988,0**	**20096,0**	**64988**	**24522,1**

The ore is transported by the motor transport to the ore shifting storage on hor. +52м, a stripping rock mass is transported to internal shifting storages on hor. +52м, +75м, +79м, +86м. Extraction-and-loadings in the motor transport are implemented by the power-shovels of Hitachi 3600, Hitachi 5500, RH - 170b on all subjacent horizons.

Before March 2015 year the trucks of Hitachi EH - 3500 ACII was exploited together with the machines of BelAZ-75131. By virtue of greater power and substantially less age they can develop more high rate in freight direction. More agreed BelAZ trucks have lower coefficient of transmissions efficiency, that stipulates lowering of speed qualities and increase of expense of fuel. During the motion upwards, on the protracted uphill Hitachi trucks following BelAZes and periodically are forced to drop the speed and speed up, that increases the trip time and fuel expenditure. At the situation of a transport zone trucks (up to 27 and more due to the BelAZes), influence of this factor increases. Additional speed losses are provided by narrow transport verges constricted by the grounds of turns at changing of directions of motion in the quarry. In this zone the BelAZes feel better, because more adapted to these terms on own sizes.

Organization of rock mass transport from lower horizons with single-sideband roads for two-sided motion additionally provides the necessity of trucks to stop in empty direction for admission of machines following in freight direction, that also results in the decline of operating speed and increase of expense of fuel. In the conditions of increasing journey time of trucks there is a decline of working time of power-shovels on loading, that along with marked factors results in the decline of prime price of mining-transport works on the whole.

In addition to increase of trip time, decline of movement rate in freight direction and increase in fuel expense, besides the decline of coefficient of readiness of practically new trucks of Hitachi there is also an overloading of trucks on 10 and more percents (useful weight makes to 200 tons). As a result, in March 2015, from 21 of Hitachi EH-3500 ACII trucks 5 machines are under repair, that also increases prime price of the mining-transport works on the whole.

In modern conditions, as the factor of decline of efficiency of work of the Hitachi EH - 3500 ACII is their development for transporting of 3-4th million tons of crumbly rock mass, that provides their unoptimal loading on a carrying capacity (120-130 tons at a passport carrying capacity 168 tons.).

On the Kachar quarry there are deviations of parameters of quarry roads from the passport ones, and also in connection with work in such terms of quarry trucks of different types (differences in their overall sizes, carrying capacity, middle rate of movement etc.) there are unplanned outages last and, consequently, decline of their productivity.

The works of technological motor transport of the Kachar quarry in straitened conditions of mining-technical and mining-geometrical parameters and exploitation of trucks of BelAZ and Hitachi in combination lead to inhibition and decline of efficiency of high-productive trucks of Hitachi.

The geometrical analysis of motorway showed that slopes on conventions not everywhere comply with a leading slope, that does not exceed 80‰ in practice. There are areas exceeding a slope in 100 ‰ and higher, that

negatively affects efficiency of work of a transport equipment, because not all trucks is identically effective on the semi-steep and horizontal areas of roads. Also during all motorway not sufficiently of horizontal areas of roads. It all those reduce efficiency of the use of trucks, because reduces the medium technical rate of movement and increase by the same, medium of trip time. For example, slope of motorway from a mark -188,9 m to the mark -196 m makes - 110 ‰, from the mark -196м to the mark -203 m - 100 ‰, from a mark -125,2 m to the mark -132,2 m - 104 ‰.

In the conditions of the Kachar quarry one of actual directions of increase of efficiency of work of trucks through upgrading of their exploitation is observance of project norms of parameters of roads. Narrowing of transport verges results in a forced decline of speeds, higher fuel consumption and enhanced wear of tires.

On the following areas of motorway one can usually depict deviations of actual parameters of motorways from a project (Figure 1 and 2).

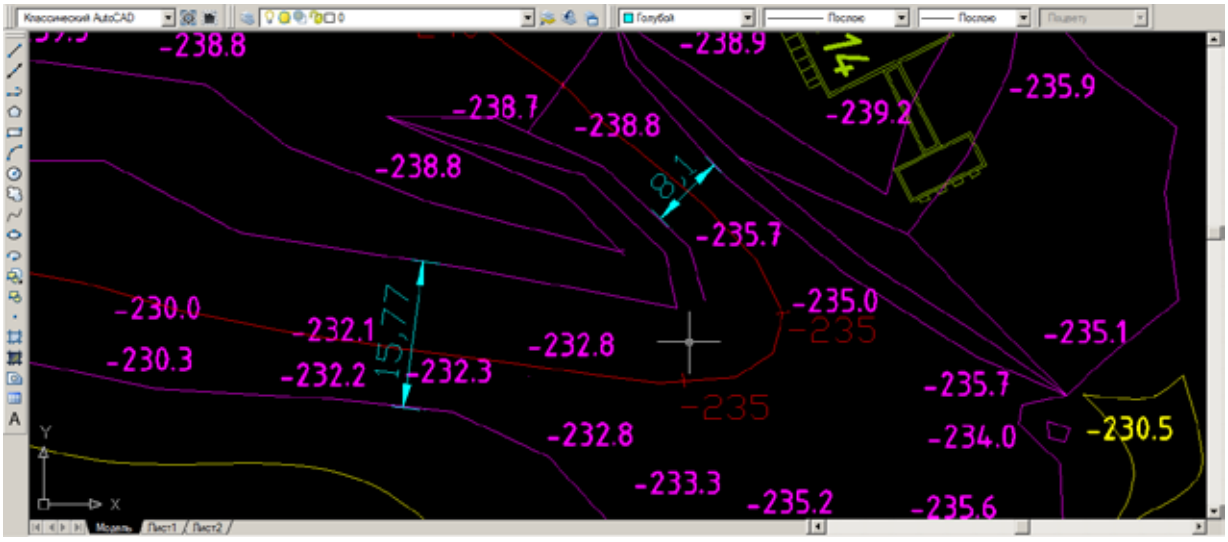

Figure 1

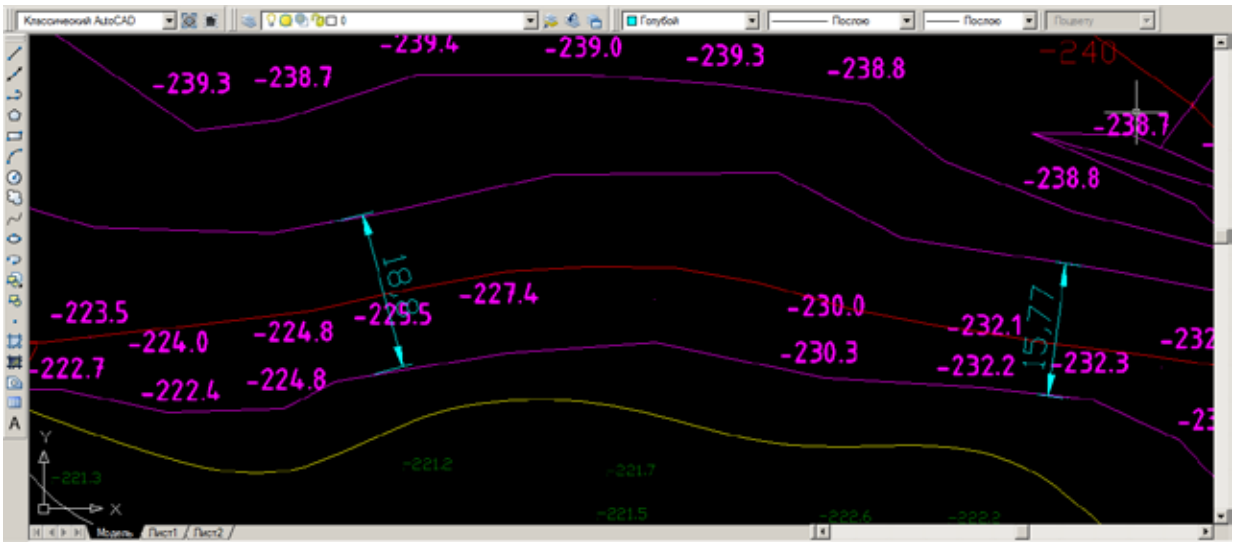

Figure 2

For example, width of convention on horizon -240 m makes 8,1м, on the area of marks -232,1 m, - a 232,8 m makes 15,77 m, width of convention on the area of marks -224,8 m, - a 227,4 m makes 18,8 m.

For creation of maximally favorable conditions of Hitachi trucks exploitation maximally maybe brings to conformity parameters of turns and width of motorways are offered. Areas of motorway, where it is needed to conduct expansion of roads in accordance with project indexes pointed in the table 2.

Table 2 - The actual arguments of motorways on the Kachar quarry

Horizons, m	Width of conventions and roads, m	Horizons, m	Width of conventions and roads, m
-238,0	8,1	-82,5	27,18
-232,1	15,77	-69,7	21,8
-224,8	18,8	-46,2	25,98
-204,4	18,78	-44,0	19,92
-203,0	16,07	-87,8	14,73
-199,2	17,93	-87,2	20,11
-196,1	13,22	-93,7 м	16,07
-190,4	14,51	-111,7	20,25
-182,5	18,62	-1,4	25,58
-177,4	13,34	-0,8	27,17
-174,2	19,34	-43,4	9,78
-167,7	18,02	-41,1	17,09
-161,6	17,76.	-56,5	11,86
-156,3	17,18	-51,8	14,15
-142,3	23,15	-71,9	16,86
-134,6	24,26	-63,2	14,8
-105,4	23,64	-83,0	13,63
-97,9	26,03	-96,8	14,85

SHORT DESCRIPTION OF RESEARCH METHODOLOGY

The primary purpose of the conducted practical research is a determination of a rational mining-transport complex of the Kachar quarry. For the achievement of the set aim the methodical providing of analysis, estimation, optimization, planning and planning of mining-transport complexes of quarries was used with the cyclic types of mining and transport equipment, based on application of logic-statistical simulation modeling, developed within the framework of corporate automated system of management by geotechnological complexes. Choice options of basic mining and transport equipment were investigated with the ground of their amount and numeral correlation, and also terms and mode of exploitation [*Mining enterprise social and economic development management, 2015*].

The basic and related decided tasks are establishment of necessary for given mining-and-geological and mining-technical conditions of operating types of trucks, definition of organization of mining and transport works, as well as definition of the mode and conditions of exploitation of motor transport [*Section modeling with railway transport, 1972, The basic principles of logical and statistical modeling simulation of excavator-automobile quarries systems, 1993*].

The quality setting experiments significantly determines efficiency of the conducted researches and authenticity of the outcoming results, conclusions and recommendations. During modeling it is important to take into account the factor of volume of a mining-transport work at his maximal values (volumes and weighted average distance of transportation of rock mass), that provides the higher degree of authenticity of results of modeling.

While establishing the optimal option of truck exploitation, the interaction up of all mark factors, with factors external in relation to trucks (quality of coverage, structure and geometry of roads, with the quantity of a mining-transport equipment and parameters of his work) is realizing. Thus, all separate factors and parameters of processes of loading, transportation and unloading are integrated in the general indexes of technological and economic efficiency of work of power-shovel-motor-car complex, that allows to definitely judge upon efficiency of choice of one or another type of truck.

DESCRIPTION OF EXPERIMENT ON THE MINING-TRANSPORT COMPLEX OF THE KACHAR QUARRY

Estimation of mining-transport possibilities of the mining-transport system of the Kachar quarry was produced on the basis of information about actual position of mining works of quarry presented by the technical department of JSC "SSGPO" as of the end of 2014 year.

The account of mining-and-geological and mining-technical factors implemented by the giving of actual or planned position of mining works in quarry space, quality and physic-mechanical descriptions of extractive rock mass on the loading items. Depending on the mining-and-geological situation produced corresponding placing of basic mining loading and unloading equipment, further, in obedience to formed ore and rock stream the structure of model of motor-car route is determined. Geometry and spatial coordinates of motor-car route was determined by the plan of mining works. The actual schemes of transport communications, parks of basic technological mining and transport equipment, existent organizations of mining and transport works on quarries, actual costs related to maintenance of basic technological processes are taken as the basis.

The calculation of prime price of work and idle time of trucks and power-shovels was produced coming from fact dates about the cost of 1 kW/h of electric power and 1 liter of diesel fuel, size of salary of machinists and

helpers of machinists of power-shovels and drivers of trucks. The size of depreciation decrees settled accounts on the actual balance of value of power-shovels and trucks, exploited in the quarry.

In the conditions of the Kachar quarry simultaneously at the moment of forming of data 6 reloading point were used for unloading of trucks. Two reloading storages on the horizon +52 m the only ore was accepted taken out from coalfaces, and reloading storages being on the horizons +52m, +75m, +79m, +86m the stripping was accepted.

Technical productive power of every units of power-shovel equipment was set coming from his actual technical state (degree of wear, coefficient of engine efficiency), own basic technological and technical parameters (time of cycle and capacity of bucket), also physic-mechanical properties of the rock mass (density of rock mass, coefficient of making light) loading by it. In the process of imitation design this given productivity will be corrected depending on time of exchange (organization of cooperation of mining and transport equipment) and useful mass of served trucks, interval of arrival of machines into the point of loading-unloading. All indicated factors are accepted by such, as it takes place on the real investigate object.

According to the present park of equipment on December 2014 year 6 power-shovels worked on loading of trucks. Extraction-and-loadings works with the motor transport is implemented by the power-shovels of Hitachi 3600, Hitachi 5500, RH – 170B (Table 3).

Table 3 – Information on forming list of power-shovels park

№	Designation	Number in park	Putting into operation	State	Residual value, mln.tenge.	Real time of cycle, sec	Additional data			
							Expenditures, thousand tenge /month		Technical on engine	
							On materials	Not taken into account	Coefficient of power utilization	Index of Efficiency
1	Hitachi EX 3600	63	2009	+	451, 822	35,0	300,00	100,00	0,30	0,85
2	Hitachi EX 3600	64	2009	+	662, 628	35,0	300,00	100,00	0,30	0,85
3	Hitachi EX 3600	65	2009	+	760, 080	35,0	300,00	100,00	0,30	0,85
4	Hitachi EX 5500	61	2008	+	621, 868	38,0	500,00	100,00	0,28	0,80
5	Hitachi EX 5500	70	2013	+	1425, 55	36,0	400,00	100,00	0,35	0,94
6	Terex RH 170-B	67	2010	+	424, 676	34,0	300,00	100,00	0,32	0,85

Information on the models of power-shovels and on the list of power-shovel park of machines in the base option of the mining-transport complex, added to the initial databases of informative programmatic-methodical complex "Cebadan-auto". Passport descriptions of machines and basic technical-economical indexes of their exploitation are here presented.

Rock mass is taken out by the trucks of Hitachi EX3500ACII and BelAZ-75131. The present list of technological motor transport park includes 34 trucks, including: Hitachi EH3500ACII – 21 units and BelAZ-75131 - 13 units. Values of coefficient of engine efficiency and transmission of trucks are accepted depending on time of machines employment. Low level of coefficient of efficiency can be explained by high middle age and physical wear of the trucks. Most trucks of BelAZ-75131 working-out the operating resource already.

In the period of collection of initial information all datas on examined trucks was added to the initial databases of informative programmatic-methodical complex "Cebadan-auto" (Table 4).

The structure of the examined scheme of the motorway accepted according to the actual situation on mining works in a quarry on the end of 2014 year is presented on a picture 5. Motor-car road periodically, as far as the change of situation in quarry space, is correcting. For researches the last version of obtained electronic version of motorway was used and therefore her authenticity has a high degree. The motorway is broken up on the plan of mining works on the sections with the different technological and technical setting, geometrical descriptions, that allows to the model with the high degree of exactness to correspond to the real position on the quarry.

One of the substantial factors influencing the work of transport vehicles and technological complex on the whole is organization of changing of drivers of trucks. In this case, the point of changing is organized on a place near the reloading point. The trucks begin to gather at the point of changing before a half of hour to completion of shift and make changing as appearance on it happens.

On trucks the speed limitations are accepted, accordingly in freight and idle directions, as it is traditionally accepted in practice. Their values are taken on maximum possible in conditions of safety, because this limitation in a substantial measure humiliates possibilities of more quality machines.

Type of road's coverage - rolled ground in a breast and on a dump, width of runway - 12,5 m, types of route section: area for a manoeuvre, area of motion and convention. The slope of motorway on the model is formed on the set three-dimensional coordinates of quarry space.

Table 4 - Information on list of trucks park

№	Model of truck	Garage number	Truck capacity, t		Volume , м3	Weight of truck, т	Wear of putting into operation	Engine		Transmission			Tires		Balance cost, thousand.tenge	Amortization	
			Nominal	Fact				N, кVt	Coef. effic.	Type	Coefficient efficiency		Cost , thousand tenge	Run of tire, thousand.km		Kind	Norm
								Nominal	Fact		Nominal	Fact					
1	EH3500ACII	750	168	172	111	141	2010	1491	0,78	EM	0,85	0,78	5 682,82	69,2	325 459,47	wear	0,1
2	EH3500ACII	751	168	172	111	141	2010	1491	0,78	EM	0,85	0,78	5 682,82	69,2	306 567,25	wear	0,1
3	EH3500ACII	752	168	172	111	141	2010	1491	0,78	EM	0,85	0,78	5 682,82	69,2	317 782,91	wear	0,1
4	EH3500ACII	753	168	172	111	141	2010	1491	0,78	EM	0,85	0,78	5 682,82	69,2	319 836,19	wear	0,1
5	EH3500ACII	754	168	172	111	141	2010	1491	0,78	EM	0,85	0,78	5 682,82	69,2	357 065,59	wear	0,1
6	EH3500ACII	755	168	172	111	141	2011	1491	0,81	EM	0,85	0,81	5 682,82	69,2	388 369,22	wear	0,1
7	EH3500ACII	756	168	172	111	141	2011	1491	0,81	EM	0,85	0,81	5 682,82	69,2	412 695,13	wear	0,1
8	EH3500ACII	757	168	172	111	141	2012	1491	0,83	EM	0,85	0,83	5 682,82	69,2	493 044,13	wear	0,1
9	EH3500ACII	758	168	172	111	141	2012	1491	0,83	EM	0,85	0,83	5 682,82	69,2	506 803,09	wear	0,1
10	EH3500ACII	759	168	172	111	141	2012	1491	0,83	EM	0,85	0,83	5 682,82	69,2	498 571,19	wear	0,1
11	EH3500ACII	760	168	172	111	141	2012	1491	0,83	EM	0,85	0,83	5 682,82	69,2	503 369,50	wear	0,1
12	EH3500ACII	761	168	172	111	141	2014	1491	0,85	EM	0,85	0,85	5 682,82	69,2	697 744,69	wear	0,1
13	EH3500ACII	762	168	172	111	141	2014	1491	0,85	EM	0,85	0,85	5 682,82	69,2	710 336,75	wear	0,1
14	EH3500ACII	763	168	172	111	141	2014	1491	0,85	EM	0,85	0,85	5 682,82	69,2	719 520,00	wear	0,1
15	EH3500ACII	764	168	172	111	141	2014	1491	0,85	EM	0,85	0,85	5 682,82	69,2	714 188,50	wear	0,1
16	EH3500ACII	765	168	172	111	141	2014	1491	0,85	EM	0,85	0,85	5 682,82	69,2	716 260,88	wear	0,1
17	EH3500ACII	766	168	172	111	141	2014	1491	0,85	EM	0,85	0,85	5 682,82	69,2	714 333,06	wear	0,1
18	EH3500ACII	767	168	172	111	141	2014	1491	0,85	EM	0,85	0,85	5 682,82	69,2	723 084,00	wear	0,1
19	EH3500ACII	768	168	172	111	141	2014	1491	0,85	EM	0,85	0,85	5 682,82	69,2	720 970,69	wear	0,1
20	EH3500ACII	769	168	172	111	141	2014	1491	0,85	EM	0,85	0,85	5 682,82	69,2	723 084,00	wear	0,1
21	EH3500ACII	770	168	172	111	141	2014	1491	0,85	EM	0,85	0,85	5 682,82	69,2	723 084,00	wear	0,1
22	BelAZ-75131	08	130	130	71,2	107	2008	1194	0,75	EM	0,85	0,75	4 471,45	88,5	17 627,00	wear	0,14
23	BelAZ-75131	09	130	130	71,2	107	2007	1194	0,65	EM	0,85	0,65	4 471,45	88,5	1 441,00	wear	0,14
24	BelAZ-75131	12	130	130	71,2	107	2008	1194	0,75	EM	0,85	0,75	4 471,45	88,5	17 990,00	wear	0,14
25	BelAZ-75131	58	130	130	71,2	107	2007	1194	0,65	EM	0,85	0,65	4 471,45	88,5	918,00	wear	0,14
26	BelAZ-75131	66	130	130	71,2	107	2007	1194	0,70	EM	0,85	0,70	4 471,45	88,5	26 684,00	wear	0,14
27	BelAZ-75131	67	130	130	71,2	107	2007	1194	0,65	EM	0,85	0,65	4 471,45	88,5	7 413,00	wear	0,14
28	BelAZ-75131	70	130	130	71,2	107	2007	1194	0,65	EM	0,85	0,65	4 471,45	88,5	2 719,00	wear	0,14
29	BelAZ-75131	89	130	130	71,2	107	2007	1194	0,65	EM	0,85	0,65	4 471,45	88,5	2 324,00	wear	0,14
30	BelAZ-75131	95	130	130	71,2	107	2007	1194	0,65	EM	0,85	0,65	4 471,45	88,5	0	wear	0,14
31	BelAZ-75131	96	130	130	71,2	107	2007	1194	0,70	EM	0,85	0,70	4 471,45	88,5	20 785,00	wear	0,14
32	BelAZ-75131	97	130	130	71,2	107	2007	1194	0,65	EM	0,85	0,65	4 471,45	88,5	6 313,00	wear	0,14
33	BelAZ-75131	98	130	130	71,2	107	2007	1194	0,70	EM	0,85	0,70	4 471,45	88,5	26 088,00	wear	0,14
34	BelAZ-75131	99	130	130	71,2	107	2007	1194	0,70	EM	0,85	0,70	4 471,45	88,5	10 294,00	wear	0,14

MODELING OF WORK OF MINING-TRANSPORT COMPLEX OF THE KACHAR QUARRY

During modelling of work of base option of power-shovel-motor-car complex of the Kachar quarry with high degree of accuracy the order of executable technological operations was reproduced. Taken into account power consumption by trucks and power-shovels, organization of cooperation of mining and transport equipment and others. As a criterion of optimality the index of specific current expenses on a 1 cube of rock mass is accepted.

For the modeling of work of base option the weighted average of height of getting up of rock mass is accepted at the level of 143 m, that corresponds to the planned indexes of 2015 year. Planned annual capacity on ore - 14 mln.t, on stripping - 51 mln.t, on rock mass - 65 mln.t.

Modeling results showed that by rational correlation of mining and transport equipment of power-shovel-motor-car complex of the Kachar quarry at that implementation of the planned mining-transport works is provided on 2015, are 6 power-shovels in the points of loading and combination of 21 trucks of Hitachi and 3 trucks of BelAZ. Option with 16 trucks of Hitachi EX3500ACII and 7 trucks of BelAZ-75131 in a complex also is interesting from the economic point of view.

For option 2, where modeling of work of technological motor transport was designed on a motorway with the increased speed limiting the rational correlation of mining and transport equipment of power-shovel-motor-car complex of Kachar quarry at the six power-shovels makes the use in a complex of 21 trucks of model of Hitachi EH-3500 ACII with specific current expenses 113,84 tenge on a 1 ton of rock mass.

When using of six power-shovels with the purpose of accomplishing the plan of works on the year the optimal number of trucks makes 25. The specifically-current expenses at such laying out will make about 113,99 tenge on a 1 ton of the taken out rock mass.

On the Figure 3 it is visually possible to see, that the motorway of the Kachar quarry has limitations on the admission and transport capabilities.

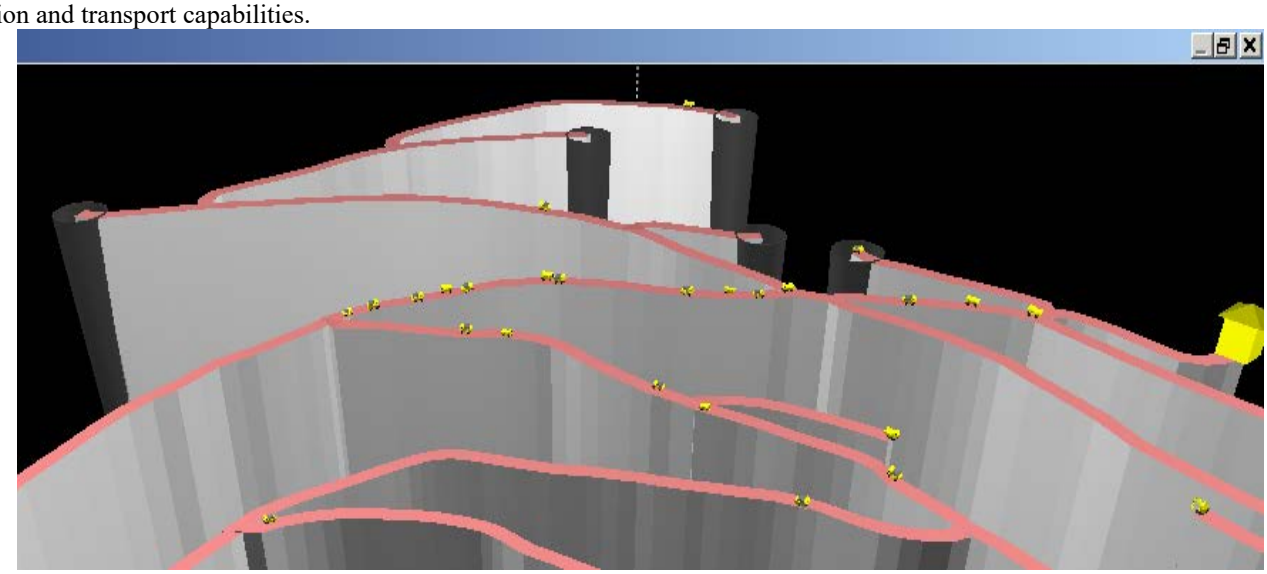

Figure 3 - The graphic viewing of modeling of work of excavator-auto complex

Limitation here is the shoulder with long 500 m from horizon +/-0 m to the horizon +35 m, at that the motorways of lower horizons intersect on horizon +/- 0 m, farther the trucks force to move with a load on the top. To that it is also assisted the variety of applied trucks. As accepted organization of work of transport (maintenance of power-shovels on loading on open-cycle), the trucks of Hitachi and BelAZ attendant lower horizons move in quarry space on the same roads.

At the graphic view of the modeling options scenario utilizing both Hitachi and BelAZ, trucks it can be concluded that the old trucks of BelAZ considerably weaker than Hitachi in terms of hauling, and, as a result, hinder to the movement of trucks of Hitachi. A low index on hauling descriptions is explained by high middle age and physical wear of trucks of BelAZ. Greater part of expenses fall on trucks of Belaz. It is explained by that most of trucks of BelAZ already are working out it's operating resource, and that challenge the increased fuel consumption and wear of tires. Specific consumption of fuel is also rising when both Hitachi and BelAZ trucks are being used.

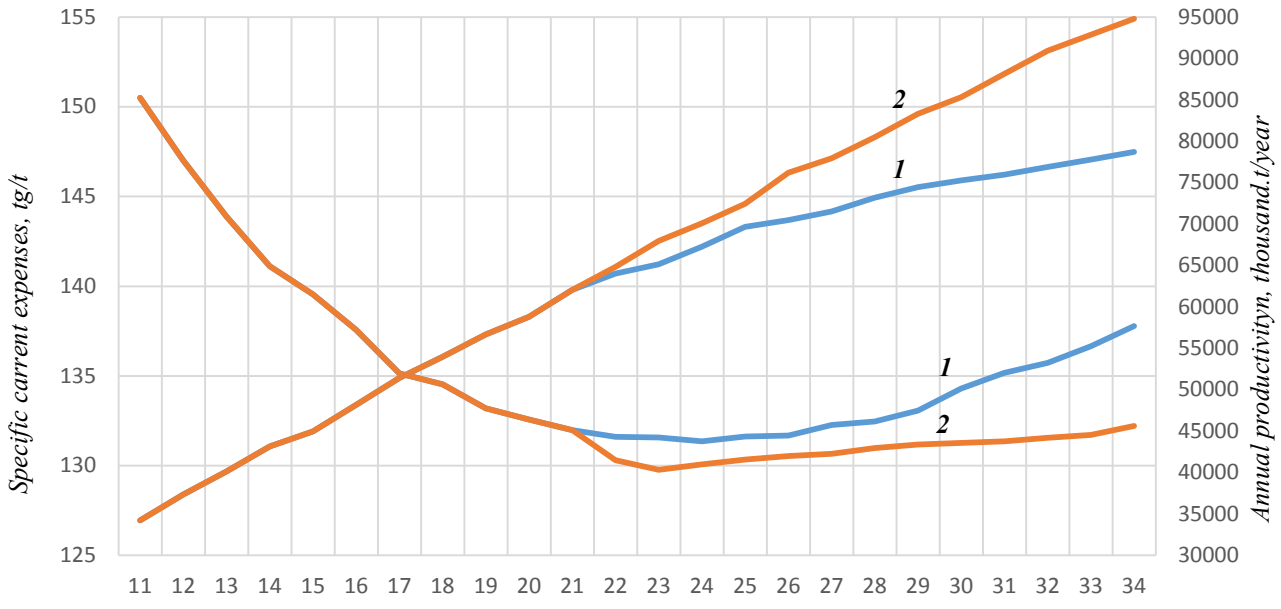

Figure 4 – Dependence of specific current consumption and productivity of power-shovel-motor-car complex of Kachar quarry from the amount of trucks: option 1 - in a complex together Hitachi EX3500 – 21 units and B elAZ-75131 – 13 units, option 2 - in a complex only Hitachi EX3500 are 34 units.

According to the results of analysis of work of mining-transport complex, the organization of works using old trucks of BelAZ-75131 with carrying capacity 130 tons and comparatively new trucks of Hitachi with a carrying capacity 168 tons after the first look are formed somewhat efficiently, but after consideration of options on a

simulation model with actual position of mining plan using together BelAZ and Hitachi trucks, one can notice, that in a chainlet old trucks brake work of more new truck, that farther more affects its efficiency and productivity of work of the mining-transport complex on the whole. To resolver this it is necessary to organize separate work of trucks on close cycle. It in a substantial measure will promote utilization of potential of high-performance trucks of Hitachi, will provide the substantial decline of expense of fuel, will promote efficiency of work of power-shovels on loading and unloading points, and on the whole will give the result of increase of the productivity of power-shovel-motor-car complex of quarry bringing down the prime price of mining-transport works.

On the preliminary results of modelling of work of power-shovel-motor-car complex for the effective use of technological motor transport of the Kachar quarry by the specialists of the "Research engineering center ERG" is offered in an ore-rocky zone maximally to eliminate crossing of trucks of different types, namely to divide front of works of present park of trucks: the trucks of Hitachi EH-3500 ACII work in an ore-rocky zone only; for the removal of loose stripping the trucks of BelAZ-75131 are used only.

As a result of undertaken studies was made decision to conduct experiments with different options. As a base on an ore-rocky zone the option of using only trucks of Hitachi EH-3500 ACII was accepted.

On the Kachar quarry the height of ore-rocky zone makes more 300 m, it stipulates the dramatic change of weighted average distance of transportation and weighted average height of getting up of rock mass during a year. It can cause the overfalls of index of specific current expenses on the power-shovel-motor-car system. In this connection options with the weighted average height of getting up of rock mass of 140 m, 160 m, 180 m, 200 m, 220 m were examined.

On the Kachar quarry there are deviations of parameters of highways from a passport (constricted single-sideband two-sided transport verges, over normative slopes and turns), that prevent to develop high-rate of motion to high-performance trucks of Hitachi EH-3500 ACII. Therefore the options with different speed limitations were examined. On the points of loading and unloading possible speed limitations were 5-15 km/hour. On turns and lower horizons possible speed limitations were 10-15 km/hour. In freight direction speed limitations were 20-30 km/hour. Speed limitations accepted on the models in empty direction maximally 20, 30, 40 km/hour, depending on interpretation of heights of road sections.

Within the framework of maximum contours of the year of 2014 and planned value of the development of mining works of the Kachar quarry on 2015, an experiment on the choice of rational technology of mining-transport works is conducted. Within the framework of calculation the conditions of development were accepted at the use 6 power-shovels in a complex with trucks of model of Hitachi EH-3500 ACII in a range from 15 to 21 units. The place of location of power-shovels on the period of miscalculation was accepted in accordance with the plans of mining works.

The results of modeling of work of power-shovel-motor-car complex of the Kachar quarry at different speed limitations on the road and weighted average height of getting up of rock mass on the level of 143 m are demonstrate in the Table 5.

Table 5 - The Results of design of work of power-shovel-motor-car complex of the Kachar quarry

№	Options*	1*	2*	3*	4*	5*
1	Amount of trucks	24	21	20	19	18
2	An amount of voyages is in freight direction	632	578	588	594	589
3	Weighted average distance, km	3,33	3,34	3,34	3,36	3,35
4	Weighted average height of getting up of rock mass, m	142,13	143,38	142,66	144,51	143,69
5	Medium shiftwork run of one truck, a km/shift	176,84	184,68	196,79	210,69	219,93
6	Medium technical rate of movement, km/h	20,36	20,85	22,82	27,05	28,49
7	Medium exploitative rate of movement, km/h	16,77	17,54	18,82	19,96	21,53
8	General expense of fuel, thous.l	50,264	47,351	44,219	40,747	38,144
9	Specific expense of fuel,g/tkm	123,78	116,89	108,22	97,76	92,48
10	Expenses on a fuel, thous.tenge	6659,9	6273,9	5858,9	5399,0	5054,1
11	Expenses on a mining-transport complex, mln.tenge.	13,589	13,069	12,516	11,905	11,395
12	- including operating costs	11,541	11,060	10,508	9,896	9,386
13	Productivity of complex on rock mass, mln.м3	23,345	23,167	23,423	23,829	23,657
14	Productivity of complex on rock mass, mln.t	62,507	62,046	62,755	63,764	63,227
15	Specific current expenses, tenge/ton	134,90	130,70	123,76	115,85	111,83
16	Economic effect, mln. tenge/year	-	260,6	699,1	1 214,	1 458,

1*-2* - speed limits on manoeuvre areas are 5 km/hour, on turns - 10 km/hour, in freight directions - 20 km/hour, in empty direction - 30 km/hour, below than horizon – 100 m according to 10 and 20 km/hour; 3* - speed limits on manoeuvre areas - 10 km/hour, in freight directions - 20 km/hour, in empty direction - 30 km/hour; 4* - speed limits on manoeuvre areas - 15 km/hour, in freight directions - 20 km/hour, in empty direction - 40 km/hour;

5* - speed limits on manoeuvre areas - 15 km/hour, in freight directions are 30 km/hour, in empty directions - 40 km/hour.

In the first base option the joint work of trucks of Hitachi EH-3500 in an amount of 16 units and BelAZ-75131 in an amount of 8 units are imitated with actual speed limitations on a route that is maximally close to the real mining-technical terms of the Kachar quarry.

In the second option the results of modeling of work of trucks of Hitachi EH-3500 in an amount 21 units are shown with actual speed limitations on the route. The modeling results show that during separate exploitation of trucks of Hitachi EH-3500 have the more best indexes. When compared to the base option the medium technical rate of movement increases on 4,6 %, the specific expense of fuel diminishes on 5,6 %, expenses on the mining-transport complex diminish on 4 %, specific current expenses diminish on 3,1 %. Here an annual economic effect makes 260,59 mln. tenge.

In the next options the results of the modeling of Hitachi EH-3500 work in the improved conditions (increase of width of highways, upgrading of travelling coverages, increase of speed limitations etc.) are shown. The modeling results show that at the improvement of external of trucks of Hitachi EH-3500 the medium technical rate of movement increases on 12-28 %, the specific expense of fuel diminishes on 12-24 %, expenses on the mining-transport complex diminish on 8-16 %, specific current expenses diminish on 8-17 %. At the moment it is possible to get the annual economic effect of 1 458,64 mln. tenge.

MESURES TOWARDS A HIGHER PRODUCTIVITY OF MINING-TRANSPORT WORKS AT THE KACHAR QUARRY

Given the results from analysis of mining-transport works Kachar quarry has a substantial potential in the increase of efficiency and decline of prime price of mining-transport works.

An important potential of decline of prime price of mining-transport works on the Kachar quarry is effective organization of work of power-shovel-motor-car park in the plan of optimization of general park quantity and quantity of going out on a shift trucks. Analysis of the state and research has demonstrated, that for providing of the pre-arranged motor transport works in the volume of 65 mln.t in a year there is not a necessity of maintenance of park of 34 and more than trucks. With this volume the park of Hitachi trucks fully manages well corresponding conditions.

On the Kachar quarry there is substantial potential of efficiency improvement and reduction of prime price of work of power-shovel-motor-car complex due to the increase of level of technic-economical politics, touching, first of all, planning and management by mining-transport works, corporate approach in cooperation of the basic structural subdivisions, related to realization of mining-transport processes.

Firstly, realization of present potential must be related to more quality basing of choice of models and numeral correlation of basic mining and transport equipment.

The second direction is creation of conditions for effective exploitation corresponding to applied today the mining and transport equipment. The project foreseen the corresponding parameters of transport verges, number of power-shovel for loading and other mining-technical terms. Motorways in the quarry, including the temporal practically do not depend on their transport ability, that results in the outages of the mining-transport equipment in the period of the planned working off.

On the mine there should a higher effective politics on maintenance of profitability of the mining-transport complex due to the timely and reasonable updating of basic technological equipment is needed.

As data shows that, there are of BelAZ-75131trucks operating in the quarry, which practically deprived their working resource, that on the hauling descriptions doesn't fully corresponds to the utilized alongside the trucks of Hitachi EH-3500. The last also doesn't go well with the existing in the quarry mining-technical parameters (constricted single-sideband two-sided transport verges, over normative slopes and turns), what the actual plans of mining works testify to. The acquisition of high-performance power-shovels of Hitachi-5500 with the volume of scoop of 29 m3 also is not conditioned and reasonable as it applies to the Kachar quarry. On the results of researches power-shovels stand more than half of time of working shift.

One of relevant means to raise efficiency of work of the Kachar quarry trucks through upgrading their external conditions is a clear observance of project norms of traffic way. Narrowing of transport verges results to a force decline of speeds, increased of fuel consumption and augmented wear of tires.

The operative monitoring of work-load of areas of highways with the subsequent ranging them on categories for more effective distribution of the distinguished facilities on their maintenance depending on the degree of loading and intensity of the use in the process of porta can become a next important and effective event. Thus, corresponding quality of the most actively used sections will provide the decline of fuel consumption, increase of rate of movement, reduction of motor-car emissions in to the atmosphere and increase of run of tires.

Decline in efficiency and technical state of trucks the Kachar quarry originates from a existing over exceeding of useful mass of trucks. As researches on models showed, and also already having an experience of analysis of the modes of exploitation of quarry trucks, speed overloaded on 10% of trucks goes down on 6-7%, and it is accompanied by the increased of fuel consumption in grams on ton-kilometer. The temporally (within the framework of working shift, day and month) increase of the productivity of power-shovel-motor-car complex is

accompanied by the increased of fuel consumption and wear of tires, and also separate knots of truck reducing the level of his technical state, coefficient of his technical readiness. That also drives to subsequent to the increasing expense of awaiting-parts and materials, expenses on repair and restoration works.

The third direction is an increase of management efficiency of mining-transport works in the quarry, including all aspects of this process: control, account, setting of norms, adjusting, planning and organization. To that end it is expedient to form the corresponding system of monitoring and control of mining-transport works, functioning in the automated mode. Within the framework of this system of monitoring it is important to define the necessary for control and account list of basic technical and economical indexes that would provide possibility of operative estimation of efficiency of the mining-transport complex functioning and measures applied on the operative adjusting of the mining-transport process.

Main important direction of perfection of technology of planning of a mining-transport process can become formed on the mine the system of operative technical-economical analysis of work of basic technological complex and making effective and maximally adapted to the conditions of equipment exploitation measures and decisions. A current situation shows that it is difficult to get certain characteristic information about work of a mining-transport complex. For example even such elementary, as a general extent of a transport scheme, extent of stationary and temporal roads, expenses on maintenance of one kilometer of highways in a quarry both on the whole and on their technological variety. It is important to pay a greater attention to the speed mode and loading on trucks.

One of possible directions to improve efficiency of a mining-transport complex work requiring additional research is application of the combined motor transport at the area "coalface-reloading storage". This method supposes the using on lower horizons the trucks of BelAZ more adapted to the existent terms, with an overload on the large-sized motor transport of Hitachi.

CONCLUSIONS

High efficiency of corporate control geotechnological complexes automated systems at the quarries, based on the operating principles of the approach depends on adequate consideration of the interaction of the main technological equipment, and modes and conditions of their expluatation. It is important to provide quality feedback in order to objectively assess the effectiveness of management decisions technical, technological and organizational plan.

REFERENCES

Mining enterprise social and economic development management (2015). Moscow.: Economics. - p.270, Kaplan A.V.

Section modeling with railway transport (1972). Moscow: Alpina Business Books- Issue 3.- pp.6-14. Anpilogov A.E.

The basic principles of logical and statistical modeling simulation of excavator-automobile quarries systems (1993). Mineral raw materials complex use. N1. pp. 3-8. Bukeikhanov D.G., Galiyev S.ZH., Zhaksybayev A.Kh.

ESTIMATION OF THE CONSTRUCTION TIME OF AIR INJECTON TUNNELS 11 AND 12 OF THE CHUQUICAMATA UNDERGROUND PROJECT

Carlos Corvalán[1], *Juan P. Vargas[1], Juan P. Hurtado[1] & Pamela Jara[1]

[1] *Universidad de Santiago de Chile*

Departamento de Ingeniería en Minas

Av. Libertador Bernardo O'Higgins 3363, Estación Central, Santiago, Chile

*(*Corresponding author: juan.vargas@usach.cl)*

24th World Mining Congress
MINING IN A WORLD OF INNOVATION
October 18-21, 2016 • Rio de Janeiro /RJ • Brazil

ESTIMATION OF THE CONSTRUCTION TIME OF AIR INJECTON TUNNELS 11 AND 12 OF THE CHUQUICAMATA UNDERGROUND PROJECT

ABSTRACT

An estimation is made of the remaining construction time of injection tunnels 11 and 12 of the Underground Chuquicamata mining complex by a stochastic simulation using the algorithm presented by Vargas *et al.* (2014).

The algorithm will be adapted to each type of rock in order to be able to simulate the construction of both tunnels. The simulations do not consider the construction of the portals because that refers to a different construction technique, considering also that they are a mathematical certainty, since they are already built.

The total simulated construction times were 1,013 and 1,004 days for injection tunnels 11 y 12 respectively. From the above it is concluded that there are 184 and 161 construction days left, respectively.

KEYWORDS

Planning, tunnels, stochastic simulation, Monte Carlo

INTRODUCTION

The Chuquicamata mine, which belongs to the Corporación Nacional del Cobre de Chile (Codelco Chile) is one of the largest copper exploitations at the world level. It is located in the Region of Antofagasta, 1,650 kilometers north of Santiago, the capital of Chile.

The Chuquicamata mine is now going through its last days of open pit exploitation. After 100 years of mining, the costs have increased as a result of the long distances over which the ore must be carried and of the increased gangue/mineral ratio, making Chuquicamata a less profitable mine.

After a number of explorations that established the existence of an amount of remnant mining resources (Codelco, 2011), called “deep Chuquicamata sulfides” that are found below the open pit operation (Codelco, 2005), it was decided to carry out an underground exploitation, changing substantially the way of utilizing this deposit. In this context various underground works are currently taking place: access and transport tunnels, extraction shafts, and air injection tunnels.

As a result of the above, the Acciona-Ossa Consortium is in charge of the construction of two air injection tunnels required for a preoperational or preparation stage of the underground mine. The two tunnels, identified as tunnels 11 and 12, are parallel and are 4,367 m and 4,349.8 m long, respectively. Furthermore, they will go through the same types of rocks, so they can be considered to have the same lithological characteristics at the time of making the simulations.

Both tunnels are being constructed simultaneously by drilling and blasting (Suorineni *et al.*, 2008).

DEVELOPMENT

From the above, the importance of these tunnels is vital for complying with the deadlines set for this project. We can therefore see the importance of estimating the construction time of air injection tunnels 11 and 12, considering that they are already being constructed.

For that purpose we will use the estimation algorithm presented by Vargas *et al.* (2014), which makes the estimation by means of a stochastic method based on the Monte Carlo method (Metropolis & Ulam, 1949; Sobol, 1994).

Methodology

The methodology of the study is divided as follows:

- Analysis of the data provided by the Acciona-Ossa consortium.
- Selection and classification of data according to the kind of rock.
- Determination of the unit operations and lengths of advance according to the kinds of rocks that will be used in the algorithms.
- Getting probability distributions for the times of the defined unit operations.
- Getting probability distributions for the advanced lengths.
- Stating the algorithms needed for the simulation of the construction times for tunnels 11 and 12 from the construction algorithms presented.
- Getting the simulated construction time for the air injection tunnels.

Description of the Tunnel Construction Project

The injection tunnels' portals or entrances are located around 6 km east of the present pit. The permanent initial infrastructure works consider the execution of two air injection tunnels, named 11 and 12, currently under construction by the Acciona-Ossa Consortium.

The sizes of the tunnels will be 10.74 m wide x 8.0 m high, with downgrade slopes of 15% and individual lengths of 4,367 and 4,322 m for tunnels 11 and 12, respectively, with orientation N80°W from the portal and N80°E from the pit.

The main work conditions used for the estimation of the construction times of the air injection tunnels are presented below:

- The working day consists of two daily shifts of 12 hours each, comprising seven working days and seven resting days, which therefore considers four work groups.
- The use of unit operations and particular advance lengths for the different kinds of rocks, CS2, CS3, CS4 and CS5, with the latter as the one with the worst quality. Therefore, estimation algorithms will be used for the different classes of rocks present.
- The construction time of the tunnels is determined by the number of shifts needed to complete the total length of the tunnel.

Implementation of the Simulation Algorithm

To estimate the construction time of the tunnels, two modifications were made to the algorithm proposed by Vargas *et al*. (2014). The first modification consists in redefining the unit operations of the original algorithm, because it considers five operations, namely:

- Drilling
- Loading of explosives
- Blasting
- Ventilation

- Mucking
- Scaling

The modification consists in editing the algorithm using new unit operations defined by the construction cycle of the air injection tunnels, which are the following seven:

- Drilling
- Blasting
- Ventilation
- Mucking
- Scaling
- Support Instalation.

The second modification is in the advance length, because the original algorithm considers a fixed advance length that is multiplied by a correction factor which, the same as the unit operations, is defined by a probability distribution based on actual advance lengths.

The introduced modification consists in that to simulate the construction time of the tunnels use is made of a probability distribution of the advance length obtained from actually registered lengths.

With these modifications the construction time simulation algorithm is obtained for each of the types of rock.

The data used for this study were provided by the Acciona-Ossa Consortium, and they consist of the daily record of the tunnels. The period of the data is from September 2012 to April 2015.

The data contain the times recorded for the different unit operations needed for the construction of the tunnels, which were recorded by the foremen of both tunnels and were introduced into a computational data base.

For the study, these data are separated and processed independently for the different kinds of rocks, Therefore, determining for the study only the kinds of rocks recorded in the l project, which are CS2, CS3, CS4 and CS5. There are no records of the CS1 class, and only four times there a record was made of class CS6, which also includes blasting time, and by design the advance in this class of rock is made by mechanical excavation, thereby causing an inconsistency for the study, so these few data were taken as rock of class CS5.

For the study, the cycle time data recorded in the tunnels up to April 5, 2015, (Table 1) were processed, and these cycle times allow the calculation of the real construction time by rock class of the tunnels up to the real advance executed. It should be mentioned that in both cases the length of the portal is not considered, since it is made by another excavation technique, and it is 17.2 m for tunnel 11 and 18 m for tunnel 12, with construction times of 68 and 54 days, respectively.

Getting the construction time of the tunnels by means of the simulation algorithms requires the already defined unit operations and advance lengths, and it also requires the probability distribution obtained from the data that compose the unit operations and advance lengths.

Table 1: Real construction time by rock class.

Rock Class / Tunnel		Real Construction Time				
		CS2	CS3	CS4	CS5	Total
11	Advance (m)	73,60	1.153,30	1.075,40	1.258,30	3.560,60
	Days	13,22	250,89	226,82	337,99	828,93
12	Advance (m)	183,80	988,10	1.268,30	1.043,20	3.483,40
	Days	53,91	211,12	250,42	310,18	825,63

Table 2: Unit operations distributions.

Unit Operation	Rock Class	Distribution	Mean (min)	Std. Devn.
Drilling	CS2	Normal	246,56	64,57
	CS3	Lognormal	197,47	86,22
	CS4	Lognormal	144,16	50,87
	CS5	Normal	82,44	29,54
Blasting	CS2	Lognormal	108,98	68,97
	CS3	Lognormal	121,83	61,29
	CS4	Lognormal	90,58	37,51
	CS5	Lognormal	68,01	21,82
Scaling	CS2	Normal	201,92	68,65
	CS3	Lognormal	179,12	64,29
	CS4	Lognormal	161,29	48,69
	CS5	Lognormal	109,47	49,17
Supporing	CS2	Lognormal	78,98	48,93
	CS3	Lognormal	97,40	66,31
	CS4	Lognormal	94,79	50,16
	CS5	Lognormal	127,17	78,76
Shoring	CS2	Lognormal	279,47	85,95
	CS3	Lognormal	391,53	177,70
	CS4	Lognormal	458,58	274,12
	CS5	Lognormal	483,46	222,96

The data of the different unit operations were processed using the Anderson-Darling algorithm, and Table 2 shows the data obtained for both tunnels.

The distributions obtained for the tunnels are entered into each of the algorithms modified for each rock class, and the simulations are carried out, considering that ventilation has a constant time, so it is not dealt with as a distribution.

Confirmation of the simulation algorithm

To confirm the correct operation of the algorithm for both tunnels, the actual executed distances of each tunnel were simulated with the obtained distributions.

Tunnel 11 gets a construction time of 829 days for 3,560 m. The simulation for this tunnel gave 830 days, which represents a negligible difference.

Injection tunnel 12 had a construction time of 826 days for 3,483 m. The simulation gave 813 days for that distance, with a relative error of 1.6%.

Both cases considered 100,000 iterations.

Simulation of injection tunnels 11 and 12

To make the simulations the total length of the tunnels was considered, even though a large part of them was already built. The reason for this decision is that we do not have an estimation of the rock classes expected in what is left of the construction, in this way preserving the rock quality percentages that have already been passed.

The weighting of the rock classes executed for the total length of tunnel 11 is carried out, which as already mentioned is 4,367 m, and the portal's length, was subtracted to perform the weighting, getting a distance of 4,349.8 m (Table 3), which is the distance to be simulated to estimate the construction time of tunnel 11. The same was done for the total length of tunnel 12, which as already mentioned is 4,322 m, getting a distance of 4,304 m (Table 4).

Table 3. Injection tunnel 11 weighting by rock class.

Class	Partial Distance (m)	%	Weighted Distance (m)
CS2	73,60	2,1%	89,91
CS3	1.153,30	32,4%	1.408,93
CS4	1.075,40	30,2%	1.313,76
CS5	1.258,30	35,3%	1.537,20
Total	**3.560,60**		**4.349,80**

Table 4. Injection tunnel 12 weighting by rock class

Class	Partial Distance (m)	%	Weighted Distance (m)
CS2	183,80	5,28%	227,10
CS3	988,10	28,37%	1.220,87
CS4	1.268,30	36,41%	1.567,08
CS5	1.043,20	29,95%	1.288,95
Total	**3.483,40**		**4.304,00**

The input data of the algorithms are the following, as presented by Vargas *et al.* (2014):

- Number of simulations: 100,000 and 200,000.
- Shift duration: 12 hours → 720 minutes.
- Length to be simulated: Distance corresponding to the rock class.

The results obtained for the simulations of both tunnels are shown in Tables 5 and 6, from which we can conclude that the value used for the planning will be that of the mean, which is very similar to the mode, as stated by Vargas *et al.* (2014). The above gives a value of 1013 days for tunnel 11 and 1.004 days for tunnel 12.

Table 5. Simulation results for injection tunnel 11.

Class	Sim No.	Lenght	Shift	Mean	Std. Devn	Mode	Minimum	Maximum
		(m)	(min)	(days)	(days)	(days)	(days)	(days)
CS2	10^5	89,9	720,0	13,4	1,4	14,0	10,5	16,5
CS3	10^5	1.408,9	720,0	290,0	9,3	290,0	272,0	311,0
CS4	10^5	1.313,8	720,0	274,4	9,6	275,0	254,0	296,0
CS5	10^5	1.537,2	720,0	435,4	12,0	436,0	405,5	416,0
Total				**1.013,2**		**1.015,0**	**942,0**	**1.039,5**

Table 6: Simulation results for injection tunnel 12.

Class	Sim No.	Lenght	Shift	Mean	Std. Devn	Mode	Minimum	Maximum
		(m)	(min)	(days)	(days)	(days)	(days)	(days)
CS2	10^5	227,10	720,00	60,58	3,52	61,00	47,00	79,00
CS3	10^5	1.220,87	720,00	251,35	4,32	252,00	229,50	269,50
CS4	10^5	1.567,08	720,00	327,22	5,26	327,00	307,00	351,50
CS5	10^5	1.288,95	720,00	365,09	5,48	366,00	341,00	388,50
Total				**1.004,2**		**1.006,0**	**924,5**	**1.088,5**

CONCLUSION

The good behavior of these algorithmos was confirmed at first by simulating the partially executed tunnels.

That led to the assumption that the simulation for both tunnels has a high degree of confidence, 1013 days for injection tunnel 11 and 1004 days for injection tunnel 12.

The simulation data obtained do not consider the construction of the portals, mainly because it is performed by drilling and blasting, but with mechanical excavation, which falls outside the simulation methodology used. The above is not important if we consider that the construction of the portals in relation to the time taken is a mathematical certainty, because they had been built, and it was 68 days for tunnel 11 and 54 days for tunnel 12.

The above means that the construction time including the portalis is 1081 days (36 months) for tunnel 11 and 1058 days (35.3 months) for tunnel 12. Considering that the construction time used so far is 897 days for tunnel 11 and 880 days for tunnel 12, it is estimated that they will be finished in 184 and 161 more days, respectively, considering the advances made to date.

REFERENCES

Codelco. (2005). *Bases técnicas: Desarrollo de obras mineras proyecto de explotación de súlfuros profundos tercera etapa.* (Bases Técnicas Licitación No. DAP CP 050-05). Calama: Codelco.

Codelco. (2011). *Minería subterránea: Pilar del futuro de codelco.* Retrieved 23/Enero, 2013, from http://www.codelco.com/mineria-subterranea-pilar-del-futuro-de-codelco/prontus_codelco/2011-05-19/170202.html

Metropolis, M., & Ulam, S. (1949). The monte carlo method. *Journal of the American Statistical Association, 44*(247), 335-341.

Suorineni, F.T., Kaiser, P.K., & Henning, J.G. (2008). Safe rapid drifting-support selection. *Tunnelling and Underground Space Technology, 23*(6), 682-699.

Sobol, I. M. (1994). *A primer for the monte carlo method* (pp. 107). Boca Raton, FL: CRC Press.

Vargas, J.P., Koppe, J.C., Pérez, S. (2014). Monte Carlo simulation as a tool for tunneling planning. *Tunnelling and Underground Space Technology,* 40, 203-209.

FEATURES OF INTERNAL STACKING DURING MINING OF STEEPLY DIPPING MINES

Drizhenko A.,[1]Anisimov O.[1], Rakishev B.[2],Moldabayev S.[2], Sarybayev N.[2]

[1]National Mining University, Ukraine
19 Karl Marx Avenue
Dnepropetrovsk, Ukraine, 49600

[2]Kazakh National Research Technical University after K.I. Satpayev
22A Satpayev Street
Almaty, Kazakhstan, 050013
*(*Corresponding author: moldabaev_s_k@mail.ru)*

24th World Mining Congress
MINING IN A WORLD OF INNOVATION
October 18-21, 2016 • Rio de Janeiro /RJ • Brazil

FEATURES OF INTERNAL STACKING DURING MINING OF STEEPLY DIPPING MINES

ABSTRACT

Offered classification of internal culm dump formation allows determining efficient method of filling mined open-pits depending on its sizes at surface and bottom sides, also at specific depth of mining with dead end track of automobile road and railways. Development of elongated mines and piling of overburden inside the mined space is achieved through phased mining and formation of an open-pit of first order. Generally during mining of round open-pit mines, track of automobile roads usually has a spiral form; thus, it is hard to form internal culm dumps in such open-pit mines. Internal stacking inside such open-pit mines could only be organized by "filling mined open-pit" scheme during mining of close ore bodies, or if large mined areas are present inside and prism stops could be equipped, then internal culm dump could be formed on the boundaries of these prisms.

KEYWORDS

Internal stacking, steeply dipping mines, filling method, overburden, elongated and round mines, order of open-pit field mining.

INTRODUCTION

Piling overburden on external culm dumps is a costly process in extraction of minerals due to the long transportation distances, overload and stacking, and also financial compensation for soil degradation near mining corporations and pollution of atmosphere due to dust and gases. At the same time, placement of waste in internal culm dumps by analogy with open-pit mines, mining flat-lying mines of brown coal, manganese ore, construction minerals, ores of nonferrous and rare metals will noticeably decrease the transportation distance and ecological impact on the environment, wherein, significantly decreasing costs of stripping (Dryzhenko et al., 2009). As a result, technical-economical indexes of surface mining of deep iron mines and other open-pit mines will be significantly improved.

Many mining corporations, extracting minerals by surface mining method, pile overburden on external culm dumps, occupying up to 30% of all land designated for mining and processing. Culm dumps are located far from boundaries of a mine field. Transportation of waste is usually done by automobile or combined automobile-railroad transport, rarely in combination with conveyor or skip hoisting.

Researches on controlling open-pit mine space formation and its working zone to create a premise for transition to internal stacking during mining of deep open-pits with limited length are given in the textbook of G.G. Sakantsev (Dryzhenko et al., 2009). Possibility and expediency of internal stacking on round open-pit mines are proved and rational limit of its usage is determined. It corresponds to mining-geological and mining technical conditions of many mined and perspective open-pit mines.

On elongated mines (these include number of contiguous mines) best technical-economical indexes are achieved during the reduction of time allocated for an open-pit mine to reach the first order of final depth with transition to internal stacking. Examples of internal stacking implementation on iron mines of Ukraine are given in the paper of A.Y. Drizhenko (Sakantsev, 2008). In the context of real conditions of many coal mines such designs were created in MNI under the supervision of P.I. Tomakov, full analysis of modern approaches for solving given problem is generalized by V.S. Kovalenko (Nikiforova & Dryzhenko, 2015).

Works of K.N. Trubetskoi, A.G.Shapar, V.G. Pshenychnyi (Kovalenko et al., 2013; Trubezkoi et al., 1994; Shapar et al., 2009; Phsnichnyi, 2012) and other scientists are dedicated to increase the efficiency of internal stacking technology during mining of steeply dipping mines.

Classification of methods and internal culm dump formation order

Culm dumps could be single and multistage. Piling of culm dumps inside open-pit mines are done on separate horizons or from surface up to full depth of mined space. They are formed temporarily with transfer of overburden from one position to another or they could be stationary. Classification of methods and internal culm dump formation order are shown in Figure 1 and Table 1.

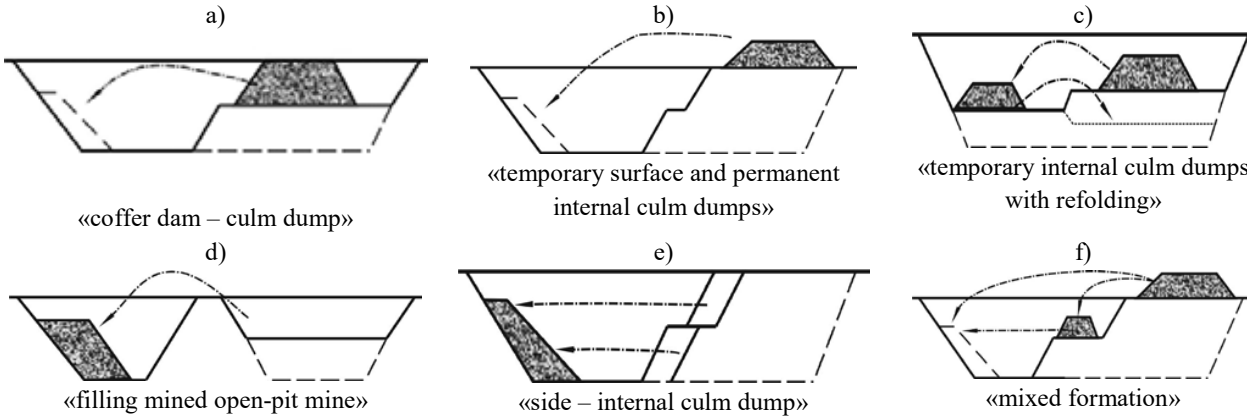

Figure 1 - Internal culm dumps formation schemes on the boundaries of mine field

Implementation of various schemes determined by sizes of a mine field, physical-mechanical features of rock mass on open-pit sides and rock mass piled to internal culm dump. Transportation of overburden could be done by automobile, railroad or conveyor transport depending on implemented technology of complex mechanization on an open-pit mine.

During transportation of rock mass with automobile transport the most effective schemes are *a, c, e* (Figure 1). For elongated open-pit mines, including oval ones, it is effective to use railroad and conveyor transport, because their usage reduce costs of overburden transportation, especially on upper horizons.

Option of internal stacking on elongated open-pit mines

Suggested classification determines the internal culm dump formation order on boundaries of an open-pit mine for any overburden transportation technology. Wherein, parameters of a mine field and its mining order play an important role. Mining operations of 1st phase are expected to be carried out till reaching the project bottom surface level and consequent 2nd phase overburden piling in its mined space during mining of a standard deep open-pit mine (Figure 2).

Table 1 – Classification of internal culm dumps formation schemes during mining of deep open-pits

№	Method of internal stacking formation	Stacking technology	Piling of culm dump in the design	Order of open-pit mining and internal stacking formation
1	Temporary placement of culm dumps ahead of the extraction operations on overburden horizons «dam – culm dump» (Figure 1, a)	Culm dump is placed on formed areas of a mine with consequent transfer to deep horizons	On mined end(s), along recumbent or suspended sides of open-pit	Culm dump is formed after mining of a 1st order open-pit
2	Temporary placement of culm dumps on the surface of a mine field «temporary surface and permanent internal culm dumps» (Figure 1, b)	Culm dump is placed on the boundaries of mining allotment on the surface and consequently is displaced inside the mine	On mined end(s), along recumbent or suspended sides of open-pit	Culm dump is formed after mining of a 1st order open-pit
3	Temporary placement of culm dumps on the boundaries of an operational zone with consequent transportation «temporary internal culm dumps with refolding» (Figure 1, c)	Internal culm dump is shifted from one position to another until reaching mine's projected bottom surface	Areas on the boundaries of mined open-pit space	Culm dump is formed during transportation of overburden by phases of mine development
4	Stationary placement of culm dumps on a mined open-pit space with transportation of overburden from adjacent open-pit mines «filling mined open-pit» (Figure 1, d)	After mining of open-pit, overburden from adjacent mines is transported and piled on the mined space	On perimeter of mined end(s), along recumbent or suspended sides of open-pit	Culm dump is formed after mining adjacent open-pit in mined space
5	Stationary placement of culm dumps with transportation of rock mass inside the mine «side – internal culm dump» (Figure 1, e)	Overburden are transported to culm dump directly from sides by transport system inside the open-pit	On mined end(s), along recumbent or suspended sides of open-pit	Culm dump is formed after mining of a 1st order open-pit
6	Combined placement of culm dump, including previous methods «mixed formation of culm dump» (Figure 1, f)	Combination of different methods of stacking and refolding of overburden	On mined and non-mined areas on boundaries of mined space of a mine field	Culm dump is formed before mining of 1st order open-pit, during its operation and during consequent operation of mine

Wherein, the size of the mined space has crucial meaning for placement of current volume of overburden of consequent mining phases of a mine. It was determined, that for open-pit bottom surface with length of 324 m and width of 528 m and project depth of 400 m, there is a possibility of storing current volume of overburden while keeping transport platforms on internal perimeter of mined space with width of 40 m for movement of dump trucks from the bottom ledge (Aben et al., 2014). Resistant prism is formed at the height of lower extraction ledge with top width of 30 m, along the lower edge of internal culm dump to avoid piling of rock mass on roads, falling from the slope of internal culm dump (Figure 3). Internal capacity between the slope of non-operating side and resistant prism is filled by overburden of current excavation.

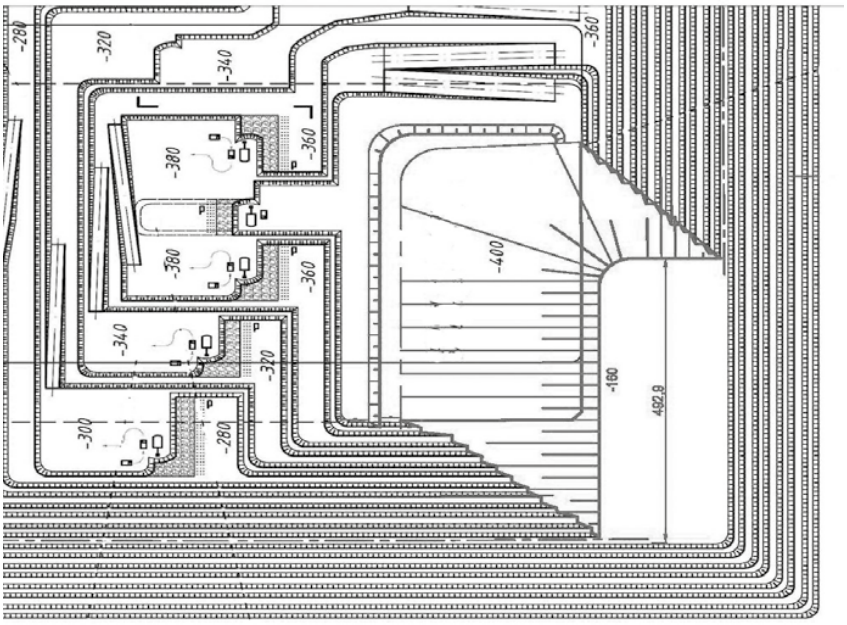

Figure 2 - Internal culm dump formation scheme on an open-pit of 1st order

Conducted research showed that, one of the effective options of mining elongated mines is the implementation of mining operations providing equal length of operation front on all ledges of working zones (Moldabayev & Rakishev, 2015). As a result of comparative analysis, selection of operational front's advancement direction of working zones' ledges perpendicular to the advancement direction of operational sides of technological layers was justified (Figure 2). Contours of mining phases on sectional view of a mine occupy several technological layers. On an open-pit of 2nd order, mining works are conducted throughout its depth, which, during double side transverse subsystem of mining, provides maximum production capacity on an open-pit of 2nd order with the best mining operations regime. It is proved, that amount of ore could be raised up to 47% if open-pit contours' separation spaces are reduced up to 2 times maximum.

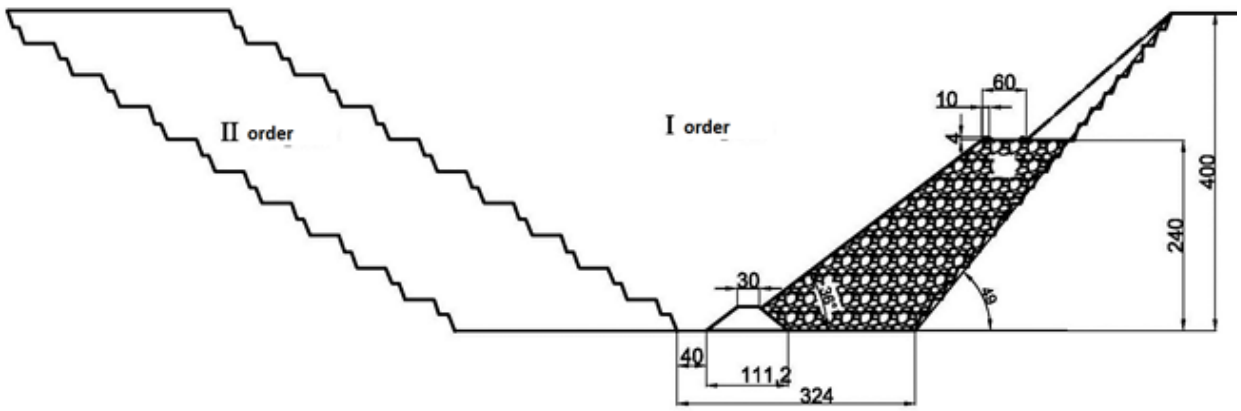

Figure. 3 - Sectional view of an open-pit with positions of 1st and 2nd phases of mining

Selection of mining phases is determined by the width of panels on daylight surface from boundaries of 1st order open-pit. With the exception of first and last phases on intermediate phases, during the set-up of contours of mining phases, amount of panels being mined on several technological layers corresponds to conduction of mining operations by double side transverse mining subsystem for the whole depth of 2nd order open-pit.

Height of the lower tier of 1st order internal culm dump is taken at the two-thirds of the open-pit's bottom surface level, which corresponds to the center of gravity of overburden excavation by footwall of mine. Resistant prism prevents scattering of rock mass during formation of internal culm dump slope; 6 mln. m^3 of waste is needed for its construction. Piling of rock mass could be performed by bulldozers or excavators with prolonged equipment. Dumping with excavators is considered to be safest method.

Second order of internal culm dump is dumped during advancement of dumping operations front in transverse direction from non-operating open-pit side by suspended side of open-pit with gap of 60 m from the base. About 22 mln. m^3 of overburden could be stored up to the level of 240.0 m in accordance with the position of mined 1st order open-pit up to the level of daylight surface. Consequently, during the advancement of mining operation's front, upper portion of the internal culm dump is displaced right after mining operations. Dislocation of automobile access tracks after advancement of mining operations front allows increasing width of the internal culm dump. Increasing its area at the surface allows dumping culm dump with height up to 60-120 m on upper area. Such operation contributes to the placement of the whole overburden from 2nd phase of mining on the mined space of an open-pit.

Significant economy of financial resources is achieved; also number of parking spots for dump trucks is decreased by reducing the waste transportation distance by 1.5 -2 km and intensity of soil degradation by external culm dumps.

Examples of industrial implementation of internal stacking on iron mines

Industrial implementation of internal stacking technology on the open-pit of JSC «Poltavskyi GOK» was conducted from 1993 to 2010 yy. Usage of internal stacking allowed reducing overburden transportation distance by automobile transport by 1.2-2.5 km; by railroad transport – 5 km. About 6 hectares of arable land were saved from degradation by external culm dumpsь.

As of 01.01.2008 on the contours of open-pit #2-bis of JSC «ArselorMittal Krivoy Rog», there are 317.1 mln. tons of non-oxidized ferruginous quartzite of first and second ferruginous horizons. Among simultaneously mined rock mass, which lie in the contours of the mine field, there are 47.35 mln.m^3 of overburden, of which, 1.35 mln.m^3 are alluvium and 46 mln.m^3 are rock mass, consisting of substandard quartzite and slate. Required capacity for overburden storage from open-pit #2-bis, considering residual loosening ratio of K_{po}=1.2, is 56.8 mln.m^3.

By data of Ore control of JSC "ArselorMittal Kriovoy Rog" overburden from open-pit #2-bis is planned to be placed on the following culm dumps (with project capacity): mined open-pit #1 – 74.6 mln.m^3; distant culm dumps – 17.9 mln.m^3; tailings storage "Mirolubovskoe" – 950 th.m^3; tailings storage "Obiedinennoe", 3rd map – 10 mln.m^3; tailings storage "Obiedinennoe", 4th map – 850 th.m^3.

Overburden and non-oxidized quartzite, being mined by open-pit #3, are placed in culm dumps #2-3and "Stepnoy", also, partially, in mined open-pit #1. Part of rock overburden (0.2 – 0.5 mln.m^3) is used for crushed stone production, which is used by GOK for its own needs.

Culm dumps #2-3 are located on watershed beam "Zelenaia" and floodplain of Ingulets river. They are dumped on main area up to the level of 146 m. Projected heights of culm dumps are 166 m. Capacity of culm dumps #2-3, according to the project solutions accepted earlier was 250 mln.m^3, including storage of oxidized quartzite - 90 mln.m^3, for overburden storage – 160 mln.m^3. Stacking of overburden was done on the western site, but due to the landslides was stooped from 1990, and according to the current materials and recommendations about the condition of given site, currently cannot be resumed.

Oxidized ferruginous quartzite is stored on separate north-eastern site of culm dumps #2-3 with the purpose of consequent usage on DOF KGOKOR. Oxidized quartzite is delivered to the culm dump by railroad transport; stacking - by excavators. Two-three culm dump deadlocks are used on the culm dump. Remaining capacity as of 01.01.08 is 35.2 mln.m^3. Additional culm dump capacity of 165.5 mln. m^3 will be needed to store oxidized quartzite till the end of mining operations.

Culm dump "Stepnoy" is located to the west of culm dump of "Novaya" mine. Area of the culm dump is 240 hectares. Maximum height of culm dump is 60 m. Transportation of overburden is conducted by railroad transport, stacking – by excavators EKG-8I; 2 deadlocks are operated. Residual capacity of culm dump "Stepnoy" as of 01.01.08 is 10.04 mln.m^3. Possibility of increasing the capacity of culm dump is depleted.Shortage of capacity for overburden storage of open-pit # 3 will be 184 mln.m^3.

According to reported data of mining-enrichment complex JSC "AMKR" average annual economic effect from implementing new method of rock mass storage in mined open-pit #1 will be around 7.2 mln. USD. Main efficiency of developing new culm dump in mined open-pit #1 comes from redistribution of overburden storage directions from open-pit #3, delivered by railroad transport. Also, height of internal culm dump of 345 m allows increasing

significantly its land capacity and to store 134.39 mln. m^3 of rock mass on an area of 111.5 hectares. Filling of open-pit mine named after Iliych by overburden of open-pit #3 JSC "AMKR" will allow storing about 732 th. m^3 of rock mass on mined territory.

Perspectives of internal stacking on round mines

Currently, in Kazakhstan, pre-project developments of implementation in mining of Lomonosov iron ore reserves are done, which is located 10 km to the north-east of Sarbaisk mine and 20 km to the north of Rudnyi city. The mine has two round areas: North-Eastern Central, which differ by structural features and nature of mineralization.

Conducted analysis shows expediency of initial mining of Central region (Rakishev & Moldabayev, 2014). In such a case, all 294.6 mln. m^3 of overburden of North-Eastern region could be placed on mined space of Central region (Figure 4). With residual loosening coefficient of 1.1, usage of mined space of Central region will be 1.01. Results of research are received by LLC «Lomonosovskoe» for further transmission to contractor for their use in project of operation production after the final approval of project conditions.

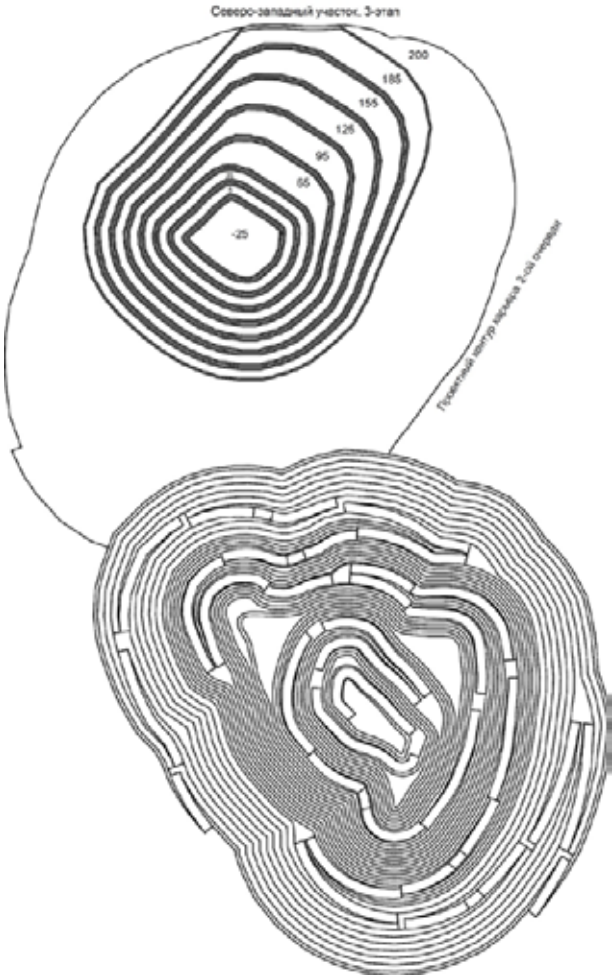

Figure 4 - Alternate mining of Lomonosov mine areas with formation of internal culm dump on mined space of Central region (below North-Eastern region)

Following schemes could be distinguished during piling overburden from the surface of an open-pit or from concentrated horizon. First scheme is intended for piling overburden on area without preliminary formation of resistant prism. In this case, to ensure safe operation of equipment in the bottom of open-pit in the region of formed culm dump area, given site should have a zone of possible culm dump dislocation or rolling out overburden lumps. Movement of transport and working personnel is prohibited in the given zone. This zone is usually transferred ahead of the depleted cut. Transfer pace of depleted cut depends on operational parameters of excavating-loading equipment, used during the formation of culm dump. Length of depleted front could be equal to its width during

initial phase. Consequently, as dumping operations progress it increases and, area under internal culm dump also changes.

Second scheme requires preliminary formation on the bottom surface of an open-pit or on base of internal culm dump of resistant prism. In cross section it might have a form of trapezium or rectangle, depending on height of a given prism and how it was formed (by bulldozer, excavator, spreaders, etc.). Height of such prism could vary from 4-6 up to 15 m. Height of culm dump or piled dump tier determines the height of preliminary formed resistant prism. Resistant prism is formed along mined side on certain distance from lower edge. Afterwards, formation of internal culm dump is initiated.

Overburden storage place is determined according to the open-pit plan, where open-pit sides are plotted, brought to non-operational design position. Transport and other communications should not be present in internal culm dump area. At least two areas are needed: upper, for placement of dumping equipment and lower – base of culm dump (design position of bottom surface of an open-pit or non-operating platform) of sufficient size.

Platform of operating dumping equipment should be connected to access tracks inside the open-pit or on the surface. Other communications are also supplied if needed. It is necessary to consider mining-geological and hydro-geologic conditions. Operating dumping platform cannot be located near open-pit sides' displacement areas.

The most feasible option of filling deep open mined area is to dump overburden from daylight surface using console spreader. In this case, possibility of using combined automobile-conveyor transport should be present during mining of iron mines of North-Western area.

CONCLUSION

Filling of mined open-pits is a main measure, leading not only to rational use of land resources during mining, but also to significant cost cuts of mineral extraction. Placement of overburden on mined space of deep open-pits minimizes transportation distance and preserves land degradation by external culm dumps. Wherein, open-pits of 1st order should be emphasized during operation of group of mines or mine fields with significant sizes, mine them up to limit contours and conduct further mining including storage of overburden on mined space afterwards.

Analysis of mining conditions of iron ore mines by surface method and internal culm dump formation order shows that offered technical solutions could be used on many open-pits, which have significant parameters of mine field. Mining order should be distinguished during operation of a group of mines. First phase of mining should be mined till the limit project depth.

REFERENCES

1. Dryzhenko A.Y., Kozenko G.V., Rykus A.A. Surface mining of iron mines of Ukraine: condition and improvement methods. – D.: NGU., 2009, p .452.

2. Sakantsev G.G. Internal stacking in deep mines. Yekaterinburg, IGD Uro RAS, 2008, p. 225.

3. Nikiforova N., Dryzhenko A.Y. Technologies of overburden rock storing in depleted or operated iron open pit mines of Ukraine // Theoretical and practical solutions of mineral resources mining. - CRC Press/Balkema. P.O. Box 11320, 2301 EH Leiden, is an imprint of the Taylor & Francis Group, London an informa business, 2015. pp. 493-504.

4. Kovalenko V.S., Artem'ev V.B., Opanasenko P.I. Soil sustaining and soil producing technologies on coal mines. Moscow, Izd-vo «Gornoe delo» OOO «Kimmeriiskii zentr», 2013, p. 440

5. Trubezkoi K.N., Peshkov A.A., Mazko N.A. Determining application areas of methods of mining steeply dipping mines using preformed mined space of an open-pit. Gornyi zhurnal, 1994. no. 1, pp. 51-59.

6. Shapar A.G., Iakubenko L.V., Piven' V.A., RomanenkoA.V. New technological solutions of mining steeply dipping mines with internal stacking for open-pits, mining steeply dipping mines. International math. conference «Forum of mining engineers». 2009, pp. 78-86.

7. Phsnichnyi V.G. Determining rational regime of mining and internal stacking for open-pit mines, mining steeply dipping mines. Vestnik Krivorozhskogo Nazional'nogo Universiteta. 2012. vyp. 31, pp. 3-6.

8. Aben Ye., Rakishev B.R., Moldabayev S.K. Minimizing the Time of reaching the Final Depth in the Pit of the First Train When Extracting the Elongated Steeply Dipping Mines. C. Drebenstedt and R. Singal (eds.), Mine Planning and Equipment Selection, Springer International Publishing Switzerland 2014. Proceedings of the 22nd MPES Conference, pp. 209 -216. Volume 1. Dresden, Germany (2013).

9. Rakishev B.R., Moldabayev S.K. «Method of surface mining of steeply dipping mineral mines with transition to internal stacking». – Innovational patent for invention of RK № 29038 by application № 2013/1337.1 от 11.10.2013г. Publ. 15.10.2014, bul. № 10.

10. Moldabayev S.K., Rakishev B.R. Rationale of working zones formation order in deep open-pits for excavator-automobile complexes // Scientific-technical magazine «Gornyi informatsionno-analyticheskyi bulleten». – Moscow: Gornaya kniga, 2015. – № 1. - pp. 27-34.

FUTURE OF UNDERGROUND COAL MINING IN BRAZIL: IMPLEMENTATION OF LONGWALL MINING

*F. A. C. Cardozo[1], M. Zampiron[1]and A. C. Zingano[1]

[1]Federal University of Rio Grande do Sul
9500 Bento Gonçalves Avenue
Porto Alegre, Rio Grande do Sul, Brazil
*(*Corresponding author: fernando.cantini3@hotmail.com)*

24th World Mining Congress
MINING IN A WORLD OF INNOVATION
October 18-21, 2016 • Rio de Janeiro /RJ • Brazil

FUTURE OF UNDERGROUND COAL MINING IN BRAZIL: IMPLEMENTATION OF LONGWALL MINING

ABSTRACT

It's been a while since the exhaustion of most economic coal deposits minable through open pit mining has encouraged the use of underground mining. Among the underground mining methods of higher productivity and lower cost is the Longwall Retreating Mining. This method is almost unknown in Brazil, but with attempts of being used in the State of Rio Grande do Sul and a new intention of being applied in a new mine. Currently the coal mining in Brazil is held by open pit method in the State of Rio Grande do Sul, and by Room and Pillars in State of Santa Catarina. Both methods have some advantage and disadvantage in terms of productivity, operation cost, recovery, and environmental issues. There is a huge coal deposit near to Porto Alegre, but it's very deep for surface mining, and conventional room-and-pillar mining could not be applied because the higher cost and low productivity. This case study is related to the use of longwall mining method for this very important coal deposit, in terms of basic infra structures, the natural characteristics of deposits, accesses and support, design of pillars, ventilation, mining planning and choice of equipment for longwall mining. The project was set up for a production of 4 Mtpa. The mining panels are 400 m wide and over 2000m long for average 2.5 m of coal seam thickness. In addition to mining it was considered 3 faces for development with miner bolter. This study showed that it's possible to development an underground coal mine that could reach the high production, and low cost.

KEYWORDS

Underground Coal Mining, Longwall, Rio Grande do Sul, Conceptual Design

INTRODUCTION

The longwall mining method is traditionally applied to underground coal mining, where the integrity of the immediately roof above the coal seam already mined is caved (Brady & Brown, 1995). This mining method is high productivity and low cost, because it's full mechanized and automated mining. When the roof caves, there is a distribution of the stresses to the face and chain pillars in both sides of the panel, which is called the abutment pressure (Peng, 2007). Figure 1 shows a sketch of a longwall mining face.

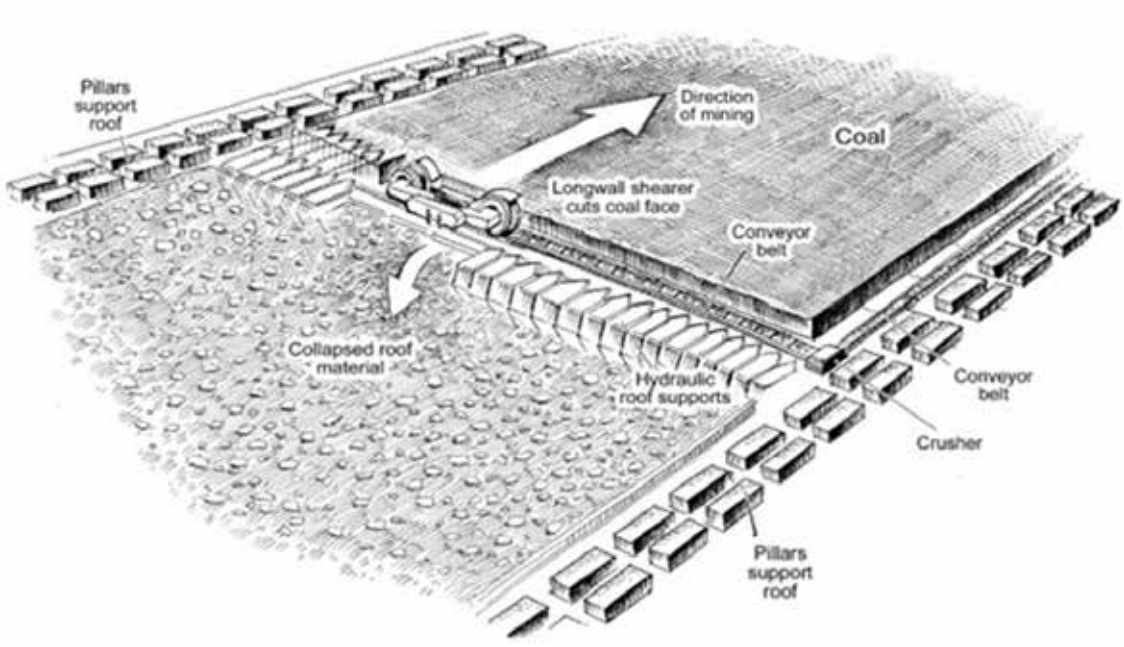

Figure 1. Perspective of a front of longwall

Currently the longwall method is known worldwide for presenting the highest productivity among all the underground coal mining methods. In 2013 the United States produced 189.2 Mton of coal using longwall which represented 53% of the coal production in underground mines. The productivity of the method was 4.15 t/hour.man (USA) against an average of 2.5 t/hour.man achieved by the other underground coal mining methods, according EIA (2015).

This study was based on the knowledge of the longwall operations worldwide applied on the Brazilian coal deposit conditions. It aims to investigate the application of longwall in a mine located in the southern of Brazil. The Triumph Mine can be considered compatible with the longwall method since it presents satisfactory thickness, flat and high continuity. Among the good geology conditions for longwall, this deposit is very important because the coal resource is more than 200 Mt of coal.

The study area is located in the municipality of Triunfo in southern state of Rio Grande do Sul, Brazil. The area is adjacent to a petrochemical complex to the Northeast, to the Jacuí Park and the Jacuí River to the South and West, respectively. Also, this area is close to Charqueadas Coal Mine, an underground operation located at this area that closed since 1990. This area, subject to mineral exploration and mining, including the mine of Charqueadas Mine, embracing an area of 39000 ha.

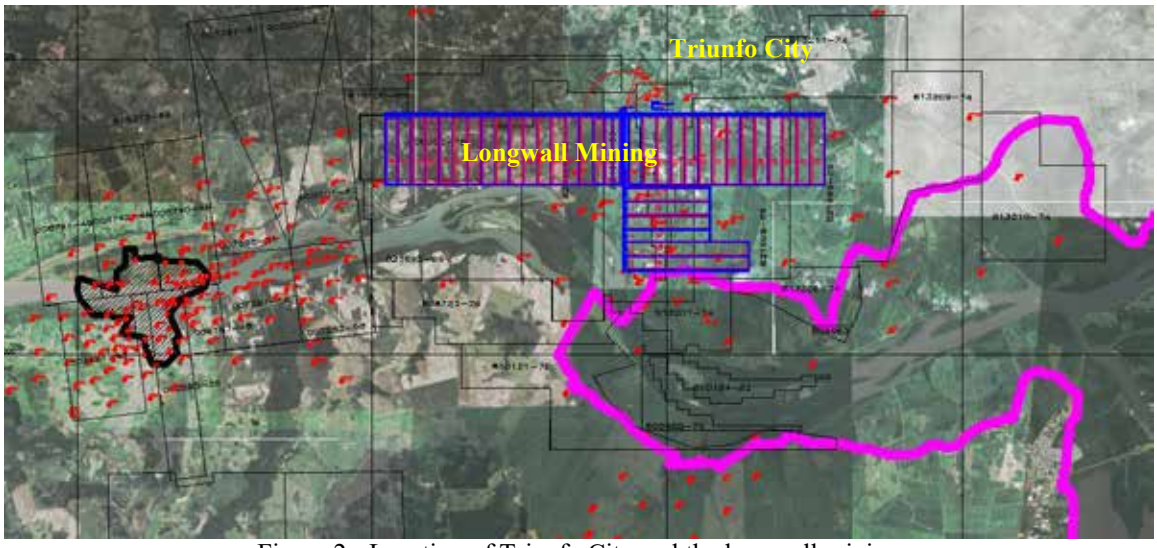

Figure 2 - Location of Triunfo City and the longwall mining

On the basis of available data, a study was conducted aiming to investigating the best technical and economic alternative to recover the coal at Triumph region. It was taking into account: minimum environmental and social impact, profitability, operation efficiency, high productivity and mineral recovery.

The existence of a large good quality coal deposit and the interest of its economic exploitation has been known for long time. Nevertheless, it was located on deeper layers when compared to the coal seams currently exploited in Brazil.

In the past, coal had been mined in more superficial deposits in Rio Grande do Sul, including surface mining, with considerable lower costs. However, the depletion of such coal reserves and the ever growing demand for coal justified the necessity to evaluate this deposit. In the 70's and 80's, the Charqueadas Mine, located about 3km west of the area in study was developed. At that the time, the main problem in coal mining was the intensive support and stabilization of the immediate roof, and floor heave.

In 2008 and 2009, a coal company carried out some exploration in the region with the plan to develop a coal mining, but due to geological conditions (mainly the quality of the immediate roof) the project was closed. The information and data of the late mining experience and the results of the more recent projects have been used in the study and evaluation of the possibility of longwall application.

LONGWALL DESIGN

Based on the few boreholes made in the coal deposit, it has been set a layer named as I2B to be mined. It was the one with the greatest continuity, fundamental factor for using this method, and also presented a consistent thickness of an average over 2.5 meters, perfect for longwall. The objective area was located outside of the environmental preservation areas and where the coal seam presented a thickness greater than 2.0 meters. A first moment the region down the river has not considered as a target, defining it as a possible area of expansion (Figure 3).

Figure 3 - Location of the area with a thickness greater than 2 m

Considering the premises of the mining method layout presented in bibliography (Peng, 2006; Bessinger, 2011) it was created the concept for longwall mine. Mining panels 400 m wide were placed in such a way to best fill the target area. The first four panels were designed with smaller width, due to the need for experimenting with the mining method.

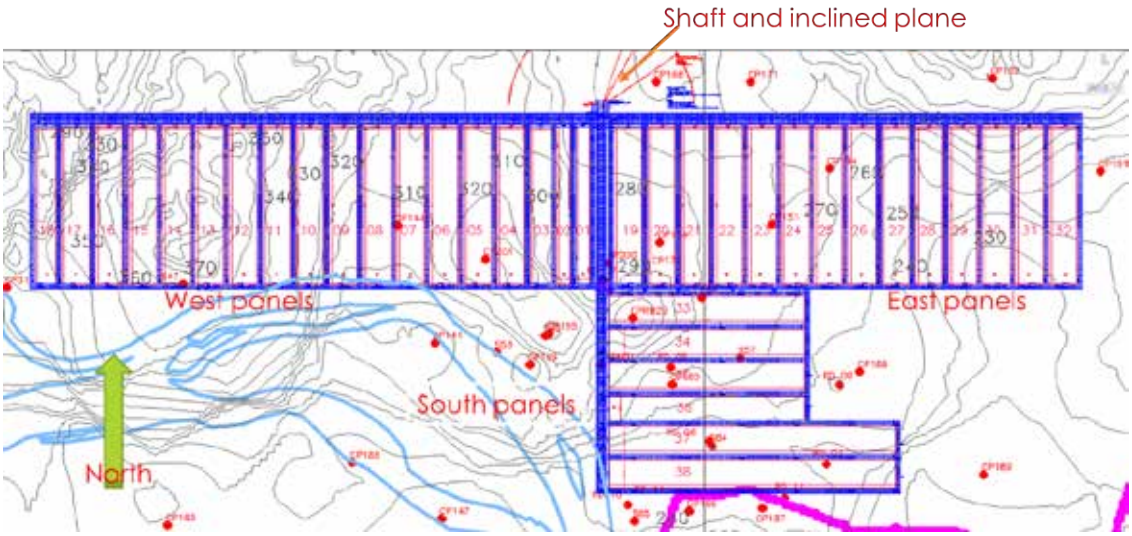

Figure 4 - General layout of the mine showing the arrangement of mining panels

The main entries pillars were designed by using the methodology proposed by Bieniawski (1963), the other pillars of tailgate, headgate and bleeder were desinged by the ALPS methodology (Mark, 1990).

According to ALPS methodology, the pillars designed at the mains 25x25m wide, and entries are 5m wide. The height was equal to the coal seam thickness of 2 meters. The average coal layer Uniaxial Compressive Resistance was considered 4.0MPa (Zingano et al., 2015) and the adopted safety factor not less than 1.5. The tailgate and headgate pillars were designed to be 30x30m and the bleeder were 28x28 meters.

To design the barrier pillars between the longwall panels and mains, the empirical methodology of 10% of the depth plus 13 meters (45ft) was adopted. In this way the pillars were estimated to reach 35 meters wide. This methodology have been successfully applied in the United Kingdom (PENG, 2008) coal mines of the. It was considered a system of three galleries in the tailgate and headgate since it had proven to be the safer.

Table 1 – Planned panels geometrical parameter

Average thinckness (I2B)		2.5				
Panel		Number of Panels	One Panel		All Panels	
Width	Length		Volume	Tons	Volume	Tons
200	2225	2	1.112.500,00	2.225.000,00	2.225.000,00	4.450.00,00
300	2225	1	1.668.750,00	3.337.500,00	1.668.750,00	3.337.500,00
400	2225	29	2.225.000,00	4.450.000,00	64.525.000,00	129.050.000,00
400	2777	4	2.777.000,00	5.554.000,00	11.108.000,00	22.216.000,00
400	4069	2	4.069.000,00	8.138.000,00	8.138.000,00	16.276.000,00
	TOTAL	38			87.664.750,00	175.329.500,00

Based on the production premises of 4 Mtpa and operational productivity, the equipment fleet was defined for both, production and development.

Table 2 - 400 meters wide longwall panels

Description	Number
Hydraulic roof support (face shield) with 1.75 m wide and two legs system	229
AFC (Armored Face Conveyor) drag chute for transport of coal (400 m)	1
Two drums Shearer (double ended shearer)	1
Stageloader for transfer of the AFC for the coal conveyor belt feeder	1
Jaw Crusher (feeder breaker) to reduce size of blocks	1
Belt feeder	1
Tractor to transport equipment (shields and shearer)	2
Scoop to transport supplies	1
Oil pumping system to support equipment and shearer	1
Track system for movement of equipment on the Panel	1
Communication system	1
Energy generator	1

Table 3 - Development galleries

Description	Number
Continuous mining with drilling rigs (miner boom)	1
Shuttle car for coal transportation until the feeder	2
Roof bolter	1
Feeder breaker (crusher and belt feeder)	1
Scoop for cleaning and supplies transporting	1
Energy generator	1

CONCLUSION

According to the conceptual model of longwall mining and to the information about the potential deposits of southern Brazil, the implementation of longwall mining have been proved for future work. It is necessary to emphasize the need of further studies, more so, about the deposit's structural geology. It could be an important obstacle to overcome in the event of applying this underground mining method. Such geological features are even more pronounced in the coal seams of Santa Catarina State compelling, in the first moment, to investigate the underground mining of the Rio Grande do Sul State coal formations.

The coal market demand over 4 Million of tons year yet to be produced in Brazil is a reasonable argument to invest more efforts in investigating the use of Longwall Mining at the Brazilian coal seams.

ACKNOWLEDGMENTS

The authors would like to thank the Universidade Federal do Rio Grande do Sul by supporting this study, the Laboratório de Pesquisa Mineral (UFRGS) for making it available the information and technical expertise and Caterpillar for making it possible the discussions with Prof. Syd Peng which inspired this work.

REFERENCES

Brady, B. H. G., Brown, E.T. (1995). *Rock Mechanics for Underground Mining*. Chapman & Hall, 2º ed, 572 pg.

Bessinger, Stephen L. (2011). *Longwall Mining*. In: Peter Darling (Org.). SME Mining Engineering Handbook. 3. ed. Usa: SME, 2011. Chap. 13. p. 1399-1415.

Cardozo, F. A. C. (2015). *Longwall: Estado da Arte, Geomecânica, Planejamento e Aplicação*. (Master's thesis) - Federal University of Rio Grande do Sul, Porto Alegre.

Energy Information Administration. (2015). *Annual coal report*. DOE/EIA-TR-20585. Washington, DC, April 2015.

Mark, C. (1990). *Pillar Design Methods for Longwall Mining*. Information Circular IC 9247. Washington, DC: U. S. Bureau of Mines.

Peng, S. S. (1992). *Surface Subsidence Engineering*. Morgantown Printer, 161 pag

Peng, S. S. (2006). *Longwall Mining*. Morgantown Printer, 2º ed, 621 pag

PENG, S.S. (2008). *Coal Mining Ground Control*. Morgantown Printer, 600 pag

Zingano, A. C., Carvalho, A., Cardozo, F. A. C. (2015). *Projeto de Lavra Subterrânea de Carvão, Jazida Triunfo: Fase de Pré-Viabilidade*. Luiz Englert Foundation's technical report, Porto Alegre. Unpublished.

IMPROVEMENTS IN SLOT RAISE OPENINGS IN CORREGO DO SITIO – I MINE

André Luiz de Almeida – Anglo Gold Ashanti
Daniel Lanna de Oliveira – Anglo Gold Ashanti
Carine Vaz Braga – Orica Mining Services
Victor Morais – Orica Mining Services
Fernando Martinez – Orica Mining Services

24th World Mining Congress
MINING IN A WORLD OF INNOVATION
October 18-21, 2016 • Rio de Janeiro /RJ • Brazil

ABSTRACT

This article presents the results of a study to increase advance in slot raise opening at Córrego do Sítio I mine, which was around 64%. The mining method is Sublevel Stoping in narrow veins, which constitutes in the opening of slot raises to create free in ore stopes. Enhancing the drilling and blasting parameters, utilizing hole deviation profile to define the firing sequence in addition to seismography and rock mechanical evaluation, it was possible to obtain advances averaging 98%.

Keywords: Slot raise, blasting, advance increasing.

INTRODUCTION

The generation of the initial free face is critical to determine the success of blasts in underground mines. In both cases, production or development, unlike the great majority of applications in open pit mines, the only free face in which the rock mass breaking process can occur is in the direction of the tunnel walls or galleries [1]. This is even more difficult when it is necessary to drill and blast upward holes, whether in the case of recovery of pillars, or the opening of stopes for ore extraction.

Successful slot raises openings for free face creation is critical to reduce the cost of the mine. Factors such as precision drilling, initiation sequence and explosive charge should be carefully designed for not result in partial or total failure of the blast, known as "freezing" [2], as occurred in some situations in the mine of study, especially in the "blind slots" openings. This operation is undoubtedly, the greatest risk activity and always presented the greatest challenge in the underground mine, both from the technological point of view as well as safety. These openings are called as blind precisely because they are not communicated with an upper level and therefore, restrict access only for the lower gallery [3].

Córrego do Sítio underground mine, owned by AngloGold Ashanti, is located in Santa Barbara, Minas Gerais and consists of three major body systems called Cachorro Bravo, Orange and Carvoaria. The mining method is Sublevel Stoping in narrow shafts, consisting in the opening of slot raises, followed by explosive loading, blasting and cleaning.

SITUATION

During the first months of 2015, some stopes in Córrego do Sítio mine were with unsatisfactory levels of underbreak and dilution, as shown in Figure 1.

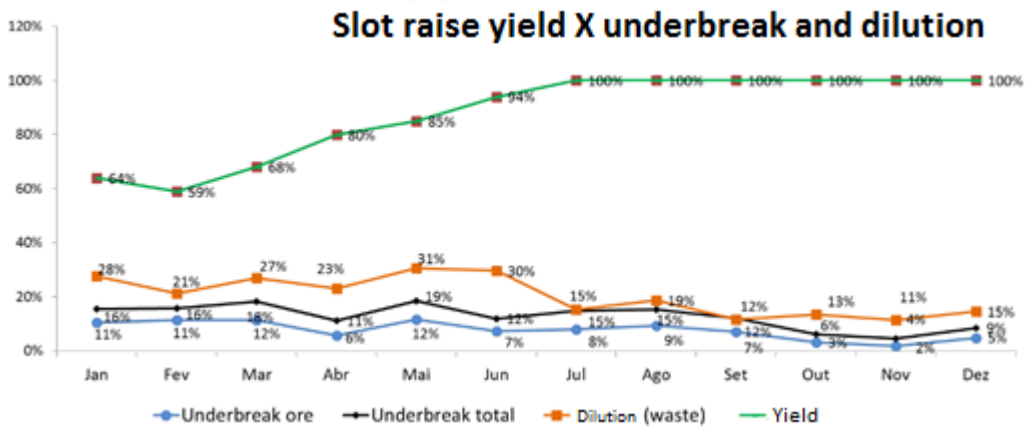

Figure 1 - *Underbreak* e dilution levels.

Among the reasons mapped as the root cause for high numbers of dilution and underbreak, the blind slot openings were appointed as a starting point for the study, since the yields were averaging 64% (Figure 2).

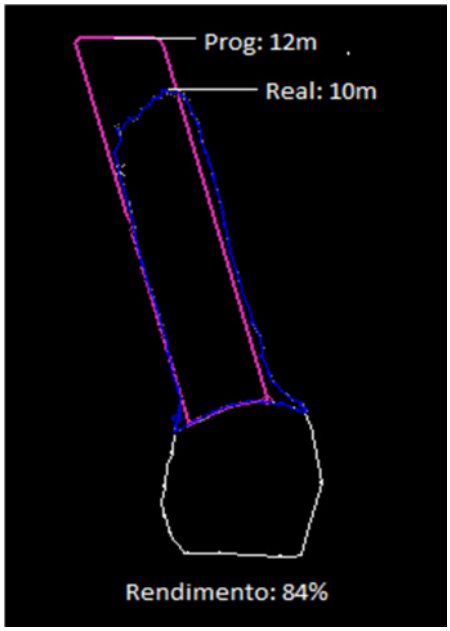

Figure 2 – Advance of slot raise opening.

As mentioned above, the initial process of free face opening has a preponderant role in the excavation's success. In this study, it was observed that due to the loss of free face and slot's yield lower than expected, this loss was propagated along the other production blasts, as shown in Figure 3.

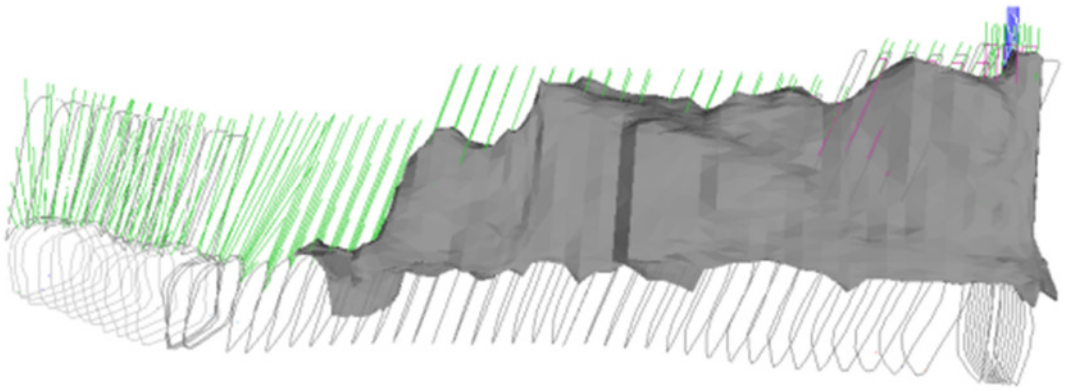

Figure 3 - Underbreak in the stope.

This situation represents a direct economic impact on the mine activities. To solve this problem, AngloGold Ashanti, in partnership with Orica Mining Services, has initiated studies to enable yield improvements in slots raise and thus reduce losses with under/overbreak.

Every month, are opened around 10 slots in Córrego do Sítio mine, distributed according to the mine planning. All drilling plans used had the same settings regardless of the type of solid, as described below:

- **Drill & Blast design (Figure 4):**
  - Slot raise: 2.4m x 2.4m
  - Large holes diameter: 5”
  - 05 large holes
  - Blasthole diameters: 2 ½” (64mm) ou 2 ¾” (70mm);
  - 16 blastholes
  - Total of holes: 21
  - Angle of holes: between 44 and 90º;
  - Iniatiation system: Exel™ SS;
  - Explosive Booster: 150g (Pentex™);
  - Package emulsion: Senatel™ Magnafrag (2 X 24’’ for 64mm blastholes, 1.1/4 X 16’’ for pneumatic cartridge loader and 2.1/4 X 24’’ for 70mm blastholes)

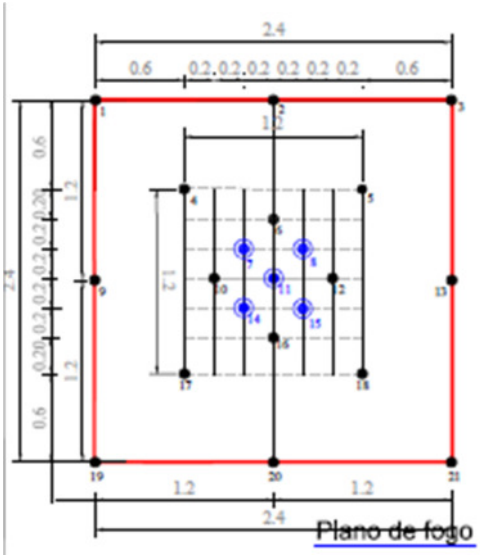

Figure 4 – Drilling design.

Moreover, it was not used the REFLEX®- EZ-AQ equipment drilling deviation control.

TECHNICAL SOLUTIONS

To achieve a yield above 95% and avoid generating underbreak, it was evaluated geomechanical features of all the lithologies based on frequency of fractures, rock mass classification and made the following recommendations:

- **Rock mass with fair/good quality, depth up to 20m (Figure 5):**
  - Slot raise: 2.5m x 2.5m
  - Large holes diameter: 6”
  - 06 large holes
  - Blastholes diameter: 2 ¾”
  - 16 blastholes
  - Total of holes: 22

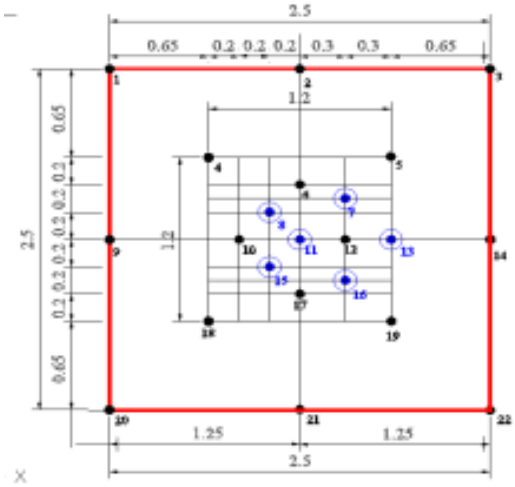

Figure 5 - Drilling plan recommendation for rock mass with fair/good quality (depth up to 20m).

- **Rock mass with poor/fair quality, depth up to 20m (Figure 6):**
  - Slot raise: 2.5m x 2.5m
  - Large holes diameter: 6”
  - 07 large holes
  - Blastholes diameter: 3”
  - 16 blastholes
  - Total of holes: 23

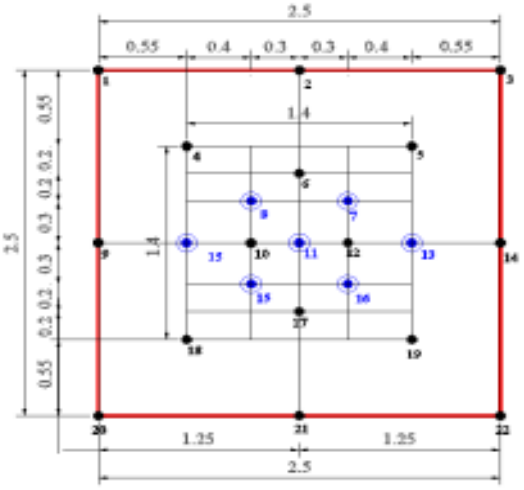

Figure 6 – Drilling plan recommendation for rock mass with poor/fair quality (depth up to 20m).

In addition to the drilling recommendations according to the rock mass quality, it was adopted a new procedure for the implementation of slots as highlighted:

- Use of REFLEX® for hole profiling, ensuring proper analysis of hole deviation for assertive definition of initiation sequence;
- Use of electronic detonator i-kon™ II, with greater delay time (up to 30.000ms);
- Use of 225g Booster (Pentex™);

- Double prime, one in the bottom hole and the second one in the half, ensuring the blasting of the entire explosive column in case of displacement of the rock mass or presence of fractures;
- Use of stemming;
- Seismography of all shots.

The use of electronic detonators (ikon™ II) provides, besides the great accuracy in shots, the application of delay times between holes that are not possible to achieve using pyrotechnic delays, and even with the most similar products on market. With the electronic initiation system ikon™ II is possible to program detonators with increments of 1 on 1 milli-seconds since 0 to 30000ms. This made this tool important to the success of this project, especially in deeper slots, as it was defined that the first four holes should have delays equivalent to 100 ms/m, allowing blasting and cleaning of holes. The remaining holes should have shorter times (50-75 ms/m) to prevent the effect of sympathy during the initiation. In some cases, the total initiation time could easily exceed 15,000ms, which is the limit value for most electronic detonators.

Changing the Booster 150g to 250g allowed generating higher detonation pressure in the bottom of the hole. The primers position should be different in adjacent holes to avoid the efect of dynamic pressure (Figure 7).

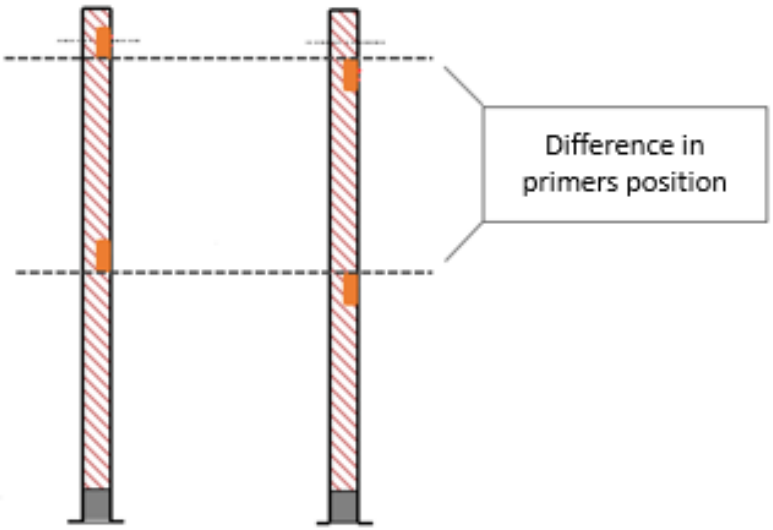

Figure 7 – Primers position.

After all suggested settings, adjustments have been made as each blast was carried out and according to the particularities of each one. As a procedure, it was adopted the diameter of 7" for large holes for all slots deeper than 9m (Figure 8).

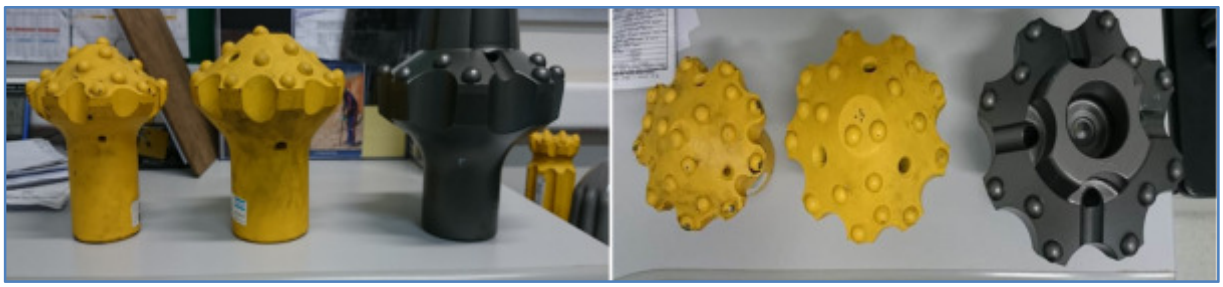

Figure 8 – New hole diameters adopted.

RESULTS

All recommendations and adjustments made in drilling and loading settings ensured yields averaging 98%, representing great benefits for subsequent activities. In addition of that, obtained a greater availability of drilling equipments to other demands of the mine, because there is no more rework for slots openings.

The profiling images below show the efficiency of techniques used and good results generated (Figures 9 and 10).

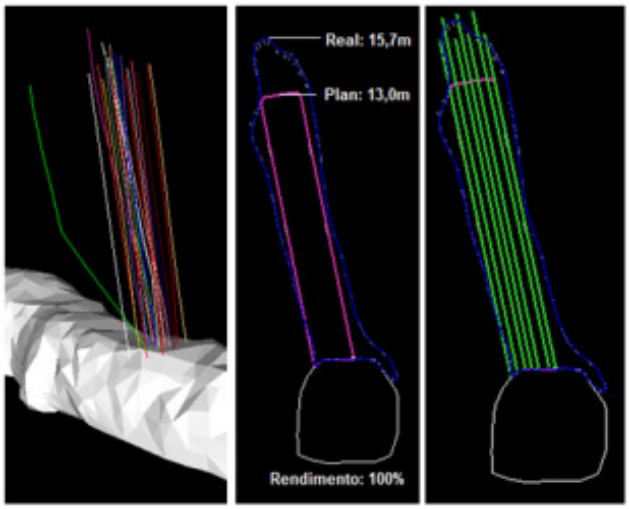

Figure 7 – Slot opening in CB 464/211 North, after adjustments in drilling and loading settings, yield of 100%.

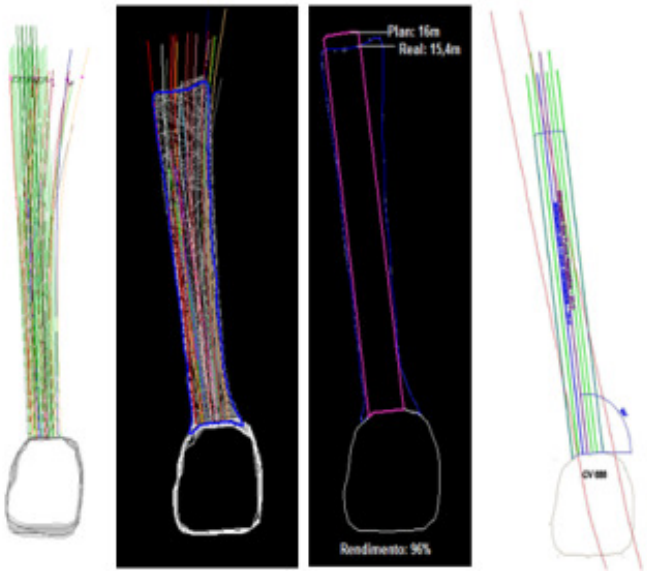

Figure 8 – Slot opening in CV 688/330 North, with yield of 96%.

CONCLUSIONS

Good results could be achieved through the implementation of new operational procedures and introduction of technology to opening slots such as:

- Audit of 100% of the holes with the use of REFLEX®.
- New loading and stemming settings.
- Implementation of new drilling designs according to the rock mass quality.
- Involvement of Geotechnical team to define the best local for slot drilling.
- Use of electronic detonators (ikon™ II), which allowed the use of greater delays.
- Slot opening in a single shot.

BIBLIOGRAPHIC REFERENCES

[1] PERSSON, P.; HOLMBERQ, R.; LEE, J. (1996), **Rock Blast and explosives engineering**, Editora CRS Press, p. 213.

[2] LIU, Q., TRAN, H. (1999), **Techniques of inverse drop raise blasting and slot drilling**, CIM Bulletin–Vol. 93, p. 45-50.

[3] SILVA, C. A. V., MOURA, J. C. B. (2008), **Nova técnica para abertura de chaminés "cegas" adotada nas minas subterrâneas da CIA. de Ferro Ligas da Bahia – FERBASA, Andorinha – BA**. Available in http://www.brasilminingsite.com.br/anexos/artigos/17_0.pdf. Accessed 25th January, 2016.

INCORPORATION OF HYDRO GEOLOGICAL ASPECTS AND OPERATIONAL CONSTRAINTS IN STRATEGIC MINING PLANNING

Marcélio Prado Fontes[1], Rodrigo de Lemos Peroni[2] and Luciano Nunes Capponi[3]

[1]*Centro Federal de Educação Tecnológica de Minas Gerais - CEFET/MG*

[2]*Federal University of Rio Grande do Sul - UFRGS*
*(*Corresponding author: peroni@ufrgs.br)*

[3]*Vale Fertilizantes S.A.*

24th World Mining Congress
MINING IN A WORLD OF INNOVATION
October 18-21, 2016 • Rio de Janeiro /RJ • Brazil

INCORPORATION OF HYDRO GEOLOGICAL ASPECTS AND OPERATIONAL CONSTRAINTS IN STRATEGIC MINING PLANNING

ABSTRACT

Developing mine sequencing involves many factors and a large amount of information, consequently the profitability of the project will strongly depend on the production schedule. A mining project may be conditioned to non-optimal sequencing, which may affect the economic results of the project and also lead to an inadequate utilization of mineral resources. During the mine sequencing it is necessary to make decisions for each block during extraction, such as: 1) whether or not a particular block should mined; 2) If mined, when it should be extracted; 3) Once extracted, how and when it should be processed. These decisions define the annual cash flow of a given project and the number of periods that the mine will be operated, impacting the project´s net present value (NPV). The decision of how many blocks should be extracted in a given period and how they should be processed not only defines the cash flow for a particular year, but also impacts on future schedules. Normally, the final pit limit is optimized for a fixed set of parameters (price, costs, resource model, etc.), knowing that changes in these parameters will have impact on the life of mine plan. Uncertainties (as grades, stripping ratio, market, groundwater level, etc.) are included only as a post-analysis of variability and sensitivity of the results of the abovementioned factors. The conventional method of sequencing a mine is divided into three main steps: First the delineation of the final pit; second, subdividing the final pit in operational pushbacks and third, sequencing blocks in each of these pushbacks, taking into consideration the mine, processing plant and market capacities. However, there are some aspects that are not necessarily incorporated into the conventional mining system, including mining ore below the water table. This aspect imposes some vertical mining advancement constraints that must be considered. The objective of this study is to demonstrate the relevance and impact on the NPV result from the groundwater as a constraint related to the need for water table drawdown, also considering grades and stripping ratio (SR) variability during the mining sequence for a phosphate mine. The methodology adopted considers adjustments when determining each pushback within the limit of the final pit, trying to respect the constraints and pursuing global profitability as the main goal of the optimization process.

KEYWORDS

Sequencing, Constraints, Groundwater Level, NPV

INTRODUCTION

Mine planning aims for the rational use of mineral deposits and project´s profitability involving the application of a set of techniques for decision-making and the selection of the best alternatives for the life of the mine, whose goal is to achieve the best production sequence. Like any other project, mining industry has the basic economic objective of maximizing its future wealth. However, it is characterized by targeting the economic use of an exhaustible, non-renewable capital good, which differentiates it from other industries. So, the maximization of future wealth should be carried out in a defined period, i.e. during the existence of the mineral reserve. In economic terms, it can be more appropriately expressed as follows: the purpose of the mining industry is to maximize the net present value (NPV) of future cash benefits throughout mine life (COSTA, 1979).

Mineral deposits have their formation dictated by natural laws which present several challenges and conflicts that should be better investigated to comply with the needs of the mining enterprise. The distribution of variables representing the quality of minerals such as grain size, grade, groundwater level and amount of waste to be removed hinder or even make the economic exploitation of a mineral deposit impossible. Problems can occur in non-planned mining, such as ore exploitation

with an average grade above the necessary, irreparably impoverishing the remaining reserve; prematurely exhaust the mine due to the removal of overburden poorly planned or immediate mining without taking into account the future of the ore availability. Another increasingly common constraint in mining operations is the control of groundwater level due to the increasingly deepening of the pit bottom which prevents mine operations in some sectors or even in the whole mine for a certain period of time.

Mine planning allows to anticipate the occurrence of problems which can be avoided in the future or, when it is not possible, at least minimize its consequences. As it is an anticipated simulation of the mining routine, this planning permits to know *a priori* the possibility of controlling quality variables, evaluate groundwater level behavior over time and the best use and allocation of mining equipment. Moreover, it enables to establish the schedule of waste generation/disposal and / or tailings, providing subsidies for better use of the mineral resource, seeking to minimize environmental impact.

Production scheduling must meet the evolution of environmental needs, the challenges offered by this development and related aspects such as: changes in government policies; changes in technology; changes in the global economic situation, including prices, workforce and raw materials; changes in the nature of competition: changes in social life and activities; drastic changes in the political situation of the region. Therefore, mining sequencing must carefully consider economic, social, environmental, political and technological factors. However, it is essential to take into account possible constraints so as not to jeopardize the viability of the enterprise.

OBJECTIVE

This paper aims at evaluating the impacts of possible constraints, especially water level, on the grade of oscillations and stripping ratio. These impacts are analyzed based on the results of NPV obtained in each mine sequencing.

METHODOLOGY

Considering mine sequencing is essential to the success of a mining entrepreneurship, the methodology used in this study focused on maximizing the financial return for the mining business, especially in the early years of mine operation. Therefore, the delineation of the final pit involves some crucial steps such as: a representative block model, well-adjusted profit function, a consistent cut-off grade with the available mineral reserves and technology. Following with the mine sequencing requires some additional input data, such as current topography; production rates and possible constraints which in this study were the following: the search of ore providing stability in the average grade fed to the process; the search for stability in SR; the vertical feed control considering the level of the groundwater level; environmental limit of pit depth; mining leases.

According to Osanloo, Gholamnejad & Karimi (2008) mining sequencing begins with the determination of production capacity, based on mine operational capacity, the estimates for operating costs and commodity prices. Then, using block model and economic evaluation of each block, an algorithm analysis of the positive blocks as well as of the overlying waste units in order of precedence is made to check if its extraction is economically justifiable. This analysis is based on cutoff grade which checks if the undiscounted profit obtained from a given ore block can pay the undiscounted cost to remove the waste blocks in its precedence. The final pit is then determined using an optimization algorithm in order to maximize the undiscounted cash flow. Within the final pit, stages are designed so that the reserve is divided into multiple nested pits. These procedures are a parameterization using revenue or cost factors to generate smaller pits, for example, from lower revenue per ton of ore, and move to higher pits with higher revenue per ton of ore. Subsequently, operational constraints are imposed to generate the so-called operational advances also known as *pushbacks* which are mining advance stages to reach the final pit and are used as guidelines during the annual production schedule planning. Before determining the extraction sequence, cut-off grade should be set in order to differentiate ore and waste allowing the production plans elaboration.

According to Dagdelen (2001), there are a number of sophisticated software packages in the mining industry which outline the final pit, perform analysis, do pushbacks design and determine mining annual plans. However, it is important to highlight that not all of these steps may be optimized

by a single program due to large changes in mathematical scale. The most common approach to this problem is dividing it into sub-problems similar to those shown in Figure 1.

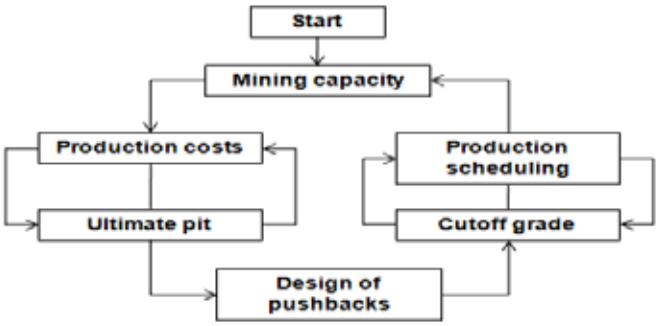

Figure 1 - Steps of traditional planning by circular analysis. Source: Dagdelen (2001).

The main point used to develop the methodology was determining and ranking the most relevant constraints after measuring the project outcome using the NPV. The structure of the methodology proposed in this paper can be seen in Figure 2. The following steps were taken: first, the determination of input block model; second, final pit definition; third, pushbacks were designed primarily with the maintenance of default input parameters suggested by the sequencing software; fourth, NPV was assessed considering only the processing plant capacity; fifth, some mining scenarios were simulated imposing constraints such as ore grade and stripping ratio both individually and later on simultaneously; sixth, the procedure was repeated by changing the number of pushbacks, starting again from pushbacks design. The new sequencing scenarios were simulated from the following number of pushbacks: 3, 5, 7, 10, 12, 15, 17, 20, 22, 25 and 100. For each of those scenarios, evaluation and comparison of NPV were carried out.

At last, groundwater level was added to establish a new final pit provided that water level elevation, given by a drawdown model at the end of mine life, overlies the original final pit bottom. Thus, the analysis considering this constraint initiated with a new ultimate pit scenario generated between the intersection of the prior pit limit and the water table. Finally, the alternatives were compared not only in terms of NPV, but also average grades fed to the plant and stripping ratio for the first 10 years of mine sequencing.

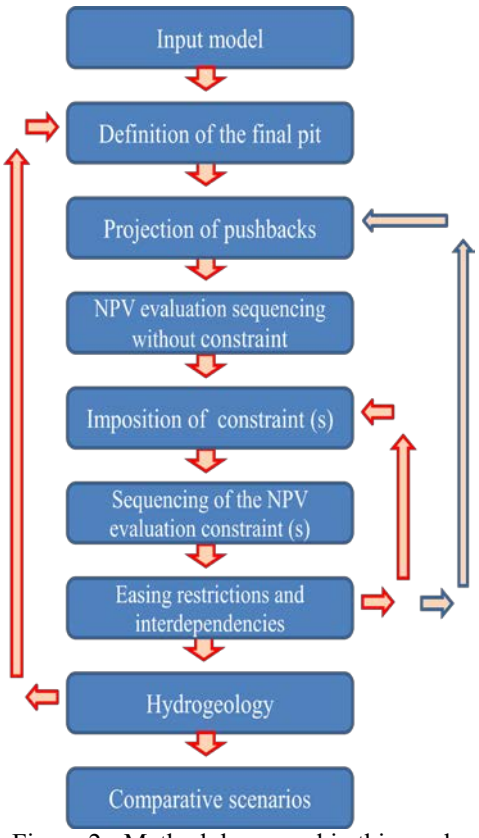

Figure 2 - Methodology used in this work.

CASE STUDY

To illustrate the methodology, a case study in a phosphate deposit located in Araxá Minas Gerais southeastern Brazil was carried out. The phosphate deposit belongs to Barreiro carbonatite complex, named F4, was designed to feed plant II in the Complex with capacity to process around 3.2 million tonnes per year. A reconstruction of the original topography of the mine within the leasing limit granted to Vale Fertilizantes was necessary. Leasing limit is a physical polygon which neither final pit nor mining operations can exceed in any mining scenarios. Figure 3 shows the topography and leasing limit.

The block model has the following dimensions: 25m x 25m x 10m (**x**, **y,** and **z,** respectively) containing 6 typologies: #1 undefined, #2 oxidized ore, #3 cemented ore, # 4 friable silica-carbonated ore, #5 hard silica-carbonated mineral rock and #6 waste. Ore consists of grouping types 2 and 3 and waste by the conjunction of the other types.

The surface drainage is calculated considering the average monthly runoff comprised by part of the total amount of rainfall in the entire area of the natural contribution area, where the mine pit is inserted, plus the runoff from the mining area of the adjacent company which flows into the pit of F4 mine. Considering historical precipitation, a minimum of 372 m^3/hour water pumping capacity is needed, reaching the flow rate of up to 1.231 m^3/hour during the rainy season. However, taking into account the maximum historical 30-year monthly precipitation, the water flow can reach rates ranging from 1.105 to 2.532 m^3/hour up to the exhaustion of the mine. In order to avoid very high flows, in the pit, a peripheral channel drain located next to crest of the final pit is usually suggested, to contain the water income from the external portion of the natural drainage area, reducing the volumes to be pumped out from the pit bottom.

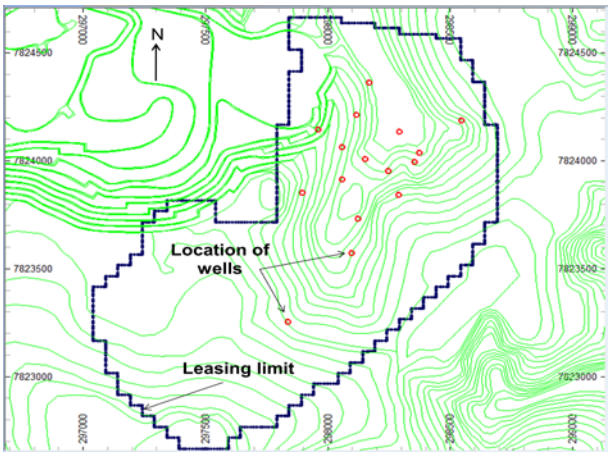

Figure 3 - F4 mine original topography as per September 2009 showing drawdown wells in red and leasing limit in dark blue.

To simulate the water level during the mine life, a numerical model of transitional arrangements was developed and calibrated for simulating groundwater level drawdown. The purpose of this process is to measure and assess the impact of drainage structures and also to guarantee the water level below pit bottom and thus quantify pumping flow rates needs and possible drawdown impacts. This type of simulation is useful to determine minimum pumping requirements during the mine advancement and also estimate the number of minimal wells and its location to achieve drawdown. The best and also more realistic scenario consists of the combination of drawdown wells with dewatering channels in the lower levels of the pit directing the runoff towards a sump located at the bottom pit where the water it is pumped out from the pit. This method is advantageous because it considerably reduces the number of required wells, although it creates operational difficulties. Figure 3 shows the location for the wells of the first 10 years of mine operation. Another important issue taken into account in this study was the environmental pit bottom limit. F4 mine is located besides Barreiro Hydro mineral Resort where there are several natural fountains. Therefore, the pit bottom cannot deepen below 980m elevation, as lowering the water level beyond this limit can interfere with the fountains flow rate.

Finally, based on the above listed data and profit function calculation (assumption made for mining and process costs, commodity price and process recovery), provided by the company and kept confidential by request, mining sequencing was carried out. The first step was to import the block model and select the working variables, in this case P_2O_5 (phosphate grade). In the subsequent step, the economic model was generated consisting of a grade block model and the economic value for each block.

Within the pit limit, the pushbacks must be sequenced according to annual ore demand respecting the available budget. This is an important step during mine planning to optimize NPV for each scenario considered. Therefore, it is also essential to manage parameters such as: average ore grade consistent with the available technology in the processing plant; waste tonnes to be removed per year; and groundwater level inside the mining areas. One alternative to control these variables in mine sequencing is to adjust pushbacks according to the variation of such constraints. After the adjustment of pushbacks, it is possible to program the sequence of annual exploitation. In this case study the first 10 years of mine operation were analyzed, due to the availability of hydro geological model information.

RESULTS ANALYSIS

Final Pit

The final pit limit represents a boundary in which ore mass and the associated amount of waste can be profitably mined, according to predefined parameters. The economic value of final pit and its respective limit are used as benchmark to compare with the later stages of sequencing, the values found in the final pit base case were 78.3 Mt of phosphate ore with a stripping ratio of 2.87 (t/t).

When the groundwater level was considered as a constraint in sequencing, it was necessary to establish a new final pit shell, since the water table surface was overlying the original final pit bottom in some places. This "new" pit bottom considered the results of the numerical model simulating the groundwater level drawdown, which was based on the number and the flow rates estimated for each drawdown well. The output surface became now the intersection between the original final pit bottom and the simulated water table. The result of the new final pit was 51.0 million tonnes of ore with 4.20 (t/t) SR.

Mining Sequencing

After importing all the data and followed all the steps described in the methodology, it is possible to choose the number of pushbacks to work with. Provided that this is an important step in mining sequencing and that the ideal value to be used is not known, a number of scenarios were simulated in order to find out the optimal number of pushbacks. Thus, the scenarios were simulated with the following number of pushbacks: 3, 5, 7, 10, 12, 15, 17, 20, 22, 25 and 100.

Mining Sequencing Without Constraints

Before start imposing constraints in mine sequencing (grade, SR and groundwater level), it is important to assess the NPV of the project to define a reference for comparison. Afterwards, mine sequencing without a constraint was performed, but controlling the ore mass to feed the processing plant. The results can be seen on the blue curve in Figure 4. All scenarios were simulated with the same software parameters, changing only the number of pushbacks. As it can be seen, when the number of pushbacks is greater than or equal to 15 and less than 25, the mine sequencing NPV reaches US$ 690 million. Considering groundwater level, when the number of pushbacks is greater than or equal to 10, the NPV of the mining sequencing varies between US$ 500 and US$ 550 million as shown by the red curve in Figure 4.

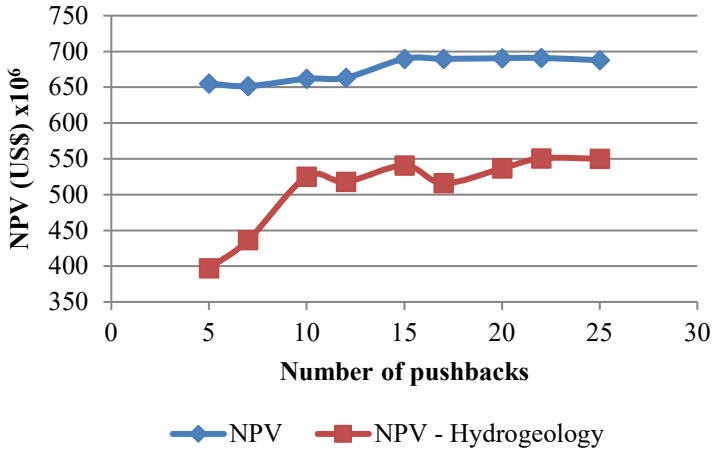

Figure 4 - Comparison of sequencing with and without hydrogeology constraints.

Mining Sequencing Considering The Grade Constraint

Normally, all treatment plants require a minimum grade so that metallurgical and mass recoveries are kept approximately stable. Figure 5 shows the results obtained from sequencing considering the average P_2O_5 grade of 11.5% with variations of ± 1%, as shown in the blue curve, the NPV varies according the number of pushbacks selected. Therefore, the highest NPV found for sequencing was using 22 pushbacks (US$ 536 million). Considering the same parameters when sequencing with water level constraint, requested pushbacks ranging from 10 to 17 obtained a level close to US$ 500 million, as it can be seen in red. But with 25 pushbacks, the highest NPV of US$ 520 million was reached according to Figure 5.

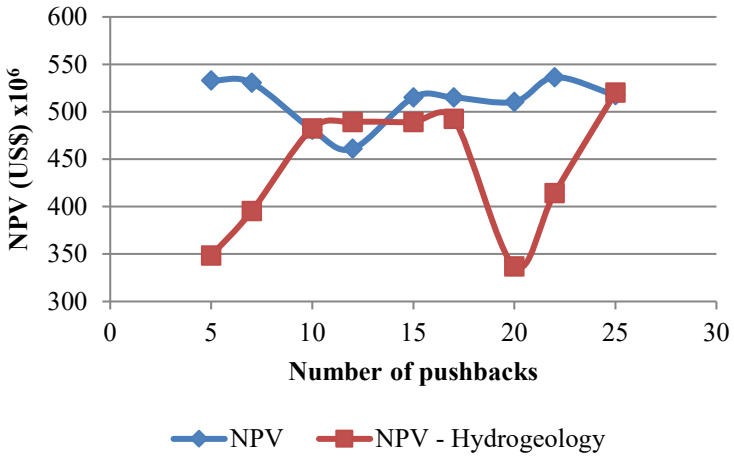

Figure 5 - Comparison of sequencing with and without hydrogeology considering P_2O_5 grade as constraint.

Mining Sequencing Considering SR As A Constraint

The waste mass to be removed can severely affect a mining project. Minimizing, stabilizing and if possible delaying the waste quantities to be moved over the years in a mining operation maximizes NPV. Figure 6 shows the result of sequencing considering SR as a constraint. It is evident that there is a tendency: the higher the number of pushbacks, the higher the NPV after sequencing. The highest NPV (US$ 643 million) was obtained when sequencing the 20 pushbacks scenario as demonstrated in the blue line. Due to the fact that the final pit, considering hydro geological constraints have less ore than the original final pit, the reduction of waste amount is not proportional to the decrease in ore amount, i.e., the increase of SR from 2.87 to 4.20 makes this aspect extremely important for the profitability of the enterprise. Figure 6 shows the behavior of SR in red after mine sequencing according to the number of simulated pushbacks. It can be observed that sequencing using 12 pushbacks provides the highest NPV (US$ 508 million).

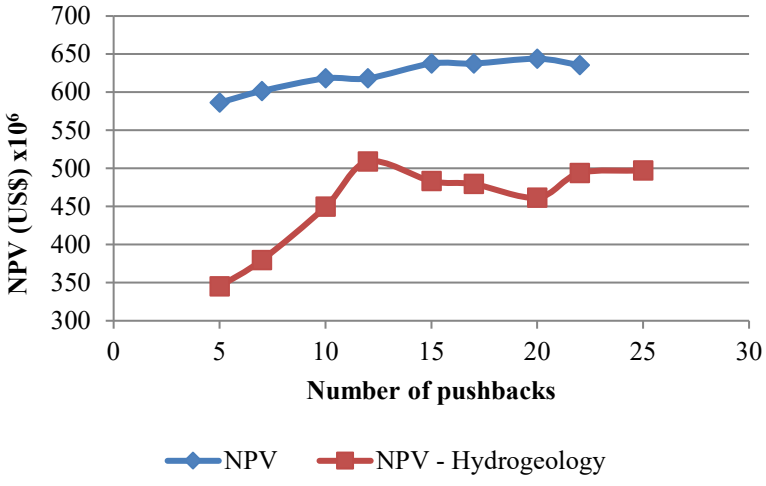

Figure 6 - Comparison of sequencing with and without hydrogeology considering SR as constraint.

Mine Sequencing Considering Grade And SR As Constraints

Mine sequencing considering grade and SR as constraints was also carried out, it is important to highlight that there is an interdependence between these two variables. By analyzing the blue curve in Figure 7 it can be noticed that, from 12 to 20 pushbacks requested, the NPV of the mine sequencing stabilizes at around US$ 600 million. Mine sequencing for 20 pushbacks achieves the highest NPV

(US$ 603 million), considering both grade and SR constraints. In an attempt to stabilize SR at a value closer to final pit SR and to obtain an average grade more consistent with the production target, NPV sequencing decreased about US$ 40 million compared to the NPV sequencing considering only SR.

Mine sequencing should be as close to the reality of mining operations as possible. Which means, a schedule that does not take into consideration all available information, like limitations in the daily mining operations, entails non-compliance with the annual plan. Hence, if the annual plan is not fully implemented, the whole mine sequencing in the following years will be compromised. The red curve in Figure 7 shows the NPV sequencing behavior considering hydrogeology, it can be observed, again, that the sequencing using 12 pushbacks provides the highest NPV (US$ 507 million).

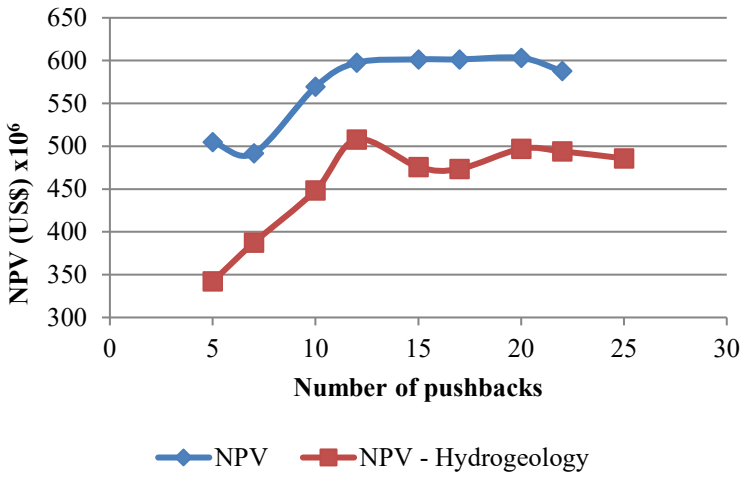

Figure 7 - Comparison of sequencing with and without hydrogeology considering ore grade and SR.

Table 1 shows a comparison of NPV for the first 10 years of the mine sequencing, without considering hydrogeology, highlighted columns (no hydro), for grade and SR (20 pushbacks); and the first 10 years of sequencing, with the same parameters, considering hydrogeology (12 pushbacks), represented in the non-highlighted columns (hydro). Although sequencing have different constraints, the NPV results, ore grade and SR at the end of 10 years are very close, indicating that the sequencing with hydrogeology was well executed. Thus, mining operation conditions are more favorable without water upwelling i.e. sequencing considering hydrology.

Figure 8 illustrates a comparison of mathematical pits in years: 1, 3, 5, and 10 for sequencing with grade and SR constraints, with and without considering hydrogeology as well as the locations of the drawdown wells planned in the simulation of the hydro geological model. The intersection of these surfaces with the groundwater level wireframe is shown in blue. This groundwater level wireframe comes from the quantity and flow of the drawdown wells. It is important to emphasize that both location and number of wells may change over time, depending on the actual pumping rates obtained. As for the bottom pit, it is evident that the pits, considering hydrogeology, have a wider area where the pumping sump can be placed.

Table 1 - Comparison of NPV results in the first ten years of sequencing with and without hydrology considering ore grade and SR as constraints.

Year	NPV (US$ x 10^6)		P_2O_5 (%)		Waste (t x 10^6)		Stripping Ratio (t/t)	
	Nohydro	Hydro	Nohydro	Hydro	Nohydro	Hydro	Nohydro	Hydro
1	0.43	63.09	12.54	12.67	30.13	11.19	9.38	3.48
2	87.83	53.54	12.53	12.19	0.49	10.51	0.15	3.29
3	63.40	61.46	12.61	13.11	7.25	9.88	2.27	3.09
4	50.93	59.20	12.51	13.70	8.78	10.88	2.74	3.40

5	51.61	47.24	13.08	12.97	9.45	10.84	2.95	3.39
6	45.45	44.86	13.08	13.15	9.65	10.21	3.02	3.19
7	42.20	35.28	13.12	12.57	9.55	10.94	2.98	3.42
8	34.51	30.48	12.59	12.23	9.09	10.70	2.84	3.34
9	29.31	27.45	12.42	12.33	9.60	10.99	3.00	3.43
10	32.38	16.24	13.19	11.01	9.41	11.11	2.94	3.47
TOTAL	**438.05**	**438.84**	**12.77**	**12.59**	**103.39**	**107.24**	**3.23**	**3.35**

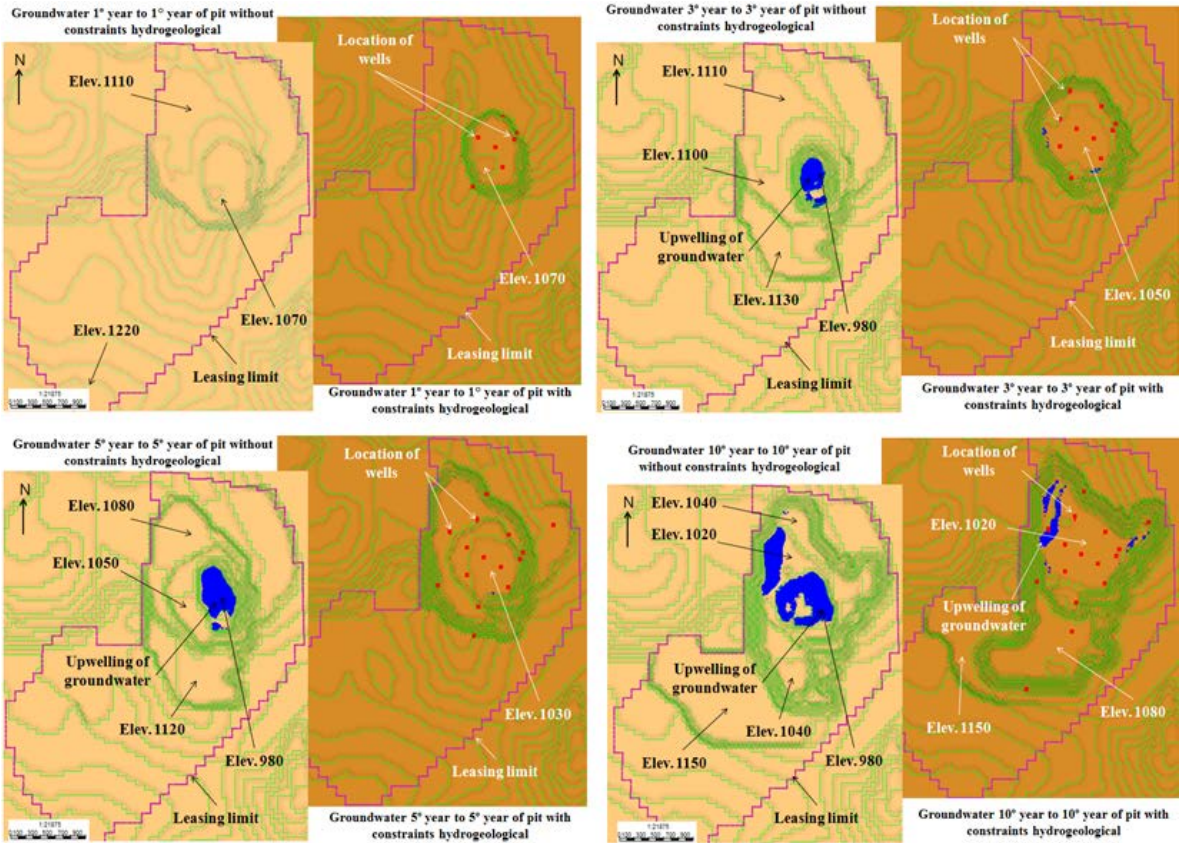

Figure 8 – Comparison of sequencing considering ore grade and SR constraints with and without hydrogeology in years 1, 3, 5 and 10

CONCLUSIONS

Mine sequencing is the core of mining planning allowing a strategic view of pits evolution over time. The constraints and their stabilization attempts have great influence on the pit geometry and hence a huge impact on the project´s NPV. Proper knowledge of the deposit and mining operation is required in the preparation of the production sequence, as fail to comply with the annual plan affects not only the current plan, but also throughout the established mining sequencing. As demonstrated in sequencing without regard to hydrogeology, the final pit has 78.3 million tonnes of phosphate ore and SR 2.87 (t/t). When sequencing without considering ore grade and SR constraints, but taking into account the annual mass fed to the processing plant, the highest NPV was US$ 690.9 million; by considering ore grade constraint, NPV was US$ 536 million. Both values were obtained in the simulation with 22 pushbacks. When SR was taken into account, the highest NPV obtained was US$

643 million with 20 pushbacks. In turn, considering both constraints, the highest NPV was US$ 603 million. Therefore, it is evident that there is an interdependence between these two variables.

In the sequencing considering hydrogeology, the final pit was rebuilt reducing it to 51.0 million tonnes of ore and increasing the SR to 4.20 (t/t). In the mine sequencing considering the annual mass of the processing plant, but without considering ore grade and SR constraints, NPV was US$ 500 million, in the simulation with 22 pushbacks. For the production schedule with the ore grade constraint, the highest NPV was US$ 520 million, with 25 pushbacks. The sequencing considering SR, the highest NPV was US$ 508 million with 12 pushbacks. Taking both constraints, ore grade and SR into consideration, the highest NPV, US$ 507 million, occurred with 12 pushbacks. Again, the interdependence between ore grade and SR constraints is evident. Due to the large impact of groundwater level on the project NPV´s, regardless the number of considered constraints, a new simulation study considering the inclusion of drawdown wells is justifiable. As a result, it may be necessary to set up a project to measure the environmental impacts in F4 mine region, which may lead to an additional request to extend the current groundwater pumping permit provided by state the environmental agency.

In order to demonstrate the accuracy of mine sequencing, considering hydrogeology, a comparison of the first 10 years of the production plan was made comparing to the sequencing without considering groundwater level. For this comparison, SR and ore grade were considered, as demonstrated in Table 1. The results are very similar as maximum variation of 4% occurred for: NPV, grade, waste and SR parameters. Although, it is important to say that the NPV results obtained are something that can be visually differentiated, presenting completely different mine sequences. Therefore, we can conclude that the groundwater level constraint (hydrogeology) for the first 10 years of sequencing is much more a matter of mining operations management and fulfillment of annual plans than financial. However, the operation of the mine is facilitated as far as water upwelling is concerned, considering the sequencing with hydrogeology.

REFERENCES

COSTA, R. R. (1979) **Projeto de mineração [Mining Project]**. 1 ed. Ouro Preto: Universidade Federal de Ouro Preto, Ouro Preto. v. 1, 286p. Apostila.

DAGDELEN, K. (2001) Open Pit Optimization - Strategies for Improving Economics of Mining Projects Through Mine Planning. In: INTERNATIONAL MINING CONGRESS AND EXHIBITION OF TURKEY, 17., 2001, Ankara. **Proceedings IMCET 2001**. Ankara: The Chamber of Mining Engineers of Turkey. p. 117-122.

OSANLOO, M., GHOLAMNEJAD, J., & KARIMI, B. (2008) Long-term open pit mine production planning: a review of models and algorithms. **International Journal of Mining, Reclamation and Environment**, v. 22, n. 1, p. 3 - 35, mar.

INTEGRATION OF AN EMPIRICAL APPROACH FOR EVALUATING THE DILUTION IN THE DESIGN OF OPEN STOPES IN DEEP MINES

*J. Robert Martel, M. Laflamme and S. Planeta

Université Laval

2325 Rue de l'Université

Québec (Québec), Canada G1V 0A6

24th World Mining Congress
MINING IN A WORLD OF INNOVATION
October 18-21, 2016 • Rio de Janeiro /RJ • Brazil

INTEGRATION OF AN EMPIRICAL APPROACH FOR EVALUATING THE DILUTION IN THE DESIGN OF OPEN STOPES IN DEEP MINES

ABSTRACT

Since the eighties, Canadian mining engineers have relied on Stability Graphs to design open stopes. Today, mines like Agnico Eagle LaRonde that extract ore using open stope mining methods at depths of 3,000 meters and greater, demonstrate that empirical methods have reached the limits of their databases. This paper discusses the principal limitations affecting the existing open stope design methods and proposes an updated version of the ELOS Stability Graph based on the results of an open stope performance study at the LaRonde mine, overcoming some of these limitations. The study is based on planning and extraction data of 1,083 stopes mined at depths ranging from 860 meters to 2,450 meters over a period of 10 years. Numerical modelling and statistical analysis of the data demonstrates a significant impact of stress ratio variation with depth on ore dilution in open stopes. These analyses led to the introduction of a new correction factor that accounts for this effect and allowed for the development of an ELOS estimation model inspired from Clark's (1998) RMR-based ELOS Stability Graph. The paper also presents how the integration of this model in a mineral reserve estimation methodology introduced by Planeta et al. (2013) can provide a powerful tool when planning and designing open stopes in deep mining.

KEYWORDS

Open stope, Dilution, Stability Graph, Estimation, Planning, Design

INTRODUCTION

The first mention of deep mining in Canada dates back to 1905, when the province of Nova Scotia passed the Deep Mines Act, through which financial assistance could be made available to mine operators wanting to deepen shafts beyond 150 meters (Udd, 2006). Nowadays, Canada is host to one of the deepest mines in the world, LaRonde, which uses open stope mining methods to depths beyond 3,000 meters. Mining at such depth implies working in a significantly challenging environment with extreme temperatures and rock stresses. More research is needed to optimise mining operations confronted with these conditions.

Starting in the 1970s, Canadian mining began favoring low-cost bulk mining methods, such as open stoping, over high-cost selective mining methods (Udd, 2006). The adoption of this new method was made possible by technological advances driven by productivity and health and safety benefits. However, the growth in popularity of open stope methods combined with the lack of appropriate design tools resulted in poor mining performance. Statistics from a 1986 Canadian mine survey revealed that 47% of open stopes mines had more than 20% dilution while 21% of mines had more than 35% dilution (R. T. Pakalnis, 1986). This situation prompted the creation and development of open stope design tools such as the Stability Graph, originally introduced by Mathews et al. in 1981, and the Dilution-Based Open Stope Empirical Design Method, presented by Pakalnis in 1986. These methods and the work done to improve stope design have helped solve problems faced by industry at that time (F.T. Suorineni, 2014). As a result, an investigation of the Canadian mining practices published in 1995, showed that 90% of ore extracted from underground mines was mined from open stopes (Potvin & Hadjigeorgiou, 2001).

Today, solutions developed by our predecessors seem to have reached their limits as mines continue to go deeper (F. T. Suorineni, Hebblewhite, & Saydam, 2014). This paper discusses the principal limitations affecting the existing open stope design methods and proposes an updated version of the ELOS Stability Graph based on the results of an open stope performance study at the LaRonde mine that overcomes some of these limitations.

CURRENT OPEN STOPE DESIGN METHODS AND LIMITATIONS

The stability of underground openings can be assessed by one or a combination of three different approaches: analytical methods, empirical methods, or numerical modelling. Based on the available literature, empirical and numerical design methods are more commonly used than analytical methods which require an oversimplification of the openings' parameters (Capes, 2009). In the last decades, advancements in numerical modelling have made this approach an unavoidable tool for the industry. However, the constitutive models that underlie numerical models cannot fully account for the complexity of the rock mass and therefore usually have to be calibrated against field observations for their predictions to be close to reality (F. T. Suorineni et al., 2014). Over the past three decades, empirical stope design techniques based on knowledge, observations, and judgment have proven to be effective tools that provide a means of overcoming the complex nature of the rock mass and the associated difficulties in defining its constitutive behavior (Capes, 2009; F.T. Suorineni, 2014). Despite any inherent weaknesses of numerical and empirical design methods, most authors seem to agree that the best results are obtained when both approaches are combined.

The most widely discussed empirical method is the Stability Graph method, originally developed by Mathews et al. (1981), and modified by others including Potvin (1988), Nickson (1992), Clark (1998), Suorineni (1998), and Mawdesley et al. (2001). The Stability Graph method is based on the relationship between the stope wall geometry, the rock mass quality, and the loading conditions. The wall geometry is represented by the hydraulic radius (HR) which is the ratio of its area to its perimeter. The rock mass quality and loading conditions are accounted for by the modified stability number (N') which is the product of four factors as follows:

$$N' = Q' \times A \times B \times C \quad (1)$$

Where:

Q' = Modified Tunneling Quality Index (NGI) with Jw/SRF set to 1 (Barton, Lien, & Lunde, 1974)

A = Stress Factor

B = Joint Orientation Factor

C = Gravity Factor

Although a majority of authors agree that the Stability Graph method accounts for the most significant factors influencing stope stability, many have discussed its limitations and proposed improvements (F.T. Suorineni, 2010). The limitations commonly identified are:

- The application of the method is limited to cases that are similar to those in the developmental databases (Capes, 2009; Henning, 2007; F.T. Suorineni, 2010, 2014);
- The Stress Factor A does not account for instability caused by relaxation (Capes, 2009; Clark, 1998; Henning, 2007; Mitri, Hughes, & Zhang, 2011; F.T. Suorineni, 2010; Wang, 2004);
- That it does not address factors such as undercutting of stope walls, drilling, blasting, fault, and time (Capes, 2009; Clark, 1998; Henning, 2007; Wang, 2004);
- That stope width is not taken into account and that the qualitative descriptions of stope stability only provide a very rough estimate of unplanned dilution (Clark, 1998; Papaioanou & Suorineni, 2015; F.T. Suorineni, 2010; Wang, 2004).

The different Stability Graphs and additional factors resulting from the proposed improvements are usually site specific (Capes, 2009; Henning, 2007; Wang, 2004), and the tendency for authors to arbitrarily choose between the original and modified stability number factors results in incomparable data that cannot be combined (F. T. Suorineni et al., 2014). Therefore, it is difficult to merge the data already collected into a larger database that could cover a broader range of cases and allow for the calibration of additional factors suggested, accounting for the effects of undercutting of stope walls, fault, and time.

Quantitative methods have been proposed to refine the estimation of unplanned dilution. In 1986, Pakalnis developed the Dilution-Based Open Stope Empirical Design Method from observations collected at the Ruttan mine. The method was an attempt to quantify dilution in different mining scenarios by relations based on Bieniawski's rock mass rating (RMR), exposure rate, and stope hanging-wall area (R. T. Pakalnis, 1986). Although this method had the advantage of indirectly accounting for time and stress through the consideration of exposure rate (Capes, 2009), its main limitation came from the direct use of dilution percentage to express unplanned dilution. Because the dilution percentage is related to stope dimensions (Planeta, 2001), the choice of this value limits the use of the method only to orebodies with thicknesses similar to Ruttan mine's.

In 1998, Clark introduced a new parameter termed ELOS (equivalent linear overbreak/slough) and incorporated it into design charts as a measurement of unplanned dilution. Clark (1998) presented a version of the ELOS Stability Graph based on the relationship between HR and N', but he also pointed out that there was very little precedence for using a Stress Factor A value other than 1. In the Potvin (1988) database, all but one of the 106 hanging-walls and foot-walls were assigned an A value of 1, the other was assigned a value of 0.9. Similarly, the Joint Orientation Factor B was assigned a constant value of 0.3 for all the observations in the database due to parallel jointing (Clark, 1998). Based on this, Clark (1998) concluded that only a gravity factor was required to develop an RMR based stability number approximately equivalent to N' and presented another version of the ELOS Stability Graph based on a relationship between HR and RMR', where the RMR value for the foot-wall is unchanged and the adjusted RMR value for the hanging-wall is calculated as follows:

$$\mathrm{RMR'} = \mathrm{RMR} \times (1 - 0.4\cos\theta) \quad (2)$$

Where:

θ = Hanging-Wall Dip

The use of ELOS Stability Graphs allows for the comparison of stope dilution independently of their dimensions. However, some authors emphasise that it is still uncertain how orebody size is accounted for in the ELOS Stability Graphs (F. T. Suorineni et al., 2014).

METHODOLOGY AND RESULTS

This section presents an updated version of the ELOS Stability Graph that has been developed to overcome some of the previously mentioned limitations and allow for an efficient estimate of open stope unplanned dilution in contemporary Canadian deep mines.

Database and analyses

The data collected from the LaRonde mine includes information regarding 1,083 stopes mined at depths ranging from 860 meters to 2,450 meters over a period of 10 years. Figure 1 presents the distributions of the observed values of stope depths and stand-up time, as well as the Geological Strength Index (GSI) (Hoek, 2006), and hydraulic radius (HR) of their hanging-walls and foot-walls.

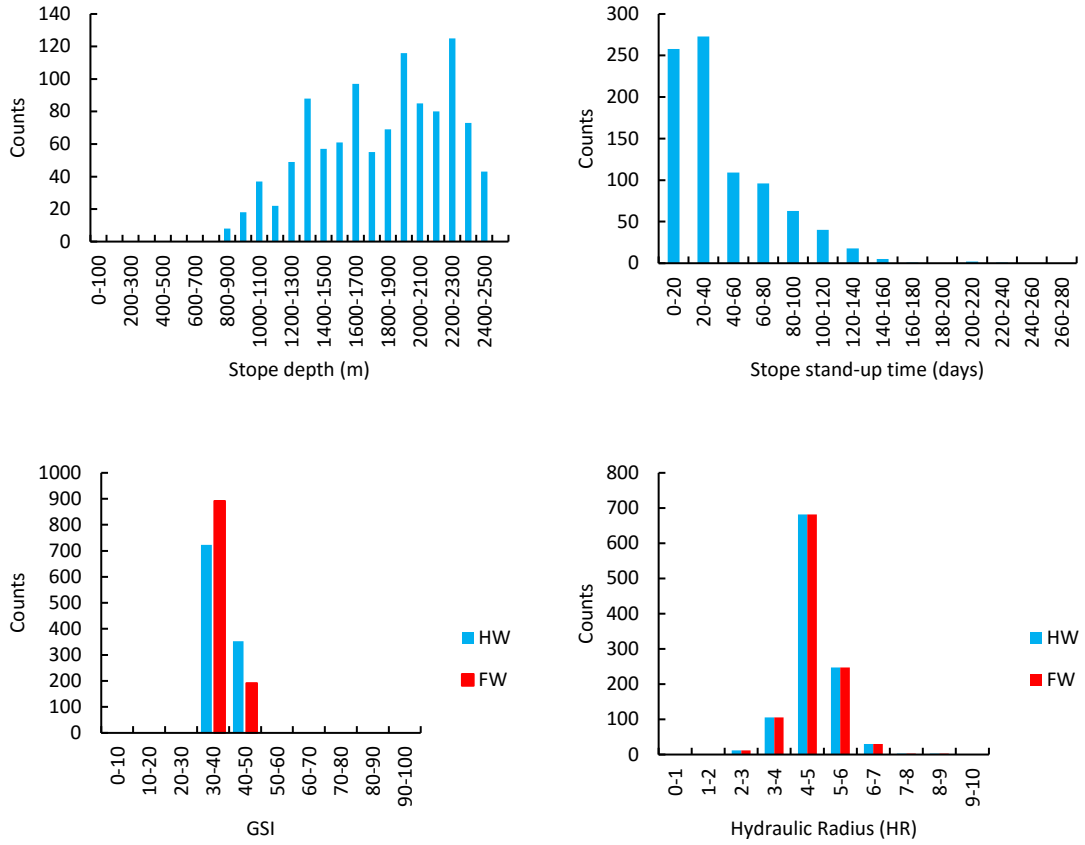

Figure 1 – Database values distributions

Local stress measurements, also included in the data collected, allows for the estimation of the *in situ* stress values and ratios. Figure 2 presents graphs showing the relationships expressing the vertical stress (σ_V), the ratio K_{max} of major horizontal (σ_{Hmax}) to vertical stresses, and the ratio K_{min} of minor horizontal (σ_{Hmin}) to vertical stresses as a function of depth for the LaRonde mine and the neighbouring properties.

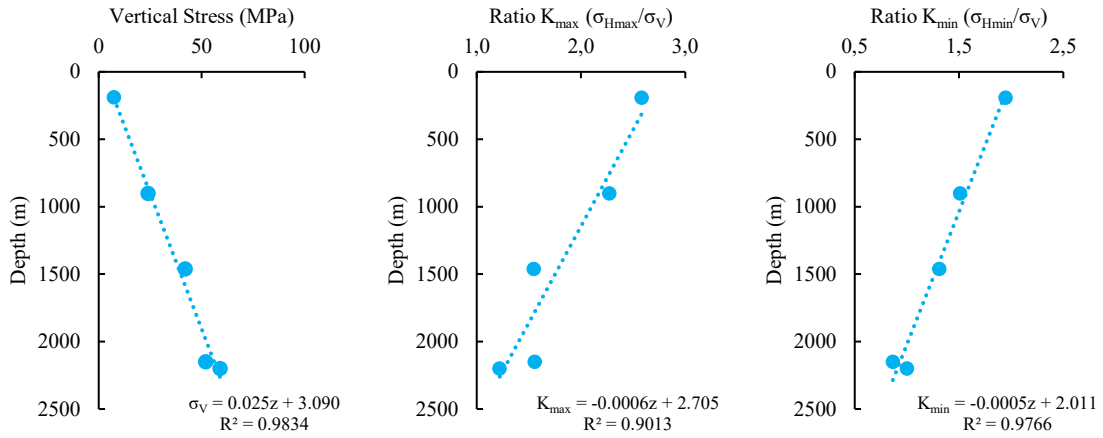

Figure 2 – Interpretation of LaRonde stress data by linear functions

The stress conditions seen at LaRonde are typical of hard rock mines in the Canadian Shield. LaRonde has a steeply dipping orebody with a strike almost perpendicular to the major stress (σ_{Hmax}) orientation and a nearly vertical minor stress (σ_V) (Arjang & Herget, 1997). It has been shown through numerical modelling that in this stress regime, hanging-walls and foot-walls generally have a zone of induced relaxation (Clark, 1998). Modelling studies indicate that for a given stope geometry, the stress ratio K_{max} dramatically affects the size of these relaxation zones which displays a strong correlation with observed ELOS values (Henning, 2007; Wang, 2004). For that reason the effect of ratio K_{max} variation with depth, as well as the effects of four other influential factors on the observed ELOS values from the stopes included in the database were investigated through a Design of Experiment (DOE) approach.

The effects and interactions due to the type of stope (primary/secondary), the ratio K_{max}, the HR, the GSI, and the stand-up time on the observed ELOS values have been analysed through a 2-level full factorial design. Figure 3 presents the results of this analysis and shows that for a confidence level of 90% ($\alpha = 0.1$) all except the stand-up time are factors that have a significant effect on ELOS.

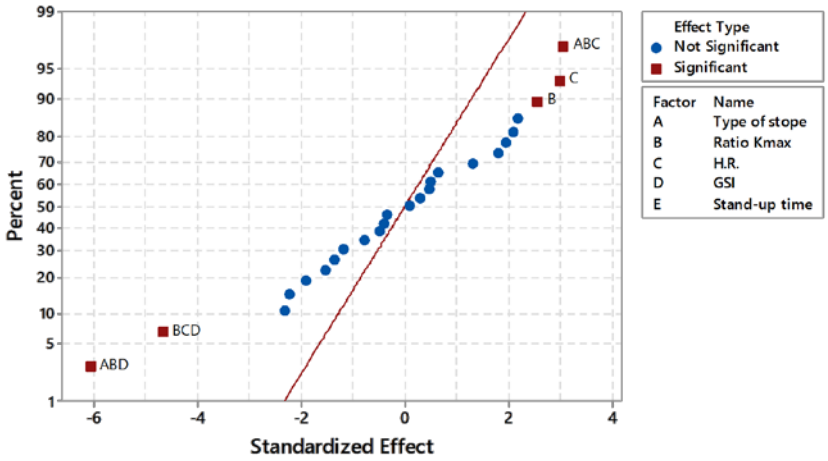

Figure 3 – Normal plot of standardized effects on ELOS ($\alpha = 0.1$)

Based on these observations, a further examination of the relationship between ratio K_{max} and ELOS allows for the introduction of a correction factor for HR, to obtain a term HR', that accounts for wall geometry and the effect of ratio K_{max} variation with depth. The adjusted HR value for the stope walls is calculated as follows:

$$HR' = 0.08\ HR \exp(1.5\ ratio\ K_{max}) \quad (3)$$

Based on the assumption that the RMR values used by Clark (1998) and GSI values are equal (Henning, 2007), a GSI' term equivalent to RMR' can be obtained by substituting the terms in equation 2. This allows for the combination of the 88 observations, originally used by Clark (1998), and the 2,158 observations from the LaRonde database to develop a ELOS Stability Graph version based on the relationship between HR' and GSI'.

ELOS estimation model

The multiple linear regression model (MLR) best fitting the 2,246 observations included in the combined database is illustrated by Figure 4 and corresponds to the following equation:

$$ELOS = 1.518 - 0.01709\ GSI' + 0.0997\ HR' - 0.001401\ GSI' \times HR' \quad (4)$$

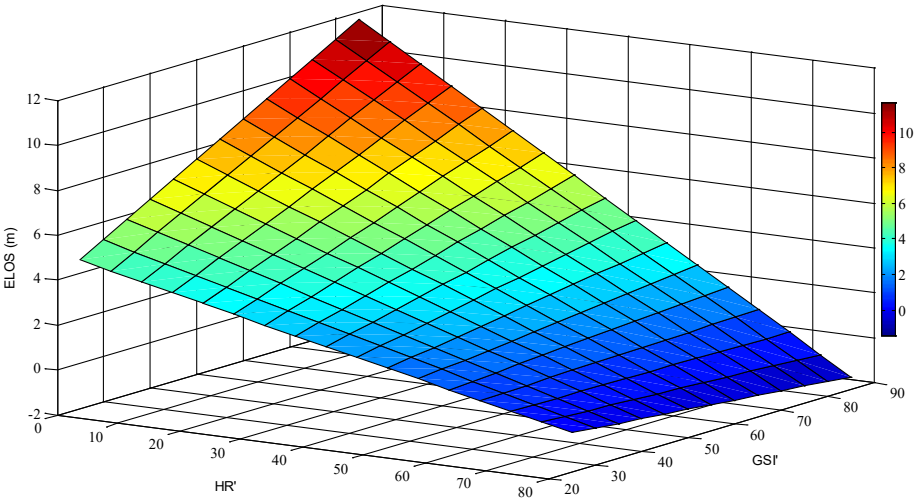

Figure 4 – GSI based ELOS Stability Graph

Although this version of the Stability Graph is more precise than previous versions, it remains a poor representation of the actual data with a standard deviation of the ELOS residuals of 1.25 m and R^2 of only 2.68%. An analysis of the ELOS residual values for the hanging-walls and foot-walls shows that their probability density functions (PDF) respect a generalized extreme value distribution type II, corresponding to equation 5 below, that can be described by a location parameter μ, a scale parameter σ, and a shape parameter k.

$$y = f(x|k,\mu,\sigma) = \left(\frac{1}{\sigma}\right)\exp\left(-\left(1+k\frac{(x-\mu)}{\sigma}\right)^{-\frac{1}{k}}\right)\left(1+k\frac{(x-\mu)}{\sigma}\right)^{-1-\frac{1}{k}} \quad (5)$$

Figure 5 shows fitted PDFs and the ELOS residual values distributions for the hanging-walls, the foot-walls, and the sum of both. These functions can be used to evaluate the probability surrounding the estimated ELOS values for a wall or for both walls of a stope. For example, by using the hanging-walls PDF one can see that there is approximately 27% probability for the real ELOS value to be more than 0.5 meter greater than the estimated ELOS value obtained with equation 4 for a hanging-wall.

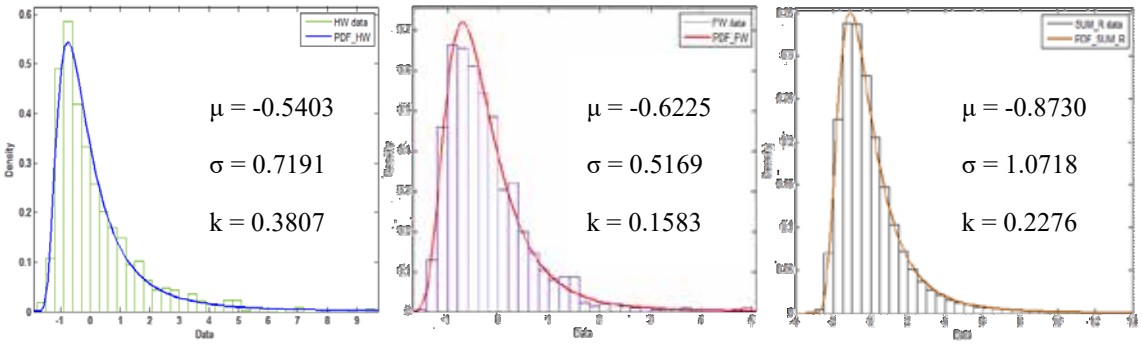

Figure 5 – Probability density functions of residuals between observed and estimated ELOS values

Integration of the model in a mineral reserve estimation methodology

It has been observed that for two different stopes, a given ELOS value can either represent an acceptable or an unacceptable level of dilution. This situation comes from the fact that an acceptable level of dilution is influenced by a great number of parameters including orebody width, as well as density and

grade of ore and waste rock (Planeta, 2001). An acceptable level of dilution is one that does not lower the average mill feed grade below the mine's tolerable return on investment. At a minimum, the average mill feed should not be lower than the mine's break-even cut-off grade (Clark, 1998). As such, a reliable methodology to quantify dilution should enable an accurate cost/benefit analysis of planned stope designs (R. C. Pakalnis, Poulin, & Hadjigeorgiou, 1995). Planeta et al. (2013) present a Mineral Reserve Estimation Methodology inspired by the NI 43-101 Canadian standard in which the previously proposed ELOS estimation model can be integrated to attain this objective. Figure 6 illustrates the process map of the proposed methodology.

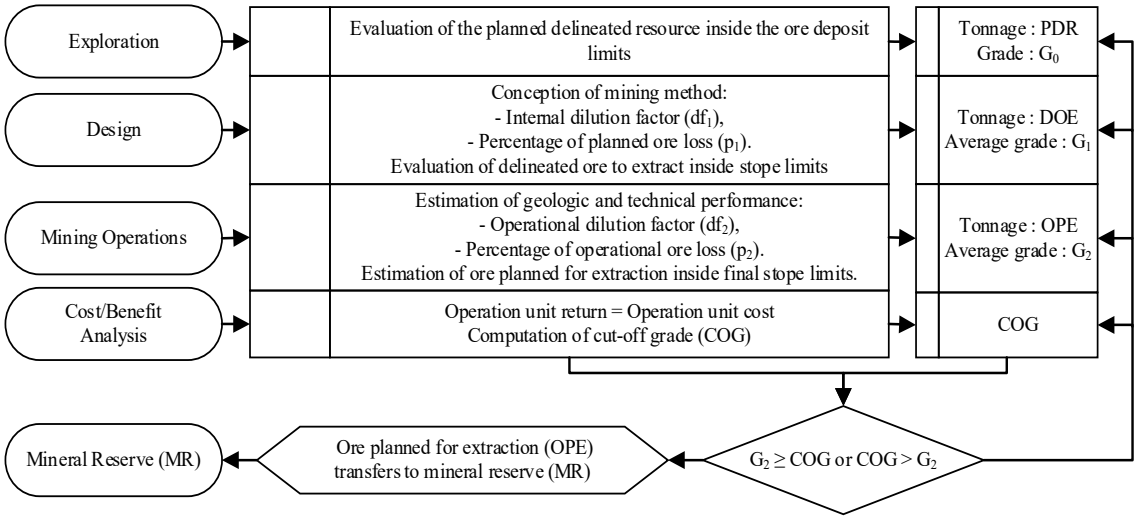

Figure 6 – Mineral Reserve Estimation Methodology (Planeta, Szymanski, & Laflamme, 2013)

Assuming a suitable knowledge of the orebody, the proposed ELOS estimation model can be integrated in the Planeta et al. (2013) methodology to estimate the operational dilution factor (df_2) and evaluate the grade (G_2) of the ore planned for extraction (OPE). The probability density functions presented in Figure 5 can then be used to approximate probability intervals for that value. Hence, the combination of this methodology and ELOS estimation model provide a powerful tool for open stope planning and design.

DISCUSSION

Empirical design methods are only applicable to conditions similar to those from which they are derived (Wang 2004). Consequently, their reliability is largely dependent on the size, quality, and consistency of their database (Suorineni, Hebblewhite et al. 2014). However, the original version of the Stability Graph (Mathews, Hoek et al. 1981) was developed from only 26 cases, the Modified Stability Graph (Potvin 1988) from 175 cases from depths ranging from 100 meters to 1,500 meters, and the ELOS Stability Graph (Clark 1998) from 88 cases from depths ranging from 75 meters to 1,100 meters. The updated ELOS Stability Graph presented in this paper is based on a much more robust set of observations than previous methods and can be applied to a broader range of conditions due to its developmental database of 2,246 observations from depths ranging from 75 meters to 2,450 meters, including 2,158 observations from LaRonde as well as the 88 observations originally used by Clark (1998).

Furthermore, for the reasons described by Clark (1998), the Stress Factor A and the Joint Orientation Factor B have not been considered in the new model. The model is based on the relationship between GSI' and HR' which efficiently accounts for rock mass quality, effect of gravity, wall geometry, and the variation of stress conditions with depth. The correction factor found in HR' accounts for the variation of stress conditions and results from the analysis of the ratio K_{max} effect on the observed ELOS values demonstrating that despite the increase of the stress component, the stope walls' stability increases as ratio K_{max} decreases with depth. This analysis begs the question, at which depth does the stabilizing

effect start to be overcome by the negative effect of high stress? To answer this, the updated model should only be used in cases similar to those included in the developmental database and further investigation is required to evaluate the effect on ELOS of decreasing stress ratios and increasing stress values at greater depths.

Many authors have stressed the fact that conventional Stability Graphs are orebody-width dependent and that they do not easily allow for the identification of what an acceptable level of dilution is for a given situation (Papaioanou & Suorineni, 2015). This paper has discussed how to address this by integrating the ELOS estimation model in a reserve estimation methodology. The probability density function of the ELOS residuals can then be used to judge the acceptability of a stope design given an adequate knowledge of the orebody.

CONCLUSION AND RECOMMENDATIONS

This paper presents the results of a study based on data collected by the LaRonde mine engineering team of the planning and extraction of 1,083 stopes mined at depths ranging from 860 meters to 2,450 meters over a period of 10 years. The analysis of these data has shown that stress ratios variation with depth has a statistically significant effect on stope wall stability and that an improved ELOS estimation model can be obtained by introducing a correction factor that accounts for this effect.

The integration of the GSI-based ELOS estimation model obtained by multiple linear regression, combined with the probability density function of the model residual, in the reserve estimation methodology presented by Planeta et al. (2013) provides a powerful decision tool to assist the planning and design of open stopes.

It is recommended that the model be used in cases similar to the ones included in the developmental database and that additional data be collected to improve the precision of the model. Studies should be done to better adjust the correction factors for gravity and ratio K_{max} and investigate the factors affecting stope stability at depths greater than 2,450 meters.

REFERENCES

Arjang, B., & Herget, G. (1997). In situ ground stresses in the Canadian hardrock mines: an update. *International journal of rock mechanics and mining sciences & geomechanics abstracts, 34*(3-4), 652. doi:10.1016/S1365-1609(97)00039-7

Barton, N., Lien, R., & Lunde, J. (1974). Engineering classification of rock masses for the design of tunnel support. *Rock mechanics, 6*(4), 189-236. doi:10.1007/bf01239496

Capes, G. W. (2009). *Open Stope Hangingwall Design Based on General and Detailed Data Collection in Rock Masses with Unfavourable Hangingwall Conditions.* (Doctor of Philosophy), University of Saskatchewan, Saskatoon, SK, Canada.

Clark, L. M. (1998). *Minimizing dilution in open stope mining with a focus on stope design and narrow vein longhole blasting.* (Maste of Applied Science), University of British Columbia, Vancouver, BC, Canada.

Henning, J. G. (2007). *Evaluation of Long-Hole Mine Design Influences on Unplanned Ore Dilution.* (Doctor of Philosophy of Engineering), McGill University, Montreal, QC, Canada.

Hoek, E. (2006). *Practical Rock Engineering*. Vancouver, BC, Canada: Evert Hoek Consulting Engineer Inc.

Mitri, H. S., Hughes, R., & Zhang, Y. (2011). New rock stress factor for the stability graph method. *International Journal of Rock Mechanics and Mining Sciences, 48*(1), 141-145. doi:10.1016/j.ijrmms.2010.09.015

Pakalnis, R. C., Poulin, R., & Hadjigeorgiou, J. (1995). Quantifying the cost of dilution in underground mines. *Mining Engineering, 47*(12), [d]1136-1141.

Pakalnis, R. T. (1986). *Empirical stope design at the Ruttan Mine, Sherritt Gordon Mines Ltd.* (Doctor of Philosophy), University of British Columbia, Vancouver, BC, Canada.

Papaioanou, A., & Suorineni, F. T. (2015). Development of a Generalised Dilution-based Stability Graph for Open Stope Design. *Journal of Research Projects Review, 4*(1), 27-33.

Planeta, S. (2001). Sources de dilution dans les mines souterraines: Methodes de calcul. *CIM bulletin, 94*(1048), 128-132.

Planeta, S., Szymanski, J., & Laflamme, M. (2013). *Méthodologie d'estimation de la réserve minérale par l'optimisation de l'information, de la planification et des pratiques minières*. Technical paper. Department of Mining, Metallurgical and Materials Engineering. Laval University. Quebec, QC, Canada.

Potvin, Y., & Hadjigeorgiou, J. (2001). The stability graph method for open-stope design. *Underground Mining Methods: Engineering Fundamentals and International Case Studies. Society of Mining, Metallurgy and Exploration, 8307 Shaffer Parkway, Littleton, CO 80127, USA, 2001.*, 513-520.

Suorineni, F. T. (2010). The stability graph after three decades in use: Experiences and the way forward. *International Journal of Mining, Reclamation and Environment, 24*(4), 307-339. doi:10.1080/17480930.2010.501957

Suorineni, F. T. (2014). *Empirical methods in mining geomechanics–Reflections on current state-of-the-art*. Paper presented at the 1st International Conference on Applied Empirical Design Methods in Mining, At Sheraton Lima Hotel & Convention Center, Lima, Peru. Conference paper retrieved from https://www.researchgate.net/publication/269984574_Empirical_methods_in_mining_geomechanics_-_Reflections_on_current_state-of-the-art

Suorineni, F. T., Hebblewhite, B., & Saydam, S. (2014). Geomechanics challenges of contemporary deep mining: A suggested model for increasing future mining safety and productivity. *Journal of the Southern African Institute of Mining and Metallurgy, 114*(12), 1023-1032. Retrieved from http://www.scielo.org.za.acces.bibl.ulaval.ca/pdf/jsaimm/v114n12/12.pdf

Udd, J. E. (2006, June 2006). *DEEP MINING IN CANADA - THE CHALLENGES AND THE OPPORTUNITIES.* Paper presented at the Proceedings of the Core Project on Deep Mining, Ottawa, ON, Canada.

Wang, J. (2004). *Influence of stress, undercutting, blasting and time on open stope stability and dilution.* (Dorctor of Philosophy), University of Saskatchewan, Saskatoon, SK, Canda.

LARGE-SCALE ROCK BLASTING IN UNDERGROUND MINING

S.D. Victorov, V.M. Zakalinskii, *A.A. Osokin

Institute of Comprehensive Exploitation of Mineral Resources Russian Academy of Sciences,
4, Kryukovsky Tupik, Moscow, 111020, Russia
*(*Corresponding author: osokin_alex-r@mail.ru)*

24th World Mining Congress
MINING IN A WORLD OF INNOVATION
October 18-21, 2016 • Rio de Janeiro /RJ • Brazil

LARGE-SCALE ROCK BLASTING IN UNDERGROUND MINING

ABSTRACT

The evolution in the explosive destruction of rock masses in underground conditions identified a number of research areas. One of them is associated with an increase in the size of the recessed unit array per charge and, consequently, in the parameters of the slugger layer. The development of scientific and technical direction based on the zoom explosive destruction of rock masses has led to a notable progress in drilling and blasting in the recent decades. A new approach to the method of calculating of the amount of charge at the breaking of large ores directional explosive charges in the underground environment through the use and development of the scale factor was required. The development of the proposed technique was based on the principle of the scale effect on the basis of the analysis of the well-known dependence of the charge on the volume of blasted rock mass and its transformation in order to obtain the same degree of fragmentation in all the volumes and terms of large-scale blasting. The principles of improving the blasting comprising theoretical questions of rational choice of specific consumption of explosives and directional blasting considering the scale of the area were investigated. A novel design of the charge is proposed, which allows controlling the action of an explosion in the new development systems with the mass forced caving and using effect of scale blasting. The use of this design of the charge for a large-scale blasting with directed action will reduce the negative seismic impact of explosion in a given direction.

KEYWORDS

Blasting, breaking, seismic action, underground mining, control.

INTRODUCTION

At present, one of the most dynamically developing industries is the mineral-energy complex of Russian industry (Trubetskoi & Viktorov, 2000). The search for new technological solutions during both typical and selective development of mineral deposits of complex structure is associated with the alteration of various grades and scales of layers (strata of mineral deposits) and interlayers of dead rocks. Drilling may be complicated by anthropogenic factors, for example, limitations on the effect of blasting impulses on underground workings in the immediate vicinity of pit boundaries. In many pits, strata of mineral deposits less than 1 m thick are removed together with host overburden rocks (dead rocks that cover mineral pools), and dead rock interlayers of the same thickness are included into development (bulk mining). This is predetermined by the limited capabilities of equipment used for separate (selective) extraction. At present, as strata of mineral deposits have been developed at most fields, interlayers with a low content of the valuable component or totally dead rocks are included into the productive layer thickness, thus reducing the quality of the raw material produced. In addition, the current ways of drilling and blasting preparation, using geological information obtained indirectly by averaged and extrapolated exploration data, do not ensure the necessary quality of drilling and blasting preparation of the rock mass for a specific terrace section. Geological factors that affect explosive fragmentation, like the geological structure of a specific block massif, are not taken into account either.

The continuous flow technology, for example, based on rotary-conveyor complexes and loading-stoping machines, manufactured by Krupp Fördertechnik, GmbH, and the Skochinskii Institute of Mining, is promising in selective field development. As applied, for instance, to coalfields in the Kuznetsk Basin, Eastern Siberia, and other similar regions, the parameters of the KSM 2000R machine have been developed (Ermakov, Burakov, & Khosoev, 2008). Trials have shown that this machinery is universal and well adapted to various mining conditions and can be efficiently used for stripping with relatively large amounts of removal, simultaneously carrying out the selective development of complex-structure strata.

TASKS OF EFFICIENT EXPLOSIVE PREPARATION

Analysis of rock mass breaking during the development of sheet mineral deposits using innovative geotechnologies has revealed the need to stiffen blasting requirements in terms of the maximally full and directional use of its capabilities. The physicotechnical parameters of efficient explosive preparation of a rock massif can be determined by solving the following problems:

- controlling explosive pulses in rock, limiting their effect on underground workings in close proximity to pit boundaries;
- the computation algorithm of rock explosive rupture at sheet deposits; and
- developing methods to control explosive fragmentation of rocks of various hardnesses in mineral deposits of complex structure.

These problems are united by a common goal whose theoretical precursors contain a corresponding (fundamental) base for the practical component of implementing a technologically controlled (directional) blasting effect in complex structural conditions.

ASPECTS OF METHODOLOGY

The explosive preparation of a rock massif during the development of mineral deposits includes the solution of many problems, including technological ones. Let us limit ourselves to one of them containing a condition for the explosive effect on rocks that affects the productivity of the mine in general. It can be reduced to the requirement of a selective explosive effect that combines the cumulative effect in certain directions and a maximal destructive (fragmenting) impact in other directions. In practice, for instance, as applied to the development of sheet deposits, this means mass blasting in pits, on the one hand, without damaging mine openings located in the blasting zone, including those in close proximity to pit boundaries, and, on the other hand, reaching the maximum of rock fragmentation. In a number of cases, the requirement of the subsequent selective separation of the blasted massif is added.

HYPOTHESIS OF CONTROL OF EXPLOSION ACTION AND IDEOLOGY OF NEW METHOD

Let us consider some issues of the mechanism of blast energy control in a rock massif by paralleled contiguous charges of different configurations, sizes, and types of explosives. Such charges, as the long practice of their use in the ore-mining industry has shown, currently have practically no technologically implementable alternatives in the control of blasting effects (Viktorov, Galchenko, Zakalinskii, & Rubtsov, 2006). The fundamental basis of the target direction of the efficient explosive preparation of a rock massif may be represented by a hypothesis based on two postulates:

- the energy of a well charge, traditionally round in its cross-section, which depends on the well-drilling method, is formed during its explosion into an explosion wave close to a symmetrical shape, which often leads to a discrepancy between mining requirements and blasting capabilities; consequently, each charge is oversized; i.e., there is excess energy not used directly; and
- if we find a way to depart from the traditionally accepted parameter of a well charge, such as the diameter, predetermined by the corresponding drilling rig, theoretically, we may design a charge of any shape, not necessarily round, in the cross-section; hence, there is one step to the formation of a blasting wave of any shape, intensity, and directionality, maximally corresponding to the mining requirements.

The combination of these postulates comprises the ideology of a new approach to the problem of improving the blasting technology during the development of mineral deposits of complex structure.

THEORETICAL BACKGROUND OF EXPLOSIVE PREPARATION

The point is that the existing methods, as estimation data analysis has shown, have turned out to be of little use due to theoretical causes. A new approach was required to the methodology of charge size estimation for ore blasting with large directional explosive charges based on the use and development of the scale effect (Viktorov et al., 2006). This is the development of the scale effect principle based on the analysis of a well-known formula,

$$Q = qV \tag{1}$$

and its transformation in order to obtain an estimation formula of the same fragmentation degree under any volumes and conditions of large-scale blasting. We have identified its main drawback: it does not take into account the degree of rock mass fragmentation, because, historically, it was derived from the problem of ground mass (volume) motion V. Its improvement consisted in representing value q as a variable dependent on its other value V, which results in a differential equation,

$$dQ = q(V)dV,$$

(2)

which takes into account the quality of rock mass fragmentation depending on the blasting volume (scale). If we know the dependences of the specific consumption of explosives on the least resistance line (LRL) for rocks of various cleavages and hardnesses, it is possible to calculate the necessary charge value, taking into account the certain fragmentation degree by a formula,

$$Q(W_1) = Q_0 + c\int_{W_0}^{W_1} q(W)WdW,$$

(3)

where Q_0 is the charge corresponding to the LRL of blasted layer W_0; c is the value of the initial area of the well pattern, corresponding to Q_0; and q is the specific consumption of explosives.

It reflects both the volume of the destroyed rock layer ($q = const$, formula 1) and, additionally, the degree of its fragmentation ($q = f(W)$ formula 3, a new factor). In practice, q depends on W to varying degrees, but it can also be independent, for example, during the breakage in broken-down ores with a size limit on the shop floor smaller than the distance sizes between cracks. Then formula (3) is identical to formula (1).

On the basis of test data analysis, formula $q = f(W)$ in formula (3) can be represented as the following dependence:

$$q = q_0 + kW^{\varphi},$$

(4)

where q_0 is the specific charge of explosives at W_0, which corresponds to the lower limit of the integral in formula (3); q is the same, but at W_1in the upper limit of the integral; kW^{φ} is a scale addition, corresponding to the increase in LRL; and k, φ are the coefficients of proportionality and immensity, respectively.

This formula was considered for all (from broken-down to relatively monolithic) ore types under the condition of obtaining an approximately equal degree of fragmentation. Its strong dependence on the degree of rock mass cleavage (~70%) has been revealed, weak cleavage depending on rock hardness f (~20%) and ~10% falling on the remaining factors. The strongest relationship manifests itself in solid or low-fractured ores, decreasing as the degree of cleavage increases (with reference to the size limit) and reaching a relative minimum in medium-fractured ores. The formula acquires a "dynamic" use, affecting flexibly (on the fly) the process of estimating the amount of explosives necessary for a mass explosion at the very beginning, since all methods of estimating explosive amounts are based on dependence (1), varying its structure relative to local blasting conditions.

The dependence tends to be controllable, since it is characterized by dynamic use compared to classical "static" formula (1), on the fly (in the beginning of estimating the necessary amount of explosives for large-scale mass blasting) and discriminatingly taking into account the geological structure of the whole block. According to the existing methods, the amount of a massif to be blasted would correspond to the other, overstated, amount of explosives, satisfying the estimation according to formula (1).

Applying the generalized law of similarity (if the fragmentation quality remains unchanged), formulas (3) and (4) may yield an expression that includes, subject to the energy principle, the values of the energy margin of explosive charges, well pattern, and LRL:

$$\frac{Q_n}{Q_o} = \frac{E_n}{E_o} = \frac{S_n}{S_o}\left(\frac{W_n}{W_o}\right)^{\varphi+2},$$

(5)

where the indices correspond to both new and old values.

This formula tracks the additive to the main charge in formula (4) that is necessary to maintain the fragmentation quality at a change in the volume of the blasted massif (the scale correction). On the basis of geological information, we may preliminarily calculate large-scale explosions for stoping under any underground conditions and without special test blasting, obtaining the same fragmentation quality as under small-scale blasting parameters. This methodological aspect can also be used in various conventional drilling-and-blasting methods after comparisons and corrections of charge values and parameters and the massif-mining unit per well charge. This need

arises during the development and design of new large-scale breakage technologies. Thus, we obtain the answer, formulated in the first postulate, relative to the true charge value, independent from its shape.

The result that satisfies the formulation of the second postulate, in practice, during mass explosions, is implemented by commutations of explosive chains and blasting sequences of typical well charges, which in simple cases solves the problem of directional or controlled blasting action.

The effect of design specifics of charges, as a rule, is reduced to a minimum due to their absence or unserviceability. The point is that principal changes have not been observed in the design of well and bore charges for a long time. In almost all cases, the breakage is done by monocharges using the expandable explosion model, when the major part of explosion energy, concentrically diverging in all directions from the charge, is carried deep into the massif. Therefore, from 50 to 70% of the total charge energy is spent on a technologically unnecessary and often harmful change in the rock massif condition outside and inside the broken volume. Great and very interesting geotechnological prospects emerge here as rock fragmentation methods are created with a sharp asymmetry of explosion energy distribution and maximum energy concentration in the direction of bare planes of the massif to be broken. The possibility of implementing this idea is associated with the well-known principle of explosion energy cumulation due to the charge shape (Lavrent'ev, 1957). Practically, this can be done by replacing a single large-diameter and large-power charge with a group (cluster) of smaller charges of the equivalent total energy. Brand new opportunities open up to control the processes of explosion energy transfer and distribution in a massif to be broken by changing the parameters and spatial position of each single change in the group. We are speaking about typical well charges, which, designed for directional action, do not affect the technology in any way.

A contiguous charge cluster is a group of wells drilled closely to one another according to a pattern and filled with an explosive composition to detonate simultaneously as a single charge and to form an explosion wave of the required shape, intensity, and direction, which are regulated by the number of wells, their location, and explosive type. As a result of the simultaneous detonation of several closely located ($d < L < 6d$) well charges, a complex process of strain wave interaction is formed in the medium. Assume that its physical nature depends on the same processes as in an elementary cell of a cluster of two contiguous charges. For two identical charges of diameter d, this picture is given in Figure 1.

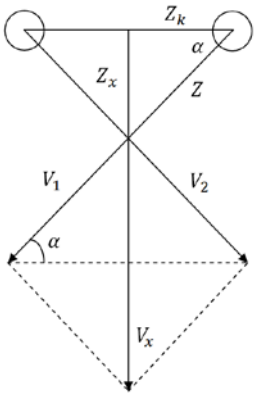

Figure 1 – Chart of the compressive wave effect of two contiguous charges

The radial component of the mass velocity for a single charge is

$$V(z) = \frac{V_0}{z^{a-1}} e^{-k(z-1)} f\left(t - \frac{z-R_0}{c}\right), \quad (6)$$

where $z = R/R_0$ is the distance from one of the charges to the observation point reduced to charge radius R_0; $f\left(t - \frac{z-R_0}{c}\right)$ is a certain time function; k is the coefficient of wave attenuation due to dissipative processes: $k = 0.5$, a broken-up massif, $k = 0.25$, a medium-fractured massif, $k = 0$, a monolithic rock; a is a coefficient that characterizes the dimension of a problem: $a = 3$, spherical, $a = 2$, cylindrical, and $a = 1$, flat case; $V(z)$ is the value of a maximal mass velocity at distance z; and V_0 is its initial value (Khristoforov & Romashov, 1967; Rodionov, Adushkin, Kostyuchenko, et al., 1971).

According to the pattern under consideration, we can obtain an expression for the maximal mass velocity component along axis x, which appears during the simultaneous explosion of two charges:

$$V_x(z) = \frac{V_0}{z^a} e^{-k(z-1)} \sqrt{z^2 - (z_k)^2}. \quad (7)$$

Equation (7) refers to the spherical ($a = 3$) and cylindrical ($a = 2$) cases. For the flat case, the speed component is zero. The maximal mass velocities, depending on various values z_k, are determined in the following way:

$$V_{max} = \frac{e^{-k(R_{max}-1)}}{R_{max}} \sqrt{R_{max}^2 - \left(\frac{R_k}{R_0}\right)^2} \quad (8)$$

where R_k is the distance from the charge to the axis.

RESULTS OF NUMERICAL CALCULATIONS

In the direction perpendicular to the charge line at different distances between them, point coordinates have been found where maximal mass velocities in the wave are reached. Tables 1 and 2 show the calculated values of R_{max} and V_{max} for various coefficients k and z_k in the range of 1-6 contiguous cylindrical charges ($a = 2$).

Table 1 – Estimated values R_{max} and V_{max} for contiguous cylindrical charges ($a = 2$)

z_k	$k = 0$		$k = 0.25$		$k = 0.5$	
	R_{max}	V_{max}	R_{max}	V_{max}	R_{max}	V_{max}
1	1.414	0.500	1.323	0.356	1.270	0.257
2	2.828	0.250	2.539	0.129	2.411	0.069
3	4.242	0.167	3.698	0.063	3.503	0.026
4	5.636	0.125	4.822	0.035	4.569	0.011
5	7.070	0.100	5.923	0.021	5.618	0.005
6	8.483	0.083	7.006	0.013	6.657	0.002

Table 2 – Estimated values R_{max} and V_{max} for an equivalent single cylindrical charge ($a = 2$)

z_k	$k = 0$		$k = 0.25$		$k = 0.5$	
	R_{max}	V_{max}	R_{max}	V_{max}	R_{max}	V_{max}
1	1.414	0.707	1.323	0.543	1.270	0.418
2	2.828	0.353	2.539	0.209	2.411	0.124
3	4.242	0.236	3.698	0.107	3.503	0.05
4	5.656	0.177	4.822	0.062	4.569	0.022
5	7.070	0.141	5.923	0.038	5.618	0.011
6	8.483	0.118	7.006	0.025	6.657	0.005

ANALYSIS OF THE DATA

The analysis of the findings has shown that the mass velocity values depend on the wave attenuation coefficient and the coefficient that characterizes a charge's geometrical shape, as well as the distance between contiguous charges. It has been established that, if contiguous charges are positioned in a line (linearly contiguous configuration), a quasi-flat (hereinafter, "flat") front is formed, which is largely affected by geometrical factors (the radius of a single well) and the type of explosives (the wave pulse length). For other cluster configurations, these factors are not decisive (Pyzh'yanov took part in these investigations).

The comparison of contiguous-charge explosions for underground and open operations have shown that explosives with low detonation speeds and stretched (the simplest) pulses, positioned in large-diameter wells, are most efficient. Charges with high detonation speeds, located in small-diameter wells, are advisable to be used in cluster configurations that form a common wave close to a cylindrical shape. Subsequently, it was necessary to give some quantitative and qualitative assessments

of the geometrical shape of the integral explosive cluster wave formed and its parameters. Various, including typical, cluster charge patterns were considered, and the geometry of the originating wave fields was calculated.

The mathematical modeling method was used to study the dependence of compressive wave parameters in a rock of the shape of a cluster charge, assuming that the total effect of several charges depends on the superposition principle. A flat case was analyzed, i.e., a case of cylindrical infinite-length charges. The main parameters for this problem were b, the well radius; R_0, the distance between charges; and T_0, the single-charge pulse length. Three basic cluster types of five charges positioned linearly semi-circularly and circularly with a charge in the center were considered. The parameters of compressive waves from a single cylindrical charge at distance R are determined by the following t-time dependence:

$$V(R,t) = \frac{1}{R^{0.5}} sin\left[\frac{\pi}{T_0}\left(t - \frac{R-b}{c}\right)\right], \quad (9)$$

where V is the mass velocity; c is the speed of elastic waves in rock; and T_0 is the wave period.

Formula (9) describes the attenuation of a harmonic wave with period T_0 against distance and time. According to the superposition principle, which is true for elastic waves, the wave for any charge position in a cluster can be calculated as the sum of the waves of separate charges. Parameter T_0 may be conventionally assumed to be associated with the explosive type used. Large T_0 values correspond to explosives with a longer time of explosive energy generation, for example, the simplest, and, vice versa, its smaller values fit better for trotyl-containing explosives. The velocity of elastic waves c in all calculations was assumed 5000 m/s. The mass velocity, and not stress, was chosen as the main parameter of the compressive wave only due to the convenience of assessment, because, in our case, it is easier to deal with a vector value than with a tensor one-comparative assessments do not change thereon.

The calculations were done using Mathematica for Windows v. 22. We calculated compressive wave parameters from five charges at observation points x_0, y_0 located at points with coordinates x_i, y_i. To assess the effect of such a combined explosion, the total radial component of the mass velocity was found at a preset distance from the center of coordinates for various angles.

The time of wave arrival to the preset point (r, a) was measured for each charge in the system, as was the amplitude of the harmonic wave, which was determined by the law of geometrical similarity for infinite-length cylindrical charges:

$$V = \frac{1}{\sqrt{r}}.$$

The radial component of velocity was calculated, i.e., the projection on the direction along the radius from the center of the charge system to the observation point (r, a), and these charge projections were summed up.

In addition to calculations, the program makes it possible to plot the resulting graphs as temporal curves both of the mass velocity wave profile of the charge system in general and of individual charges in observation points, located at different distances from the cluster and between its charges. For better clarity of the velocity distributions near the charge system and assessment updates, 3-D curves of the mass velocity were plotted.

Computed data were analyzed by three chosen directions: along the semisphere's diameter and on both sides of it. The analysis showed that the selective action of an explosion in the chosen direction could be reached depending on the distance between the charges and the length of initial pulse T_0. The real process of explosion development complies with more complex laws than the picture based exclusively on the elastic model. However, the quantitative side of the interaction of several explosions during the analysis of elastic solutions manifests itself sufficiently clearly and correlates with the above qualitative side of this process.

We also solved the problem that considered the dynamics of the resultant quasi-flat wave caused by the explosion of contiguous charges. The significant effect of the geometrical parameters of a cluster charge on the stress field was established. Parameter T_0 turned out to be important; it determined the pulse of a single-charge explosion and the closely related explosives. This makes the control of the direction of a cluster of paralleled contiguous well charges principally possible by varying its geometrical and physical parameters and can be taken as the basis for revealing the explosion mechanism.

Using the obtained results and the assumption of the general integral wave, which is formed during the explosion of a cluster of paralleled contiguous well charges, Huygens' principle is applicable, and let us monitor the wave front development with time. In the case under consideration,

of interest is the well-known consequence: as it moves away from the source, the spherical wave becomes increasingly flatter, and, if we assume that the source is infinitely distant, the wave front at the extreme will turn into a plane, which moves evenly at velocity V. Figure 2 reflects the formation of the resultant front during the explosion of contiguous charges in the rock.

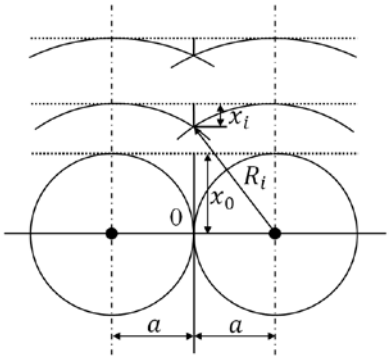

Figure 2 – Assessing the interaction of the explosion waves of contiguous charges

Initially, the fronts of cylindrical shapes develop independently until they meet at a point in the middle of the line that passes through their centers. From this moment, there is a physical process called the interaction of fronts, which is expressed in the continuous formation of the resultant common aggregate front with the curvature quickly decreasing to a practically flat (quasi-flat) front. If we designate a value that characterizes the degree of deviation from the line that connects the centers of the chargers as x and the distance from the center of the charge to the point where the waves meet at the speed of sound, $c = const$, as R_i, we will obtain the dependence of value $x \equiv x_i$ in time:

$$x_i = a\left(n - \sqrt[2]{n^2 - 1}\right), \quad (10)$$

where $n = \frac{R_i}{a}$.

The relative values and $\frac{x_i}{a}$ were calculated by formula (10), and by these values we may judge about the stages of the quasi-flat front formation on a line that coincides with LRL if we specify the threshold or criterial value of the characteristic of the flat front, i.e., value x_i.

The quasi-flat wave's characteristic was calculated for the real values of the cluster parameters, $a = 0.2\ m$ and $h \geq 2$. These data were used to plot the formation profiles of the quasi-flat wave at various distances from the charge line. It was established that, at a distance of 1 m, the formation of the common resultant quasi-flat front starts, which, as this distance increases, approaches a linear flat shape, which stably persists for the real geotechnological LRL values from 4 to 10 m.

These findings were compared to the results of explosions of contiguous charges in acrylic plastic in (Simha, Holloway, & Forney, 1983). It was noted that the external shape of the integral wave field in the direction perpendicular to the charge line had a clear-cut view. As an example, Figure 3 shows the drilling pattern in a cluster that forms a directional explosive wave at a mining enterprise in Western Siberia (Eremenko, 2013).

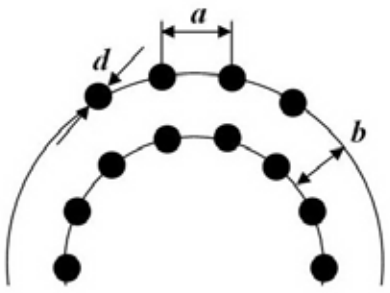

Figure 3 – The cumulative form of the arrangement of contiguous charges in a block to be exploded, which forms a directional explosion wave

By changing the number of charges in the group, their positions, and the type of explosives, it is possible to control the energy flow of a single charge, which at the time of explosion is the cluster, and to form stress fields of various intensities and in various directions, depending on the goals and requirements of mining technologies. In particular, it is possible to improve the quality of rock massif fragmentation compared to equivalent charges. In addition, there is a fundamental difference in the explosion mechanisms of typical and cluster contiguous charges, since, in the latter case, the massif is destroyed not by a direct stress wave but by a new substance – an integral wave formed at a distance from the geometrical perimeter of the equivalent charge. In total, the effect of recreation or formation of a charge and wave of a shape noncircular in cross-section is reached. This is the practical implementation of the idea of abandoning the circular cross-sectional shape of a charge, traditional for mining, for fuller correspondence with various explosion conditions and mining requirements.

From the above, ratio $d\sqrt{n} \geq D$ follows, according to which, the fragmentation efficiency of a cluster explosion consisting of n parallel contiguous well charges of diameter d exceeds or equals the explosion result of an equivalent charge of large diameter D.

The development of solid mineral deposits inevitably leads to situations when technological problems of mining production can be solved efficiently only with the help of directional blasting methods. Alongside the fact that explosive preparation for stoping during the development of various mineral deposits differs mainly only in taking into account the mining and geological specifics of a deposit, some open pit development has its specific features [9]. Analysis has shown that the presence of a scientifically justified and technologically feasible method of explosion control and, consequently, the development of the method and algorithm for calculating controlled explosive rock fragmentation, for instance, at sheet deposits allows for solving practically any mining problem.

Demonstrative is the experience of underground mass breaking at the Gornaya Shoriya mines, when outlining directional contiguous cluster charges are used to form in an ore block the central vertical concentrated large-mass charge of a special design close to a cylindrical shape. Other charges are positioned at a certain distance around it and are detonated first. Explosion control consists in directing the explosion wave toward the previously caved worked-out space by using compensation chambers and newly formed free surfaces. In addition, the quality of fragmentation of an outlined ore block improves considerably, and the seismic effect of a powerful underground explosion increases significantly. The determination of blasting parameters requires dependences based on historical prerequisites, and examples of various designs of directional cluster contiguous well charges were given in (Viktorov, 2013; Viktorov, Eremenko, Zakalinskii, & Mashukov, 2005).

CONCLUSION

Thus, we considered the following aspects of the effectiveness of a large-scale action of an explosion in the development of mineral deposits:

- evolutionary, showing the dynamics of the mining sector in the development of mineral deposits with the justification of new technological solutions;
- mining and technology, which includes analysis of various technologies and methods of system development leading to the selection of the most promising areas;
- theoretical, based on a new approach when considering energy management mechanism of the explosion in the mountain range;
- analytic, outlining the equations for calculating dependencies for methods of calculating the parameters of blasting technology using molds downhole contiguous charges forming the directional blast;
- practical, demonstrating the use of the proposed technology at some mining enterprises in Russia;
- potential introducing a specific contribution to the development of physical and technical basics in the development of various mineral deposits.

ACKNOWLEDGMENTS

The study was performed by a grant from the Russian Science Foundation (project 16-17-00066).

REFERENCES

Eremenko, A.A. (2013). Совершенствование технологии буровзрывных работ на железорудных месторождениях западной Сибири [Improving Drilling and Blasting Techniques at Western Siberian Iron Ore Fields]. Novosibirsk, Russia.

Ermakov, S.A., Burakov, A.M., & Khosoev D.V. (2008). Изыскание новых технологических решений селективной отработки Эльгинского угольного месторождения [Exploring New Technological Solutions to the Selective Development of the Elga Coalfield]. Moscow, Russia.

Khristoforov, B.D., & Romashov, A.N. (1967). Определение параметров волны сжатия в скальном грунте [Determining compressive wave parameters in rock formations]. Novosibirsk, Russia." Combustion, Explosion and Shock Waves, No. 1.

Lavrent'ev, M.A. (1957). Кумулятивный заряд и принцип его работы [Cumulative charge and the principle of its operation]. Moscow, Russia. Uspekhi Mat. Nauk, No. 4 (1957).

Rodionov, V.N., Adushkin, V.V., Kostyuchenko, V.N., et al. (1971). Механический эффект подземного взрыва [Mechanical Effect of an Underground Explosion]. Moscow, Russia.

Simha, K.R., Holloway, D.S., & Forney, W.L. (1983). Dynamic photoelastic studies on delayed presplit blasting. Julea, Sweden. *First Inter. Simp. on Rock Fragmentation by Blasting*.

Trubetskoi, K.N., & Viktorov, S.D. (2001). Современные физические и технические проблемы разрушения горных пород [Contemporary physical and technical problems of rock destruction]. St. Petersburg, Russia. *Collected Papers of II International Conference "Physical Problems of Rock Destruction." St. Petersburg, September 25–29, 2000* (SanktPeterburgskii Gornyi Institut, St. Petersburg, 2001), Vol. 148 (1).

Viktorov, S.D., Eremenko, A.A., Zakalinskii, V.M., & Mashukov, I.V. (2005). Технология крупномасштабной взрывной отбойки на удароопасных рудных месторождениях Сибири [Large-Scale Blasting Technology at Siberian Bump-Hazardous Ore Deposits]. Novosibirsk, Russia.

Viktorov, S.D., Galchenko, Yu.P., Zakalinskii, V.M., & Rubtsov, S.K. (2006). Разрушение горных пород сближенными зарядами [Rock Destruction by Contiguous Charges]. Moscow, Russia. Ed. by K.N. Trubetskoi (Nauchtekhlitizdat, Moscow, 2006).

Viktorov, S.D. (2013). Образование субмикронных частиц при горном производстве и новый метод оценки катастрофических явлений [The formation of submicron particles in mining and a new method of assessing catastrophic phenomena]. Moscow, Russia. Herald Russ. Acad. Sci. 83 (2), 128.

LONGWALL TOP-COAL CAVING MINING IN EXTREMELY INCLINED THICK COAL SEAM

Jiachen Wang[1, 2], *Jinwang Zhang[1, 2]

[1]*China University of Mining and Technology, Beijing*
D11, Xueyuan Road, Haidian District
Beijing, China 100083

[2]*Coal Industry Engineering Research Center of Top-coal Caving Mining*
D11, Xueyuan Road, Haidian District
Beijing, China 100083
*(*Corresponding author: jinwangzhang@hotmail.com)*

24th World Mining Congress
MINING IN A WORLD OF INNOVATION
October 18-21, 2016 • Rio de Janeiro /RJ • Brazil

LONGWALL TOP-COAL CAVING MINING IN EXTREMELY INCLINED THICK COAL SEAM

ABSTRACT

It is one of the challenges in China's coal industry to extract extremely inclined thick coal seam (thickness < 20m) safely and efficiently. Practice of extracting such coal seam by longwall top-coal caving (LTCC) mining technique in Dayuan coal mine is introduced in this paper. The instability behavior of roof strata, surrounding rock control and top-coal drawing mechanism in extremely inclined thick seam are analyzed. Loading of shields differ greatly in different locations of the working panel due to the asymmetrical collapse of roof strata and inhomogeneous filling in gob. The coal face stability can be improved by increasing the setting load and capacity of shield supports. Practical performance shows that united reinforcement on opening floor by bolt, steal belt and metal mesh and reinforcement on the tailgate and top-coal at upper part of the panel by cable bolt can ensure the stability of surrounding rock and the safety of mining activity effectively. The drawing process of top-coal shows significant asymmetrical characteristics and recovery ratio shows "π" shape distribution along the seam dip direction. Top-coal in the middle of the working panel has a higher recovery ratio than the upper and lower parts.

KEYWORDS

Extremely inclined coal seam, mining method, longwall top-coal caving, top-coal recovery ratio

INTRODUCTION

Extremely inclined thick coal seam refers to that the dip angle of coal seam is greater than 45° and the thickness is greater than 3.5m. The types of coal seams can be divided into two categories: 1) when the thickness of coal seam is greater than 20m, the coal seam can be extracted by the sublevel top-coal caving mining method. As shown in Figure 1, the seam (seam thickness H_c) was divided into several sublevels (sublevel height H_L) and was mined one by one sublevel. A fully mechanized mining face (face height H_p) was installed at the bottom of each sublevel and the top-coal was drawn through the window at the rear of the caving shield. 2) When the thickness of coal seam is less than 20m and the dip angle is less than 60°, the coal seam can be extracted by longwall top-coal caving (LTCC) mining method (Figure 2).

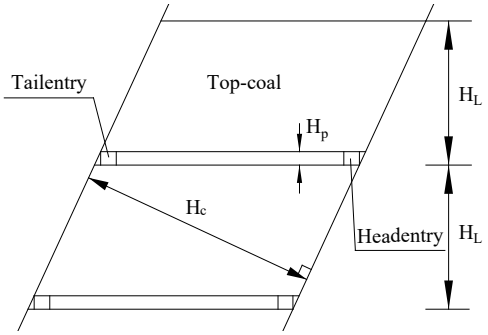

Figure 1 – Schematic diagram of sublevel top-coal caving mining

To ensure the stability of shield supports and cutting equipment, the headgate is drilled along the seam roof for decreasing the dip angle of lower part of the panel. Figure 2 shows the cross-section view of the panel 1201 in Dayuan coal mine, Shanxi province, China. The average dip angle of the coal seam is 48° and its thickness is 6.8m with seam depth varying from 242.6m to195.6m. The coal seam belongs to the Taiyuan formation of Upper Carboniferous. The overburden strata in ascending order are mudstone (0~0.5m), siltstone (0~8.0m) and sandstone (3.61~10.24m). The seam floors are argillaceous siltstone and siltstone (Wang et al., 2016b).

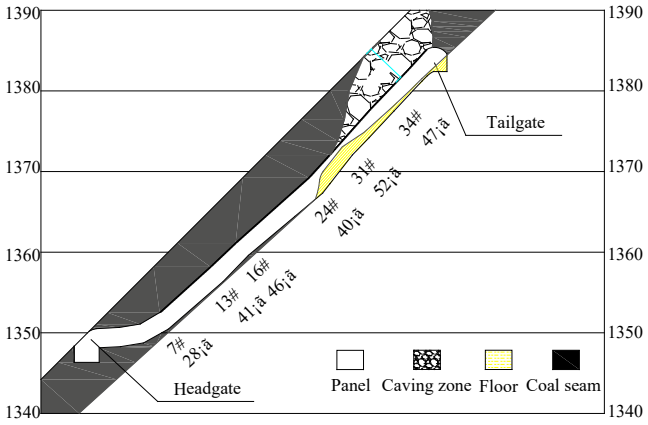

Figure 2 – Cross-section view of the panel 1201 in Dayuan coal mine

FAILURE PATTERN OF ROOF STRATA

Physical simulation and numerical simulation were employed to analyze the movement and collapse of overlying strata in extremely inclined seam, as shown in Figure 3. During the mining and caving process, the collapsed rock from immediate roof moved down to fill the lower part of the gob area. A voussoir beam structure developed in roof strata sagged down, supporting the overlying roof strata with the collapsed rock together. The collapse angle of the lower strata is 57°, while that of upper strata is 65°.

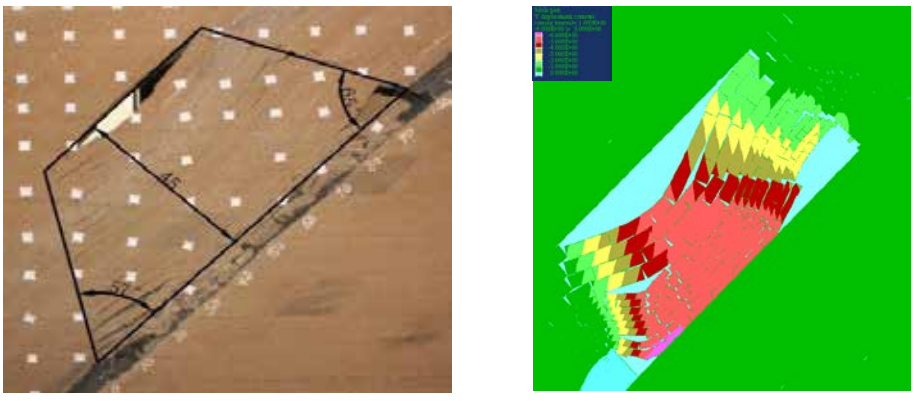

(a) Physical simulation (b) Numerical simulation

Figure 3 – Strata movement during the mining process

The overlying strata movement during LTCC mining in extremely inclined thick coal seam was simulated by Universal Distinct Element Code (UDEC). The result is shown in Figure 3b.

Numerical simulation result is in good agreement with that of physical simulation. The failure patterns of overlying strata in the upper part of the panel are mainly tensile and shear failure. The caved immediate roof slides down to fill the lower part of gob area. It forms a densely filling segment in the lower part, uneven filling segment in the middle part and no filling segment in the upper part of the panel (see Figure 4a).

According to the previous physical simulation and numerical simulation, the shape of collapsed roof strata along the seam dip direction is parabola; and the roof strata can be divided into three segments as shown in Figure 4a. In no filling segment (upper part of the panel), the fracture and instability of roof strata will result in dynamic load on the shield supports. In densely filling segment (lower part), the collapsed rock in the gob and supports share the load from overlying strata. Supports load distribution in the uneven filling segment (middle part) also shows uneven characteristics. Support near no filling segment has a higher load.

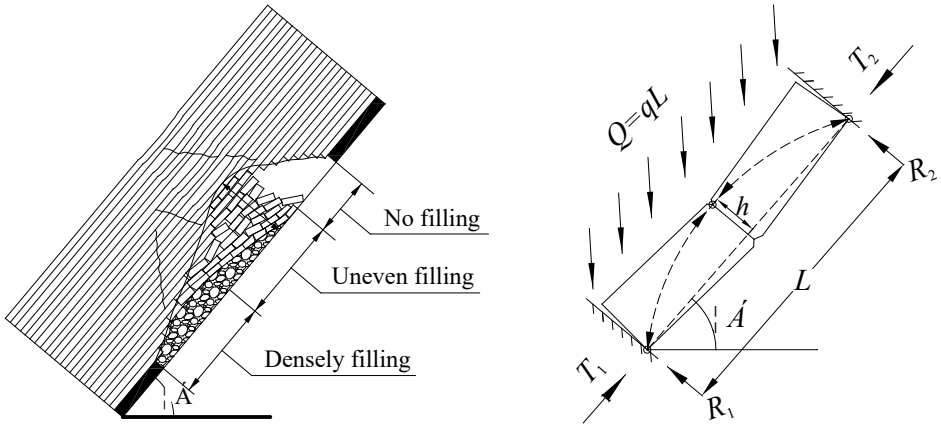

(a) Roof collapse pattern (b) "Voussoir Beam" structure along the dip direction

Figure 4 – Collapse characteristics of roof strata

Before the roof collapse occurred, the "Voussoir Beam" structure along the dip direction formed. According to the equilibrium condition of beam structure, the reaction forces of the upper and lower ends (T_1, R_1, T_2, R_2) can be calculated. The presence of dip angle reduced the vertical roof pressure. The downward sliding force of overlying strata increases the force T_1 along the tilt direction and decrease T_2 at the upper end. So sliding instability occurs easily at the upper end.

SURROUNDING ROCK CONTROL

Not only the coal face and T-junction, but the floor and tailgate need to be controlled to ensure the stability of the working panel in extremely inclined thick coal seam with LTCC mining technique, so it is more difficult to control the surrounding rock in extremely inclined LTCC than in flat condition.

Coal face Shear Failure

There are mainly two types of coal face failure: tension failure and shear failure. The shear failure is a much more common type when the strength of coal is relatively low (UCS≤20MP). The shear failure surface is always a curved surface and its general model is shown in Figure 5 (Wang et al., 2016a). According to the Mohr-Coulomb strength theory, the ratio of the anti-slide force T to slide force S on the shear surface ab is defined as stability coefficient F_S. If $F_S < 1$, then the coal face shear failure occurs; otherwise, the coal face is stable.

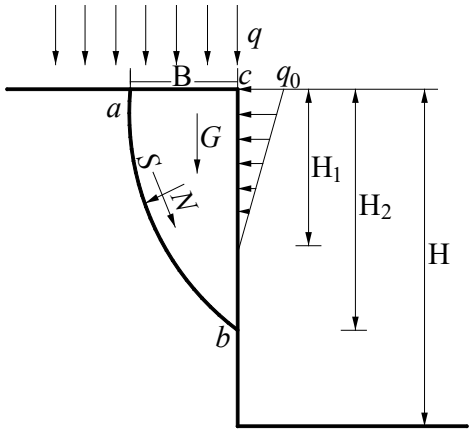

Figure 5 – The mechanical model of coal face shear failure

Where S is the slide force on the shear surface ab; N is the positive pressure on sliding surface; T is the anti-slide force on the sliding surface; q is the load collection degree of roof pressure on coal face; L is the length of sliding surface; q_0 is the horizontal force of protecting plate to coal face; q_0 is load collection degree of protecting plate; H is the height of coal face; H_1 is the height of protecting plate; H_2 is the height of coal face failure; G is the gravity of sliding body.

Mechanical analysis shows that reducing the roof load on coal face and increasing the cohesion of coal have a significant effect on the improvement of coal face stability. However, the internal friction angle of coal, the horizontal force of shield support and the height of protecting plate have limited effects on the coal face stability. Reducing the roof load on coal face and increasing the cohesion of coal are two effective measures for improving the coal face stability, which can be realized by increasing the setting load and capacity of shield support and infusing water into coal seam.

Reinforcement of Panel Floor

The panel floor may slide due to the large dipping of working face, especially during the face-installing period. The slide always occurs in the upper part of the panel face as shown in Figure 6a. Figure 6b shows the contour of shear strain increment and velocity field distribution of the upper panel floor, which is obtained from numerical calculation. The FOS value means factor of safety. To ensure the stability of set-up room, the opening floor was reinforced by bolt and steal belt after metal mesh placement (see Figure 7).

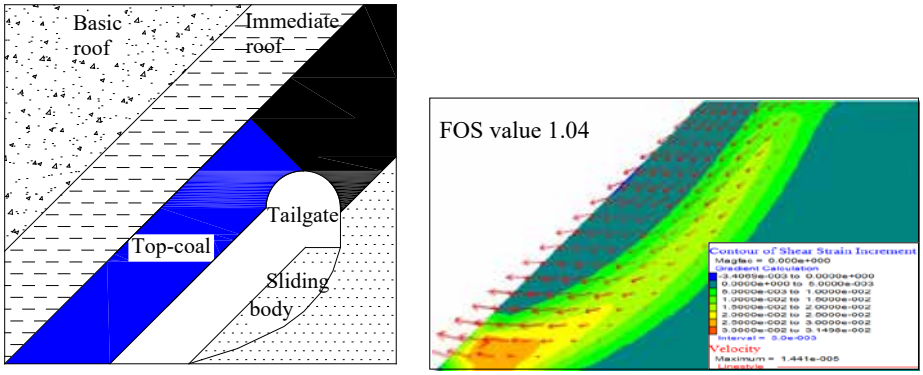

(a) Sliding of upper floor (b) Shear strain distribution

Figure 6 – Stability analysis of floor

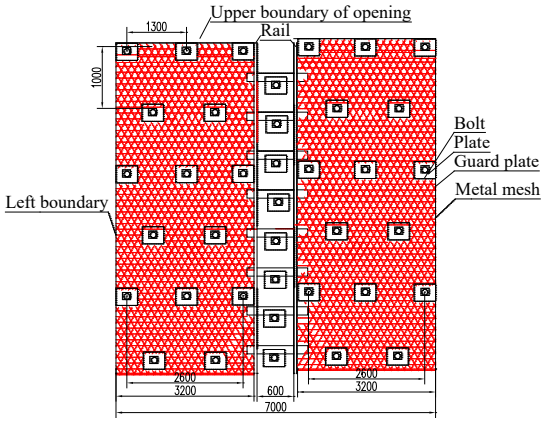

Figure 7 – Reinforcement of opening floor

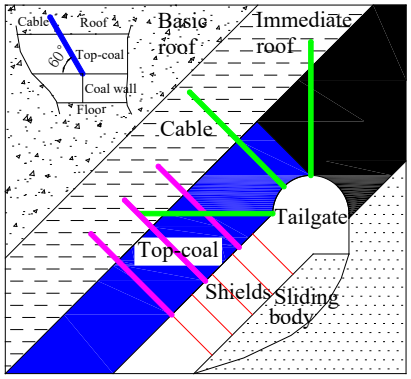

Figure 8 – Reinforcement of tailgate and top-coal

Reinforcement of Tailgate

Five-shield-wide top-coal in the upper side of panel remains undrawn in order to keep the stability of equipment and drawing process. At the same time, to avoid the tailgate damage resulting from the overdrawing of top-coal in the upper part of the panel, parts of the tailgate and top-coal was reinforced by cable bolt, as shown in Figure 8.

TOP-COAL DRAWING MECHANISM

As LTCC mining face in extremely inclined thick coal seam is extremely rare around the world, researches on top-coal drawing mechanism are not common. In this paper, 3D physical simulation and numerical simulation were employed to analyze the top-coal drawing mechanism. At the same time, the field observation of top-coal recovery ratio is carried out by using self-developed Top-coal Tracking Device (TDD).

Physical Simulation Experiment

Figure 9a shows the 3D physical simulation by self-developed top-drawing device and its

final state. A total of 1890 marked particles were set in the upper part of the top-coal before the drawing process. The spatial layout of marked particles is shown in Figure 9b. The drawing body can be obtained by analyzing the spatial coordinates of marked particles that were drawn out. Drawing bodies of shield No. 7, No. 8, No. 9 and No. 10 were shown in Figure 10.

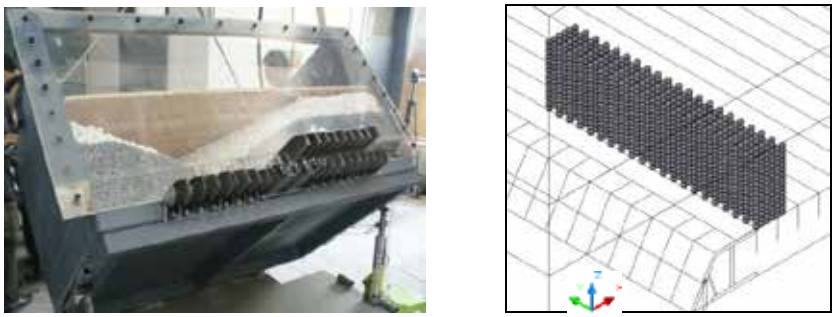

(a) 3D experiment test device (b) Layout of marked particles

Figure 9 – 3D top-coal drawing experiment

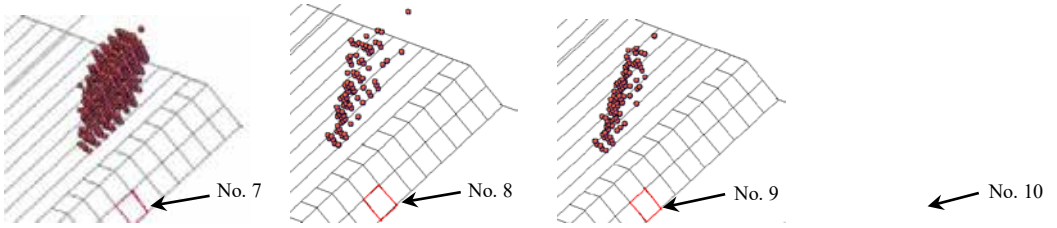

(a) Shield No. 7 (b) Shield No. 8 (c) Shield No. 9 (b) Shield No. 10

Figure 10 – Drawing body's spatial shape of different shields

We can see from Figure 10 that when the top coal-was drawing from top to bottom, the first drawing shield (shield No. 7) has the largest drawing volume. This is because not only the top-coal above the shield No. 7 but also parts of top-coal above the shield No. 1-6 were drawn out through the drawing window of shield No. 7. However, the drawing volume of shield No. 8, No. 9 and No. 10 is very small. Due to the large dip angle of the panel, the drawing bodies of different shields all have an obvious developing tendency towards the upper side of the panel face. Such a characteristic of drawing body will cause the overdrawing of top-coal in the upper part of the panel face, which has a great impact on the stability of the tailgate. The overdrawing phenomenon increases the tailgate (beneath the top-coal) deformation and makes it very difficult to maintain.

According to the total number of marked particles that were drawn out, the overall recovery ratio was calculated (75.93%). Variation in top-coal recovery ratio along the direction of the face advancing is very small. The top-coal recovery ratios fluctuated between 75.00% and 82.00%. The minimum value is 64.76% and then it tended to be stable around the average value.

Along the seam dip direction (parallel to the faceline), the distribution of top-coal recovery ratio is shown in Figure 11. It shows "π" shape distribution in the 3D loose top-coal drawing experiment. That is to say that the middle part of the panel has a higher recovery ratio than the lower and upper parts in extremely inclined thick coal seam with LTCC mining. Also, the recovery ratio in

lower part is much less than that in the upper part. These are unique characteristics of extremely inclined LTCC compared to falt LTCC (Wang et al., 2015).

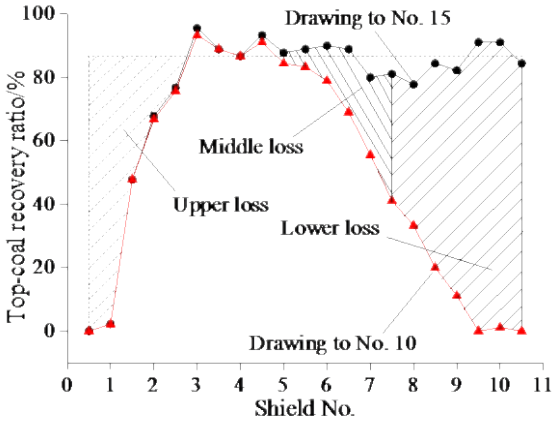

Figure 11 – Distribution of top-coal recovery ratio along the dip direction (parallel to the faceline)

Numerical Simulation

The numerical model of extremely inclined thick coal seam with LTCC mining was established by Particle Flow Code (PFC). The boundary of top-coal and contact force distribution after several drawing processes is shown in Figure 12. During the drawing process, the boundary of top-coal always shows asymmetric characteristics due to the influence of coal seam dip angle. Boundary near the lower end is steep and short while that near the upper end is gently sloping and relatively long.

Figure 12 – Boundary of top-coal and contact force sides

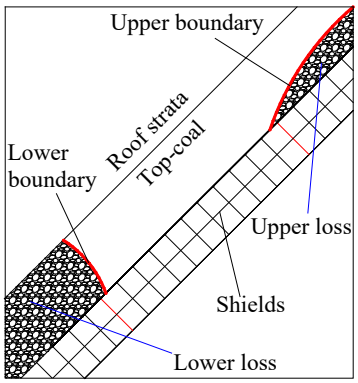

Figure 13 – Top-coal loss at upper and lower

During the top-coal drawing process, the shape difference between upper and lower boundary is obvious, which will cause the overdrawing of top-coal in the upper part of the panel and insufficient drawing of top-coal in the lower part, as shown in Figure 13. This is the root cause of the difference value of top-coal loss at upper and lower sides of panel and the "π" shape distribution of top-coal recovery ratio along the seam dip direction (see Figure 11) in extremely inclined seam with LTCC mining method.

Field Observation of Top-Coal Recovery Ratio

The field observation of the top-coal recovery ratio was conducted in Dayuan coal mine by using a self-developed top-coal tracking device (TTD). The markers with radio frequency identification tags were installed in the top-coal above the shield by drilling boreholes between two neighboring canopies. Location of different boreholes is shown in Figure 14a. Markers with different IDs were located every 0.5 m in height in the borehole (see Figure14b). The spatial coordinates and ID information of the markers were recorded after the installation completed.

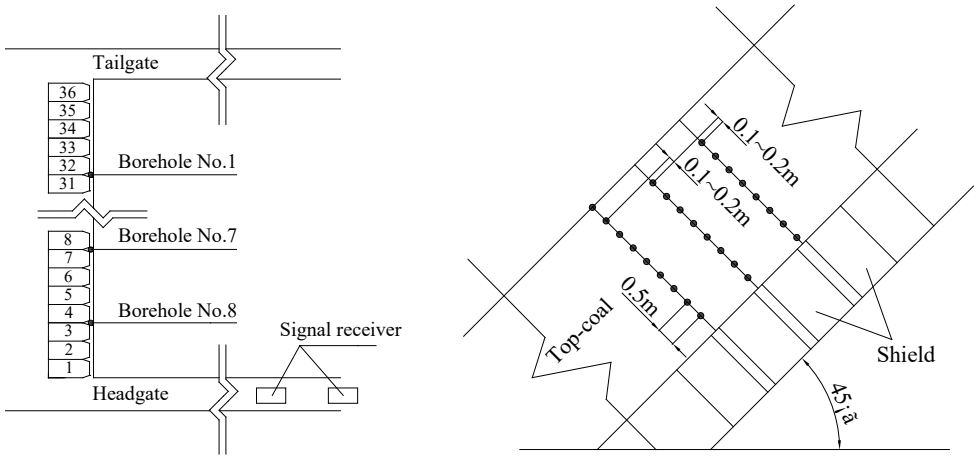

(a) Location of the boreholes (b) Layout of markers

Figure 14 – The observation scheme of recovery ratio testing

During the face advancing and top-coal drawing process, markers were drawn out from the drawing windows with the top-coal and then removed by the armored chain conveyor. The signal receiver mounted on the belt conveyor in the headgate picked up the signals that can identify the number and sequence of individual markers, and the recovery ratio of top-coal was calculated (Wang et al., 2014). The field observation result shows that the top-coal recovery ratio is 75.68% and its distribution also has "π" shape characteristic along the dip direction, which agrees with the result of similar simulation experiment (75.93%).

CONCLUSIONS

(1) When mining extremely inclined thick coal seam with LTCC method, the shape of collapsed roof strata along the seam dip direction is parabola due to the asymmetrical roof collapse. The roof strata can be divided into three sections according to the filling extent: no filling segment, uneven filling segment and densely filling segment. Generally speaking, the shields in upper part of the panel face (no filling segment) have the largest loads, followed by those in the middle part of the panel. Shields in the lower part have the minimum loads. The supporting resistance of shields in the upper part shows relatively severe fluctuations because roof strata in this area has an obvious dynamic impact tendency.

(2) The coal face stability can be improved by increasing the setting load and capacity of

shield supports. Practical performance shows that united reinforcement on opening floor by bolt, steal belt and metal mesh and reinforcement on the tailgate and top-coal at the upper part of panel face by cable bolt can ensure the stability of surrounding rock and the safety of mining activity effectively.

(3) The drawing process of top-coal shows significant asymmetrical characteristic in extremely inclined seam with LTCC mining. It is very difficult to control the top-coal drawing process because of the uneven flowing of top-coal above the shield canopies. So keeping the shields having uniform stress by effective controlling of the top-coal drawing process is one of the important measures to improve the shields stability.

REFERENCES

Wang, J., Yang, S., Li, Y., Wei, L., & Liu, H. (2014). Caving mechanisms of loose top-coal in longwall top-coal caving mining method. *International Journal of Rock Mechanics and Mining Sciences*, 71, 160-170.

Wang, J., & Zhang, J. (2015). Study on top-coal recovery ratio distribution law of longwall top-coal caving mining in steeply thick coal seam. *Coal Science and Technology (Chinese Language)*, 43, 1-7.

Wang, J., Yang, S., & Kong, D. (2016a). Failure mechanism and control technology of longwall coal face in large-cutting-height mining method. *International Journal of Mining Science and Technology*, 26, 111–118.

Wang, J., Yang, S., Li, X., & Yang. J. (2016b, July). Roof movement and loading calculation of longwall top-coal caving mining in extremely inclined thick coal seam. *Proceedings of the 35th International Conference on Ground Control in Mining*, Morgantown, WV, USA.

METHANE IN POLISH COAL MINES – METHODS OF CONTROL AND UTILISATION

N. Szlązak[1], D. Obracaj[1], *M. Borowski[1], J. Swolkień[1], M. Korzec[1]

[1] Agh University Of Science And Technology
Faculty Of Mining And Geoengineering
Mickiewicza av. 30, 30-059 Kraków
*(*corresponding author: borowski@agh.edu.pl)*

24th World Mining Congress
MINING IN A WORLD OF INNOVATION
October 18-21, 2016 • Rio de Janeiro /RJ • Brazil

METHANE IN POLISH COAL MINES - METHODS OF CONTROL AND UTILISATION

ABSTRACT

Methane hazard often occurs in hard coal mines and causes very serious accidents and can be the reason of methane or methane and coal dust explosions. History of coal mining shows that methane released from the rock mass to the longwall area was responsible for numerous mining disasters.

In Poland coal seams are mined in 30 mines only by means of underground longwall system of excavation. All kinds of natural hazards, that can occur in underground environment, are present in Polish coal mines. Total output of hard coal production in 2014 was 72,5 million tons, of which 78% came from gassy coal seams.

The quantity of methane captured in Polish coal mines is growing every year. In 2014 the amount of captured methane exceeded 37% of mines' absolute methane bearing capacity. Owing to adequately selected ventilation and methane drainage systems, the effectiveness of methane drainage process reached up to 70%. The paper presents the methane drainage efficiency for different systems used in Polish coal mines.

Methane captured by drainage system is utilized in varying degrees. It is worth noting that this tendency has been increasing each year. In 2014 about 70% of captured methane brought economical benefits. The paper presents the ways of methane utilization and the work to be undertaken in improving its development. In Poland, depending on the methane quality and quantity, the CMM is used in various projects. They include heat production through gas combustion in boilers or technological installations (e.g. coal drying plant), cogeneration of power and hot water, cogeneration of power and technological steam, cogeneration of power and factor of drying process, cogeneration of heat, cool and power and electricity generation in combined systems.

KEYWORDS

Methane hazard, control of methane, longwall ventilation system, system of longwall methane drainage, utilization of methane

INTRODUCTION

The main source of methane are coal deposits because it is autochthonous gas and is closely related with carbonification and forming of coal deposits. Degree of methane saturation in coal deposits depends on numerous factors; mainly on presence or lack of insulating layers in cover deposit that allow or do not on degasification and easily methane outflow into surroundings.

Conducting mining works in coal deposits of high methane hazard without using of special measures to combat (ventilation, methane drainage) could be impossible. Control of methane hazard depends also on other co-occuring natural dangers for which used preventive actions eliminate methane hazard prevention. (Karacan & Riuz at al. 2011, Szlązak & Korzec, 2010, Szlązak & Borowski at al. 2014). Safety in mines excavating coal deposits highly saturated with methane depends on the correct estimation of methane hazard, drawn up forecasts, conducted observations, hazard control as well as undertaken prevention measures.

Predictive methane action includes identification and control methods of methane hazards as well as means of combating the explosive accumulation of methane in longwall workings.

METHANE HAZARD POLISH COAL MINES

Methane in coal deposits constitutes a serious threat to safety in underground coal mines. Geological conditions of methane occurrence in coal seams, as well as the low permeability of Polish coal, without mining exploitation, cause the low methane release. The amount of methane released is closely related with the range of conducted mining works; actual exploitation as well as excavation in site construction (Szlązak et al., 2011; Szlązak et al., 2015).

Methane explosions are responsible for many deadly mining disasters. 18 accidents connected with ignitions or explosions of methane took place between 2009 and 2014; 25 miners lost their lives, 40 were seriously injured and 31 were slightly wounded. These happenings occurred in longwalls

using “U” as well as “Y” ventilation system and are presented in the Table 1.

Tab. 1. Summary of the events related to methane ignition in Polish coal mines between 2010 and 2014 (WUG, 2010-2014)

Mine	Year	Reason
„Mysłowice-Wesoła” Ruch Wesoła	2010	methane ignition accumulated in longwall gob; caused by spontaneous coal combustion
„Krupiński”	2011	methane ignition caused by mechanically generated sparks
„Murcki-Staszic” Ruch Staszic	2011	methane ignition caused by violent methane emission from rock mass
„Bielszowice”	2011	methane ignition outflowing from fractured rock mass
„Murcki-Staszic” Ruch Staszic	2013	methane ignition caused by mechanically generated sparks
„Murcki-Staszic” Ruch Staszic		methane ignition caused by friction between belt’s elements and sandstone rocks under the shearer
„Rydułtowy-Anna”	2013	methane ignition caused by sparks generated by coal mining operations
„Knurów-Szczygłowice” – Ruch Szczygłowice	2013	methane ignition caused by sparks generated by coal mining operations
„Sośnica-Makoszowy” Ruch Sośnica	2013	methane ignition caused by open fire
„Sośnica-Makoszowy” Ruch Sośnica		local spontaneus combustion in coal pillar
„Borynia-Zofiówka-Jastrzębie” – Ruch Zofiówka	2013	methane ignition caused by sparks generated by coal mining operations
„Chwałowice”	2014	methane ignition caused by blasting
„Budryk”	2014	methane ignition caused by sparks generated by coal mining operations
„Bielszowice”	2014	methane ignition caused by sparks generated by coal mining operations
„Mysłowice-Wesoła” Ruch Wesoła	2014	the Commission appointed by State Mining Authority is investigating the reason of fire

Methane ignition was one of the main reason of fatal accidents in 2014 in mining industry.

In Poland in 2012, coal extraction amounted 72,5 million tons and was coducted in 30 coal mines (according to Industrial Development Agency). 21 were methane mines, of which 15 exploited hard coal deposits of high methane hazard. The annual output from methane seams was 56,7 million Mg (it is 78,2% of total output, which means 3% increase compared to 2012) and from non-methane seams was 15,8 million Mg (21,8% of total output). In 2014 exploitation was performed by means of 200 longwall panels, 166 of them were methane seams (83%) and 42,5% classified into high methane hazard.

During coal production about 891,2 million m^3 of methane is generated (absolute methane bearing capacity) thus meaning 1 695,6 m^3CH_4/min (including 1 084,7 m^3CH_4/min emitted along with ventilation air). Table 2 presents the development of methane bearing capacity in Polish coal mines in years 2004-2014 and the amount of methane captured by drainage system and utilized.

Picture 1 also presents the growth of methane emission compared to 1997. The increase of methane bearing capacity of coal mines, despite the decline of coal output, has been observed in recent years. That tendency is caused by higher methane content of coal seams as well as increased mining of methane coal seams.

Tab. 2. Summary of absolute methane bearing capacity, VAM, methane drainage and methane utilized for the last 5 years (GIG, 2003-2010; WUG, 2010-2014; Szlązak & Borowski et al., 2015)

Lp.	Years	2010	2011	2012	2013	2014
1	Number of coal mines	32	31	31	30	30
2	Coal output, mln Mg	76,1	75,5	79,2	76,5	72,5
3	Absolute methane bearing capacity, mln m^3/year	834,9	828,8	828,2	847,8	891,1
4	Ventilation air methane (VAM), mln m^3/year	579,0	578,6	561,5	571,2	570,1
5	Methane obtained from drainage system, mln m^3/year	255,9	250,2	266,7	276,6	321,0
6	Amount of utilized methane, mln m^3/year	161,1	166,3	178,6	187,7	211,4
7	Methane emission to the atmosphere, mln m^3/year (line.4+line.5-line.6)	675,3	662,5	650,2	660,1	679,7

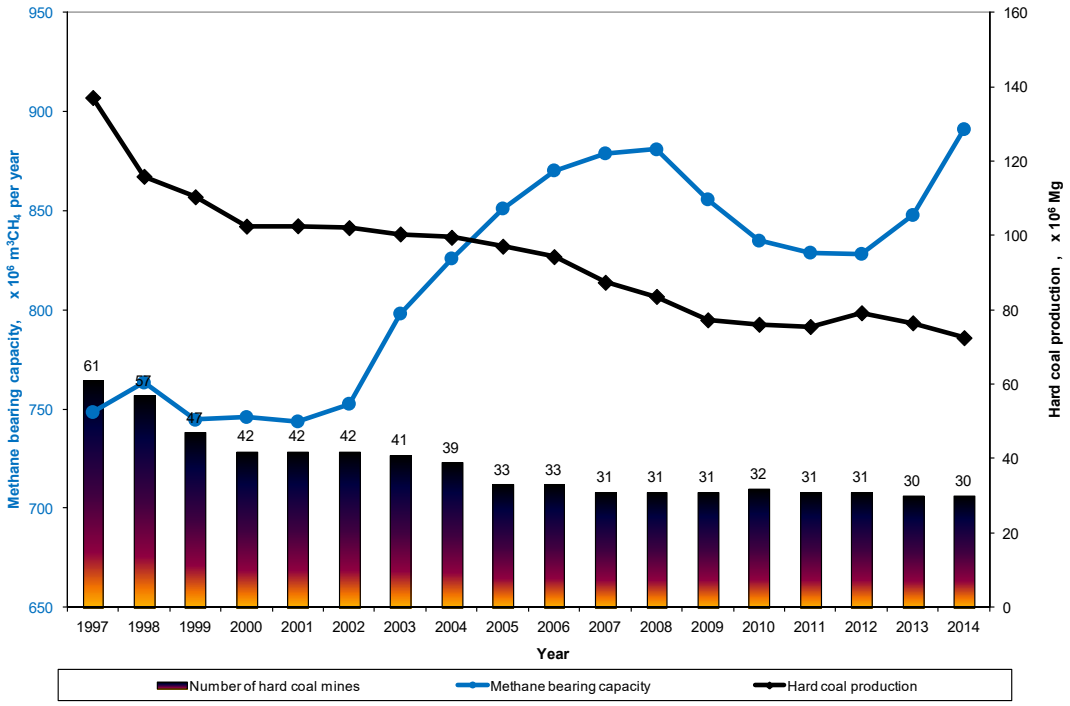

Fig. 1. Summary of changes in the production volumes and methane bearing capacity in hard coal mines between 1997 and 2014.

Selection of methane prevention is closely related to longwall ventilation systems. Ventilation system should be depended on predicted methane bearing capacity of longwall workings and chosen at the design stage.

LONGWALL VENTILATION SYSTEMS

In Polish coal mines the longwall system from the boundaries of the deposit is commonly used. It allows to get high output concentration at relatively low investment outlays. The exploitation system needs the selection of longwalls ventilation system.

Presently ventilation systems from the boundaries are most frequently used (Fig. 2):

- system U,
- system Y:
  - with reblowing,
  - with parallel ventilation roadway,
  - with air carrying away in two directions.

The paper presents two mainly used longwall ventilation systems and the principles of their selection depending on natural hazards.

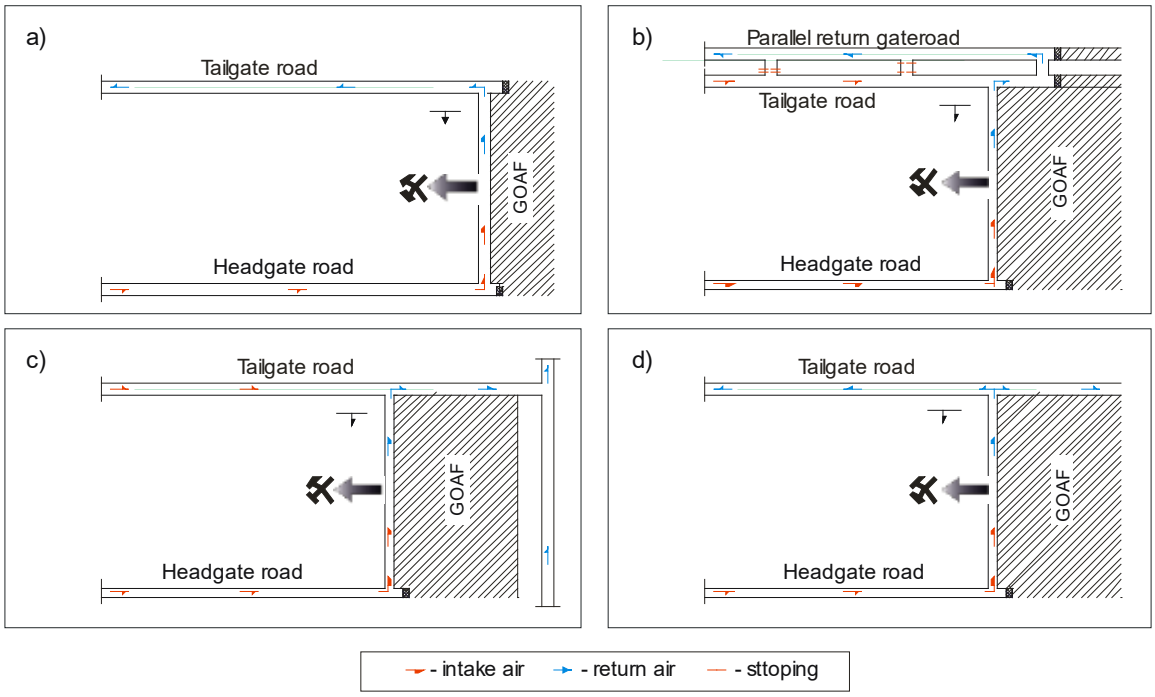

Fig. 2. The most popular panel ventilation systems in Polish hard coal mines a) U ventilation system, b) Y - return side ventilation system with parallel return gateroad c) Y - return side ventilation system, d) Y - return side ventilation system (bleeder system),

U system ventilation is generally employed. 131 out of 166 longwalls in methane mines were ventilated by U system in 2014 (WUG, 2010-2014). The methane mines use a set of preventive actions in order to meet safety requirements. These include intensive ventilation, methane drainage, methane monitoring and extra ventilation equipment (Szlązak et al., 2011; Szlązak & Borowski et al., 2015).

U ventilation system from the boundaries limits the control of methane hazard due to lack of possibility to effective methane drainage (Szlązak et al., 2008; Szlązak et al., 2011; Szlązak & Borowski et al., 2015). Fighting methane hazard in seams of low thickness is particularly difficult. There are difficulties in supplying the adequate air amount to longwall face then.

The system effectively limits the progress of coal spontaneous combustion. It ensures limited air-flow through gobs and lowers the fire hazard only in case of proper longwall extraction advance. The complicated tectonics of deposits and geological disturbances might cause problems in obtaining the longwall extraction advance that minimizes fire hazard. In case of endogenous fire in gobs, the system makes its containing difficult. The system is irrelevant in extremely tough conditions, when there is serious methane hazard with limited longwall extraction advance and spontaneous combustion of coal occurs. It causes difficulties in effective combating of coexisting mining hazards.

It happens that methane bearing capacity during exploitation is significantly higher than estimated in the technical project. Therefore, the replacing U system with Y system is necessary but generates additional costs (second ventilation roadway).

U ventilation system is generally used in longwalls with low methane explosion danger; with high methane bearing capacity the system can be used only including effective methane drainage (Szlązak et al., 2008; Szlązak & Borowski et al., 2015).

Y ventilation system (various types) is used to fight serious methane hazard. The system is appropriate both in highly and lowly methane saturated coal seams; the same applies with fire hazard or its lack. Also these longwalls achieve the record level of advance and output. In 2014 “Y” system ventilated 27 out of 166 longwalls in methane mines.

Y ventilation system with tailgate heading is used in low thickness deposits in hazardous methane conditions. It allows to move methane concentration away from longwall face. The air is supplied by two parallel roadways. After the longwall is ventilated, the gasses are mixed with fresh air and removed. Y ventilation system with air distribution in two directions is convenient for longwall panels of low and medium thickness (Szlązak et al., 2008).

Y ventilation system with parallel ventilation heading is used in extremely conditions. The air

is supplied by means of bottom gate and the outlet of longwall is reblowing from the tailgate heading. In the first phase the air is guided from the longwall to gobs and next set-up entry between two tailgate excavations towards upper heading. The main advantage of this system is the possibility of extra air-flow supply and its control what simplifies methane drainage of over- and underlying coal deposits.

SYSTEMS OF LONGWALLS METHANE DRAINAGE

Methane drainage of rock-mass is the most effective method of controlling methane hazard as it ensures the reduction of methane outflows into the working areas. The method that has proved the most efficient is draining methane from rock-mass and gobs and transporting it to the surface through pipelines, using the depression from drainage station pumps. Although this method ensures the desired parameters of ventilation, it imposes certain requirements concerning the methods of opening up the coal seams.

There are two methods of methane drainage in so far applied technologies. The first method involves drilling boreholes, called methane boreholes, from tailgate roadway to an unstressed zone in roof or floor layers of a mined seam. The location and parameters of the boreholes depend on the exploitation system and the way of longwall ventilation.

The second method is based on drilling drainage galleries in seams situated under or over the mined seam therefore is called overlying or underlying drainage method.

Defining of desorption zone caused by exploitation is necessary during methane drainage of the adjacent coal seams. Drainage holes should be situated in stress-relieved zone while not crossing the crack zone. In Polish conditions, the method of calculating the slope angles of the drainage boreholes, presented in the figure 3 below, produces good results.

The location of drilled boreholes is dependent on mining and ventilation systems of longwalls. Research results of drainage efficiency in longwall workings with different ventilation methods were presented in the publications: Szlązak et al., 2014; Szlązak & Borowski et al., 2015.

An analysis concluded that the highest effectiveness of methane drainage has been achieved by means of Y ventilation system with parallel ventilation heading and “U” system with overlying drainage gallery. In case of classic U ventilation system of longwall panel, over time, boreholes drilled from the tailgate roadway behind the longwall front are lost. It is caused by degradation of ventilation heading and because shielding pipes are placed in close proximity to the longwall gobs. In relation to the parallel tailgate roadway, the pillar between roadways allows to get permanent air-tightness of drain holes that results in obtaining a gas mixture with higher methane concentration.

Table no. 3 presents the average efficiency of methane drainage between 2002 and 2012 in Polish coal mines depending on methane bearing capacity of longwall panel.

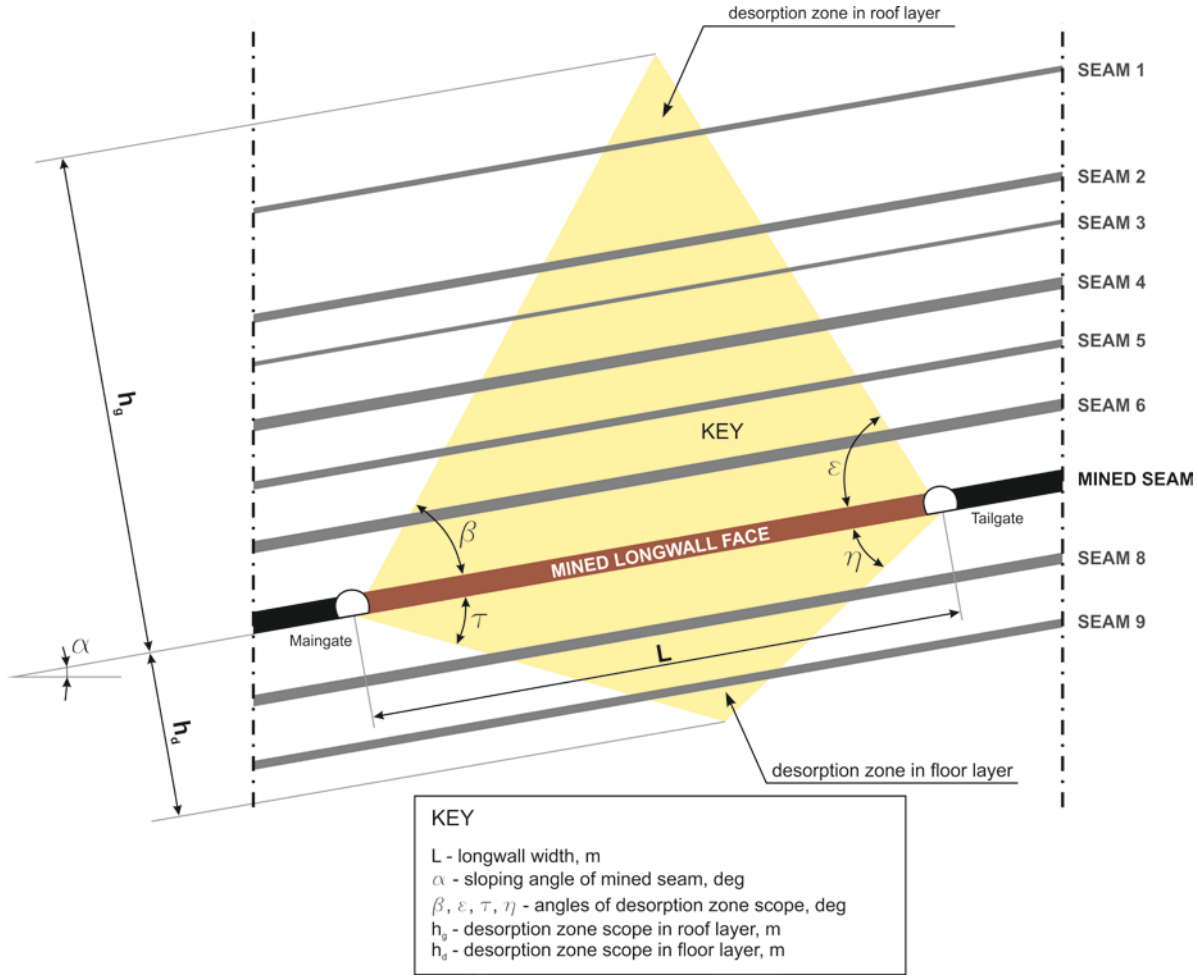

Fig. 3. Determining the methane desorpion zone during longwall's exploitation based on work by G. Flügge'a (Szlązak et al., 2014; Szlązak et al., 2015)

Tab. 3. The relations between the efficiency of methane drainage in longwalls and the type of the ventilation and drainage systems in Polish coal mines in the last 10 years.

Breakdown	Methane bearing capacity, m^3/min									Average drainage efficiency, %
	<10	10-20	20-30	30-40	40-50	50-60	60-70	70-80	>80	
Longwalls ventilated U system	38,5	39,0	40,6	38,3	48,8	64,0	x	x	x	41,2
Longwalls ventilated Y system	33,8	43,7	52,4	56,1	49,9	46,2	57,9	x	x	48,7
Longwalls with a parallel roadway and ventilated U system	x	x	58,0	60,1	62,2	64,2	64,5	68,3	71,5	63,9
Longwalls with drainage gallery and ventilated U system	49,0	58,6	60,2	62,6	68,4	64,7	68,6	68,8	76,0	63,4

x – oznacza, że nie stosowano takiego systemu odmetanowania w danym zakresie metanowości

The average efficiency of methane drainage in longwalls in the years 2002-2012 was 54%. The lowest efficiency (41%) was in longwalls with low level of methane bearing capacity ventilated with U system. In contrast, the highest average methane drainage (63%) was achieved in ventilated longwalls with a parallel roadway and with overlying drainage gallery. The efficiency of methane drainage in longwalls ventilated Y system was 49%.

In Table 3 the yellow colour presents the efficiencies of methane drainage, which do not provide safe work conditions due to high methane emission. Regarding the efficiency of methane drainage

that has been obtained, the ventilation air methane (VAM) in longwalls ventilated U system should not exceed 15 m^3CH_4/min.

RECOMMENDATIONS FOR EXPLOITATION DESIGN PROCESS HAVING REGARDS TO AEROLOGICAL HAZARDS

Planning of the specific coal extraction should be the multiple stage process and executed in the right order with respect to the security of all mining operations. These consist of:

- Preliminary identification of threats – assessment made on the basis of specific natural conditions and mining works carried out so far in the area (measurement of methane content in proximity to mined coal seams).
- Preparation of a conceptual design of the exploitation – selection of exploitation system, technical equipment, technology and production plan.
- Detailed diagnosis of threats – it is preparation of forecast concerning the threat development, taking into account the results of first phase of identification, conditions of preliminary project and design of hazard monitoring system (kind and location of sensors, safety systems, etc.).
- Revisions of design intents – following the verification of conceptual design's criteria with threat forecasts and monitoring project after making the necessary changes.
- Planning of preventive works to reduce different threats – including corrected design assumptions and dominant danger.
- Preparation of technical project - following the verification of design assumptions with plans of preventive works after making the necessary changes.

This planning mode tends to eliminate or at least reduce the unpredictability that usually results in financial loss or even dangerous accidents.

Guidelines on planned hard coal exploitation, taking into account the methane hazard, may be specified as follows:

1. Before starting the design process of exploitation in new coal seams, the level of natural hazards, that save as the basis for a conceptual design, should be identified.
2. The conceptual design for coal deposit's extraction or its parts highly saturated with methane must include forecast of methane bearing capacity that determines the selection of ventilation system and development of guidance on the prevention of methane hazard.
3. The technical project should contain the further detailed forecast of methane bearing capacity together with the possible ventilation solutions to combat danger.
4. The longwall workings with methane bearing capacity estimated to be greater than 10 m^3CH_4/min should be equipped with methane drainage systems. Methane drainage of the longwall workings can be conducted if the predicted methane bearing capacity is lower than 10 m^3CH_4/min – depending on the mining and geological conditions.
5. To effectively fight methane hazard and successfully conduct methane drainage, one of four ventilation systems may be applied. The principle of proper choice of methane drainage and ventilation systems can be indicated on the basis of results presented in Table 3.
6. System with methane drainage gallery can be used if above the mined coal seam there is thin one (that cannot be exploited) and is situated at a distance corresponding to 5 times the thickness of the deposit (however, not be less than 12 m above the mined one). In other cases, it is considered not to be appropriate to use this method.
7. Selection of parameters and location of the boreholes should be dependent on chosen longwall ventilation system, predicted methane bearing capacity and demarcated methane desorption zone.
8. Methane drainage project should include:
   - calculations of the required pressure in boreholes,
   - dimentioning of the installation and the selection of pipeline diameters,
   - selection of the monitoring system and control of the mixture distribution in methane drainage network.
9. Every time after identification of required quantity of methane captured in new ventilation area, mine methane drainage network should be tested in regard to its methane-capture capability. Needed value of pressure (negative pressure) must be supplied in pipelines due to flow resistance of gas mixture (methane-air) and required pressure (depression) in all openings of boreholes.

CAPTURED OF UTILIZATION METHANE

Methane hazard in hard coal mines generates an increase in operating costs. This is related to financial outlays assigned for methane prevention and the obligation to conduct methane drainage to reduce the level of methane explosion hazard. The gas produced during mining operations can be either high quality gas (such as released in advance of mining) or low methane concentration such as VAM. Although methane drainage is costly, it is worth noting that it can be used directly to supply or generate energy, which in turn can deliver economic returns for the mine, even bring further benefits.

Ways of methane utilization are presented in Table 4. Activities applied depending on the gas source in technological process of coal producing were also included in the table (Karacan & Riuz at al. 2011, Szlązak & Borowski et al. 2015).

Tab. 4. Ways of CMM utilization

Technology	*gas recovered from ventilation air (VAM)*	*gas recovered from mined coal seam*	*gas recovered from virgin coal seams*
Recovery units	fans	vertical shafts, horizontal boreholes	vertical boreholes
Recovery equipment	fans, pipeline system	boreholes and/or surface equipment, compressors and pumps	boreholes and/or surface equipment, compressors and pumps
Calorific value	low (CH_4 content< 1%, usually < 6%	average (10-30 MJ/kg)	high (to 37 MJ/kg)
Ways of utilization	in the air to combust in boilers, piston engines or gas turbines; conversion to electricity and heat in reactors (flow-reversal oxidizers)	energy production; transmission to natural gas network (after enrichment process), direct using (e.g. industrial)	similar as mined coal seams; in addition as raw material for chemical industry
Availability	first group of technologies available, the second in demonstration stage	technologies available	technologies available
Applicability	utilization possibility dependent on local conditions	widespread use, depending on the location	dependent on the technology of excavation, finance and location
Methane utilization rate	recovery 10 – 90%	up to 50%	up to 70%

At present, most of Polish coal mines have methane drainage systems. These actions are designed to ensure a sufficient level of methane safety or for technological reasons (methane captured by drainage system results in lower emissions to longwall workings).

Depending on the quality and volumes of extracted methane, it can be used in variety of projects, including (Szlązak & Borowski et al. 2015):

- energy generation/energy recovery
  - heat production (technological and heating needs)
  - electricity production,
  - combined systems (production of electricity, heating and cooling),
- gas transmission ouside the mine,
- gas production that meets natural gas network standards,
- liquefaction process.

In Polish mines' conditions, methane is being extracted in places where mining operations are carried out. Due to constantly changing mining conditions, methane supply can fluctuate in quantity and quality. The firedamp of unstable quality and quantity parameters cannot be sent to gas network. It would entail using a costly process of purification and enrichment.

Systems enabling the economic use of captured methane should be located as close to the mines as possible. In that case, power generation may involve heat production or electrical energy and waste heat in the so-called cogeneration systems. The tri-generation systems enable additionally production of chilled water.

Type of fuel that is burned significantly affects the operations of devices. Not all devices available on the market can be powered by CMM. A decisive factor for changeable use of fuel are Wobbe index, methane number and combustion rate. The minimum methane content is usually also required. For the purpose of enabling the motor power, relevant design changes in the power supply

and combustion chambers are necessary. Adapting operations are mainly linked to changes of compression ratio and average pressure of recirculation system and, in certain cases, also changes of mixture's homogenization degree and the ignition energy. Design changes are mostly performed in cylinder head and result in combustion chamber's shape. The simplest modifications concern changes in chamber's volume and advanced ignition timing. More complicated adjustments relate to power supply system, adequate turbulence for efficient mixing in combustion chamber, variations in the composition of the mixture, and finally an increased quantity of spark plugs. Nevertheless, despite these issues, piston engines are commonly used in installations powered by specialty gases. Motor power and its efficiency reduce when gas captured by drainage system is used.

Methane liberated during coal mining may be recovered and used in network gas production. This will, however, require the use of technology to upgrade methane parameters in order to meet the pipeline quality standards.

An alternative way to develop coal mine methane is the process of its purification and liquefaction (LNG). Liquefied natural gas contains 97% methane and 3% N_2 and, after the re-gasification, has effectively identical characteristics with network natural gas. The main difference is that LNG produced from methane recovered via methane drainage systems do not contain higher hydrocarbons and water that is removed before starting the cryogenic processes.

Methane released into longwall workings is directed, along with ventilation air, to mine's shafts. There is a limited number of technologies that can beneficially use the dilute methane emitted from mine ventilation shafts (VAM). These include:

- thermal flow-reversal reactor (TFRR),
- catalytic flow-reversal reactor (CFRR),
- methane concentrator,
- gas turbines (CGT i CCGT),
- micro turbines,
- hybrid turbines,
- others.

Most of these technologies allow the use of VAM at concentration 0,3-0,6%, some require higher quality drained gas but there are methods that are able to process methane concentration from 0,1%. Research efforts are underway at international level to make greater use of VAM.

Installation for VAM utilization consist of the following components:

- device for taking mixture of air and methane from ventilation shaft
- device for mixture transport,
- reactors to methane burn (produce heat and exhaust gas),
- heat exchangers water-gas (possibility to use thermal energy),
- chimneys to release exhaust gases.

In Australia, the BHP Biliton Illawarra Coal West Cliff Ventilation Air Methane Project (WestVAMP) - which became operational in 2007 and is the first power station in the world that uses the extremely dilute methane from West Cliff Mine to produce electricity and to reduce greenhouse gas emission (Karacan & Riuz at al. 2011). The plant generates five megawatts of electricity taking 250 000 m^3/h of VAM (methane concentration 0,9%).

CONCLUSIONS

Before starting the design process of exploitation in new coal seams, the level of natural hazards, that save as the basis for a conceptual design, should be identified. The conceptual design for coal deposit's extraction or its parts highly saturated with methane must include forecast of methane bearing capacity that determines the selection of ventilation system and development of guidance on the prevention of methane hazard.

The technical project should contain the further detailed forecast of methane bearing capacity together with the possible ventilation solutions to combat danger. Therefore, it is suggested that the longwall workings with methane bearing capacity estimated to be greater than 10 m^3CH_4/min should be equipped with methane drainage systems. Depending on the mining and geological conditions, methane drainage of the longwall workings may be conducted if the predicted methane bearing capacity is lower than 10 m^3CH_4/min.

To effectively fight methane hazard and successfully conduct methane drainage process, one of four ventilation systems may be applied, according to the following conditions:

- longwalls ventilated U system with projected absolute methane bearing capacity up to 25 m^3CH_4/min,
- longwalls ventilated Y system with projected absolute methane bearing capacity up to 50 m^3CH_4/min,
- longwalls with a parallel roadway and ventilated U system with projected absolute methane bearing capacity exceeding 25 m^3CH_4/min,
- longwalls with drainage gallery and ventilated U system with projected absolute methane bearing capacity exceeding 25 m^3CH_4/min.

System with methane drainage gallery can be used if above the mined coal seam there is thin one (not intended to exploit) and is situated at a distance corresponding to 5 times the thickness of the deposit (however, not be less than 12 m above the mined one). In other cases, the application of this method is no longer economically justified.

REFERENCES

GIG, 2003-2010 – Raporty roczne (2003-2010) o stanie podstawowych zagrożeń naturalnych i technicznych w górnictwie węgla kamiennego. Główny Instytut Górnictwa. Katowice.

Karacan C. Ö., Ruiz F. A., Cotè M., Phipps S., 2011: Coal mine methane: A review of capture and utilization practices with benefits to mining safety and to greenhouse gas reduction. International Journal of Coal Geology, 86(2-3), 121-156.

Szlązak N., Borowski M., Obracaj D. 2008. Directions of changes in ventilation system of longwalls with attention on reduction ventilating hazards. Mineral Resources Management, Volume 24, issue 1/2.

Szlązak N., Korzec M., 2010 – Zagrożenie metanowe oraz jego profilaktyka w aspekcie wykorzystania metanu w polskich kopalniach węgla kamiennego. AGH Journal of Mining and Geoengineering, r. 34, z. 3/1, 163–174.

Szlązak N., Borowski M., Obracaj D., Swolkień J., Korzec M., 2011 – Metoda oznaczania metanonośności w pokładach węgla kamiennego. Wydawnictwa AGH, Kraków.

Szlązak N., Borowski M., Obracaj D., Swolkień J., Korzec M., 2014: Selected issues related to methane hazard in hard coal mines. Ed. by N. Szlązak. AGH University of Science and Technology Press, Krakow, 148.

Szlązak N., Borowski M., Obracaj D., Swolkień J., Korzec M., 2015: Methane drainage in coal mines. Odmetanowanie górotworu w kopalniach węgla kamiennego. Wydawnictwa AGH, Kraków 2015.

WUG, 2010-2014 – Stan bezpieczeństwa i higieny pracy w górnictwie w latach 2010-2014. BIP 2010-2014, WUG Katowice.

METHODOLOGY FOR DIMENSIONING UNDERGROUND EXCAVATIONS IN STRATIFIED ROCKS THROUGH ANALYTICAL FORMULATIONS AND COMPUTATIONAL MODELING

*A.N. Ávila
Universidade de São Paulo
Universidade Federal de Ouro Preto
*(*Corresponding author: arloavila@gmail.com)*

R.P. Figueiredo
Universidade Federal de Ouro Preto
Departamento de Engenharia de Minas
Campus Morro do Cruzeiro
Ouro Preto, Minas Gerais, Brazil

24th World Mining Congress
MINING IN A WORLD OF INNOVATION
October 18-21, 2016 • Rio de Janeiro /RJ • Brazil

METHODOLOGY FOR DIMENSIONING UNDERGROUND EXCAVATIONS IN STRATIFIED ROCKS THROUGH ANALYTICAL FORMULATIONS AND COMPUTATIONAL MODELING

ABSTRACT

Some minerals, such as coal and potash, are extracted from stratified sedimentary rocks, usually by underground mining. To safely calculate the excavations, geotechnical studies are required in order to ensure that the openings made do not collapse. The dimensions of the excavations are frequently calculated by using a numerical tool such as the elastoplastic finite element software Phase2 (Rocscience Inc.). However, for being an analysis tool, Phase2 does not directly provide the most appropriate dimensions for an excavation project. It should be used only to confirm if a previously developed project is adequate or not. We hereby propose a different method of design for dimensioning underground excavations in stratified rocks. We have assessed the use of an analytical method to calculate the optimal width of an underground excavation. Using Mathcad software (Mathsoft Inc.), we employed mathematical models to design theoretical mining projects for strata with three different types of behavior: (1) embedded beams on rigid supports, (2) simply supported beams on rigid supports, and (3) beams on flexible supports. We compared the solutions from the three models with one another and with the respective results obtained with Phase2. The correlation for each pair of analytical-numerical results proved that the analytical method is more efficient for designing excavations. While the analytical method readily provides the adequate width of the excavations, the numerical method requires a trial-and-error approach, which is a slow process, in which the dimensions of the excavation are varied until the necessary level of stability is achieved. Therefore, a logical and effective strategy for the design of an excavation should include the use of an analytical tool to calculate its dimensions followed by the use of a numerical tool to verify these dimensions.

KEYWORDS

Underground excavation, underground mining, bedded rocks, sizing, computational modeling.

INTRODUCTION

In underground mines, the voids left by the extraction of rock cause disturbances in the surrounding rock mass. In the decompression zones that are established around the excavations, the rock mass is likely to break, since the rock tends to expand toward the voids created. A good knowledge of the mechanical behavior of the excavated rock can contribute to a safer mining operation as well as to a lower cost with rock supports.

The elastoplastic finite element software Phase2 (Rocscience Inc.) can be used for analysis of an underground excavation stability. However, this computational method has been frequently applied in designing excavations despite it is an analysis tool for projects already developed. By trial and error, various dimensions of the excavations are simulated on the software until an acceptable level of stability is achieved. This is a slow, inaccurate and imprecise technique.

We propose the application of analytical methods that are more efficient than the numerical method mentioned above, to calculate the proper width of an excavation in layered rock mass. Thus, we will consider three possible behaviors for a rock mass of this sort: (1) as embedded beams on rigid supports, (2) as simply supported beams on rigid supports, and (3) as beams on flexible supports. For each

of these three behavioral hypotheses, we will present excavation design equations that will be used in theoretical mines planning. The results of this sizing will be compared with each other and with the results of Phase2 software.

MECHANICAL BEHAVIOR OF THE ROOF OF EXCAVATIONS IN HORIZONTALLY BEDDED ROCKS

In excavations whose roof is directly below the rock horizontal layering, the thinnest layer near the opening tends to detach from the rock mass, flex down and break in the upper surface of its ends and on the center of the bottom surface. Thicker layers and under horizontal stress layers are more stable. The collapse of a layer leaves cantilevers as supports for the layer above. Then, each layer above the roof forms a progressively shorter beam. The end result of the continuing collapse of the beams is a stable trapezoidal opening (Goodman, 1989, p.233). “In the case where the beams thin upwards, the strata will not separate directly above the opening - providing the elastic properties of the beams are equal. Conversely, if the beams thin downwards, strata separation will occur immediately above the roof.” (Hudson & Harrison, 1997, p. 362).

In this paper, just the tensile ruptures (Figure 1) described above will be considered. However, beyond the tensile rupture, Jeremic (1985, p.109) presents other types of roof collapse.

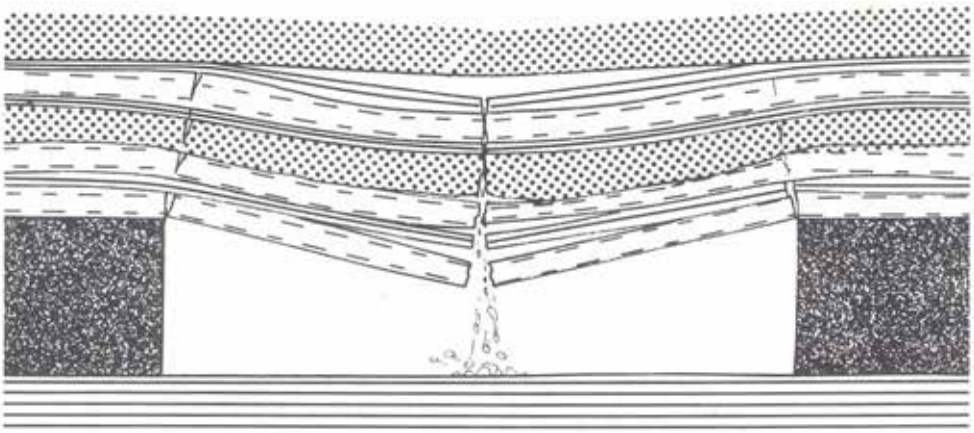

Figure 1 - Roof break by layer traction. Source: Jeremic (1985)

The most important factor in stratified rocks excavations design, in most cases, is the maximum acceptable roof span without support. The stability and the supports demand can be verified by an elastic analysis of beam bending, calculating the maximum tensile stress gravitationally induced by the weight of the layers and their maximum deflections (Hudson & Harrison, 1997, p. 362).

Jeremic (1985, p.10) points out that sedimentary rocks are anisotropic. Accordingly, the preferred direction of the openings may have a much greater effect on the stability of the mine than the format of the excavation. The theory of excavations in sedimentary strata tends to rely on the classical approach of elasticity, homogeneity and isotropy of the materials and the stress distribution in an infinite solid beam. It is recognized that a difficulty exists in adopting considerations of inhomogeneity due to oblique anisotropies.

Mathematical Relations for Rigid Supports

Obert and Duvall (1967, p. 518) argue that the critical stresses in elastic stratified rocks can be determined by the theory of embedded beams or plates loaded gravitationally. For these authors, there are two cases to consider, depending on the relative values of the load per unit length ratio on the flexural

stiffness (*q/EI*) of two beams. If this ratio for the top beam is smaller than that for the lower beam, then each beam acts independently. This is equivalent to layers of the same rock in which the thicker layer lies on top of the thinner one. When the thinner layer lies on top of the thicker one, i.e., the upper layer has a larger ratio, the lower layer will partially support the load of the upper beam.

In the first case above and in situations in which the roofs consist of a single layer, the following equations may be used, respectively, to calculate maximum deflection and maximum tensile strength of each layer:

$$\eta_{max} = \frac{\gamma L^4}{32Et^2} \tag{1}$$

$$\sigma_{max} = \frac{\gamma L^2}{2t} \tag{2}$$

where γ is the unit weight of the rock, L is the length of the layer, t is the layer thickness and E is Young's modulus.

The maximum deflection occurs at the center of the beam and the maximum stress occurs on the upper surface of the beam ends. These formulas can be used for beds inclined up to 10°. As the rocks are much less resistant to traction than to compression and shear, only tensile stresses must be considered in determining the width of an excavation (Obert & Duvall, 1967, p. 519).

Obert and Duvall (1967, p.154) also determine formulations for the second case. However, these equations are not presented in this paper.

The equation (2) may be transformed into the following sizing formula:

$$L_{max} = \sqrt{\frac{2T_0 t}{\gamma F_s}} \tag{3}$$

where T_0 is the tensile strength of the rock and F_s is tensile safety factor, which can be obtained by the formula:

$$F_s = \frac{T_0}{\sigma_{max}} \tag{4}$$

For Obert and Duvall (1967, p. 490), an acceptable tensile safety factor is in the range of 4 to 8. The lower value is applied for short-lifespan openings and the greater value is applied for openings that must be kept as long lasting openings.

According to Pariseau (2007, p. 246), the assumption that the beams of roofs of excavations are embedded is inaccurate. The ends of the beams are neither entirely fixed nor free. The author's approach involves both the equations for embedded beams as the equations for simply supported beams. Here are the formulas for simply supported beams:

$$\sigma_{max}(SS) = \frac{3}{4}\frac{\gamma L^2}{t} \tag{5}$$

$$L(SS) = \sqrt{\frac{4}{3}\frac{T_0}{F_s}\frac{t}{\gamma}} \tag{6}$$

$$\eta_{max}(SS) = \frac{5}{32}\frac{\gamma L^4}{Et^2} \tag{7}$$

Pariseau (2007, p.246) suggests that it would be more accurate consider the roof as a blade rather than as a beam and, therefore, use $E/(1-\upsilon^2)$ in the formulas, rather than E. Thus, a lower deflection would be obtained. However, the difference is less than 10% for Poisson ratio in the range of 0.20 to 0.30. Obert and Duvall (2007, p.519) believe that the theory of the blades should be applied only on roofs which length over span ratio is less than two.

Mathematical Relations for Flexible Supports

Stephansson (1971, p.7) presents mathematical solutions for roofs of horizontally stratified rocks based on the theory of elastic beams on elastic supports. Initially, the author introduces the formulas for the modulus of the foundation and for the flexural rigidity. "The modulus of the foundation characterizes the deformability of the elastic support. For homogeneous elastic abutments the modulus is given by:

$$c_u = \frac{E_u}{h(1-\upsilon_u^2)} \tag{8}$$

where E_u is the modulus of elasticity, υ_u Poisson's ratio, and h the height." (Hofer & Menzel, 1964, apud Stephansson, 1971, p.9).

The flexural rigidity, according to the theory of plates, is given by:

$$K = \frac{EI}{1-\upsilon_1^2} \tag{9}$$

where $I = H^3/12$ is the moment of inertia, E is Young's modulus, and υ_1 is Poisson's coefficient of the layer.

The roofs of a layer are divided into two types depending on the ratio between thickness (H) and width (l) of the roof. For thin layers roofs, $H < l/5$, the deformations due to shear stress can be neglected. A monolayer roof of infinite length is considered partially supported by elastic supports and subjected to a uniformly distributed load, $p = H \times \gamma$ (where γ is the specific weight of the layer) and/or any other uniform pressure, e.g., water pressure (Stephansson, 1971, p.12). For the layer section $0 \leq x \leq l$, which is above the excavation, the author presents the following equations for the deflection, y, and bending moment, M:

$$y = \frac{p}{c_u}\left[\alpha^4 x\left(\frac{x^3}{6} - \frac{x^2 l}{3} - \frac{lx}{\alpha} - \frac{l}{\alpha^2}\right) + l\alpha^3\beta(1+\alpha x)^2 + 1\right] \tag{10}$$

$$M = -\frac{px^2}{2} + \frac{pl}{2}\left(x + \frac{1}{\alpha} - \alpha\beta\right) \tag{11}$$

$$\alpha = \left(\frac{c_u}{4K}\right)^{\frac{1}{4}} \tag{12}$$

$$\beta = \frac{\frac{l^2}{6} + \frac{l}{\alpha} + \frac{1}{\alpha^2}}{(\alpha l + 2)} \tag{13}$$

The stresses are obtained by $\sigma_x = Me/I$, where e is the distance from the neutral axis (Stephansson, 1971, p.16).

Within the range $l/5 < H < l/2$, the influence of shear stresses can no longer be neglected. The deflection of the layer is affected by the bending moment and shear, increasing the deflection and tensile stress (Stephansson, 1971, p.20). Here are the equations for this situation:

$$y = \frac{px}{2K}\left[\frac{x^3}{12} - \frac{lx}{2}\left(\frac{x}{3} + \frac{1}{\alpha} - \alpha\beta\right) + a(l - x) - \frac{l^3}{24} + \frac{l^2}{2}\left(\frac{l}{4} + \frac{1}{\alpha} - \alpha\beta\right)\right] + y_{II} \tag{14}$$

$$M = -\frac{px^2}{2} + \frac{pl}{2}\left(x + \frac{1}{\alpha} - \alpha\beta\right) + a \tag{15}$$

$$r_1 = \sqrt{\frac{1}{2K}\left[ac_u + \sqrt{a^2(c_u)^2 - 4Kc_u}\right]} \tag{16}$$

$$r_2 = \sqrt{\frac{1}{2K}\left[ac_u - \sqrt{a^2(c_u)^2 - 4Kc_u}\right]} \tag{17}$$

$$y_{II} = \frac{(r_1^2 + r_1 r_2 + r_2^2)\left[\frac{pl}{2K}\left(\alpha\beta - \frac{1}{\alpha} + \frac{1}{r_1 + r_2}\right) - \frac{a}{K}\right]}{r_1^2 r_2^2} + \frac{pl}{2Kr_1 r_2(r_1 + r_2)} + \frac{p}{c_u} \tag{18}$$

$$a = \frac{3I}{H(1 - v_1)} \tag{19}$$

Stephansson (1971) also determines equations for multilayer roofs. However, these equations are not presented in this paper.

METHODOLOGY AND RESULTS

There were nine excavation situations supposed in a dolomite, stratified and isotropic rock, of high rigidity and high resistance, which occurs in a given Brazilian zinc mine. The adopted rock behaves elastically up to approximately the peak resistance. Thus, such a rock fits perfectly to the assumptions of the theoretical formulations and has the following characteristics:

$\gamma = 0{,}03\ MN/m^3$
$E = 49815\ MPa$
$\nu = 0{,}26$
$T_0 = 11{,}1\ MPa$

Considering t_1 as the thickness of the lower beam, t_2 as the thickness of the upper beam, and L as the width of the excavation, we considered the following situations:

Table 1 - Dimensions of the excavations

EXCAVATION	I	II	III	IV	V	VI	VII	VIII	IX
L (m)	7	17	20	7	7	17	17	20	20

t_1 (m)	1,25	2,25	2,75	1,25	1,25	2,25	2,25	2,75	2,75
t_2 (m)				2,5	2	2,5	2	2	2,5

The excavations IV, V and VI are under two layers with each one acting independently, supporting their own weight. For them, only the calculations for the bottom layer will be presented, which is the most fragile. To calculate the optimal width (L_{max}), the value eight will be adopted for the safety factor. Stephansson's (1971) equations require the height of excavation be determined, that is, the height of the walls, which represent the elastic supports. We adopted a height of 10 meters for all of the excavations. We performed all of the calculations using the Mathcad software, by Mathsoft Engineering & Education Inc.

Results Obtained Through the Analytical Methods

For the situations described above, taking the equations under the approaches of layers behaving like embedded beams on rigid supports, like simply supported beams on rigid supports and like beams on elastic supports, we obtained the results shown in Tables 2 and 3.

Table 2 - Comparison table of safety factors and the optimal spans of the excavations

EXCAVATIONS	RIGID SUPPORTS				ELASTIC SUPPORTS	
	EMBEDDED BEAMS		SIMPLY SUPPORTED BEAMS			
	F_S	L_{max} (m)	F_S	L_{max} (m)	F_S	L_{max} (m)
I	18,88	10,75	12,59	8,78	18,37	10,69
II	5,76	14,43	3,84	11,78	6,98	16,23
III	5,09	15,95	3,39	13,02	6,19	18,41
IV	18,88	10,75	12,59	8,78		
V	18,88	10,75	12,59	8,78		
VI	5,76	14,43	3,84	11,78		
VII	5,19	13,69	3,46	11,18	7,55	17
VIII	4,08	14,28	2,72	11,66	6,13	20
IX	4,67	15,28	3,11	12,47	6,69	20

Table 3 - Comparative table of maximum deflections and maximum stresses of the excavations

EXCAVATIONS	RIGID SUPPORTS				ELASTIC SUPPORTS	
	EMBEDDED BEAMS		SIMPLY SUPPORTED BEAMS			
	η_{max} (m)	σ_{max} (Pa)	η_{max} (m)	σ_{max} (Pa)	η_{max} (m)	σ_{max} (Pa)
I	$2{,}89 \times 10^{-5}$	$5{,}88 \times 10^{5}$	$1{,}45 \times 10^{-4}$	$8{,}82 \times 10^{5}$	$1{,}32 \times 10^{-4}$	$6{,}04 \times 10^{5}$
II	$3{,}11 \times 10^{-4}$	$1{,}93 \times 10^{6}$	$1{,}55 \times 10^{-3}$	$2{,}89 \times 10^{6}$	$8{,}32 \times 10^{-4}$	$1{,}59 \times 10^{6}$
III	$3{,}98 \times 10^{-4}$	$2{,}18 \times 10^{6}$	$1{,}99 \times 10^{-3}$	$3{,}27 \times 10^{6}$	$1{,}05 \times 10^{-3}$	$1{,}79 \times 10^{6}$
IV	$2{,}89 \times 10^{-5}$	$5{,}88 \times 10^{5}$	$1{,}45 \times 10^{-4}$	$8{,}82 \times 10^{5}$	$1{,}59 \times 10^{-4}$	
V	$2{,}89 \times 10^{-5}$	$5{,}88 \times 10^{5}$	$1{,}45 \times 10^{-4}$	$8{,}82 \times 10^{5}$	$1{,}64 \times 10^{-4}$	
VI	$3{,}11 \times 10^{-4}$	$1{,}93 \times 10^{6}$	$1{,}55 \times 10^{-3}$	$2{,}89 \times 10^{6}$	$9{,}78 \times 10^{-4}$	
VII	$3{,}45 \times 10^{-4}$	$2{,}14 \times 10^{6}$	$1{,}72 \times 10^{-3}$	$3{,}21 \times 10^{6}$		$1{,}47 \times 10^{6}$
VIII	$4{,}97 \times 10^{-4}$	$2{,}72 \times 10^{6}$	$2{,}48 \times 10^{-3}$	$4{,}08 \times 10^{6}$		$1{,}81 \times 10^{6}$
IX	$4{,}34 \times 10^{-4}$	$2{,}38 \times 10^{6}$	$2{,}17 \times 10^{-3}$	$3{,}57 \times 10^{6}$		$1{,}66 \times 10^{6}$

For excavations VII, VIII and IX, according to the theory of elastic supports, we calculated just the values for the lower layer, which is the most unstable. Stephansson's (1971) equations to calculate the bending moment in the situation of two layers being the upper one of higher flexural rigidity have dimensional compatibility errors. The first term in both equations is dimensioned as a negative power of length, instead of force times length. That fact has made it impossible to calculate the maximum stresses of excavations IV, V and VI, as well as the safety factors and the optimum widths. There is also a dimensional mismatch in the formula for calculating deflection of the situation of double layers in which the flexural stiffness of the upper layer is smaller. In the numerator of the expression, the dimensionless term αx is added to the width *l*. Thus, it was impossible to calculate the maximum deflection of the excavations VII, VIII and IX.

Using Table 3, we identified the most conservative results for each parameter of each excavation. By dividing the results from each of the three methods by the most conservative result, we obtained a factor of variation. The closer to the most conservative result, the closer to one the value of the variation factor will be. Table 4 was then created:

Table 4 - Comparison of the variation of results in relation to the more conservative

EXCAVATIONS	RIGID SUPPORTS				ELASTIC SUPPORTS	
	EMBEDDED BEAMS		SIMPLY SUPPORTED BEAMS			
	η_{max}	σ_{max}	η_{max}	σ_{max}	η_{max}	σ_{max}
I	0,20	0,67	1,00	1,00	0,91	0,68
II	0,20	0,67	1,00	1,00	0,54	0,55
III	0,20	0,67	1,00	1,00	0,53	0,55
IV	0,18	0,67	0,91	1,00	1,00	
V	0,18	0,67	0,88	1,00	1,00	
VI	0,20	0,67	1,00	1,00	0,63	
VII	0,20	0,67	1,00	1,00		0,46
VIII	0,20	0,67	1,00	1,00		0,44
IX	0,20	0,67	1,00	1,00		0,46

Results Obtained Through the Numerical Method

We carried out computer modeling trying to obey all the assumptions of the theory in a finite element software (Phase2). We considered the materials elastic and subject only to the mass forces. In nature, the rock masses are pre-tensioned by gravity. Therefore, we introduced a first shaping stage in order to allow gravity to act on the model, before digging. We simulated the hypothesis of interfaces without resistance between layers annulling friction, cohesion and tensile strength of the joints of the models. Figure 2 illustrates the boundary conditions and the mesh used. We obtained the values of stresses by plotting the horizontal stresses of the models, as in figures 3 and 4.

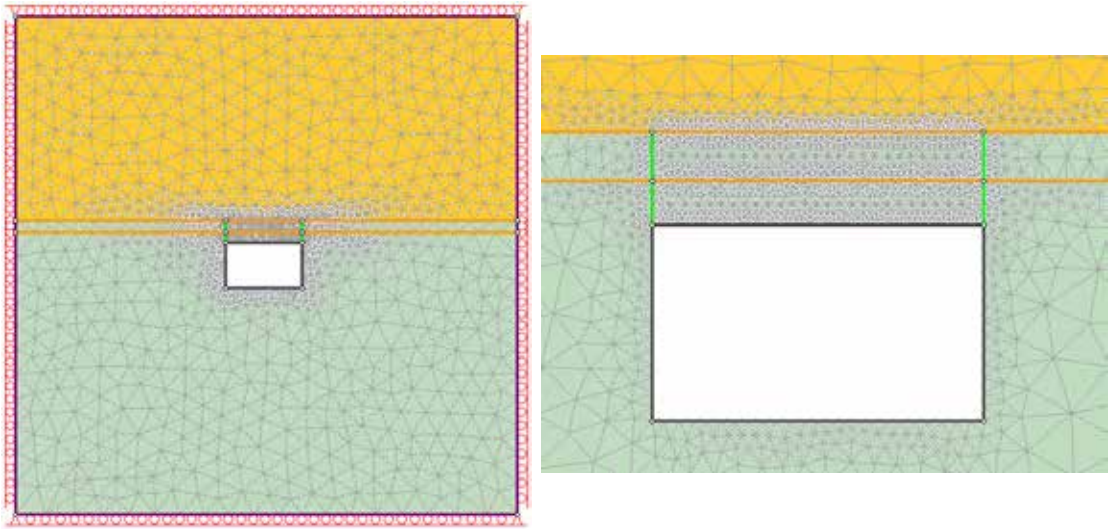

Figure 2 - Kinematics restriction imposed to the external boundaries and typical mesh model (left); and discretization level used in the models (right)

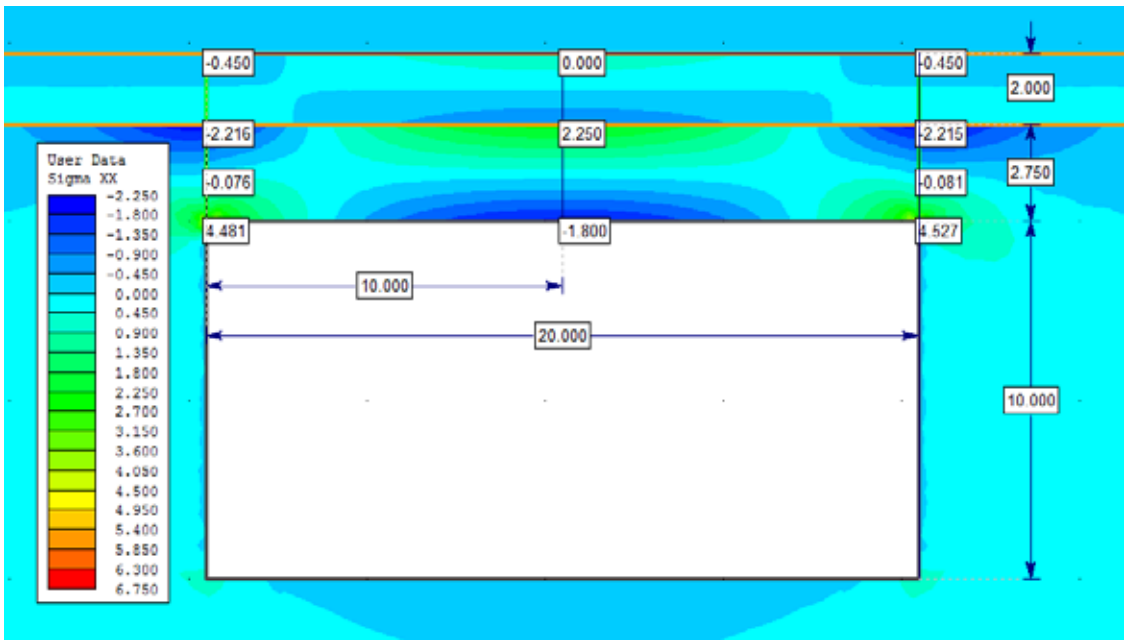

Figure 3 - Horizontal stresses in excavation VIII

As with the excavation V (Figure 4), some points of the models showed unexpected tensions (zero or opposite sign). This fact was repeated in various parts of the excavations I and IV and in the upper layers of the excavations VI, VII and IX. It is believed that these inconsistencies should be attributed to the difficulty in defining the mechanical parameters of the interfaces of the layers. We created Table 5 using Table 3 and the values of horizontal stresses calculated by using Phase2.

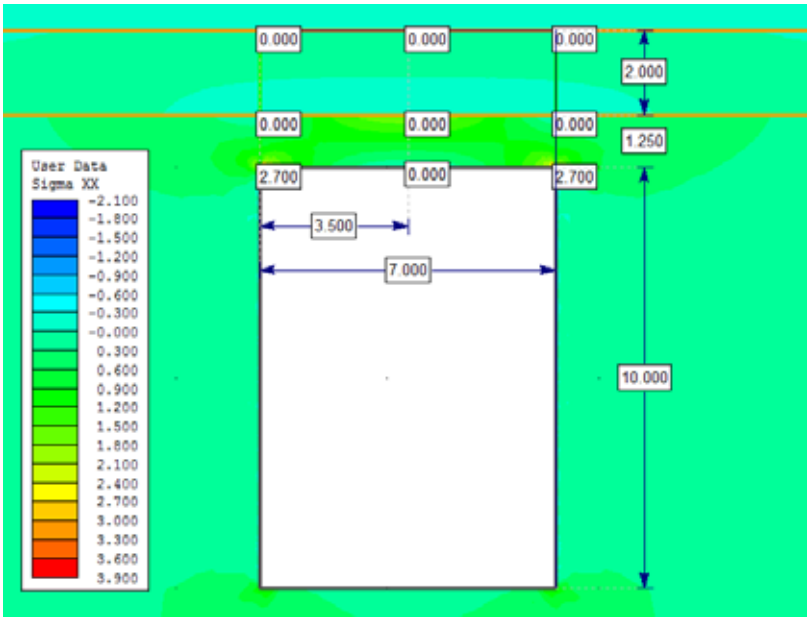

Figure 4 - Horizontal stresses in excavation V

Table 5 - Comparative table of the results from the analytical and the numerical methods

EXCAVATIONS	ANALYTICAL METHODS			NUMERICAL METHOD
	RIGID SUPPORTS		ELASTIC SUPPORTS	
	EMBEDDED BEAMS	SIMPLY SUPPORTED BEAMS		
	σ_{max} (Pa)	σ_{max} (Pa)	σ_{max} (Pa)	σ_{max} (Pa)
I	$5{,}88 \times 10^5$	$8{,}82 \times 10^5$	$6{,}04 \times 10^5$	0
II	$1{,}93 \times 10^6$	$2{,}89 \times 10^6$	$1{,}59 \times 10^6$	$1{,}33 \times 10^6$
III	$2{,}18 \times 10^6$	$3{,}27 \times 10^6$	$1{,}79 \times 10^6$	$1{,}48 \times 10^6$
IV	$5{,}88 \times 10^5$	$8{,}82 \times 10^5$		0
V	$5{,}88 \times 10^5$	$8{,}82 \times 10^5$		0
VI	$1{,}93 \times 10^6$	$2{,}89 \times 10^6$		$2{,}25 \times 10^6$
VII	$2{,}14 \times 10^6$	$3{,}21 \times 10^6$	$1{,}47 \times 10^6$	$2{,}06 \times 10^6$
VIII	$2{,}72 \times 10^6$	$4{,}08 \times 10^6$	$1{,}81 \times 10^6$	$2{,}22\times 10^6$
IX	$2{,}38 \times 10^6$	$3{,}57 \times 10^6$	$1{,}66 \times 10^6$	$2{,}35\times 10^6$

RESULTS DISCUSSION

Observing Table 4, it is noted that the results for maximum deflection and maximum stress for the hypothesis of the simply supported beams were the most conservative in most situations. The maximum deflections calculated by the hypothesis of embedded beams were the least conservative in all the excavations. Often, the hypothesis of flexible supports showed the lowest values of maximum stress. Therefore, Stephansson's (1971) equations allow the design of wider excavations.

No value found by using the formulas for the maximum deflection and maximum stress differed more than about twice from the value found by using the formulas of other theories, except in one case (see Table 3 and Table 4). There was a large discrepancy in the results of maximum deflection from the theory

of embedded beams that in most cases were about five times smaller than the results from other theories. However, the maximum stresses from the theory of embedded beams did not differ much from the other theories, since it was just 50 % lower than the stresses of the simply supported beams theory and always greater than the stresses of the flexible supports theory, reaching a maximum difference of about 50 %.

Comparing the results of the numerical method with the results of analytical methods in Table 5, it is noted that the values are very similar, apart from those found for excavations I, IV and V. These three excavations are the narrowest of all and have in common the seven-meter width. In other excavations, the values of simply supported beam theory were the most differentiated from the numerical method results, reaching a difference of 121 %, in excavation III.

CONCLUSIONS

In this work, we presented analytical methods that readily indicate the optimal width of excavations with roof under sub-horizontal bedded rocks. Obtaining the adequate width by using the numerical method involves a lengthy process. In the computational model, the size of the excavation must be changed several times until one that meets the desired stability standards is found.

There was a correlation between the analysis of the excavations performed with Phase2 and the results from the theoretical formulations. This correlation proves that the analytical methods may be employed in the design of excavations. Therefore, it is advisable that Phase2 be used only for verification of pre-defined projects. To design excavations, the application of analytical methods has proved to be more convenient.

REFERENCES

GOODMAN, R.E. (1989). *Introduction to rock mechanics* (2nd. ed). New York, NY: John Wiley & Sons.

HÖFER, K.H., & MENZEL, W. (1964). Comparative study of pillar loads in potash mines established by calculation and by measurements below ground. *International Journal of Rock Mechanics and Mining Sciences*, *1*(2), 181-198.

HUDSON, J.A., & HARRISON, J.P. (1997). *Engineering rock mechanics: An introduction to the principles*. Oxford, England: Elsevier.

JEREMIC, M.L. (1985). *Strata mechanics in coal mining*. Rotterdam, Netherlands: A. A. Balkema.

OBERT, L., & DUVALL, W.I. (1967). *Rock mechanics and the design of structures in rock*. New York, NY: John Wiley & Sons.

PARISEAU, W.G. (2007). *Design analysis in rock mechanics*. London, England: Taylor & Francis.

STEPHANSSON, O. (1971). Stability of single openings in horizontally bedded rock. *Engineering Geology*, *5*(1), 5-88.

NPV ANALYSIS OF MULTIPLE SURFACE CONSTRAINTS FOR PIT EXPANSION SCENARIOS

*B. T. Kuckartz[1], and R. L. Peroni[1], L.N. Capponi[2]

[1] *Federal University of Rio Grande do Sul – UFRGS. Mining Engineering Department*
Avenida Bento Gonçalves, 9500, Bloco IV Prédio 75
Porto Alegre, RS, Brasil.
*(*Corresponding author: brukuck@hotmail.com)*

[2] *Vale Fertilizantes S.A.*
Rodovia MG - 341, Km 25.
Tapira, MG, Brasil

24th World Mining Congress
MINING IN A WORLD OF INNOVATION
October 18-21, 2016 • Rio de Janeiro /RJ • Brazil

NPV ANALYSIS OF MULTIPLE SURFACE CONSTRAINTS FOR PIT EXPANSION SCENARIOS

ABSTRACT

The operation and management of large surface mines are very difficult and complex tasks. To optimize the entire operation the engineers must deal with several technical aspects and constraints, like orebody modelling, reserves estimation, determination of blending necessity, optimum and operational pit designs, operational costs, environmental issues, among others. In this sense, locating surface infrastructures is one of the most critical mine planning concerns, considering there is always the dilemma between approximating to the pit the processing plant, waste dumps and tailings dam, for example, to reduce the operational costs. It is clear that this approximation might interfere with future pit expansions in new favorable scenarios, but at certain point in time the decision was taken to guarantee the operation feasibility. In such cases, impacts on project's NPV are inevitable and must be deal with caution, evaluating several alternative scenarios to design a strategy to maximize profitability. Relocating waste dumps, stockpiles or mine facilities might be expensive, however it allows pit expansions that will pay for the relocation process and still generate value. The aim of this study is to evaluate, through NPV comparisons considering different scenarios with multiple constraints, the possibility of moving waste piles and infrastructure buildings from their current position and/or defining priorities to after measuring the impact that each constraint represents on the project´s profitability. The methodology will be applied to a phosphate mine, to determine the best alternative from a long-term mine planning perspective.

KEYWORDS

Mining planning, surface constraints, NPV, ultimate pit.

INTRODUCTION

Large surface mines represent a great challenge in terms of planning, operation and management. To optimize the entire operation the engineers must deal with several technical aspects and constraints, like orebody modelling, reserves estimation, optimum and operational pit designs, determination of blending necessity, equipment allocation and maintenance, environmental issues among others. Besides these technical aspects, the managing the cash flow and risk during production is a critical part of mining as well as an important part of a strategy to develop new and existing operating mines (Dimitrakopoulos, Martinez & Ramazan, 2007).

The long-term planning engineers consider many of these variables in the early stages of a mining project, therefore decisions involve a high degree of uncertainty of future demands. Moreover, the further the periods are, the greater is the uncertainty (Albach, 1967). In order to obtain the best operational and economic results is important to raise a well-based pit optimization and production scheduling study, given these variables impact on projects´ economics.

The majority of these variables are modified with time in consequence of uncertain prices, unpredictable global markets, and unforeseeable changes in foreign exchange rates, and may jeopardize the operation feasibility (Deutsch, González & Williams, 2015). To deal with them is essential to make many assumptions regarding costs behavior with time. Depending on costs fluctuation, optimum pit may vary altering the total amount of reserves and therefore forcing drastic shifts in production schedule that, according to Ramazan and Dimitrakopoulos (2013), can modify significantly the project´s NPV.

Defining ultimate pit limit is a fundamental problem in mine planning and decisions on this subject will endure to the end of the mine life. According to Cacceta and Hill (2003) ultimate pit limit of a mine is the contour, which is the result from extracting quantities of ore and waste material and reaches the best profitable scenario for operation. As the ultimate pit is based on uncertain parameters and is the reference for the operation to reach the end of the mine life, it affects directly on where infrastructures will be placed to avoid intersecting the pit limits blocking ore and future pit expansions (Deutsch et al., 2015).

Considering the possibility of pit expansion or reduction with time due to the variables mentioned before, engineers must choose surface facilities location with caution once is not easy to relocate these structures. There is always the dilemma between approximating surface facilities to the pit, like the processing plant, waste dumps and tailings dams, to reduce operational costs. It is possible that this approximation might interfere with future pit expansions in new favorable scenarios, but at certain point in time the decision might be taken probably to guarantee the operation feasibility.

The aim of this study is to evaluate, through NPV comparisons considering different scenarios with multiple constraints, the possibility of moving waste dump piles and infrastructure buildings from their current position and/or defining relocation priorities after measuring the impact that each constraint represents on the project´s profitability. The methodology will be applied to a phosphate mine, to determine the best alternative from a long-term mine planning perspective.

MINE HISTORICAL

According to the Vale Fertilizantes' resources report (Júnior, 2010) the operation started in 1938. Ore composition was mainly by apatite with grades around 20% in a residual material layer. In the end of the 60's, the residual material was depleting and the new source of apatite were the carbonatites found underneath, with mean grade of 5.5%. This forced an update on the process plant, which started to use flotation. At this stage, the apatite was no longer the only relevant mineral, sharing its economic importance with sub products like magnetite and limestone. In 1972, the company built a cement factory to use the limestone tailings with MgO grade below 4.5%, and in 1974 were installed units to produce sulfuric and phosphoric acids.

Many different carbonatites comprise local geology in a cylindrical shape inserted in the waste volcanic rock, called Jacupiranguito. A detailed scale study revealed the occurrence of five different carbonatite intrusions in distinct ages. Currently the ore zone model (phosphate rocks composed by calcite and dolomite carbonatites) contains 14 different lithologies (Figure 1), separated in 5 groups according to their spatial location and mineral similarities. Table 1 shows the relation between grades, lithologies and final products.

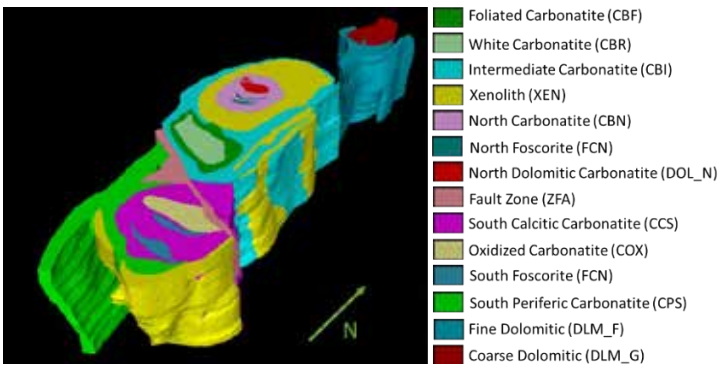

Figure 1 – Ore zone local geology model. Dimensions are 1.13 km (0.70 mi) longitudinal and 0.4 km (0.25 mi) transversal

Table 1 - Ore classification according to cut-off grade and lithology

Ore Type	Cut-off Grades (%)		Lithologies	Calcareous Tailings Application
	P2O5	MgO		
A	≥ 3.00	≤ 4.00	CPS, CCS, FCS, CBI, CBF, CBR, CBN, FCN	Phoscalcium
B	≥ 3.00	> 4.00 and ≤ 5.00	CPS, CCS, COX, ZFA, FCS, CBI, CBF, CBR, CBN, FCN	Cement
C	≥ 3.00	FREE	CPS, CCS, COX, ZFA, FCS, CBI, CBF, CBR, CBN, FCN, DOL_N, XEN, DLM_F, DLM_G	Magnesia

Currently the pit bottom is located at elevation -140 m (-459.3 ft) and engineers expect to lower to -270 m (-885.8 ft) and probably deeper. The pit is almost entirely developed in fresh and competent rock, which allows a general slope angle around 54°, using benches of 10 m (32.8 ft) and 20 m (65.6 ft) height. Although the ore and waste rocks have good geotechnical parameters, many surrounding surface structures limit pit expansion. There are three waste dump piles blocking the advances to the east, southeast and southwest directions.To the south , there are also the crushing system, homogenization piles and process plant (Figure 2).

Figure 2 - Overall view of the pit location and the surrounding surface structures

To lower vertically the pit bottom it is mandatory to relocate some of these structures. The only horizontal advance direction, which is not blocked by any physical constraint, is to north/northwest, in a region called Mesquita Sampaio where exploration found high MgO grades though.

METHODOLOGY

The present study aims the evaluation, through NPV analysis, of different scenarios considering several surface facilities and its interference with the mine to find the most profitable alternative for future pit expansions. This will be carried out with a block model containing grades of P_2O_5 and MgO (interesting minerals for processing plant) estimated using ordinary kriging, and six constraints (one mining claim limit, three waste piles and two other surrounding infrastructures groups) as shown in Figure 3.

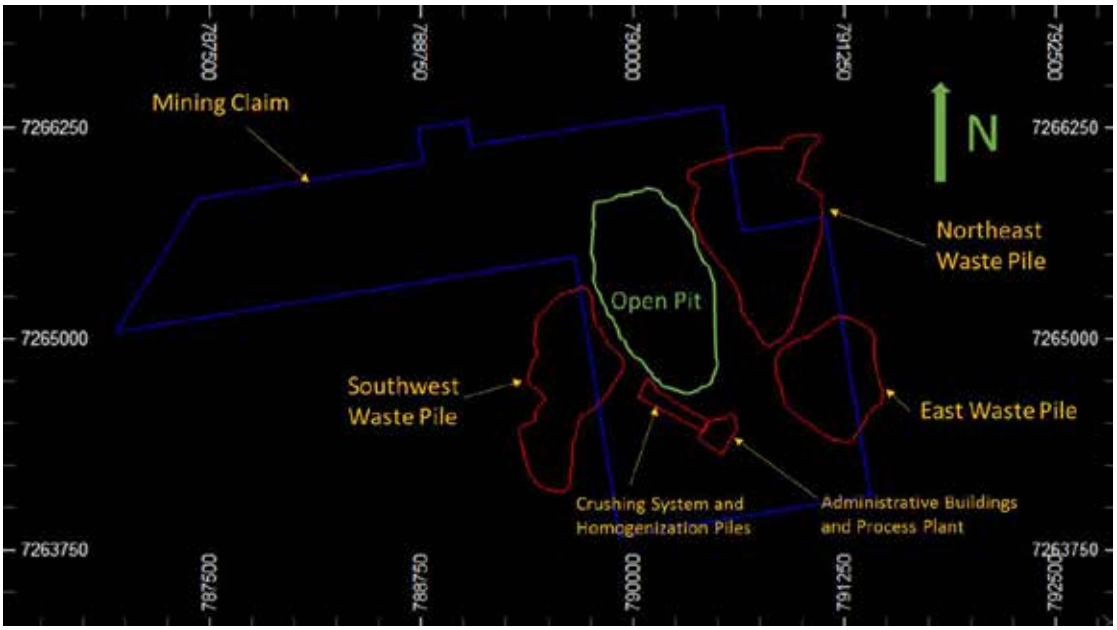

Figure 3 - Location of each constraint considered in this study and the current open pit limit

We considered eight different scenarios in this study, one of them considers to keep mining according current situation (all constraints applied) and another one is the unconstrained scenario to determine the maximum and minimum usage of mineral resources and perform its NPV assessment. Table 2 contains descriptions of all scenarios and some combinations of the six surface constraints (as presented in Figure 3). It is important to say that all scenarios consider the mining claim limit as a hard boundary for every analysis. Having said that, S0 would be the "unconstrained" case to serve as a reference of maximum outcome in terms of mineral resources usage and consequently created the expectation to be converted into ore reserves if the limitations (or constraints) can be overcome.

Table 2 - Constraints combinations considered in each evaluation scenario.

Scenario	Constraints Considered
S0	Mining Claim
S1	All (current mine situation)
S2	Northeast and east Waste Piles
S3	All Waste Piles
S4	All Waste Piles + Process Plant + Administrative Building
S5	Crushing System + Homogenization Pile + Process Plant + Administrative Building
S6	Southwest Waste Pile
S7	East and Southwest Waste Piles

For all scenarios were generated optimized pits through Lerchs-Grossmann algorithm, a well-stablished ultimate pit limit problem approach. After that, for the best scenarios, which means the ones

that generated the most attractive NPVs, we followed with a mine scheduling to assess, rank and determine the most advantageous scenario.

RESULTS AND DISCUSSION

The results from the pit optimization are listed in Table 3 and contains NPV, ore tonnes, stripping ratio, pit bottom elevation and average grade for the main minerals considered in this analysis. The NPV results are shown in percentage of a reference case, it was taken the unconstrained scenario (S0) to be the optimistic base case in terms of liberation of all constraints.

Table 3 - Results for ultimate pits containing NPV, Strip Ratio, pit bottom elevation and P2O5 and MgO grades. NPV values normalized to S0 (higher result).

Scenario	Ore Mass (Mt)	NPV (%)	Stripping Ratio	Pit Bottom Elevation m (ft)	P_2O_5 (%)	MgO (%)
S0	193.4	100.00	2.50	-420 (-1378)	4.32	8.16
S1	87.7	83.70	1.76	-300 (-984)	5.31	7.66
S2	129.7	95.90	1.91	-320 (-1050)	5.34	6.69
S3	105.0	91.40	1.78	-300 (-984)	5.38	7.08
S4	105.0	91.40	1.78	-300 (-984)	5.38	7.08
S5	139.5	91.30	2.49	-400 (-1312)	5.23	6.98
S6	148.5	96.10	2.51	-375 (-1230)	5.35	6.52
S7	148.8	96.00	2.39	-375 (-1230)	5.36	6.60

Figure 4 shows the amount of tonnes and strip ratio. From all eight scenarios, S0 has the highest NPV value and we used it as a reference to normalize the other scenarios results for comparison. S0 also contains the highest total tonnes (waste plus ore), which was expected, given the has only one constraint (mining claim). However, 72% of all contained tonnes are waste material and 12% of this waste is landfill, therefore the relocation costs may lower substantially the NPV for this scenario. Besides, the average grade for apatite contained in ore blocks is the lowest amongst all scenarios.

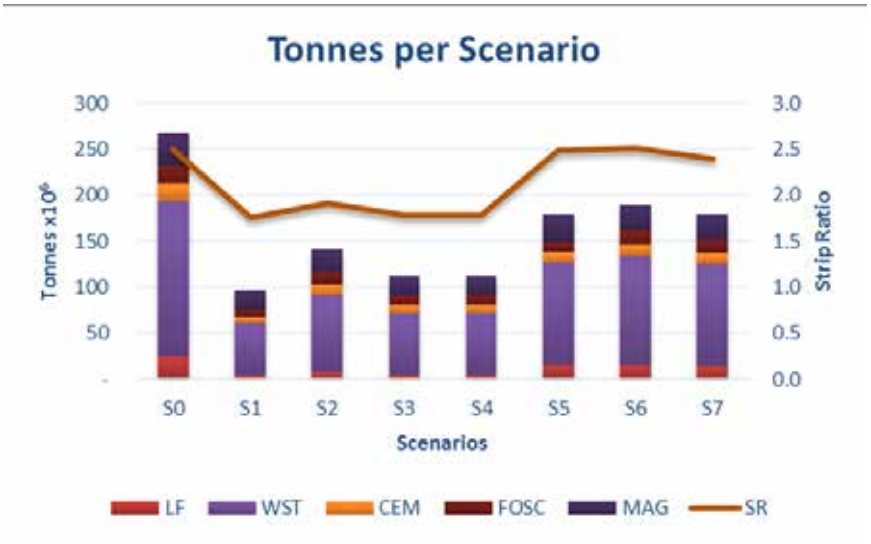

Figure 4 - Total tonnes per scenario and the respective proportion of tonnes of LF (landfill), WST (waste), CEM (cement), FOSC (phoscalcium), MAG (magnesia), SR (strip ratio)

As expected, S1 presented the worst results regarding NPV and total tonnes. This result indicates that surface structures are really blocking significant amount of ore and consequently it reflects on project´s NPV. Ultimate pit bottom is located at elevation -300 m (-984 ft) and, therefore, to deepen the pit it is essential to relocate or unblock some of the surface structures. Even though

geotechnical studies demonstrate the local geology is comprised of competent rock making possible to work with 20 m (65.6 ft) bench height and a very steep face angle (75° to 80°), the presence of unmapped joints or fractures, underground water flows, overload around pit walls and other aspects may become a huge concern for pit stability and safety.

S3 and S4 presented the same results. In S3, were kept all waste piles as constraints and disregarded the crushing system, homogenization piles, process plant and administrative building. S4 considers the same situation, just in addition to the waste piles, were kept process plant and administrative building as constraints. The ultimate pit surface for both scenarios are identical and it is possible to conclude that the processing plant and/or administrative building (leaving waste piles as constraints) will not provide any additional profit or increase in reserves. In fact, looking at Figure 5, it can be noticed that the only scenario in which the processing plant and administrative building need to be moved is S0.

Scenarios S6, S7 and S2 presented the best NPV results, respectively, compared to S0. However, it is important to realize that even though S2 presents the lowest NPV it has also the lower stripping ratio among these four scenarios. Is also important to highlight that in all situations is necessary to relocate the crushing system and homogenization piles. The only scenarios where it does not happen are S1 and S5 by definition, where the crushing system is considered as one of the constraints. Figure 5 also shows the crushing system relocation necessity.

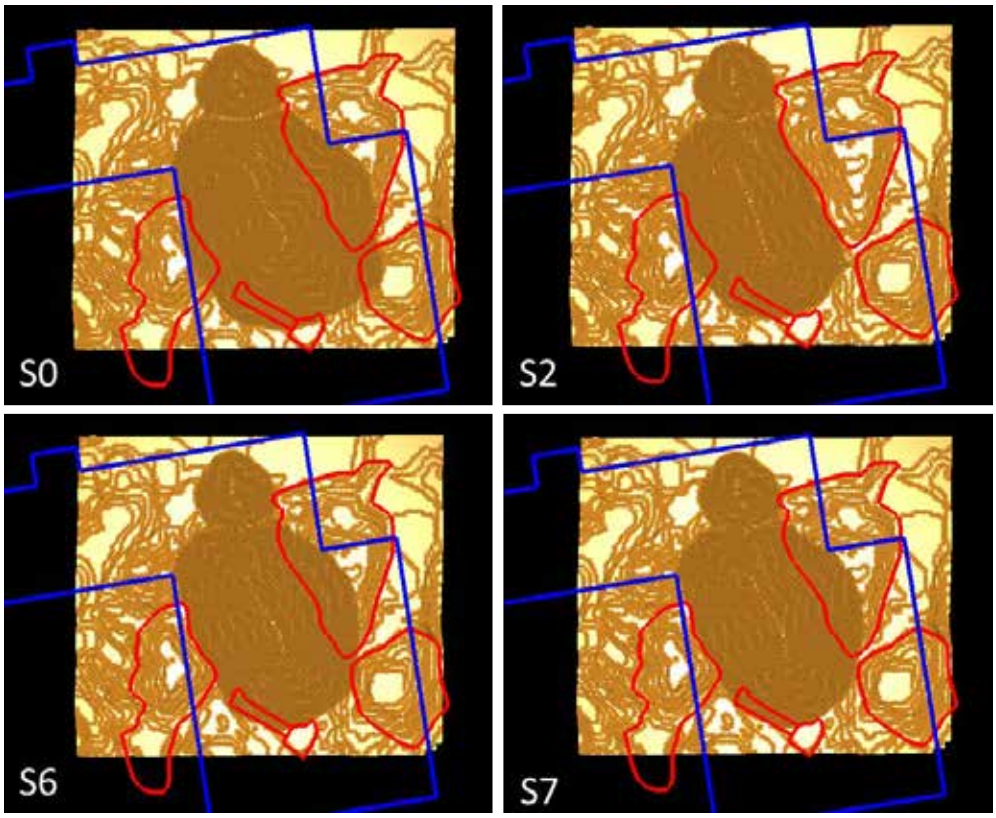

Figure 5 – Visual comparison between footprints of the four selected ultimate pit scenarios and the constraints considered

After choosing these four scenarios, the scheduling process was carried out to verify the resulting ranking from previous analysis. The scheduling was performed according to the mine production necessity and also trying to keep stable the yearly stripping ratio and feed grades. Table 4 shows the results obtained after sequencing the scenarios, along the results from S1 pit for comparison in case no physical constraint is released and consequently no relocation will be done.

Table 4 - Scheduling results for the four best scenarios after scheduling. NPV values are normalized according scenario S0 result

Scenario	Mine Life (yr)	NPV (%)
S0	38	100.0
S1	17	95.5
S2	25	107.0
S6	29	101.1
S7	28	102.4

Scenario S0 turned out to be the worst case after scheduling procedure. Scenarios S6 and S7 switched rank position. The necessity to move east and northeast waste pile in S6 implies relocation of approximately 3.0 Mt more landfill than in S7, causing a reduction on NPV.

Scenario S2 became the most attractive solution at this point. It presented 7% increase NPV compared to S0 and 11.5% when compared with S1 scenario. Despite the total tonnes in the S2 ultimate pit is 20% to 45% less than in S0, S6 and S7, the necessity to relocate landfill and move waste in the first 3 years is 37.5%, 21.7% and 9.4% lesser, respectively. It occurs due to keeping northeast and east waste piles as constraints.

CONCLUSION

The results presented in this paper show the importance of studying as many alternatives as possible in cases where surface structures are interfering with the pit limit. Some of these surface structures such as east and northeast waste piles demonstrated to be good opportunities to increase the project´s NPV. Moving them increases significantly mineral resources recovery but, in the other hand, the necessity of relocation in the first years penalizes NPV. Other surface structures, like processing plant and administrative buildings, do not seem to be huge constraints as, in various scenarios, pit limits do not intersect them.

Moving crushing system along with homogenization piles and southwest waste pile seems to be the best alternative as demonstrated in this preliminary study. However much of the resources will be left in place and a pit design would be necessary to determine the amount of ore that would be left behind before a decision is taken. In S2 situation, the pit bottom will reach the elevation of -320 m (-1049.8 ft) while the modeled orebody reaches -600 m (-1968.5 ft).

It must be considered in all scenarios the relevance of availability of areas to waste relocation and/or waste removal. As could be seen in Figure 2, the constraints are exactly where they currently are because the juggle to deepen the pit and reducing operational costs. This is a hard constraint and the decision passes through this assessment.

As future developments, geostatistical simulation should be included in further studies to insert grades uncertainty and risk analysis, so better decisions regarding projects profitability could be made. It is also interesting to evaluate the possibility of transition for underground operation, as is not possible to reach some of the resource even in the deepest ultimate pit scenario.

REFERENCES

Albach, H. (1967). Long range planning in open-pit mining. Management Science, col. 18, no. 10, June.

Caccetta, L., & Hill, S. P. (2003). An application of branch and cut to open pit mine scheduling. Journal of Global Optimization, vol. 27, pp. 349-365.

Deutsch, M., González, E., & Williams, M. (2015). Using simulation to quantify uncertainty in ultimate-pit limits and inform infrastructure placement. Mining Engineering, vol. 67, No. 12, pp.49-55.

Dimitrakopoulos, R., Martinez, R. L., & Ramazan, S. (2007). A maximum upside / minimum downside approach to the traditional optimization of open pit mine design. Journal of Mining Science, vol. 43, No. 1.

Júnior, A. F. (2010). Estimativa de teores do modelo de blocos de curto prazo da Mina de Cajati [Grades estimation of the short-term block model of Cajati Mine] (Technical Report). Vale Fertilizantes.

Ramazan, S., & Dimitrakopoulos, R. (2013). Production scheduling with uncertain supply: A new solution to the open pit mining problem. Optim Eng, vol. 14, pp. 361-380.

OBJECT MAP AS A MEAN OF CREATING COMPLETE INVENTORY OF INFRASTRUCTURE IN UNDERGROUND MINES

A. Dyczko and D. Galica and E.J. Sobczyk and J. Kicki and J. Jarosz

[1]Mineral Energy and Economy Research Institute of the Polish Academy of Sciences
J. Wybickiego 7, 31-261 Krakow, Poland
([*]Corresponding author: jjot63@gmail.com)

24th World Mining Congress
MINING IN A WORLD OF INNOVATION
October 18-21, 2016 • Rio de Janeiro /RJ • Brazil

OBJECT MAP AS A MEAN OF CREATING COMPLETE INVENTORY OF INFRASTRUCTURE IN UNDERGROUND MINES

ABSTRACT

With current coal market being so unstable it is the main objective of Polish mines to cut costs of excavation. This will, in time, allow them to cep a stable income. No mine is the same that is why differed solutions are needed. One of world's biggest bituminous coal producers – Bogdanka Coal Mine with the help of The Mineral and Energy Economy Research Institute of the Polish Academy of Sciences is trying to gather all the information on mines underground infrastructure in one place. This project is ongoing since 2013. It is widely known that the biggest treasure of all mines is its underground infrastructure and excavation machines. It is highly important, for the authors of this paper, to be able to have a quick access to all possible information on the machines installed in mine. This allows for more effective management of the whole mining process.

There are many definitions of Object Map. For the authors of this paper it is a single platform installed with a 3D carto-metric map of underground shafts, corridors, was that includes underground infrastructure, and extra, numeric information placed in connected database.

The Object Map presented in this article allows for:

- giving definitions on types of objects and there properties,
- attaching and fulfilling data base that can be used to cep geometric information's,
- resenting selected information's on underground mas,
- creating thematic maps that allow to present only selected elements and there attributes,
- data exchange with financial systems,
- exchanges of maps (files including maps),
- visualization of technical objects, defined by their functionality (in full or default versions).

Objects in mentioned maps are being stored in appropriate data base. That includes bought graphic information and attributes. The user's interface is based on CAD like solutions.

KEYWORDS

Hard coal mining, mine infrastructure, map of objects, Bogdanka Coal Mine

INTRODUCTION

The current situation in polish coal market has forced mining companies to minimize costs of production. This is done in order to obtain a constant income with coal prices decreasing. Every mine is forced to implement its own special solutions to mitigate this problem. Since 2013 coal mine Lubelski Węgiel „Bogdanka" S.A. in cooperation with The Mineral and Energy Economy Research Institute of the Polish Academy of Sciences (MEERI PAS) is implementing a project consisting of gathering key information on underground infrastructure and resources (Karlikowski, Parzniewski, &Galica, 2015). It is a widely known fact that one of every mines most prized possessions are machines and underground infrastructure. In authors opinion knowing what kind of machines does the mine possess and fast, easy access to detail information on their placement is a key factor in effective mine production management.

The cooperation between LW „Bogdanka" S.A. and MEERI PAS has produced a so-called Object Map – a IT data base based system that covers all information on underground infrastructure. Implementing this system in to Bogdankas' IT infrastructure allows for integration of information on mines assets so allowing for better managing of existing underground infrastructure.

OBJECT MAP – SYSTEMS STRUCTURE

There are many definitions of Object Map. According to the authors and Object Map is a compact and homogeneous IT platform that includes a 3D map of the corridors, drafts and shafts of the mine and places infrastructure and machines in them. Detailed information's are placed in attached data base. Object map is undergoing consist maintenance and improvements in order to provide the user with as many current information's on underground infrastructure as possible. Currently with the use of Object Map a user is able to:

- define object types and there properties,
- fill the data base with detailed geographic and description information that will define the object within the data base,
- present chosen parts of mining maps on top of object map,
- display layers of parts of object map in accordance to the attributes,
- define users profile,
- exchange data with financial and accounting systems,
- exchange of map documentation,
- visualization of technical objects on the map with regard to their functionality (basic and full information).

Elements (objects) of Object Map are being stored in a data base (that includes graphical and description information). Bentley Map and Bentley PowerMap are used for displaying map information. This system provides a means of integrating information from Maincoal data base and financial data base.

In order to fulfill a conception of this project a detail plan of implementation was prepared and done. The schematic in figure 1 shows the overview of the system.

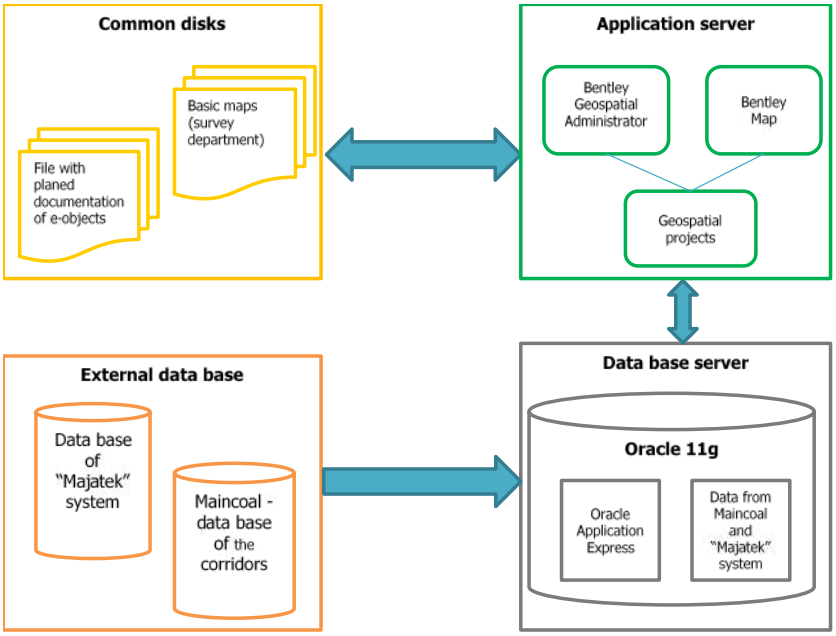

Figure 1. Object map of LW "Bogdanka" S.A. – schematic

The users of this system are categorized by the division they are working at. After the division is identified, software automatically decided upon the tools that would be used for editing the Object Map. Every user is entitled to edit only given parts of the project.

OBJECT MAP TOOLS FOR IMPROVING INVENTORY PROCESS

Object Map system deals with various data types this is why a few software applications are used. All drawings and maps are done in CAD-base systems Bentley MicroStation. Objects are defined

by administrators in Geospatial Administrator. Implementing object in to the map are done in Bentley Map. The last software used in described system is GeoWeb Publisher, that allows for all kinds of data (CAD files, raster files, information on relation within data base, objects in 3D data bases, technical documentation etc.) to be published by web browsers (fig. 2).

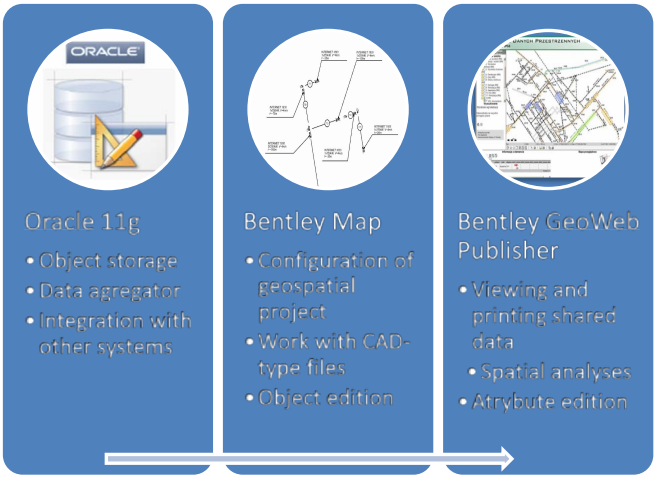

Figure 2. Applications used while creating Object Map

Every division of the mine is working on separate parts of gathered information. This is why some extra tools ware constructed for each division in order to make works faster and easier. For example, mechanics division was given tools for implementing into Object Map elements such as belt conveyers, conveyers engine, sieving machines etc. and also objects connected with energy transportation including drainage like pipelines, fire water supply pipelines, drainage pipelines, air-condition pipelines, bolts, manometers etc.. Similar tools have been provided for drawing suspended frictional railway, floor mounted railway, railroad station, and railroad crossings. Moving objects such as locomotives are being assigned to the underground rail stations (fig. 3).

The inventory method that was installed during construction of Object Map remained unchanged turnout the project, only the display method has been modified. It is important to mention at this point that before Object Map underground machines have been drown into a full metric survey map, also technical information was attached as a description. This has made maps hard to read in places where many machines ware stored. On top of that it was impossible to estimate the number of such machines is separate tunnels or levels of the mine. There is also no automatic way of finding specific objects. Object map provides a way of storing all technical information in a database and allows for finding specific descriptive and generate reports on chosen topics.

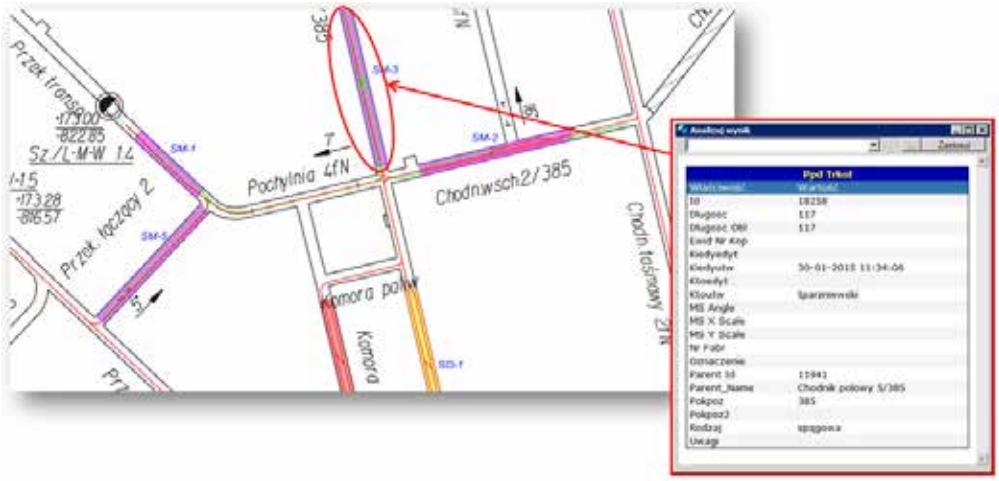

Fig. 3. Displaying information on objects that appears after clicking on it
– the example being underground railway

Object Map is entering the field where previously some other still working software was implemented. MainCoal system, and data base for storing information on fixed assets is working in Bogdankas IT infrastructure. The same information as in those two are being stored in Object Map. Cohesion of the system was one of the conditions of implementing this system. APEX application was produced in order to generate reports from Object Map, MainCoal and fixed assets base.

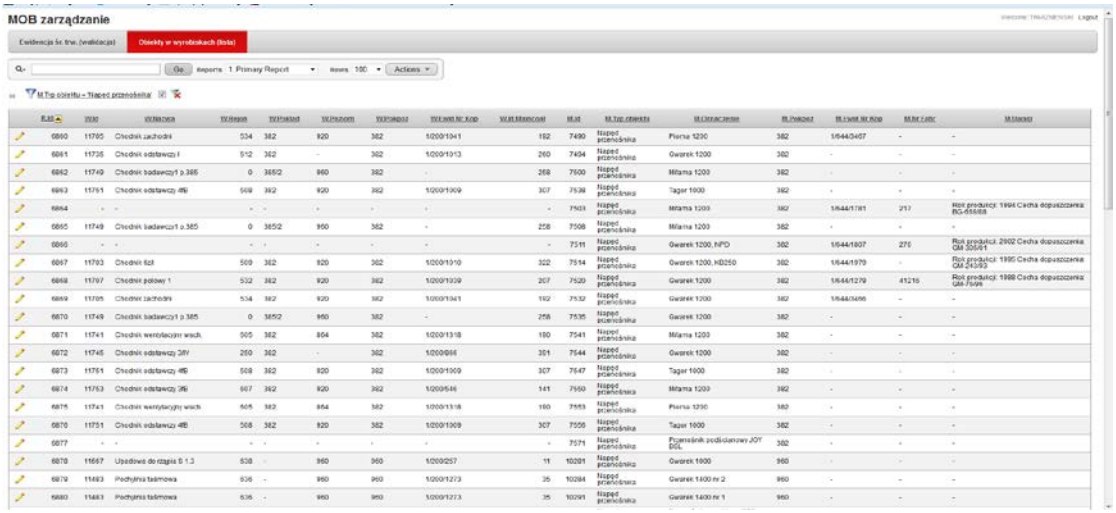

Fig. 4. Example of a report generated from 3 databases – Object Map, MainCoal and fixed assets base

INVENTORY PROCESS OF UNDERGROUND INFRASTRUCTURE

Inventory is a process that allows for generating information or placement, value and existence of the assets (Winiarska, 2004). There are many ways of conducting inventory however they need to be edited in order to fulfill the needs and specifics of a company. Since described process was placed in an underground mine it was done by onside inventory. It took two stages, first an onside inventory was done and results implemented in to the software, second results ware compared with inventory list provided by separate underground divisions.

Also timetable of inventory was separated in to 2 stages:

- I stage – included level 990 in Stefanów, 960 in Bogdanka and 864, 910, 960 in Nadrybie.
- II stage – included levels 382, 385/2 and 391, and also update of inventory of levels 864, 910, 960 and 990.

Ist stage, that was finished by the time of writing, included inventory of almost 50,000.00 m of underground corridors.

The object of this inventory ware:

- belt conveyors,
- pipelines:
  - fire water supply,
  - main drainage,
  - main air-condition,
  - comperes air,
- additional energy supply,

– floor mounted railway,
– suspended frictional railway:
  - railway stations,
  - goods station,
  - loading station,
– rail transport terminal.

Process of placing object to the Object Map consists of 3 easy to perform stages (fig. 7):

1. Placing object on a map.
2. Assigning attributes to the object.
3. Saving data that automatically sends it to the base.

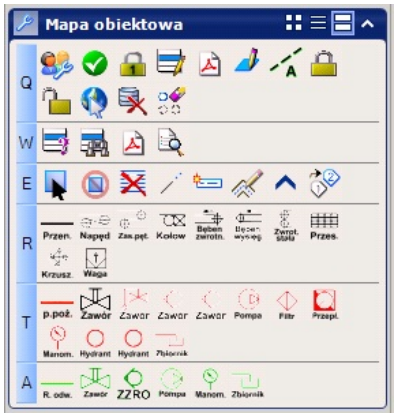

Figure 1. Tools of object map implemented for underground rail transport

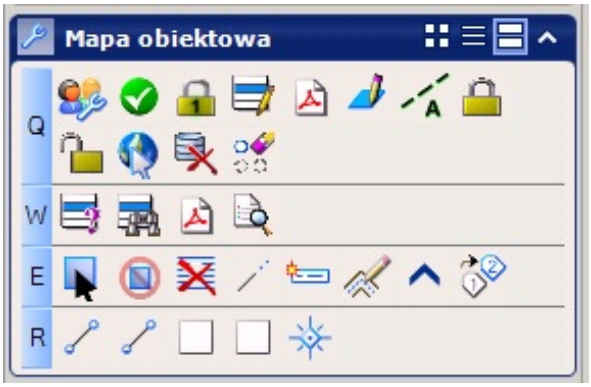

Figure 2. Tools of object map implemented for belt conveyors and pipelines

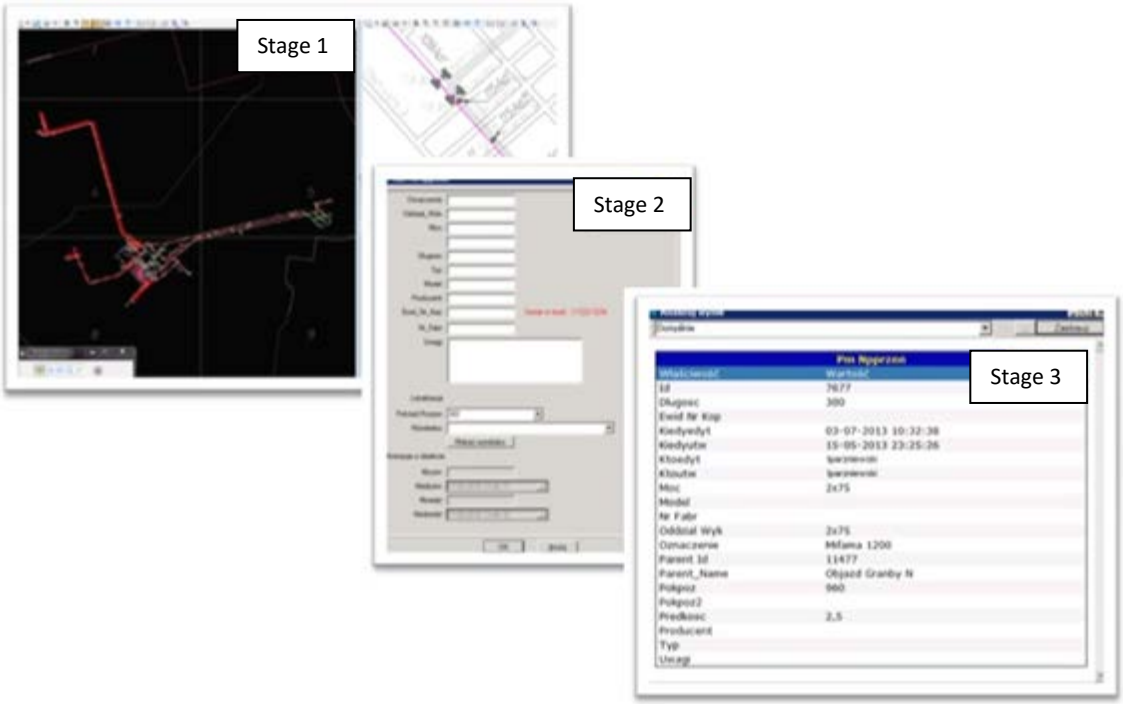

Figure 7. Process of placing object to the Object Map

SUMMARY

Object Map is undoubtedly a system that helps with monitoring the inventory of underground mine tunnels. Detail inventory allows for providing reliable information that can be stored in Object Map system. This system allows for full control of underground assets and there proper usage. Once control over assets is possible, control over costs of production is easy. It is easy to find objects, machines in a chooses corridor and estimate there value for tax purposes. Plans for near future involve providing the system access to WebGIS and adding more, technical information on stored objects. The authors also plan to improve methods of onside inventory by providing better ways of marking machines.

REFERENCES

Karlikowski S., Parzniewski T., Galica D. (2015). *Wdrożenie mapy obiektowej kolejnym krokiem na drodze inwentaryzacji majątku dołowego w LW „Bogdanka" S.A.*, Proceedings of the School of Underground Mining. Kraków, IGSMiE PAN.

Winiarska K. (2004). *Organizacja inwentaryzacji w firmach prowadzących księgi podatkowe i księgi rachunkowe*. Difin.

OPTIMIZATION OF THE ROCK MASS IDENTIFICATION METHODOLOGY FOR MINE DESIGN IN POLAND

*S. Fabich[1], D. Nitek[1], A. Waligóra[1], M. Rajczakowska[1], S. Świtoń[1]

KGHM CUPRUM Ltd. R&D Centre
ul. Gen. Wl. Sikorskiego 2-8
53-659 Wroclaw, Poland
(Corresponding author: sfabich@cuprum.wroc.pl)

24th World Mining Congress
MINING IN A WORLD OF INNOVATION
October 18-21, 2016 • Rio de Janeiro /RJ • Brazil

OPTIMIZATION OF THE ROCK MASS IDENTIFICATION METHODOLOGY FOR MINE DESIGN IN POLAND

ABSTRACT

This paper deals with an optimal scope of rock mass identification for deep mines in Poland. Firstly, a history of rock mass testing for polish mine design is presented, from 1966 to recent years. Testing programs are described, evaluated and compared in terms of their usefulness are complexity. Advantages and disadvantages of each testing approach are demonstrated. The rock mass characterization necessary for the deep mine design is introduced with respect to the traditional and modern design methods including numerical simulations. Technological aspects of shaft sinking method as well as the geological information about the investment region and their influence on the rock mass investigation program are emphasized. Finally, taking into consideration past experience and all the specified criteria, an optimal rock mass testing procedure is proposed including laboratory and in-situ measurements.

KEY WORDS

Rock mass identification, Poland's Copper Belt, shaft design

INTRODUCTION

Vertical shafts are a primary means of access to the ore body within Poland's Copper Belt Mines. Due to the fact that they operate for many years, the design of a proper shaft concrete lining, which provides the stability of the excavation while maintaining its functionality, is a crucial matter. The design should be performed taking into account the actual geological conditions preceded by a detailed borehole examination. Another important task is the execution of the access to the deposit, being directly connected to the completion of the planned investment on time, which depends on a properly chosen shaft sinking method. The choice of sinking method that is safe and, at the same time, economically optimal, requires a detailed rock mass investigation. During rock mass identification process, there is always a possibility of making mistakes, especially in the case of difficult geological conditions, which may result in a misinterpretation of e.g. ground water table, the inflow of water and gas to the excavation or the geomechanical parameters of the rock mass.

The purpose of the identification of the geological conditions and properties of the rock mass within the access to the deposit, is to gather a set of data allowing to choose the shaft execution technology. The information obtained during the geological investigation should, in addition, give the possibility to determine the mining methods for the particular rock layers and select a proper concrete lining. On the other hand, the procedures of the rock mass investigation depend on the shaft concrete lining design methodology assumed. In 70s, fulfillment of the regulations from the standards was obligatory in Poland. Nowadays, the designer has freedom to choose the design method and the guidelines presented in the current Polish Standards, PN-05015 and PN-G-05016, are only one possible design procedure. An alternative way is the computer aided engineering. The two aforementioned approaches have major differences. The Polish Standard methodology assumes that the loading on the concrete lining consists in the pressure from the weight of the rock mass and ground water table. In order to calculate the rock mass pressure, the apparent angle of internal friction and critical depth are introduced. The computer aided engineering takes into account the interaction between the concrete lining and the rock mass. Here, the numerical solution of the boundary problem is applied within the theory of the elasto-plastic medium. This model corresponds to the properties and behaviour of the real rock mass. Currently the choice of the engineering software for the shaft design is large. With the use of those programs it is possible to, e.g. model the 3D structure of the rock mass, analyze the interface concrete lining-rock mass, calculate the properties of the rock mass based on the laboratory test results for the intact rock samples, perform the statistical analysis of the rock mass discontinuities and joints, etc.

Depending on a chosen design methodology, a different set of input parameters is required. In Poland, the rock mass identification procedures are dedicated to the standard design method. Development of the computer aided design, with the variety of rock mass models and features that can be implemented, did not bring any revolution to the laboratory or in-situ testing programs. What is more, the technological progress in geophysical equipment and easier access to the advanced machinery, has not resulted in a more detailed and optimized for engineering purposes rock mass investigation. Therefore, there is an urgent need to reevaluate and update the existing testing methodology and, most importantly, its scope. The selection of the necessary rock mass testing program for Polish Copper Belt conditions is a first step to increase the efficiency of the functional rock mass analysis. The goal of this article is to estimate a set of rock mass parameters which can be useful for the design and execution of the mine shafts for deep copper ore deposits in Poland. This will lead to the development of the new, economically optimal, engineering solutions. In addition, it may significantly decrease the time of the investigation which is a factor directly affecting the start of the design work and, as a consequence, sinking of the shaft.

POLAND'S COPPER BELT MINES

Currently the copper ore extraction in Poland is done only in Foresudetic Monocline area. Due to the nature of copper ore deposit at the Foresudetic Monocline (pseudo-stratified type of the deposit) the current model of ore extraction is based on the vertical shafts. Currently, 1250 m deep shaft sinking process with 650 deep freezing zone, lasts approximately five years. Due to technology of shaft's sinking which is currently being used in the Foresudetic Monocline area, where the deposit is deeper and deeper (1200 ÷ 1700 m), revenues from extracted copper ore will be delayed. To achieve the target was set in the KGHM Strategy (annual production rate of 700 gigagrams of copper concentrate), it is necessary to open new parts of the deposit. Besides of KGHM's foreign assets, the greatest prospects for exploitation in Poland are the new parts of the orebody in Foresudetic Monocline and in the Grodzieck Syncline.

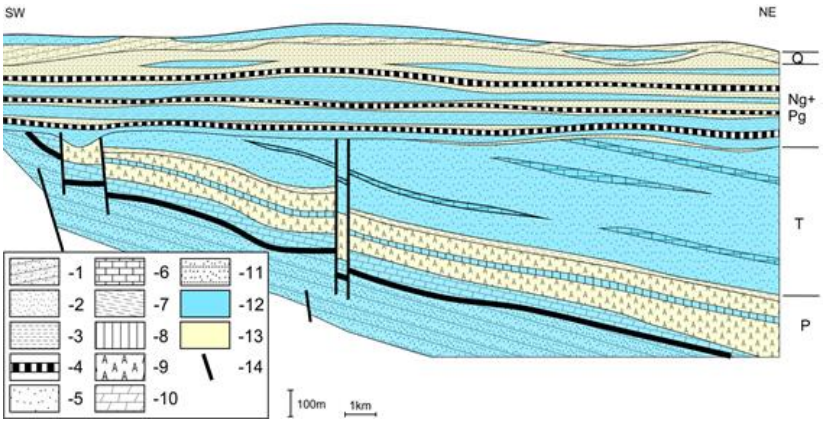

Figure 1 – Poland's Copper Belt hydro-geology schematics. 1- loam, 2- sand, 3- clay, 4- lignite, 5- Triassic sandstone, 6- limestone (oolitic, sandy), 7- claystone, 8- dolomite, 9- anhydryte, 10- limestone, 11- permian sandstone, 12- water-bearing layers, 13- isolation layers, 14 – faults

For the purpose of the exploitation of the Foresudetic Monocline, thirty shafts have been executed during 1968 ÷ 2013. The depth of the shafts is from 495 to 1,250 m. In total around 29 kilometers of shafts have been executed. At the moment, the thirty-first shaft is being sank to reach the depth of 1,340.7 m. The geological conditions of the Foresudetic Monocline are complex with high waterlogging in the range of 312 ÷ 690 m. The deeper the rock mass, the lower the waterlogging with increase of mechanical parameters increase. Due to the high waterlogging and weak rock mass parameters within the interval of 312 ÷ 690 m, the rock mass is subjected to freezing process and, usually in this range the watertight tubing shaft lining is designed. Below this depth the shafts are sank with traditional methods and the lining is made of monolithic concrete.

Shafts are located in the specific structure of the rock mass as well as in the difficult hydro-geological conditions. There are two thick layers of sedimentary rocks (from the top) - Cenozoic and

Permian. The elder of those is build out of a thick series of concise Triassic and Permian rocks. It consists of mottled and Rotliegend sandstones as well as clay shale, anhydrite, limestone and dolomite, and in some parts Zechstein rock salt.

Cenozoic rock is made up of Tertiary and Quaternary deposits of the total thickness of ~ 283 to ~ 500 m. These rock is loose (soil) and cohesive mostly saturated with water (quartz sands, gravel and clay, with intrusions of lignite – a few meters thickness).

The deposit of copper within the Polish copper mines shafts is at depths from 600 to 1200 m.

Strictly connected with geological structure are also hydrogeological conditions. Basically there are two major water bearing structures:

- Cenosoic water in loose Quaternary, Neogene and Paleogene rock structures,
- Permian-Triassic water in hard, porous, fissured rock structures as well as in clay shale, limestone, molted sandstone, with water circulation.

These complexes are different in regards of lithological parameters, underground water chemical compounds and other hydrogeological parameters. The Cenosoic water complex is placed between ground surface and the depth from ~283 to ~497 meters.

In the profile there is one valuable feature. It can be observed that each layer is separated with an impermeable layer. There is only few direct hydraulic relations between layers, and it is observed at the contact between Triassic and Cenosoic layers.

DESING METHODS FOR SHAFT LINING IN POLAND

In Poland the design of shaft lining is done based on guidelines presented in Polish Standards. However, their application is not obligatory. The standard design methodology helped to execute a number of shafts which still operate without any problems. On the other hand, it is a well-known fact that the necessity to access deeper deposits, makes the standard regulations insufficient due to the fact that they simplify the problems concerning, e.g. tectonic stresses, which, at greater depths (below 800 m), have a significant influence on the loading of the shaft and, as a consequence, its stability. Therefore, it is advised to supplement the standard design procedure with the computer-aided one, allowing to take into account a lot of factors which were previously indirectly considered by applying correction coefficients. Nevertheless, it needs to be underlined that the methodology presented in the standards must not be neglected – the computer-aided methods should only be a supplementation, conducted parallel to the standard calculation.

The standard design method

The development of mining industry in Poland was associated with the construction of a number of shafts to access the deposits. Therefore, in order to facilitate and regulate the design methodology, a standard method has been prepared. The standard guidelines cover all the works connected to the design of the shaft lining, i.e. the geological investigation, sampling of the rock material, laboratory investigation scope, determination of the loading from the rock mass and, finally, design of the lining thickness.

The shaft design methodology is presented in two Polish Standards, namely PN-G-05016:1997 *Mine Shafts. Lining. Loads* and PN-G-05015:1997 *Mine Shafts. Lining. Guidelines for Design.* The former gives the guidelines for loading calculation based on the solutions of the limit states of the theory of plasticity with the Coulomb-Mohr failure criterion modified by application of material coefficients in order to take into account specific geological and mining conditions. In addition, based on the results of model tests, the theories prepared *ad hoc* were introduced, allowing to determine and modify the loading plots along the shaft. The horizontal pressures from the rock mass on the shaft concrete lining can be calculated according to the following formula:

$$p_n = \sigma_{zy} \cdot \tan^2\left(45° - \frac{\varphi}{2}\right) \quad (1)$$

where p_n is the horizontal pressure, σ_{zy} is the vertical stress from the weight of the rock and φ is the apparent angle of internal friction:

$$\varphi = arc\tan\left(\frac{R_{cs}^{(n)}}{10}\right) \tag{2}$$

where based on the loading calculated according to the formula mentioned above, Polish Standard gives the relation for the thickness of concrete shaft lining:

$$d_b = a\left\{\sqrt{\frac{R_{bb}}{R_{bb} - mp\sqrt{3}}} - 1\right\} \tag{3}$$

where a denotes internal radius of the shaft circular lining, R_{bb} is the design value of concrete uniaxial strength, m is the correction coefficient and p is the design loading determined according to Eqn. (1).

Computer-aided design methods

In Polish Standards it has been assumed that the rock mass loads the lining which has to be "durable" enough to withstand this load. This approach has some limitations. It does not take into account the interaction between the shaft lining and the rock mass, and, as a consequence, the fact that the loading on the shaft lining increases while the shaft sinking is progressing (phase excavation). In addition, the standard method does not take into consideration the horizontal in-situ stresses in the rock mass. The standards were originally developed for the Upper Silesia coal mines' conditions. The deeper the shafts, the more questionable the usage of the standard design procedures becomes. Recently there is an extensive development of the computer-aided engineering, namely numerical methods allowing, e.g. to model the rock mass and liner interaction or analyze different cases of loading.

All the inconveniences associated with the design of the mine shafts according to the standard methodology can be solved with the use of numerical modelling. There is a number of software not only facilitating the concrete lining design (RS^2, FLAC) but also allowing to determine the design parameters of the rock mass form the laboratory tests conducted on the intact rock samples (RocData). In addition, it is possible to analyze the rock mass with the use of block theory (Goodman & Shi, 1985) – Unwedge software – by taking into account discontinuities spacing and properties. The numerical methods give the possibility to take into account, e.g. lining-rock mass interface, tectonic stresses in the rock mass, rock bolts etc. As a result the stresses in the support can be estimated as well as the plastic zone range or the forces occurring in the rock bolts (Fig. 2).

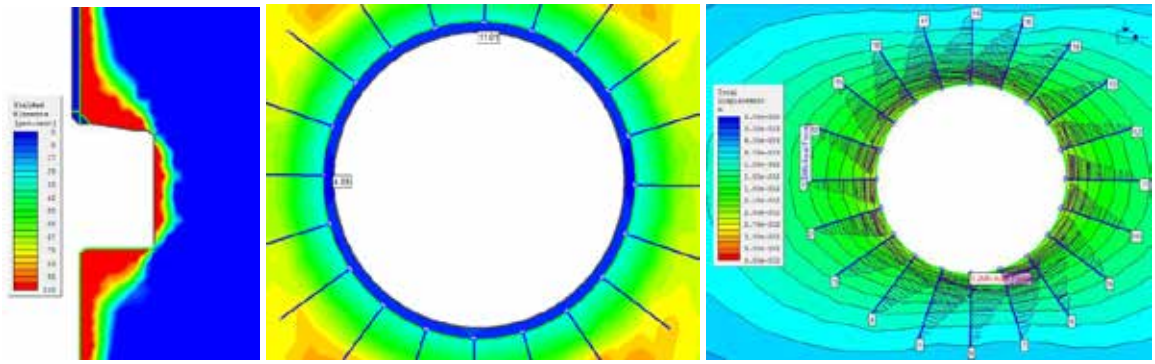

Figure 2 – Example of the numerical calculation of the shaft lining. From the left: plastic zone range in the shaft station, stresses in concrete support and calculation of the axial force in the rock bolts (Fabich et al, 2015)

Depending on the type of software, different models and failure criterions are available. However, the most important element in the numerical analysis is the "scaling" of the rock parameters – from the intact rock to the rock mass. This is a major difference between the computer-aided approach and the

standard one. Therefore, it is necessary to identify the input parameters necessary to perform the scaling procedure which can then be applied as input parameters for the numerical model.

In Table 1 the calculation results of the stresses in the shaft concrete lining are presented. Two methods were applied, namely Polish Standard design method and numerical calculation with the use of finite element method. It is visible that the results according to standard methodology are significantly lower. Of course those two methods cannot be compared directly due to a different calculation approach and differences in the input parameters. However, this example shows clearly that it is worth implementing both of the methods in order to achieve a safe design.

Table 1 – Calculation example according to Polish Standard and computer-aided design method

Rock type	Layer thickness [m]	Mid depth [m]	Stresses in concrete support [MPa]	
			Numerical calculation	Polish Standard method
Rhyolite	96	1605	9.2	6.6
Quartz-Diabase	18	1662	19.7	6.6
Metasediment	4.5	1673	11.2	6.2
Metagabbro	25.5	1688	15.3	6.2
Rhyolite	60	1731	10	7.1
Quartz-Diabase	24	1773	24.5	7.1

OPTIMIZATION OF THE ROCK MASS IDENTIFICATION METHODOLOGY

Overview of the evolution of the rock mass testing in Poland's Copper Belt

The design of the shaft lining requires a proper rock mass investigation. Throughout the years, in Poland the scope of the rock mass testing was strictly connected to the geological law regulations as well as the previously mentioned standard shaft lining design methodology. For the purpose of this research, the geological documentation from the years 1960–2009 has been reviewed in order to assess the changes in the rock mass testing procedures.

It has been observed that the scope of rock mass investigation did not significantly change over the years. This phenomenon is most likely associated with the fact that the design method remained the same as well. In addition, the testing methodology, e.g. uniaxial compression test, triaxial test, was also constant with time. The only visible difference comes with the development of new equipment over the years. In recent documentation there are results from various geophysical surveys. However, their direct application for the engineering/design purposes is unproven. In order to find the differences, an attempt has been made to perform a quantitative analysis of the scope of tests. The results of this analysis are presented in Figure 3.

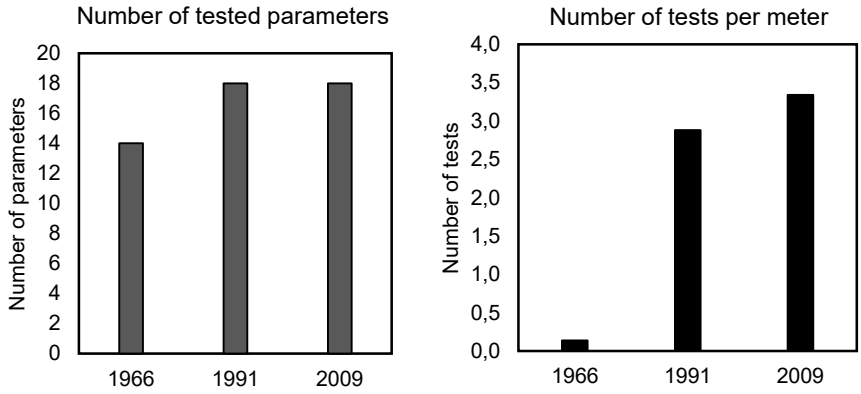

Figure 3 – Quantitative analysis of different geological documentations

It is clearly visible that the number of tests differ with time. What is more, in case of older geological documentations, the total number of tests was significantly lower as well as the number of tests per meter. The reason for this might be the level of knowledge about the rock mass at that time and lack of necessary investigation methods or access to the equipment. The only element that remained relatively constant is the number of tested parameters. This is due to the fact that the design methodology did not change over the years and there was no need to verify other parameters of the rock mass.

The parameters required for the standard design procedure are presented in Figure 4. The input data for the shaft lining loading are assumed based on the results of the laboratory tests for intact rock. There is no transition between the intact rock and rock mass parameters. The standard requires the macroscopic evaluation of the core extracted from the borehole in order to determine the weak zones of the rock mass. The physical as well as mechanical parameters have to be examined, therefore the uniaxial and triaxial compression test and tensile strength test are to be performed.

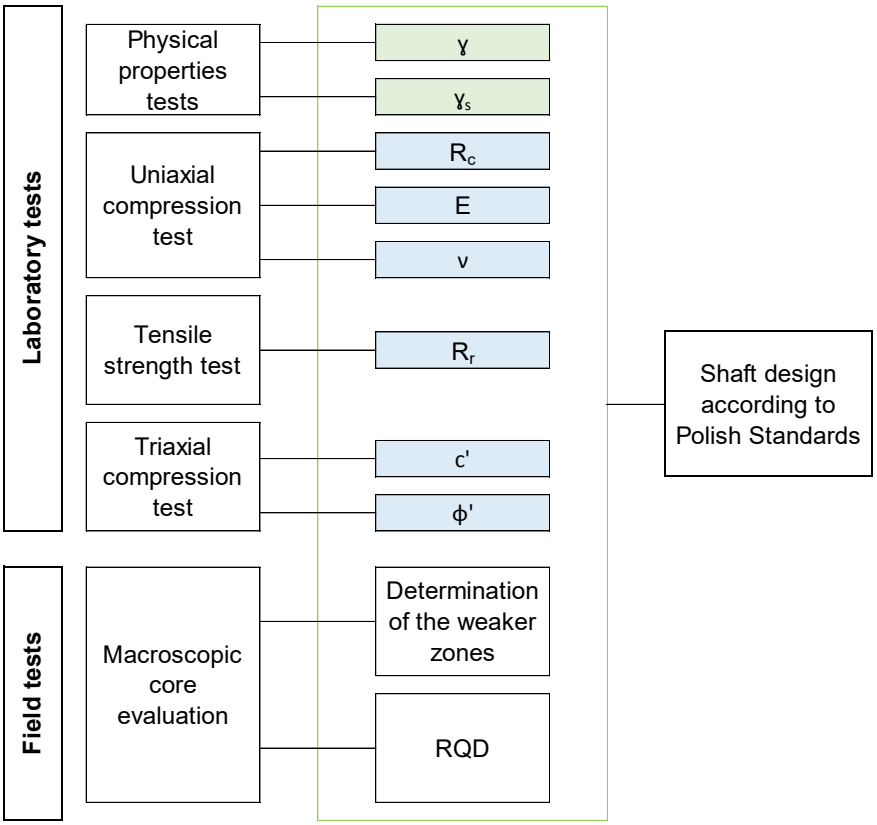

LEGEND:

γ_n - volume weight
γ_s - specific weight
R_c - Uniaxial Compressive Strength
E - Young Modulus
ν - Poisson ratio
ϕ' - angle of internal friction
c' - cohesion

Figure 4 – Input parameter for the standard design method.

It is worth mentioning that the friction angle obtained from the laboratory tests is not directly applied in the calculation of the loading. It is useful for estimation of the limit depth – the depth where the loading value stabilizes.

Development of a new recommended rock mass identification methodology

As it was mentioned earlier, due to the limitations of the standard design methodology, it is recommended to supplement it with the computer-aided methods. They give significantly more possibilities to analyze the phenomena which are neglected or simplified in the standard method. However, the set of parameters being the outcome of the rock mass investigation process, presented in previous section, is not sufficient for the numerical modelling. Therefore, in this chapter a new set of rock mass characterization procedures is proposed (Fig. 5).

The primary assumption for the new testing methodology is the, previously mentioned, scaling procedure of the intact rock properties to the rock mass ones. This can be done with the use of Hoek and Brown empirical criterion which takes the following form (Hoek et al, 2002):

$$\sigma_1' = \sigma_3' + \sigma_{ci}\left(m_b\frac{\sigma_3'}{\sigma_{ci}} + s\right)^a \tag{4}$$

where σ_1' and σ_3' are the major stress components, σ_{ci} denotes Uniaxial Compressive Strength and s, a, m_b are the empirical rock mass characteristics which can be evaluated with the use of Geological Strength Index (GSI) rock mass classification (Marinos & Hoek, 2000), introduced by Hoek and Brown. The additional formulas and details regarding the aforementioned criterion as well as its history can be found in (Hoek & Brown, 1980; Hoek, 1990; Hoek & Brown 1997; Marinos & Hoek, 2000; Hoek et al, 2002; Hoek & Marinos, 2007).

In order to acquire the rock mass parameters (Eqn. [4]), which can be implemented in the numerical model, the intact rock properties are required. Therefore, a specific set of laboratory tests has to be performed, i.e. triaxial test and uniaxial compression test. Then, Hoek and Brown criterion is fitted to the results of the tests, resulting in the computation of the parameters $\boldsymbol{m_i}$ and $\boldsymbol{\sigma_{ci}}$. Next, the Hoek and Brown Classification is used – the parameters of the Hoek and Brown criterion are calculated, namely $\boldsymbol{s}$, $\boldsymbol{a}$, $\boldsymbol{m_b}$. Additionally, the Coulomb-Mohr criterion can be fitted to the data as a straight line. The outcome of this procedures is a set of rock mass parameters: friction angle, cohesion, global Uniaxial Compressive Strength (Hoek et al., 2002), Uniaxial Compressive Strength, Tensile Strength and Elastic Modulus (Hoek et al., 2002).

Due to the fact that the numerical software gives a possibility to model jointed rock mass, unlike the Polish Standard method, an additional set of parameters is needed. For this purpose, it is important to perform borehole surveying with the use of geophysical methods such as acoustic or optical borehole logging. As a result of these tests, information regarding the joint spacing as well as joint orientation can be gathered. What is more, in order to have a full set of input parameters, the mechanical properties of the rock mass discontinuities have to be obtained. This can be done by performing the direct shear test and fitting a chosen criterion, e.g. Barton-Bandis, Power Curve, to the data. As a result, cohesion and friction angle of the joint are calculated (Fig. 5).

It is extremely crucial to remember about the tectonic stresses which can also be implemented in the computer-aided design. Distribution of tectonic forces is complicated by geological factors, with the added uncertainty in that there is no constraint on the total force, as is the case of gravity loads. Plate motions, interactions at plate boundaries and within plates are all driven by tectonic forces. What is more, the magnitude and orientation of the forces changes over geological time. It is to be expected, therefore, that the magnitude and orientation of these forces may vary considerably within geological systems (Sugawara et al., 2003). Unfortunately, a trustworthy in-situ stresses analysis has not been performed yet in Poland's Copper Belt.

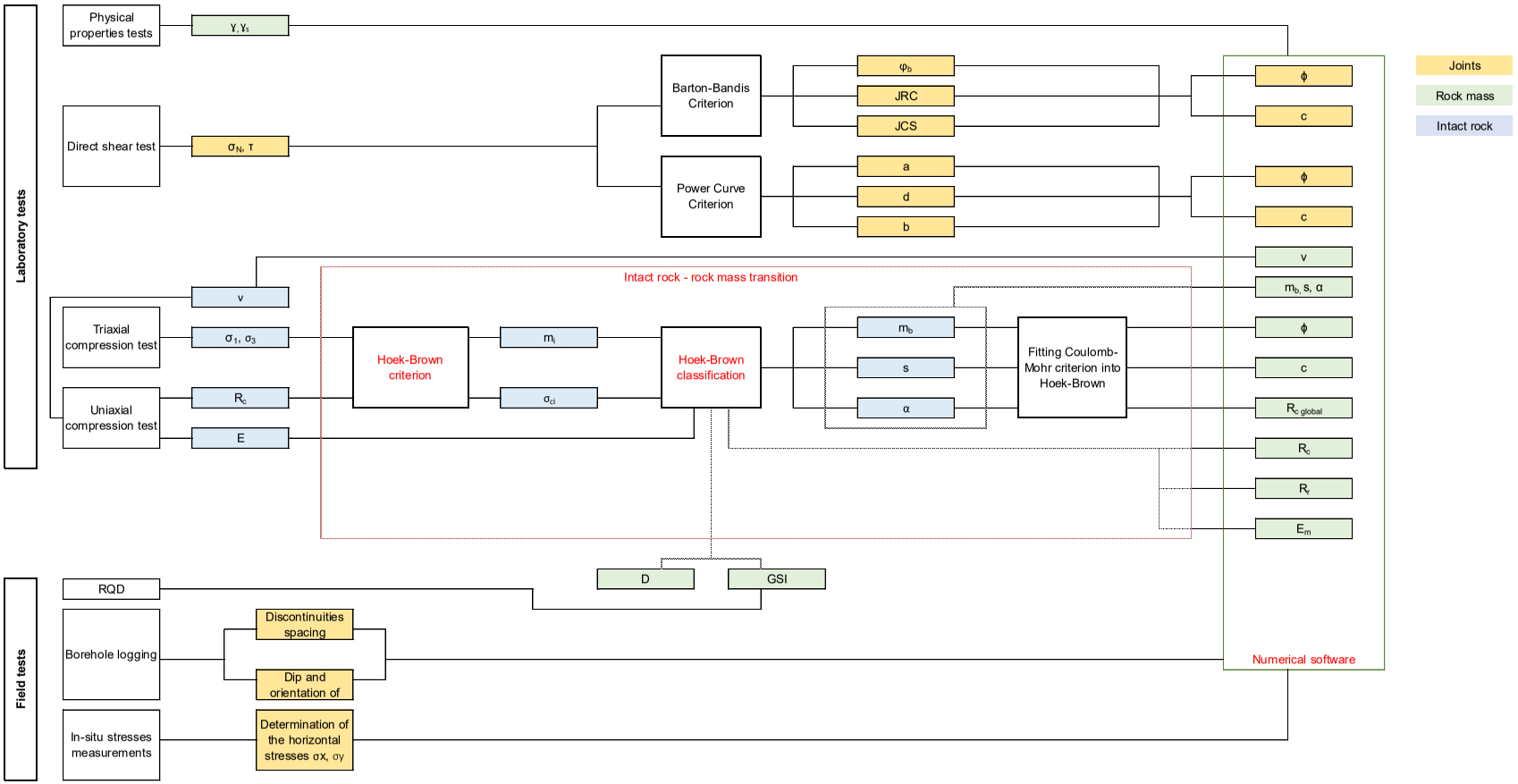

LEGEND:

γ - volume weight
γ_s - ciężar właściwy
σ_1, σ_3 - principle stresses
σ_N - normal stress
R_c - Uniaxial Compressive Strenght
τ - shear stress
E - Young Modulus
ν - Poisson ratio
m_i - Hoek-Brown parameter for the intact rock
σ_{ci} - Uniaxial Compressive Strength of the intact rock
D - disturbance factor
GSI - Geological Strength Index
m_b - reduced Hoeka-Brown parameter for rock mass
s, α - Hoeka-Brown criterion constants
φ_b - friction angle od the joint slip surface
JRC - Joint Roughness Coefficient
JCS - Joint Compressive Strength
a, d, b - Power Curve model parameters
ϕ - angle of internal friction
c - cohesion
R_r - Tensile Strength
RQD - Rock Quality Designation

Figure 5 – Scaling procedure from intact rock to the rock mass parameters.

Another important aspect that may influence the rock mass investigation scope is the choice of shaft sinking technology. In the presence of water level, which has to be evaluated based on the hydrogeological investigation results, the rock mass may require freezing. Therefore, it is important to assess the thermal properties of rock before and after freezing as they may vary with the rock type, etc. In addition, the mechanical properties of the frozen should also be checked, namely the compressive strength at different temperatures. Obtaining this information will allow to perform the freezing design (Fig. 6).

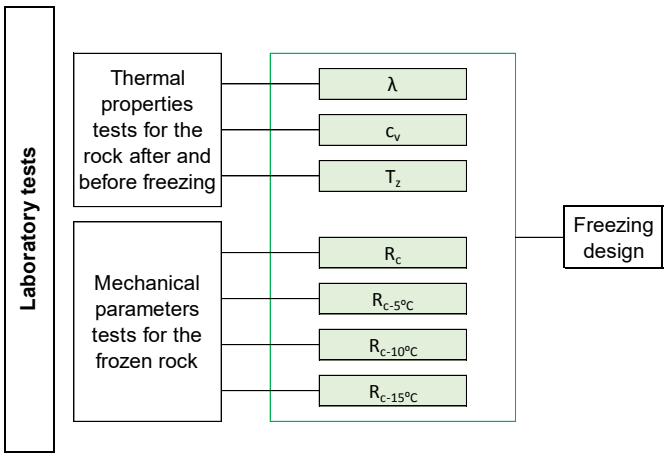

LEGEND:

λ - thermal conductivity coefficient

c_v - volumetric heat capacity

T_z - freezing temperature

R_c - Uniaxial Compressive Strength

$R_{c\,(-5,\,-10,\,-15)}$ - Uniaxial Compressive Strength for the rock frozen in temperatrues: -5, -10 and -15 deg.

Figure 6 – Scaling procedure from intact rock to the rock mass parameters.

SUMMARY

In the paper, an optimal scope of rock mass identification was analyzed for deep mines in Poland. The geological conditions corresponding to the Poland's Copper Belt area were presented. Technological aspects of shaft sinking method as well as the geological information about the investment region and their influence on the rock mass investigation program were emphasized. Polish standard design methodology for the shaft lining was described. The general rules as well limitations of this method were shown. In addition, the computer-aided design capabilities and advantages were demonstrated. The rock mass characterization necessary for the deep mine design was introduced with respect to the traditional and modern design methods including numerical simulations. Finally, taking into consideration past experience and all the specified criteria, an optimal rock mass testing procedure was proposed including laboratory and in-situ measurements.

The article presents the current problem regarding rock mass investigation program. As it was shown, almost nothing has changed in the rock mass characterization since 1960s in Poland. It is obvious that the reason for this is that the traditional design method presented in Polish Standards did not change over the years. However, taking into account the technological evolution, development of new modern equipment as well as the appearance of computer-aided design software on the market, it is very surprising that the rock mass investigation scope was not updated. The analysis of the geological documentation from the Poland's Copper Belt indicated that the current rock mass recognition scope requires reorganizing as it is not fully correlated with the current design methodology. In addition, it does not include the rock parameters necessary for the numerical modelling and computer-aided design, which take into account the transition between the intact rock results and rock mass properties. Therefore in this article a new set of procedures was presented, which could become the guidelines for both the designers as well as the geologists.

The following conclusions can be drawn from the study:

i. The standard method is the major and fundamental design procedure in Poland as it has been verified over the years. However, this procedure has also some limitations. Therefore, in complex cases, it should be supplemented by the use of numerical methods.
ii. Due to the significant influence of the design method on the rock mass investigation, the decision regarding the scope of the geological and geomechanical investigation should be a matter of consultation between the geologists and the shaft designers in order to find the most optimal solution.
iii. The numerical methods, on the contrary to the standard procedure, are based on the rock mass parameters. Therefore, they require the transition between the laboratory results obtained for the intact rock to the rock mass properties. This can be done by applying the Hoek-Brown criterion and GSI classification.
iv. The parameters of the rock mass, i.e. joint properties, tectonic stresses etc., are neglected in the Polish Standards. However, they play a crucial role in the shaft lining design and can be implemented in the numerical modelling. Therefore, despite the additional costs that it may generate, they should be added to rock mass investigation program.
v. In the case of the shaft sinking technology that requires rock mass freezing, it is necessary to include rock thermal properties, e.g. thermal conductivity, heat capacity, in the investigation scope.
vi. It is predicted that application of the investigation scope proposed in this article may significantly decrease the time needed for the execution of the shaft as well as the costs associated with the preparation of the rock mass for shaft sinking.

REFERENCES

Fabich, S., Bauer, J., Rajczakowska, M., & Świtoń, S. (2015). Design of the shaft lining and shaft stations for deep polymetallic ore deposits: Victoria Mine case study. Mining Science, 22.

Goodman, R. E., & Shi, G. H. (1985). Block theory and its application to rock engineering (p. 338). Englewood Cliffs, NJ: Prentice-Hall.

Hoek, E., Carranza-Torres, C., & Corkum, B. (2002). Hoek-Brown failure criterion-2002 edition. Proceedings of NARMS-Tac, 1, 267-273.

Hoek, E., & Brown, E. T. (1980). Empirical strength criterion for rock masses. Journal of Geotechnical and Geoenvironmental Engineering, 106(ASCE 15715).

Hoek, E., & Brown, E. T. (1997). Practical estimates of rock mass strength. International Journal of Rock Mechanics and Mining Sciences, 34(8), 1165-1186.

Hoek, E. (1990, June). Estimating Mohr-Coulomb friction and cohesion values from the Hoek-Brown failure criterion. In International Journal of Rock Mechanics and Mining Sciences & Geomechanics Abstracts (Vol. 27, No. 3, pp. 227-229). Pergamon.

Hoek, E., & Marinos, P. (2007). A brief history of the development of the Hoek-Brown failure criterion. Soils and rocks, 2, 1-8.

Marinos, P., & Hoek, E. (2000, November). GSI: a geologically friendly tool for rock mass strength estimation. In ISRM International Symposium. International Society for Rock Mechanics.

PN-G-05016:1997 Mine Shafts. Lining. Loads

PN-G-05015:1997 Mine Shafts. Lining. Guidelines for Design

Sugawara, K., Obara, Y., & Sato, A. (Eds.). (2003). Rock Stress' 03: Proceedings of the Second International Symposium on Rock Stress, Kumamoto, Japan, 4-6 November 2003. CRC Press.

OPTIMIZATION OF WINNING BLASTING PARAMETERS CONDUCTED FOR GROUP OF FACES, AIMING FOR ELASTIC WAVE EFFECT AMPLIFICATION

**[1]P.P. Mertuszka, [1]W.M. Pytel and [2]K. Szczerbiński

[1]*KGHM CUPRUM Ltd. Research & Development Centre*
2-8 Sikorskiego Street
53-659 Wrocław, Poland
*(**Corresponding author: pmertuszka@cuprum.wroc.pl)*

[2]*KGHM Polska Miedź S.A., Polkowice-Sieroszowice Mine*
Kaźmierzów 100
59-101 Polkowice, Poland

24th World Mining Congress
MINING IN A WORLD OF INNOVATION
October 18-21, 2016 • Rio de Janeiro /RJ • Brazil

OPTIMIZATION OF WINNING BLASTING PARAMETERS CONDUCTED FOR GROUP OF FACES, AIMING FOR ELASTIC WAVE EFFECT AMPLIFICATION

ABSTRACT

The exploitation of flat copper ore deposits in Polish deep underground mines is performed primarily by the use of drill-and-blasting technology. Each day in Poland a few hundred mining faces are fired out using this method which seems to be relatively well suited to the hardness of the local rocks and to local mining/geological conditions.

Besides, blasting works are also recognized as an active method of seismic events prevention, conducted as group strain-release blasting within potentially instable main roof strata and in pillars - if they are able to accumulate high amount of strain energy. A significant number of recorded dynamic (seismic) events can be clearly and directly explained by the blasting works' effects. Unfortunately, at present time, these operations are conducted intuitively – on a trial-and-errors basis, rather than upon an intentional and scientifically justified approach, so they are not effective enough as they could be. Furthermore, non-electric detonators used presently for production, usually do not allow to achieve a sufficient accuracy in actually realized firing time-delays and therefore in the future they are planned to be generally replaced by the electronic type of detonators.

As a one of seismic hazard reduction measures, a special kind of group winning blasting conducted with appropriately selected delays between the successive face-detonations is proposed in the paper. This approach is expected to be able to amplify purposely the energy of rock mass vibration within the area which has been *a priori* indicated by the 3D FEM modeling as a potentially instable. The entire multi-faces blasting operation should conclude with the rock mass possibly distressing manifested as a seismic event. The analyses have been supported by a 3D FEM dynamic modelling of multi-face blasting in different configurations of space and time coordinates (number of faces, sequences and delays of blasting, etc.). The presented numerical examples taken from "Polkowice-Sieroszowice" mine indicate that the release of seismic energy accumulated in the rock-mass may be accelerated using the proposed method. Amplification of elastic waves by smartly designed multi-face winning blasting has revealed itself to be a promising new mean of seismic and rockbursts hazard reduction.

KEYWORDS

Rock Mechanics, Blasting Works, Numerical Modeling

INTRODUCTION

Having the increasingly tighten geological and mining conditions in which extraction of copper ore deposits in Poland is conducted, ensuring an effective and safe mining presently becomes a key task and a significant challenge for mine operators. New geomechanical hazards has been identified under these conditions, particularly those related to induced seismicity, which are mostly attributable to high stress values, lower deformability and higher strength of rocks surrounding a deep deposit. Therefore, more attention should be paid on a dual role played by multiple-faces blasting operations, since it is a technology providing sustainable high production and on the other hand it is a measure applied for the rockburst hazards prevention.

The Authors' overall goal was to develop and implement such firing patterns for the group winning blasting process which may produce the effect of wave amplification due to the interference of post-blasting seismic waves (Kabiesz, Lurka & Drzewiecki, 2015). This should increase the capability of inducing stress relief, manifested as a seismic event in a rock mass being mined. As a result, the development of an appropriate group winning blasting procedure may help to develop an effective method which would assist, better than methods used so far, in the stability control in underground workings as well as mitigate risks associated with the dynamic effects of the rock mass pressure. By the use of electronic detonators, it is possible to achieve a precise delay time between the detonation of explosives in the individual mining faces. Their implementation into mining operations is a technological milestone which has revolutionized the work of blasting engineers in underground mines. It may be also be expected that the blasting method described above may provide the amplification of vibrations in a specific location in the main roof strata where the strength hypotheses

based on the actual stress-strain state within a rock mass indicates a close location in respect of limit boundary surface.

BLASTING TECHNIQUES IN ROCKBURST HAZARD CONDITIONS

Hazardous situations, due to the dynamic effects of rock mass pressure, represent an essential problems for the mining operations in Polish copper mines. These effects mostly include tremors, rockbursts, and stress relief. The applied blasting method is one of the most effective approaches allowing for dealing with such hazards in the mines of the Lower Silesian Copper Belt (LGOM) in Poland. The following blasting operations are conducted there:

- Group winning blasting of mining faces (with possibly greatest number of blasted faces);
- Stress relief in solid ahead, by blasting-off the explosives in additional holes of enlarged length and diameter, done separately or together with blasting the faces;
- Relief blasting in pillars able to cumulate the stress;
- Relief blasting in the roof and floor strata.

Inducing stress relief in a rock mass by blasting methods involves eliminating simultaneously the roof support along quite a long mining front (Butra & Kicki, 2003) while at the same time reducing the horizontal component of stress in the same stratum. This may create an additional load applied to the subsequent, already heavily loaded stratum face, which may cause stress relief and rockburst (Figure 1).

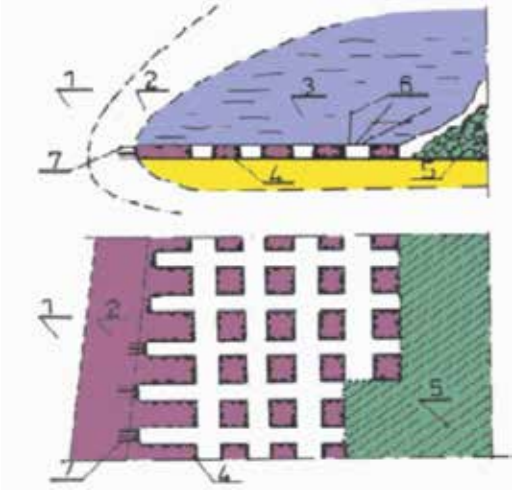

1 – unmined rock-mass,
2 – zone of mining pressure effect,
3 – stress relieved and delaminated rock-mass,
4 – bed (pillar) solid in post-critical state,
5 – cave-in forced by blasting,
6 – caving blasting holes,
7 – face blasting holes.

Figure 1 – Method of provoking strong seismic tremors and rockbursts in LGOM mines (Butra & Kicki, 2003)

This can be achieved by the simultaneous blasting of several faces located close to each other. Stress relief blasting operations – which can be carried out independently from regular blasting operations, can disturb the works in the operational fields, and, above all, also generate higher costs. To increase the inducing efficiency during the relief blasting operations, the so-called cut-stress relief holes of enlarged length and diameter are also frequently used. An example of such a stress relief blasting procedure is shown in Figure 2. In addition to the detonation of explosives in normal blasting holes of 3-4 meters, a large-diameter stress-relief explosive charge (about 30 kg of explosives in the hole) with a diameter of 127 mm is blasted in the mine face using the first or the last time delay. This allows overloading the mine faces with explosives and increasing the burden.

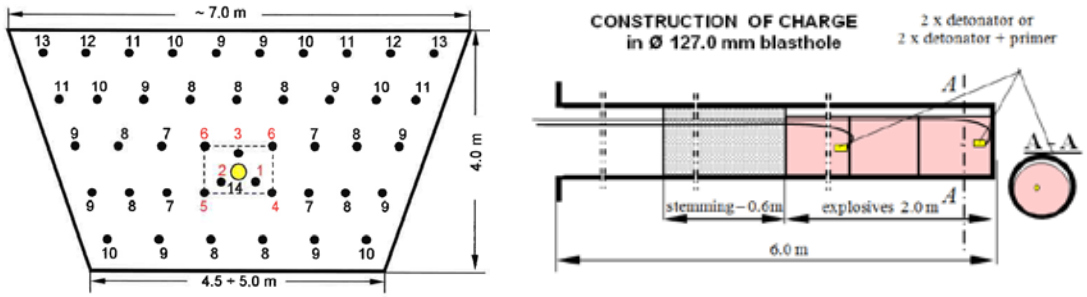

Figure 2 – Typical drilling, firing pattern, and construction of charges in an additional relief-cut hole

Rock mass provoking through the use of simultaneous (i.e. detonated theoretically at the same time in all the faces) blasting works has proved to be a partially effective method of rockburst prevention in LGOM mining conditions. The blasting works usually provoke a large number of recorded dynamic events. These stress relief events are classified as provoked events if they occur immediately after mining face detonation or after a period of minimal waiting time following the blasting works.

Figure 3 – Effectiveness of the seismic events provoking from point of view of the number of events (top) and their energy emission (bottom) in "Rudna" mine in the years 2011-2015

Figure 3 shows a 5-year summary of tremors of the energy $E_s > 10^3\ J$, recorded within the "Rudna" mine between 2011 and 2015, subdivided into the spontaneous (S) tremors and those provoked (P) by blasting works. These data prove that during the last 5 years the percentage ratio of spontaneous versus provoked tremors have changed significantly, both from point of view of number

of tremors and energy emitted as well. The presented data show that the effectiveness from point of view of number of tremors inducing by blasting operations has remained at approximately the same level of about 25% over the first four years, however it has increased up to 38% in 2015. In contrast, if we consider the seismic energy of tremors we may observe that during the considered years the energy dissipated by multi-face blasting has dropped down dramatically from about 48% to 25% in 2015. If we consider exclusively tremors of the energy greater that 10^6J, we may get an effectiveness of equal to 24% (number) and only 12% (energy), what one may treat as a kind of setback. This also means that in the last year in the "Rudna" mine, only the narrow portion of the observed high-energy tremors were really provoked. This is an evidence that the current blasting technique is not a very effective method which may be applied for rock mass distressing.

Nevertheless, inducing stress relief in a rock mass by intelligently designed simultaneous blasting works is still a chance for better controlling the time of occurrence of mining tremors. In selected mining divisions stress relief in a rock mass induced by simultaneous blasting of a large number of mining faces still constitute a significant percentage of tremors occurred in the absence of the mining crew, i.e. immediately after blasting during the post-blasting waiting period.

OPTIMIZATION OF BLASTING PARAMETERS OF MINING FACES

Despite the above-listed reservations, one may expect that the development of an appropriate group blasting procedure may help to obtain an effective method to assist both with the stability control of underground workings as well as with the mitigation of risks associated with the dynamic effects of the rock mass pressure. Selection of the proper blasting parameters, in addition to the use of modern blasting agents, may favor an easier elastic energy relieve from the rock mass and a significant increase of the burden.

When discussing the optimization of blasting parameters, one should consider which parameters are to be included in the blasting works model. At first glance, the following parameters should be taken here into account: (a) the number of mining faces detonated in one cycle and their spatial location, (b) the number and distribution of blasting holes in the individual mining face scale, (c) the diameter and length of blasting holes and their inclination, (d) the type (energy) of explosives, (e) the applied delays between each initiated blasting faces, and other less important things. While these parameters may be instantly included in the model as its parameters, certain limitations are encountered when translating their variability into mining conditions. So, the developed method may be effective only when it cannot cause disturbances in the mining process. Analyzing each of the above mentioned parameters, those which on-site conditions make optimization impossible can be forthwith eliminated. Finally, to maintain mining operations safe and effective, the following factors should be taken into consideration in the analysis (Pytel et. al., 2014):

1) the number of operational faces blasted per one cycle;
2) the spatial location of the mining faces;
3) delays applied between each detonating mining face (delays in group of mining faces scale, not individual faces).

While the first two parameters does not require any special measures aside from an appropriate operating plan, the last one involves implementing the most advanced technological solutions in the form of electronic detonators. The use of electronic detonators ensures exceptionally precise time delays with a practically unlimited number of time delay degrees – this may lead to the generation of a wave that would help to achieve stress relief in a rock mass.

The specific geological structure of the overburden, something which is typical in LGOM copper mines, favours strong seismic events occurrences. The material of the specific geological strata is characterised by high strength and low deformability. From the geomechanical point of view, the occurrence of dynamic events is determined by the high stress-strain state of the material surrounding the mine workings, i.e. low load bearing capacity margin. This means that even a slight additional load in the form of adverse stress changes – according to the accepted strength hypothesis – may lead to instability in a certain area of the workings. An instability may occur due to a dynamic impulse. This impulse may be created by the detonation of explosives, i.e. blasting of a mining face or a group of mining faces. Therefore, for the purpose of this paper, it has been assumed that the roof strata immediately in front of the blasted faces includes an area where the detonation of explosives at a group of faces, may cause a significant change in the level of stress or/and deformation (Pytel, Mertuszka & Cenian, 2015).

Assuming that the velocity of a seismic wave in a rock mass is approximately 5,000 m/s, and the analyzed mining parcel is located at a depth of about 1,000 m, the seismic wave generated by the

detonation of explosives will reach the surface of earth in 0.2 s. Such a high wave velocity means that the amplification effect by blasting a group of mining faces is only possible with relatively short and precise delays of several milliseconds between the individual faces/groups of mining faces. Bearing in mind that today the total firing time (the activation time of all detonators) is about 4-5 seconds, this time interval is too long to consider a mining face as a single dynamic impulse. On the other hand, it should be noted that the essential aim of the blasting works is rock excavation. Therefore, it is proposed to implement drilling and firing patterns with a stress relief hole of enlarged length and diameter (see Figure 2). To achieve a "single" dynamic impulse, these holes should be provided with electronic detonators and blasted with the first time delay.

GEOMECHANICAL ANALYSIS OF ROC KMASS BEHAVIOUR WITH IDENTIFICATION OF THE AREAS PRONE TO INSTABILITY

Computer simulations of the propagation of an elastic wave generated by group winning blasting operations were performed using a computation model based on the geometry of the mine workings in the area of block D-IE within the G-54 division, in the "Polkowice-Sieroszowice" mine, at a time when stress relief event in a rock mass has achieved the energy of $E_s = 2.1x10^7\ J$. This phenomenon has taken place on 13 December 2011 immediately after blasting a group of 26 mining faces. The objective of the presented analysis was to determine the overall stress/deformation states within the analyzed mining parcel prior to the event and afterwards to judge if the geometry of the mine workings could favor the likelihood of the occurrence of instability in the rock mass. As a basic physical model for the problem, the multi-plate overburden model has been accepted (Figure 4). It was assumed that the overburden strata consists of several homogeneous rock plates reflecting the real lithology in the area and the technological and remnant pillars work effectively within a post-critical phase (elastic-plastic with strain softening behaviour). To illustrate the effect of mining face geometry, the G-54 mining district located at a depth of 1,018 m has been modelled in 3D FEM code. A mining system with roof deflection and the use of dry backfill with 50% compressibility was assumed. The averaged geological data over the considered area and the estimated rock mass parameters are given in Table 1.

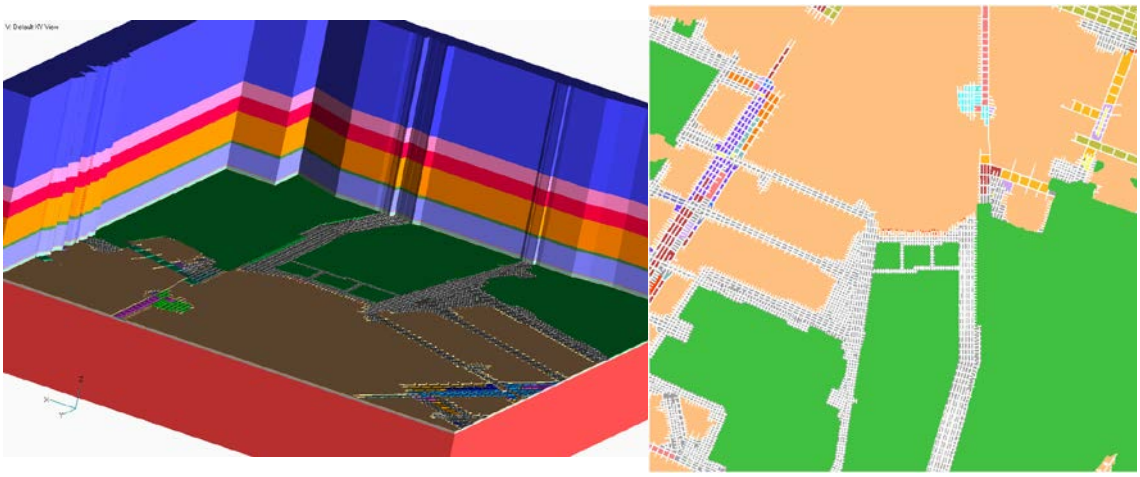

Figure 4 – General view FEM numerical model of rock mass (left) and view of the analysed FEM model of G-54 "Polkowice-Sieroszowice" mine's district (right) at the mine workings level

Table 1 – Geological data in the analyzed area

Rock type	Thickness (m)	σ_c σ_{cm} (MPa)	σ_r σ_{tm} (MPa)	σ_t σ_{sm} (Mpa)	E_s $E^{(r)}$ (MPa)	Poisson's ratio ν	LEVEL
Motley Sandstone	311	76.5 11.51	3.55 0.13	13.8 2.07	20000 5000	0.15	ROOF STRATA
Clayey Shale/Sandstone	103	36.0 1.73	1.7 0.002	4.75 0.21	13500 3375	0.18	
Main Anhydrite	100	93,1 19.53	6.4 0.24	17.9 3.12	56100 14025	0.24	

Breccia	10	36.0 1.73	1.7 0.002	4.75 0.21	13650 3375	0.18	
Basic Anhydrite	73	95.5 19.53	5.47 0.24	15.28 3.12	54600 13650	0.25	
Calcareous Dolomite III	4	121.8 40.71	8.15 0.55	18.3 6.11	52900 13225	0.25	
Calcareous Dolomite II	10	149.2 63.96	9.60 0.89	22.38 7.64	58300 14575	0.26	
Calcareous Dolomite I	2	214.7 149.6	14.3 2.15	30.0 18.44	96200 24050	0.25	
Copper ore	2.4	116.4	6.9	19.8	16400 8200	0.23	EXTRACTION RANGE
Grey Sandstone	7	25.1	1.10	4.8	9400 4700	0.16	FLOOR STRATA
Quartz Sandstone	200	17.9	0.9	3.40	5100 2550	0.13	

- $\sigma_{cm}, \sigma_{tm}, \sigma_{sm}$ compression, tension and shear strengths for rock mass, assessed according to Hoek's (2007) approach
- estimated laboratory results $\sigma_t = \omega \cdot \sigma_c$, where ω based on Lis (1996) equals: 0.16 for anhydrites, 0.15 for dolomites, 0.19 for sandstones and 0.12 for clayey shales

Geomechanical problem solution and results visualization were based on the NEi/NASTRAN (2009) computer program code utilizing FEM in three dimensions. It was assumed that all of the materials reveal linear elastic characteristics, except for rocks comprised within pillars which exhibit elastoplastic behaviour with strain softening. The entire numerical models general boundary conditions and were described by displacement based relationships. More information on the applied solution method may be found elsewhere (Pytel, 2003). A non-linear calculation procedure was applied, including an adaptive phase (elastic solutions with successive modification of overloaded pillars and an iterative procedure for selection of pillars for which the vertical load σ_z was greater than the critical value σ_p, and subsequently using a constant residual load σ_r instead of such pillars) and a final phase (verification of safety margins within the roof layers). The displacement boundary conditions were formulated as follows: no vertical displacements of the bottom layer in the model and no movements in the direction perpendicular to the lateral walls. The external load was divided into the following two groups: the self-weight load of the tertiary and quaternary formations (represented by the load $\sigma_z = 9.67$ MPa distributed evenly on the upper edge of motley sandstone) and the self-weight load of the other rocks represented by material characteristics, including the density (gravitation).

Numerical experiments permitted the determination of the overall stress/deformation states which were used afterwards for quantitative characterization of the actual level of safety using the indicators called safety margins related to different failure criterions (Pytel, 2010; Pytel & Pałac-Walko, 2015). In this paper safety margin F_τ spatial distribution has been calculated utilizing the maximum shear hypothesis which may be presented as follows:

$$F_\tau = \varepsilon_{nr} - \left(\varepsilon^d_{\tau,max} + \varepsilon^s_{\tau,max}\right) \tag{1}$$

where: $\varepsilon_{\tau,max} = \frac{\gamma_{max}}{2} = max\left(\left|\frac{\varepsilon_1-\varepsilon_2}{2}\right|, \left|\frac{\varepsilon_2-\varepsilon_3}{2}\right|, \left|\frac{\varepsilon_3-\varepsilon_1}{2}\right|\right)$,
$\varepsilon^d, \varepsilon^s$ – values of strain due to dynamic and static effects, respectively,
$\varepsilon_{nr} = 0.005$ – assumed limit value of the destructive shear deformation,
$\varepsilon_1, \varepsilon_2, \varepsilon_3$ – principal strain.

The value (positive or negative depending on the strength hypothesis involved) of any safety margin indicates the likely occurrence of instability in the rock mass. The selected results of calculations are shown in Figures 5.

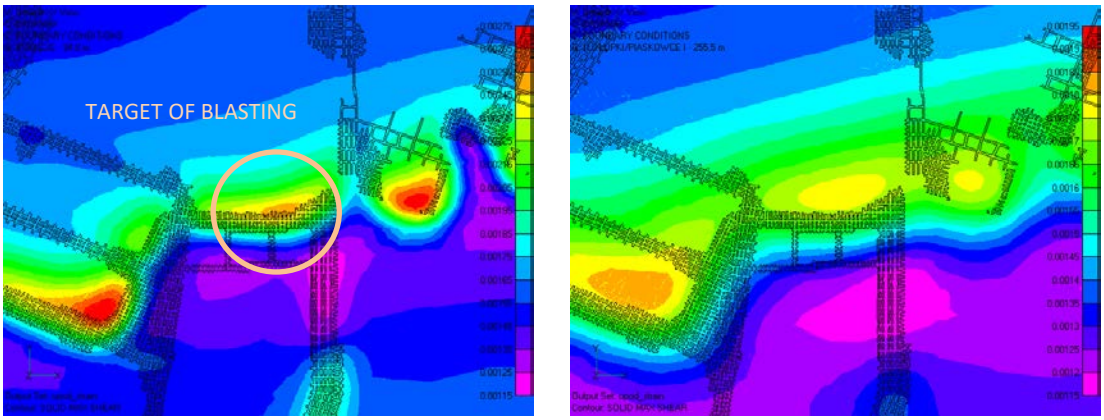

Figure 5 – Calculated values of safety margin contour 94 m (left) and 255.5 m (right) above the immediate roof strata based on a maximum shear strain hypothesis

The analysis indicates that the main roof instability may occur first in the breccia layer which is located at 94 m above the roof of the workings as shown by the minimum value of the safety margin at this level. This was determined based on the hypothesis of greatest shear deformations. The potential for risk exhibits also the clayey shale layer with sandstone (at 225.5 m above the roof strata). Based on the above, it may be concluded that an additional load in the form of a stress change in the roof layer – due to a dynamic impulse such as group winning blasting of mining faces – could lead to instability in the mine workings as well as to of high-energy tremors occurrence within the identified areas of the main roof strata. The knowledge on the areas in which the safety margins indicate that an instability event occurrence is very likely makes it possible to verify the results obtained using the developed numerical model.

NUMERICAL SIMULATIONS OF GROUP WINNING BLASTING

The above presented geomechanical analysis confirmed that the group blasting operations of 13 December 2011 could lead to induced tremors which were registered while firing of a group of mining faces. The blasting works were simulated by applying hydrostatic pressure within a finite elements comprising the fired out faces in which the detonation of explosives were represented by the pressure increasing from 0 to 5 GPa within 1 ms, and decreasing after detonation linearly to zero within the next 4 ms. In the subsequent simulations it was assumed that all of the analyzed faces were provided with an additional large-diameter hole and an electronic detonator which could be given a precisely defined time delay.

For the purpose of this paper, all of the analyzed faces were numbered from 1 to 33 (Figure 6), and then a total of several tens of group blasting configurations were simulated with different parameters, i.e. the number of mining faces blasted per one cycle, their spatial location and delays between sequentially blasted faces or groups of mining faces. The time delays were determined based on a geometrically determined distance between the analyzed group of mining faces and the point (area) characterized by greatest shear deformations (Figure 5). It was assumed that seismic waves travelling from the number of blasting faces will reach the mentioned area at the same time.

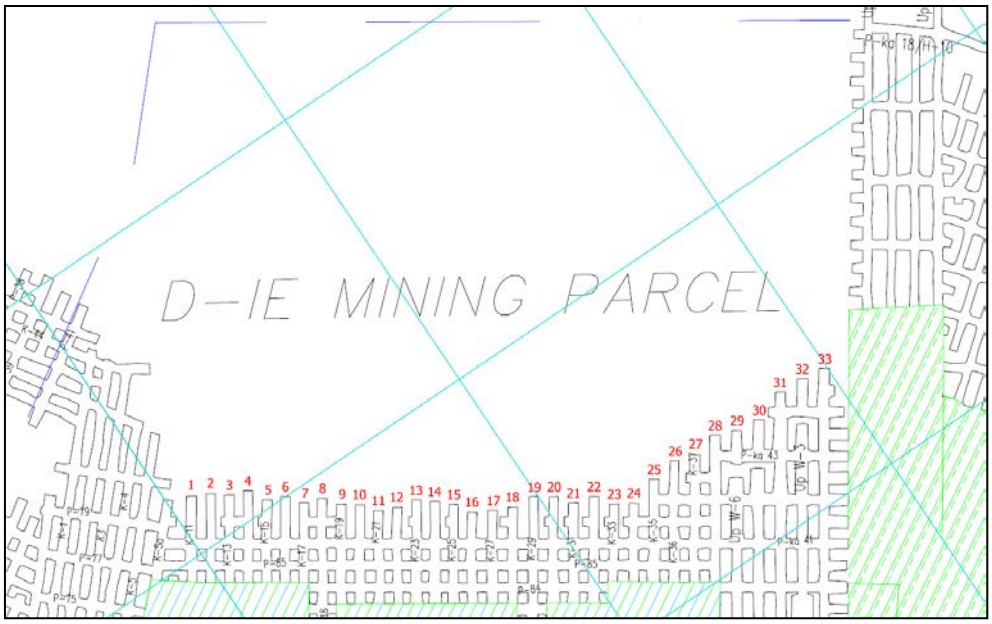

Figure 6 – Spatial location of analyzed mining faces within D-IE mining parcel

The seismic wave velocity in the rock mass of 5,800 m/s was accepted as an average value based on the results of passive tomography measurements carried out at periodic intervals in the LGOM mines.

The most characteristic scenarios were selected among the simulations. Six different cases are presented within the framework of this paper:

- Case 1 – immediate firing of 18 mining faces (no delays);
- Case 2 – geometrically determined delays (18 mining faces);
- Case 3 – immediate firing of 24 mining faces (no delays);
- Case 4 – geometrically determined delays (24 mining faces);
- Case 5 – immediate firing of 33 mining faces (no delays);
- Case 6 – geometrically determined delays (33 mining faces).

Changes in the safety margins at specific points of time within 0 to 100 ms after the firing of the first mining face have been presented in the form of graphs (Figure 7). The analysis included the changes in the safety margins at the site determined by numerical methods, characterized by the greatest shear deformations located above the roof of the workings at 96.4 m in breccia strata.

DISCUSSION OF THE ANALYSIS RESULTS

The changes in the safety margins at the stress accumulation sites, as determined by numerical methods, indicate that the blasting of a group of mining faces leads to a certain disturbance of the static state of stress and deformations. Some of the analyzed scenarios are characterized by significantly greater changes – when compared to the initial status – than in other scenarios. Case 6, in which the blasting of a group of 33 faces was simulated, is an example of this. This scenario involved 7 degrees of time delay, determined geometrically based on the distances from the previously determined sites exhibiting the potential risk of instabilities. A similar situation is observed in case 4, which simulated the blasting of a group of 24 faces with 7 degrees of time delay, however, these results' values differ from those obtained in scenario 6.

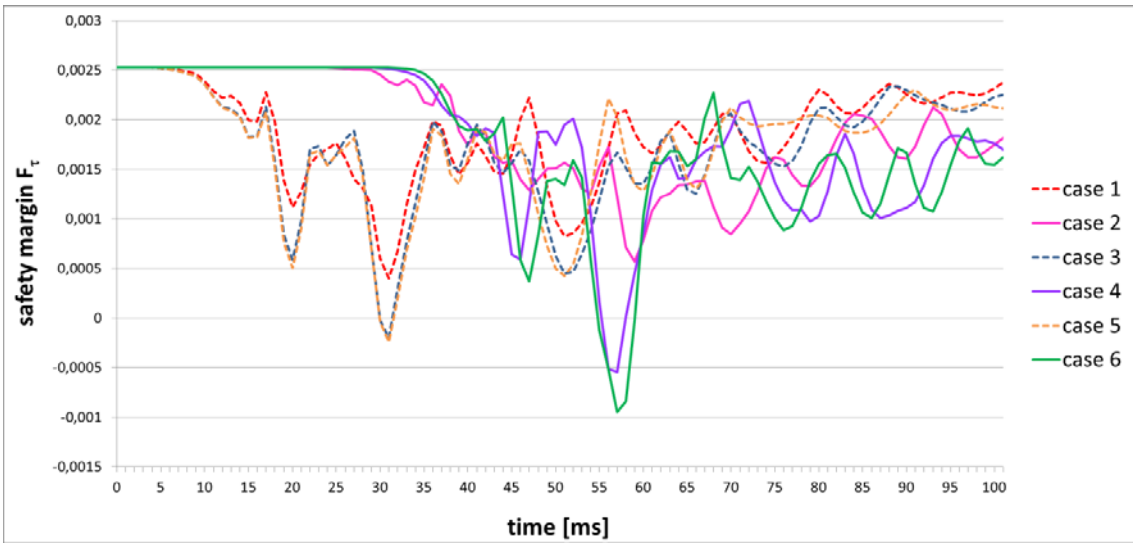

Figure 7 – Changes of safety margin F_τ values for cases 1÷6

DISCUSSION OF THE ANALYSIS RESULTS

The changes in the safety margins at the stress accumulation sites, as determined by numerical methods, indicate that the blasting of a group of mining faces leads to a certain disturbance of the static state of stress and deformations. Some of the analyzed scenarios are characterized by significantly greater changes – when compared to the initial status – than in other scenarios. Case 6, in which the blasting of a group of 33 faces was simulated, is an example of this. This scenario involved 7 degrees of time delay, determined geometrically based on the distances from the previously determined sites at the potential risk of instabilities. A similar situation is observed in case 4, which simulated the blasting of a group of 24 faces with 7 degrees of time delay, however, these results' values differ from those obtained in scenario 6.

Taking into account that the 'in minus' change in the safety margins may indicate potential of rock mass instability within the analyzed area, the determined safety margins (based on the maximum shear strain hypothesis) confirm an existing risk of rock mass destruction due to the high shear deformation level. The instability associated with an excessive shear strain represented by the utilized strength criterion (Eq. 1) points to a very likely occurrence of instability, especially at the level of 94 m above the roof of the workings, even though the primary (static) values of the safety margins determined by this method have not reached negative values. The greatest decrease in the safety margins is observable in scenario 6 at 94 m above the roof of the workings, where the value of the safety margin decreased of about 0.0035 as compared to the pre-blasting values (see Figure 7).

CONCLUDING REMARKS

The copper ore deposit in Poland is mined at increasingly greater and greater depths, and therefore mining operations are conducted in more and more challenging and difficult geological and technological conditions. Very often, mining is accompanied by dynamic events such as rock mass tremors, rockbursts and stress relief. These phenomena are extremely difficult to both predict and analyze due to their short duration and unpredictable time of occurrence. Furthermore, since no satisfactory results have been achieved by the implementation of different types of mechanical excavating systems suitable for copper ore deposits, there is still a need for continued efforts to improve the effectiveness of drill and blasting technics of mining.

The detonation of explosives generates a propagating shock wave which may cause a serious damage to a material body that is encountered on its way. This wave (mechanical vibrations) is usually considered to be a side effect that has a destructive impact on the immediate surroundings. However, in this specific case, blasting operations are considered as one of the most effective active methods for dealing with rockburst hazards as the waves generated by blasting operations interfere with each other, amplifying or reducing amplitudes in given areas. As a result, it is possible to control, at least to a

certain extent, the blasting phases which in turn may control the time and place of occurrence of an induced dynamic effect.

The primary objective of this paper was to develop an appropriate method for group blasting operations in order to provide an effective tool that would assist, by amplifying the elastic wave, with the control of stability of underground workings. This may permit mitigating risks associated with the dynamic effects of the rock mass high pressure. Additionally, the applied numerical methods have revealed themselves to be very effective in the verification of the "primary" conditions, i.e. stress and deformations within the analyzed area of the rock mass. For this purpose, the effects of selected parameters on the formation of an elastic wave generated by the detonation of explosives in the mining face have been evaluated. As a result, several noteworthy conclusions were formulated. The most important outcomes are as follows:

- The presented results of numerical modelling have proved that there is a clear relationship between the applied delay of charges detonation and the and the stress-strain time-dependent changes within rock mass.
- Controlling the blasting delay from the individual sources permits correcting the safety margins at a specific point of the analysed area.
- Changes in the distribution of the sum of values of safety margins characteristic for the static and for the load due to the detonation of explosives indicate that there is room for intentional inducing instabilities within a rock mass.
- Changes in the number of faces, their spatial location and the sequence (delays) of face blasting operations per a one cycle have a considerable impact on the spatial distribution of safety margins within a rock mass.
- Elastic wave amplification observed in the areas located immediately above the faces which are to be blasted, has proved the usefulness of this approach applied in the future for rockburst hazard prevention, especially in high stress level areas.
- The tracking of the changes in the safety margins, determined on the basis of selected strength hypotheses, permits determining the sites with instability risks which may then be purposely induced with a given time-sequence blasting at a group of mining faces.

A prerequisite for obtaining reliable results based on computer calculations that describe the analyzed effect with acceptable accuracy is – in addition to the sufficient knowledge of the modeling methods – the adequate data which will provide the reliable representation of rock mass behavior in the extreme load conditions. Thus, the potential of laboratory testing of rocks with a view to determining their mechanical properties under dynamic load is recognized to be of significant importance. Therefore, the proposed numerical model, in which the shock wave is used as the load-inducing basic factor, should also involve the dual character of deformation and strength properties of materials under static load or alternatively under dynamic load.

ACKNOWLEDGEMENT

This paper has been prepared through the Framework 7 EU project on "Innovative Technologies and Concepts for the Intelligent Deep Mine of the Future (I^2Mine)", Grant Agreement No. 280855. The authors also wish to acknowledge the support of the Polish Ministry of Science and Higher Education.

REFERENCES

Butra, J., & Kicki, J. (2003). *Ewolucja technologii eksploatacji złóż rud miedzi w polskich kopalniach [The evolution of exploitation of copper ore deposits in Polish mines]*. Biblioteka Szkoły Eksploatacji Podziemnej. Kraków, Poland: Biblioteka Szkoły Eksploatacji Podziemnej.

Hoek, E. (2007). *Practical Rock Engineering.* Retrieved from https://www.rocscience.com/learning/hoek-s-corner/books.

Kabiesz, J., Lurka, A., & Drzewiecki, J. (2015). Selected methods of rock structure disintegration to control mining hazards. *Archive of Mining Sciences, Vol. 60, No.3,* 807-824. doi: 10.1515/amsc-2015-0049.

Lis, J., Fabich, S., Kijewski, P., Kokot, B., Szadkowski, T., Maćków, B., Struzik, H. (1996). *Opracowanie i wydanie nowej edycji katalogów fizykomechanicznych cech skał złożowych i otaczających występujących w obszarach kopalń LGOM [Preparation and publication of the new edition of the catalogue of physical and mechanical properties of ore zone rocks and*

surroundings typical for LGOM mines] (Research Work No. U-138/NG/95). Wrocław, Poland: "CUPRUM" Research & Design Center of Copper.

NEi/Nastran (Version 9.2) [Computer software]. Westminster, CA: Noran Engineering, Inc.

Pytel, W. (2003). Rock Mass – Mine workings interaction model for polish copper mine conditions. *International Journal of Rock Mechanics & Mining Sciences, 40,* 497-526.

Pytel, W. (2010). Room and pillar mine workings design in high level horizontal stress conditions. Case of study from the Polish underground copper mines. In F. Xie (Ed.), *Rock Stress and Earthquakes* (pp. 505-511). London, Great Britain: Taylor & Francis Group.

Pytel, W., Mertuszka, P., & Cenian, B. (2014). Rockmass de-stressing by blasting in LGOM mines conditions. *Proceedings of the International Conference on Drilling and Blasting Technology* (pp. 37-48). Balatonkenese, Hungary: Hungarian Society for Blasting Technology.

Pytel, W., Mertuszka, P., & Cenian, B. (2015). Group Winning Blasting as a Rockburst Control Method. *Proceedings of the 15th International Multidisciplinary Scientific GeoConference SGEM, Vol. III* (pp. 353-360). Albena, Bulgaria: STEF92 Technology Ltd.

Pytel, W., & Pałac-Walko, B. (2015). Geomechanical safety assessment for transversely isotropic rock mass subjected to deep mining operations. *Canadian Geotechnical Journal, 52(10),* 1477-1489.

OVERBURDEN MOVEMENT IN MULTIPLE-SEAMS LONGWALL MINING

*Yang Li, Huaqun Wang, Kangning Zhang

School of Resources and Safety Engineering, China University of Mining and Technology, Beijing
D11, Xueyuan Road, Haidian District
Beijing, China 100083
*(*Corresponding author: liyangcumtb@163.com)*

24th World Mining Congress
MINING IN A WORLD OF INNOVATION
October 18-21, 2016 • Rio de Janeiro /RJ • Brazil

OVERBURDEN MOVEMENT IN MULTIPLE-SEAMS LONGWALL MINING

ABSTRACT

The multiple coal seams mining is one of the big mining issues in western China. The theoretical analysis and filed measurement are applied to study effect of interburden on the overburden movement during the mining process of lower coal seams. This study is focused on the effects of thickness and lithology, the proportion of hard rock, the ratio of the overburden thickness to the interburden thickness (OB/IB). In this paper, the amount of strata movement is calculated based on the key strata theory. A theoretical calculation method is put forward to calculate the roof fracture height. The results indicate that the ratio of the upper strata thickness to the interburden thickness（OB/IB） is not the dominative factor for overburden movement, especially in the mines in western China which features shallow buried depth and thin roof. Further research reveals that the fracture development in the roof strata is determined by the mining height and the property of roof strata. The breaking of thick and hard interburden could result in the instability of roof strata. The proportion of hard rock in the middle seam is irrelevant to movement of overlying seam.

KEYWORDS

western China, multiple coal seams, interburden, overburden movement, lower group coal

INTRODUCTION

The western China, including Inner Mongolia and Xinjiang, boast 40% of the Chinese total reserves, and as a result, massive projects in this area have been carried. Currently, the mining activity is gradually started in the lower No.2 and No.3 workable seam. Meanwhile, new technical issues have been also appeared in the mining process of multiple coal seams. As shown in Table.1, these issues can be divided into two major aspects: geological factor and mining factor. Due to these challenges, mining conditions and overlying seam movement of longwall panel are more complex.

Table.1 – Seam interaction factors in multiple-seam mining

Factors		**The research contents in this paper**
Geological factor	Mining factor	Interburden
The changes of thickness and structure of overlying seam	The adaptability of traditional mining method in multiple coal seam	The thickness and structure of interburden
water disasters Caused by Fracture connection	The stress concentration on the coal pillar	The proportion of hard rock in interburden
The different of thickness and structure of interburden	Support and the arrangement of roadway	The ratio of the overburden thickness to the interburden thickness
The dip Angle and the thickness of coal seam	The gob above the lower seam	

To date, extensive studies in this area have been carried out. YaoBanghua et al. studied the multiple coal seams mining, they found the lower seam mining can lead to the development of original

fractures. Majid summarized five kinds of calculating model to predict the fracture height. He thought the fracture height is 6.5-24 times of mining height in the short term after mining and the fracture height is 11.5-46.5 times of mining height when the roof stabilized. Ellenberger et al. studied the effect of ratio of overburden thickness to the interburden thickness（OB/IB）on overlying seam movement in both open pit and underground mines. The results show that the movement overlying seams declines when OB/IB is less than 7 and increase dramatically when OB/IB is more than 16. Haycocks et al. studied the lithology of the middle seam. They found the exploitation of upper coal seam influence the facture development and strata movement if the middle seam is relatively soft. These researches enrich the theories of multiple seam mining and promote the development of multiple seam mining. But the effect of middle seam on overlying seam movement during the mining of lower group coal seam is still a challenge.

In the paper, we explored the effect of interburden on the overlying seams during the mining process of lower group coal. Theoretical derivation, numerical simulation and filed test are applied to study effect of interburden on the movement of overlying seam based on different types of hard rock. Our analysis focuses on the effects of thickness, lithology, the proportion of hard rock, and the ratio of overburden and the interburden (OB/IB) as is shown in Figure.1. The movement and breaking mechanism are studied, which provides an important reference for the shield design of lower coal seam mining.

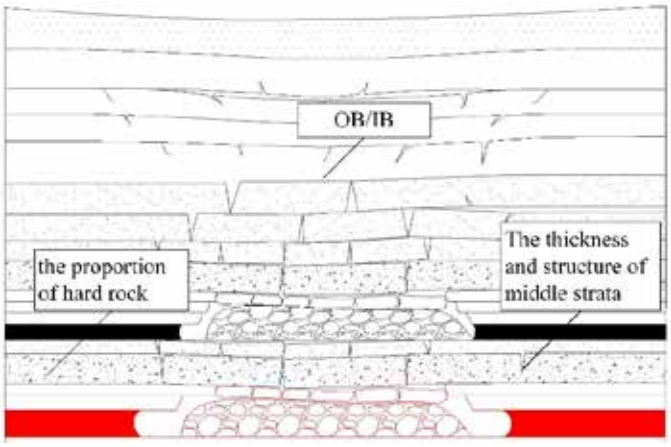

Figureure 1 – The research content of this paper

BACKGROUND

The study is based on four typical underground coal mines in the western diggings. The thickness, OB/IB value and the proportion of hard rock in middle seam are shown in Table.1. To be specific: the thickness of middle seam are listed as follows: 7m in Halagou coal mine, 6m in Kaida coal mine, 10m in Shigetai coal mine, 28m in Bulianta coal mine. Different OB/IB value of the four coal mine are also studied: 6.2 in Bulianta coal mine, 7.2 in Kaida coal mine, 8.2 in Shigetai coal mine, 9.4 in Halagou coal mine. The proportions of hard rock in the middle seam of the four coal mines are also different: 0% in Kaida coal mine, 70% in Shigetai coal mine, 80% in Bulianta coal mine, 100% in Halagou coal mine.

Table.2 –The data of the overburden and the interburden

	Upper coal seam	The depth of the upper coal seam/m	Lower coal seam	The depth of the lower coal seam/m	The type and thickness of interburden /m		The proportion of hard rock in interburden/%	OB/IB
Shigetai	1-2 lower	79	2-2 upper	92	Fine sandstone mudstone	7 3	70	8.2
Halagou	1-2 upper	66	1-2	75	Fine sandstone siltstone	4 3	100	9.4
Bulianta	1-2	182	2-2	215	siltstone Fine sandstone mudstone siltstone mudstone	6 12 4 3 3	80	6.2
Kaida	6-2 upper	54	6-2	66	argillaceous sandstone	8	0	7.3

THEORETICAL DERIVATIONS

(1) Analysis on breaking of hard rock

With the advancement of the longwall face, the breaking of immediate roof first occurs and then the span of the roof keeps extending until the first breaking of hard rock. The roof strata is simplified into a clamped beam, according to elastic solution, the first breaking span of hard rock seam is given by:

$$l = h\sqrt{\frac{2\sigma_t}{q}} \qquad (1)$$

After the first breaking of the hard rock, with the advancement of the panel face there will be periodic breaking of the hard rock. The roof strata are simplified into a cantilever beam, and the periodical breaking span of hard rock layer is given by:

$$L=h\sqrt{\left(\sigma_t+\frac{1}{5}\right)/3q} \qquad (2)$$

Where: l is the first breaking span, m; L is the periodic breaking span, m; σ_t is the tensile strength, MPa ; q is the loading from overlying seams, MPa ; h is the thickness, m .

The first breaking span and the periodic breaking span of hard rock seam in the four coal mines are shown in Table 3.

Table.3 –The first breaking span and the periodic breaking span of hard rock seam

Coal mine	Hard rock types	The first breaking span /m	the periodic breaking span /m
Shigetai	Fine sandstone	39.6	11.2
Halagou	Fine sandstone siltstone	27.5 19.8	11
Bulianta	Fine sandstone siltstone	41.1 28.9	17.1

Kaida	argillaceous sandstone(soft rock)	19.0	9

(2) The development height of fracture

After the coal seam is excavated, the overlying seams will collapse layer-by-layer. The excavation creates a free space between the falling rock and the roof seam. The bulking property of falling rock will make the height of the space decreases continuously. Through the derivations of multiple seams, the free height of the space is given as follow:

$$l_n = \begin{cases} M_{下} - \sum_{i=1}^{n-1} h_i(k_i - 1) & n < z+1 \\ M_{下} + M_{上} - \sum_{i=1}^{n-1} h_i(k_i - 1) & n > z+1 \end{cases} \qquad (3)$$

Where: l_n is the free height of the space of No.n layer, m; $M_{上}$ is the mining height of the upper seam, m; $M_{下}$ is the mining height of the lower seam, m; h_i is thickness of the corresponding layer, k_i is bulking coefficient of the corresponding layer.

And the maximal deflection of the roof layer is given as follows:

$$\omega_n = \frac{5q_n l_n^{\,4}}{384E_n I_n} \qquad (4)$$

The cross section of the strata as a rectangle, and the moment of inertia is given as follows:

$$I_n = \frac{a_n^{\,3} h_n}{12} \qquad (5)$$

where: ω_n is the maximal deflection of the roof layer, m; q_n is the loading from overlying seams, kN/m; l_n is the breaking span of the rock beam, m; E_n is the elastic modulus, kPa; I_n is the moment of inertia, m^4; a_n is the width of rock section, m;

By comparing the maximal deflection of the roof layer and the height of the free space, if $\omega_n \geq l_n$, the strata would keep its plastic state due to the restriction of free space.

For the lower coal seam mining, When the value of n within the interburden, if:

$$M_{下} \leq \sum_{i=1}^{n-1} h_i(k_i - 1) + \frac{5q_n l_n^{\,4}}{384E_n I_n} \qquad n < z+1$$

The fracture height H is:

$$H = \sum_{i=1}^{n-1} h_i \qquad n < z+1 \qquad (6)$$

When the value of n beyond the interburden, if:

$$\begin{cases} M_{下} > \sum_{i=1}^{n-1} h_i(k_i - 1) + \dfrac{5q_n l_n^4}{384E_n I_n} & n < z+1 \\ M_{上} + M_{下} \le \sum_{i=1}^{n-1} h_i(k_i - 1) + \dfrac{5q_n l_n^4}{384E_n I_n} & n > z+1 \end{cases}$$

The fracture height H is:

$$H = \sum_{i=1}^{n-1} h_i \qquad n > z+1 \qquad (7)$$

where: h_i is the thickness of the corresponding strata, m; H is the fracture height, m.

The relationship between the advancement of longwall panel and the fracture development height, the following results can be obtained by the above theoretical derivations.

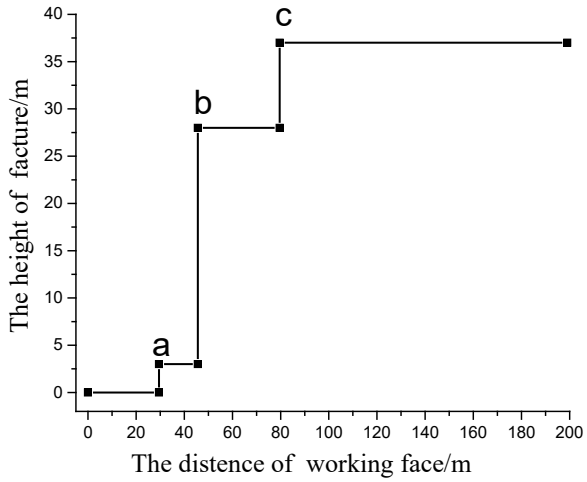

Figure 2 –The fracture development process of Shigetai coal mine

The fracture development process of Shigetai coal mine is shown in Figure.2. The results show that the height of fractured zone is 3m when the advancement is 30m and the immediate roof collapses at Point a. The hard rock seam first breaks when then advancement reaches 46m and the height of the fractured zone develops to 28m at Point b. The height of the fractured zone develops peaks at 37m when the advancement is 80m at Point c.

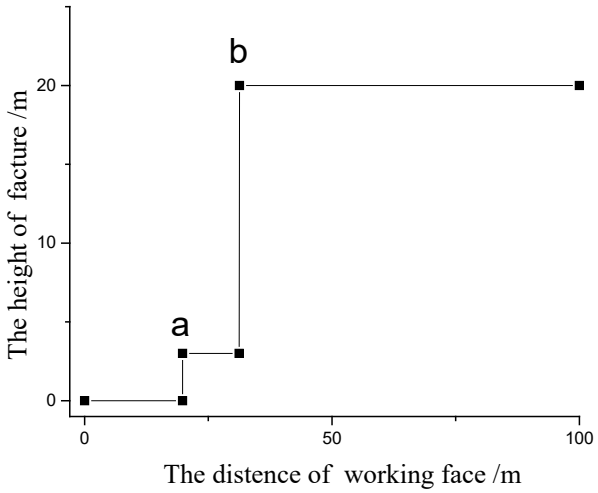

Figure 3. – The fracture development process of Halagou coal mine

The fracture development process of Halagou coal mine is shown in Figure.3. The results show that the height of fractured zone is 3m when the advancement is 20m and the 3-meter-thick siltstone seam collapses at Point a. The 4-meter-thick fine sandstone seam breaks when the advancement is 31m and the fracture zones triggered by lower group and upper coal seam mining are connected at Point b. The height of the fractured zone develops peaks at 20m

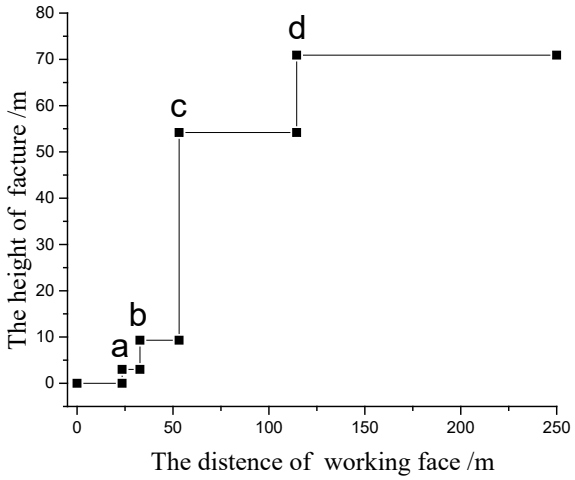

Figure 4 – The fracture development process of Bulianta coal mine

The fracture development process of Halagou coal mine is shown in Figure.4. The results show that the height of fractured zone is 3m when the advancement is 24m and the 3-meter-thick immediate roof collapses at Point a. The height of the fractured zone reaches 9 m when the 3-meter-thick siltstone seam collapses at Point b. When the advancement reach 53m, the fracture zones triggered by lower group and upper coal seam mining are connected and the 12-meter-thick fine sandstone seam breaks at Point c. The height of the fractured zone is 54m at this point and then peaks at 71m when the advancement is 114m at Point d.

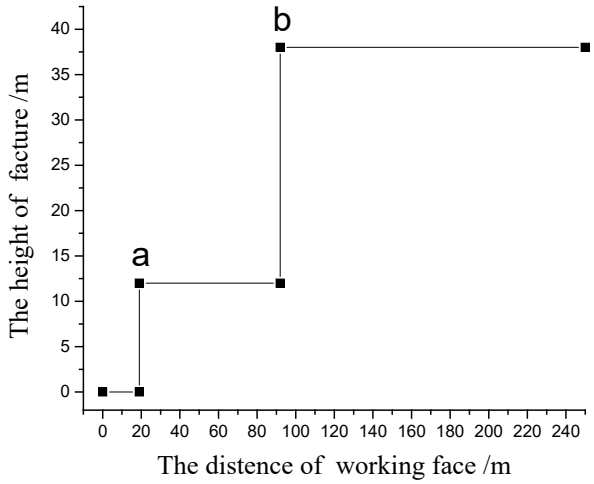

Figure 5 – The fracture development process of Kaida coal mine

The fracture development process of Kaida coal mine is shown in Figure.5. The results show

that the height of fractured zone is 12m when the advancement is 19m and the shaly sandstone roof collapses at Point a. The height of fractured zone is 38m when the advancement is 92m at Point b. The fracture height of the mines are shown in the table 4.

Table 4 – The fracture development height of the four coal mines

Mines	The ratio of hard rock in interburden/%	OB/IB	The thickness and type of the interburden/m		The advance distance of the panel face/m	The height of fracture/m	Description of the fracture and roof
Shigetai	70	8.2	Mudstone	3	30	3	The first breaking of immediate roof
					46	28	Fine sandstone(hard rock) is broken, fracture conduction occurred, first weighting occurred
			Fine sandstone	7	80	37	Fracture reach to the highest position
Halagou	100	9.4	Silk sandstone	3	20	3	Silk sandstone(hard rock) is broken
			Fine sandstone	4	31	20	Fine sandstone(hard rock) is broken, fracture conduction occurred, first weighting occurred
Bulianta	80	6.2	Mudstone	3	24	3	The first caving of immediate roof
			Silk sandstone	3	33	9	Silk sandstone(hard rock) is broken
			Mudstone	4	53	54	Fine sandstone(hard rock) is broken, fracture conduction occurred, first weighting occurred
			Fine sandstone	12			
			Silk sandstone	6	114	71	Fracture reach to the highest position
Kaida	0	7.3	Argillaceous sandstone	8	19	12	Argillaceous sandstone(soft rock)is broken
					92	38	Fracture reach to the highest position

FIELD TEST

The supporting capacity data were collected in the four coal mines during the mining process and compared with the calculated results. Statistical data as shown in the table 5

Table 5 – Supporting capacity data in the four coal mines

Mines	First weighting interval/m	Periodic weighting interval /m
Shigetai	48.8	11.6
Bulianta	44.1	15.3
Halagou	48.5	16.3
Kaida	20	9.8

Shigetai: During the mining of 2-2 coal in the lower coal seam, the supporting capacity is monitored at 6 selected hydraulic supports in 1 month. The monitored data indicates that the first weighting occurs when the advancement reaches 48.8m and the span of periodical weighting is 10m. The supporting pressure peaks at 47.1 MPa and the minimum value is 44.4 MPa. The average

supporting pressure is 45.7 MPa. The peak value of supporting pressure show little change. The distribution of the supporting pressure of the panel face advancing 136m is shown in the Figure 6. From the Figureure we can conclude that the highest of the supports pressure reach to 53 MPa. This brings difficult to the shield supports

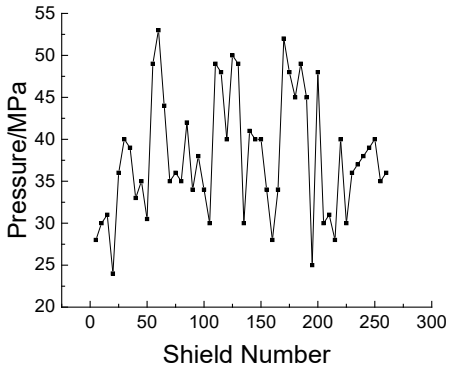

Figure 6 – The distribution of the supports working resistance

Halagou: The breaking span of the immediate roof of 101 longwall panel in the 1-2 upper coal seam is 11-12m. The average span of first breaking in main roof is 44.1m. The breaking spans show significant change and the loading is intensive.

Bulianta: During the mining process in 32301 longwall panel of lower 2-2 coal seam, the average span of first breaking in main roof is 48.5m. The span of periodical loading is 12.9m.

Kaida: During the mining of 6-2 coal seam, the first breaking occurs when the advancement is 20m. The supporting resistance is between 25MPa-30MPa. Cutting roof happens occasionally within the range of tens of hydraulic support in the middle of the longwall panel and the supporting resistance could reach more than 40 MPa.

The theoretical calculatio and field test agree well. The height of the fractured zone varies in different mining height and overlying strata properties. To be specific: the height of the fractured zone in Bulianta coal mine where the coal seam thickness is 7.5m is 70m and it in Halagou coal mine where the coal seam is 2-meter thick is 20m. For Shigetai coal mine and Kaida coal mine where the coal seams are both 2m, the heights of the fractured zone reach reach 40m. The results show that the mining height is the dominative factor to the height of fractured zone. And when the mining heights are same, the property of roof rock is the deciding factor. In the Halagou coal mine where the proportion of hard rock in middle seam is 100% and the Kaida coal mine where there is no hard rock in middle seam, the overlying seam movements are both serious.

Morsy et al. proposed that the effect of ratio of upper strata thickness to the interburden thickness（OB/IB）on overlying seam movement is dominative. While in our study, the movement of overlying seams in Shigetai coal mine where the OB/IB value is 8.2 is gradual but it in Kaida coal mine where the OB/IB value is 7.3 is dramatic. Therefore, the dominative factors of overlying seam

movement are not only OB/IB value but also the property of middle seam and thickness.

CONCLUSION

(1) A method of calculating fractured zone height is proposed through comparing the maximal deflection and the free space. This provides the basis for the theoretical calculation of the roof fracture height of the panel face.

(2) The height of fractured zone is decided by the mining height and it increase with the increasing of mining height. The property of overlying seam also has significant effect on the fracture development. If there is a hard rock with large thickness in the overlying strata, the development of the fracture will be affected by the hard rock.

(3) During the mining of lower group mining, the ratio of the upper strata thickness to the interburden thickness（OB/IB） is not the dominative factor for overlying seam movement, especially in the mines in western diggings which features shallow buried depth and thin roof.

(4) For the interburden, the thick and hard rock have a decisive influence on the movement of the overlying strata. At the same time, the proportion of the hard rock in the interburden is not closely related to the movement of the overlying strata: when the middle rock is hard rock, the overlying strata movement may also be intense.

ACKNOWLEDGEMENT

The paper is supported by the National Natural Science Foundation of China (Grant Nos. 51404275 and U1361209), the Fundamental Research Funds for the Central Universities (2013QZ03).

REFERENCE

Yao BH, Zhou HF, Chen L. (2010) Numerical simulation about fracture development in overlying rocks under repeated mining. *Journal of Mining & Safety Engineering*, 27(3): 443-447.

Majdi A, Hassani F P, Nasiri M Y. (2012) Prediction of the height of distressed zone above the mined panel roof in longwall coal mining . *International Journal of Coal Geology,* 98: 62-72.

Ellenberger JL, Chase FE, Mark C. (2003) Using site case histories of multiple seam coal mining to advance mine design. *In: Proceedings of the 22nd international conference on ground control in mining*. Morgantown, WV. p. 59–64.

Haycocks C, Zhou Y. (1990) Multiple-seam mining – A state-of-the-art review. *In: Proceedings of the 9th international conference on ground control in mining*. Morgantown, WV. p. 1–11.

Morsy K, Yassien A, Peng SS. (2006) Multiple seam mining interactions–a case study. *In: Proceedings of the 25th international conference on ground control in mining*. Morgantown, WV. p. 308–14.

H. Yavuz. (2004) An estimation method for cover pressure re-establishment distance and pressure distribution in the goaf of longwall coal mines. *Int J Rock Mech Min Sci*, 41, pp. 193–205

PANNEL OPENING IN SUBLEVEL OPEN STOPE MINING USING MODELING SOFTWARE

R.F. Massabki[1]

[1]Blasting engineer – Orica Brazil

663 Salmão Avenue, 9th Floor

São José dos Campos – SP

(ricardo.massabki@orica.com)

24th World Mining Congress
MINING IN A WORLD OF INNOVATION
October 18-21, 2016 • Rio de Janeiro /RJ • Brazil

PANNEL OPENING IN SUBLEVEL OPEN STOPE MINING USING MODELING SOFTWARE

ABSTRACT

This paper addresses the use of advanced modeling software for the optimization and sequencing of an underground panel opening applied in a sublevel open-stope mining method. The study took place an underground mine in Brazil in 2015.

The work focused on the following aspects for optimization: minimum number of blast events to mitigate human exposure to the stope and increase mining productivity; evaluation of optimum blast volume to allow free-flowing of blasted material; minimize over-break and damage in the walls in initial blasts for the preservation of unblasted drill holes; and optimization of muckpile movement and minimize under-break in the long holes and final blasts.

Using the Orica Blast Design Assistant™ software, it was possible to create blasting scenarios considering multiple blast volumes with different loading and initiation schemes, and using the Distinct Motion Code (DMC) module of the software where it was possible to estimate the bulking effect on blasted material. This module also provides an estimate on the muckpile movement and blasted material flow. The damage and over-break was predicted using the Hellfire module on the same software.

With the aid of the advanced predictive modeling software, it was possible to design larger blasts with increased volumes, allow the panel to be opened with less blast events, increase productivity, permit less human exposure to the open stope, and minimize overbreak compared to previous free-face openings on the same mine.

As a result, the designed blasts performed with considerable improvements regarding over-break, compared to previous panel openings. The larger blasts also allowed the bottom-layer of the panel to be delivered 2 weeks ahead of schedule (33% improvement in productivity)

KEYWORDS

Underground mining, modeling, sublevel open stope

INTRODUCTION

Traditionally, the underground mining industry rely on practical rules of thumb to design underground panel opening blasts. Although it is extremely helpful to use such rules as a revision method, it relies on previous results and experiences, which may be insufficient to achieve optimum productivity and safety performance.

This work place in a sublevel open stope limestone mine located in Brazil. Previous panel openings made on the mine took an average of one year, and the crew reported several issues regarding over break and loss of pre-existent drilled holes, under break in following blasts due to incomplete explosive charge of lost blast holes, and other delays and safety concerns.

In November/2015, Orica was invited to review some of the blast designs and, together, provide a solution for some of the pitfalls encountered in previous panel openings.

METHODOLOGY

The original designs consisted of nine blasts (five on the West side, and four on the East side) intended for the opening of the funnel bottom layer of the open stope. The shots were would be loaded from the bottom of the panel (level 280)

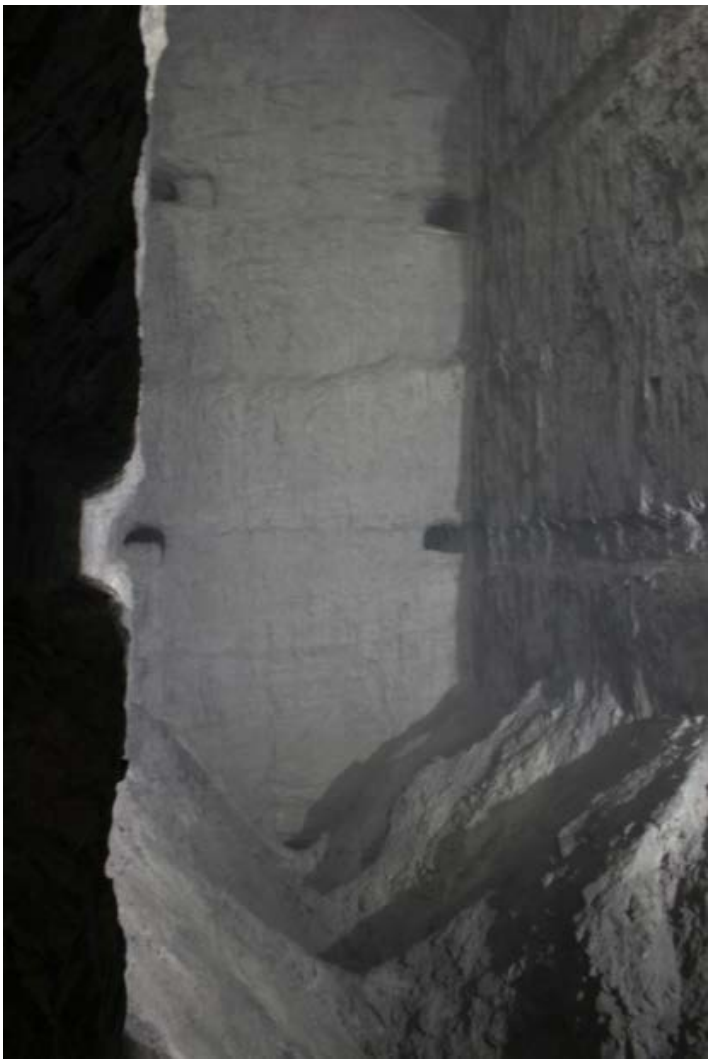

Picture 1 – Picture of 110m high, 40m wide panel

To evaluate the original designs, Orica technical crew reproduced the scenarios and implemented in the software Blast Design Assistant™. The following parameters, including Distinct Motion Code parameters (Hawke, 2011), were used to consider the rock mass:

Table 1 – Rock Parameters used

Parameter	Vallue
Rock	Limestone
Rock Mass properties	Jointed to Massive
Density (kg/m³)	2700
Young Modulus (GPa)	20

UCS (MPa)	200
Tensile Streght (MPa)	6
DMC absorption factor	0,4
DMC In-place Damping	0,3

Orica Technical and Operational crew evaluated the designs using the following key process indicators.

Number of blasts

The main focus of the study was to reduce number of blasts to minimize human exposure to the stope, since the shots would have to be loaded by the access on the bottom gallery. A smaller number of blasts would also increase mine productivity, speeding up the process for the creation of a new production front.

Material Flow

Another critical factor for the effectiveness of the blast designs, the optimum material flow is dependent of a number of factors, such as blast volume, material bulking, fragmentation and backwall angle.

Over break

Since the blast holes are drilled throughout the panel, it is important to maintain damage levels to the remaining blast holes to the minimum, avoiding blast hole loss, and potential under break in sequential blasts

Under break

The under break is an important factor, as it may impact subsequential blasts with higher burden and decrease fragmentation, it may also lead to material loss if it becomes inaccessible for drilling and blasting.

OPERATIONAL RESULTS

Using these indicators as guidelines, Orica tested several different scenarios and was able to reduce the number of blasts to six. Picture 2 shows the shape of the six designs and also exemplifies the loading designs of blasts 3 and 5.

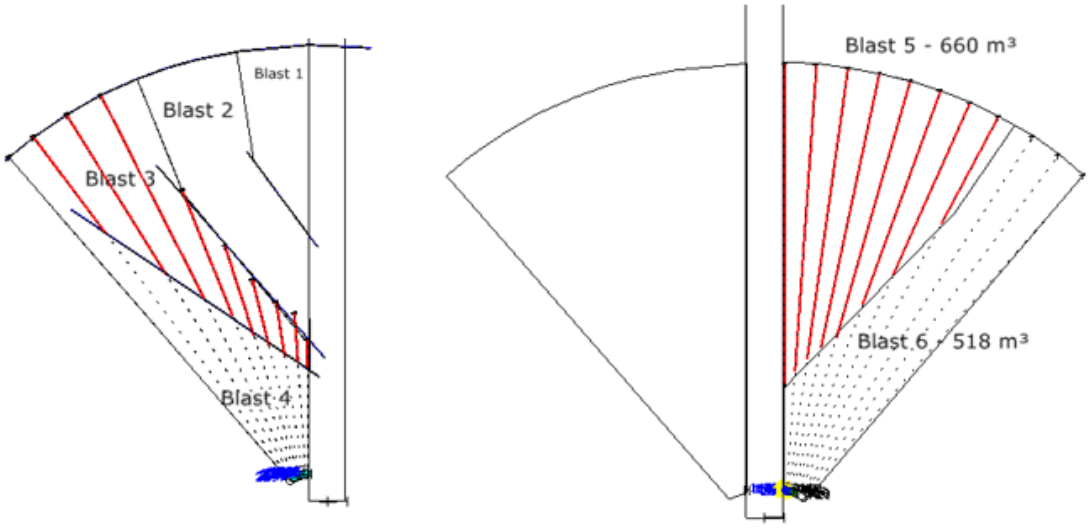

Picture 2 – Blast Designs proposed

The designs take into account each of the previous indicators to allow, considering by the same order:

Number of blasts

Blast number one was designed to fill approximately the volume of the Raise Bore hole at the middle of the panel, taking into account bulking effect. Blast number two was designed to occupy the volume of the Raise Bore hole, plus the space created by Blast number one, so it could be slightly bigger. As the void increased, the available volumes for blasts increased as well.

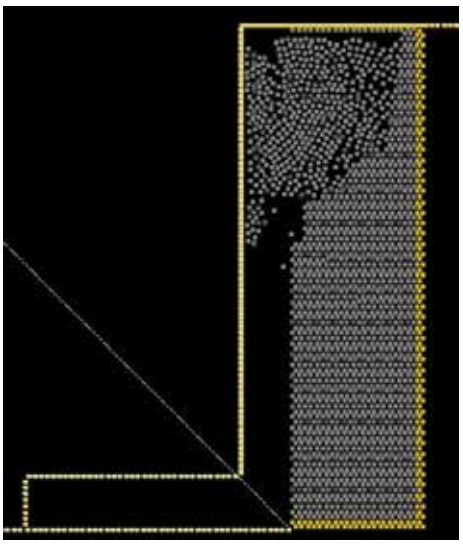

Picture 3– Screenshot of the Distinct Motion Code calculation results

Material Flow

To make sure the blasted material could flow easily, the back wall was designed to have an inclination greater than 50º at least. To avoid oversized material to interrupt material flow, powder factor was kept at very high values (around 1kg/ton). Material flow and bulking was also simulated using a Distinct Motion Code module existing in the Blast Design Assistant™ software.

Over break and under break

To mitigate the effect of over break, a minimum distance between charged holes and pre-drilled uncharged hole was kept of at least 25 hole diameters. Damage to uncharged blast holes were also simulated using the Hellfire module of the Blast Design Assistan™. The uncharged blastholes had velocities bellow 2Vc at all points. The Hight Powder factor, as well as the complete charge of all back wall holes allowed the under break to be minimized as well

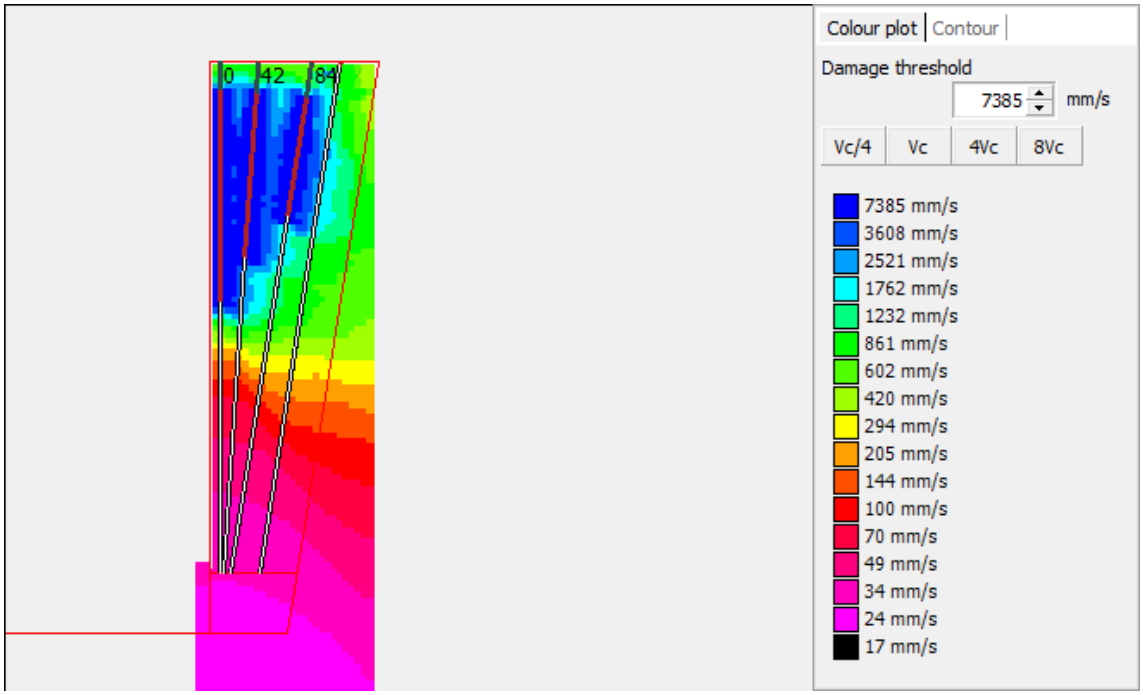

Picture 4 – Evaluation of damage on blast hole with Hellfire Module

With the aid of the modeled designs, it was possible to create bigger blast, minimizing number of blast events, human exposure to the stopes, as well as increasing productivity. Compared to the original designs, the number of events decreased 33%, which on field represented the blasts were performed 2 weeks ahead of schedule. Regarding loading operations, the designs showed perceptible improvements regarding blast holes preservation.

Picture 5 – Loading operation

Picute 5 – Results of West Backwall after blast 4

CONCLUSION

In the recent years, more and more the industry is required to run effectively with lower costs, maintaining and improving levels of safety. The solution for these ongoing demands passes thought better understanding of the processes with a more comprehensive approach.

This article showed that with the application of specific softwares and know-how may allow for the blasting operation to be performed more safely and productively.

Thus, with the contribution of the application of modeling software, it is possible to design and model several scenarios, having a good and quick indication for optimum blast design.

ACKOWLEDGMENTS

I would like to acknowledge the mine operational crew and site supervisor Cezar Gaiofatto for the help and support throughout the project. I would also like to acknowledge Sergio Maier, senior blasting technician and Geraldo Cordeiro, underground operations subervisor for technical counseling and guidance that led the results to be achieved.

REFERENCES

Hawke, S. (2011), Blast Design Assistant™ – Introduction workshop, Orica Australia Pty Ltd, Austrália, 1 CD-ROM.

PLANNING OF MINING OPERATIONS IN AN UNDERGROUND COAL MINE

*E. Brzychczy

AGH University of Science and Technology,
Faculty of Mining and Geoengineering,
Cracow, Poland
*(*Corresponding author: brzych3@agh.edu.pl)*

24th World Mining Congress
MINING IN A WORLD OF INNOVATION
October 18-21, 2016 • Rio de Janeiro /RJ • Brazil

PLANNING OF MINING OPERATIONS IN AN UNDERGROUND COAL MINE

ABSTRACT

In the light of current crisis in the mining industry, companies are forced to increase efficiency of a mining process. Some of activities in this area should be carried out already at the mine planning phase. After mine construction, the only possibility to introduce changes into process exists during the planning of mining operations.

In the paper selected issues of the underground mine planning are presented. A proposal of method for operations' planning in underground coal mine with longwall system is described. Main assumptions of developed method (CPRG) as well as case study are presented.

KEYWORDS

Mine planning, mining operations, optimization, CPRG method, OPTiCoalMine calculation service

INTRODUCTION

Mining process, especially underground, is one of the most complex production and logistic processes. Main conditions of the mining activity which have great influence on a production and economic results are:

- geological conditions and natural hazards,
- used technologies and complex, expensive machinery,
- working staff,
- market situation.

Nowadays, when the market situation is very difficult, mining companies are struggling to survive by, among others, increasing efficiency of the process.

Increase of the process efficiency has to be taken into consideration during the mine planning. Chosen solutions in this stage affect (often irreversibly) production and economic results. After mine construction, planners have limited possibilities in this area. One of the opportunities to increase efficiency of the process is modeling and optimization of operations during planning stage.

Great meaning in the area of planning has supporting methods and tools. Quite detailed reviews of mine planning methods are presented in (Topuz & Duan, 1989; Newman, Rubio, Caro & Eurek 2010). Some proposals regarding underground mine planning and production optimization are presented in (Barbaro, Ramani, 1986; Carlyle, Eaves, 2001; Chanda 1990; Epstein, Gaete, Caro, Weintraub, Santibanez, Catalan, 2003; Fava, Millar, Maybee, 2011; Jawed, 1993; Kumral, 2005; Newman, Kuchta, 2007; Pendharkar, Rodger, 2000; Rahal, Smith, Van Hout, Von Johannides 2003; Sarin, West-Hansen, 2005; Smith, Sheppard, Karunatillake, 2003; Snopkowski, 2002; Trout, 1995; Winkler, 1998; Yun, Liu, Chen, Huang, 1990).

In the paper a new proposal for operations' planning in underground coal mines with longwall system is presented. The CPRG method includes multi-option analysis concerning various possibilities of equipment allocation to planned longwalls with simulation approach.

UNDERGROUND MINE PLANNING AND OPTIMIZATION PROBLEM

The mine planning is one of the basic phases in a mine life cycle (Figure 1).

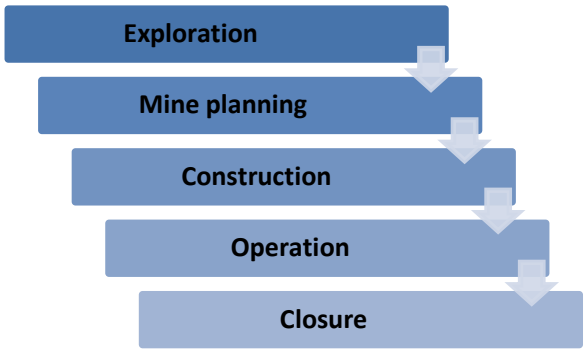

Figure 1 – General scheme of the life cycle of a mine
Source: own work

Mine planning, in a scope of underground mining, concerns a spatial mine model. The mine model includes: surface model and underground model.

Because of specific conditions, more difficult and complex in the mine planning is the underground part. Planning process of the underground model of a coal mine could be divided into the following parts:

- planning of a main development,
- planning of mine levels,
- planning of a seam development.

Planning of the main development includes choice of the development (shafts, inclined drifts), location of the main development excavations in the mining area, designation of their functions and equipment.

Planning of the mine levels includes division of the deposit into levels (ventilation and mining), with the assumptions of their vertical height and depth, the number of simultaneously working levels and the sequence of seams' exploitation.

Planning of the seam development includes design of the development model (excavations in the rock or/and in the seam), according to selected development structure.

The mentioned issues have strategic meaning for the mine activity and they are carried out at the mine planning stage. Solutions chosen at this stage have influence on:

- a construction period of a mine,
- an amount of resources trapped in pillars,
- a ventilation system of a mine,
- a length of transport roads.

Mentioned elements in the long period affect efficiency of the mining process and are rather irreversible from technical and technological point of view. Therefore, after construction phase of the mine, the planners have limited possibility of changing the resultant efficiency of the process in this area.

In the operation phase of a mine planners have possibility to increase efficiency of the mining process by optimization of mining operations.

In a coal mine using the longwall system, optimization of mining operations in longwall panels includes selection of the longwalls' operation order, choice of an equipment and assumption of operations' rate of advance.

Mining operations which have to be planned in a single longwall panel include: preparatory operations, equipping, exploitation and liquidation. Each of the operation has own rate of the operation advance depending on mining and organizational conditions, technology, staff qualifications and used equipment.

Therefore, the optimization problem could be defined as follows: *Which equipment should be used in mining operations under conditions of designed excavations in a coal mine and what should be the rate of the operation advance according to the adopted objective function?*

To solve this problem CPRG method was developed (Brzychczy E., 2011).

CPRG METHOD

The main assumptions of the CPRG method are:

- in the underground mine (or group of mines) coal is mined by the longwall system,
- planned longwall panels are connected by time dependencies and form so called production series,
- in the planned longwall panels three types of operations are carried out: equipping, exploitation and liquidation operations. Preparatory operations (like cutting the deposit into longwall panels) are excluded,
- a rate of exploitation advance is a random variable with normal distribution (determined on the data analysis of similar operations carried out in the past),
- one of the optimization criteria - the minimization of a coal output deviation from target values in analyzed period is proposed,
- evolutionary algorithm as optimization technique is used.

The general scheme of the method is presented in Figure 2.

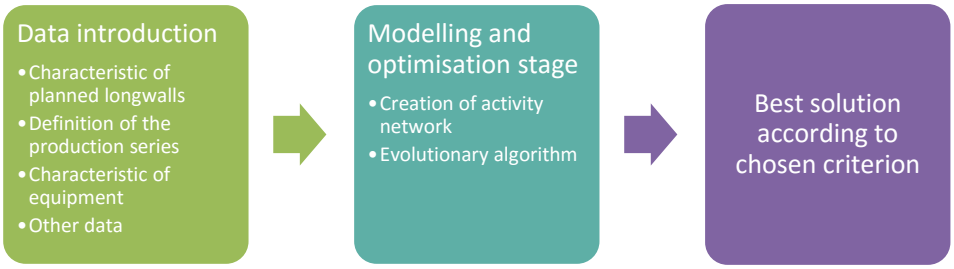

Figure 2 – General scheme of the CPRG method
Source: own work

The characteristic data of the planned longwall include:

- length of the longwall panel [m],
- length of the longwall face [m],
- height of the longwall face [m],
- volume weight of coal [Mg/m3].

The definition of the production series includes:

- order of the longwall panels forming production series,
- start date of the operations in the production series.

The characteristic of the planned equipment include:

- elements of the longwall complex (i.e. shearer, longwall conveyor),
- possibilities of allocation in the planned longwalls (allocation matrix) with estimation of allocation probability,
- average rate and possible deviation of the exploitation advance in the planned longwalls [m/day].

The other data include:

- coefficient of losses,
- duration of equipping and liquidation operations [months],
- planned output [Mg/month],
- analyzed period [months].

In the CPRG method as optimization technique evolutionary algorithm is used. Standard evolutionary algorithm is generic, iterative and probabilistic algorithm that maintains population P of N individuals in each iteration (generation). Each individual represents a potential solution to a problem that has to be solved. Individuals reproduce themselves with use of genetic operators: crossover and mutation, generating offspring. In the evolutionary algorithm natural selection mechanism is applied. A comparison of individual fitness to environment leads to competition for survival and reproduction. Evaluation of the fitness is expressed by a value of the objective function. Selective advantage exists for those individuals of higher fitness (de Castro, 2006). Stopping criterion of the algorithm could be a maximum number of generations or no improvement in a population at a given time.

In the CPRG method as the base for calculations of the fitness function value, an activity network is created. Activity network enables a time projection of operations in the planned longwalls according to initial data of each individual. Individuals differ in equipment allocation to planned longwalls. After multiple simulations of the rates of exploitation advance in the planned longwalls (according to assumed distributions of the random variables), value of the fitness function is calculated. Then individuals are rated and selected for a mutation stage (as parental individuals). In the mutation stage, random changes of the longwall complexes in the planned longwalls are done. In the developed algorithm two types of mutation are possible: micromutation – change is done in a one longwall and macromutation – changes are done in all planned longwalls at once. After evaluation of offspring individuals according to value of the fitness function, the selection of individuals to the next generation is carried out. As a result of algorithm operation, the best solution according to optimization criterion is found.

Main assumptions of the CPRG method were realized in a calculation service - OPTiCoalMine (Brzychczy 2014). The current version of the service (Java application) is implemented in a Virtual Laboratory GridSpace2 and shared on the ACK Cyfronet server as a part of the Polish Grid Infrastructure (OPTiCoalMine, 2016). Implementation of the developed algorithm into grid structures allows access to great computational power, which is essential for complex optimization problems. In case of the operations' planning such tool significantly reduces the time of calculations.

CASE STUDY

The presented example concerns three underground coal mines in a selected mining company. Characteristics of the planned longwalls, production series and allocation matrix are presented in Tables 1 and 2.

The other input data were assumed as follows:

- coefficient of losses – 0,85,
- volume weight of coal – 1,3 Mg/m^3
- duration of equipping and liquidation operations – 3 months,
- analyzed period 1.03.2017 – 28.02.2019.

Detailed data about longwall complexes are presented in Table 3. Target output is presented in Table 4.

Table 1 – Selected input data

Mine no	Production series	Longwall panel	Length of the longwall face [m]	Height of the longwall face[m]	Length of the longwall panel [ml]	Allocation matrix					
						Z1	Z2	Z3	Z4	Z5	Z6
1	c1	404	161	2.45	808.3	0,9	0,1				
		405	161	2.45	808.3	0,9	0,1				
		406	161	2.45	808.3	0,9	0,1				
		407	111	2.85	726	0,9	0,1				
		408	111	2.85	726	0,9	0,1				
	c2	409	204	1.85	823	0,9	0,1				
		410	204	1.85	823	0,9	0,1				
		411	204	1.85	823	0,9	0,1				
		412	215	2.85	708	0,9	0,1				
		413	215	2.85	708	0,9	0,1				
	c3	501	173	3.7	1021	0,9	0,1				
		502	173	3.7	1021	0,9	0,1				
		503	173	3.7	1021	0,9	0,1				
2	c4	414	248	3.9	1010	0,1	0,5	0,3	0,1		
		415	247	3.4	950	0,1	0,5	0,3	0,1		
	c5	416	247	2.5	1200	0,1	0,5	0,3	0,1		
		417	297	2.35	330	0,1	0,5	0,3	0,1		
	c6	418	244	1.75	970	0,1	0,5	0,3	0,1		
		419	200	1.85	660	0,1	0,5	0,3	0,1		

		320	249	1.98	810	0,4	0,4	0,1	0,1
	c7	321	238	1.92	630	0,4	0,4	0,1	0,1
		322	213	2	600	0,4	0,4	0,1	0,1
		323	241	2.44	1420	0,4	0,4	0,1	0,1
3	c8	324	154	2.39	760	0,4	0,4	0,1	0,1
		325	152	2.11	760	0,4	0,4	0,1	0,1
		420	208	1.98	1030	0,4	0,4	0,1	0,1
	c9	421	240	2.86	940	0,4	0,4	0,1	0,1
		422	161	1.96	960	0,4	0,4	0,1	0,1

Source: based on (Brzychczy, Napieraj & Sukiennik 2015)

Table 2 – Selected input data

Mine no	Production series	Average rate of exploitation advance [m/day]						Standard deviation of exploitation advance [m/day]					
		Z1	Z2	Z3	Z4	Z5	Z6	Z1	Z2	Z3	Z4	Z5	Z6
		5,79	3,73					1,57	0,61				
		5,79	3,73					1,57	0,61				
	c1	5,79	3,73					1,57	0,61				
		5,79	3,73					1,57	0,61				
		5,79	3,73					1,57	0,61				
		5,79	3,73					1,57	0,61				
1		5,79	3,73					1,57	0,61				
	c2	5,79	3,73					1,57	0,61				
		5,79	3,73					1,57	0,61				
		5,79	3,73					1,57	0,61				
		5,79	3,73					1,57	0,61				
	c3	5,79	3,73					1,57	0,61				
		5,79	3,73					1,57	0,61				
	c4	6,43	5,95	4,05	5,62			1,86	1,49	1,02	1,57		
		6,43	5,95	4,05	5,62			1,86	1,49	1,02	1,57		
2	c5	6,43	5,95	4,05	5,62			1,86	1,49	1,02	1,57		
		6,43	5,95	4,05	5,62			1,86	1,49	1,02	1,57		
	c6	6,43	5,95	4,05	5,62			1,86	1,49	1,02	1,57		
		6,43	5,95	4,05	5,62			1,86	1,49	1,02	1,57		
		6,57			5,43	3,76	5,1	1,99			1,38	0,58	1,50
	c7	6,57			5,43	3,76	5,1	1,99			1,38	0,58	1,50
		6,57			5,43	3,76	5,1	1,99			1,38	0,58	1,50
		6,57			5,43	3,76	5,1	1,99			1,38	0,58	1,50
3	c8	6,57			5,43	3,76	5,1	1,99			1,38	0,58	1,50
		6,57			5,43	3,76	5,1	1,99			1,38	0,58	1,50
		6,57			5,43	3,76	5,1	1,99			1,38	0,58	1,50
	c9	6,57			5,43	3,76	5,1	1,99			1,38	0,58	1,50
		6,57			5,43	3,76	5,1	1,99			1,38	0,58	1,50

Source: based on (Brzychczy, Napieraj & Sukiennik 2015)

Table 3 – Elements of the longwall complexes

Complex no	Shearer	Conveyor
Z1	JOY 4L	RYBNIK 850
Z2	KSW 880EU	RYBNIK 850
Z3	KGE 750	JOY AFC
Z4	KSW 460	RYBNIK 850
Z5	KGE 710FM	RYBNIK 850
Z6	KGS 345N	HB 3E74

Source: based on (Brzychczy, Napieraj, Sukiennik 2015)

Table 4 – Target output in analyzed period (thousand Mg)

Year/Month	I	II	III	IV	V	VI	VII	VIII	IX	X	XI	XII
2017			300	300	300	250	250	250	250	250	300	300
2018	300	300	300	300	300	250	250	250	250	250	300	300
2019	300	300										

Source: own work

The mentioned data were entered to OPTiCoalMine calculation service. The following parameters of the evolutionary algorithm were assumed:

- number of individuals in a base population – 200,
- parents quantity – 100,
- number of simulations – 100.

The convergence of the evolutionary algorithm is presented in Figure 3.

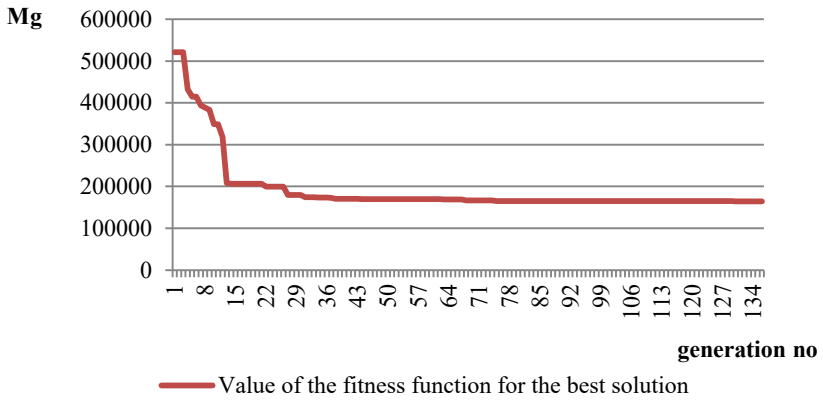

Figure 3 – The convergence of the evolutionary algorithm
Source: own work

As a result of the calculations the best solution was found in 130th generation with the fitness function value equal to 164,460 Mg.

The allocation of equipment to planned longwalls and rates of exploitation advance in the best solution are presented in Table 5.

Table 5 – Allocation of equipment in the best solution

Mine no	Production series	Longwall panel	Longwall complex	Average rate of exploitation advance [m/day]
1	c1	404	Z1	6,71
		405	Z1	4,19
		406	Z1	5,92
		407	Z1	7,36
		408	Z1	3,94
		409	Z2	4,54
		410	Z1	3,24
	c2	411	Z1	4,86
		412	Z1	6,04
		413	Z1	4,85
	c3	501	Z1	4,17
		502	Z2	6,62
		503	Z1	4,22
	c4	414	Z3	5,82
		415	Z2	5,32
2	c5	416	Z2	6,46
		417	Z3	8,14
	c6	418	Z2	4,83
		419	Z2	7,62
	c7	320	Z6	3,45
		321	Z6	5,17
		322	Z4	5,20
		323	Z4	6,25
3	c8	324	Z4	4,22
		325	Z1	5,71
	c9	420	Z5	8,25
		421	Z5	7,95
		422	Z5	6,58

Source: own work

Deviations of the calculated output from target values in the chosen solution are presented in Figure 4.

Figure 4 – Coal output and planned values in the best solution
Source: own work with use of OPTiCoalMine

The presented solution is characterized by quite small deviations from the target values. Noticeable the overproduction in the first part of 2017 year could be a buffer for deficiencies in the second half of the year. Very valuable information gives the range (marked in red) as a risk measure,

which is associated with the realization of the mining process in the planned longwalls (based on historical data).

Additionally, on the basis of detailed results a schedule of planned operations could be done with use of a scheduling software.

The OPTiCoalMine calculation service is available for scientists after completion of application procedure, described at http://www.plgrid.pl/en.

CONCLUSIONS

Increasing efficiency of the process during mine operation phase should be taken into consideration during the modeling and optimization of mining operations at the planning stage.

In the paper, method for operations' planning in underground coal mine with longwall system is presented. Main advantages of the presented solution are:

- multi-option analysis concerning various possibilities of equipment allocation to planned excavations,
- simulation approach enabling determination of operations' advance rate in the planned longwalls allowing achievement of the target output,
- risk analysis, which is associated with the realization of the mining process in the planned longwalls (based on historical data),
- modern, effective optimization technique,
- access to large computing power (into grid structures),
- short calculation time.

Results of the calculations could support a decision making process concerning the growth of mining process efficiency according to better equipment allocation and increase of productivity. The presented solution could be used also in modelling and optimization of cutting the deposit into longwall panels or determination of production series order.

ACKNOWLEDGEMENTS

This paper presents results of research conducted at AGH University of Science and Technology

REFERENCES

1. Barbaro, R. & Ramani, R. (1986). Generalized multiperiod MIP model for production scheduling and processing facilities selection and location. *Mining Engineering*, 38 (2), 107–114.
2. Brzychczy E. (2014). A modern tool for modelling and optimisation of production in underground coal mine. In M. Bubak, J. Kitowski & K. Wiatr (Eds). *eScience on distributed computing infrastructure: achievements of PLGrid Plus domain-specific services and tools*. (pp. 317–344) Springer International Publishing.
3. Brzychczy, E. (2011). The planning optimization system for underground hard coal mines. *Archives of Mining Sciences*, 56 (2), 161–178.
4. Brzychczy E., Napieraj A., & Sukiennik M. (2015). Modelowanie i optymalizacja wydobycia w kopalniach węgla kamiennego z wykorzystaniem struktur gridowych. *Przegląd Górniczy*, vol.71, no 8, 2–7.
5. Carlyle, W. M. & Eaves, B. C. (2001). Underground planning at Stillwater Mining Company. *Interfaces*, 31 (4), 50–60
6. Castro de, L.N. (2006). *Fundamentals of Natural Computing. Basic concepts, algorithms and applications*. Chapman & Hall/CRC, Boca Raton.
7. Chanda, E. K. C (1990). An application of integer programming and simulation to production planning for a stratiform ore body. *Mining Science and Technology*, 11 (2), 165–172.
8. Epstein, R., Gaete, S., Caro, F., Weintraub, A., Santibanez, P. & Catalan, J. (2003). Optimizing long term planning for underground copper mines. *Proceedings Copper 2003, 5th International Conference*, vol I, (pp. 265–279). Santiago, Chile, CIM and the Chilean Institute of Mining.
9. Fava, L., Millar, D. & Maybee, B. (2011). Scenario evaluation through mine schedule optimisation. In: R. Kuyvenhoven, E. Rubio & M. Smith (Eds.) *Proceedings of the 2nd International Seminar on Mine Planning* (pp. 1–10). Gecamin, Santiago, Chile.
10. Jawed, M. (1993). Optimal production planning in underground coal mines through goal programming: A case study from an Indian mine. In J. Elbrond & X. Tang (Eds.). *Proceedings*

24th International Application of Computers and Operations Research in the Mineral Industry (APCOM) Symposium (pp. 44–50). CIM, Montréal.

11. Kumral, M. (2005). Reliability-based optimisation of a mine production system using genetic algorithms. *Journal of Loss Prevention in the Process Industries*, 18 (3), 186–189.
12. Newman, A. & Kuchta M. (2007). Using aggregation to optimize long-term production planning at an underground mine. *European Journal of Operation Research,* 176 (2), 1205–1218.
13. Newman, A., Rubio, E., Caro, R., Weintraub, A. & Eurek, K. (2010). A review of operations research in mine planning. *Interfaces*, 40 (3), 222– 245.
14. OPTiCoalMine, 2016 – https://docs.plgrid.pl/display/PLGDoc/Energetyka%3A+OPTiCoalMine
15. Pendharkar, P. C. & Rodger, J. A. (2000). Nonlinear programming and genetic search application for production scheduling in coal mines. *Annals of Operations Research*, 95 (1–4), 251–267.
16. Rahal, D., Smith, M., Van Hout, G. & Von Johannides A. (2003). The use of mixed integer linear programming for long-term scheduling in block caving mines. In F. Camisani-Calzolari (Ed). *Proceedings 31st International Application of Computers and Operations Research in the Mineral Industry (APCOM) Symposium* (pp. 123–131). SAIMM, Cape Town.
17. Sarin, S. C. & West-Hansen, J. (2005). The long-term mine production scheduling problem. *IIE Transactions*, 37 (2), 109–121.
18. Smith, M., Sheppard, I. & Karunatillake, G. (2003): Using MIP for strategic life-of-mine planning of the lead/zinc stream at Mount Isa Mines. In F. Camisani-Calzolari (Ed). *Proceedings 31st International Application of Computers and Operations Research in the Mineral Industry (APCOM)* (pp. 465–474). SAIMM, Cape Town.
19. Snopkowski, R. (2002). Longwall output plan considered in probability aspect. *Archives of Mining Sciences*, 47 (3), 413–420.
20. Topuz, E. & Duan, C. (1989): A survey of operations research applications in the mining industry. *CIM Bulletin*, 82 (925), 48–50.
21. Trout, L. (1995). Underground mine production scheduling using mixed integer programming. In *Proceedings 25th International Application of Computers and Operations Research in the Mineral Industry (APCOM) Symposium* (pp. 395–400), AusIMM.
22. Winkler, B. (1998). System for quality oriented mine production planning with MOLP. *Proceedings. 27th International Application of Computers and Operations Research in the Mineral Industry (APCOM) Symposium* (pp. 53–59), Royal School of Mines, London, England.
23. Yun, Q., Liu, J., Chen, Y. & Huang G. (1990): Optimization of planning and design in underground mines. *Proceedings 22nd International Application of Computers and Operations Research in the Mineral Industry (APCOM) Symposium* (pp. 255–260), Berlin, Germany

PRELIMINARY GEOMECHANICAL STUDY OF QUARTZITE FROM KAOLIN SMALL MINES AT SÍTIO POLAR, JUNCO DO SERIDÓ, STATE OF PARAÍBA, BRAZIL

* L.L. Maia[1], P.H.A. Lima[1], V.A. Genuíno[1], F.F. Vieira[1], M.A. Niccio[1], F.W.H. Vidal[3]

[1]Universidade Federal de Campina Grande – UFCG – UAMG
R. Aprígio Veloso, 882
Bairro Universitário, Campina Grande – PB
*(*Corresponding author: leandromaia@hotmail.com.br)*

[3]Centro de Tecnologia Mineral – CETEM
Av. Pedro Calmon, 900
Cidade Universitária, Rio de Janeiro - RJ

24th World Mining Congress
MINING IN A WORLD OF INNOVATION
October 18-21, 2016 • Rio de Janeiro /RJ • Brazil

PRELIMINARY GEOMECHANICAL STUDY OF QUARTZITE FROM KAOLIN SMALL MINES AT SÍTIO POLAR, JUNCO DO SERIDÓ, STATE OF PARAÍBA, BRAZIL

ABSTRACT

Kaolin is one of the main rocks exploited by small mining companies in the region of the city of Junco do Seridó, state of Paraíba. It occurs in form of pegmatite seams filling fractures on Quartzite following Patos lineation. The extraction is done from surface using excavators and manual picks creating sub vertical openings. In order to perform a preliminary geomechanical study on Quartzite, host rock of Kaolin, in the location of Sítio Polar, city of Junco do Seridó, we used rock mass classification systems Rock Mass Rating (RMR) and Rock Tunnelling Quality Index (Q) combined to a correlation of Point Load Strength Test Index to Uniaxial Compressive Strength. Results from rock mass classification and point load strength index agree with rock mass characteristics observed on field, indicating a stable slope for open pit operations and the need of support systems for underground excavations. The simplicity of structures makes easier to predict and analyse stability and behaviour of rock mass, in this case, requiring less local knowledge to achieve reasonable conclusions. Point Load Strength Index correlated to Uniaxial Compressive Strength (UCS) showed accurate results confirming the efficiency and convenience of using Point Load Test against UCS tests. This study aims the improvement of the local economy and social development of miner municipalities in the region of the Borborema Pegmatitic Province, providing a first approach to rock mass characteristics that can utterly contribute to more robust mining design projects.

KEYWORDS

Quartzite, Kaolin, Rock Mechanics, Geomechanics, Mining, Rock Mass Classification, Point Load Index Test, UCS, Paraíba.

INTRODUCTION

Junco do Seridó is known in the state of Paraiba, Brazil, as a miner potential municipality. The main rock and mineral substances extracted in the region are Kaolin, Quartzite, Quartz, Feldspar, Mica, Tantalite and Tourmaline. Many of these extractions are small sized operations in which there is few technical support mainly due to the small output and low selling prices. However, some of the mines are operational for many years and have reached a technical level that satisfies buyer's requirement for the final product. Still, improvements on safety, mineral prospection, mining planning, mineral processing and rock mass stability studies can make the production safer, add value to the final product and improve the performance of mining operations.

These improvements are considered a challenge for The Federal University of Campina Grande (UFCG) which has been developing studies along with the Centre of Mineral Technology (CETEM) aiming the improvement of the local economy and social development of miner municipalities in the region of the Borborema Pegmatitic Province.

This paper focuses on the characterization and classification of the enclosing Quartzite of Kaolin surface extraction at Sítio Polar, in the municipality Junco do Seridó, by using the rock mass classification methods Rock Tunnelling Quality Index, Rock Mass Rating and correlations of Point Load Index tests to Uniaxial Compressive Strength tests.

The study provides a first approach to rock mass characteristics that can utterly contribute to robust mining design projects, which aim to present alternative Kaolin extraction methods, and database for feasibility studies.

Borborema Pegmatitic Province

Located between the states of Paraíba and Rio Grande do Norte, this province was originally denominated Borborema Pegmatitic Province by Scorza (1944) to designate the main area of occurrence of mineralized pegmatites in the northeast of Brazil. Geological exploration in the region started during World War II because of the necessity to provide industrial minerals and metals for arms industry. This province is worldwide known as one of the most important sources of Tantalum, Niobium, Beryllium, Kaolin and Gems, in which Paraíba Tourmaline represents the main valuable gem explored.

Local Geology

The Borborema Pegmatitic Province (PPB) occurs in the context of the Seridó range of Rio Grande do Norte Domain (Borborema Province), including occurrence of pegmatites of varied mineralogy hosted in quartzite from formation Equador, Seridó Group. The survey area is dominated by Quartzite, Kaolin pegmatites and residual soil, which outcrop in the area along the Serra da Borborema in an elongated topographic elevation in the direction N-NE. The Quartzite in the region are light coloured, fine grained composed by quartz, muscovite, feldspar and opaque accessories.

From satellite imagery analysis and findings in the field, we observed that rocks of the Seridó range and the associated pegmatites have an E-W trend in the southern portion, while in the central portion presents a NNE-SSW trend, which systematically bend to N-S in the northern portion. Brittle structures occur secondarily affecting mainly the pegmatite. This tectonic is represented by faults and fractures striking towards E-W, NW-SE and N-S. Veins mineralized in Feldspar or Kaolin may be associated with such fractures. In the area of study, the Sítio Polar, for example, veins of Kaolin Pegmatite fill E-W fractures.

The structural behaviour of pegmatite strongly reflects the influence of Patos Lineation and local shear zones striking NNE-SSW. Regional folds with various styles, occur with E-W direction fold line associated with regional transcurrent E-W, especially Patos Lineation.The Map 1 summarizes structural geology and topography of the region.

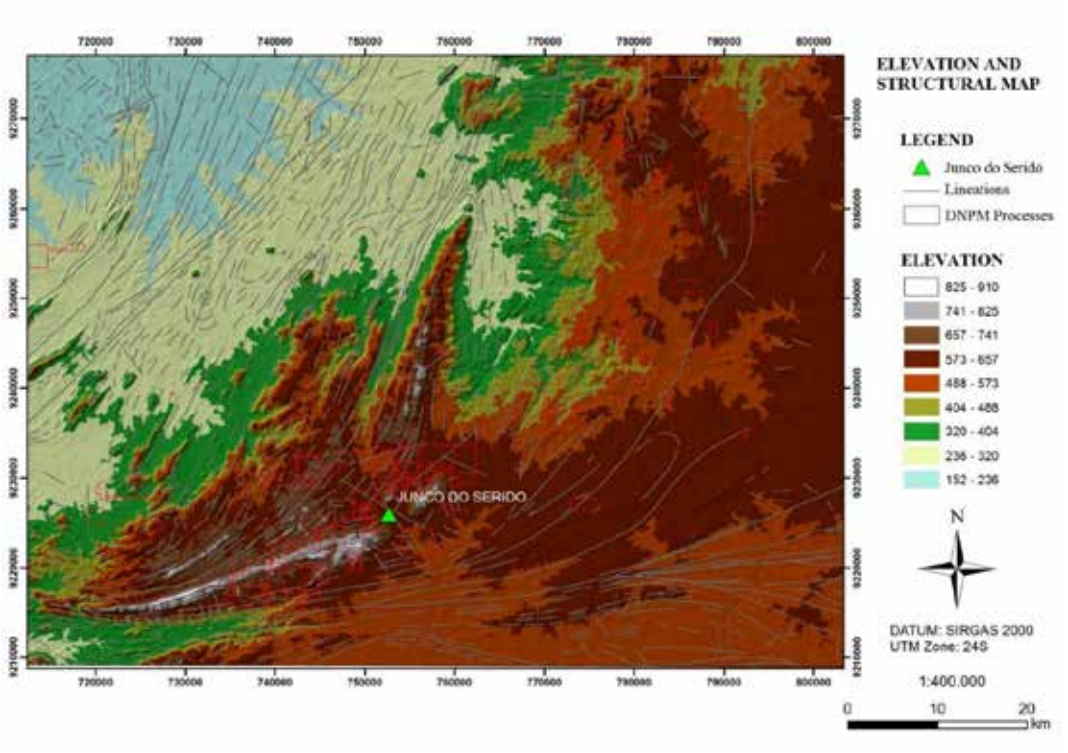

Map 1 – Elevation and Structural Map (Vieira, 2015)

Rock Mass Classification

In early stages of a mining project, when there is little or no database available, using rock mass classification methods contribute on the first approach for determining general rock characteristics. The information gathered by classification methods are relevant to give an overview of the rock mass strength, deformation, possible failure mechanisms and support requirements. As projects progresses and more information is acquired, classification can be updated and used in conjunction with new available data, making it more accurate.

The study area presents kaolin mines operating for decades. However, rock mass classification has not been performed, being mines stability assessed by local experienced miners. According to Hartman (2002), a rock mass classification needs 'local knowledge' from the engineer or geologist, which means a familiarity developed over many years working on a particular rock mass and therefore being able to interpret and collect data reliably. The simpler the structures presented in a rock mass, the less complex the classifications are, thus 'local knowledge' become easier to acquire. For example, a homogeneous rock mass which has well defined structures takes less field work and experience to classify and understand the responses to excavations than a massive jointed, heterogeneous rock mass. In this way, it is possible combine the local knowledge of the miners with the information retrieved from classification methods and then improve mining stability.

The rock mass study presented in this paper consists of a single lithology, the quartzite. It occurs in sub-horizontal layers with east-west fractures, following Patos lineation, intruded by Kaolin Pegmatite. The exploitation of the intruded pegmatite, a very common practice in the region, exposes faces of quartzite and the simplicity of the main structures. When used in conjunction with more elaborated design procedures, rock mass classification can be an important tool to ensure a safe operation and to avoid production losses. Therefore, the study here provided has one of its objectives to serve as a contribution for future robust stability and feasibility studies.

METHODOLOGY

In this study, we defined three different openings for taking measurements and samples. The data acquired is composed by: Rock Quality Designation (RQD), traverse orientation, rock type, joint dip and dip direction, structure type, joint spacing, roughness, JRC roughness, planarity, joint filling, aperture, persistence, visible ends and water condition. Map 2 represents the openings of study, topography and mining concessions.

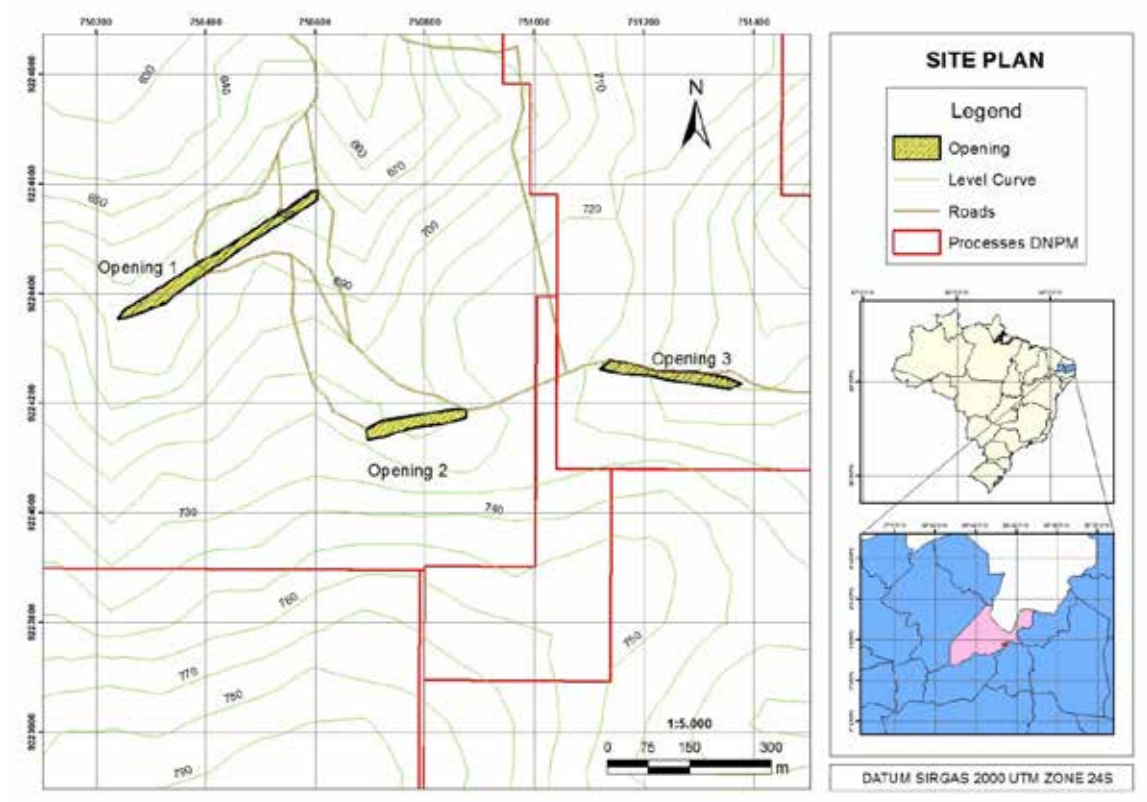

Map 2 – Area of study

The data acquired in the field is then translated to technical language for evaluating rock mass strength. The application of this method brings Quartzite rock mass particularities to a technical language worldwide spread for rock mass classification which will facilitate further studies in the near future.

Figure 1 – Opening 1 and 2

Figure 2 – Opening 2 and 3.

Rock Tunneling Quality Index

Barton et al. (1974) proposed an index for determining the necessity of tunnelling support according to rock mass characteristics, the Rock Tunnelling Quality Index, also known as Q-Barton. The numeric value of the index varies in logarithm scale from 0.001 to 1000 and is defined by equation 1:

$$Q = (RQD/J_n) * (J_r/J_a) * (J_w/SRF) \quad (1)$$

Where RQD is Rock Quality Designation, J_n the joint set number, J_r the roughness number, J_a the alteration number, J_w the water reduction factor and SRF the stress reduction factor. In summary, Q is a measure of bock size (RQD/J_n), inter-block shear strength (J_r/J_a) and active stress (J_w/SRF). According to Hartman (2002), this method is of easy application, simple in measuring critical factors to stability such as block size, inter-block shear strength and active stress, and gives a simple relation to decide whether support systems are needed or not.

Rock Mass Rating

Developed by Bieniawsky (1976), the Geomechanics Classification or the Rock Mass Rating (RMR) considers six parameters to classify a rock mass: Uniaxial compressive strength of rock material, RQD, spacing of discontinuities, condition of discontinuities, ground water conditions, and orientation of discontinuities. Each parameters score is sum and result in a RMR value that varies from 0 to 100. The system is applied by dividing rock mass in structural domains, which are defined by changes in rock type, faults and other major structural features. Significant changes in spacing and characteristics of discontinuities may also divide rock mass in smaller domains.

Point Load Strength test (PLT)

According to Hoek (1977), the Unconfined Compressive strength is undoubtedly the geotechnical property that is most often quoted in rock engineering practice. It is widely understood as a rough index which gives a first approximation of the range of issues that are likely to be encountered in a variety of engineering problems including roof support, pillar design, and excavation technique. However, performing a Uniaxial Compressive Strength test is often expensive and difficult because of sample preparation requirements such perfectly parallel endings and specific proportions.

In this context the Point load strength test (PLT) has been widely accepted as an efficient empirical tool for indirect estimation of the UCS through the calculation of a rock strength index (Is_{50}). It is a simple, easy handed experiment which can be carried out quickly in the field and with relatively very low cost and easy sample preparation requirements.

In order to standardize the results obtained by point load strength tests, the International Society of rock mechanics (ISRM) established in the ASTM D 5731 – 05, a basic procedure to acquire the data and calculate the Point Load Strength Index (Is_{50}). According to it, the test can be performed in core samples (with the load platens parallel or perpendicular to the diameter – Axial or diametral tests respectively) or using block or irregular lump samples. In this study, we used block samples in the calculation of Is_{50}. The standard calculation for block and irregular lump samples is provided as:

$$I_s = P / D_e^2 \quad (2)$$

Where I_s is the uncorrected point load strength index in MPa, P the Failure load in Newtons. D_e^2 is defined by equation 3:

$$D_e^2 = (4 \times W \times D) / \pi \quad (3)$$

Where W = Width and D = Height in mm.

As the standard sample for this test is defined as diametral cylinders with approximately D equal to 50 mm and width equivalent to 0.3 D to 1.0 D for axial tests and greater than 1 D for diametral, the uncorrected point load strength index is calculated when samples have diameters different than 50 mm or in case of block and irregular lump tests. In order to provide an approximation to the standard core diameter a correction factor is applied according to the equation 4.

$$I_{s50} = F \times I_s \quad (4)$$

Where I_{s50} is the standard Point load strength index and F can be obtained as shown by the equation 5:

$$F = (D^2_e / 50)^{0.5} \quad (5)$$

The experimental study was performed using the ROCTEST TELEMAC Point Load Tester PIL -7, shown in figure 3.

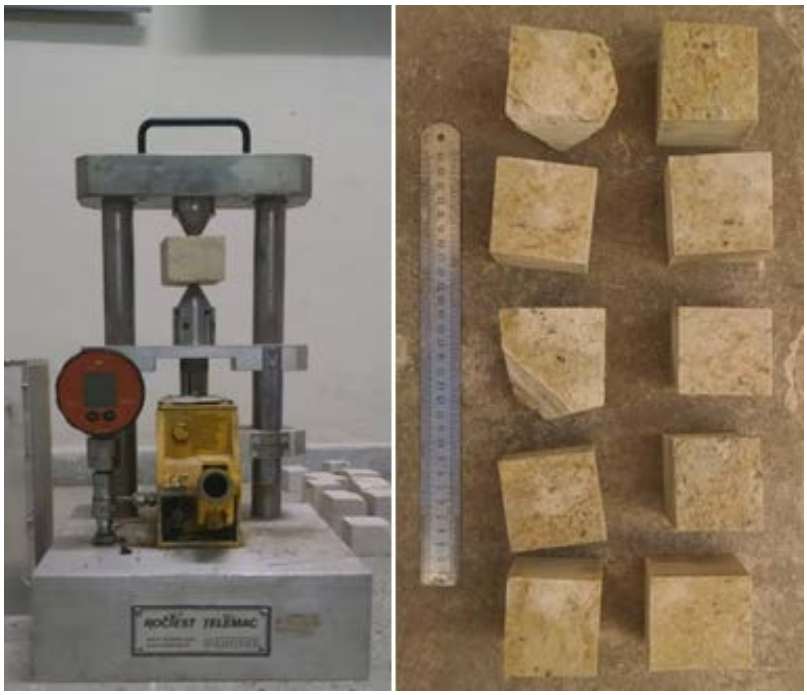

Figure 3 – ROCTEST TELEMAC and cut samples

RESULTS AND DISCUSSION

The structures observed on the field are predominantly horizontal, therefore RQD in this direction retrieves 100% score, while a vertical measurement depends on joint spacing which is mostly constant and varies abruptly in altered packages. RQD mean score is 85.

In general, the traverses are composed by quartzite sub-horizontal layers of variable width (0.5m to 1m). The face of the traverses represents a sub-vertical fracture striking towards E-W filled by Kaolin Pegmatite. The joints have aperture, length, filling conditions, spacing and rock strength well defined and constant, with some small altered portions. Such portions, and its structures, are not considered as different sets of joints considering that they have the same orientation, despite the discrepancy observed on joint spacing and rock strength. In this occasion, altered packages are not representative for the general classification of the rock mass, being the result of alteration processes that seldom occur in the surface of small portions of the rock mass.

Figure 4 – Weathered package on traverse 3

We considered then four set of joints for the rock mass: Quartzite layers, sub-horizontal with dip direction varying due to surface undulation (green); two sub-vertical joints with azimuths of 230 and 330 (yellow and blue); and a 10 azimuth joint dipping 48 degrees to east (red). Figure 5 shows the set of joints represented on a stereogram.

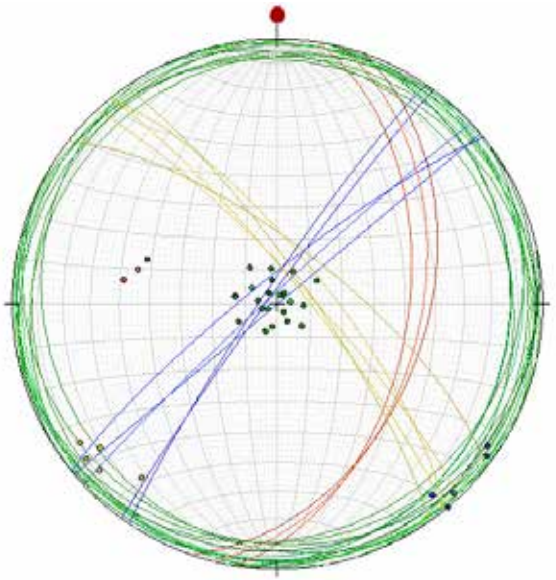

Figure 5 – Stereogram of the four main set of joints

As many structures are sub-horizontal, a frequency diagram of strike or dip direction would not be meaningful since they would vary abruptly according to quartzite layers undulation. Therefore, a dip rosette diagram is presented in figure 6.

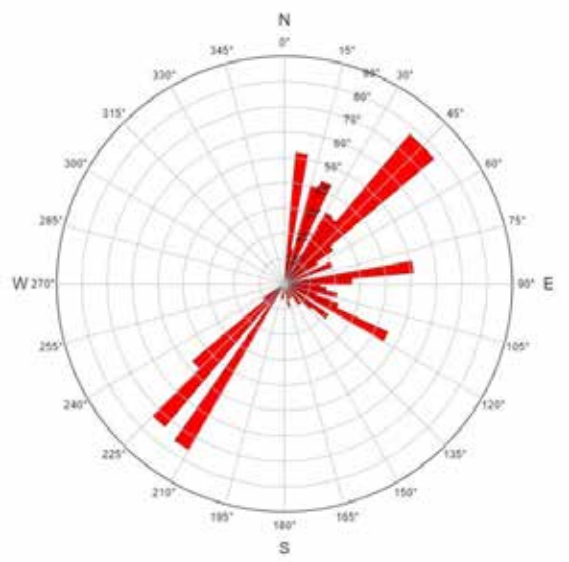

Figure 6 – Rose diagram on dip of structures

It is important to notice that the combination of yellow and blue joint sets on figure 5 indicates the possibility of a wedge failure occur, which is confirmed by wedges already failed towards north observed in the field. In joint contacts we observed thick layers of kaolin. The spacing of discontinuities varies from 0.5 m to 1.0 m with undulated, slightly rough and dry surfaces.

Figure 7 – Wedge failed at opening 1

Rock Tunneling Quality Index Results

Given all the considerations above about rock mass characteristics, the Rock Tunnelling Index Q scored 1.7 class D, poor rock. Considering underground excavations height of 4 meters and an Excavation Support Ratio (ESR) of 1.6 for permanent mining openings, the red square in the figure 7 represents the Q index and support requirements for the rock mass studied.

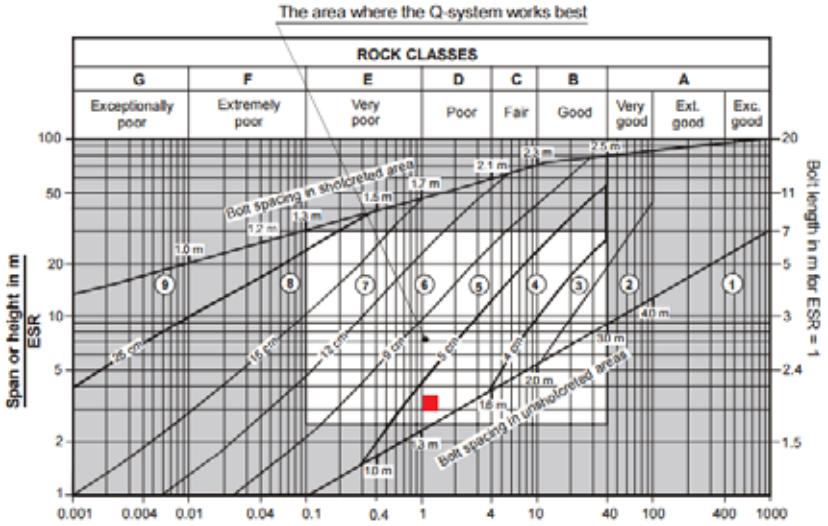

Figure 8 – Q rock support diagram (Palmstrom et al., 2002)

This rock support diagram suggests fibre reinforced shotcrete and bolts with five to nine centimeters of diameter spaced 1.3 meters.

Point Load Strength Test results

The interpretation of Point Load Index Strength and its most precise correlation with the unconfined compressive strength (UCS) has been issue of extensive debate amongst many authors. Bieniawski (1975) tested a range of different lithology and came up with the relationship presented in the equation 6.

$$UCS = 23 \times I_{s50} \quad (6)$$

However, as there is a wide range of rock type occuring naturally, from extremely weathered and loose to stiffer and compact, there is also a huge variety in the relationship expressed by equation 6 which can change from one lithology to another. In order to address such variability and sharpen Bieniawski approximation, many studies have been conducted for samples from the same rock type. Singh and Singh (1993) conducted a study to identify the correlation between UCS and PLT of Quartzite rocks, achieving similar results to those expressed by Bieniawski (1975). Equation 7 shows Singh and Singh (1993) expression.

$$UCS = 23.27 \times I_{s50} \quad (7)$$

There are some samples which are highly weathered retrieving very low Is_{50} values. But they appear to happen only in the contact zone between Kaolin and Quartzite, therefore represent only a small portion of the rock mass.

The following table presents results of PLT test after correction using Sing and Sing equation. Samples tested are from middle and top of openings, thus called as being from intermediate zone and top zone.

Table 1 – Intermediate zone UCS

Intermediate Zone	I_s (MN/m²)	I_{50}	UCS (MPa)
Average	0.06	0.45	10.40

Table 2 – Top zone UCS

Top Zone	I_s (MN/m²)	I_{50}	UCS (MPa)
Average	0.04	0.30	6.95

Rock Mass Rating Results

Given an average UCS of 8 MPa, RQD 85%, 0.6 m average joint spacing, a slightly rough and weathered surface with an average aperture of < 1 mm, considering that rock mass is dry and joints orientation unfavourable for tunnels, result in 57 RMR score which represents a moderate rock quality class III.

CONCLUSIONS

Patos Lineation and local shear zones striking NNE-SSW strongly influences structural behaviour of the pegmatite. Regional folds with various styles, occur with E-W direction hinge line associated with regional transcurrent E-W. This tectonic is represented by faults and fractures striking towards E-W, NW-SE and N-S. The veins mineralized in Feldspar or Kaolin are associated with such fractures in the area of study, the Sítio Polar, where the veins of Kaolin Pegmatite fill E-W fractures.

The rock mass studied in this paper consists of a single lithology, Quartzite. The exploitation of intruded pegmatite, regionally a very common practice, exposes faces of quartzite and the simplicity of main structures. A combination of joint sets indicates the occurrence of wedge failure, which is confirmed by two wedges already failed towards north observed in the field.

All results from rock mass classification and point load strength index converge to rock mass characteristics. We expected results indicating a stable slope for open pit operations and the need of support systems for underground excavations, expectations all confirmed by test results. Again, considering simpler structures makes easier to predict and analyse stability and behaviour of rock mass, requiring less local knowledge to achieve reasonable conclusions.

This study aims the improvement of the local economy and social development of miner municipalities in the region of the Borborema Pegmatitic Province providing a first approach to rock mass characteristics that can utterly contribute to more robust mining design projects, which aim to present alternative Kaolin extraction methods, and database for feasibility studies.

REFERENCES

BARTON, N., LIEN, R. and LUNDE, J. (1974). Engineering classification of rock masses for the design of tunnel support, Rock mechanics, Vol. 6. No. 4, pp. 189-236

BIENIAWSKI, Z.T. (1975). The point load test in geotechnical practice. Eng. Geol., pp. 1-11.

GENUÍNO, V.A. (2015). Pesquisa mineral qualitativa do pegmatito do alto do feio (paraíba) com ênfase em aspectos geológicos, mineralógicos e econômicos [Qualitative mineral prospection of Alto do Feio Pegmatite (Paraíba) with emphasis on geological, mineralogical and ecomical aspects]. Universidade Federal de Campina Grande, Campina Grande, PB.

HARTMAN, W. & HANDLEY, M. F. (2002). The application of the Q-Tunnelling Quality Index to rock mass assessment at Impala Platinum Mine, The Journal of The South African Institute of Mining and Metallurgy, pp 155-166

PALMSTROM A., BLINDHEIM O.T. and BROCH, E. (2002). The Q-system – possibilities and limitations. Norwegian National Conference on Tunnelling, pp. 41.1 – 41.43. Norwegian Tunnelling Association.

SCORZA, E.P. (1944). Província Pegmatítica da Borborema [Borborema Pegmatitic Province]. DNPM/DGM, Report 112, Rio de Janeiro, RJ, page 55.

SINGH, V.K. & SINGH, D.P. (1993) Correlations between point load index and compressive strength for Quartzite rocks. Geotechnical and Geological Engineering.
VIEIRA, F.F.; ARAUJO, M.F.S. ; LIMA,E.N.M. and SANTOS,L.C.M.L. (2015). Identificação de controles estruturais no Seridó Paraibano e Potiguar através de sensoriamento remoto [Identification of structural controls on Paraíba and Potiguar Seridó by remote sensoring]. In: XV Simpósio Nacional de Estudos Tectônicos - IX International Simposyum on Tectonics, Vitória. Anais do XV Simpósio Nacional de Estudos Tectônicos, 2015.

RISK ANALYSIS APPLIED TO UNPLANNED DILUTION IN OPEN STOPE MINING METHODS

Paulo André Charbel [1], Márcio Muniz de Farias [2], Hernán Eduardo Martínez Carvajal [2,3] and André Pacheco de Assis [2]

(1) Instituto Federal de Goiás
Coordenação de Mineração
Rua 75, nº 46, Centro
Goiânia, Brasil
(pauloanch@gmail.com)

(2) Universidade de Brasília
Campus Universitário Darcy Ribeiro, Departamento de Engenharia Civil e Ambiental
Brasília, Brasil
(carvajal@unb.br)
(muniz@unb.br)
(aassis@unb.br)

(3) National University of Colombia at Medellín
Faculty of Mines, Department of Civil Engineering
Medellín, Colombia
(carvajal@unb.br)

24th World Mining Congress
MINING IN A WORLD OF INNOVATION
October 18-21, 2016 • Rio de Janeiro /RJ • Brazil

RISK ANALYSIS APPLIED TO UNPLANNED DILUTION IN OPEN STOPE MINING METHODS

ABSTRACT

The unplanned dilution in open stope mining methods has significant implications on the economic viability of a mine. Due these economic implications, an academic study was developed at Vazante Mine to quantify the unplanned dilution by numerical simulations and, to carry out a risk analysis applied to unplanned dilution. The Vazante Mine is a zinc underground mine owned by Votorantim Metais, situated in Vazante, Minas Gerais State, Brazil. This work comprises of three parts: geomechanical and operational mine characterization; numerical simulations of open stope mining and; risk analysis applied to unplanned dilution. The first one, geomechanical and operational mine characterization, consists in presenting the natural variability of rock mass geomechanics parameters and the variations of mining operationals conditions, which are essential conditions for numerical simulations and risk analysis.The second one, numerical simulations of open stope mining, consists in estimating the unplanned dilution as random variable, considering the natural variability of rock mass geomechanical conditions and the variations of mining operationals conditions. The last part, risk analysis applied to unplanned dilution, consists to change the open stope design from deterministic to probabilistic analysis. In risk analysis, the probability of ocurrence of unplanned dilution associated to the economic impact over the mining operationals costs is fully described. The objective is to demonstrate that the unplanned dilution discription by risk analysis is closer to real conditions than the unplanned diluiton discription by deterministic analysis. Consequently, the combined action of risk analysis and professional experience can be considered fundamental condition to make a decision about the optimal open stope dimensions.

KEYWORDS

Unplanned dilution, open stope design, numerical simulation, risk analysis

INTRODUCTION

In underground mining, the ore dilution is one of the key measures to control the production quality. The dilution represents a contamination of ore with non-ore material. In open stope mining, there are two types of dilution, planned and unplanned (Figure 1). The planned dilution (internal dilution or primary dilution) refers to the material below the cutoff grade that lies within the stope designed limits (mining lines). This dilution is inherent in the mining method selected. The unplanned dilution (external dilution or secondary dilution) refers to the material below the cutoff grade, beyond the stope designed limits (mining lines), that is added to the ore as a consequence of: sloughing from stope walls, hanging wall and footwall; blast over-break; and unexpected excavation of backfill (Scoble & Moss, 1994; Tatman, 2001). Although both dilutions are important to mining design, only unplanned dilution will be considered in this work.

The unplanned dilution has significant implications on the economic viability of a mine. First, it increases the mining operational costs, because there will be more tons of non-ore material to be loaded, transported, crushed, processed and stored as tailings (Pakalnis *et al*., 1995). Second, the increase of ore dilution reduces the ore recovery in processing plant, as observed by Tatman (2001). Therefore, the unplanned dilution reduces the net present value (NPV) of each ore block mined, what reduces the cash flow

of a mining company. For this reason, the unplanned dilution estimates, at the mine planning phase, are important variables to an efficient open stope design, since this dilution is related to the size of the stopes, among other factors.

The open stope design, in all underground mines, aims to plan largest possible stopes, in order to reduce the stope numbers to maximize the economic viability of mining operations. However, the bigger the stope, the greater is the unplanned dilution. So, the aim of open stope design is to dimension stopes as large as possible with minimum acceptable level of unplanned dilution. It should be observed that the acceptable level of dilution differs from site to site, because this level depends on the ore grade, the grade of the dilution material, costs and metal prices (Pakalnis *et al*., 1995).

To design the stopes, mining companies, around the world, use empirical and/or numerical methods. Both of them have advantages and disadvantages. The challenge is to predict the unplanned dilution quantitatively for each size of stope, at the mine planning phase, in order to design stopes, as large as possible, with an acceptable level of unplanned dilution. In the empirical methods, the design of open stope is based on previous experience. One of the most known empirical methods is the stability-graph method. In spite of widespread use of empirical methods, the employment of numerical methods has increased in the last decades. In different way from empirical methods, the numerical simulation describes the rock mass stress-strain behavior, around the open stope. The description of this behavior contributes to understand the physical phenomenon of the sloughing from the stope walls (hanging wall and footwall), which permits to correlate the unplanned dilution to the size of open stope, by numerical simulations.

Due the economic implications of unplanned dilution on the economic viability of a mine and the challenge of quantifying this dilution, an academic research has been developed in the Vazante mine. This mine is a zinc underground mine, owned by Votorantim Metais, situated in Vazante town, Minas Gerais State, Brazil. The mining method is the vertical retreat mining (VRM). The objectives of research have been two: first one, quantify the unplanned dilution by numerical simulations, considering the natural variability of geomechanic parameters and the variation of mining operational conditions; second one, based on the results of the numerical simulations, propose a risk analysis applied to unplanned dilution, in order to contribute to optimization of the open stope design.

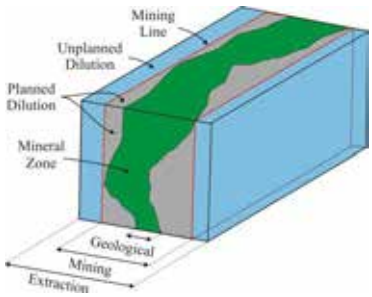

Figure 1 – Planned and unplanned dilution (Scoble & Moss, 1994).

METHODOLOGY

To develop this academic research in the Vazante mine, a three steps methodology was proposed. The first one consisted in analyzing the geomechanic conditions, rock mass parameters and mining operational conditions. The objective was to characterize the variables that had influenced the unplanned dilution, in this underground mine. The second one involved numerical simulation of open stopes excavations. The objective was to quantify the unplanned dilution, considering the natural variability of geomechanic parameters, and the variations of mining operational conditions. The last part comprised the risk analysis applied to unplanned dilution, using the results from numerical simulations. The objective was to demonstrate that the risk analysis is a robust tool able to support the optimization of open-stope design, since the risk analysis consists in quantifying the costs of unplanned dilution and assess its probability of occurrence, for each size of stopes. These three parts of the academic research are described below, where

the last two parts are emphasized. However, before describing them, the causes of the unplanned dilution and its calculation are briefly discussed.

CAUSES OF THE UNPLANNED DILUTION

From the researches conducted by Pakalnis (1986) and Potvin (1988), different studies, about the factors influencing the unplanned dilution in open stope mining, as Scoble & Moss (1994) and Clark (1998), among others, have been developed. Based in these works, the factors, that influence the unplanned dilution, can be separated in two groups: rock mass geomechanical conditions; and mining conditions. The first one, rock mass geomechanical conditions, encompass intrinsic factors and extrinsic factors of rock mass. The intrinsic factors relate to intact rock parameters and discontinuities conditions of rock mass and the extrinsic factors relate to the stress state and to the underground water flow conditions. The second one, the mining conditions, relates to the open stope mining aspects, as the size of stopes, the blasting vibrations, among others, which could induce disturbances on the rock mass conditions around the open stopes.

CALCULATION OF UNPLANNED DILUTION

Pakalnis (1986) conducted a survey of 22 mines throughout Canada about the calculation of unplanned dilution. Nine different ways of calculation have been identified in these mines (Table 1). It should be observed that in Table 1, the terms, waste and ore, respectively, refer to the unplanned dilution (external dilution or secondary dilution) and to the ore planned to be mined. Among these different calculations, the equations (1) e (2) are those widely used in the Canadian mining practices. The equation (1) is more sensitive than equation (2), to quantify the unplanned dilution. For this reason, the equation (1) is recommended as a standard measure of unplanned dilution (Pakalnis *et al*., 1995; Tatman, 2001). In the Vazante mine, the calculation is based on the equation (2), so in this academic study, both of the equations, (1) and (2), were used to calculate the unplanned dilution.

Table 1 – Calculation of unplanned dilution (modified from: Pakanis *et al*., 1995).

D = (Tons waste mined)/(Tons ore mined)	(1)
D = (Tons waste mined)/(Tons ore mined + tons waste mined)	(2)
D = (Undiluted in − situ grade as derived from drill holes)/(Sample assay grade at drawpoint)	(3)
D = (Undiluted in − situ grade reserves)/(Mill head grades obtained from same tonnage)	(4)
D = (Tonnage mucked − tonnage blasted)/(Tonnage blasted)	(5)
D = Difference between backfill tonnage acctually placed and theoretically required to fill void	(6)
D = Dilution visually observed and assessed	(7)
D = ("x" amount of meters of footwall slough + "y" amount of hanging wall slough)/(ore width)	(8)
D = (Tons draw from stopes)/(Calculated reserve tonnage)over the last ten years	(9)

*D = Dilution. The dilution is generally expressed as a percentage.

GEOMECHANICAL AND OPERATIONAL MINE CHARACTERIZATION

The mine characterization has consisted of reliable estimates of the rock mass geomechanical parameters and a clear definition of the mining operational conditions. Both of them have been used as input data for the unplanned dilution analysis by numerical simulation. Thus, the underground mine characterization is divided in two topics, geomechanical characterization and operational characterization.

Geomechanical Characterization

The geomechanical characterization has consisted in describing the rock mass intrinsic and extrinsic conditions. The intrinsic conditions refer to the intact rock and discontinuities characteristics of the ore and country rocks. The extrinsic conditions refer to the rock mass initial state of stress.

The mineralization is located in a shear zone that cuts across a sequence of carbonate rocks. Three lithologies have been identified: ore breccia, carbonate breccia and carbonate rocks (Figure 2). The

engineering geological mapping has showed that the joint sets, in each lithology, are closely spaced and among them, there isn't a joint set significantly weaker than the others. Therefore, considering permissible departures from the ideal, the rock mass can be treated as isotropic and continuum medium. For the ore breccia, carbonate rocks and carbonate breccia in the footwall, the geomechanical parameters have been considered as deterministic parameters (Table 2). For carbonate breccia in the hanging wall, lithology that is responsible for the unplanned dilution, rock mass deformability modulus (E_{RM}) and unconfined compression strength (UCS) have been considered as random and independent variable and other parameters as deterministic parameters (Table 3). The aim in considering E_{RM} and UCS as a random variable is evaluate the effect of natural variability of rock mass geomechanical conditions on the unplanned dilution. These geomechanical parameters, described in the Table 2 and Table 3, have been obtained from the laboratory tests on small-scale intact rock samples and by the RocLab software. About the failure process, around the open stopes, it has suggested that carbonate breccia behaves as a brittle rock. Finally, the initial state of stress has been estimated considering the weight of the rock above, and the ratios (k_H and k_h) of horizontals to vertical stress equal to 1 (k_H) and 0,7 (k_h), respectively, perpendicular and parallel to the orebody strike.

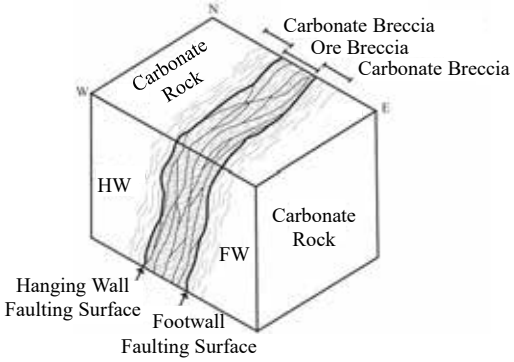

Figure 2 – Geological model (modified from IPT, 1994).

Table 2 – Geomechanical parameters of ore breccia, dolomitic rock and carbonate breccia in the footwall.

Lithology	E_{RM} (GPa)	ν	UCS (MPa)	m_b	s	a	γ (MN/m^3)
Ore Breccia	13	0,2	108	2,829	0,0020	0,509	0,035
Carbonate Rock	30	0,2	124	2,966	0,0117	0,503	0,027
Carbonate Breccia	10	0,2	101	3,012	0,0016	0,510	0,030

E_{RM} is deformability modulus, ν is Poisson's ratio, UCS is unconfined compressive strength, m_b, s and a are Hoek-Brown strength parameters and γ is unit weight.

Table 3 – Geomechanical parameters of carbonate breccia in the hanging wall.

Lithology	E_{RM} (GPa)		ν	UCS (MPa)		m_b	s	a	γ (MN/m^3)
	Mean	SD		Mean	SD				
Carbonate Breccia	10	2	0,2	101	35	3,012	0,0016	0,510	0,030

E_{RM} is rock mass deformability modulus, SD is standard deviation, ν is Poisson's ratio, UCS is unconfined compressive strength, m_b, s and a are Hoek-Brown strength parameters and γ is unit weight.

Operational Characterization

The operational characterization has consisted in describing the open stopes positions and their geometrical dimensions, stope mining sequence, mining rate, blasting effect (D) and backfill characteristics. The stopes considered in this analysis came from four panels isolated from the others mine stopes. These four panels are known as 9140, 9100, 9060 A and 9060 B.

The open stopes relative position and geometrical dimensions and the stope mining sequence and mining rate are described, respectively, in the Figure 3 and Figure 4. The factor D, proposed by Hoek *et al.* (2002), allows to estimate the effects of blast damage on the geomechanical parameters of rock mass, by empirical relationships. The estimates of the factor D and extents of damage zone, in the open stopes walls,

are represented in the Figure 5. In order to evaluate the influence of the blasting effect on the unplanned dilution, it has been considered variations for the factor D, 0,4 and 0,0, on hanging wall of the ore block 9140, beyond the value equal to 0,8, that represents the real case. The factor D equal to 0,0 means no perturbation on the geomechanical parameters of hanging wall, so the unplanned dilution in this case is due only to geomechanical conditions. And the factor D equal to 0,4, means an intermediate perturbation, between real case (D=0,8) and the last hypothesis (D=0,0), on the geomechanical parameters of hanging wall. At least, observes that the backfill is comprised by waste rock, whose the geomechanical parameters have been estimated equal to 300 MPa, for deformability modulus, and 0,2, for Poisson's ratio.

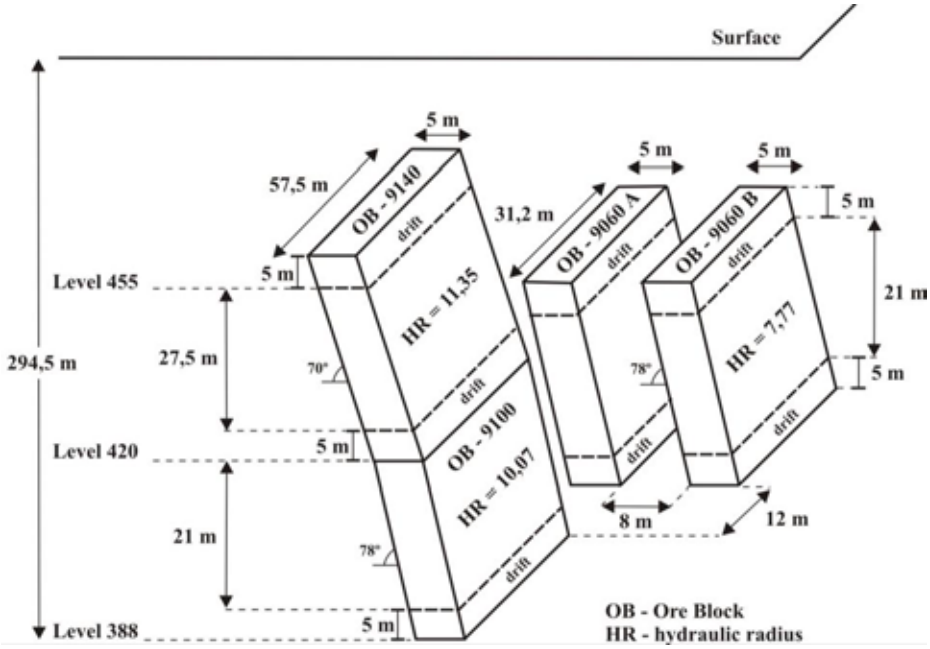

Figure 3 – Relative position and geometry of the open stopes (Charbel, 2015).

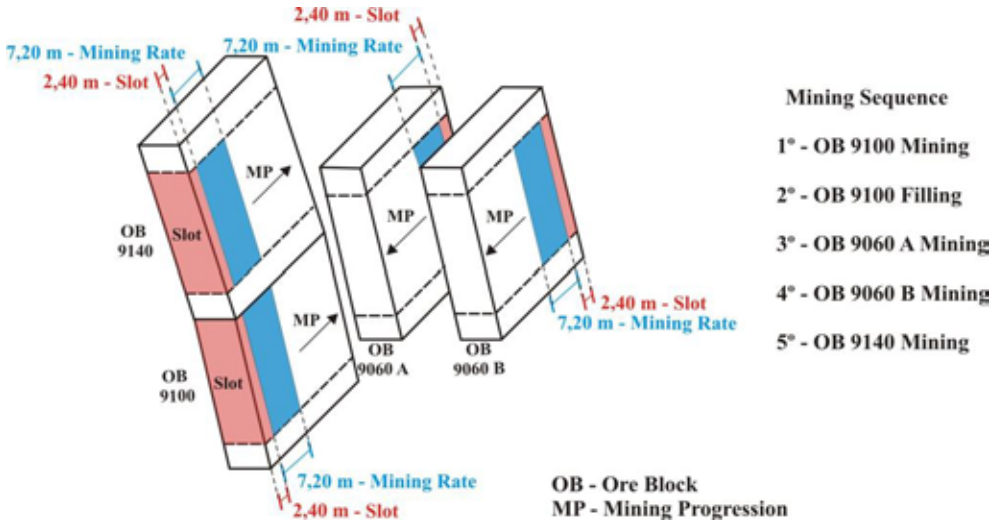

Figure 4 – Stope mining sequence and mining rate (Charbel, 2015).

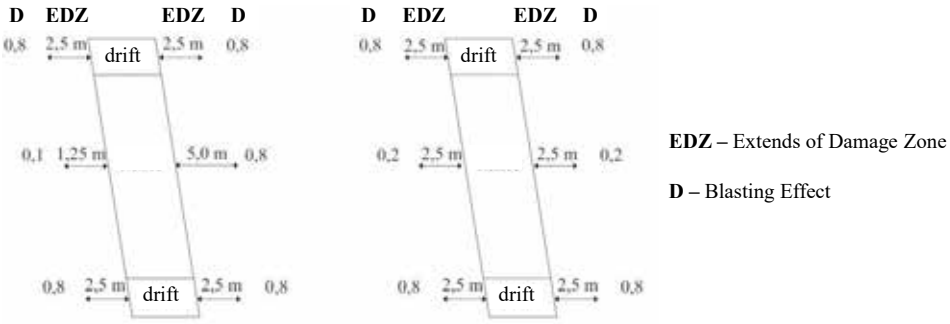

Figure 5 – The factor D and the extents of damage zone in the open stopes walls (Charbel, 2015).

NUMERICAL SIMULATION

The numerical simulations have been used to describe the unplanned dilution in the ore block 9140, considering the natural variability of the E_{RM} and UCS of the hanging wall, and the variations of the blast damage. These analysis has been accomplished using the CESAR-LCPC 3-D, a finite element program. The discription of the numerical simulations is separated in five topics: numerical model; open stope mining simulation; quantifying unplanned dilution using numerical simulation; variability of geomechanical parameters and operational conditions; and numerical simulations results.

Numerical Model

The numerical model, that represents the four isolated panels (9140, 9100, 9060 A and 9060 B), is comprised by a physical model, finite element mesh, constitutive model and pre-mining stress state, among others aspects, all of them described in the following text.

The physical model encompasses the geological model (Figure 2), the geomechanical parameters (Table 2 and Table 3) and the relative position and geometry of the four panels (Figure 3). The finite element mesh has showed 121.125 nodes (Figure 6) and the tridimensional elements used has been hexahedral and pentahedron with eight and six nodes, respectively.

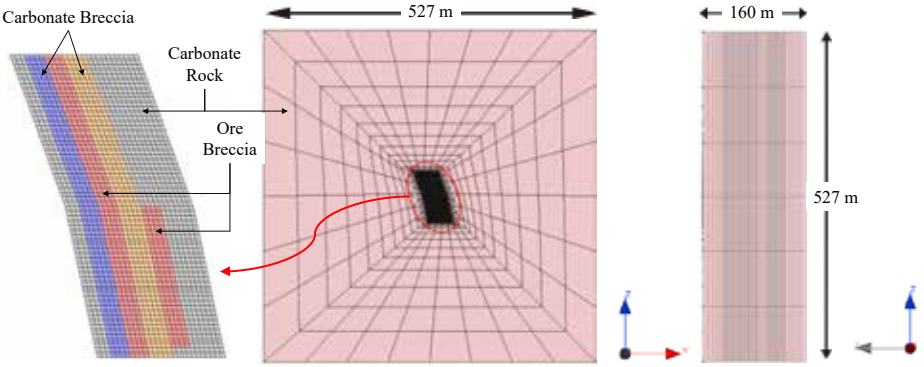

Figure 6 – Finite element mesh (Charbel, 2015).

The constitutive model employed is the elastic perfectly plastic (EPP) model with Hoek-Brown failure criterion, which applies to isotropic and continuum medium. Hajiabdolmajid *et al*. (2002) observed that, around underground opening where there is low confining stresses, the EPP models have not been successful in predicting the extent and depth of brittle failure. In spite of the carbonate breccia behaves as a brittle rock, the EPP model has been used, because there was not another constitutive model applied to rocks available in the program. At last, the pre-mining stress state corresponds to initial state of stresses indicate in the geomechanical characterization.

Open Stope Mining Simulation

The mining numerical simulation has consisted in reproducing the stope mining sequence and mining rate as described in the Figure 4. At the same time, the blasting effect on geomechanical parameters has been considered to the rocks around the underground excavations, in each excavation stage. As result of mining, overstressed zones will appear in the open stopes hanging wall, and plastic strains will be verified in these zones, always when the induced stresses surpass the rock mechanical strength. The detailed analysis of these regions become important, because the unplanned dilution is associated to the plastic strain zones.

Quantifying Unplanned Dilution Using Numerical Simulation

The unplanned dilution occurs inside the plastic strain zones around the open stopes, specifically in the Vazante mine, this dilution restricts to the hanging wall. To determinate the unplanned dilution by numerical simulation, back-analysis of the performance of the open stope 9140 (Figure 3 and Figure 4) has been used as a benchmark case. From this back-analysis, correlations between the rock mass stress-strain behavior and the observed behavior had been obtained by comparative analysis. The rock mass stress-strain behavior came from the mining numerical simulation, considering the mean values of the E_{RM} and UCS for carbonate breccia in hanging wall. The observed behavior came from the cavity monitoring system (CMS) applied to real condition of the open stope 9140. And the comparative analysis has consisted in evaluating the stress, strain, displacement ranges around the open stopes, or another ranges from numerical outputs, that can describes better the boundaries of unplanned dilution verified by CMS in the real case. The numerical output range, that represents better the real boundaries of the unplanned dilution, became the behavior indicator for quantifying this dilution.

In this research, the comparative analysis, between stress-strain and observed behaviors, showed that horizontal displacement above 1 cm has been the numerical output range, that better represents the volume of the unplanned dilution (Figure 7). Therefore, this horizontal displacement value has been assumed as behavior indicator for unplanned dilution, which means that, all the region in the open stope hanging wall, that shows a horizontal displacement equal or above 1 cm represents a potencial volume of unplanned dilution. This behavior indicator has been used in the following analyses, to evaluate the influence of the variations of the operational conditions and the natural variability of the geomechanical parameters on the unplanned dilution, in the open stope 9140. The possibility of using plastic strain or stresses as behavior indicator, became difficult, possibly, because the EPP models aren't adequate to predict the extent and depth of brittle failure, as observed by Hajiabdolmajid *et al*. (2002).

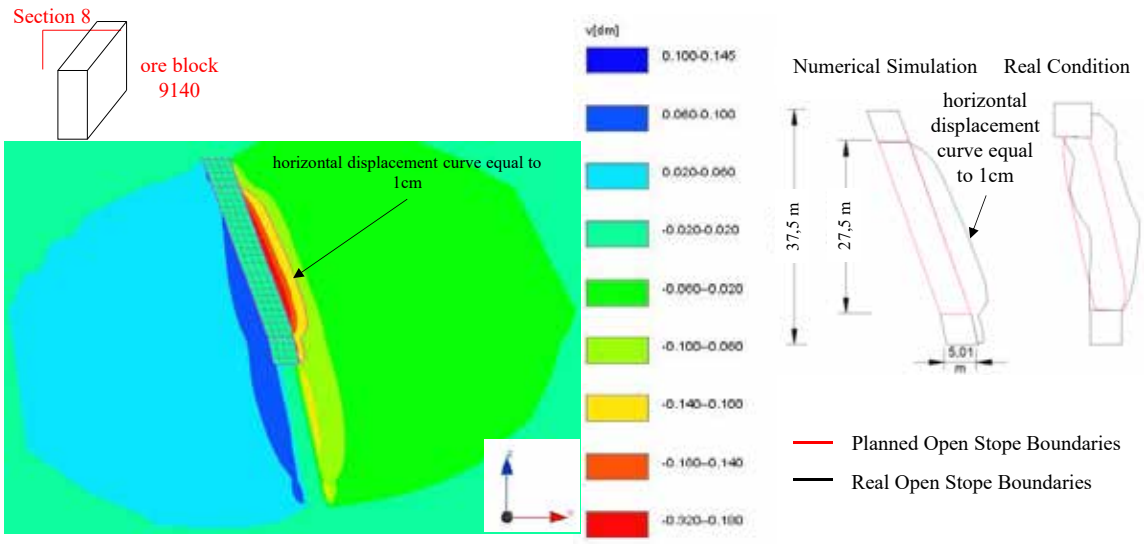

Figure 7 – Behavior indicator for the unplanned dilution (Charbel, 2015).

Variability of Geomechanical Parameters and Operational Conditions

The numerical simulations are deterministic analysis, hence, to consider the influence of the variations of the operational conditions and the natural variability of the geomechanical parameters on the unplanned dilution, in the ore block 9140, twelve analysis have accomplished.

These twelve analyses have been separated in three groups, where each group represents, respectively, the different blasting effects (D), 0,8, 0,4 and 0,0. The aim was to consider the variations of the operational conditions. Based on the point estimate method, a probabilistic method published by Rosenblueth (1981), four analyses have been performed for each operational condition (Figure 8), to consider the influence of the natural variability of the E_{RM} and UCS of the hanging wall on unplanned dilution.

Thus, the unplanned dilution has been quantified for each operational condition, considering the natural variability of geomechanical parameters, consequently the unplanned dilution has became described as a random variable, no more as a deterministic variable (Figure 8).

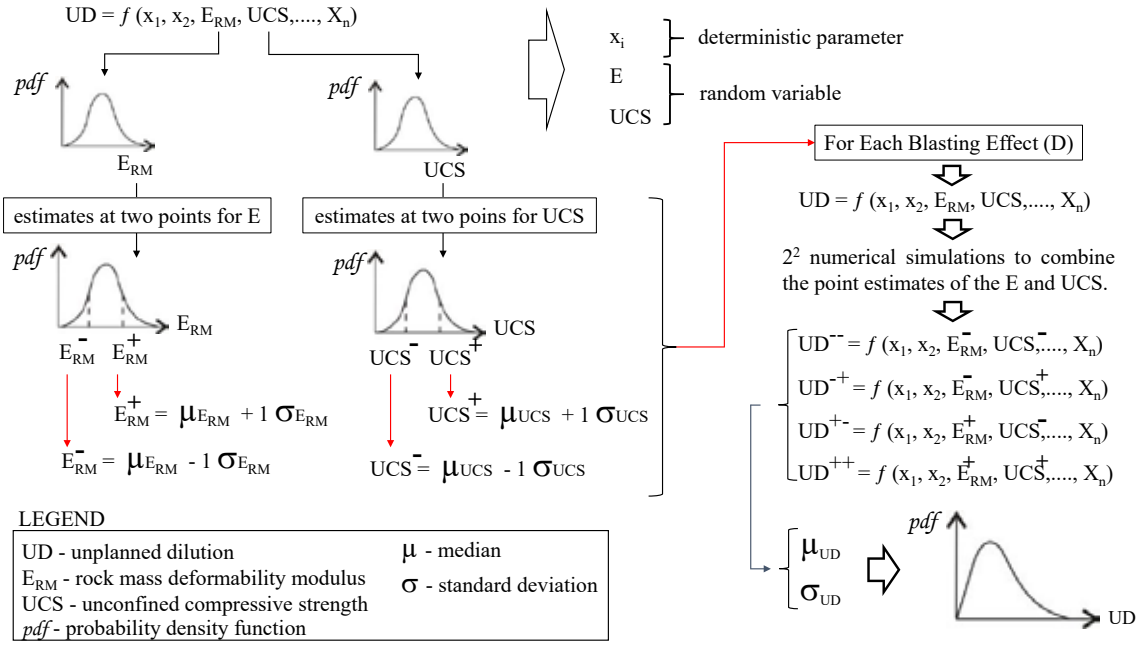

Figure 8 – Variability of geomechanical parameters and operational conditions applied to simulation.

Numerical Simulation Results

The unplanned dilution, in the ore block 9140, has been treated as random variable and represented by a probability density function (PDF). The PDF curve describes the relative likelihood of the unplanned dilution assume a particular value. As, the unplanned dilution has been analysed for three blasting effect conditions, there are three PDF curves, one for each operational condition (Figure 9). From these PDF curves, the mine planning can evaluate the likelihood of achieving the unplanned dilution targets for each operational condition. It should be noted that, the unplanned dilution has been calculated using the Equation (2) showed in the Table 1. Although the PDF curves (Figure 9) demonstrate the variability of the unplanned dilution, as a consequence of the variations of the operational conditions and the natural variability of the geomechanical parameters, a broader evaluation can be obtained by a risk analysis applied to unplanned dilution.

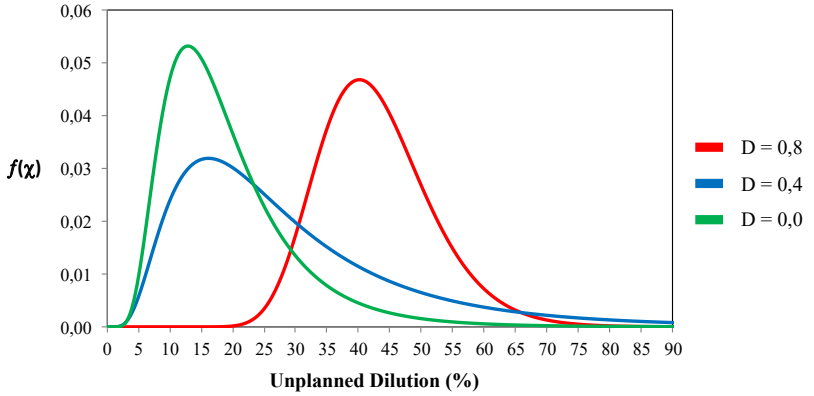

Figure 9 – Unplanned dilution PDF curves for each operational condition (Charbel, 2015).

RISK ANALYSIS APPLIED TO THE UNPLANNED DILUTION

The risk analysis proposed to the unplanned dilution, briefly, consists in correlating the likelihood in achieving the unplanned dilution targets with the mining costs (Figure 10). The risk analysis graphic has been divided in six unplanned dilution regions (Figure 10), what allows objective evaluations about the influence of variations of the operational condition on the unplanned dilution (Table 4), considering the natural variability of the geomechanical parameters. In this risk analysis, the values for unplanned dilution target and mining costs are hypothetic values, not real. Similar analysis could be performed to others operational conditions, such as, the size of the open stopes.

Thus, the risk analysis applied to unplanned dilution associated to the professional experience could become an efficient methodology to design the mine open stopes and to choose the operational conditions more adequate to open stope mining, in order to achieve the unplanned dilution targets.

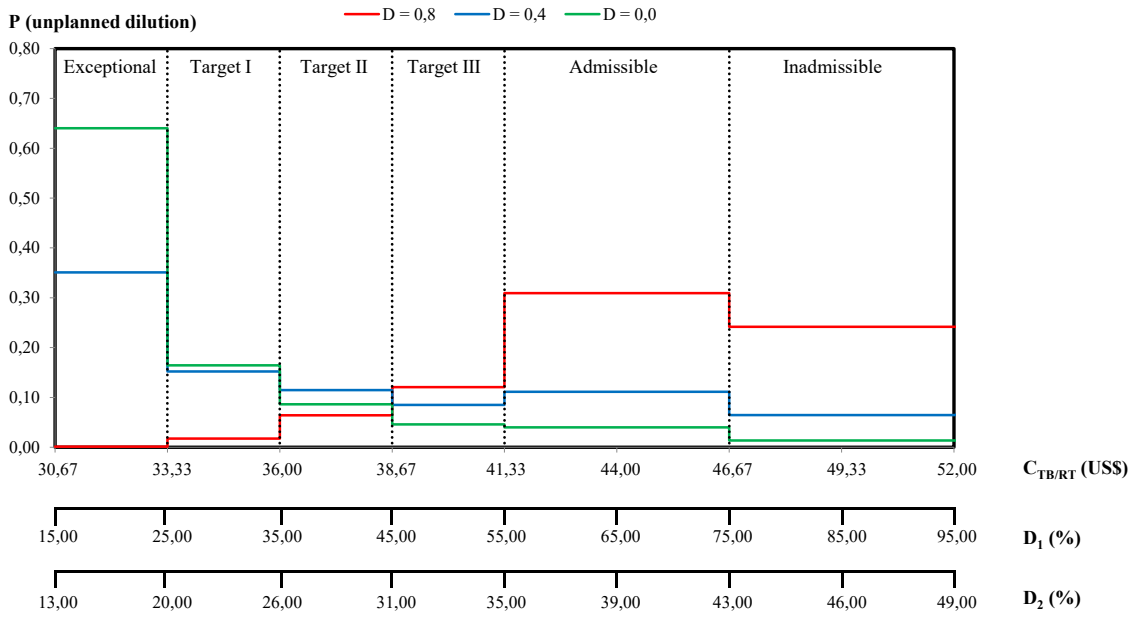

$C_{TB/RT}$ – Transport e beneficiation costs per rock tons inside the limits of the planned open stope

D (%) – unplanned dilution expressed in percentage

D_1 (%) = [(Tons waste mined) / (Tons ore mined)] x 100 D_2 (%) = [(Tons waste mined) / (Tons ore mined + tons waste mined)] x 100

Figure 10 – Graphical representation of the risk analysis applied to unplanned dilution (Charbel, 2015).

Table 4 – Relationship between unplanned dilution scenario and blasting effect (Charbel, 2015).

Scenario	Unplanned Dilution Range (%)	Occurrence Probability (%)			
		D	0,8	0,4	0,0
Exceptional	< 20%		0,1	35,1	64,0
Target I	20% - 26%		1,7	15,2	16,4
Target II	26% - 31%		6,4	11,5	8,6
Target III	31% - 35%		12,1	8,5	4,6
Admissible	35% - 43%		30,9	11	4
Inadmissible	> 43%		48,8	18,7	2,4

CONCLUSIONS

This academic research has been restricted to four isolated open stopes in the Vazante mine, so it is necessary to use this approach in a larger number of open stopes, in order to evaluate its generalization capability. In spite of this, two observations could be considered. First, the numerical simulation of the open stope mining, considering variations of the operational conditions and the natural variability of the geomechanical parameters, allows to estimate the unplanned dilution, with more accuracy. Second, the risk analysis applied to unplanned dilution associated to professional experience can aid a decision-making process in the open stope design, in order to achieve the unplanned dilution targets.

ACKNOWLEDGMENTS

The authors would like to thank the Votorantim Metais company and their professionals allocated in the Vazante mine for the valuable help in this work. We also want to acknowledge CAPES and CNPq for the financial support to this research.

REFERENCES

Clark, L.M. (1998). Minimizing Dilution in Open Stope Mining with a Focus on Stope Design and Narrow Vein Longhole Blasting. MASc thesis, University of British Columbia, Department of Mining and Mineral Processing Engineering, 336.

Charbel, P.A. (2015). Gerenciamento de Risco Aplicado à Diluição de Minério. Tese de doutorado em geotecnia, Universidade de Brasília, Departamento de Engenharia Civil e Ambiental, 406.

Hajiabdolmajid, V.; Kaiser, P.K.; Martin, C.D. (2002). Modelling brittle failure of rock. International Journal of Rock Mechanics and Mining Sciences, 39, 731-741.

Hoek, E.; Carranza-Torres, C.; Corkum, B. (2002). Hoek-Brown failure criterion – 2002 edition. Proceedings of NARMS-TAC conference, Toronto, 1, 267-273.

IPT – Instituto de Pesquisas Tecnológicas (1994a). Assessoria em geomecânica na mineração subterrânea de Vazante – Vazante, MG. Relatório Nº 32 032, 58.

Pakalnis, R.T. (1986). Empirical Stope Design at the Ruttan Mine, Sherritt Gordon Mines Ltd. PhD. thesis. University of British Columbia, Department of Mining and Mineral Processing Engineering, 276.

Pakalnis, R.C.; Poulin R.; Hadjiogeorgiou, J. (1995). Quantifying the cost of dilution in underground mines. SME Annual Meeting, Denver, CO, 1136-1141.

Potvin, Y (1988). Empirical Open Stope Design in Canada. PhD. thesis, University of British Columbia, Department of Mining and Mineral Processing Engineering, 350.

Rosenblueth, E. (1981). Two-points estimates in probabilities. Appl. Math. Modelling, vol. 5, 329-335.

Scoble, M.J. & Moss, A. (1994). Dilution in underground bulk mining: implications for production management. Mineral Resource Evaluation II: Methods and Case Histories. Geological Society Special Publication, Nº 79, 95-108.

Tatman, C.R. (2001). Mining dilution in moderate – to narrow – width deposits. SME Underground Mining Methods. Engineering Fundamentals and International Case Studies. Edited by William Hustrulid and Richard L. Bullock. Published by Society for Mining, Metallurgy, and Exploration, Inc. (SME) Littleton, Colorado, 615-626.

SEISMIC INTENSITY INDUCED BY MINING IN RELATION TO WEAK EARTHQUAKES

G.Mutke[1], J. Dubinski[2]

[1]*Asst. Prof. Dr eng., Central Mining Institute (GIG), Poland, 40-166 Katowice, Pl. Gwarkow 1, +48 2592189, +48 2596533, gmutke@gig.eu*

[2]*Prof. Dr.eng., Central Mining Institute (GIG), Poland, 40-166 Katowice, Pl. Gwarkow 1, +48 2592222, +48 2596533, jdubinski@gig.eu*

24th World Mining Congress
MINING IN A WORLD OF INNOVATION
October 18-21, 2016 • Rio de Janeiro /RJ • Brazil

SEISMIC INTENSITY INDUCED BY MINING IN RELATION TO WEAK EARTHQUAKES

ABSTRACT

Seismicity induced by mining activity occurs in several European mining basins (Cesca et al. 2013). The strongest mining tremors reached magnitude 4.5, horizontal ground motion velocity PGV_{Hmax} up to 10 cm/s and horizontal ground motion acceleration PGA_{H10} up to 0.25g (g- gravity force). The damages caused by this seismicity refer mainly to the decorative elements and only in individual cases very light damages of individual structural elements of buildings are noted (Zembaty et al. 2015, COMEX RFCS project). In case of weak earthquakes the above mentioned ground motion values, PGV, correlate to VI degree of Mercalli instrumental intensity (MMI) and PGA correlate to VII degree of MMI (Wald et al. 1999). It means possibility to cause damage of structural elements and endanger to the stability of the whole load-bearing structure of the weak buildings.

The differences in the ground motion characteristics are visible only in time duration and dominant frequency in both cases (Mutke et al. 2008). Usually for mining seismic events in epicentral zone only single high-level peak of PGA or PGV are recorded. The relation PGA/PGV for mining tremors reaches usually values from 10 to 80 and for weak earthquakes only up to 15. More than 95% of mining seismic events in epicenter distance are characterized by time duration t_{Hv} less than 3 seconds and frequency content higher than 5 Hz. These records were described by low intensity, even when the PGV values exceed 8 cm/s and PGA values exceed 0.15g. Because of the shorter duration time of mining tremors also the Arias intensity parameters are smaller than for earthquakes of the same magnitude. The estimation of damaging effects of vibrations caused by mining seismic events using the MM instrumental intensity scale leads to their overestimation. Therefore the new Mining Seismic Instrumental Intensity Scale (MSIIS-15) in the frame of scientific project "COMEX", financed by Research Fund for Coal and Steel, has been developed.

MSIIS-15 is two-parameter scale based on instrumentally measured peak horizontal ground velocity, PGV_{Hmax} and the duration time of tremor, t_{Hv}. These parameters are correlated with the observed impact of ground motions on buildings, technical infrastructure and the perceptibility of vibrations by people. The macroseismic observations are arranged in six described in detail seismic intensity degrees. The MSIIS-15 is very useful scale, because allows to define the liability of the mine company for the damages.

KEYWORDS

induced seismicity; mining; instrumental-intensity scale,

INTRODUCTION

In the Polish part of the Upper Silesian Coal Basin (USCB), seismic activity is observed in 19 mines and seismic events and rockbursts are recorded by mine-owned local underground seismological networks. In the case of USCB area the strongest tremors, i.e. with a local magnitude M_L >1,5, are recorded by the Upper Silesian Regional Seismic Network (USRSN) consisting of 20 three-component seismic stations located over the area of the USCB (Stec 2007). The USRSN recorded hundreds of strong mining-induced tremors (with hypocentres located near extraction fronts) as well as the more rarely occurring stronger tremors of regional character which are mainly located in faulting zones (Dubiński et al. 1999; Dubiński and Stec 2001; Mutke and Stec 1997; Stec 2007). The mechanisms of strong mining induced

tremors are similar to those of weak earthquakes and they are usually triggered by mining ongoing close to the faults (Cesca et al. 2013; Alber and Fritschen 2013; Kozłowska et al. 2016). In 2015 over 1000 tremors with a local magnitude M_L >1,5 occured in the Upper Silesian Coal Basin (Stec 2016)

SEISMICITY IN UPPER SILESIA COAL BASIN

The tectonic seismic events triggered by mining in the USCB area are characterised by magnitudes ranging from 3 to 4.5 and they are weak when compared with earthquakes (Marcak and Mutke 2013). They have peak ground velocity amplitudes PGV in their epicentral zone up to 0.10 m/s and vibration acceleration PGA up to 2.5 m/s^2. The frequency of the dominating vibrations phase in the epicentre is rather high and ranges from 1Hz to 10 Hz. The residents of areas touched by such tremors are particularly sensitive to these frequencies. Moreover, these frequencies are close to the resonance frequencies of buildings. The duration of vibrations in the epicentral zone is in the case of induced and triggered seismicity considerably lower when compared to weak earthquakes and ranges between 0.5s and 10s. The low values of PGV and relatively high value of PGA of the ground motion combined with short duration time of vibrations, cause that the response of buildings to the mining seismic events is not such strong and damages of their load-carrying and other structural elements are not observed. After the strongest tremors only damage to the decorative elements of the buildings located in the epicentre and strong feeling of vibrations by the residents of this area take place. In some cases slight damage to structural elements and falling of chimneys are observed. This kind of damages took place during the Janina M_L3.8 seismic event and the seismogram of this event is presented in figure 1. The fallowing vibration parameters were monitored in epicentral area : PGV = 0.066 m/s; PGA = 1.8 m/s^2; very short duration of velocity ground motions - 1.2 s; frequency of main phase vibration's was below 5 Hz. The falling of chimneys was observed after this seismic event in more than 100 buildings in poor technical conditions (Figure 2). In hundreds of buildings were observed damages to decorative elements (cracks in the plaster, sliding off roof tiles)

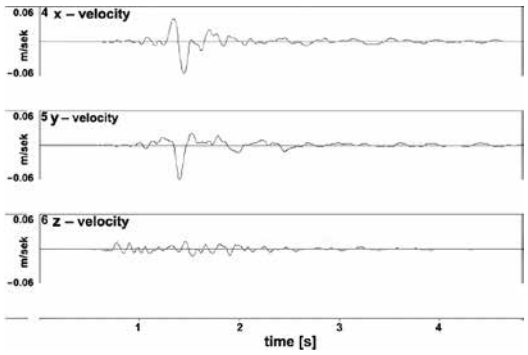

Figure 1. Janina mine seismic event velocity seismogram – tectonic seismic event triggered by mining on 30 of September, 2016 with magnitude M=3,8 recorded in the epicentral area.

Figure 2. Characteristic damage to the buildings located in the epicentral area after the seismic event dated on 30 of September 2015 (Janina Mine)

PGA-TO-PGV RELATIONS IN THE EPICENTRAL ZONE FOR STRONG MINING-INDUCED TREMORS AND EARTHQUAKES

A comparative analysis of the characteristics of ground motion produced by the seismic events induced and triggered by mining in the USCB and the L'Aquila earthquake and VI degree of MMI scale is presented in Figure 3. The strongest seismic event triggered by mining in the USCB in 2015 was Janina tremor on 30 of September with the local magnitude M_L=3,8. The strong mining-induced tremors (thin line) are distinctly different as regards the PGA/PGV values from similar relations developed for earthquakes (Dubiński and Mutke 2011). In case of earthquakes, the records of their vibration velocities PGV show relatively much larger values at a given acceleration of PGA. A good example of such trend is shown between VI degree instrumental values of PGA and those for seismic events triggered by mining in Janina Mine.

In the case of VI degree of instrumental Modify Mercalli (MMI) the vibrations are felt by all and many are frightened. Some heavy furniture can move; falling plaster and chimneys are observed as well as slight damages. Similar slight damages were noted during seismic event in Janina Mine, but PGA values was recorded one degree higher than in VI degree of MM scale and velocity PGV one degree lower (Wald et al. 1999). To better correlate macroseismic observation and seismic parameters of mining seismic events, the new Mining Seismic Instrumental Intensity Scale (MSIIS-15) has been elaborated.

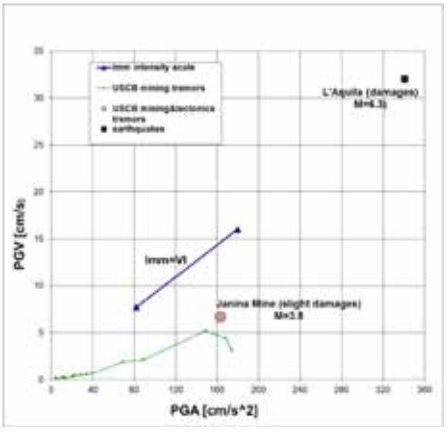

Figure 3. Relation between vector of peak accelerations, PGA and vector of peak velocities ground motion, PGV for the Janina ML=3.8 seismic event triggered by mining and mining-induced tremors in the USCB, strong earthquakes in L'aquila (ML=6,3) and MMI instrumental intensity scale parameters (degree VI).

In order to explain the differences between the regional mining-tectonic tremors in the USCB (which usually cause slight damage to non-load-bearing parts of buildings in the epicentral area) and the mining-induced tremors (that usually do not cause any damage), there was calculated the ratio of vibrations PGA to PGV. The mining-induced as well as the mining-tectonic tremors in the USCB are characterised by a PGA/PGV ratio ranging from 10 to 80, whereas for earthquakes the ratio varies between 5 and 15. This is one of the characteristics that are different in the epicentral zone for mining-induced seismic events and earthquakes (Dubiński and Mutke 2011).

MINING SEISMIC INSTRUMENTAL INTENSITY SCALE – MSIIS-15

The Mining Seismic Instrumental Intensity Scale (MSIIS-15) was developed under COMEX project (COMEX project, Mutke et al. 2015). The basic assumption of this scale is based on the GSI_{GZW} scale elaborated earlier by the Central Mining Institute (GIG) and applied in 2008 in mines belonging to Polish Coal Company (KWSA) (Dubiński and Mutke 2011, Mutke et al. 2008). The MSIIS-15 is applied to assess the impact of vibrations caused by seismic events induced by deep mining on buildings, linear objects of the underground infrastructure, levels of nuisance of used buildings and the perceptibility of vibrations by people. The vulnerability levels of historical buildings and impact of mining seismic events on the old shallow mining (caving, voids, chambers and tunnels) were also tested.

The MSIIS-15 scale combines instrumental measurement parameters of shaking with observed macroseismic effects. These macroseismic observations and instrumentally recorded parameters are arranged in six descriptive seismic intensity degrees. MSIIS-15 is a two-parameter scale and categorizes a seismic event induced by mining to a certain instrumental intensity degree, based on the maximum horizontal amplitude of vibration velocity, PGV_{Hmax} and the duration time, t_{Hv} (Mutke et al. 2015). This scale allows for an approximate assessment of the impact of mining tremors on buildings, within the range from harmless vibrations to vibrations causing damages to non-structural and decorative elements up to slight structural damages. The biggest damages observed during mining tremors concern damages of individual construction elements that don't compromise the stability of the buildings (Zembaty et al. 2015; Pohl and Sroka 2006; Holecko and Mutke 2010).

During the development as well as during the verification of the scale, various characteristic buildings were identified, including the weakest buildings with un-reinforced structures and those in poor technical condition (for example, the buildings located in the area of the previous mining activities and subjected to a process of subsidence). Therefore, the determined limits of the intensity degrees of the MSIIS-15 scale include also the harmful impact of mining tremors on typical buildings having the weakest structures and being in a poor technical condition

The short form of MSIIS-15 scale, is presented in table 1 and is intended to give a much generalized view of the scale. The full version of MSIIS-15 scale was presented in Deliverable 1.4 of COMEX project.

Table 1. The short form description of intensity degrees of the MSIIS-15 scale

MSIIS-15 Intensity I_{MSIIS}	Vibration velocity (mm/s) for short time duration impact ($t \leq 1.5$ s)	Vibration velocity (mm/s) for long time duration impact ($t > 1.5$s)	Perceived shaking	Potential damage
I	≤5	≤5	Not felt or weak felt	none
II	5 - 20	5 - 10	Felt indoors by many people, outdoors by few. Dishes rattle, hanging objects begin to swing.	*Buildings in good technical conditions:* None. *Buildings in poor technical conditions:* first slight extension

				of existing cracks
III	20 - 35	10 - 25	Felt strongly indoors by many people. Weak shaking of the whole building. Open window and door may close.	Intensification of existing damages *Buildings in poor technical conditions:* first new damages to non-structural decorative elements
IV	35 - 50	25 - 40	Felt strongly by most people. Many people are frightened and run outdoors. Furniture may be shifted. Rocking of the whole building.	Damage to decorative elements (cracks in plaster, loosening and sliding of individual roof tiles) *Buildings in poor technical conditions:* extensive damage in the decorative elements. First slight damage to structural elements
V	50 - 70	40 - 60	Felt very strongly by most people. Most people are frightened and try to run outdoors. A few people lose balance. Objects fall from shelves in large number.	Slight single structural damage- do not endanger to the stability of building *Buildings in poor technical conditions:* Many slight damages to structural elements - do not endanger to the stability of building
VI	70 - 110	60 - 100	Most people have a problem with balance. Fear and panic. Heavy objects and furniture, can fall over. Objects fall from shelves in large number	Cracks to many walls of buildings. Structural damages which do not endanger the stability of the whole load-bearing structure of the building

Impact of mining seismic events on the old shallow mining

Threshold values of the velocity parameter PGV, to classify hazard of potential instability of the old shallow mining tunnels or shafts and creation of new cracks in bedrock under seismic events, are following (Kotyrba & Mutke, 2015) :

- tunnels in fractured rock - PGV > 0.04 m/s
- tunnels in intact rock – PGV> 0.200 m/s

Historical building

Mining tremors in degree I of MSIIS ($PGV_{Hmax} \leq 0.005$ m/s) are harmless to historical structures as well as in the case of single mining seismic events exceeding this intensity level (number of seismic events <100). In the case of numerous mining seismic events exceeding intensity I (number of seismic events ≥100), the level of first slight damage to historical buildings is at lower level of $PGV_{Hmax} = 3$ mm/s.

In figure 4 there is presented Janina M_L3.8 seismic events on the background of the MSIIS-15 scale. The recorded parameters showed instrumental intensity in the V degree of the MSIIS-15 scale. The V degree intensity of MSIIS-15 is in good correlation with macroseismic damages observed for this seismic event.

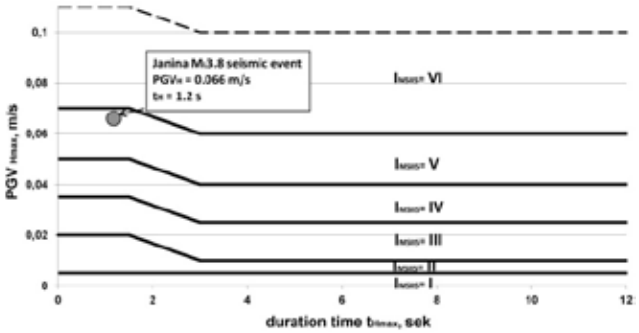

Fig. 4. Intensity degrees of the MSIIS-15 scale and Janina Mine seismic event on this scale

SUMMARY

The experience gained during the last 40 years of monitoring and analysing the mining seismicity in the Polish coal basins indicates that there are two basic types of seismic events:

- mining induced tremors – that are mainly connected with bursts of strong rock strata close to an extraction front or coal bump in the seam (Stec 2007),
- tectonic earthquake triggered by mining (Cesca et al. 2013; Marcak and Mutke 2013),

The seismic events of tectonic type occur rarely and are more hazardous at the surface. The hazard mainly manifests itself by causing discomfort to the residents and inconsiderable damage to the decorative elements of the buildings located within the epicentre area. In some cases slight structural damages are observed.

The characteristics of the strongest seismic events triggered by mining in the Upper Silesian Coal Basin are as follow: local magnitude from 3.0 to 4.5, frequency of mine phase from 1.0 Hz to 10 Hz, PGV up to 10 cm/s and PGA up to 250 cm/s^2, the duration of the main vibration phase from 0.5 s to 10 and are several times shorter than those of the earthquakes. The PGA/PGVs of the earthquakes featured a value range from 5 to 15 whereas the mining-induced tremors a range from 10 to 80. The presented seismicity induced or triggered by mining show that the assessment of vibration effects in buildings have to be a two-parameter assessment, i.e. incorporate the velocity vibration PGV and time duration of ground motion.

Based on the GSI_{GZW} scale which is used by the Polish coal hard mines, Mining Seismic Instrumental Intensity Scale (MSIIS-15) was developed under COMEX RFCS project. The MSIIS-15 scale combines instrumental measurements parameters of shaking with observed macroseismic effects according to above mentioned idea. These macroseismic observations are arranged in six descriptive seismic intensity degrees. It is very useful scale, because it allows the use of a number of seismic observations in the mining regions, to assess the expected damage distribution and the scope of liability of industry. Therefore this scale can be used to assess the seismic hazard in mining areas.

REFERENCES

Alber, M. & Fritschen, R. (2013). Rock mechanical analysis of a ML=4 seismic event induced by mining in the Saar District, Germany. Geophysical Journal International, 186(1), 359-372. DOI: 10.1111/j.1365-246x.2011.05047.x.

Cesca S., Dost B., Oth A. 2013: Preface to the special issue “triggered and induced seismicity: probabilities and discrimination. J. Seismol. (2013) 17. Pp1-4. DOI 10.1007/sl 10950-012-9338-2.

Dubiński J., Mutke G., Stec K.: 1999. Source characteristics of the mine tremors from the Upper Silesian Coal Basin – Poland. Proc. of the 9th International Congress on Rock Mechanics. ISRM, vol. II, Paris, pp. 1039-1047.

Dubiński J., Stec K. 2001. Relationship between focal mechanism parametrs of mine tremors and local strata tectonics. Proc. of the 5th International Symposium on "Rockbursts and Seismicity in Mines", Sandton, RSA, ed. A.A. Balkema Publishers. pp.113-118.

Dubiński J. and Mutke G. 2011: Selected relations between earthquakes and mining seismic events recorded in Polish coal mines. Proceedings of 22nd World Mining Congress Istambul-2011. Editor Dr Sinasi Eskikaya. Volume-I. pp. 350-357.

Holecko J., Mutke G. 2010: The mining seismicity influence on surface in ostrava-karviná coalfield - first results of monitoring with new seismic network. Colloquium on Geomechanics and Geophysics

Kotyrba A. & Mutke G. 2015: Impact of deep mining on shallow voids stability and sinkhole hazard. AIMS 2015 - Fith Int. Symp.: Mineral Resources and Mine Development. RWTH Aachen University. Vol 14, pp.561-567. (ISBN 978-3-941277-22-9)

Kozłowska M., Orlecka-Sikora B., Rudziński Ł., Mutke G. 2016: Atypical evolution of seismicity pat-terns resulting from the coupled natural, human-induced and coseismic stresses in a longwall coal mining environment. International Journal of Rock Mechanics and Mining Sciences (2016), pp. 5-15. DOI information: http:/dx.doi.org/10.1016/j.ijrmms.2016.03.024

Marcak H., Mutke G. 2013, Seismic activation of tectonic stresses by mining, Journal of Seis-mology. Vol. 17,Issue 4, pp 1139-1148..DOI 10.1007/s10950-013-9382-3. (ISSN 1383-4649).

Mutke, G., Stec, K. 1997: Seismicity in the Upper Silesian Coal Basin, Poland: Strong regional seismic events. Proc. 4th Int. Symp. :Rockbursts and Seismicity in Mines, ed. S.J. Gibowicz. Rotterdam, A.A. Balkema, 213-217.

Mutke G., Dubinski J., Barański A Lurka A.., 2008: Intensity Scale of Mining Seismic Events – GSIGZW . International Conference in Cracow: Near Surface 2008 - "The 14th European Meeting of Environmental and Engineering Geophysicists" .DOI: 10.3997/2214-4609.20146266

Mutke G., Chodacki J.,Muszyński L., Kremers S.,Fritschen R. 2015: Mining Seismic Instrumental Intensity Scale MSIIS-15 – verification in coal basines. AIMS 2015 - Fifth Int. Symp.: Mineral Resources and Mine Development. RWTH Aachen University. Vol 14, pp.551-560. (ISBN 978-3-941277-22-9)

Pohl F., Sroka A. 2006: Neuer Klassifizierungsansatz fur Gebaude Gegenuber bergbaubedingten Erderschutterungen – Entwicklung und Erfahrungsbericht. 7. Geokinematischer Tag. 11 und 12 Mai. S. 222-246

Stec K. 2007: Characteristics of Seismic Activity of the Upper Silesian Coal Basin in Poland. Geophysical Journal International, Blackwell Publishing Ltd, V 168 str. 757–768

Stec K.: 2016, Zagrożenie sejsmiczne. W: Raport roczny o stanie podstawowych zagrożeń naturalnych i technicznych w górnictwie węgla kamiennego 2013. Seismic hazard. In: Yearly report (2015) on the natural and technical hazards in hard coal mining. Ed. J. Kabiesz. Główny Instytut Górnictwa, Katowice.

Wald, D.J., Quitoriano, V., Heaton, T.H., & Kanamori, H. (1999). Relationship between Peak Ground Acceleration, Peak Ground Velocity, and Modified Mercalli Intensity in California. Earthquake Spectra, 15(3), 557-564.

Zembaty Z., Kokot S., Bozzoni F., Scandella L., Lai C.G., Kuś J.,Bobra P., 2015: A system to mitigate deep mine tremor effects in the design of civil infrastructure.International Journal of Rock Mechanics and Mining Sciences. Vol. 74 (2015) 81-90.

COMEX (RFCR-PR-11012): Complex Mining Exploitation: optimizing mine design and reducing the impact on human environment. www.comex.eu.

SUPPORT PERFORMANCE IN CONDITIONS OF DYNAMIC LOAD

Stanisław Prusek; Wojciech Masny; Zbigniew Lubosik*; Andrzej Pytlik
Central Mining Institute
Plac Gwarków 1
40-166 Katowice
Poland
*(*Corresponding author* z.lubosik@gig.eu)

24th World Mining Congress
MINING IN A WORLD OF INNOVATION
October 18-21, 2016 • Rio de Janeiro /RJ • Brazil

SUPPORT PERFORMANCE IN CONDITIONS OF DYNAMIC LOAD

ABSTRACT

The extraction of coal deposits or other minerals often results in dynamic phenomena in the form of rock mass tremors and rock bursts. In the south of Poland, in the Upper Silesian Coal Basin (GZW), as mining activities go deeper underground, in many cases the hazards get more and more serious. Some of the most significant threats are tremors and rock bursts induced by mining activities. In the Upper Silesian Coal Basin, between 2003 and 2014, there were 14,202 tremors in total. In 2014 half of the hard coal output in Poland originated from seams located in areas where rock mass tremors occur.

This paper presents selected results of investigations on support performance in dynamic load conditions in one Polish hard coal mine. The investigations consisted of the underground testing of steel arch yielding support performance in a gateroad (described by load on support, its deformation and PPV measurements), laboratory testing of different support elements (rockbolts, hydraulic props and spray-on-liners) and the reproduction of those measurements and tests and additional analyses by means of numerical modelling codes (FLAC 2D and ANSYS).

The analysis confirmed that the role of dynamic load on support is highly important to ensure its proper performance, the functionality of the gateroad and the safety of the mine crew during coal extraction.

All research was carried out under the project entitled "Innovative Technologies and Concepts for the Intelligent Deep Mine of the Future - I2Mine" financed by the European Union (7th Framework Programme).

INTRODUCTION

The Project entitled “Innovative Technologies and Concepts for the Intelligent Deep Mine of the Future - I2Mine” was carried out in the years 2011-2015 as part of the 7th Framework Programme of the European Union. Twenty three institutions from ten European countries took part in the project consortium. The team from Glowny Instytut Gornictwa carried out two out of the ten work packages. The model of a waste-less mine was developed in the first work package. Also information for the assessment of the impact of traditional and waste-less mines on the social and business environment was gathered. The results of the second work package are presented in this paper. The work conducted was related to the phenomenon of dynamic load influence on the support of underground workings and their close surroundings. This issue has significant meaning when considering the occupational safety of underground workers. All activities in I2Mine were performed in close cooperation with the industrial partner, Kompania Weglowa SA, the biggest coal producer in Europe.

BACKGROUND

Hard coal deposits in Poland are mined in two coal basins, namely the Lublin Coal Basin (LZW) and the Upper Silesian Coal Basin (GZW). The Lublin Coal Basin is located in the south-eastern part of Poland, near the border with Ukraine. Currently, one coal mine - LW Bogdanka, operates there. The Upper Silesian Coal Basin is located in the south of Poland near an urban agglomeration, with Katowice as its centre. Mining operations in the Upper Silesian Coal Basin have been conducted for over 200 years.

In 2015, there were 30 underground hard coal mines operating in Poland, which produced 72.5 million tons of coal. The basic hard coal mining system is a longwall system with single gateroads. In 2014, there were 118 longwalls in operation (Cybulski and Malich 2015) and the average depth of mining operations was slightly over 700 m. In all of the mines coal is produced in multiple seams which often results in an increase in rock burst hazard due to the influences of previous exploitation, such as: the edges or residues of previously mined seams. There are also other hazards which affect extraction in Polish coal mines, these being: seismic, caving, gas, dust, water, climate, radiation and fire.

The significant depth of extraction and the stress concentration caused by the interaction of edges or remnant pillars in previously mined-out seams, causes a presence of seismic activity and rockburst hazard in the mines. Between 2003 and 2014 (figure 1) hard coal mining operations in the Upper Silesian Coal

Basin resulted in approximately 14,000 tremors with seismic energy of E ≥ 105 J (local magnitude, ML≥1.7) and 32 rock bursts which caused material and personnel losses. In recent years, 19 tremors have had energy of E ≥ 108 J, and two had E ≥ 109 J (Stec, 2015).

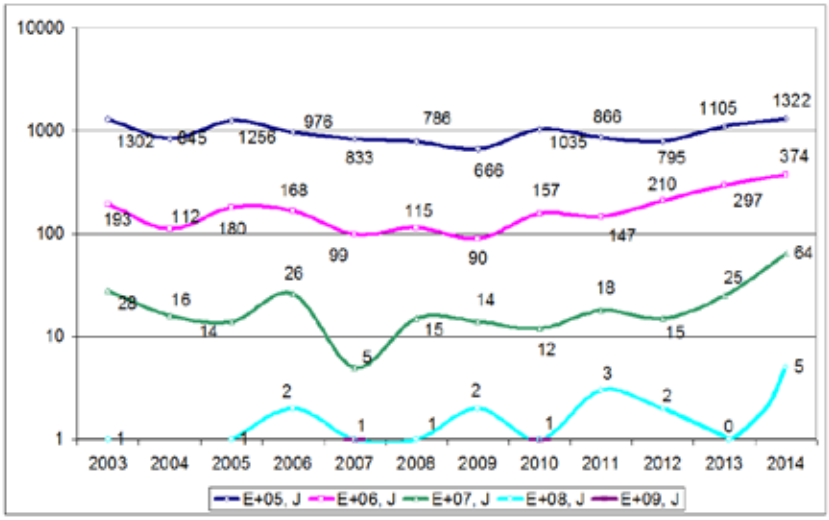

Fig. 1. The number of rock mass tremors in the Upper Silesian Coal Basin in the years 2003-2014 (Stec 2015)

Table 1 shows the production of coal in Poland between 2003-2014, including the seams mined in areas with rockburst hazard, the number of rockbursts, the number of accidents and the length of damaged workings (Patyńska 2015).

Table 1. Total hard coal production, production from seams located in rockburst areas, the accident rate, the number of rockbursts, accidents, and the length of the mine workings damaged due to rockburst from 2003 to 2014 - (Patyńska 2014)

Year	Total production	Extraction from seams located in rockburst areas		Accident ratio (accidents/ /extraction)	No. of rockbursts	Accidents caused by rockburst		Consequence in mine workings	
	millions of tones		% to general			Fatal	Other (severe and minor)	destroyed and after rock fall, m	damaged, m
2003	100,4	41,80	40,90	0,18	4	2	16	110	145
2004	96,9	39,20	39,40	0,11	3	0	11	0	358
2005	99,5	41,01	41,20	0,13	3	1	12	0	270
2006	94,5	42,15	44,60	0,25	4	4	20	0	510
2007	87,4	44,61	49,43	0,11	3	0	10	0	530
2008	83,6	41,92	50,12	0,31	5	0	26	0	710
2009	77,5	34,33	43,80	0,06	1	0	5	0	101
2010	76,1	35,84	47,04	0,18	2	2	12	30	87
2011	75,5	34,25	45,36	0,08	4	1	6	0	168
2012	79,2	37,60	47,47	0,04	1	1	2	170*	210*
2013	76,5	36,90	48,25	0,07	1	0	5	50	113
2014	72,5	36,00	49,66	0	1	0	0	160	390

*- Approximate data

The data presented in Table 1 shows that from 2004 to 2014 hard coal production decreased from 100.4 million to 72.5 million tons. During this period, 39% to 50% of coal production came from seams located in rockburst areas. The number of rockbursts ranged from 1 to 5, resulting in 125 minor to severe accidents, and 11 fatalities. As a result of rockbursts, between 520 m and 3.200 m (length) of mine workings were destroyed or damaged.

UNDERGROUND TESTS

To make in situ measurements of dynamic load on the support of a roadway, a measuring system which enables the continuous monitoring of load on support and roof bolts was developed in the Central Mining Institute (meeting the requirements of the ATEX 94/9/WE directive for equipment and systems used in potentially explosive atmospheres). A system operation diagram is presented in Figure 2, and Figure 3 shows the location of its elements in the mine working (Prusek, Masny 2015).

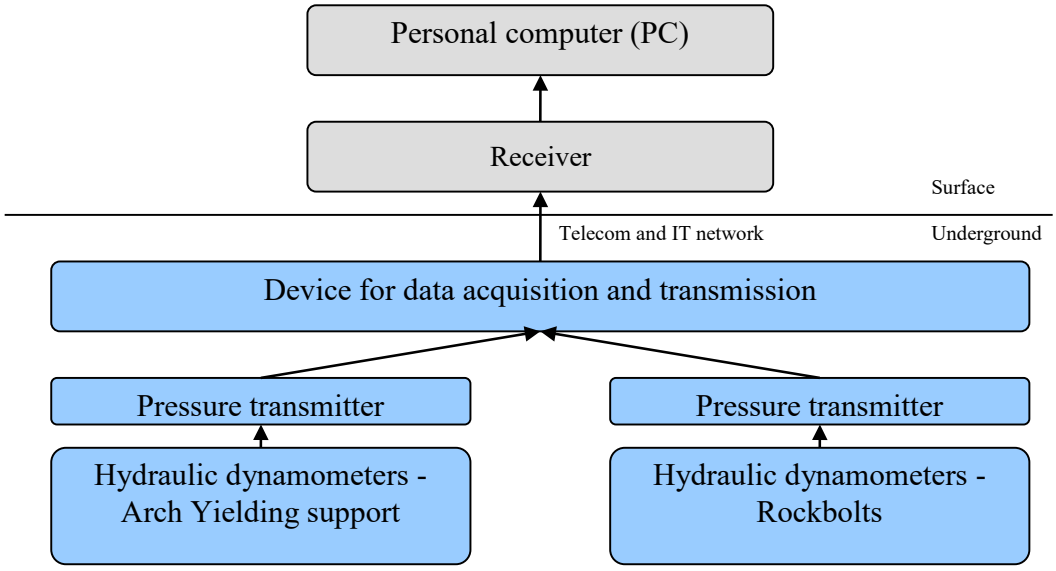

Fig. 2. Simplified diagram of a system measuring static and dynamic load exerted on support and rock bolts (Prusek, Masny 2015)

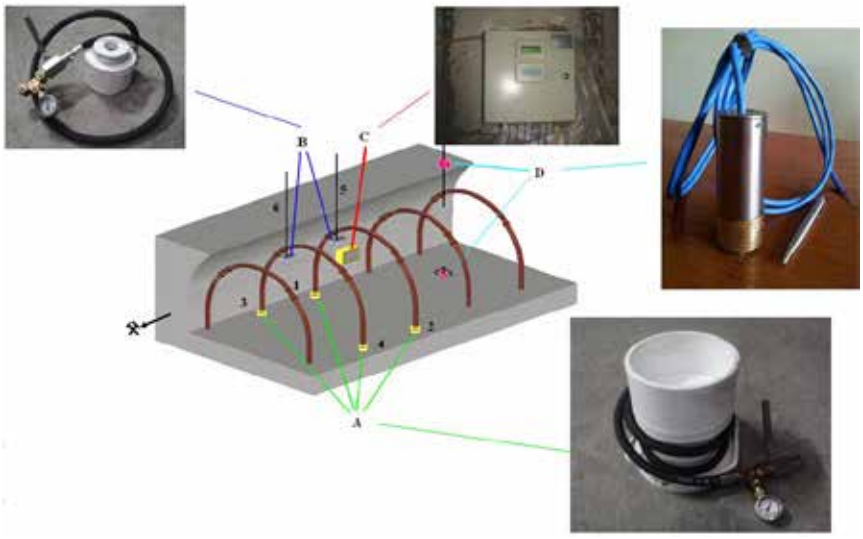

Fig. 3. Diagram of the measurement area: A – dynamometers under steel arches, B – dynamometers on bolts, C – device for data acquisition and transmission, D – PPV seismometers (Mutke, Masny, Prusek 2016)

As visible in Figures 2 and 3, hydraulic dynamometers, both under the feet of an arch support and on the rock bolts e.g. flexible dynamometers, are connected to pressure transmitters. Additionally, for control purposes, there is a manometer for each of the dynamometers. Measurement signals from the pressure transmitters are collected by a device for data acquisition and transmission and then they are sent to the surface with the telecom and IT network in order to be finally recorded on a PC with specially installed software. Signals

from PPV seismometers (DLMPPV type) are connected to tremor receiver DLM-SO, located in the geophysical station (Prusek, Masny 2015).

This system of monitoring load exerted on supports was used in two bases located in one of the mines of the Upper Silesian Coal Basin. In total, it worked in underground conditions for 195 days. Figure 10 shows graphs of the load exerted on the dynamometers located under the feet of steel arches D1÷D4 and on roof bolts D5÷D6 during underground measurements in base I (78 days). The base was located approximately 25 m behind the longwall entry.

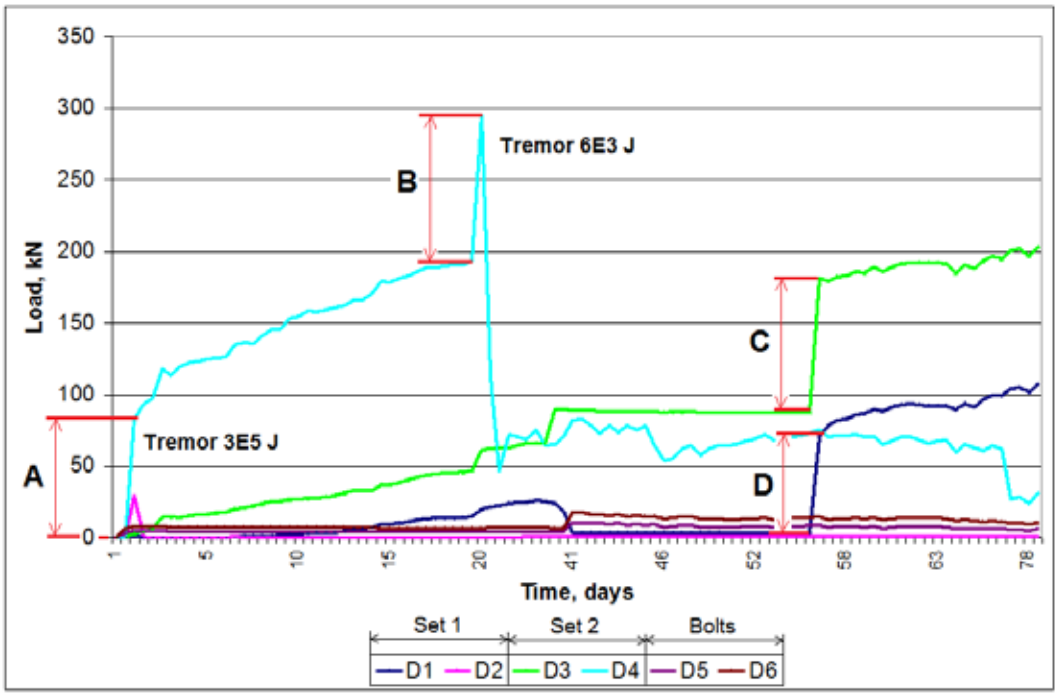

Fig. 4.Changes in load exerted on steel arches D1÷D4 and on rock bolts D5÷D6: A - load increase due to tremor energy 3E5 J, B - load increase due to tremor energy 3E5 J, C, D - load increase due to front abutment pressure (Mutke, Masny, Prusek 2016)

Having compared the load and tremor parameters measured, two tremors were selected which undoubtedly resulted in an increase in load on the roof support. They are marked A and B in Figure 4. Data concerning the two phenomena is presented in Table 1.

Table 1. Results of measured load on support and mining tremor parameters (Mutke, Masny, Prusek 2016)

Date, time	Increase in load on ŁP roof support and rock bolts [KN]						Seismic energy of tremor [J]	Distance between tremor source (focus of tremor), and station in mine working [m]	Dominant frequency of vibrations [Hz]	PPV W, [m/s]
	Dynamometers under roof support ŁP				Dynamometers on rock bolts					
	D1	D2	D3	D4	D5	D6				
2013.11.05, 17:38:39	1.1	28	2.5	82	1.9	1.9	3E5	132	30	0.110
2013.11.25, 16:16:43	5	0	14	100	0	0	6E3	60	35	0.046

LABORATORY TESTS

Research concerning different types of support used in underground coal mines has been conducted over many years in the Central Mining Institute. Usually the tests are carried out by exerting static or dynamic loads on the support. Technical specifications of the dynamic test facility enables the examination of components with dimensions up to 5×2×6 m (height × width × length) by direct impact of a free moving mass from 1,000 to 20,000 kg. The maximum impact energy is 500 kJ, and the initial setting load of the hydraulic cylinders may be up to 2 MN (Pytlik, Masny, Prusek 2016).

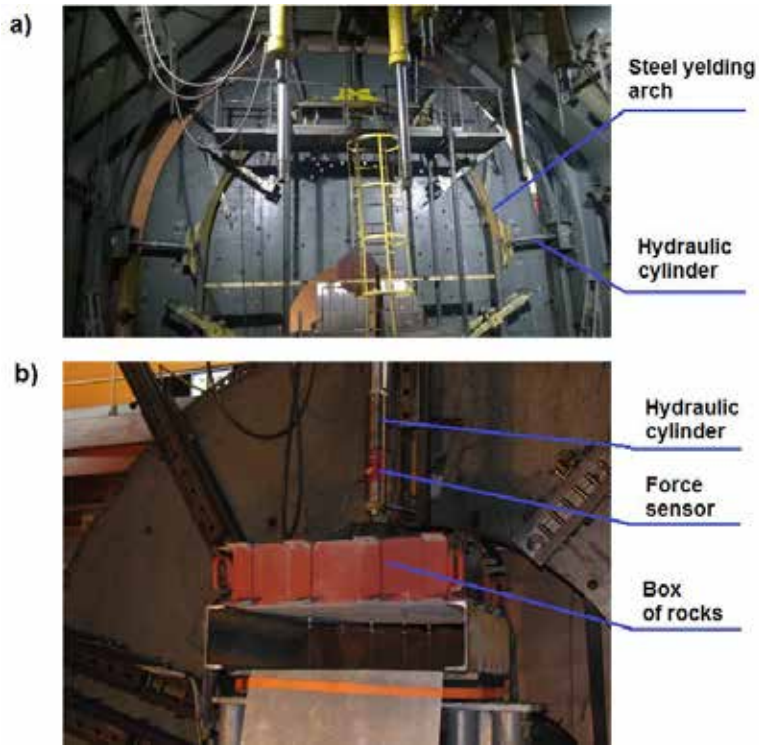

Fig. 5. The test facilities at the Central Mining Institute (GIG), a - facility for testing the steel arches in real scale; b - facility for testing the lining support (e.g. shotcrete, TSL) (Pytlik, Masny, Prusek 2016)

In the framework of the project I2Mine the following elements of support used in Polish underground mining industry were selected for the dynamic load tests:

- hydraulic props,
- yielding bolts,
- lining support (e.g. shotcrete).

The aim of the tests was to determine the performance, in the form of a load vs. time graph of the selected support under dynamic load, for various values of impact energy and, based on these values, the determination of dangerous values of load leading to their destruction. As a result of the work, a catalogue containing the performance characteristic of the tested support under dynamic loads has been prepared.

In the hard geological and mining conditions of Polish collieries, SHC type hydraulic props with valve batteries are commonly used as support elements. In real life conditions they often get damaged due to impact-like dynamic load. The phenomenon is caused by the insufficient flow rate of typical valve batteries used in SHC type props - figure 6.

Fig. 6. Destruction of an SHC prop with a working release valve and destruction of sealing in the area above the piston of the prop due to the inadequate performance of the valve (Pytlik 2015b)

An example of performance graphs of SHC-40 type hydraulic props under dynamic load is presented in Table 2.

Table 2. An example of performance graphs of SHC-40 type props under impact-like dynamic load (Pytlik 2015b)

TABLE 1 Type and kind of prop/ Type of valve battery /Producer	drop weight / beam, kg	p_{max}, MPa	kinetic energy of impact, kJ	h, m	Performance $p=f(t)$	Notes
SHC-40 W13 / GIG-PUMAR type battery (prototype) spring-loaded (cylindrical) ϕ4.5mm fluid jet diameter PUMAR HYDRAULIKA	4,000/ 3,300	65.4 70.3 75.6 81.6 87.7	10.8 12.9 15.1 17.2 21.5	0.5 0.6 0.7 0.8 1.0	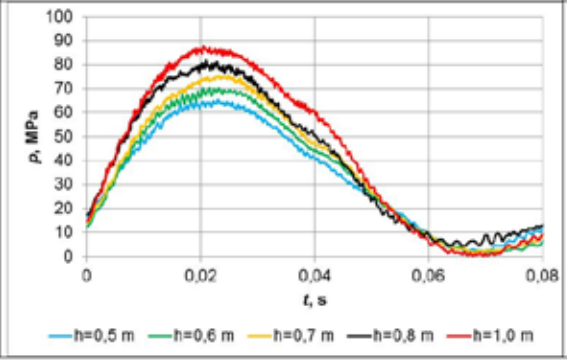	Prop was not destroyed

A laboratory test of the bolt, according to GIG methodology, was performed in two stages. The first stage contains the examination of the bolts' mechanical components. Bolts which passed the first stage of research are tested in step II. In this stage a bolt is bonded to the steel cylinder (Pytlik 2015a). The scheme of the test for this step is shown in Figure 6.

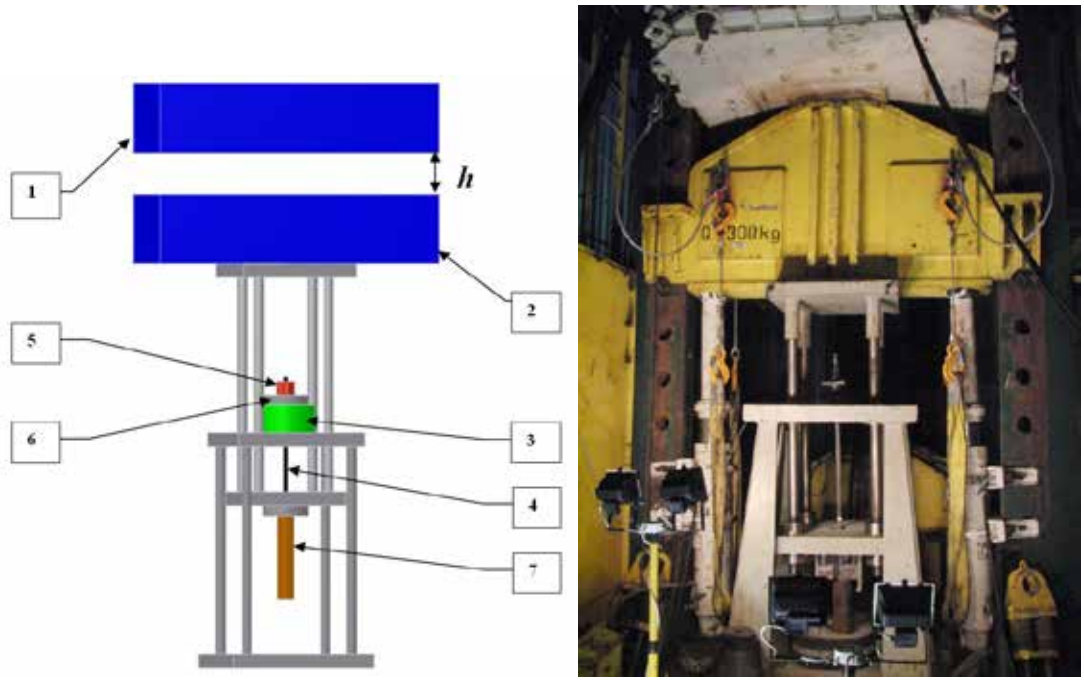

a b

Fig. 6. The test facility prepared for testing in Phase II of the dynamic load on the bolt in steel cylinders: a - scheme; b - photograph; (1) the free falling mass (m1), (2) traverse (with mass m2), (3) a force sensor (4) bolt rod (5) bolt nut (6) bolt washer (7), steel cylinder (Pytlik, Masny, Prusek 2016)

In Figures 7 and 8 the exemplary results of yielding bolts tests with impact speed vu of 0.7 m/s after 14 and 21 days after bonding have been shown.

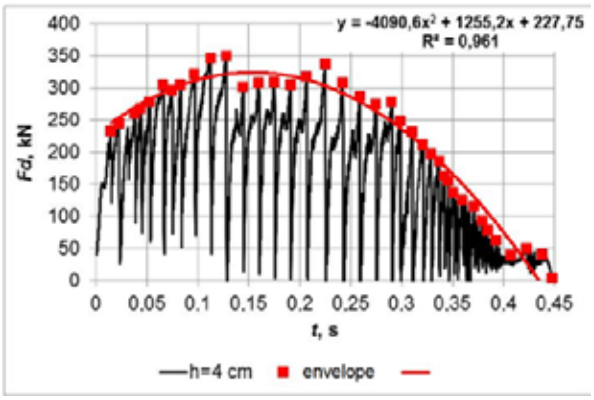

Fig. 7. Graph of dynamic resistance force (Fd) in time (t) for yielding bolt at the impact speed vu of 0.7 m/s (h=0.04 m, 14 days after bonding) (Pytlik, Masny, Prusek 2016)

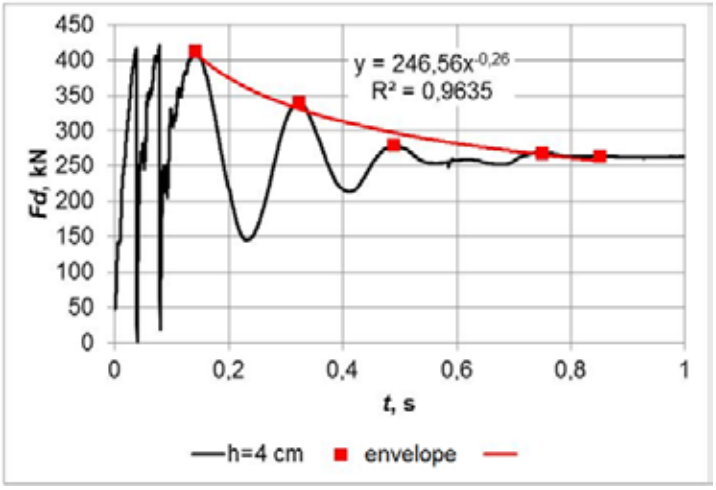

Fig. 8. Graph of dynamic resistance force (Fd) in time (t) for yielding bolt at the impact speed vu of 0.7 m/s (h=0.04 m, 21 days after bonding) (Pytlik, Masny, Prusek 2016)

The test carried out after 14 days of bonding showed that there was no damage to the mechanical parts of the bolt but the wires protruded fully from the cylinder due to the shearing of the wires-binder connection. 21 days after bonding, the wires had protruded from the cylinder to a length of 27 mm. The laboratory test was described as positive.

The last tested elements were the lining support (eg. shotcrete or TSL). This type of support is commonly used in mining and tunnelling, most often as a temporary support, to improve stability and reinforce mine workings as well as to seal them against gases and water.

An example of the performance graphs of lining support under dynamic load is presented in Table 3.

Table 3. An example of performance graphs of the lining support under dynamic load (Pytlik 2015b)

TABLE 3						
Type and kind of liner	Mass of striker / beam, kg	F_{max}, kN	E_k, kJ	s, cm	Performance $F_d=f(l)$	Notes
TSM70 g=46 mm + MSM g=4 mm	4,000/290	55.7	0.4	1	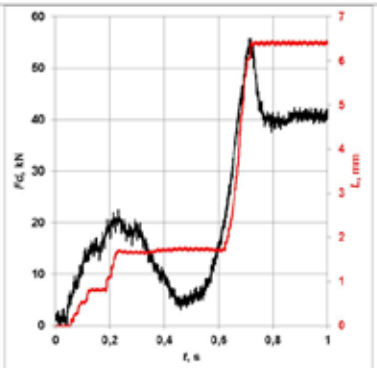	Lining stable. Slightly cracked.

Typical destruction of hybrid lining support i.e. type TSM 70 bond with an MSM membrane is presented in the photos in Figure 9.

a **b** **c**

d **e** **f**

Fig. 9. Example of deformation and destruction of hybrid lining: TSM 70 bond with an MSM membrane (Pytlik 2015b)

NUMERICAL MODELLING

Numerical modelling aimed at the analysis of the behavior of powered roof support under the influence of dynamic phenomena was carried out using FLAC software based on the method of finite differences and ANSYS software based on the finite element method. Additionally, original software developed in the Central Mining Institute, which makes it possible to determine the balance of forces in particular elements of the roof support, was used for mapping the powered roof support in the FLAC software - Figure 10.

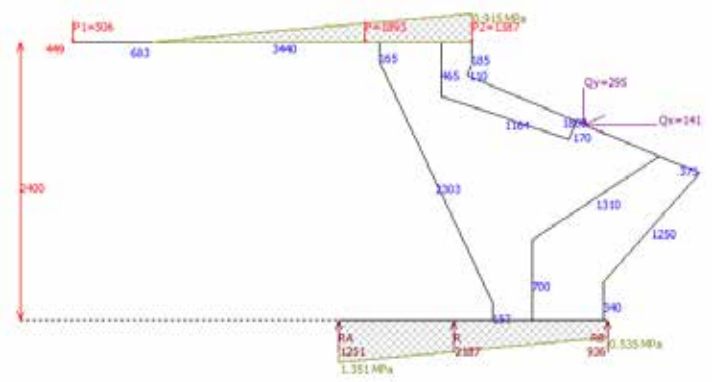

Fig. 10. Pressure distribution at the canopy and base of the powered roof support

Calculations were made for several variants of roof displacements corresponding to dynamic phenomena with different values of peak rock mass particle velocity (PPVw) - both for if the dynamic impulse is described with a sinusoid (PPVw = 0.25; 0.5; 0.75; 1.0 m/s) and the actual values (chapter 3) measured in situ (PPVw = 0.038; 0.046; 0.049; 0.110; 0.122 m/s).

Among other things, model deformations, stress components and their distribution under the applied load were obtained as a result of the calculations. Figure 10 presents the distribution of reduced stresses designated according to the Huber-Mises-Hencky hypothesis. The graphs in Figure 11 present peak values resulting from the applied load as well as the change in pressure in the legs of the roof support.

a)

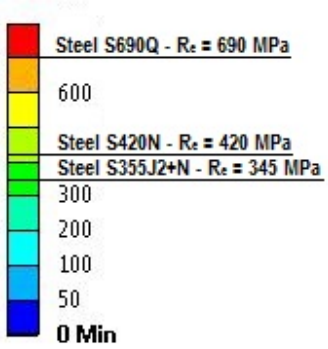

b)

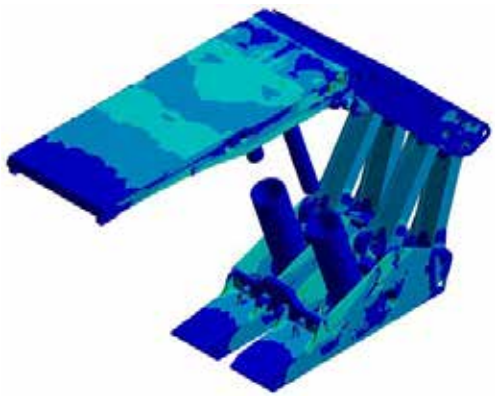

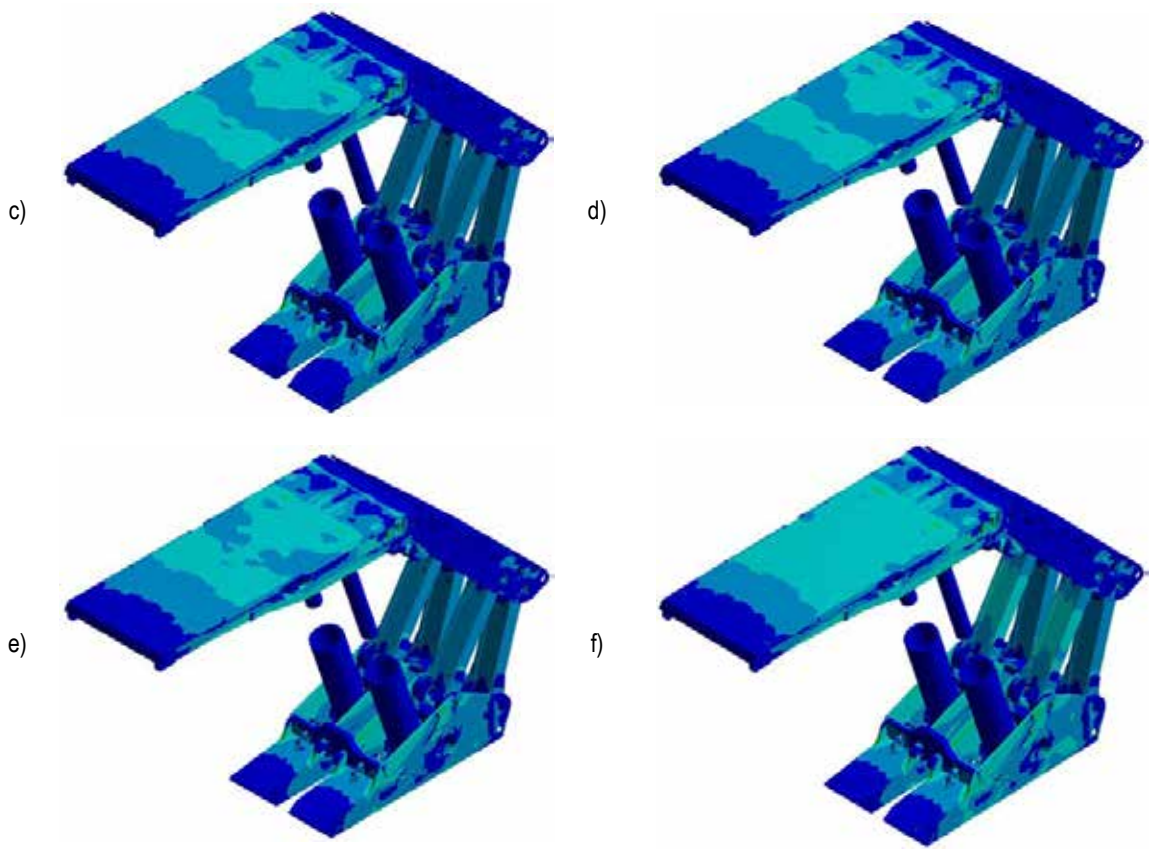

Fig. 10. The comparison of stress distribution reduced in the section of the powered roof support upon the application of roof displacements with a variable amplitude related with the dynamic impulses measured in situ: a) legend - Huber-Mises-Hencky reduced stresses [MPa], b) PPVw = 0.038 m/s, c) PPVw = 0.046 m/, d) PPVw = 0.049 m/s, e) PPVw = 0.11 m/s, f) PPVw = 0.122 m/s - impulse triggered by the detonation of an explosive (Witek et. al 2015)

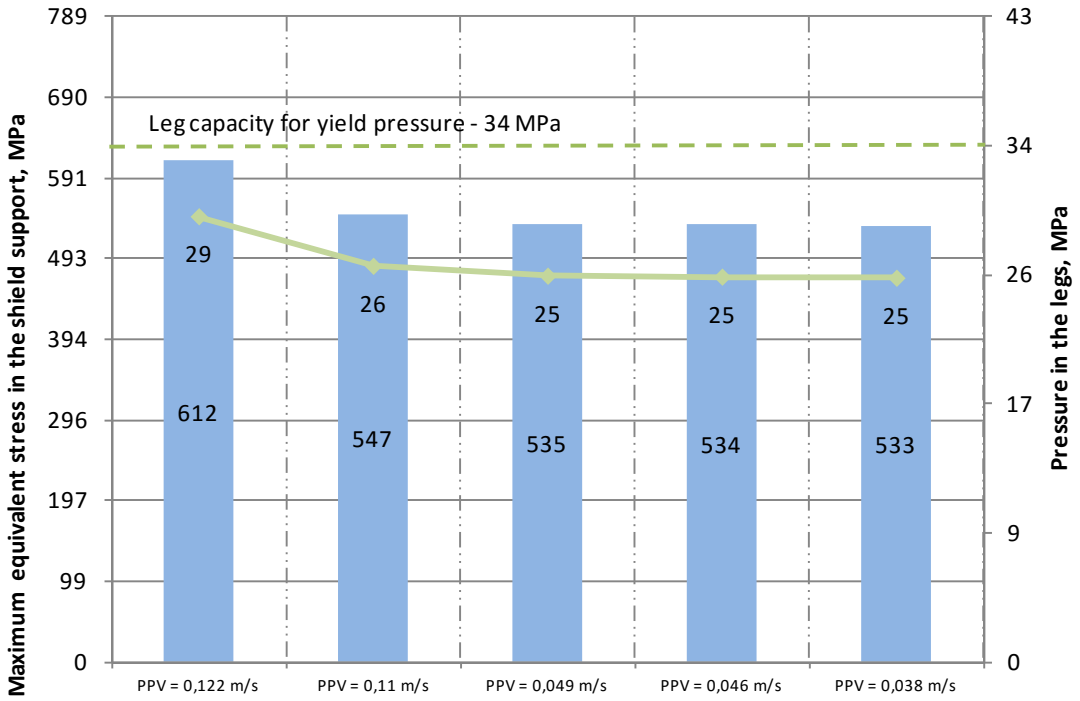

Fig. 11. Peak values of reduced stresses in the section of the powered roof support together with corresponding values of pressure in the legs for particular PPVw values measured in situ (Witek et. al 2015)

As visible in Figures 10 and 11, each of the analyzed impulses caused a specific increase of reduced stresses in the structure of the powered roof support and simultaneously an increase of pressure within the space under the piston of the leg.

Upon analysis of the actual dynamic phenomena and the related measured PPVw values, it can be stated that when the PPVw values are lower than 0.049 m/s, the changes in the reduced stresses in the steel constituting the structure of the powered roof support as well as the pressures in the space under the piston are so small that they should not have a negative impact on the longwall.

SUMMARY

Complicated mining conditions in Polish coalmines resulting from multiple seam extraction mean that, despite decreasing production, seismic activity remains at a constant level. The occurrence of high-energy rockmass tremors, induced by mining operation, can affect the safety of underground exploitation. Apart from the typical consequences of dynamic phenomenon in terms of mine workings and support damage, it can also results in the injury of workers.

The continuous load monitoring system, designed for standing and rockbolt support in areas of rock mass tremor occurrence, can provide information about the behaviour of the support, including boundary stress states. This information allows mine managers to take appropriate actions, e.g. the installation of additional reinforcements. The monitoring system was successfully tested underground for a period of 195 days.

The information concerning the characteristics of support operation in conditions of rockmass tremor occurrence is not of less importance. The testing rig of the Glowny Instytut Gornictwa allows for the performance of multi-optional tests which take into account variable energy as well as different characteristics of the element tested (e.g. construction, operational height range, setting pressure). Knowledge about support and its elements' performance during dynamical tests allows for its further effective application in underground workings.

Highly valuable information in the scope of mining support affected by dynamic loading can be gained from numerical calculations. As presented in this paper, the analysis of whole shield support is possible in terms of both stresses in elements and under piston pressure in hydraulic props. After the development of adequate models, the analysis of different variants is far less means and time consuming than laboratory tests.

To summarize, it can be stated that mining operations in conditions of rockmass tremor occurrence requires the involvement of many complementary techniques and methods. Only a holistic approach can assure an appropriate safety level.

REFERENCES

Cybulski K., Malich B. (2015): Zagrożenie pyłowe.: Raport roczny o stanie podstawowych zagrożeń naturalnych i technicznych w górnictwie węgla kamiennego 2014 (Dust hazard: Yearly report on basic natural and technical hazards in hard coal mining in 2014). Ed. Kabiesz, J., Central Mining Institute, Katowice, Poland. pp. 41-60.

Mutke G., Masny W., Prusek S. (2016): PPV as an indicator of dynamic load exerted on the support of underground workings. Acta Geodynamica and Geomaterialia (in print).

Patyńska, R. (2015): Zagrożenie tąpaniami. W: Raport roczny o stanie podstawowych zagrożeń naturalnych i technicznych w górnictwie węgla kamiennego 2014. (Rockburst hazard. In: Annual report (2014) about the state of natural and technical hazards in hard coal mining). Ed. Kabiesz, J. Central Mining Institute, Katowice, Poland. pp. 96-106.

Prusek S., Masny W. (2015): Measurement of dynamic load exerted on support of workings in Polish coal mines. Aachen International Mining Symposia, 5th International Symposium – Mineral Resources and Mine Development, RWTH Aachen, pp. 295-308.

Pytlik, A. (2015a): Odporność dynamiczna kotwi górniczych (Dynamic capacity of rockbolts). Occupational Safety and Environmental Protection in Mining No 04/2015. Publisher: State Mining Authority. pp. 28-35.

Pytlik, A. (2015b): Tests of selected types and elements of support under dynamic load. Deliverable 3.3. Report - I2Mine. GA No 280855, Główny Instytut Górnictwa, Katowice (not published).

Pytlik A., Prusek S., Masny W. (2016): The methodology for laboratory testing of rock bolts used in underground mines under dynamic loading conditions. Journal of the Southern African Institute of Mining and Metallurgy (in print).

Stec, K. (2015): Zagrożenie sejsmiczne. W: Raport roczny o stanie podstawowych zagrożeń naturalnych i technicznych w górnictwie węgla kamiennego 2014. (Seismic hazard. In: Annual report (2014) about the state of natural and technical hazards in hard coal mining). Ed. Kabiesz, J., Central Mining Institute, Katowice, Poland. pp. 82-95.

Witek M., Szot Ł., Masny W., Prusek S. (2015): Recommendations of improved ground control practice for safe deep underground Mining - Deliverable 3.2. Report - I2Mine. GA No 280855, Główny Instytut Górnictwa, Katowice (not published).

THE APPLICATION OF LASER SCANNING IN THE PROCESS OF CONSTRUCTING A MINE DRIFT NUMERICAL MODEL

Jakub Janus[1]

Strata Mechanics Research Institute of Polish Academy of Sciences,
30-059 Krakow, Poland
*(*Corresponding author: janus@img-pan.krakow.pl)*

24th World Mining Congress
MINING IN A WORLD OF INNOVATION
October 18-21, 2016 • Rio de Janeiro /RJ • Brazil

THE APPLICATION OF LASER SCANNING IN THE PROCESS OF CONSTRUCTING A MINE DRIFT NUMERICAL MODEL

ABSTRACT

Knowledge of the air flow in the mine drifts is important for the safety and efficiency of work in mine. In this area are many problems that have not been solved in a satisfactory way. More and more often in this area progress is made through simulations using computational fluid dynamics methods. Several comparison of simulation and measurement data indicate, that for a given class of problems must be chosen optimal methodology for modeling. For many problems, there are sets of instructions regarding the whole process of modeling - building model geometry, build computational meshes, choice of turbulence models. But so far there was not developed a universal method of solving the numerical simulations for mine drift. The process of formulating appropriate recommendations to carry out numerical simulations in the mine environment, which guarantee god results compared to measured data is still expand.

One of the obstacles in creating the guidelines for solving numerical simulations for mines is to create a geometric model that credible representative the mine drift geometry. Therefore, nowadays the geometry model of mine drift is not a reflection of the object but relatively coarse representation. During creating a model there are same simplifications of the object description. Simplify are often necessary to obtain a clear picture of the phenomenon studied and to shorten the numerical calculations. However, knowledge about the impact of such simplifications on changes in calculation results is required. One of the conditions necessary to acquire this knowledge is to obtain accurate information about the geometry of the mine drift. Classical methods of measurement require a large amount of time and work of many people. To obtain enough data about the object is necessary to use modern methods of measurement like laser scanning.

The paper presents the results of laser scanning in the form of spatial representation of mine drift. Based on the resulting point cloud shows how to build a numerical model of mapping the geometry of the mine drift in order to conduct numerical calculations.

KEYWORDS

laser scanning, TLS, numerical fluid mechanics, numerical model geometry

INTRODUCTION

The knowledge of airflows in mine drifts is essential when it comes to safety and efficiency of mining activities. There are many problems in this field that have not yet been solved satisfactorily, or could still be solved in a better way. More and more often, however, some progress can be achieved due to simulations that make use of the methods of numerical fluid mechanics. Numerous comparisons of simulations and measurement data show that, for each selected group of problems, a best practice should be chosen. For many problems, there exist best practice guidelines which refer to the whole process of modelling – i.e. building the geometry of the model, building calculation nets, choosing the right turbulence model. Yet, so far, no universal method has been developed, and the process of formulating proper guidelines for conducting numerical simulations in underground conditions – which, unlike measurement data, guarantee satisfactory results – is still underway.

In the process of numerical simulations, three essential operating stages can be distinguished:

- pre - processing – preparation for calculations;
- processing – solving the problem;
- post-processing – processing the calculation results.

The stage of preparation for calculations includes activities due to which it becomes possible to solve a given problem using a computer. The geometry of the calculation area should be designed, and then a numerical net covering this area should be generated. Subsequently, the type of boundary conditions for the calculation area should be determined, together with the physical parameters of the airflow. As far as airflow problems in underground conditions are concerned, one of the obstacles preventing determination of proper guidelines for numerical simulations is creating a geometrical model that would correspond with the geometry of mine drift in a reliable way. Thus, at present, the geometry of the model of mine drift is not an accurate projection of the object in question, but its rough representation. While constructing a model, the description of the object is simplified. Such simplifications are often necessary if we want to obtain a clear image of the investigated phenomenon and shorten the duration of numerical calculations. Still, we need to know in what way such simplifications will influence the accuracy of the obtained calculation results. One of the conditions essential for obtaining this knowledge is getting detailed information about the geometry of the mine drift. Classic measurement methods require a huge investment of time and effort of many people, who frequently work in conditions that pose a threat to their health and lives.

In order to obtain an adequate amount of data about a given object, it is necessary to search for new measurement methods that would make it possible to quickly obtain sufficiently accurate information needed to map the objects – also the objects whose shape is complicated, and which are difficult, or sometimes even impossible to measure by means of classic measurement methods.

NUMERICAL SIMULATIONS PERFORMED ON GEOMETRICAL COMPLICATED NUMERICAL MODELS

The geometry of mine drift poses a lot of problems in the process of creating numerical models. With some standard measurement techniques at our disposal (a meterstick, a laser rangefinder), it is really difficult to map such elements as:

- mine drifts intersections,
- floor uplifts,
- mine drifts convergence,
- deformation of arch-yielding supports
- uneven placing of arch-yielding supports
- presence of mining equipment, such as band conveyors, mining combines, stone-dust barriers, hydraulic installations, or pipelines.

A good example of an attempt to map the geometry of an mine drift characterized by a complex structure is the descending gallery IV-S at the outlet of the longwall 303-S PN in the KWK Murcki-Staszic hard coal mine (as illustrated in Figure 1). In the inflow section of the gallery, there were numerous sources of airflow disturbances, such as palisade of props, cribs, and a pile of mining output.

On the basis of photographic documentation and measurements carried out with a meterstick, the stage of pre-processing – aiming at creating a geometrical model of the investigated section of the mine drift – was initiated. The total length of the calculation area (as illustrated in Figure 1) was 24 m. The calculation area encompassed:

- a section secured by arch timbering/steel arching, from the inlet to the first set, with the props not taken into account,
- a pair of emergency stopping sets, whose spacing and dimensions corresponded to the data about the mine,
- props.

A section of the mine drift between cribs and a side wall

A fragment of the cross-section of the mine driftwith no obstacles

The crew placing sacks

The state after placing the barrier

Figure 1 - A photograph of the descending gallery IV-S,
an outlet of the longwall 303-S PN, the KWK Murcki – Staszic hard coal mine

A section between the second set and the outlet encompassed the measurement cross-section and the place where a barrier consisting of sacks had been built. Here, the arches were initially supported with props. To the left (looking in the direction of air inflow), there was a pile of mining output that remained after the process of sorting out the sole. Further down the section, cribs were used (apart from props) to support the arches (as illustrated in Figure 2). The model takes into account their dimensions, as well as their irregular placement.

A constant cross-section was assumed, corresponding to the measurement cross-section – local narrowings connected with the presence of sets and soil uplifts excluded. The geometry of the model includes a lot of elements presented in a detailed way. It was assumed that, in the section before the first set, it was not necessary to take into account the presence of props, as their impact is minor when compared to other obstacles to the airflow, located closer to the measurement cross-section.

The obtained calculation results (Krawczyk, , Janus, 2015) showed some differences in the readings of the numerical simulation in relation to the measured values of the airflow velocity – in particular, for the measurement points located close to the cribs. This is explained by the highly diversified geometry of the mine drift and the elements occurring in the investigated section. The more exact mapping of these elements is virtually impossible.

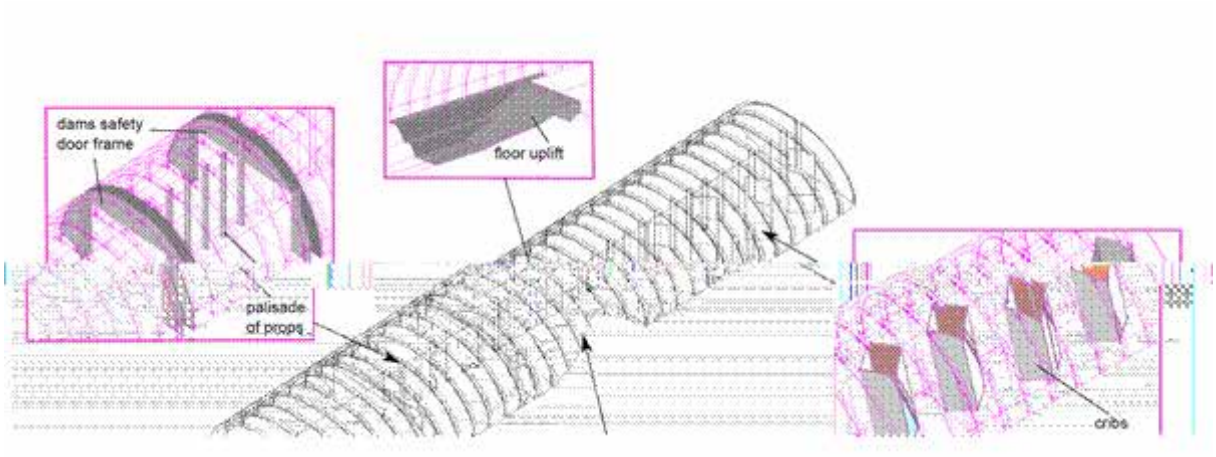

Figure 2 - A numerical model of the descending gallery IV-S
an outlet of the longwall 303-S PN, the KWK Murcki – Staszic hard coal mine

On the basis of numerical simulations carried out for the underground conditions, the following conclusions can be formulated:

- numerical simulations carried out for mine drifts characterized by complicated geometry do not yield results that would be satisfactory in relation to measurement results,
- with the applied techniques for measuring the mine drift geometry (a meterstick, a laser rangefinder), it is impossible to represent the numerical model in geometrical terms in a satisfactory way,
- in order to obtain most accurate simulation results in relation to measurement results, one has to ensure that the very process of numerical modelling is long enough.

TERRESTIAL LASER SCANNING

The constant development of new technologies resulted in the proliferation of methods previously restricted for a very narrow group of users. An example of such a technology is the reverse engineering and its tools, i.e. 3D scanners. The abilities of this equipment, combined with the advantages of the CAD systems, create new, previously unattainable possibilities (Baścik 2013; Zokoła - Szewioła, Wiatr, 2013).

Terrestrial Laser Scanning (TLS) is a technology used to obtain information about the shape of an object, based on very fast determination of the coordinates X, Y, Z – a huge number of points called a cloud of points. The cloud of points oriented in space, obtained in the course of the scanning process, makes it possible to generate – in a very fast and accurate way – a three-dimensional model of the scanned object. Due to the development of the software, the processing of such a substantial amount of data becomes more efficient. Also, we are provided with a tool for various types of analyses, which becomes better and better with time.

Usually, a TLS system includes a transmitter, i.e. a module generating the laser light (a diode), a whirling mirror system whose task is to ensure an even angular deviation of a laser beam and „scattering" it over the surface of objects. The instrument also includes an optical telescope by means of which the reflected returning rays are concentrated, and a detector which transforms the energy from light into an impulse recorded in a registration module (a memory card) and a console. The transmitter and the detector are managed by a control unit, which, in turn, is managed by a microprocessor. The instrument rotates around its own axis, with a fixed rotation angle, which ensures obtaining the assumed resolution.

The functioning of a laser scanner is based on the phase method of measuring distances, based, in turn, on the properties of the wave emitted by the laser. The instrument emits a laser beam of a known frequency („emited light"), which – after meeting the object – comes back to the instrument

(„returning light"). The phase of the „returning light" was compared to the phase of the known frequency. The difference between the two peak values is known as a „phase shift".

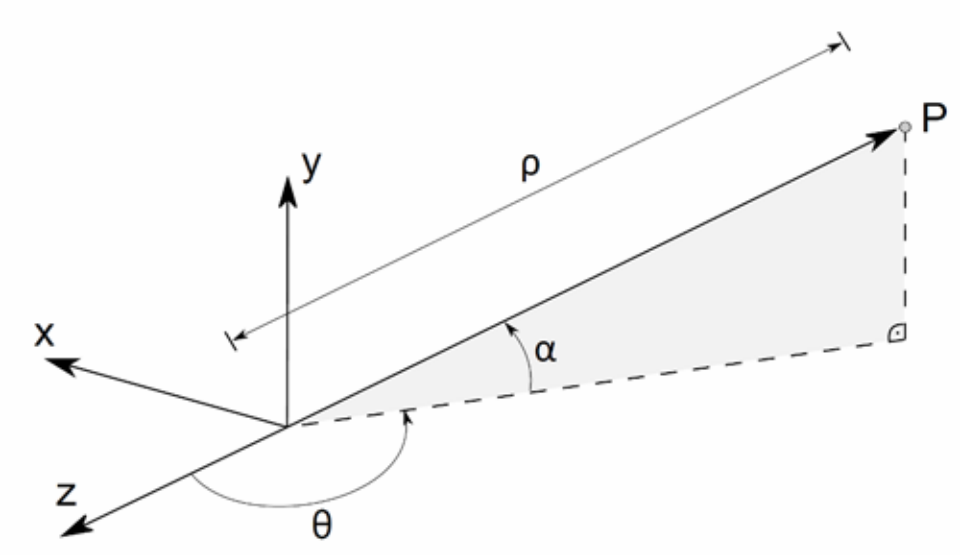

Figure 3 - The functioning of TLS – a schematic representation

This is a polar measurement method, in which the location of a given point is determined by means of the horizontal and the vertical angle, as well as the distance from the measured point. The angles are determined on the basis of the location of the mirrors scattering the laser beam. In order to establish the location of the point P, one has to know: the length of the ray ρ, and the values of the angles α and θ (as illustrated in Figure 3). The scanners measuring the phase shift are regarded as some of the most accurate instruments for laser scanning destined for commercial purposes, as they make it possible to obtain the desired data very quickly, and generate scans characterized by a very high resolution.

The Measuring Equipment

In the measurements of the geometry of a gallery in mine drift, one of the commercially available 3D scanners was used, i.e. the FARO Focus 3D laser scanner. It is a most compact instrument, whose dimensions are mere 0,24x0,20x0,10 m, and whose total weight is 5 kg. The range of the instrument is 0.6 m – 120 m; the laser beam falls – at the angle of 90° - on the surface whose reflectance is 90%. The scanner is characterized by a high speed of the measurement – from 120,000 points per second to 976,000 points per second, depending on the scan resolution. The measurement error is ± 0.002 m. The visual field of the instrument is 360^0 in the horizontal plane and 305^0 in the vertical plane. The laser power is 20 mW, the wave length – 905 nm, and the typical value of the beam divergence is 0.16 mrad. During measurements, all the data is recorded on an SD card, and therefore it can be transferred to a computer safely and easily.

The Measurement Site

Measurements performed by means of a 3D scanner were carried out in the ZG Sobieski mine, in the Grodzisko cross-cut gallery, level 300. As the measurement site, the neighborhood of a turn was chosen, which gave the researchers vast measurement possibilities (Lipecki, 2010).

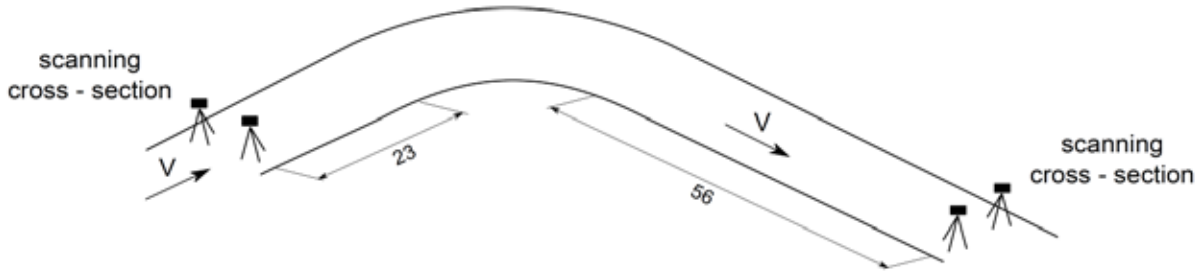

Figure 4 - Schematic layout of the scanning cross - sections

Due to the complex structure of the mine drift (floor uplifts, clamps in the lining, the arch - yielding supports, a turn), it was necessary to choose proper sites for measurements performed with a 3D scanner. In order to map the geometry of the gallery in the best possible way, a double scanning site in the cross-section of the mine drift was established. One of the elements in the cross-sections were pipelines running underneath the roof. Performing measurements in one site only would result in emergence of the so-called dead spaces – areas in the shadow of the pipelines where laser has no access. The scanning sites were placed at the left and the right sidewall, which made it possible to minimize the areas where no scanning was performed. Subsequently, the researchers had to determine the measurement cross-sections and place the proper number of markers, which link the scans from consecutive sites and place them in a chosen set of coordinates. In order to obtain a full spatial model of the mine drift, the whole section of the gallery was divided into 11 scanning cross-sections, which resulted in 22 measurement sites. First scanning cross-section was 23 meters before turn, last scanning cross - section 56 meters after turn (as illustrated in Figure 4).

Processing The Data Provided By Laser Scanning

Processing the data provided by laser scanning can be referred to as pre-processing. As part of processing the measurement data, one has to prepare the data for further activities (Krawczyk, Kula, 2013). At this stage, one of the most important processes is orienting a cloud of points by combining several clouds of points (obtained from particular measurement sites) into one set of data. After that, the cloud of points is filtrated, which involves cleaning, removing the measurement noises and discontinuities. If the obtained cloud of points poses some difficulties from the perspective of further processing because of its dimensions (a large number of points), it is recommended that a number of points should be reduced in order to limit the exploitation of the computer resources and accelerate the remaining activities.

As a result of laser scanning of the geometry of the Grodzisko cross-cut gallery, pre-processing of the obtained cloud of points and reduction of the number of points, a very detailed, digital mapping of the whole space of the scanned gallery section – comprising 152,000,000 points – was obtained (as illustrated in Figure 5, 6).

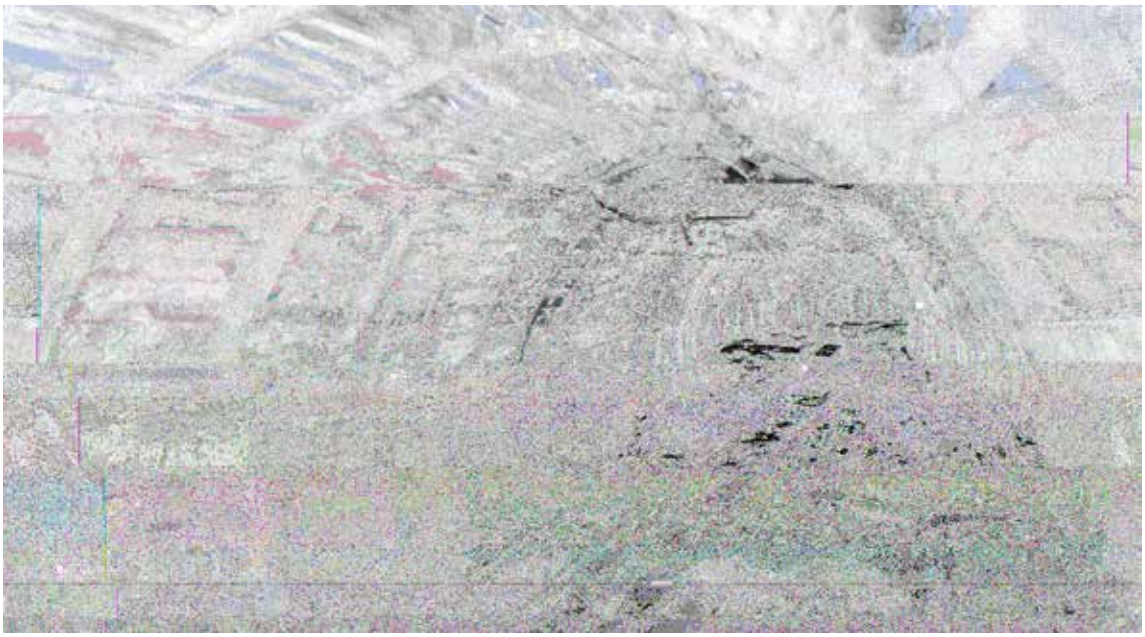

Figure 5 - View "inside" the straight section of mine drift before turn

Figure 6 - View "inside" the straight section of mine drift nearby turn

CREATING OF THE NUMERICAL MODEL GEOMETRY BASED ON THE RESULTS OF LASER SCANNING

Way to create the numerical model geometry is presented on the example of mapping the geometry of hydraulic hose and pipe, located in the vicinity of the roof.

The process of scanned geometry mapping consist of several steps during which it is necessary to use the software for post - processing the point cloud and software in the CAD environment. The first step, aimed at facilitating of mapping the geometry, is process of separating

from the point clouds the individual elements (group of points). This process reminds CAD software capabilities, which give the possibility to divide the model into individual layers. The model of point clouds has been divided in to 3 layers: arch-yielding supports, floor, hydraulic hose and pipe.

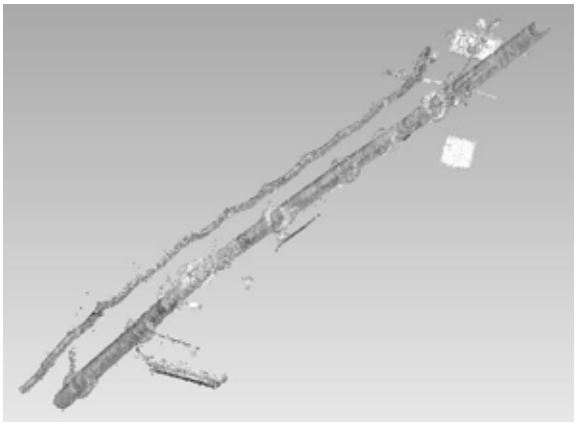

Point clouds of hydraulic hose and pipe

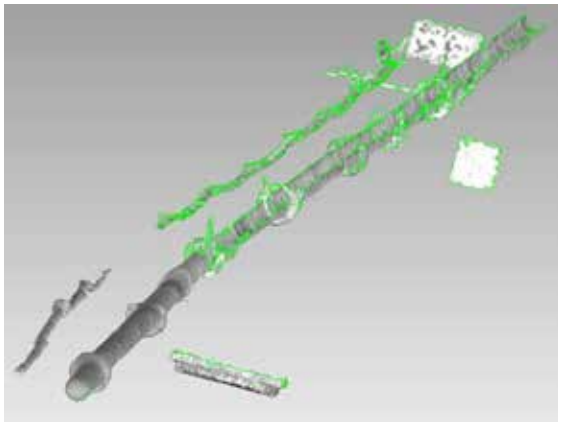

3D model after triangulation process

Figure 7 - Steps of mapping geometry from point cloud

The next step of mapping the geometry model is triangulation of point clouds. This procedure consist the connecting the individual points into triangles. Usually, programs that generate triangle mesh use for this process its own algorithm, however, because of the many errors occurring during triangulation requires manual adjustment of the generated object. Thus prepared model has been exported to a file in the CAD environment, which allowed the passage to the design stage.

The design process involves making a number of cross - sections through the 3D model. This solution allows to create cross - section lines by the individual components of the model. Due to the occurrence of dead spaces – areas and distortion model in the triangulation process, cross lines are not accurate enough to build a geometric model. Therefore, it is necessary to draw precise lines based on cross - section lines, which reflect the cross 0 section of the model. In the case of pipelines and hydraulic hoses, lines will be in the form of a circle. Next step is to determine the leading line of the hole and pipe (connecting the means of all circles) to map arrangement of elements in the mine drift geometry. The last step is creating a geometrical model, using CAD function, based on the resulting cross - section lines and leading lines.

As a result of work geometrical model of the hydraulic hose and pipe were obtained. Model is an accurate representation of the geometry, shape, running along the roof and located of the cross - section of mine drift.

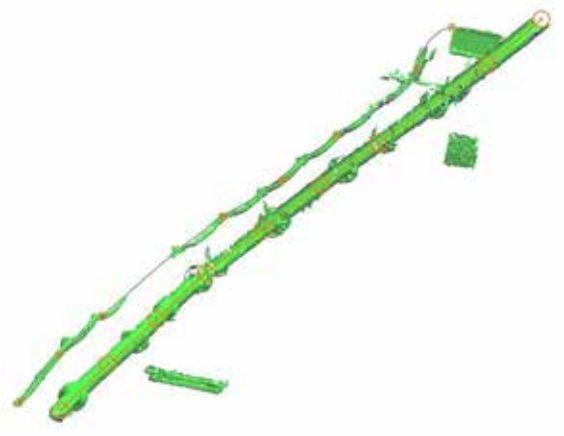

Cross - sections through the 3D model

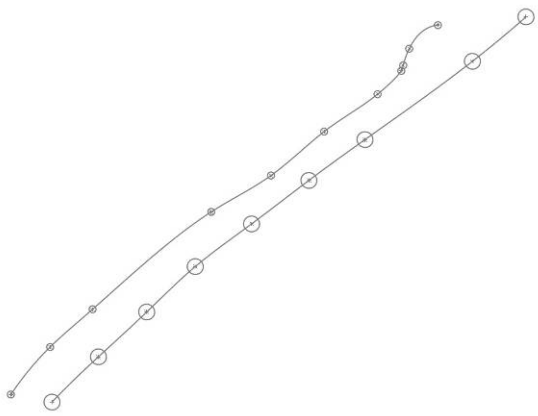

View of cross - section lines and leading lines

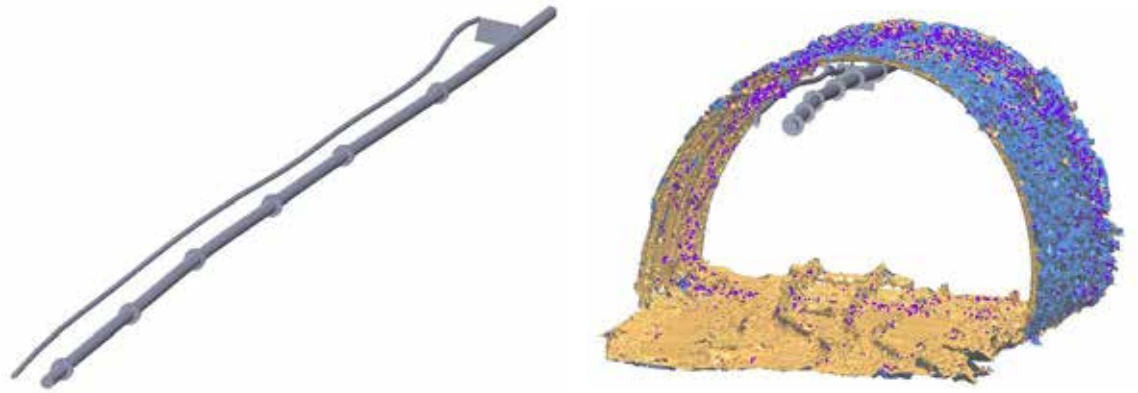

Geometrical model of hydraulic hose and pipe Located model in cross - section of mine drift

Figure 8 - Steps of mapping geometry of numerical model in CAD software

CONCLUSIONS

The article presents an innovative way of using the results of laser scanning to build numerical models geometry. TLS allows to quickly obtain a sufficiently accurate information needed for mapping objects also those that are complex in shape, and where measurements using conventional methods are extremely difficult and even impossible. Classical methods of measurement in order to obtain enough information about complex shape, requires a lot of time and effort, work of people often in conditions that threaten their health and life.

Analysis of the resulting point cloud can determine the suitability of laser scanning to obtain a spatial model of mine drift. The rationale for such thesis is very complicated measurement process and ability to achieve high accuracy of the model.

Based on the resulting point cloud and process of mapping the geometry conclusion could be drawn:

- construction the geometry model of mine drift using TLS is much more efficient compared to conventional measurement techniques,
- accuracy of the results obtained (2 mm) is sufficient to apply to the model the computation grid of suitable size
- results of measurements in the form of point clouds allow for an accurate representation to the geometry of mine drift for numerical targets,
- resulting point clouds can also be used to calculate the cross section area of the mine drift and flow rate of air

REFERENCES

Baścik, M. (2013). 3D laser scanning in underground mines - practical experience. *School of Underground Mining 2013, The Mineral And Energy Economy Research Institute of Polish Academy of Sciences*

Krawczyk, A., Kula, R. (2013). Analysis of variants of arc - suscesible case models of mining excavations in view of computer processing. *Annals of Geomatics, Vol. 11, No. 5*

Krawczyk, J., Janus, J. (2015). Velocity field in the area of artificial generated barrier on the mine drift floor. *Polish Mining Review , No 11*

Lipecki, T. (2010). Leaser scanning measurement of mining equipments geometry and deformation. *Polish Mining Review, No 7-8*

Sokoła-Szewioła, V., Wiatr, J. (2013). Application of laser scanning method for the elaboration of digital spatial representation of the shape of underground mining excavation. *Polish Mining Review , No 8*

THE IMPORTANCE OF A SIMULTANOUS OCCURRENCE OF NATURAL HAZARDS IN POLISH COLLIERIES

*Z. Burtan

AGH University of Science and Technology, Krakow, Poland
Faculty of Mining and Geoengineering,
Al. Mickiewicza 30, 30-59 Krakow
*(*Corresponding author: burtan@agh.edu.pl)*

24th World Mining Congress
MINING IN A WORLD OF INNOVATION
October 18-21, 2016 • Rio de Janeiro /RJ • Brazil

THE IMPORTANCE OF A SIMULTANOUS OCCURRENCE OF NATURAL HAZARDS IN POLISH COLLIERIES

ABSTRACT

The coal mining sector in Poland is exceptional throughout the world in that underground mining operations are accompanied by nearly all natural hazards which are the main cause of major accidents. The simultaneous occurrence and interaction of these hazards, which is known as associated hazards, is significantly more dangerous than in the case of a divergent occurrence. A coincidental occurrence of hazards can furthermore result in a collision of applied prevention measures and their effects. In other words, mitigation of one hazard can contribute to an intensification of other hazards. This article presents the mining conditions of Polish collieries and discusses their impact on the intensification of natural hazards.

The article describes the scale of hazard-induced dangerous occurrences such as methane fire and explosions, coal dust explosions, endogenous fire, coal bumps and rock and gas outbursts. The article highlights the aspects that lead to the coincidence of natural hazards and their intensification thereof. In reference to hazards associated with methane emissions, self-ignition of coal and seismic activity, the article discusses numerous examples of interaction between prevention of hazards and their incompatibility. The analysis confirms the thesis that natural hazards that occur simultaneously can greatly influence safety of Polish collieries.

KEYWORDS

Coal mining, simultaneous occurrence of natural hazards, occupational health and safety in the mining sector

INTRODUCTION

Coal in Poland, which is mainly extracted in the Upper Silesian Coal Basin, occurs in complex geological and mining conditions. Mining operations are usually conducted at increasing depths and in difficult climatic conditions, and they are often carried out in problematic areas such as areas of geological disturbances, areas of earlier mining activities and mining remnants, residual parts of deposits, and regions with high methane activity. Poland's emphasis on indigenous coal deposits, which are mainly extracted by the longwall mining system with the roof control by caving-in, is furthermore characterized by a high mining concentration, based on a full mechanization of mining, loading and transportation of coal. A large share of mining operations in Poland comes from a sublevel exploitation, too. The aforementioned as well as other conditions influence the occurrence and intensification of natural hazards such as methane fire and explosions, coal dust explosions, endogenous fire, coal bumps and rock and gas outbursts.

A simultaneous occurrence of these hazards, which can further increase the risk of mining operations, is indeed a characteristic feature of the Polish mining industry. The impact of natural hazards can be especially noticeable in the Upper Silesian Coal Basin where an interaction of various hazards may often result in dangerous occurrences and fatal accidents. A coincidental occurrence of risks might furthermore lead to a collision of their prevention measures. In other words, mitigation of one hazard can contribute to an intensification of others.

GEOLOGICAL AND MINING CONDITIONS AND TECHNICAL FACTORS DETERMINING THE OCCURRENCE OF NATURAL HAZARDS

Coal production in 29 Polish collieries, including 28 collieries located in the Upper Silesian Coal Basin, reached the level of 75,2 million tons in 2015 (figure 1). Because of depletion of some coal reserves, limited production capacities of mines, increased production costs and lower demand for domestic coal, the coal production levels in Poland are now gradually decreasing and the number of operating mines is becoming lower, too (table 1, figure 1) (Report of the State Mining Authority, 2016).

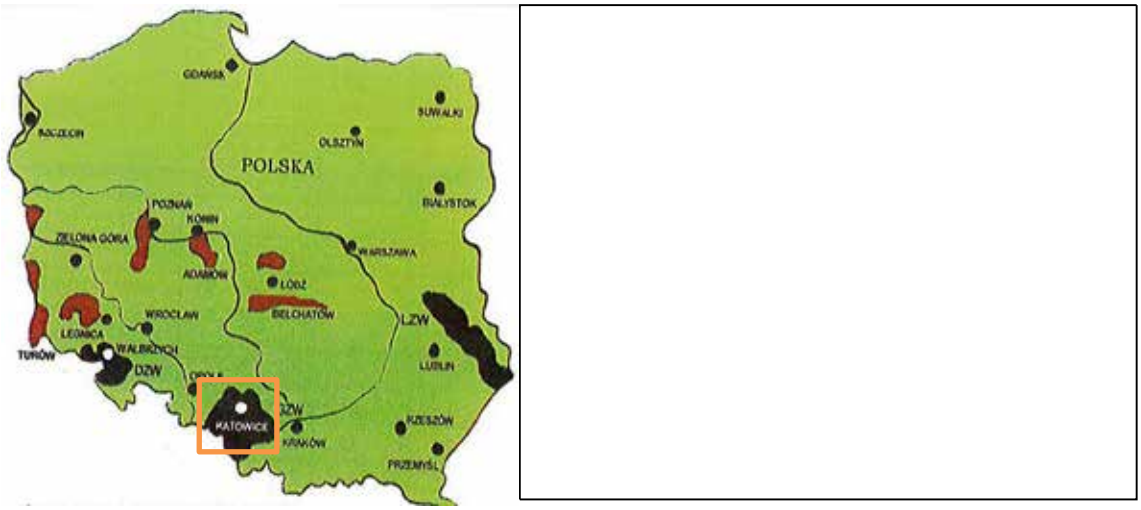

Figure 1 – Coal mines in the Upper Silesian Coal Basin
(Source: National Geological Institute)

Table 1 – Characteristics of the coal mining sector in Poland in 2001-2015

Year	2001	2003	2005	2007	2009	2011	2013	2015
Total output $\cdot 10^6$ [Mg]	102,6	100,5	97,0	87,5	77,4	75,5	76,5	72.2
Numbers of mines	42	41	33	31	31	31	30	29

Such decreases, both in production levels and in numbers of mines, have not translated into a decrease in the occurrence of most natural hazards; a state fostered by complex geological and mining conditions and a regional concentration of production, resulting from mining activities, conducted in the neighboring basin.

Depth of the deposit

Mining of available coal deposits in the Upper Silesian Coal Basin is now continued at increasing depths. Presently coal is mined at depths exceeding 1200m, and in a few collieries the mining operations are pursued below 1000m. The average mining depth approaches 760m (Report State Mining Authority, 2016). Coal mining at increasing depths leads to stress increase in the rock strata, reduced strength of coal in the deposits and increased strength of neighboring rocks, higher temperature of rocks, increased methane capacity of coal deposits. The strength of coal deposits decreases with depth and rock porosity becomes reduced, too leading to reduction of their permeability to gas. These negative effects impact on the rock burst and roof collapse hazard levels, climatic conditions, methane emissions, rock and gas outbursts hazard.

Structure and physico-chemical properties of coal seams and surrounding rocks

Coal in Polish collieries is mined from Carbon deposits formed as silts- mudstone- sandstone formation with coal seams. In the case of most coal types, their strength tends to decrease with depth while strength of surrounding rocks tends to increase, this increase is more apparent in sandstones than in silts. The thick-layer structure of the rock strata at greater depths, revealed by the presence of thick and compact sandstone and mudstone strata in roof formations, becomes the frequent cause of high-energy ($A_s \geq 10^5$J) rock bursts that might consequently lead to mining tremors. Mining in thick-layer structures furthermore increases the risk of tremors and endogenic fires.

Physico-chemical properties of coal seams and surrounding rocks such as methane capacity, dust volatility, tendency to self-ignition, geothermal gradient, thermal conductivity coefficient, degree of humidity, sorption ability of rocks, gas permeability, tendency to sparking, which are all characteristic for most of coal deposits and rock stratas in the Upper Silesian Coal Basin, are critical for the risk of methane and dust explosions, spontaneous fire, climatic conditions, and rock and gas outbursts. Mechanical properties of rocks such as strength, brevity and elasticity, on the other hand,

condition the risk of mining tremors and rock and gas outbursts.

Geological disturbances

Tectonic disturbances are the most frequent and least favorable amongst numerous irregularities found in coal deposits. Large-thrust faults often determine the boundaries of mining operations and hence the panel geometry and parameters of the mining system, at the same time leaving a lot of residues. Multi-desk mining exploitation in Poland often occurs in geologically disturbed regions. The occurrence of faults affects on primary state of stress in the rock strata and intensifies seismic activity of rocks. In many cases, high seismic energy mining tremors, which were the cause of catastrophic coal bumps, took place in the neighborhood of large-thrust faults. Mining operations in the neighborhood of faults and other geological disturbances can furthermore enhance the risk of spontaneous fires, methane emissions and rock and gas outbursts.

Previous mining activities and residues areas

Because of the multi-seam structure of coal deposits in Poland and the mature age of Polish collieries, earlier mining activities and mining remnants are of paramount importance for mining exploitation. These remnants (including goafs, pillars or edges) are responsible for increasing the primary state of stress in the rock strata, at the same time intensifying the risk of mining tremors and rock and gas outbursts.

The inevitable necessity to conduct mining operations in goafs, pillars, edges, and residual areas is highly problematic for the majority of Polish mines, and particularly for those that have already used their deposits. Mining exploitation conducted in these areas is inextricably linked with the risk of fire, mining tremors, methane and rock outbursts, and their coincidental occurrence.

The size and concentration of coal exploitation

For economic reasons, mining companies in Poland tend to ensure the maximal coal production from the smallest possible number of operating units. Such understood concentration of coal production is ensured by well-designed mining systems, and most importantly by favorable conditions of coal deposition. Nonetheless, one has to bear in mind that nowadays coal mining occurs in less favorable geological and mining conditions. Concentration of coal production, which is achieved with the use of longwall mining and at a high speed of exploitation front, is also responsible for an intensification of natural hazards such as climatic rock burst hazard, methane emissions and mining tremors. In 2015 mining production in Poland was conducted by 194 longwalls, amongst which 22 longwalls were at the highest risk of methane and coal dust explosions and mining tremors (Report State Mining Authority, 2016).

Sub-level mining

Sub-level mining, which is often conducted to reduce operational costs, is done through directing air downwards to mining pits. Such a method is increasingly used in Polish coal mines; at present 26 out of 29 mines conduct their mining operations below the level of development, including 4 mines that conduct sub-level mining only. A large proportion of coal, accounting now for nearly 50% of the total output, is obtained from sub-level mining. The increasing use of sub-mining goes hand in hand with an increase of depths at which the method is conducted, currently reaching 200m (Report State Mining Authority, 2016). Sub-level mining, which is now conducted on a large scale thanks to the possibility of lengthening air channels, to a larger extent influences the likeability of methane-induced explosions, fire and adverse climatic conditions. Sub-level occurrences of fires, mining tremors, methane emissions or coal dust explosions can make an evacuation of mining crews more difficult (Burtan et al., 2008).

An analysis of the influence that geological and mining conditions have on the occurrence and intensification of natural hazards suggests that specific conditions can have a simultaneous impact on a larger group of hazards (table 2).

Table 2 – Concurrent conditions that influence the risk of hazards occurring jointly

Geological and mining conditions	Impact on hazards that can occur jointly					
	Methane	Coal dust	Fire	Climatic	Mining	Rock and

		explosions		hazards	Tremors	gas outbursts
Depth of exploitation	+	=	+	+	+	+
Structure and mechanical properties of rock strata	=	+	+	=	+	+
Physico-chemical properties of coal and surrounding rocks	+	+	+	+	=	+
Tectonic disturbances	+	=	+	=	+	+
Previous mining activities and residues	+	=	+	=	+	+
Size and concentration of production	+	+	– / +	+	+	=
Sub-level mining	+	=	+	+ / –	+	+

Type of influence: + increase, – decrease, = none, – / + depending on a situation
Shadow field indicates the compatibility of impact

Geological conditions such large depths at which mining operations are conducted and physico-chemical properties of coal and surrounding rocks as well as mining conditions such as a high concentration of coal-production all intensify the risk of hazard-induced occurrences. Hazards that are likely to occur jointly and are determined by the aforementioned elements include methane, fire and tremors hazards.

LEVELS OF NATURAL HAZARDS AND THEIR SIMULTAENOUS OCCURRENCE

Methane emissions

Methane emissions and coal dust explosions present major threats to ensuring safe and effective coal mining in Poland (table 3). 22 out of 28 collieries operating in the Upper Silesian Coal Basin are threatened by methane emissions, with 15 collieries belonging to the IV (the highest) category of methane emission risk. In 2015, 161 (83%) out of 194 longwalls operated in deposits with high methane activity, including 91 longwalls (47%) belonging to the IV category of methane emission risk. The proportion of coal production from gassy mines tends to increase steadily, now approaching approximately 78%. In 2015 the methane emission hit the level of 933 mln m^3, released in the consequence of mining operations. When related to the production levels, that yields the ratio of 12.9m^3/Mg and an approximate 1775,15m^3 of methane released in one second. In the KWK „Pniówek" colliery, which is characterized by the highest concentration of methane, more than 100 mln m^3 of methane is released every year (2015r. - 116 mln m^3). Despite productivity cutbacks and reduction of the number of operating mines, the aforementioned values represent the largest values of methane emissions in the history of Polish mining (Report State Mining Authority, 2016).

Amongst all the hazards discussed in this paper, the methane hazard has been the major cause of fatal accidents (Burtan, 2010). Since 1990 methane ignitions and explosions caused 93 casualties. Although compared to other hazards, methane-induced accidents generally do not occur very often, the accidents, which have occurred in the past couple of years and were caused by methane explosions and outburst, involved other risks, too. Methane ignitions and explosions were often caused by fires and mining tremors whilst methane ignitions resulted in coal dust outbursts (table 3) (Kabiesz, 2002; Report State Mining Authority, 2016). Sudden methane emissions were also triggered by tremors and coal bumps whilst methane and rock outbursts lead to high methane emissions (table 5).

Table 3 – Selected fatal accidents that involved the methane hazard

Year	Coal Mine	Casualties	Simultaneous occurrence of hazards
1961	KWK „Polska"	9	Methane and coal dust explosion
1974	KWK „Silesia"	34	Methane and coal dust explosion
1974	KWK „Anna"	0	Tremor, methane and coal dust explosion
1985	KWK „Niwka-Modrzejów"	5	Methane and coal dust explosion
1987	KWK „Mysłowice"	17	Methane and coal dust explosion
1990	KWK „Halemba"	20	Methane explosion and attack

2002	KWK „Rydułtowy”	3	Methane ignition and coal dust explosion
2002	KWK „Pniówek	1	Methane ignition
2003	KWK „Sośnica”	3	Methane ignition
2003	KWK „Brzeszcze”	1	Methane ignition
2006	KWK „Halemba”	23	Fire, methane and coal dust explosion
2008	KWK „Mysłowice Wesoła”	2	Fire, methane and coal dust explosion
2008	KWK „Borynia”	6	Methane explosion
2009	KWK „Wujek” ruch „Śląsk”	20	Fire, methane and coal dust explosion
2011	KWK „Krupiński”	3	Methane ignition
2014	KWK „Mysłowice Wesoła”	5	Methane ignition

Coal dust hazard

The risk of coal dust explosion is present in all collieries. In years 1922-2015 there have been 35 coal dust ignitions and explosions, including 16 occurrences caused by methane explosion and 2 occurrences caused by fire. Coal dust explosions are generally associated with the presence of methane. When methane concentration increases, the lower limit of coal dust tendency to explosion is reduced. Although coal dust explosions, alongside methane emissions and endogenous fires, are the major cause of catastrophic accidents, in recent years there have been only a few coal dust explosions (table 4) (Kabiesz, 2002; Report State Mining Authority, 2016). Such a low number of coal dust explosions can be owed to effective dust control strategies that were put in place. The last coal dust explosion not involving any other risks was reported in 2002, which occurred after 15 years from the previous explosion and was void of any methane explosions.

Table 4 – Coal dust explosions that were not caused by methane explosions

Year	Coal mine	Casualties
1956	KWK „Łagiewniki”	8
1967	KWK „Wawel-Walenty”	4
1972	KWK „Szczygłowice”	0
1979	KWK „Dymitrow”	34
1982	KWK „Dymitrow”	18
1987	KWK „Mysłowice”	18
2002	KWK „Jas-Mos”	10

Typically, during the mining, hauling and loading processes about 2% of the mined material turns into coal dust, so enhanced dust explosion risk is associated with the mechanisation of most operations and increased concentration of coal production.

Fire hazard

Endogenous fires commonly occur in all collieries of the Upper Silesian Coal Basin. Apart from the coal’s natural tendency to self-ignition, there are many factors that further enhance the risk of fire: increased mining depth affecting the primary state of stress (leading to the formation of fracture zones) and increased temperature of rocks. The number of fires in Poland was very high in the 50ties (200÷450 annually), and it has gradually decreased in the past years. In the last 10 years the number of fires oscillated between 3 to 11 fires per year (figure 2) (Report State Mining Authority, 2016).

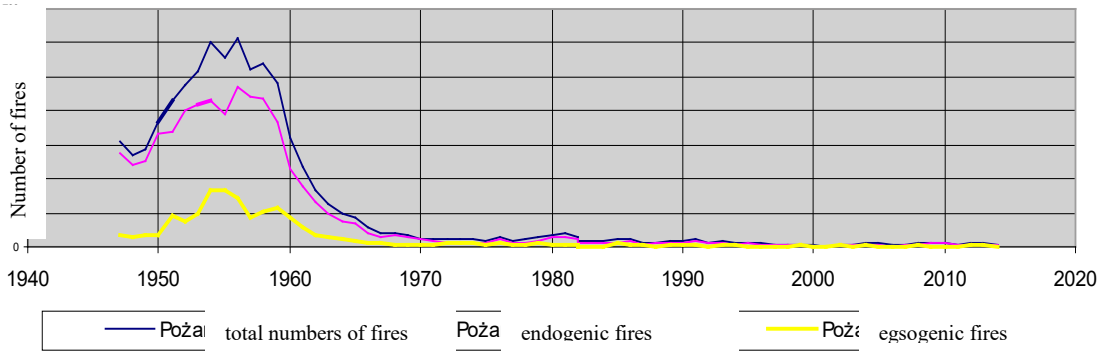

Figure 2 – The number of fires in coal mines in years 1947-2015
(Source: Report State Mining Authority, 2016)

Despite decreasing number of fires, the fire hazard is one of the most frequent cause of hazard-induced dangerous occurrences. Nevertheless, fires occurred in 2004 did not involve any casualties, which confirmed the efficiency of their fast detection by the CO-metric system (Burtan, 2012).

Mining of burst prone to seams, rock bursts and the applied preventive measures might further enhance the fire hazard. Methane control measures also increase the risk of fire, particularly because of the intensified air supply along the headings they provide. As noted above, fires are often the cause of methane ignitions and explosions which may further result in dust coal explosions.

Rock burst and bumps hazard

Rock bursts and tremors are experienced now in a growing number of collieries. In 25 out of 28 currently operated collieries coal is mined from burst-prone seams, and 14 collieries are classified as those belonging to the highest (III) category of risk. Mining in burst-prone seams has increased in recent years, in 2015 reaching 51% of the total coal production. It has to be noted that 16% of production comes from the collieries characterized by the highest category of risk. Seismic risks have also increased and is now at the highest ever rate of the total energy of registered tremors, currently reaching 9,7GJ. In recent years the rock burst and bumps hazard has revealed in the form of more than a thousand (2015 – 1548) of high-energy tremors (energy of $>10^5$J) and a few tremors and coal bumps in a year. Selected accidents which were caused by rock bursts and tremors are presented in Table 5 (Report State Mining Authority, 2016).

Table 5 – Selected accidents caused by rock burst and tremors

Year	Coal Mine	Tremor energy [J]	Casualties
1984	KWK „Czerwone Zagłębie”	$2x10^6$	3
1984	KWK „Powstańców Śląskich”	$1x10^7$	8
1985	KWK „Siemianowice”	$6x10^7$	6
1986	KWK „Bobrek”	$7x10^6$	9
1986	KWK „Zabrze-Bielszowice”	$1x10^6$	3
1987	KWK „Śląsk”	$2x10^6$	4
1991	KWK „Halemba”	$1x10^7$	5
1992	KWK „Porąbka Klimontów”	$1x10^7$	4
1993	KWK „Miechowice”	$3x10^5$	6
1995	KWK „Nowy Wirek”	$5x10^7$	5
1996	KWK „Zabrze-Bielszowice’	$5x10^7$	5
2002	KWK „Wesoła”	$3x10^7$	2
2004	KWK „Halemba”	$3x10^7$	-
2005	KWK „Bielszowice”	$8x10^6$	1
2006	KWK „Rydułtowy-Anna”	$1x10^8$	-
2006	KWK „Pokój”	$9x10^7$	4

2007	KWK „Zofiówka”	$8x10^7$	-
2008	KWK „Bielszowice”	$8x10^5$	-
2008	KWK „Halemba-Wirek”	$1x10^7$	-
2010	KWK „Rydułtowy-Anna”	$7x10^5$	1
2011	KWK „Jas-Mos”	$2x10^6$	1
2012	KWK „Marcel”	$9x10^7$	1
2013	KWK „Piekary”	$3x10^7$	-
2014	KWK „Borynia-Zofiówka-Jastrzębie”	$9x10^7$	-
2015	KWK „Wujek” ruch „Śląsk”	$4x10^9$	2
2015	KWK „Halemba-Wirek”	$9x10^6$	-

Reduction of the number of rock bump occurrences (In years 1980÷95 there has been 7÷29 rock bumps reported per year) to several incidents yearly is the result of an efficient coal bump preventive strategy resulting from better management of mining projects and enhanced methods of coal bumps risk assessment.

Shocks, tremors and coal bumps are often followed by methane emissions to the galleries and mine workings whilst coal bumps lead to the enhanced risk of endogenous fires, due to the stopping of the mining front. Furthermore, most rock burst and coal bump control strategies contribute to fire hazard, too.

Rock and gas outburst hazard

Rock and gas outbursts are regarded as the most dangerous natural hazards in underground mining. The most threatened collieries were the collieries situated in the Lower Silesia Coalfield, which were closed in the 1990s. Increased level of methane and coal outburst risk is encountered in 4 collieries belonging to the Jastrzębie Coal Holding extracting coking coal, where major methane and coal outbursts were reported in 2002, 2005 and 2012 (table 6) (Kabiesz, 2002; State Mining Authority, 2016).

Table 6 – Rock and gas outbursts in the Upper Silesian Coal Basin

Year	Coal Mine	Casualties	Methane emissions [m^3]	Methane concentration [%]	Weight of rocks [Mg]
1979	KWK „Manifest Lipcowy”	0	400	-	5
1979	KWK „Manifest Lipcowy”	1	2170	-	15
1984	KWK „Zofiówka”	0	450	-	-
1984	KWK „Zofiówka”	0	250	-	-
1984	KWK „Zofiówka”	0	5 000	-	95
1986	KWK „Brzeszcze”	0	300	-	10
1987	KWK „Pniówek”	0	19 700	-	-
2002	KWK „Pniówek”	0	52 000	85	250
2005	KWK „Zofiówka”	3	10 200	50	350
2012	KWK „Budryk”	0	340	37	35

All the outbursts occurred in excavation corridors during the preparatory and development phases, and the majority of them (including the last three) took place on faults. The rock and gas outburst hazard is largely influenced by mining at larger depths, in outburst-prone seams, in residual areas and in the neighbourhood of faultings. The state of stress in the rock strata increases with depth, at the same time the strength of coal seams tends to deteriorate while their methane-bearing capacity increases and coal permeability to gas becomes lower, which further enhances the risk (Burtan, 2010).

TYPES OF INTERACTION BETWEEN HAZARDS OCCURING SIMULTANEOUSLY AND THE INCOMPATIBILITY OF THEIR PREVENTION

On the basis of past experiences and the analysis of the possible coincidence of natural hazards, it is possible to distinguish two types of interaction between threats (Kabiesz, 2002):

- **direct interaction**; when an accident caused by one hazard increases the intensity of the other hazard or leads to an accident, caused by other risks;
- **indirect interaction;** when technology of mining operations or prevention of one hazard increases the intensity of other hazards. A situation in which measures successfully applied to prevent one risk come into conflict with other hazards is often termed as the **incompatibility of prevention**.

Direct interaction

Examples of direct interaction in which an accident caused by one hazard increases the intensity of the other hazard include (table 7):

Table 7 – Direct interaction between hazards occurring jointly

Hazard-induced occurrences	Interaction with other hazards or with accidents caused by other hazards				
	Methane	Coal dust explosions	Fire	Tremors	Rock and gas outbursts
Methane explosion		+	+	=	=
Coal dust explosion	=		+	=	=
Endogenic fire	+	+		=	=
Tremor/Bump	+	+	+		+
Rock and gas outbursts	+	+	+	+	

Types of interaction: + increase of risk/cause of an accident, = none
Shadow field indicates interaction

- tremors/bumps may intensify; the methane hazard (by an increased flow of methane into mining workings), the coal dust hazard (by an increase of dust), the fire hazard (by an increased cracking and fracturing of unmined coal),
- retention of longwalls after tremors as a result of prolonged ventilation of unmined coal and goafs can intensify the endogenic fire hazard;
- methane and rock outbursts intensify the methane and coal dust hazards through an increases flow of methane and increased level of dust in workings;
- increased risk of fire as a result of air migration to goafs and unmined coal following a retention of longwalls which results from tremors;

Examples of interaction between natural hazards include (table 7);

- endogenic fire leading to methane and coal dust explosions;
- endogenic fire leading to an explosion of fire, gas and coal dust explosions;
- tremors leading to methane explosions and/or coal dust explosions;
- tremors triggering gas and rock outbursts;
- methane and rock outbursts leading to an explosion of methane and/or a coal dust explosion.

Indirect interaction

A specified technology of mining, which is often used to prevent the occurrence of natural hazards, can at the same time mitigate one hazard and intensify the other. The components of that technology include (table 8) (Kabiesz, 2002; Konopko et al., 2013):

Table 8 – Indirect interactions influenced by the technology of mining used in Poland

Components of mining technology	Interaction with natural hazards				
	Methane	Coal dust explosions	Fire	Tremors	Rock and gas outbursts

Mining	mechanical	–	+ / –	–	+	+
	blasting	+	+ / –	+	–	–
Roof protection	caving-in	+	=	+	–	–
	backfilling	–	–	–	+	+
Speed pace of exploitation	fast	+	+ / –	–	+ / =	+
	slow	–	+ / –	+	– / =	–
Main and tail gates system	single flement	+	+	–	–	–
	multi flement	–	–	+	+	
Explotation with layers	down the roof	–	+	+	+ /–	–
	back fililing	+	–	–	+	+
Intensity of ventilation	big	–	+	+	=	=
	small	+	–	–	=	=
Ventilation of excavations	suction	–	–	+	=	=
	force	+	+	–	=	=
Ventilation of longwall faces	along unmined coal	+	+ / –	–	=	=
	along goafs	–	+ / –	+	=	=

Type of interaction: + intensification, – mitigation, = none, + / – / = depending on a situation
Shadow field indicates interaction of hazard

- mining of unmined coal interacting with the methane, fire, coal dust, tremors and gas and rock outbursts hazards; blasting used to limit the risk of tremors and gas and rock outbursts can also intensify the methane and fire hazard. Sparks generated by combines and an improper conduct of blasting can both trigger methane and coal dust explosions,
- methods used to liquidate goafs interacting with the methane, fire and tremors risks; caving-in used to reduce the risk of tremors can intensify the methane and fire risks,
- speed of advancing excavations and exploitation fronts interacting with the methane, fire and tremors risks; reducing the advance of excavations in order to reduce the risk of tremors can intensify the risk of fire,
- ventilation of excavation interacting with the methane risk and coal dust risk; suction ventilation used to reduce the risk of coal dust can intensify the methane risk;
- ventilation of longwalls interacting with the methane and fire risks; an increased intensity of ventilation along goafs conducted to reduce the methane risk can intensify the risk of fire;
- multi-flement main and tail gates system resulting from leaving coal pillars can intensify the risk of fire and tremors.
- exploitation of thick-layered deposits conducted down the roof by caving-in, which is aimed at reducing the risk of tremors, can intensify the methane and fire risks; exploitation with back filling can on the other hand reduce the methane and fire hazards while intensifying the risk of tremors.

Incompatibility of prevention

Prevention measures applied to mitigate or eliminate one risk can often intensify the likeability of the other (table 9) (Kabiesz, 2002; Konopko et al., 2013).

Table 9 – Incompatibility of preventions of natural hazards

Methods of prevention	Interaction with natural hazards				
	Methane hazards	Coal dust explosion	Fire	Tremors	Rock and gas outbursts
Intensity of ventilation	–	+	+	=	=
Ventilation along goafs	–	=	+	=	=
Methane drainage in coal seams	–	=	+	=	–
Caving-in method	+	=	+	–	–

Destressing exploitation	–	=	+	–	–
Small rate of longwall face advance	–	–	+	– / =	–
Relieving blasting	+	–	+	–	–

Type of interaction: + intensification, – mitigation, = none, – / = depending on a situation
Shadow field indicates interaction of hazard

Past experiences of Polish collieries suggest that an incompatibility of prevention can most likely occur in the case of prevention of the methane, endogenic fire and tremors hazards.

– Prevention measures successful at mitigating the methane hazard, such as high intensity of ventilation, ventilation along goafs, methane drainage in coal seams and small rate of longwall face advance may intensify the risk of endogenic fires.
– Prevention measures successful at mitigating the risk of tremors, such as destressing exploitation (subexploitation of seams), relieving blasting, caving-in and small rate of longwall face advance can have an adverse impact on the mitigation of the fire risk.

The incompatibility of prevention measures that are mutually exclusive generates the need to optimize prevention and subordinate its means to the hazard which poses the greatest danger in specific conditions. Such a danger is often termed namely the "dominant hazard". The "dominant hazard" is determined by a very high level of risk, specified as the highest classification. The choice of dominant hazard should be also determined by its likeability to cause fatal accidents and its tendency to have an adverse impact on other risks, especially when more than one hazard is considered to be the dominant one. One should also take into consideration potential direct interactions between hazards with the highest intensity of their occurrence.

The methane hazard, endogenic fires and tremors are considered to be the most common hazards in the Polish mining sector.

CONCLUSIONS

The distinctive feature of the mining sector in Poland is that underground mining operations are threatened by nearly all natural hazards whilst the scale and intensity of their occurrence seems to be growing each year. That applies mostly to hazards associated with methane emissions, self-ignition of coal seams, coal dust explosions, seismic activity of the rock strata and methane and coal outbursts. The high level of natural risks and growing tendency of their occurrence significantly impact on safety of Polish collieries, their employees and mining operations. Dangerous accidents caused by the coincidental occurrence of natural hazards may not only lead to accidents but put heavy constraint on mining activities. Decommissioning certain parts of deposits may in turn reduce the production capacity of mines, and in some cases may even shorten their life span (Burtan, 2012). Since a particular prevention successful at mitigating one risk can have an adverse impact on the other, it is recommended that a selection of least-incompatible prevention measures should become a priority in activities aimed at improving safety of Polish collieries.

REFERENCES

Burtan Z., 2010 – *The influence of natural hazards on occupational safety in Polish collieries.* Mine Safety and Efficient Exploitation Facing Challenges of the 21st Century. International Mining Forum 2010. p. 81 – 90. Huainan, China. Published by: CRC Press/Balkema.

Burtan Z., 2012 – *Wpływ zagrożeń naturalnych na stan bezpieczeństwa w kopalniach węgla kamiennego w latach 2001-2010*. Bezpieczeństwo Pracy i Ochrona Środowiska w Górnictwie, nr 1 (209)/2012, str. 16 – 22. Katowice. (in Polish)

Burtan Z., Zorychta A., Chlebowski D., 2008. – *Trends in the development of preventive measures against natural hazard in Polish collieries.* Underground Mine Environment, Session „Ground Control & Rock Burst". 21st Word Mining Congress & Expo 2008. p. 143 – 151. Kraków-Katowice-Sosnowiec.

Kabiesz J., 2002 – *Charakterystyka skojarzonych zagrożeń górniczych w aspekcie ich oceny oraz doboru metod prewencji*. Prace Naukowe GIG. Katowice. (in Polish)

Konopko W. et al., 2013 – *Bezpieczeństwo pracy w kopalniach węgla kamiennego*. *Tom 2: Zagrożenia naturalne.* GIG. Katowice. (in Polish)

WUG (Wyższy Urząd Górniczy - State Mining Authority), 2016 – *Ocena stanu bezpieczeństwa pracy, ratownictwa górniczego oraz bezpieczeństwa powszechnego w związku z działalnością górniczo-geologiczną w 2015 roku*. Katowice. (in Polish)

Artykuł zrealizowano w ramach działalności statutowej AGH nr 11.11.100.005.

THE STABILITY GRAPH FOR OPEN STOPE DESIGN – RECENT DEVELOPMENTS

*F.T. Suorineni

School of Mining Engineering
UNSW Australia
Kensington, Sydney
NSW 2052, Australia
*(*Corresponding author: f.suorineni@unsw.edu.au)*

24th World Mining Congress
MINING IN A WORLD OF INNOVATION
October 18-21, 2016 • Rio de Janeiro /RJ • Brazil

THE STABILITY GRAPH FOR OPEN STOPE DESIGN – RECENT DEVELOPMENTS

ABSTRACT

The stability graph was introduced by Mathews et al. (1981) in Canada for open stope design below 1000 m depths. The feasibility of the concept was proven with only 26 case histories from 3 mines. The work of Potvin (1988) popularized the use of the method following an increase in the database from 26 case histories to 175 and calibration of the conceptual stability graph factors to account for stress, joint defect orientation and gravity. This work resulted in increased confidence in the use of the method. Key developments have since included use of statistics (Nickson, 1992; Hadjigeorgiou et al., 1995; Diederichs and Kaiser 1996; Suorineni et al., 2001; Mawdesley et al., 2001) to objectively define the transition zones between the different stope stability state clusters. Trueman and co-workers have also increased the stability graph database to an impressive number of 483 case histories. Other developments have focused on accounting for missing factors that will improve the predictive reliability of the method such as accounting for faults (Suorineni et al. 1999a, b) and improvement in the determination of the shape factor (Milne et al., 1996). Noting that the stability graph only expresses the stability state of stopes qualitatively and that quantifying the amount of stope failure is important, Clark and Pakalnis (1997) introduced the Equivalent Linear Overbreak Slough (ELOS) stability graph that provides average potential depths of stope surface failure. There is continuing interest in the stability graph around the world. This paper provides an up to date status of the stability graph and presents a quantitative dilution-based stability that is independent of orebody width. The Suorineni (1998) fault factor is further validated with case histories and seen to be effective in improving the predictive reliability of the design method when stopes are close to faults and shear zones.

KEYWORDS

Stability graph, Open stopes, New developments, Dilution-based stability graph

INTRODUCTION

To date, the definition of mass mining remains vague just as it was 12 years ago when Brown (2004) noted that despite the widespread use of the term clear definitions of what it means clear definitions of what it means are not readily available. The first attempt to define mass mining was given by Hustrulid in 2000 at GeoEng2000. In Hustrulid's view large-scale mining (mass mining) refers to any mine producing greater than 5,000 tpd. Mining methods cited by Hustrulid to capable of meeting this target include:

- Panel caving (of course including block caving)
- Sublevel caving
- Sublevel stoping

Brown (2004) argues that Hustrulid' s lower limit of 5,000 tpd may be too low and suggested underground mass mining should be taken to involve production rates of more than 10,000 tpd. By Browns definition, open pits mining 30,000 tpd are included in mass mining. Thus, mass mining includes the following mining methods:

- Open pit mining
- Panel caving
- Block caving'

- Sublevel caving and
- Sublevel stoping.

There is a need to differentiate between sublevel stoping in narrow vein orebodies and that in large / massive orebodies. The category of orebodies intended in the inclusion of sublevel stoping in mass mining refers to application of the method to wide or massive orebodies and excludes narrow vein orebodies. Of course this brings to fore the other argument of what is difference a narrow vein orebody and a massive orebody. Suorineni (2010) revealed through the literature that the definition of what is a narrow vein in the mining context appears to be continental, national and individual dependent. In this context the width of a narrow vein ranges between less than 2 m to 10 m wide. He suggested an appropriate definition of a narrow vein should be both geometry and technology dependent. Based on this point of view Suorineni (2010) defined a narrow vein orebody as one with thickness ≤2 m.

At the mass mining 2016 website (http://www.massmin2016.com/) the question is asked "What is mass mining?" The answer to this question starts with the following opening paragraph:

"The definition of mass mining in some ways depends upon when you ask the question and the context in which it is asked. In its simplest form, mass mining refers to large-scale mining, at high tonnage rates, of large deposits of the world's important commodities. The size of these deposits is typically defined by substantial dimensions in all three directions. Characteristically, mass mining entails deployment of the available technology to support an operation of significant scale and degree of mechanization for its time."

Thus the definition of what makes mass mining remains as confusing, if not more, as it was nearly 20 years ago despite the four-year conference series on this all important mining technique.

The stability graph method for open stope mining (bulk mining method) was developed by Mathews et al. (1981) at the beginning of the shift from surface to underground bulk mining, for application to wide orebodies. Based on definitions mass mining by Hustrulid (2000) and Brown (2004) open stope mining seems to form the lower bound for mass mining methods.

THE STABILITY GRAPH METHOD

The stability graph method for open stope design was introduced approximately three and a half decades ago by Mathews et al. (1981). The various developments following the introduction of the method in these 35 years is proved in Suorineni (2010 with further details in Suorineni (2011). Potvin (2014) points out common errors in the use of the method, including the graph by Hadjigeorgiou et al. (1995) for sliding; noting out that it should not be applied to vertical walls. The method became popular following the expansion of the original database from 26 case histories from 3 mines (complemented with 29 cases from the literature) to 176 case histories from 32 mines and the re-calibration of the stability number factors by Potvin (1988).

The stability graph (Figure 1) is a plot of a stability number (N') (Equation (1)) against a shape factor (S), also referred to as Hydraulic Radius (HR) (Equation 2).

$$N' = \frac{RQD}{J_n} x \frac{J_r}{J_a} xAxBxC \quad (1)$$

Where N' is the modified stability based on the calibrated stability graph factors A, B and C by Potvin (1988). A, B and C are the calibrated stability number factors referred to as Stress factor, Joint defect factor and Gravity factor respectively. RQD is the rock quality designation, J_n is the joint set number, J_r is the joint roughness number and J_a the joint alteration number as defined for the tunneling quality index Q in Barton et al. (1974). Factors A, B and C are determined from empirical charts provided in Figure 2.

$$HR = \frac{Stope\ surface\ area}{Stope\ surface\ perimeter} \quad (2)$$

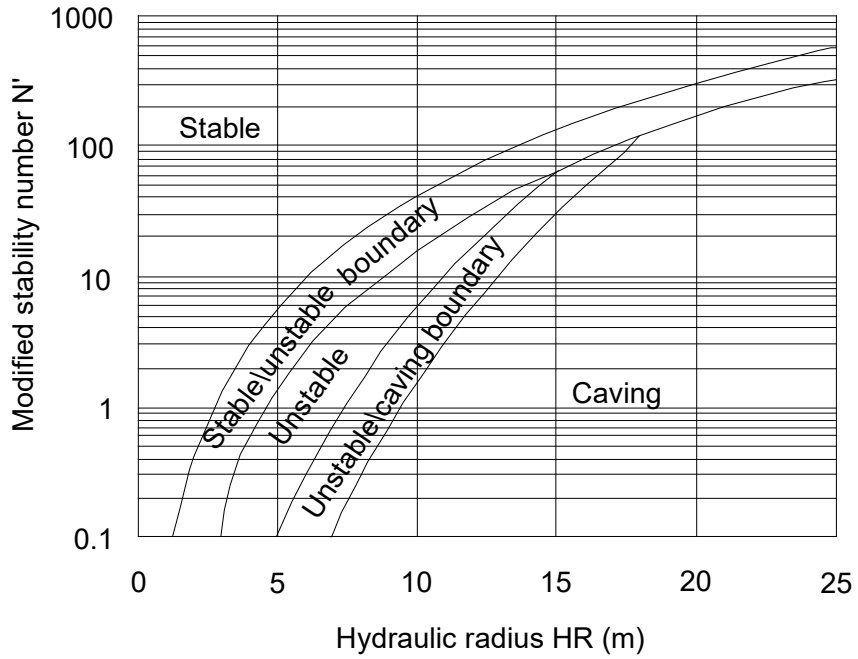

Figure 1. The stability graph (after Nickson 1992).

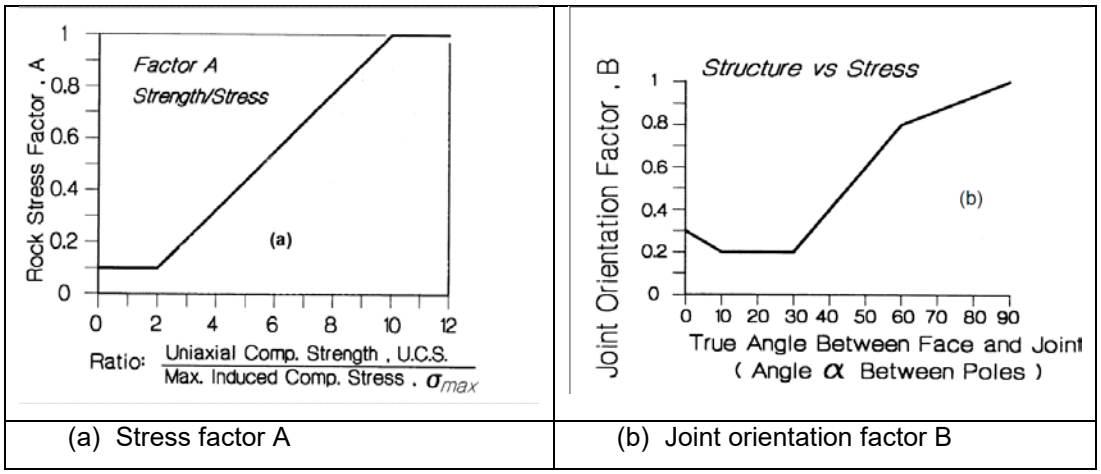

(a) Stress factor A | (b) Joint orientation factor B

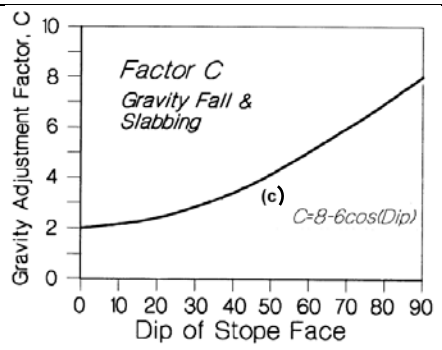

(c) Gravity factor C

Figure 2. Charts for determining factors A, B and C (Potvin, 1988) in Equation (1).

In the stability graph method, each stope surface's stability (Figure 3) is considered independently and the stope is stable if all surfaces are stable and failed if any surface fails. Thus in Figure 1, the Stable zone means any stope surface plotting there has a high probability of being stable, the Unstable zone implies a stope surface has a high probability of being unstable while the Cave zone means the stope surface plotting in this area has a high probability of caving. Caving, in the context of the stability graph implies 30% of a given stope surface will slough (Diederichs and Kaiser, 1996) and differs from the continuous unravelling implied in caving as in block or panel caving.

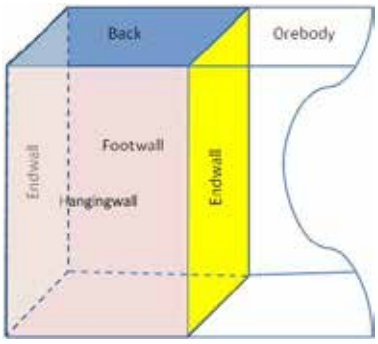

Figure 3. Stope illustrating stope surfaces for independent assessment of surface stabilities in stability graph.

LIMITATIONS OF THE STABILITY GRAPH

Key limitations of the stability graph are discussed by several authors and summarized in Suorineni (2010, 2011). Suorineni (2011) also presents the main assumptions underlying the stability graph method. The most discussed limitation prior to 1998 was the graph not taking into the presence of faults in the vicinity of stope surfaces. As a consequence of this serious limitation, Suorineni (1998) developed a fault factor for incorporation into the stability graph application. Following this development, for stope surfaces close to faults the stability N' is given by Equation (3).

$$N' = \frac{RQD}{J_n} x \frac{J_r}{J_a} xA.B.C.F \tag{3}$$

Where F is the fault factor. The rest of the parameters are as defined earlier in Equation (1).

The fault factor (Figure 4) was calibrated against various case histories including Kidd Mines (Suorineni et al., 2001a) and Detour Lake Mine (Suorineni et al. 1999). These case histories clearly showed the importance of the fault factor and why faults close to the vicinity of stope surfaces resulted in wrong predictions of the stability state of such stopes.

Here is the hidden implication. What is described as the Stable Zone in the stability graph is not universal across mines and in the industry. The stability of a stope is dependent on what dilution level is acceptable at a given mine depending and depends on what is mined. For example, if at a given mine the acceptable dilution level is 10% stopes with 10% dilution will be classified as Stable. At another mine where the acceptable dilution is 20% stopes with this dilution level will be classified as Stable. However, in the mine where 10% is the acceptable dilution a dilution level of 20% the stope may be classified as Caved. Figure 5 demonstrates this logic. In Figure 5, planned dilution is compared with observed dilution. A dilution of 10 % and 15% is accepted at different parts of this mine. Therefore, stope surfaces with dilution levels greater than these at the respective locations in the mine will be considered Unstable or Caved depending on how much the accepted dilution level is exceeded. Therefore, the use of qualitative zones to describe stope stability states in the stability graph can be misleading.

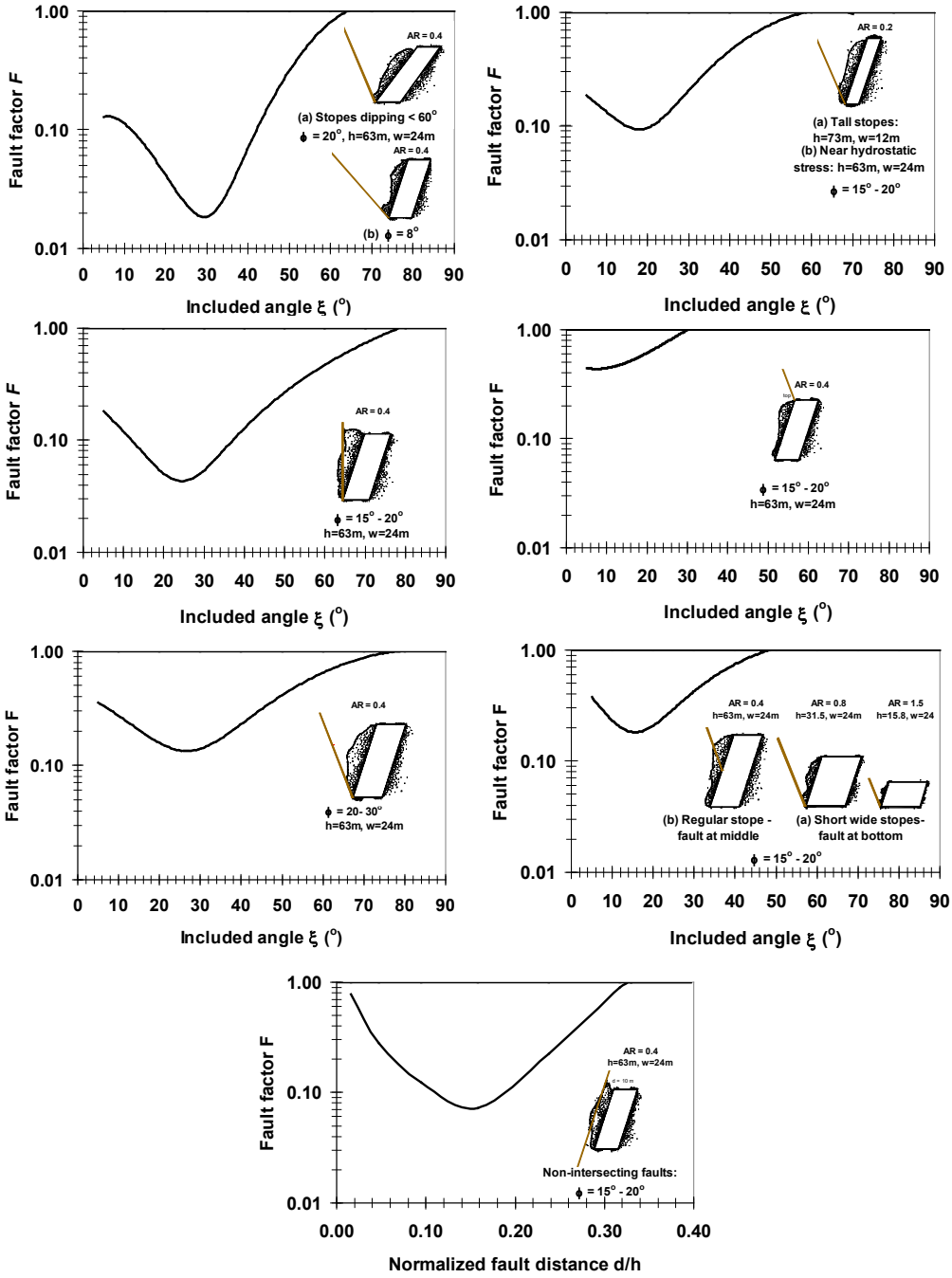

Figure 4. Fault factor determination charts (Suorineni, 1998).

The stability states of open stope surfaces plotted on the stability graph can best be described as probable or most likely. Hence, Diederichs and Kaiser (1996), Suorineni (1998), Trueman et al. (2000) have used statistics to interpret the stability states of stope surfaces on the stability graph. What is remains a challenge and never discussed until recently (Papaioanou and Suorineni 2015, 2016) is the factor that the stope stability states are purely qualitative with hidden implications.

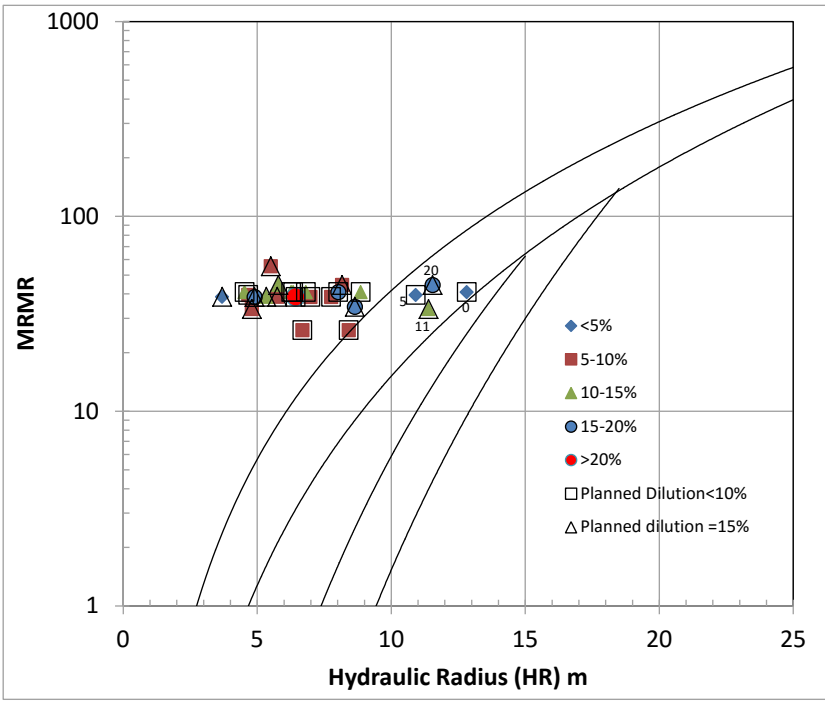

Figure 5. Comparison of planned dilution and observed dilution illustrating issues with quantitative definitions of stope surface stability states.

RECENT DEVELOPMENTS

Various types and forms of stability graphs have emerged since 1981 in attempts to increase or enhance the success rate in the use of the method for predicting the stability of designed stopes. Other developments are for different applications of the method such as cablebolt design Potvin and Milne (1992) and Diederichs et al. (1999). Clark and Pakalnis (1997) developed the Equivalent Linear Sloughage (ELOS) stability graph for application to narrow veins. The ELOS (Equation (4)) stability graph (Figure 6), unlike the conventional stability graph for bulk mining, is quantitative and expresses dilution as average overbreak in the stope wall. This graph is an improvement to the qualitative stability graph but only applies to narrow vein orebodies since it is developed from a database compiled from narrow vein mines.

$$ELOS = \frac{Volume\ of\ \ Slough\ \ from\ Stope\ Surface}{Area\ of\ \ the\ Stope\ Surface} \tag{4}$$

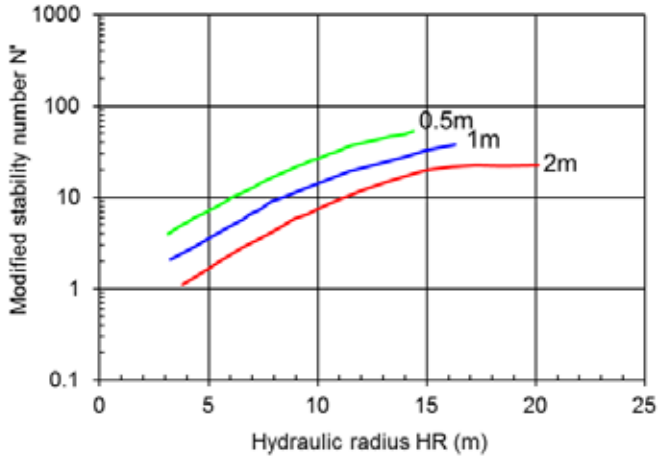

Figure 6. ELOS stability graph (Clark and Pakalnis, 1997).

Common errors in the use of the stability graph for open stope design have been pointed out in Potvin (2014) and include the use of spreadsheets to automate the process.

The stability graph is also a 3D plot in a 2D space. The third dimension in the stability graph is qualitative three descriptions of the stope surface stability states: Stable, Unstable and Cave. A 3D quantitative dilution plot is demonstrated in Figure 7 in two different forms as scatter plot and a surface plot. Figure 7 appears more attractive than the 2D plot of the stability graph, in particular when it accounts for quantitative dilution. Figure 7 shows that, higher dilution occur at lower N' values and at higher hydraulic radii.

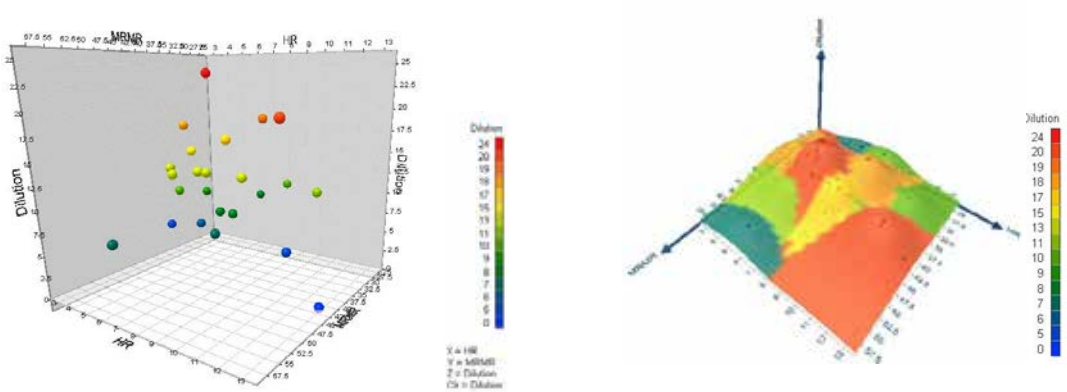

(a) 3D scatter plot (b) 3D surface plot

Figure 7. 3D representation of stability graph (a) Scatter plot and (b) Surface plot.

Recently, the Author's group have developed quantitative dilution-based stability graph (Papaioanou and Suorineni 2015, 2016; Suorineni et al. 2016). A generalized quantitative stability graph has more attached value to miners and mine planners as they appreciate dilution numbers more and their implication to the profitability of the operation than merely knowing whether a stope is Stable, Unstable or Cave as in Figure 1, in the case of the conventional stability graph by Mathews et al. (1981). More importantly, the quantitative stability graph eliminates the misuse of the conventional stability graph that was developed for bulk mining of large orebodies and the ELOS stability graph developed for narrow orebodies. Experience has shown that the use of the two graphs seems to be dictated by choice rather than dependent on type of orebody which should govern their use. The quantitative stability graph eliminates this potential problem. More details on this issue can be found in Papaioanou and Suorineni (2016). Thus, the quantitative

dilution-based stability graph can be described as unified stability graph, being a unification of the conventional stability graph for wide orebodies and the ELOS stability graph for narrow vein orebodies.

Challenge in the dilution graph development

There are two obvious challenges to the development of a quantitative dilution-based stability graph. The first challenge is that a new database has to be developed as the available stability graph databases namely, Potvin's database and Trueman and co-Workers database do not include quantitative dilution. Second, one will have to overcome the varying definitions of dilution in the metal mining industry. Table 1 shows the various definitions of dilution.

Table 1. Dilution definitions (Pakalnis, 1986)

Parameter	Equation	Equation number
Dilution 1 (%)	$\frac{(\text{Tons waste mined})}{(\text{Tons ore mined})+(\text{Tons waste mined})}\text{x}100$	(5)
Dilution 2 (%)	$\frac{(\text{Tonnage mucked})-(\text{Tonnage blasted})}{(\text{Tonnage blasted})}\text{x}100$	(6)
Dilution 3 (%)	$\frac{(\text{Backfill tonnage placed})-(\text{Theoritically required backfill})}{(\text{Theoritically required backfill})}\text{x}100$	(7)
Dilution 4 (%)	$\frac{(\text{Hangingwall ELOS})+(\text{Footwall ELOS})\,(\text{m})}{(\text{Orebody width})\,(\text{m})}\text{x}100$	(8)
Dilution 5 (%)	$\frac{\text{Waste tons mined}}{\text{Ore tons mined}}\text{x}100$	(9)
Dilution 6 (%)	$\frac{\text{Undiluted insitu grade reserves}}{\text{Mill headgrades from same tonnage}}\text{x}100$	(10)

Table 1 provides a summary of the various definitions of dilution from Canadian mine practices. Scoble and Moss (1994) reported that Equations (5) and (9) in Table 1 are commonly used in the Canadian hard rock mining operations. Pakalnis et al. (1995) suggest that Equation (9) be adopted as Equation (5) is insensitive to wall sloughage. Other mines around the world (Including Australia) will inadvertently use one of these definitions for its dilution calculation. Clearly, the table shows dilution is normally measured as a percentage. The multiple definitions of dilution in Table 1 also shows different mines can have different definitions of unplanned dilution which presents a challenge in what dilution really means as these definitions can give entirely different values for the same volume of waste overbreak.

The challenge of getting stope information with corresponding dilution levels was overcome with granted access to various mine data both locally and internationally. The second challenge was more daunting but was resolved at mine sites through discussions with planning and ground control engineers. Over 300 case histories have been compiled to date. The quantitative dilution-based stability graph is based on cavity monitoring surveys (CMS) and mine plans. As planned stopes, are compared with actual stopes to determine dilution values which are then compared with values from the mine and emerging differences discussed with mine staff and resolved. CMSs enable volumes (tonnages) of waste rock to be determined and compared with original stope designs to determine dilution percentages. In the same process ELOS

based dilution values can also be determined based on estimated depths of failure. The later however, has the limitation of being orebody width dependent.

Quantitative dilution-based stability graph

A quantitative dilution-based stability graph is developed by plotting the dilution data in the N'-HR space that the stability graph used. However, rather than describe stope stability states qualitatively, these are described quantitatively with dilution numbers as percentages. The dilution levels are categorized arbitrarily based on what most miners will commonly quote, namely: <5%, 5-10%, 10-15%, 15-20% and >20%. More categories could be added or removed if desired. The intervals could also be expanded or reduced.

As suggested earlier the 3D stability graph is further explored with a given mine dilution data in terms scatter plots and surface plots as shown in Figure 8. The 3D plot shows that dilution is higher at lower N' and at higher HR for the data shown. This exploratory 3D plot seems to be encouraging and appears to make more sense than the 2D plot and in this case, more so because of the quantitative nature of all the three axes.

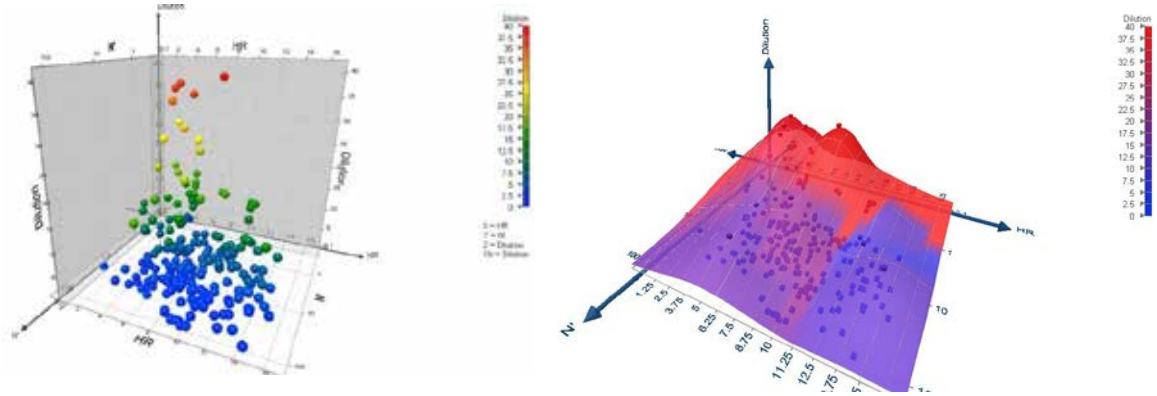

(a) Scatter plot (b) Surface plot

Figure 8. 3D stability graph showing dilution, HR and N' (a) Scatter plot and (b) Surface plot.

The same data presented in Figure 8 is plotted in the conventional stability graph (Figure 9) and shows in addition to the Stable, Unstable and Cave zones the dilution categories.

Similar the conventional qualitative stability graph in which stope surfaces with similar stability states form clusters that can be separated by eyeballing and more objectively by statistical methods, the stopes surfaces belonging to the same dilution categories can be separated. Suorineni (1998) used the Bayesian likelihood statistic to define the boundaries between the three stope surface stability states in the conventional stability graph while Mawdesley et al. (2001) used the Logistic regression approach. For more details on these methods the interested reader is referred to these works. Figure 9 is an example application of the Bayesian likelihood statistic for defining boundaries between dilution categories and further details can be found in Suorineni et al. (2001a).

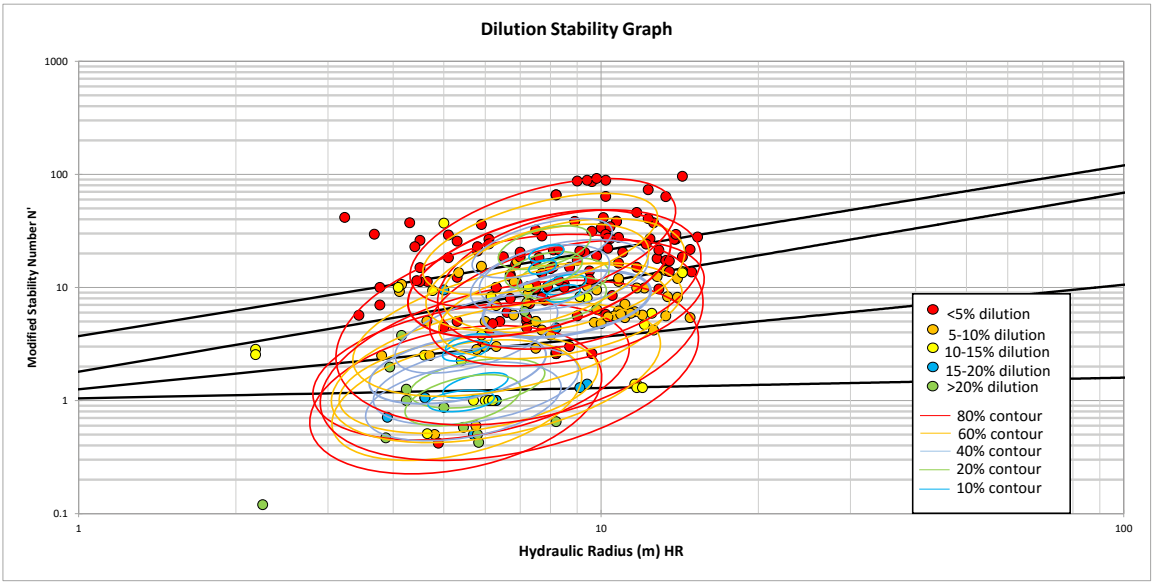

Figure 9. Use of Bayesian likelihood statistic discriminant analysis to define boundaries between dilution categories.

Fault factor F

One of the most frequent complaints about the stability graph following its development in 1981 was that it did not account for the presence of faults close to the stope surfaces. Presumably, because the Q-system, one of the factors on which the method is based does account for faults, it was assumed that there was no need for a separate fault factor in the design method. However, field experience with the method over the years following its development showed that there was indeed need for a separate fault factor. Suorineni (1998) developed a fault factor to fill this gap. The fault factor *F* further degrades *N'* when stope surfaces being assessed are close to a discrete fault or shear zone. In this case the stability *N'* is as defined in Equation (11). The fault factor was calibrated against case histories from Kidd Mine in Timmins and details can be found in Suorineni et al. (2001b).

$$N' = \frac{RQD}{J_n} x \frac{J_r}{J_a} xAxB.C.F \tag{11}$$

Recent experiences at a mine in Australia in which the orebody is intersected by several faults and shear zones showed that the stability of the stopes was largely impacted by the presence of these discrete geological structures. Immediate interest was attracted on upon discussions with mine staff on their realization that indeed a fault factor exists that should be taken into account in the assessment of open stope surfaces when these were close to faults and shears. The stability of stopes at the mine was analyzed with and without the factor. The results are shown in Figure 10 and Figure 11 with and without fault factor respectively.

Following industry feedback on the use of stability graph that the most

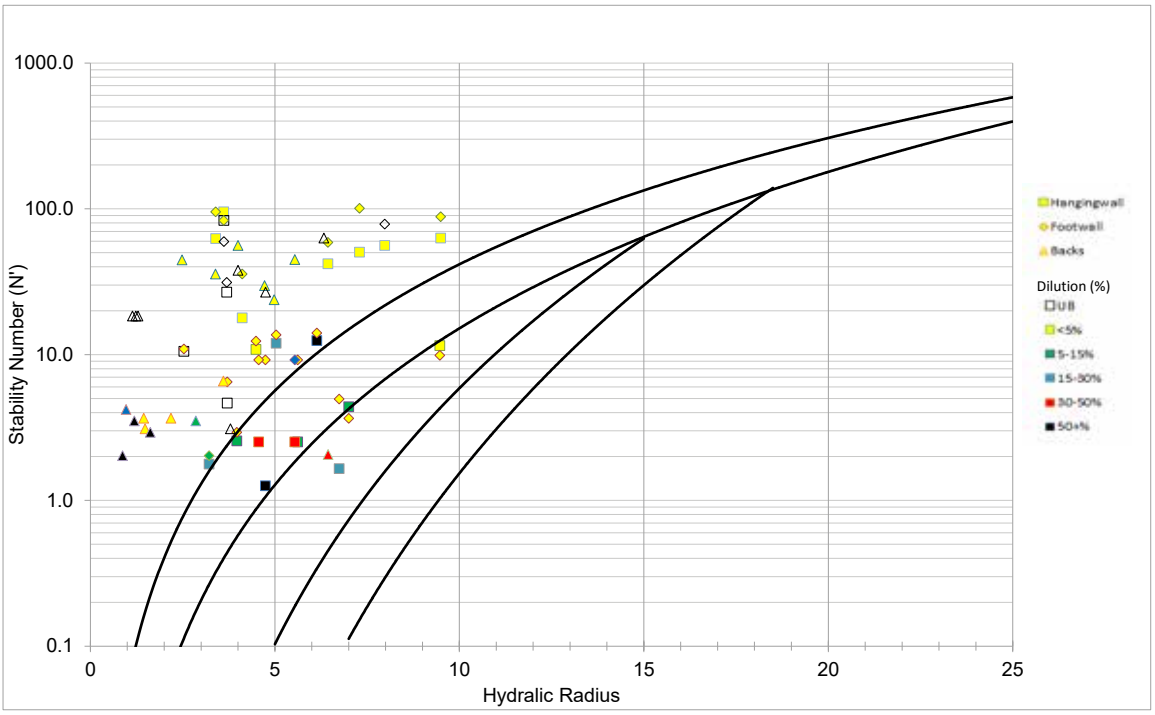

Figure 10. Stability of stopes without fault factor (Suorineni et al. 2016).

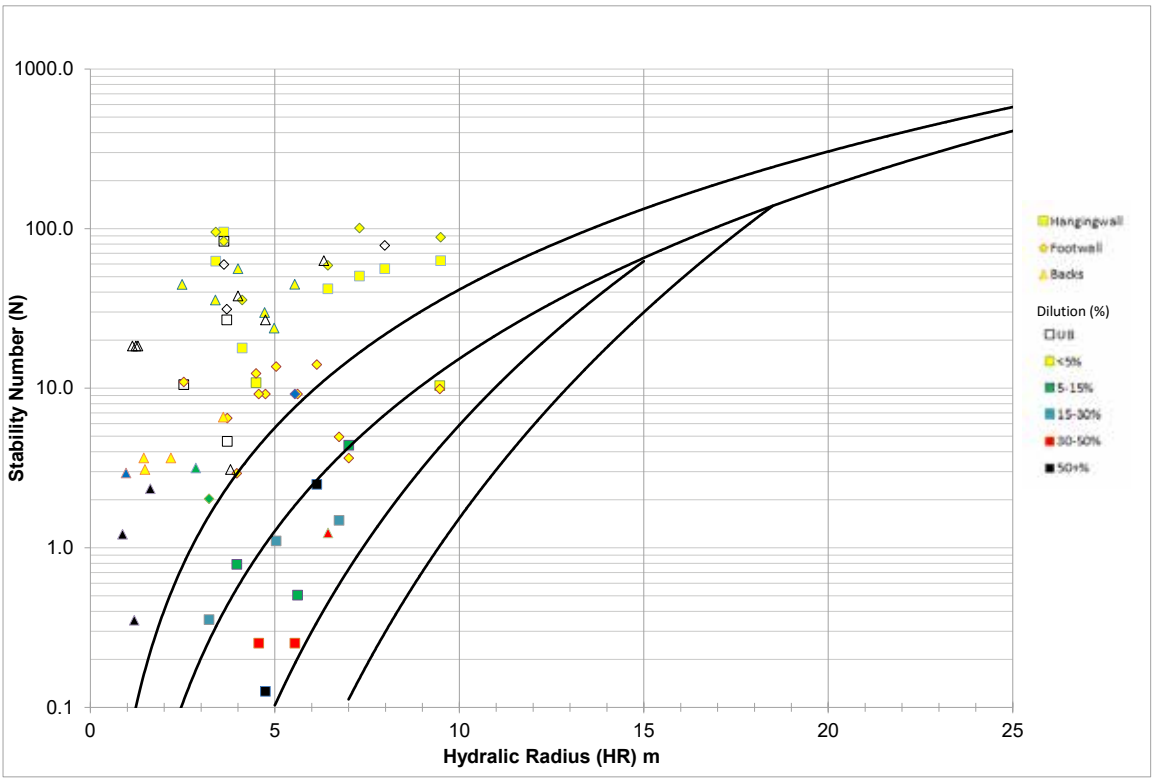

Figure 11. Stability of stopes with fault factor (Suorineni et al. 2016).

Comparison of Figure 10 and Figure 11 shows clear impact of the fault factor on improving the reliability of the stability graph in predicting stope stability and dilution. However, the graphs also show that the fault factor is inefficient in improving the stability of stope backs when these surfaces are affected by faults. This limitation has earlier been pointed out (Vallejos, per. Comm.) from experiences in Chile.

This limitation of the fault factor not being effective for stope backs affected by faults has been reviewed. The review reveals that in the development of the fault factor no scenario was considered for stope backs. The original stope-fault geometry relationship used in the development of the fault factor is shown in Figure 12. Further work is currently being conducted to extend the fault factor to cover stope backs.

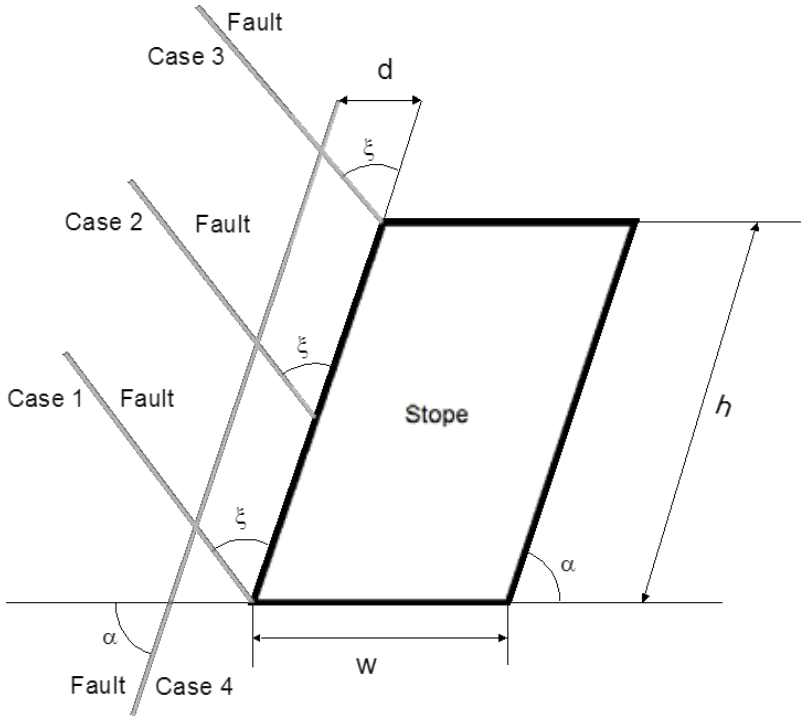

Figure 12. Original stope-fault geometry scenarios considered in fault factor development (Suorineni, 1998).

Updated quantitative dilution-based stability graph

The first quantitative dilution-based stability graph was published in Papaioanou and Suorineni (2016). Suorineni et al. (2016) provides the updated version. Figure 13 and Figure 14 show the updated quantitative dilution-based stability graph with and without the dilution numbers. As previously argued, Figures 13 and 14 can be used for the design of open stope sizes based on what a mine operation considers as its acceptable dilution which can differ even in the same mine as demonstrated in Figure 5. Boundaries between dilution categories as based on Bayesian likely statistic.

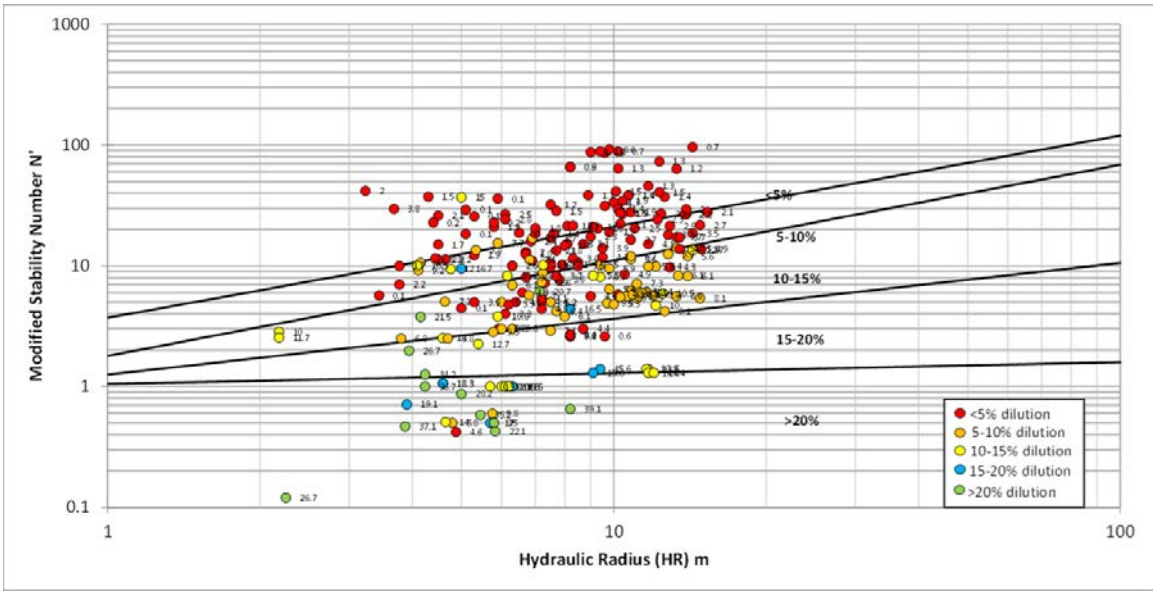

Figure 13. Updated quantitative dilution-based stability graph with dilution labels (Suorineni et al. 2016)

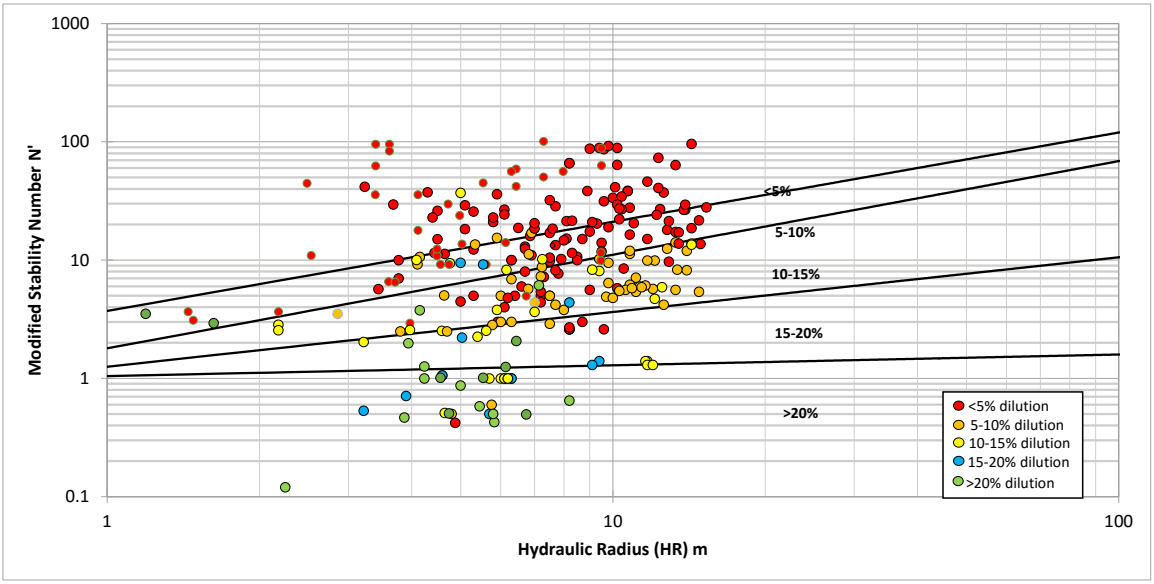

Figure 14. Updated quantitative dilution-based stability graph without dilution labels (Suorineni et al. 2016)

CONCLUSSIONS AND RECOMMENDATIONS

This paper provides an update on the stability graph with focus on recent developments. Recent developments include further guidelines on the proper use of the method a common mistakes often made as provided in Potvin (2014). More importantly, there is shift from the qualitative stability graph to a quantitative dilution-based stability graph. The quantitative dilution-based stability graph can be described as a unified stability graph in that merges the difference between the bulk mining stability graph that must only be applied to wide orebodies and the ELOS stability graph that only applies to narrow vein orebodies.

Alternative representations of the stability graph are also examined in the paper, recognizing that the graph is more meaningful when plotted in 3D space. This alternative representation has potential benefits and should be further explored for practical applications.

The fault factor is further demonstrated to be effective in designing stopes close to faults and shear zones. However, when stope backs are affected by faults, the factor is ineffective and adjusted the back of stopes for reliable stability performance prediction.

Further work is recommended to determine adjustment factors to stope backs close to faults and shear zones. It is also recommended that the quantitative dilution-based stability graph be used for its obvious benefits. Like any empirical methods, more data is welcome to increase the database and improve confidence in the data.

ACKNOWLEDGEMENTS

The Author wishes to acknowledge the School of Mining Engineering for initially providing funds through the School Research Grant scheme to support the research. He also acknowledges the contributions of many of his students including Lewis Baird and Alexander Papaioanou. He is also deeply indebted to the various mines that gave access to their data and sacrificed production time to discuss the data. Efforts from the international community in contributing data are especially appreciated and special mention goes to my Chilean colleagues.

REFERENCES

Barton, N., Lien, R. and Lunde, J. 1974. Engineering classification of rock masses for the design of tunnel support. Rock Mechanics 6(4), pp. 189-236.

Brown, E T, 2004. Geomechanics: the critical engineering discipline for mass mining, in Proceedings Fourth International Conference and Exhibition on Mass Mining (MassMin 2004) (eds: M A Alfaro and A Karzulovic), pp. 21–36 (Instituto de Ingenieros de Chile: Santiago).

Clark, L.M., and Pakalnis, R.C. 1997. An empirical design approach for estimating unplanned dilution from open stope hangingwalls and footwalls. 99th CIM-AGM, Vancouver, CD-Rom.

Diederichs, M.S and Kaiser, P.K. 1996. Rock instability and risk analyses in open stope mine design, Can. Geotech. J. 33, pp. 431–439.

Diederichs, M.S., Hutchinson, D.J. and Kaiser, P.K. 1999. Cablebolt layouts using the modified stability graph, CIM Bull. 92, pp. 81–86.

Hadjigeorgiou, J., Leclair, J. and Potvin, Y. 1995. An update of the stability graph method for open stope design, in Proceedings CIM AGM, Rock Mechanics and Strata Control session, Halifax, Nova Scotia.

Henning, J.G. and Mitri, H.S. 2006. Numerical modelling of ore dilution in blasthole stoping. Int J Rock Mech Mining Sci 44(5), pp. 692–703.

Hustrulid, W. 2000. Method selection for large scale underground mining, in Proceedings Third International Conference and Exhibition on Mass Mining (MassMin 2000) (ed: G Chitombo), pp. 29–56 (The Australasian Institute of Mining and Metallurgy: Melbourne).

Matthews, K.E.., Hoek, E., Wylie, D., and Stewart, 1981. Prediction of stable excavation spans for mining at depths be-low 1000 m in hard rock. CANMET DSS serial no: 0SQ80-00081., Canada.

Mawdesley, C.A., Trueman, R. and Whiten, W. 2001. Extending the Mathews Stability Graph for Open-stope Design, Institution of Mining and Metallurgy, Mining Technology, 110(1), pp. 27–39.

Nickson, S.D. 1992. Cable support guidelines for underground hard rock mine operations. M.A.Sc. thesis, The University of British Columbia., 223 p.

Pakalnis RC (1986) Empirical stope design in Canada. Ph.D. Thesis. University of British Columbia, 276 p.

Pakalnis, R.C, Poulin, R. and Hadjigeorgiou, J. 1995. Quantifying the cost of dilution in underground mines. Mining Eng pp. 1136–1141.

Papaioanou, A. and Suorineni, F T, 2016. Development of a generalized dilution-based stability graph for open stope design. Transactions of the Institutions of Mining and Metallurgy: Section A; Mining Technology. http://dx.doi.org/10.1080/14749009.2015.1131940.

Papaioanou, A. and Suorineni, F.T. 2015. Development of a generalised dilution-based stability graph for open stope design, Journal of Research Projects Review, 4(1):27–33 (Mining Education Australia).

Potvin, Y. 1988. Empirical open stope design in Canada. PhD Thesis, University of British Columbia, 350 p.

Potvin, Y. 2014. The modified stability graph method; more than 30 years later. 1st International Conference on Applied Empirical Methods to Mine Design, Lima, Peru, 7 p.

Potvin, Y. and Milne, D. 1992. Empirical cable bolt support design, in Proceedings International Symposium on Rock Mechanics, Sudbury.

Scoble, M.J. and Moss A. 1994. Dilution in underground bulk mining: Implications for Production Management, mineral resource evaluation II, methods and case histories, Geological Society Special Publication No. 79, pp. 95–108.

Suorineni, F T, 2011. Factors influencing overbreak in the Barkers orebody, Kundana Gold mine: narrow vein case study. Paper by: P.C. Stewart, R. Trueman and I. Brunton, 2011: Mining Technology, vol. 120(2), pp. 80-89. Letter to the Editor, Transactions, Institution of Mining and Metallurgy (Section A): Mining Technology.

Suorineni, F., Papaioanou, A., Baird, L. and Hines. D. 2016. A Dilution-based Stability Graph for Open Stope Design, MassMin2016, In Print.

Suorineni, F.T. 2010. The Stability Graph After Three Decades in Use: Experiences and the Way Forward. International Journal of Mining, Reclamation and Environment, 24(4), pp. 307–339.

Suorineni, F.T. Tannant, D.D., Kaiser, P.K. and Dusseault, M.B. 2001b. Incorporation of a fault factor into the stability graph method: Kidd mine case studies. Mineral Res. Eng. 10, pp. 3–37.

Suorineni, F.T., 1998. Effects of Faults and Stress on Open Stope Design. PhD thesis (unpublished), University of Waterloo, Waterloo.

Suorineni, F.T., Tannant, D.D. and Kaiser, P.K. 2001a. Likelihood Statistic for Interpretation of the Stability Graph for Open Stope Design. International Journal Rock Mechanics and Mineral Science, 36(7): 891–906.

Trueman, R., P. Mikula, P., Mawdesley, C. and Haries, N. 2000. Experience in Australia with the application of the Mathews method of open stope design, CIM Bull. 93, pp. 162–167.

UNDERGROUND EXPLOITATION OF NATURAL STONE IN CROATIAN LAYERED DEPOSITS

*Ivan Cotman

KAMEN d.d. (Ltd.)
Trg slobode 2
52000 Pazin, Croatia
*(*Corresponding author: razvoj@kamen.hr)*

24th World Mining Congress
MINING IN A WORLD OF INNOVATION
October 18-21, 2016 • Rio de Janeiro /RJ • Brazil

UNDERGROUND EXPLOITATION OF NATURAL STONE IN CROATIAN LAYERED DEPOSITS

ABSTRACT

Croatia is known in the natural stone world as producer of limestone natural stone blocks for more that few thousand years. Main centres of natural stone mining activity are the southern part of country with generally whitish limestone , and northern part of the country from Istrian peninsula with beige limestone New environment regulations were the decisive factor which “forced” the miners to start thinking about underground exploitation. Initiative temptations were started in 1995 in the Cretaceous layered limestone on Istrian peninsula in the quarry of Kanfanar. During the last two decades, room and pillar method of exploitation with irregular distribution of the pillars was developed and approved , and in the same time related machine producer companies from Italy developed special machines adjustable for underground exploitation of natural stone blocks. From the mining point of view, the considerable problems of rock mechanics were encountered related to the designing the open spaces and pillar sections and distribution in underground surroundings disturbed by various systems of discontinuities and other undesired properties of excavated rock. Excavation with self supported roof was main challenge and the main goal to develop high and economical method of exploitation. For final estimation of all necessary parameters needed to design safe and productive method of exploitation, many laboratory tests and tests " in situ " were conducted with the aim to estimate basic physical-mechanical properties of rock such as: compressive strength , tension strength , Young modulus of elasticity and others. Parallel to those “in situ” tests, all necessary control measurements of stability were conducted and followed from the beginning up today. A particular problem underground mining by this method due to the multiple entry and exit to the underground mine were ventilation of the underground spaces, and that was resolved by movable ventilation stations.

KEYWORDS

Dimension stone, Natural stone, Quarry, Underground mining, Room and pillar

INTRODUCTION

Natural stone mining is still “unrecognised child” of mining industry. In certain countries this kind of exploitation is already inserted in mining filed; in few countries this branch belong to the quarrying and in certain numbers of countries it is not estimated yet as mining or quarrying. World mining of dimensional stone blocks date from earliest human history, and it is growing every year. With the possible exception of wood or mud, stone was almost certainly the first construction material used by man. Stone houses and wal1ed cities existed before the Bronze Age; and stonemasons were among the earliest artisans. The earliest constructions that we know were made of consisted undressed stone, boulders, and rubble-materials which did not require quarrying. The cyclopean stone fortress wall at Mycenae is an excellent example of the use of such undressed stone. The building and decorative crafts took on new significance with the discovery of the new methods for quarrying and polishing rock. Using tools of wood and hard stone the Ancient Egyptians extracted rocks of impressive size from the quarry at Aswan. Wooden pegs were placed in a row of holes and wetted with water. The water caused the pegs to expand, forcing the rock to break along the line of the holes. Another early quarrying method utilized a combination of the principles of heat and strain. Fires would be lighted along a previously marked line in the rock. After the rock had been sufficiently heated the fires would be simultaneously quenched. The contraction caused by the sudden cooling would cause rifts to occur in the rock. These rifts would be further widened by means of wedges and levers until blocks of stone would become detached. With further development of industry and with appearance of the new modern machines (electricity, drilling machines, compressors, loaders, wire saws etc,) technology of natural stone block extraction rises. First big step in industrial exploitation of block was

application of abrasive fed wires in the quarries. On the end of last century this wire was replaced with wires with diamond segments mounted mounted on the wire. That was revolution in mining technology which rises the productivity. As a consequence of applications of chain cutters in coal mines, in the same time, new types of cutters were developed for dimensional stone extraction. These chain cutter machines were equipped with widia or diamond segments, and for extremely abrasive rocks diamond belts were developed. Most of the quarries were working as open pit quarries, but with applications of modern chain cutters, in few last decades the number of new underground quarries were opened. Total production of natural stone (Figure 1) is growing significantly every year in physical units and in financial values as well. Total gross world product in the year 2013 was 74.000.000.000 USD (Montani, 2015).

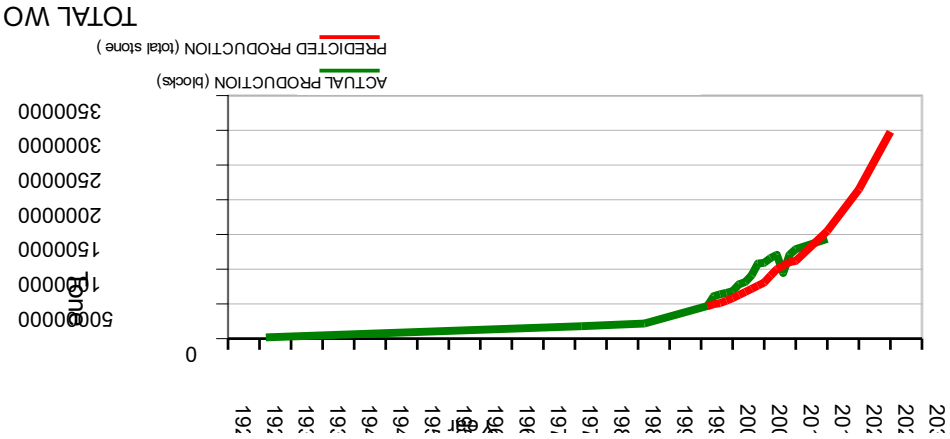

Figure1 – Total world production of natural stone

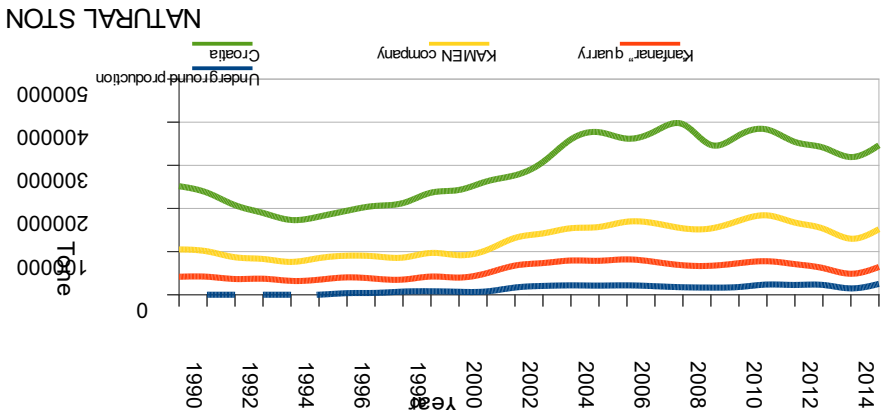

Figure 2 – Croatian natural stone production

The present production of dimension stone in Croatia is approximately 350,000 tpa (Fig.2), mostly limestone. The quarries are located predominantly in the coastal regions of Istria and Dalmatia, (Fig.3) famous for tourism, which presents a new challenge for mining industry. Croatia has numerous

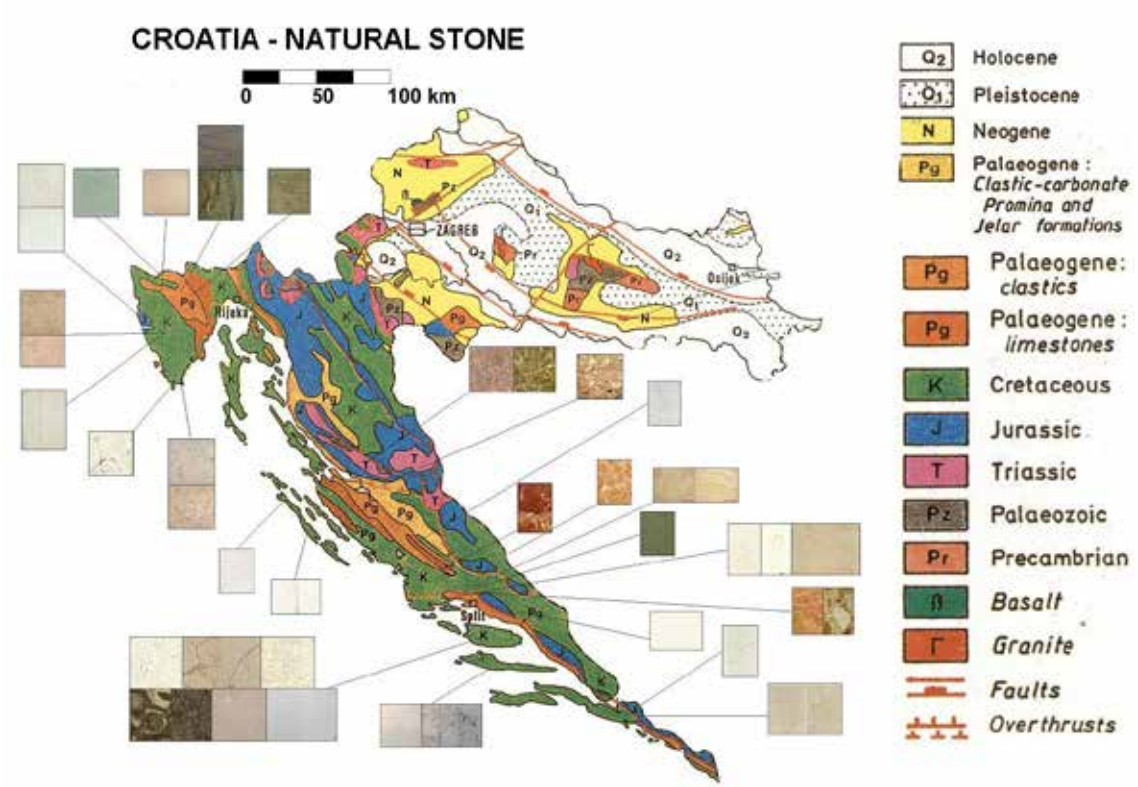

Figure 3 – Natural stone of Croatia

historical monuments, which is proof of a high level of culture in stone applications. Old traces of Roman exploitation and old Roman quarries can be found, and well-preserved public buildings, basilicas and temples are in the coastal region of Istria and Dalmatia. The amphitheater in Pula (First Century AD), besides those in Rome and Verona, is one of the best preserved in the world. It was built of stone from the quarry near the village of Vinkuran, the oldest quarry in Croatia. From the numerous ancient towns and buildings in the Dalmatian coastal region let us mention the Diocletian Palace complex in Split (4th Century BC), the residence of Gaius Aurelius Valerius Diocletius. This valuable ancient building is known as the “symphony in stone”. Its principal building material is limestone from the island of Brač, where old quarries still exist today. Limestone from the island of Brač called "Veselje" or "marble from Brač", is well known in the USA as one of the building materials for the White House in Washington, while Istrian limestone (often called istrian marble) was using as building material at Columbia University, NewYork, Carnegie complex Pittsburg and etc. City of Venice is build of Istrian stone - limestone type Orsera.

Company "KAMEN" d.d. from Pazin, Istra, Croatia , is a company whose predominant activity is quarrying, transforming, cladding, trading and all other activities connected with dimensional stone (Vujec et al. 2000). Company is producing about 35000 m^3 of blocks, from which, about 50% is use for proper factory and another 50% is exporting all around the world. All quarries are settled on Istrain peninsula, which is composed from the Jurassic and Triassic limestone (Fig. 4). The deposits are represented with layered, sedimentary structure, generally inclined about 0^0 - 10^0 in direction East-Northeast. Quarry, called "Kanfanar" (Fig. 6) is consisting of five smaller quarries, named from K- I up to K-V. Lower Triassic sedimentary limestone is object of quarrying, and it is represented by six layers with various thickness from 0,8 meters up to 1,55 meters. Total useful thickness for ornamental stone purposes is about 6.8 meters in total. Overburden is represented also by limestones, but with different physical-

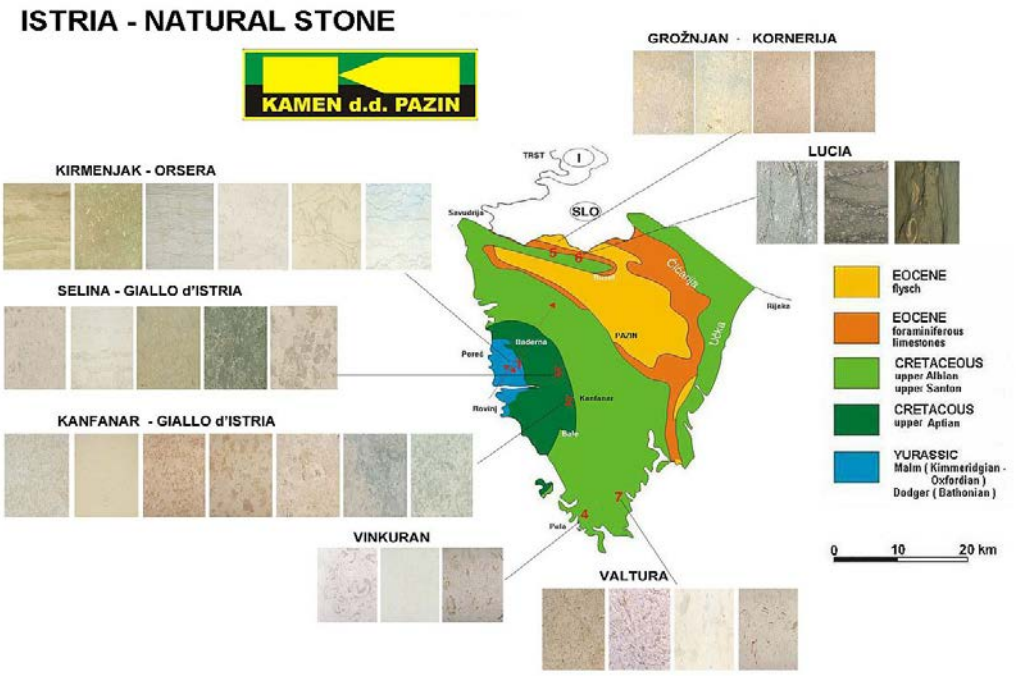

Figure 4 – Natural stone of Istrian peninsula

mechanical properties, and with advancing with exploitation, overburden is rising up to 20 to 25 meters. Foot-wall is also represented with limestones but with different physical-mechanical properties (Cotman, 2006). The limestone of the Kanfanar quarry represents rhythmical alternation of micrite and oncolite, in which two cycles may be distinguished. Strata's are limited in height with closed strata lines, and are numbered from n^0 1 up to n^0 6. Due to higher organic matter in micrite, their colour is darker than light/brown and yellowish colour of micrites, and thus they are easily seen on the polished slabs.

BASIC PRINCIPLES OF UNDERGROUND EXCAVATION

The term "natural stone block" means a piece of stone in regular parallelepiped shape with lengths from (2,0-4,0)m, width about (1,0 – 2,0)m and height (1,0 – 2,0)m with unique texture, colour, adequate density, without visible cracks and without internal cracks. Such block has a commercial value and ready for further transformation in slabs. Volume of the block very often depend of the tectonic state of the deposit and also form the traffic regulations (same countries do not permit LKW transport heavier than 23 tones). Because of that it is very important to know maximum about microtectonics state of the deposit. In layered deposits, as in our case, the stratification lines are limiting factor for height or width of the blocks. Using special machines for underground mining openings, three artificial planes are created (sides of the block). Knowing that deposit has 2 – 3 systems of cracks, and applying three new cutting surfaces without no respect of existing system of cracks, very often the utility factor of excavation can be economically unjustified and lead the quarry to the closing. Because of that, respecting actual cracking system of the deposit, and adjusting direction of excavation "using" one or two crack direction is of height importance. Very often the cracks can "help" in excavation and diminish the cost of cutting. Using the explosives in limestone deposit is not advisable because great possibility of destroying internal consistency of the stone block. For predicting the direction of excavation adequate Cotman stereo diagram (Kosov ,2001) is in use (Fig.6). In the natural stone production, the cracks are divided in two groups: cracks which has influence on the future volume of the block and cracks which has influence on the internal structure of the blocks. For the purpose of excavation and design of mining plan first group should be analyse carefully. In the Kanfanar quarry "crack index" vary from (0,092 – 0,196) m' of the cracks/ m^2 per total mined area with stratification lines not included. To obtain "healthy" blocks, mine excavation has to avoid the cracks what

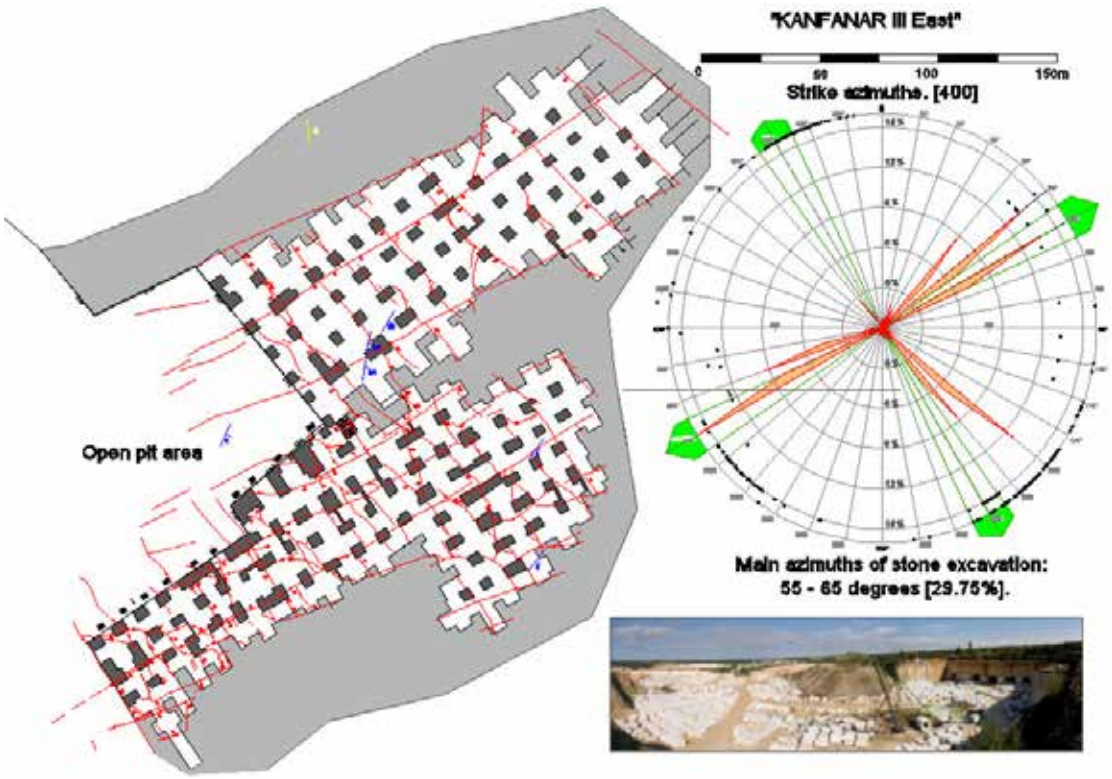

Figure – 6 Kanfanar III quarry, mine plan with crack set stereogram

has, as a consequence, pillar positioning on the places with the cracks and in various section shapes. Because of all of this factor, underground mining method selected is "room and pillar with irregular distribution of the pillars". Excavation must be followed "day per day" with improving the crack distribution on the plan. Future positions of the pillar and chambers, excavation and advancements is planned according the rule "design as you go" with the future assumed position of the discontinuities..

Before 30 years, the diamond wire make a revolution in the quarries and mining technology as well as in productivity and in financial profitability. Up today, these machines are the "number one" machines in the open pit quarries, but in last decade the development of chain saw cutters with the possibility to cut horizontal, inclined and vertical cuts ,rise and facilitate the actual methods of excavation stone blocks in open pit quarries. Speed of cutting is still advantage for diamond wires (about 10 m^2/hour), but chain cutters speed of cutting in underground achieve up to (4-6) m^2/hour. Cutting length of chain cutters in vertical cuts up to (8 – 9) m, and horizontal cuts up to 4.0 m, and the possibility of "dry" cutting make new additional step in technology. Combination of use diamond wire with chain cutters eliminates for about 90% drilling in the quarries and rise the productivity in quarries. Newest cutting machines mounted on tractors with the cutting length up to 3.5 m, and with maximum cut height of 2.5 m becomes irreplaceable for secondary transformations and shaping the natural stone blocks. Cutting tool on these machines are generally widia plaques, very hard polycrystalline materials or diamond segments. Depending of the type of rock for cutting tool must be chosen very carefully. With new underground quarries, diamond wire shows few sever disadvantages, and among them, consumption of the water is the biggest. Development of underground mining, forced mining machine industry to accompanied these movements with new products for natural stone industry. For underground applications main machine producers from Italy (Benetti, Carrarra and Fantini, Rome) start to produce new types of stone cutting machines adjustable for underground use (Fig,7; Fig.8;Fig.9;Fig.10). The chain cutters can work without necessity of the water (as cooling medium during the cutting process), but for the moment, only in case of working with hard metal plaque as cutting tool on chain saw (which is a case in majority limestone and marble quarries). That is great advantage in compare with other cutting and drilling machines. Even for

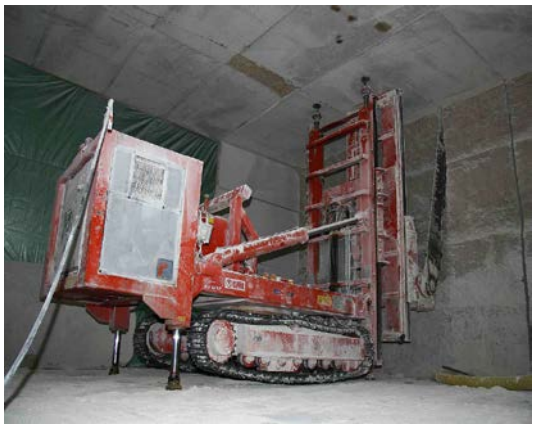

Figure 7 - Fantini GU-70 chain cutter

Figure 8 - Faintini SV-C chain cutter for back cut

Figure 9 – Benetti chain cutter TCM 988 940

Figure 10 – Benetti diamond belt cutter TCM

the limestone with height percent of flint or other types of height abrasive stone with quartz crystals, diamond belt cutters or "classical" chain cutters equipped with diamond segments makes underground excavation possible (Cotman, (2005). In case of cutting with diamond tools, use water in working process is inevitable, and in lot of cases caused certain problems connected to the environment and health of workers (humidity)..The great disadvantage is length of the horizontal cut, which is limited generally to 3.5 m which is enough for the future length of the stone block. In Croatian underground exploitation Fantini chain cutters type GU-70 and SVC- 50 are in use. Effective capacity of cutting in Kanfanar limestone is (2-4) cm/min with duration of widia plaque is (5-10)m^2 /insert. "Back" cut is made by splitting using hydraulic pillows because the rock breaks well. Whole process in use is a "dry" cutting without water use. Minimum section of the pillar is 12,5 m^2 with minimal width of 3,5, while mined maximal excavation ratio is 1 : 7. With the utilization factor of (35 – 45)%, monthly productivity of stone blocks is (130-150) m^3/ men. System of ventilation (Fig.11) is compressed, installed by using the movable ventilator stations consisted of 4 independent ventilators with capacity of (1,5 – 45) m^3/s each. Exploitation of the blocks is done by using Catterpillar loader 988 equipped with quick-coupling tool and ceramic filter type PFS (ing.G.M.Shurz Gmbh, Germany) which eliminates dangerous diesel particles. "Bosh number" never exceeds value of 0,25. Underground openings were designed by using Obert-Duvall formulas (Obert-Duvall, 1967) for openings in laminated rock, roof parallel to lamination. For the physical-mechanical properties of rock, for the initial phase of the project , values obtained from the laboratory testing according European norms (EN

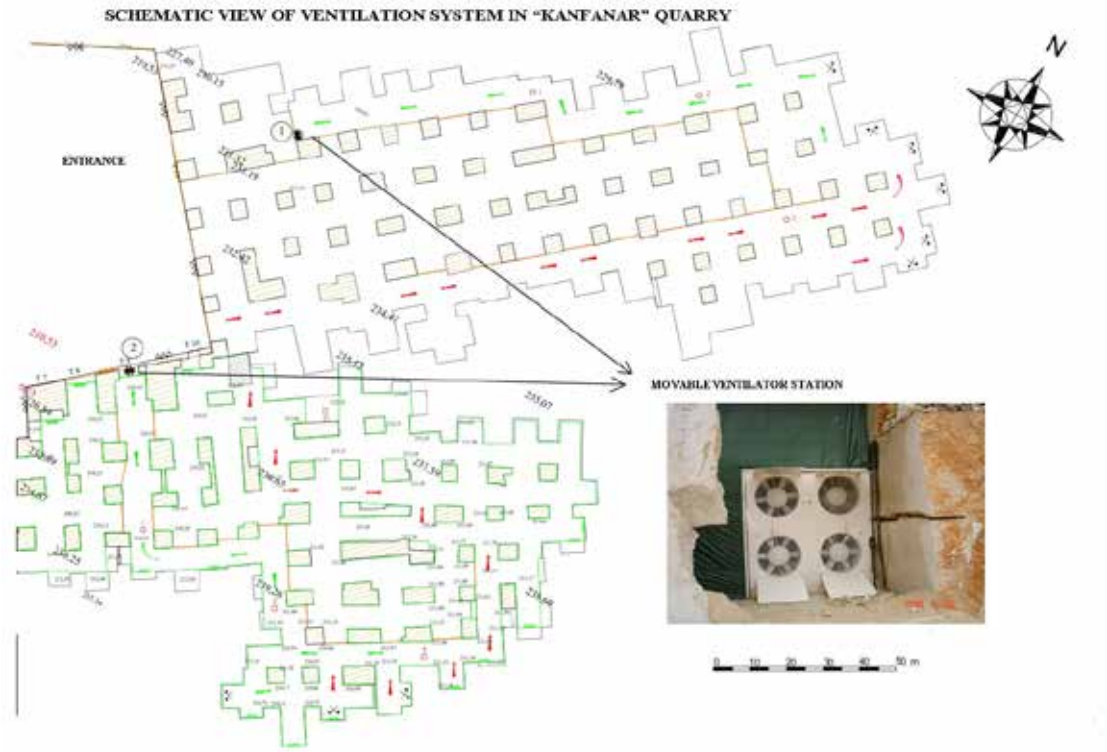

Figure 11 – Ventilation system of "Kanfanar III " quarry

1936, EN 13161,EN 12372) were taken in account for analytic calculations. Values presented within these norms are not real values, for rock mechanic calculation, because the results were obtained on very small samples, and they are excessive in comparative with real situation. These values were reduced according to the coefficient from Table 1 (N.Panjukov, 1965), which can be applied in case of lack or insufficient number of data. Using corrections from the Table 1, initial mining plan were created and exploitation starts in the year 2006. Parallel to the analytic calculation for the initial project , numerical calculation were done too by using software Phase^2 by using GSI index according to the Hoek-Brown criteria (Hoek,2007). Initial GSI factor was assumed to be (60 - 70) Space distribution of the cracks were recorded directly on the site. Immediately after start , initial measuring were started; convergence of the roof, horizontal and

Table – 1 Reduction coefficient for laboratory values considering the tectonic state of rock

Characteristics of cracking for observed rock	Reduction coefficient		
	k_{min}	k_{max}	$k_{average}$
The dense net of cracks in all directions divided the rock to a large number of unbonded pieces	0,000	0,100	0,0005
The dense net of open cracks in all directions	0,001	0,02	0,005
Dense cracking	0,01	0,04	0,02
Cracking above average	0,01	0,08	0,06
The average cracking (open and closed cracks every 20 -30 cm)	0,08	0,12	0,1
Under the medium cracking	0,12	0,3	0,2
A net of deep cracks spaced on the 30 - 50 cm; small number of open cracks	0,3	0,4	0,35
Rocks with small number of cracks. Closed cracks	0,4	0,6	0,5
There is almost no microcracks	0,6	0,8	0,7
The monolithic rocks with no signs of cracking	0,8	1	0,9

vertical stress in the pillars and relative deformation of the cracks with "in situ" measurements. Parallel to this measurements, new laboratory tests were conducted according ISRM recommendations on the Faculty of Mining, Geology and Petroleum engineering , Zagreb. Results obtained by ISRM testing were additionally corrected according to the "scale effect" (significantly reduction of the values in comparison

with increase of the volume of the sample). The result of these measurements, corrected with the "scale effect", can bee seen in Table 2 (column "project"). "In situ" measurements were conducted during the next 10 years and final results are presented (red numbers) in Table 2. Final control calculation were done using numerical analyses with the values obtained by measuring "in situ" using software SAP2000.(Hrženjak,2014) and compare them with initial data used in original mining plan (Tab.3).

In the quarry were fixed 19 points for a measuring relative movements on the "open" cracks and measurements were done using MEBA mechanical extensional meter with precision of 0,02 mm and deform-meter with precision of 0,01 mm. Measuring convergence of the roof were observed on 6 fixed points with INTERFELS type L convergence-meter. Rock stress and module of deformability are continuously followed on 6 points (3 for vertical stress and 3 for horizontal stress) using hydraulic pillows (Benetti hydro-bag Model 645 – 90 x 90 cm), digital manometer type DMC (AEP Transducer s.r.l. Italy) with resolutions of 0,2 bar and deformation measurements were conducted using GEOCON model 4450 Displacement Transducer. Method of measuring were conducted according ASTM norms

(D-4729-08). Changes in rock stress is measuring continuously on another 2 fixed points (boreholes) using hydraulic cells for the boreholes GEOCON Model 3200 with hydraulic pillows (50 x 226) mm with tubing of 800 mm. For pressure measuring serve the GEOKON GK- 403 Vibrating wire readout with resolution 0,002MPa and precision of 0,02MPa. On two additional points same measurement is performed by using hydraulic bag (Benetti hydro-bag Model 645 – 90 x 90 cm), cemented (SikaGrout 212) in horizontal cut, and measurement is followed using GEOKON GK- 403 Vibrating wire readout. The measuring is continuously followed up today. With the technology which is in use in underground exploitation, new method for measuring the tensile strength in the rock mass is developed, by using hydraulic pillows and measuring the pressure during the break the "back side " of the block (Hrženjak et alt., 2008). This method will be developed in the future for estimation the cohesion of the "closed cracks". Additional problem what was encountered during the exploitation is that the sections of the pillars very often are not rectangular and they have various shapes. Existing formulas for calculate stress in pillars are based on relationship between width and height of the pillar; generally for rectangular pillars. In present case, of underground exploitation with irregular distributed pillars with various shapes, is very difficult using these formulas in practice. For analytic calculation of the stress in such shaped pillars, the new expression, which will connect the height of the pillar and moment of inertia for the section, will be of great help. In that case it will be possible to calculate maximum height of the pillar (before bending) for certain section area . First experimental test are already done and expression is under development.

CONCLUSION

Underground method room and pillar with irregular distributed pillars, guided by the system "design as you go", is approved in layered limestone quarry as height productive and safe method. In last 15 years there were no accidents, caused due to the stability of the underground spaces. A system of movable fan station fully meets and provides sufficient quantities of clean air in both cases (working with electrical powered machines and with use of diesel loaders). Outbye excavation method applied , is an adequate method having in the mind that the during advanse excavation, the pillars and the chambers have dimensions larger than projected and thus provides additional security fot the staff and equipment. Definitive dimensions (projected) of the pillars and rooms will be designed during retread works. During the excavation is necessary to inscribe and follow the cracks on mining plan with the purpose of predicting locations for future pillars (bad material) and future rooms (healthy natural stone) to achieve height yield and maximum safety. Main guide rules for excavation are: respecting maximal exploitation ratio, respecting miniml area section of the pillar and maximal projected span. Stress measurments, convergency and relative movements of the discontinuities is continuos process followed by the specialists. System of measuring internal stresses "in situ" and tensile stregth "in situ" are giving the real results and will be done in the future too. After 15 years of observing, obtained data are sufficient for analytical or numerical calculations and their results were confermed in practice. Future efforts will be foxused to determine expression for analythic stress calculation of various shaped pillars on the base of their sections area. All around accepted recomandation for planing section of the pillar with ratio width/height equal 0,5 (Esterhuizen et al., 2011) probably is good for underground cool or ore mining, but for natural stone mining these ratio must be restuddied and reconsidered having in the mind that natural stone underground mining takes place in a healthy and consistent rocks in surroundings without application of any vibrations caused by blasting.

REFERENCE

ASTM (2008): Standard test method for in situ stress and modulus of deformation using flatjack method, D 4729-08. ASTM International, West Conshohocken, USA.,

Cotman, I. (2006): Glavni rudarski projekt podzemne eksploatacije arhitektonsko-građevnog kamena na eksploatacijskom polju „Kanfanar-jug". Kamen d.d. Pazin, Pazin (unpublished)

Cotman, I. (2005): Improved method of excavation layeres deposits in underground stone mine, 20th World mining congress & EXPO 2005, Teheran, Iran

Esterhuizen, G.S., Dolinar, D.R., Ellenberger, J.L., Prosser L.J:(2011): Pillar and roof span design guidelines for underground stone mines, NIOSH, Pittsburg, USA

Hoek E. (2007): Practical rock engineering. Rocscience Inc., http://www.rocscience.com, Toronto.

Hrženjak P., Cotman I., Z.Briševac (2008): Geotechnical investigation for designing underground natural stone mines, 21th World mining congress & EXPO 2008, Krakov, Poland. CRC Press, Balkema pp 197-206

Hrženjak P. (2001): Izbor ulaznih veličina u postupcima numeričkih proračuna pri podzemnom otkopavanju kamena. Magistarski rad. Sveučilište u Zagrebu, Rudarsko-geološko-naftni fakultet, Zagreb.

Hrženjak P. (2014): Istraživanje stabilnosti podzemnih prostorija kamenoloma asrhitektonsko-građevnog kamena na eksploatacijskom polju "Kanfanar-jug", Mining,Geological and Petroleum University, Zagreb (unpublished)

ISRM (1979b): Suggested methods for determining the uniaxial compressive strength and deformability of rock materials. *International Journal of Rock Mechanics, Mining Sciences & Geomechanics Abstracts*. Vol. 16, pp. 135-140.

Kosov.A (2001): GEOL_DH rel.8.71 and KAI-2001, AutoCad software for geologist and miners, Magadan , Russia

Kovačević-Zelić, B.,Vujec, S., Cotman, I. (1996): Numeričke analize podzemne eksploatacije arhitektonsko-građevnog kamena. *Rudarsko-geološko-naftni zbornik*. Vol. 8, pp. 91-97.

Montani C. (2015) XXVI Report marble and stones in the world, Aldus casa di edizioni, Carrara

Obert, L., Duvall, W.I. (1967): Rock mechanics and the design of structures in rock. *John Wiley & Sons. Inc., New York.*

Panjukov P.N. (1968): Inžinjerska geologija, Beograd, *Građevinska knjiga*

Vujec S., Cotman I., Hrženjak P. , Petzel M., (2000): Criteria for design and stability control in underground production of natural stone, 18th World mining congress & Mine 2000 Expo, Las Vegas, Nevada, USA

UNDERGROUND MINING. THE DIFFERENCE BETWEEN OPTIMAL AND REAL

*Paul Tim Whillans
1142 Rose Street
Vancouver, Canada V5L 4K8
(*paul@whillansminestudies.com)
Tel: +1 (604) 250-1119

Paul Tim Whillans
Principal
Whillans Mine Studies Ltd.

24th World Mining Congress
MINING IN A WORLD OF INNOVATION
October 18-21, 2016 • Rio de Janeiro /RJ • Brazil

UNDERGROUND MINING. THE DIFFERENCE BETWEEN OPTIMAL AND REAL

ABSTRACT

An underground mining study that is done in accordance with NI43-101, JORC or similar reporting code is generally assumed by the public to be representative, independent and impartial. However, it has been well documented by academics and professionals in our industry that there is a sharp difference between the forecasts presented in these underground studies and the actual costs when a mine is put into production. [i] [ii] [iii] [iv] [v] [vi] [vii] [viii] [ix]

For underground mines, the risks associated with obtaining representative information are much greater than for surface mining and the cost of accessing underground ore is also proportionally much greater. There is a pressing need to align expectations, by improving the accuracy of projections. This will result in reduced risk to mining companies and investors and provide more reliable information to government agencies, the public, and more importantly, the communities in which the proposed mine will operate.

The objective of this article and an article currently being written titled “Mining Dilution and Losses” is to:

- Identify some specific points where underground mining studies are generally weak;
- Show that a number of the practices currently in use in our industry create an unacceptable level of risk to the investor, resulting in a spiralling loss of confidence in the way we do business;
- Describe briefly the effects of overly optimistic studies;
- Outline specific changes that are necessary to overcome these challenges; and
- Stimulate discussion leading to better standards that can be pro-actively implemented in Latin America and elsewhere.

KEYWORDS

Mine Economics, Mining Risks, Mining Risk Assessment, Mining Studies, Feasibility Studies, NI43-101, Underground Mine Planning, Underground Mining Studies, Mine Economic Assessment

INTRODUCTION

Mineral project reporting guidelines such as NI 43-101 were created to prevent fraud and standardize reporting for mineral projects. The guidelines for sampling and geological reporting are well defined, but the quality of reports is highly variable with regard to mine economics. T.Lwin and J.Lazo of Export and Development Canada have indicated that capital expenses average 40% over budget for underground projects and that since 2009 this trend has been increasing. There are other components to underground studies some of which are identified in this article that also trend toward optimism and lead to a composite effect larger than that which is apparent by reviewing capital costs. Some key indicators that the author has found easy to identify are:

- Capital Cost Estimation;
- Time and resources to reach full production;
- Mill throughput;
- Dilution and Mining losses;
- Mine unit costs (if they are provided); and
- Contingencies

ELEMENTS THAT CONTRIBUTE TO OVERLY OPTIMISTIC MINING STUDIES

Intention

An important challenge to achieving an impartial mining study with appropriate accuracy is the perception of those working within the mining business of what these studies are meant to achieve. We are people of action and the natural collaboration in moving the project to the next phase dominates our industry. Endemic among the published studies are overly optimistic estimates of costs, mining rates and the grade of mineral delivered to the processing plant. Negative studies don´t get published.

Client Consultant Relationship

Here are some notes on the client / consultant relationship which affect reliability in reporting and costs to the investor:

- There is a requirement to use what are called “industry best practices”, but this is too often interpreted as a need to stay in line with what others are doing.
- There is a lack of appropriate training, appropriate in-depth or relevant experience and/or knowledge among some of those performing mining studies;
- There are budget constraints, lack of time and sometimes a lack of interest in getting to more representative results;
- There is the role of overconfidence in our own work as demonstrated by Daniel Kahneman [1] [x] and in some cases, ethics in producing overly optimistic studies;
- Draft cost models may be delayed many months which sometimes delays bad news; and finally
- If a client doesn´t like the numbers presented by the consultant they may shop for another consultant who will give them more favourable numbers;

Difficulty with Benchmarking

In operations where historical information is lacking, there are two approaches to scheduling and cost estimation; benchmarking and base principles calculations. A combination of both is always required.

For benchmarking to be representative, comparisons must be made to operations with similar characteristics, including comparable orebody dip, width and continuity, similar ground conditions, similar mining methods, preferably in the same country. Benchmarking requires an in-depth knowledge of conditions at the operations being investigated and there is a lack of professionals with appropriate experience or time to perform these comparisons. Operating mines are disinclined to share detailed cost and productivity information because it may ultimately have an effect on share prices. It goes without saying that in spite of its reliability, benchmarking is not being used as frequently as it should.

Extensive work on benchmarking reserve tonnage vs. production rate has been done by K.R. Long, [xi] W.D. Menzie, D.A. Singer, C.R. Tatman [xii] and H.K. Taylor, (Taylor´s Rule and subsequent revisions) on numerous mining operations. A recent revision is shown in Figure 1 below. This benchmarking work is increasingly being ignored because it indicates lower production rates than are often considered desirable.

Benchmarked numbers already include availability, utilization and all possible contingencies compared to calculated values, an important reason why they may appear too conservative or pessimistic to a client. This forces the consultant to resort to base principles calculations, ***a method which by its nature will yield overly optimistic results if not tempered with experience and understanding, the calculations are done properly and the appropriate allowances included***.

---

[1] "Overconfident professionals sincerely believe they have expertise, act as experts and look like experts. You will have to struggle to remind yourself that they may be in the grip of an illusion." Daniel Kahneman; nytimes.com 2011-10-23

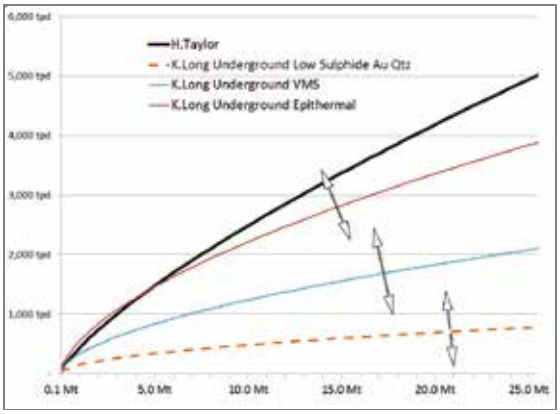

Figure 1: Taylor´s Rule compared with Findings by Keith Long for Underground Mines

Information from Suppliers

Information from suppliers is normally backed up by field tests but suppliers are also mindful that for products to sell themselves they must be shown in the best light, so test conditions tend to be optimal. Here are just a few examples of information from suppliers that deserve consideration:

Diesel machine suppliers may not be transparent about the need to de-rate for altitude because there is a loss of machine power associated with derating and if a client doesn´t understand the need to de-rate, this information could result in the loss of a sale. Ventilation is affected when machines are not appropriately de-rated, but operating mines may not make the connection between de-rating and poor ventilation. This is part of the reason some mines require workers to wear filtered breathing masks (which incidentally can be uncomfortable to wear all the time and lead to questionable compliance.)

Ventilation fan suppliers may try to provide a fan for use at 90% efficiency, but in reality, it is very hard to optimize fan efficiency to that level as actual underground conditions tend to be highly variable.

Suppliers of ventilation ducting will often focus on operational improvements rather than the parameters they have provided for calculating ducting performance. Rips in vent tubing, installation challenges and human error in installation of ducting are part of the reality of operations and are exacerbated by the pressing economies of reducing the dimensions of mine accesses. It takes the experience of someone who has measured actual pressure drops in operating mines, is aware of the frequency and size of the inevitable rips in the ventilation tubing, of how tubing is normally hung and based on this experience, can make a calculation of the size and type of the required fan and ducting and the resulting airflow at the face.

Cost databases are available that will provide estimates for fuel consumption, parts and maintenance. The source of this information comes from suppliers. The suppliers need to show their machinery costs when things work as they should. (i.e.: No operator abuse, good roadways, appropriately sized muck, no oversize, well-maintained machines, LHDs not used as taxis.)

Ventilation Considerations

Exposure to diesel fumes has long been a source of study [xiii] because of its effect on worker health. The following factors impact worker health and are normally underestimated or ignored in mining studies:

- Underestimation of fleet size is the most important factor leading to poor mine ventilation.
- Sulphur content in diesel fuel is an important factor affecting health. Some countries have maximum permissible levels set as high as 500ppm.
- In many countries, it is common for mines to use equipment that has not been designed for underground use. Some of these machines will have much higher levels of emissions.
- At higher altitudes, de-rating of diesel machinery ceases to be effective as a means of reducing contaminants. [xiv] Mining Regulations for some countries do not require any adjustments or derating to diesel machinery for higher elevations or additional ventilation.

Precise vs. Representative

Underground rock has not been optimized, yet we spend a lot of time trying to optimize our computer modelling of it. The modelling will give us astounding precision and frequently we are misled by believing it gives more reliable results. However, a step by step strategic approach involving others will usually lead to more representative results faster, as complemented by the power of computing.

Computer modelling of dilution skins has become more common, yet in almost every case, the *amount* of dilution towers in importance over the grade of the dilution. A small effort into determining the *amount* of dilution by doing some simple sketches can save a lot of time.

Geotechnical block modelling relies on composites which are weighted average values. If the rock has a high variability in geotechnical properties, compositing will result in a smearing that gives a false impression of homogenization and frequently an over estimation of rock stability.

Animations of the mining schedule are the wave of the future because everyone from the miner to the manager can immediately understand the sequence of work to be done. However, it is often difficult for the operators of this software to gain in-depth experience in operating mines and currently there is a *severe lack of knowledge of alternate processes and of how the process of design could be sequenced strategically involving others, to get to reliable answers faster*. For example in one recent case, an entire mine schedule was completed without first figuring out the sequence of steps and how long it takes to mine a typical stope.

If the resource is inferred, [2] it means that we´re not absolutely sure it´s there, it´s a well-informed guess, so why do a detailed design? Don´t forget to include a factor for upgrading the resource from inferred to indicated. [3]

Geological block models are usually based on diamond drilling and calibration of the model to underground mapping, underground sampling and production output to the mill is uncommon.

For some, the purpose of variography is to make the deposit looks better.

If the distance between drill holes is 30m will the result will be any better if the size of the blocks in the block model is reduced from 5 x 5 x 5 metres to 1 x 1 x 1 metre?

Underestimation of Mining Dilution

Operations personnel will often refer to over-break, (the unintended waste rock that falls into an opening after a blast), when speaking about dilution, sometimes excluding all other factors because it is what they are struggling to control and it is where their attention is focused. In fact, dilution comes from at least 14 different sources. There can be great pressure from mine operators and clients of mining studies to show lower numbers for dilution.

Here again, “best industry practice” does not mean what everyone else is doing. Nor should it mean a number that is defendable among peers. Best industry practice is experience, knowledge, clarity, transparency and above all in-depth understanding to serve the best interests of potential investors and raise the credibility of our industry.

If a mining study has been done well, all categories of dilution will have been considered. The following are listed briefly and will be explained in an article currently being written titled “Mining Dilution and Losses”:

- Decisions made during modelling, design and execution;
- Variability of the contact;
- Over-break;
- Variability of grade;
- Mine by lithology or grade;
- Visibility of the contact;
- Minimum mining width;
- Islands of waste in the mineral;

[2] Infer = well informed guess, speculate, surmise, hint, imply, suggest

[3] 30% to 70% of inferred pass to indicated

- Notching above and below sublevels;
- Impact of flatly - dipping structures;
- The necessity of providing an arched stable back;
- Floor dilution;
- Backfill dilution; and
- Alternating use of raises as orepass and wastepass

Underestimation of Mining Losses

Dilution has become such an important topic that mining losses are overlooked. Reducing dilution will often result in increased mining losses, a shortening of mine life, and increased proportional cost of accessing new areas. In the context of this document, Mining Loss includes mineral that is part of the mineral reserve that for any reason is not mined. Many mining studies will simply peg the numbers at 10% to 15% for mining losses which in most cases, is a serious underestimation. We have identified to date, 16 factors that contribute to mining losses which are included in the PowerPoint Presentation accompanying this article and will be described in more detail in an upcoming article dealing with Mining Dilution and Losses.

Overestimation of Availability

Availability is divided into three categories. Machine, Labour and Ambient.

Machine availability is not the same as mechanical availability. It includes not only the time that the machine has been fixed but accounts for the time when the operator had to be reassigned to another task if the machine was not available at the start of shift and it will therefore be a lower number than mechanical availability. Mining studies often set mechanical availability between 85 and 90% which in itself is high and does not consider the actual availability of the machine to the operation.

For labour availability, there is a tendency to look at holidays and shift schedules and a few other items. All conceivable reasons for not being at work, including training need to be included as well as worker substitution in case of absence. Effective work time needs to be included. This is affected by travel time, shift fatigue and cultural factors. Assignment needs to be included, in other words the frequency with which an operator is in fact assigned to their primary task, which of course varies according to the skill of the worker.

Ambient availability is often not even considered. For those of us who have worked underground we know there are shifts where nothing seems to work. Those shifts when a truck broke down in the ramp and people were reassigned to work in another area that didn´t have air or water and they found out the air and water lines had rusted out. The frequency of these type of events and more minor ones is also referred to as System Availability. If possible, measure it. Our experience indicates the numbers may be significant.

Pushing the Limits of Design

Figure 2 below, shows a tool for calculating the size of mine openings for remote entry, The Mathews Stability Graph and compares typical design criteria to historical data from an operating mine. [xv] It can be seen that over 20% of the stopes that plot within the “stable zone” experienced caving. The method not at fault, but it is based on ***probability of stability***, and therefore does not reflect the fact that a small portion of stopes that experience failure might have an enormous impact on the mine schedule and production. Indeed, there are many factors that affect stability that are difficult to consider in the planning stage. These include unexpected faulting or human error in the design and execution of drilling and blasting.

We have visited only one mine where the design was conservative enough that stope failures were extremely rare. As a consequence mine production was more predictable. Working against these prudent efforts at conservatism are:

- Overly optimistic predictions that make it their way into the budget (that´s where the problems start);
- Operations personnel who see advantages to increasing stope size.
- Lack of appropriate knowledge or experience

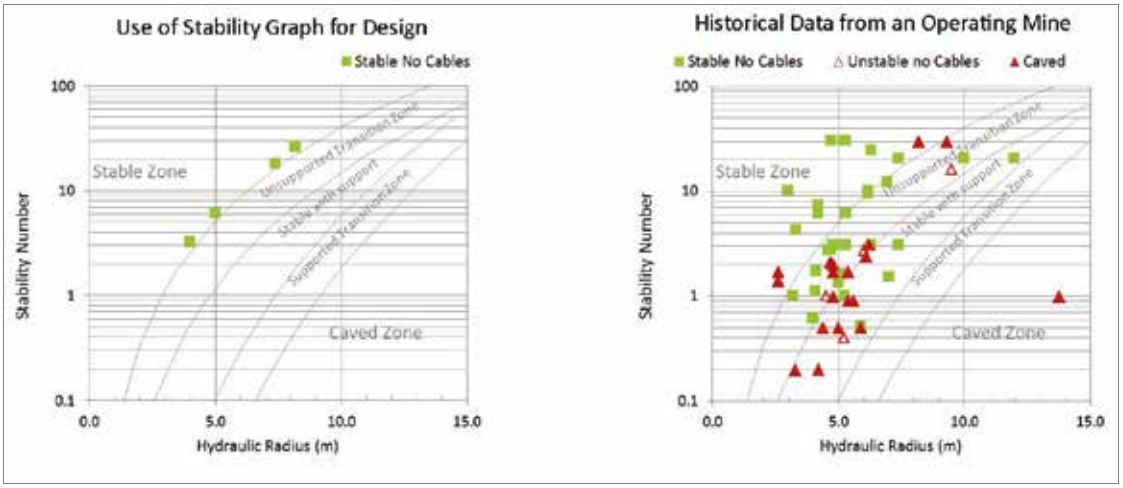

Figure 2: Use of Modified Mathews Stability Graph. Design vs. Historical Data

Interpretation of Project Sensitivities

Spider graphs (see below) may be used to represent the viability of a project showing different variables.

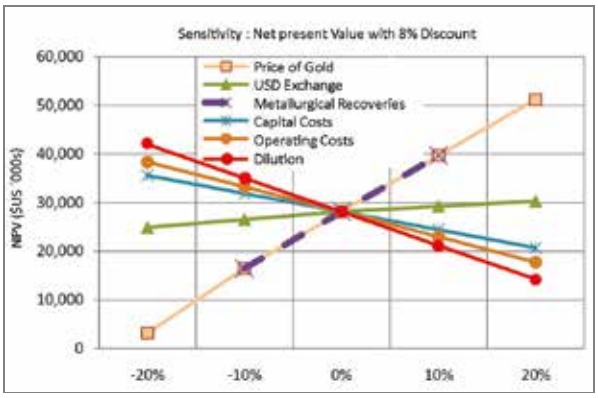

Figure 3: Project Sensitivity

There is an implied level of accuracy of +/- 20% for this graph done for a Pre-Feasibility Study based on a mine plan has been "optimized". In a mining operation, there is more often than not a combination of factors that can combine to increase the impact on project viability and a discussion should be included on the effect and likelihood of *various factors working in combination*. A Simulation such as the Monte Carlo *will not pick up on the composite effect of variables working in combination* unless the probability of that occurrence is identified.

If in the example of Figure 3, the capital costs were underestimated by 40%, the chances are high that operating costs and sustaining capital are also underestimated. That being the case, almost for sure the production ramp up time has been underestimated. Therefore, if Figure 3 above meets current standards in our industry, there would be no project.

Contingencies

There is currently much confusion on the meaning of contingency and how it should be included. Studies should quantify each area where contingencies need to be applied and discuss the composite and cumulative effect of these contingencies. Contingencies should be applied for errors of technical services, mine management, supervision as well as miners.

IMPACT ON MINE OPERATIONS

The problems faced by operating mines are lessened by appropriate infrastructure such as travel ways, ventilation raises, drainage pumping and backfill in the planning phase combined with realistic scheduling and costing. So for a mine to operate properly and predictably, the plan should be achievable. Mistakes compound when the schedule is too optimistic.

An unrealistic mine plan puts mine operators under tremendous pressure so when problems arise, reactions will be based on short term requirements. For example, if ore is buried under oversize when a stope fails, operators may pressure to fill the stope leave the ore and start mining the next stope to ensure the flow of production. The same operators may also decide to blast a few extra rings in a longhole stope to get more ore which in turn might lead to stope failures. These risks may appear reasonable in the short term but as an operating policy it is disastrous. It takes a very senior person to step in and halt that tendency. Just a few caved stopes can have an enormous impact on the schedule. Lower grade stopes may be abandoned after a cave and the stope backfilled, burying the ore in the hope for better results in the next stope in the sequence. Mucking may continue in higher grade stopes which may fill every nook and cranny with oversize but the resource allocation for handling the oversize is high and work in other areas of the mine will suffer.

Here is another actual case example of the type and flavour many of us have seen before:

- A bypass ramp was needed to connect two areas of the mine to ease haulage and ventilation. This required significant extra resources to keep up to the budget schedule for production preparations.
- The increase in expenditures from the ramp bypass required a *doubling* of the cut-off grade to pay for the extra capital development and the higher-than-predicted operating expenses. This sterilized parts of the orebody.
- Press release stated that the mine was achieving better grade than predicted. Confidence in the orebody had increased and as a result, a decision had been made to increase capital expenditure. All waste development was then capitalized so that operating costs could be brought down to what was considered reasonable. The increased mineral losses brought about by the increase in cut-off grade weren´t considered of prime importance because the geologists would find additional ore to compensate for the loss. Summary, the investor was misled on the true state of the mining operation.

IMPROVEMENTS TO BEST PRACTICES / REGULATORY FRAMEWORK

Regulations should clearly state that mining studies should “present a representative economic assessment to diminish investment risk and align expectations of investors, local communities and governments” in addition to providing transparency on environmental impacts and labour relations.

Studies should include a list of all other consultants who have worked on the project and their recommendations whether those studies have been published or not.

An account of the attempts at benchmarking with similar operating mines should be encouraged but terms of reference for benchmarking need also to be developed;

State the need to include illustrations to show calculations for mining loss and dilution.

Quantify each item in the list of dilution, mining losses as well as machine, labour and ambient availability;

Studies should include a discussion on how proposed mill throughput compares to Taylor´s Rule and subsequent revisions;

Risk Analysis in summary and conclusions should include a discussion on the composite effect of combining project sensitivities.

The meaning and use of contingency needs to be defined and should include operational errors;

Each element contributing to dilution and mining losses needs to be quantified and sketches need to be included in reports.

Each aspect of Machine, Labour and Ambient availability should be quantified;

Qualified Persons (QPs) are not experts in everything and humility is necessary in seeking information from those who know more about areas where the QP´s knowledge may be weak. QPs should be

encouraged to consult underground miners, supervision, electricians and technicians who know more about aspects of their work.

Consultants who have experience tracking their planning as a mine has moved into production are few and far between. If they have this experience it should be stated. We need to plan for a future melding of the worlds of consulting and mine operations.

Mining unit costs (such as cost per metre of development) should be stated and it should be stated what indirect costs these numbers include and what has been designated as indirect or fixed costs.

Encourage as a best practice, an early provision of a draft cost model by the consultant so the client can see up front how the project progresses and to prevent the delayed release of bad news.

Inferred Resources = inferred planning no more stope-by-stope detailed designs. Include the resource upgrade factor. (30% to 70% of inferred tonnes make it to indicated)

Encourage the use of max / min cost calculations as is done in the field of rock mechanics.

The Qualified Person for mining or geotechnical must look at the drill core.

CONCLUSIONS

We are undergoing a crisis of credibility that is reflected in the difficulty in funding new projects. Our next big hurdles are:

- Align mining studies with reality using the points listed in this document by improving reporting methodology and standards and thus gain credibility, trust and confidence from investors, governments and local communities;
- The above will only happen if those working on studies are more closely linked with underground and have an in depth understanding of the challenges of the environment; and
- We need to pay careful attention to ventilation and long term health issues.

Improvements in the reliability of underground mining studies would mean that companies can follow through more frequently on promises to shareholders. That would improve trust in our industry and make it easier to raise funds for mining projects. Trust has implications in our relationship with governments, communities and employees as it becomes easier for these groups to make their own plans and commit to mining projects.

ACKNOWLEDGEMENTS

Special thanks to Larry Smith as well as to the following people for providing valuable guidance: Finley Bakker, Will Bawden, Icent P. Brown, Michael Cullen, Callum Grant, Keila Málaque, George McIsaac, David Silverstein, Michèle Soregaroli.

REFERENCES

[i] LWIN, T. LAZO, J. 2016-05 Capital Cost Overrun and Operational Performance in the Mining Industry. Management and Economics Society, CIM Toronto

[ii] BULLOCK, R.L. 2011-04. Accuracy of feasibility study evaluations would improve accountability. Mining Engineering, pp. 78–85.

[iii] MACKENZIE, W. and CUSWORTH, N. 2007-06. The Use and Abuse of Feasibility Studies. Project Evaluation Conference Proceedings, Melbourne. Australasian Institute of Mining and Metallurgy.

[iv] MCCARTHY, P 2013 Why Feasibility Studies Fail AMC Consultants AusIMM Melbourne Branch

[v] RUPPRECHT, S. 2004 Establishing the Feasibility of Your Proposed Mining Venture. South African Institute of Mining and Metallurgy

[vi] SMITH, L.D. 2015-05 Where are we going in this handbasket? MES Discussion Group and personal correspondence.

[vii] SHILLABEER, J. GYPTON C. 2003-09-09 Reducing Project Risk Following Completion of the Feasibility Study. Mining Risk Management Conference Sydney Australia

[viii] HAUBRICH, C. 2014-03 Completion Risk Why Building a Mine on Budget is so Rare PDAC

[ix] THOMAS, P. SORENTINO, C. 2015-04 The Valuation of Mineral Projects Presentation to GPIC/AIG

[x] KAHNEMAN, D. 2011 Thinking, Fast and Slow. Farrar, Straus & Giroux. ISBN 978-1-4299-6935-2.

[xi] LONG, K.R. 2009 A Test and Re-Estimation of Taylor´s Empirical Capacity–Reserve Relationship, Natural Resources Research, Vol. 18, No. 1, DOI: 10.1007/s11053-009-9088-y and personal correspondence

[xii] TATMAN, C.R. 2001. Production rate selection for steeply dipping tabular deposits. Mining Engineering. pp.62

[xiii] ATTFIELD, M. SCHLEIFF, L. Lubin, J. et al 2011 The Diesel Exhaust in Miners Study: A Cohort Mortality Study with Emphasis on Lung Cancer. Published by Oxford University Press

[xiv] WALLACE K.G. JR. and CODOCEO V.O. 1997; Ventilation Planning at the El Indio Mine, Proceedings of the 6th International Mine Ventilation Congress

[xv] CULLEN, M. 2016 Personal Correspondence

VIOLENT COAL PILLAR COLLAPSE

*A.C. Zingano

Federal University of Rio Grande do Sul
Av. Osvaldo Aranha, 9500
Porto Alegre, Brasil
*(*Corresponding author: andrezin@ufrgs.br)*

24th World Mining Congress
MINING IN A WORLD OF INNOVATION
October 18-21, 2016 • Rio de Janeiro /RJ • Brazil

VIOLENT COAL PILLAR COLLAPSE

ABSTRACT

Pillar collapse has been studied for several years, and can be classified in two types: squeeze and violent pillar collapse, or controlled and uncontrolled pillar collapse. The underground coalmines in Brazil have been consider shallow underground mines, because the overburden thickness varies between 50 to 400 meters. For this reason, the coal pillar must be designed for permanent pillar to avoid subsidence and groundwater problems. In the last years, many pillar failures occurred; being one violent collapse and the others squeezed failures. All of them were considered massive pillar collapse because many pillars were failure. Some other cases the In the case, the violent pillar collapse the width-to-height (w/h) ratio was less than three, but the pillar safety factor (SF) is more than 1.3. The most impressive case was a cascade pillar collapse, where about 100 pillars were failure in less than three hours. The objective of this study is to determine the mechanism of pillar collapse for this violent pillar collapse, and compare to other case where failure did not occurred. Both cases are similar because they are in inclined coal seam, shallow overburden, and also low coal seam strength. Three-dimensional numerical models were built to study these cases and determine the cause of the pillar collapse. It means, if the cause was the width-to-high ratio or the inclination of the coal seam. Convergence monitoring and numerical model were applied to combine field data and theoretical approach to simulate the pillar collapse. The results showed that not only the geometry of pillar was the cause of the pillar failure. Other parameters, mainly dip of the coal seam and presence of structures as fractures and faults may affect the strength and failure mechanism of pillar.

KEYWORDS

Coal pillar, pillar failure, numerical model

INTRODUCTION

Fifty-two percent of Brazilian coal production comes from underground mining that uses the room-and-pillar method. Ground control problems, such as roof fall, pillar failure and floor heave are very common and tend to increase when the mining companies face production and geological problems. The overburden thickness varies between 40 and 700 m, and under these conditions, coal pillars should be designed as permanent structures to avoid subsidence and groundwater problems.

During 1998 and 2003, four pillar failures occurred in different coal mines. Usually, the pillar failure was caused by problems in the pillar design, blasting design and the panel width. Zingano et.al., (2004) presented a case study about pillar collapse in inclined coal seam. In this case pillar collapse, about 100 pillars collapsed in less than three hours, and 700 more pillars collapsed over the next six weeks. The mine was closed shortly thereafter because the collapse had affected the stability of the entire mine. Figure 1 shows the mining section where the violent pillar collapse occurred. The collapse began at top of the section where the pillars, where the dip angle of coal seam was about 10 degrees. The section is developed between three faults (red lines in figure 1), and these faults may prevent part of vertical stress from being transferred to the rock mass around the section. Figure 2 shows some pictures taken from the section that was occurred the pillar collapse.

The objective of this paper is to analyze the mechanism of the behavior of the immediate and main roofs, and the arc-effect. The analysis will take into account the properties of the rock masses that are the immediate roof and main roof, and pillar and entry dimensions, and thickness of the coal seam.

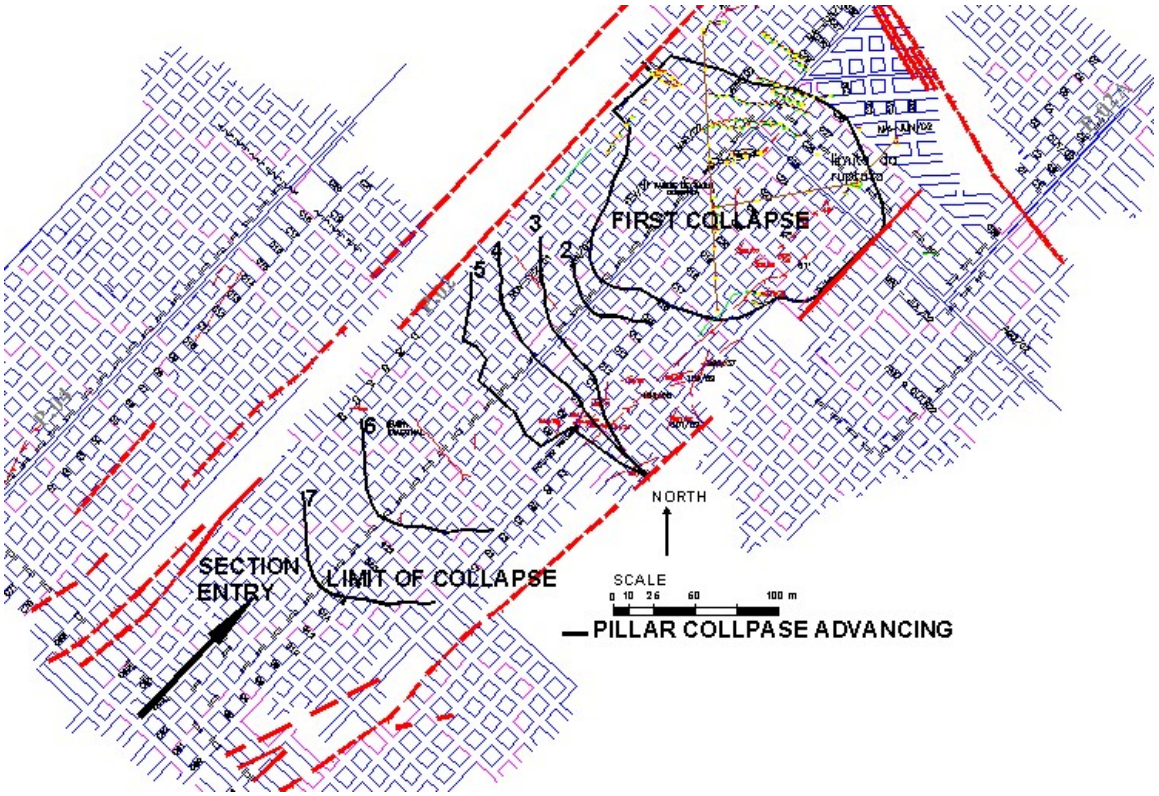

Figure 1 – Mine section where the violent pillar collapse occurred.

Figure 2 – Some pictures from pillar collapse.

The study starts with a description of geology and structure of the Bonito coal seam, which will influence the stability and failure mechanisms of the pillars and the behavior of the roof. Next the study analyzes the mechanism for this case study with instrumentation and numerical modeling to understand and simulate the mechanism of the arc-effect.

GEOLOGICAL SETTING

Two different coal seams within the Rio Bonito Formation are mined in Santa Catarina State. The first is the Barro Branco Seam which is about 1.5- to 2.3-m-thick, and the second is the Bonito Seam which

is about 2.5- to 5.5-m-thick. The Bonito coal seam is located at the bottom of the upper part of the Rio Bonito Formation, and, sometimes, it conforms to paleo valleys, under the Formation. As a consequence, the Bonito coal seam has many faults and fractures that cross the seam (Figure 1), and the dip angle of the seam varies from 0 to 15 degrees. The magnitude of fault movement varies from few centimeters to many meters. Moreover, excavation of the entries and cross-cuts forms blocks of rock in pillars, which can slide and fall into the entry. This block sliding has caused accidents with injuries and problems with pillar stability. Figure 3 shows the geological detail and the thickness of various rock layers in the immediate roof and floor of the Bonito coal seam. The immediate floor comprises siltstone, lying above stronger siltstone and sandstone layers. The immediate roof is laminated sandstone about 3 m thick overlain by a 10 m thick layer of massive sandstone. The average thickness of the coal seam is 3-4 meters.

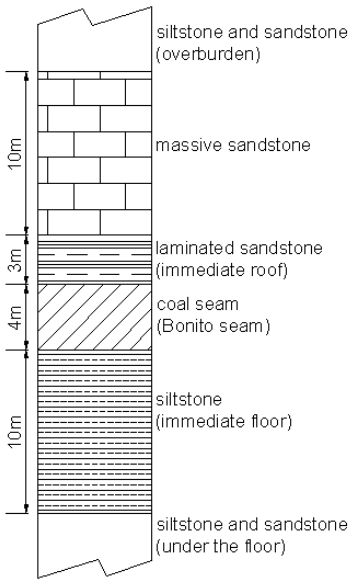

Figure 3 – Geological detail in the roof and floor around the Bonito coal seam (thicknesses in meters).

VIOLENT PILLAR COLLAPSE

Violent pillar collapse has been studied by different authors (Zipf, 1992; Mark, 1999; Peng, 1986; Salamon and Ozarevsc, 1970; Salamon, 1970; Khair and Peng, 1985). The nature of pillar collapse is governed by the stiffness of the surrounding rock and the width-to-height (w/h) ratio of the coal pillar (Mark, 1999; Salamon and Ozarevicz, 1970). Figure 4 shows the relation between safety factor determined by ARMPS and the w/h ratio. It can be observed in this figure that violent pillar occurred only when the w/h ratio is below three and the safety factor is below to 1.5 (Mark, 1999).

A pillar with low w/h ratio has low confinement in its center. Then, the immediate consequence is the reduction of pillar strength, and the increasing of probability of the violent pillar collapse. The pillar failure mode proposed by Wagner (1974) will get a higher velocity of failure for a pillar with w/h<3 than a pillar with w/h>3. Zipf (1992) presented an analysis of pillar failure that distinguishes between violent and nonviolent pillar failure based on local mine stiffness. A stable (nonviolent) failure occurs when the stiffness of rock mass is smaller than the stiffness of the coal pillar, and a violent pillar failure occurs when the stiffness of the pillar is greater than the stiffness of the surrounding rock mass.

Determining safety factor

Empirical methods are usually applied to pillar design in Brazil. The empirical approach used is the Salamon-Munro method (Salamon and Munro, 1967), where the rock mass strength (σ_{cm}) is 7.12 MPa (1032 PSI) (Equation 1). Vertical stress (σ_v) over the pillar is estimated by the tributary area method

(Equation 2), where C is the sum of the pillar width and entry span, H is overburden thickness and γ is the rock mass density. All the units are in the International System.

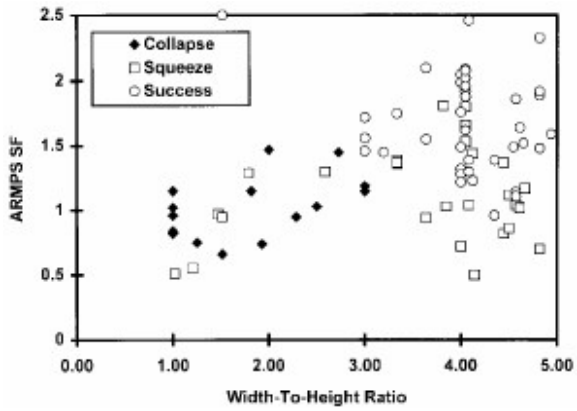

Figure 4 – Violent and squeeze collapse based on ARMPS safety factor and w/h ratio (Mark, 1999).

The geometry of the pillar and width are the following: overburden thickness is 60 m, pillar width is 8 m, pillar high is 4 m and entry span is 5 meters. The w/h ratio for the pillar is 2; therefore, the pillar is in the zone of probable violent collapse.

$$\sigma_v = \gamma H \frac{C^2}{w^2} \quad (1)$$

$$\sigma_p = \sigma_m \frac{w^\alpha}{h^\beta} \quad (2)$$

Considering the parameters above, the vertical stress over the pillar is 4.28 MPa and the pillar strength is 7.48 MPa. Therefore, the safety factor is 1.75. The safety factor indicates that the pillar is stable, but the w/h ratio is only 2. This last parameter should be the cause for any instability of the pillar. In other sections of the mine, in which the dip of the coal seam is about 0 degrees and the overburden thickness is the same, the pillars with the same dimensions were stable.

The empirical method approach considers that the seam should be flat, i.e., the dip angle of the coal seam should be about zero degree. In the location where the pillar collapse started, the dip of the coal seam was about 10 degrees. Therefore, the vertical stress was not normal over the pillar. There was a normal component and a tangential component of the vertical stress on the pillar. Figure 5 shows the stress distribution on the pillar, including the components of the vertical stress due to inclination of the coal seam.

The stress distribution in a pillar in an inclined seam is different from a pillar in a flat seam. The tangential component of vertical stress modifies the stress distribution in the pillar and the displacement of the down dip rib is larger than the displacement of the other rib sides. The rib side located at the bottom of the inclination of the seam shows cracks, which is indicative of this displacement. Figure 6 shows a picture of cracks at the rib side of the pillar and the displacement monitored by an extensometer.

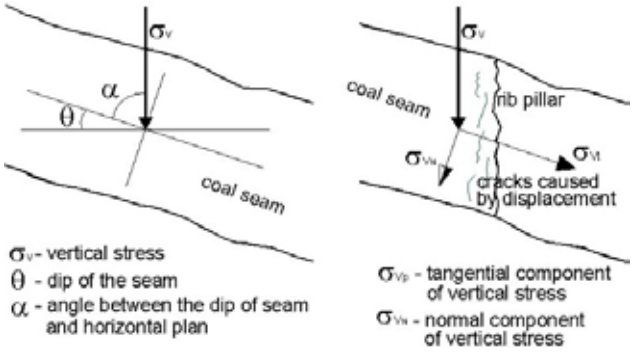

Figure 5 – Vertical stress components.

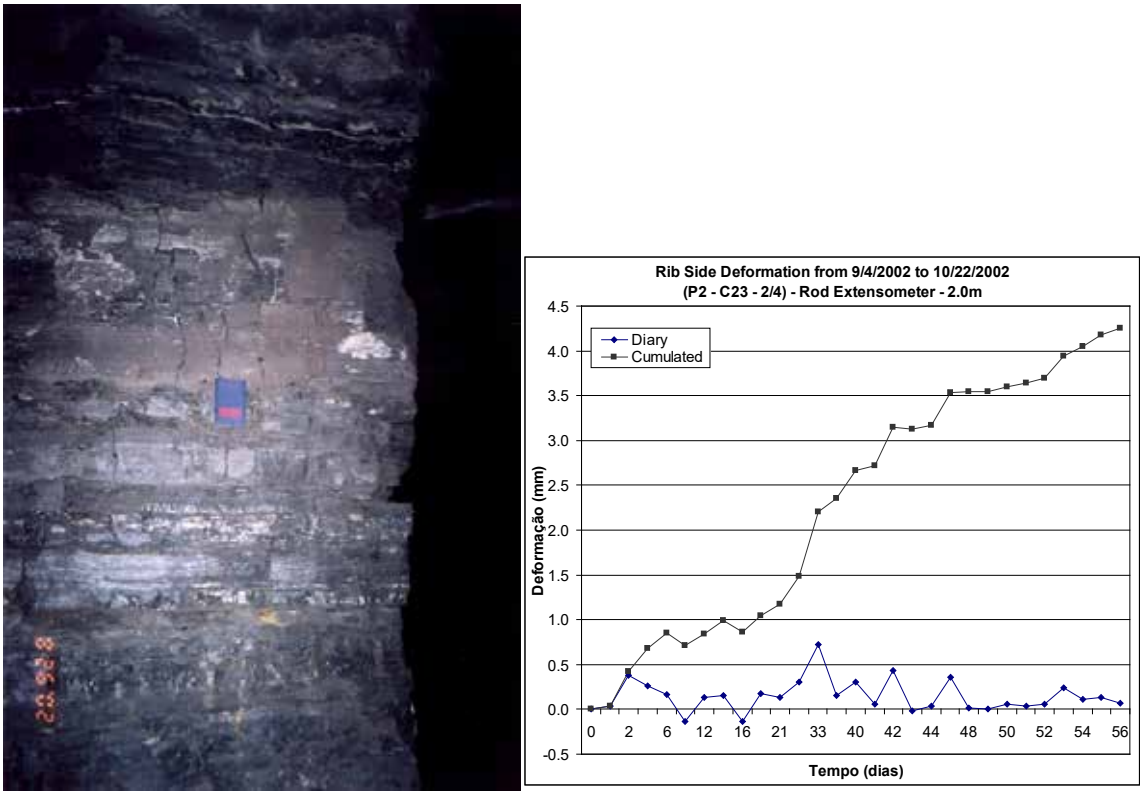

Figure 6 – Picture of cracks at rib side of pillar and the displacement monitoring.

Material properties

The material properties are described in table 1. All the rocks have Mohr-Coulomb elastic-plastic behavior. As we can see, the Young's modulus (E) of the roof is higher than the coal seam, but the E of the floor is nearly the same. Therefore, there is a different situation, when the coal pillar is surrounded by a stiffer rock mass and other with the same stiffness of the coal seam.

The numerical model is a two-dimensional plane strain model, since the objective of this study is to understand the deformation behavior in the plane of the model. Therefore, out-of-plane strains are not considered.

Table 1 – Material properties used for numerical modeling.

Rock	Young's Modulus (GPa)	Poisson Ratio	Friction Angle (degrees)	Cohesion (MPa)
Laminated-Sandstone	14.4	0.18	25.56	5.96
Siltstone	3.60	0.22	31.82	1.70
Coal	3.50	0.25	21.33	1.39
Coal-Blast	1.27	0.25	11.23	0.40

Initial stresses

The virgin vertical and horizontal stresses and the ratio between them are necessary to simulate the rock behavior surrounding mine openings in the numerical model. Various factors can change the horizontal to vertical stress ratio, such as tectonic influence, anisotropy of the rock mass and topography variations (Cornet, 1993). The rock mass in this study is a sedimentary formation affected by tectonic pressures. This situation makes the rock mass strongly anisotropic and heterogeneous. The relationship between vertical and horizontal stress based on the Poisson ratio cannot be applied in this case study. In-situ measurements of the stress field magnitude in this region of Brazil are not available. It was assumed that the initial stress ratio is 2.0, due to erosion of the overburden and tectonic pressure. Vertical and horizontal pressures are applied at the boundary (or limits) of the model. The vertical stress calculated based on an overburden thickness of 60 meters and the horizontal stress is twice the vertical stress.

THE ARC-EFFECT

After the collapse began in the region of the inclined seam, the collapse continued toward the entry to the section (Figure 1). The advance of the violent collapse had a velocity about one or two lines of pillars per day, with one or two days of intervals, when there was no pillar failure. The pillar collapse stopped 45 days after its beginning. During this period of collapse, it was possible to install extensometers with the objective of monitoring the roof to floor convergence and analyzing the behavior of the roof while violent pillar collapse was occurring. The advance of the collapse is caused by two main reasons: (1) the stress transferred from failed pillar to intact pillar, and (2) the stress transferred by the unbroken roof.

Another issue observed in this pillar collapse was the behavior of the immediate and mains roof near the collapse limit. When it is close to the collapse limit roof convergence and pillars compression occur. Conversely when it is far from the collapse limit divergence and pillars decompression occur. This behavior was observed by the instrumentation installed closed to the collapse (Figure 7 and 8). This behavior is called arc-effect.

During this period of collapse, it was possible to install extensometers with the objective of monitoring the roof to floor convergence and analyzing the behavior of the roof while violent pillar collapse was occurring. The advance of the collapse is caused by two main reasons: (1) the stress transferred from failed pillars to intact pillars, and (2) the stress transferred by the unbroken roof. Extensometers #1 and #2 measured different behavior in the immediate roof. Extensometer #1 shows convergence of the roof, while extensometer #2 indicates divergence of the roof. Figure 13 shows the charts of accumulated deformation for extensometers #1 and #2, where negative values indicate convergence and positive values indicate divergence. At the extensometer #1, when the line turns vertical, it means that the pillar failed.

The immediate roof is three meters of laminated sandstone. It is overlain by 10 meters of massive and very strong sandstone. These two sandstone seams are very competent. Therefore, while the pillar collapse was propagating toward the entry of the section, the immediate roof collapsed, but the massive sandstone did not break, i.e., it remains intact and only set on the failed pillars and immediate roof.

This different behavior can be explained by the fact that the massive sandstone and the laminated sandstone did not break. The laminated sandstone (immediate roof) broke only when the pillars were totally failed. This phenomenon of convergence and divergence occurred because the unbroken massive sandstone would reach an equilibrium due to deformation, and behaves like a beam. This behavior is called the arc-effect. Figure 9 shows the arc-effect, where there is zone of compression (convergence) and decompression (divergence).

The consequence of the arc-effect is that there is a separation between immediate roof and pillar (Figure 7), and confinement of the pillar center induced by vertical stress is completely lost. The pillar ribs slough and pillar strength decreases greatly. As the collapse advances, the arc-effect advances along with it. The pillars were subjected to decompression first, followed by compression. Because these pillars had low confinement of the pillar center and low strength, they did not support the vertical compression imposed by the roof, and the pillars started to fail. This pillar failure is a violent failure

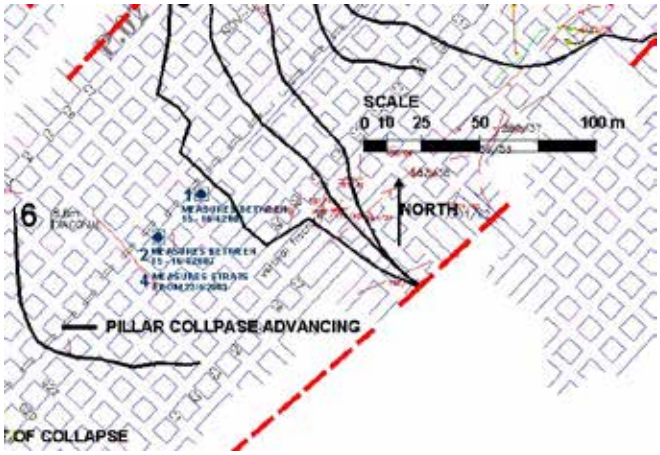

Figure 7 – Location of the extensometers

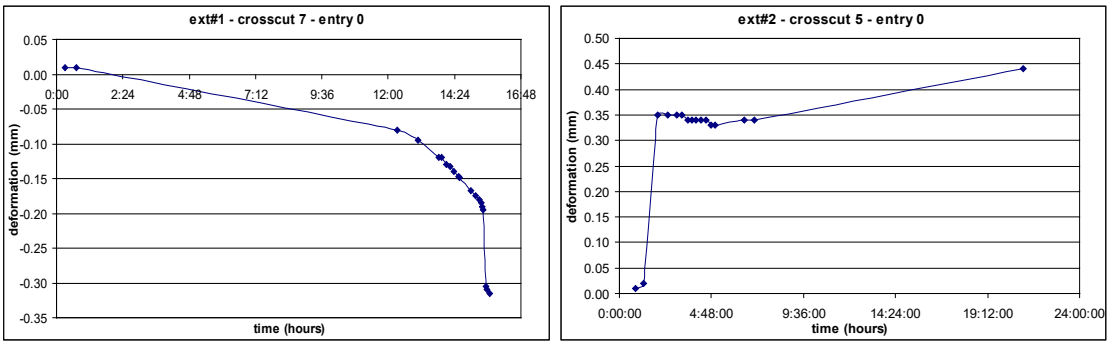

Figure 8 – Extensometer #1 and #2 showing convergence at extensometer #1 and divergence at #2.

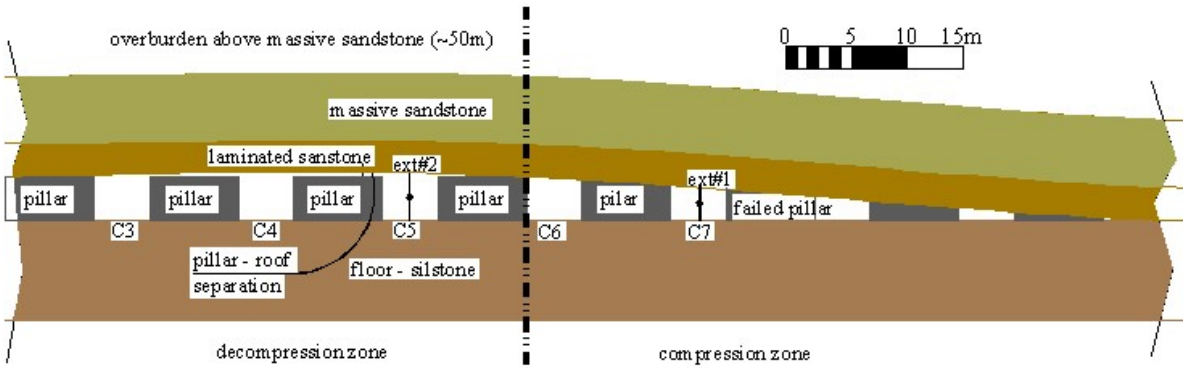

Figure 9 – Arc-effect for a very strong roof

MODELING THE ARC-EFFECT OF THE ROOF

As shown in figure 7, the arc-effect occurred due to high deformation (convergence) of the roof in the collapse area, and consequent separation of immediate roof from the top of pillar. This separation is caused by the pillar collapse and the high convergence of the roof in the collapse zone. At the zone around the limit of the collapse zone, the immediate and main roofs did not fail. Therefore, they exhibit divergence deformation in order to reach stress equilibrium, causing the separation between roof and top of pillar.

Two-dimensional numerical model was applied to simulate the arc-effect at the limit of collapse zone. The pillar collapse is simulated by taking off the elements that represent pillars and then the roof deform such that it causes separation between roof and top of pillar.

The difficulties in building this model are associated with correct definition of mining sequence and geomechanical properties of each stratum and the interface between immediate roof and top of pillar. The model simulation employed FLAC-2D, version 7.

Model Geometry and sequence

The numerical model simulates the separation of the roof from the top of the pillar at the zone around the collapse zone, caused by pillar failure and large deformation of immediate roof. The geometry of the model is shown in figure 10, and the thickness of each seam is based on figure 3.

The objective is to simulate the behavior of a coal pillar subjected to field stress (horizontal and vertical stress) and the evolution of the failure due to excavation, and stress redistribution.

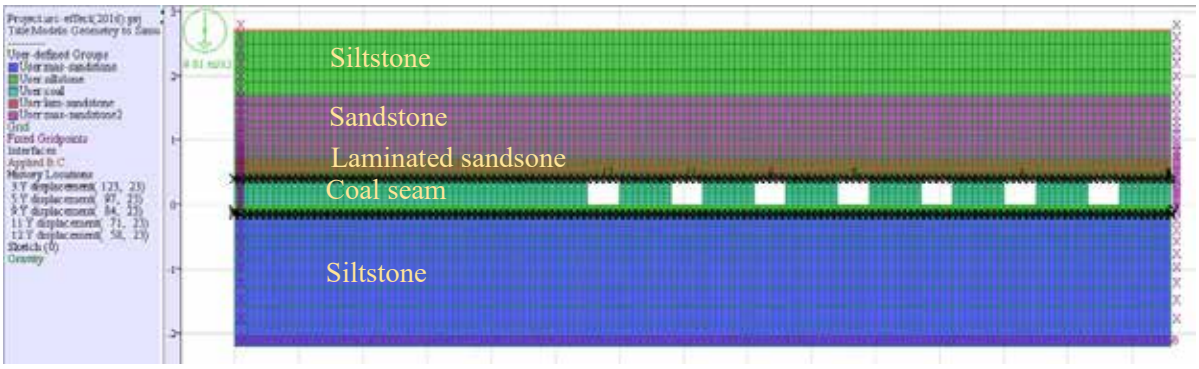

Figure 10 – Geometry used in the numerical model (distances in meters).

The numerical modeling plane is parallel to the axis of the section (Figure 1) and aligned to the advancing direction of pillar collapse. The results of this analysis determine the behavior of the roof at the zone around the collapse and the influence of separation between roof and top of pillar over the stress distribution in the pillar. The numerical model shows the behavior of the roof in response to the stress distribution and large deformation due to pillar collapse. To monitoring the displacement of the roof during the collapse of pillar, the nodes of the elements that represent the roof were monitored by history command on FLAC. One node in each entry was monitored.

Figure 11 shows the displacement of the roof in entry of the model, since entry in the collapse zone till the entry in the decompression roof. As we can observe, the roof in the collapse zone is convergent and the roof in the decompression zone is divergent. The displacement charts of roof in the entries #1 and #2 show that there were divergences about 1.9 mm, while in the entries #3, #4 and #5 the displacement were 1.4m, 2.5cm and 5.5mm in convergence, respectively. The limit between convergence zone and divergence zone moves forward together with the collapse of pillar. Therefore, the pillars will be in different situation of decompression and compression, depending on the distance from the pillar collapse zone. Comparing the charts from the instrumentation (Figure 3) and the graphics from the numerical simulation of figure 8, it shows that the simulation exhibit quite the same behavior as that of the instrumentation. The difference is that the instrumentation was installed some days after the beginning of the event, and also the reading of the instrumentation was very dangerous.

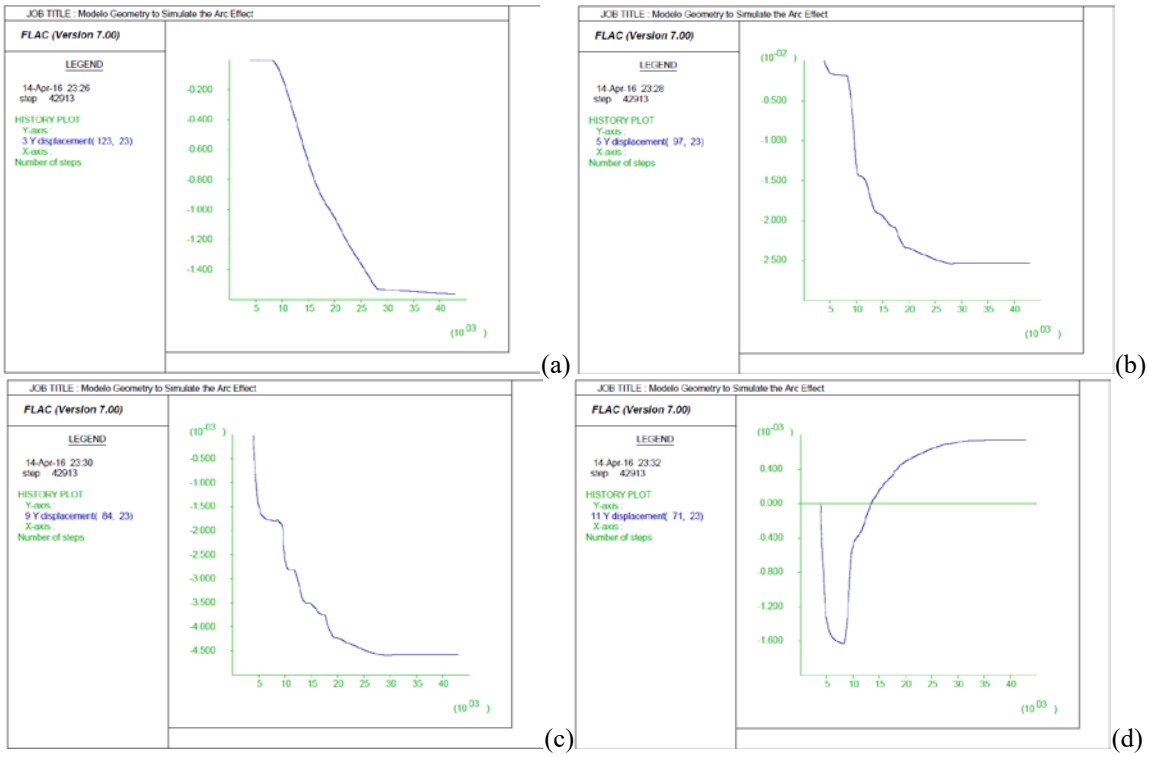

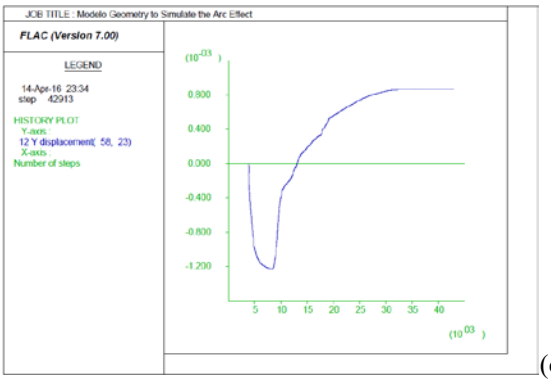

(e)

Figure 11 – Displacement of the immediate roof at entries (a) #5, (b) #4, (c) #3, (d) #2 and (e) #1.

Figure 12 presents the vertical stress distribution in the immediate roof (laminated sandstone) and pillars. It is possible to observe that at the limit between convergence and divergence zones the vertical stress is maximum and decreases in the direction of the divergence zone. When the roof separates from the top of pillar, the pillar loses the pressure and consequently the confinement at the center of pillar. The numerical model represents this separation and the loss of confinement Figure 9 also shows the stress distribution in the pillars subject to compression and decompression. Based on the results of numerical modeling, the average stress in a pillar in compression state is about 7 MPa, and that of decompression state is between 0 and 2 MPa.

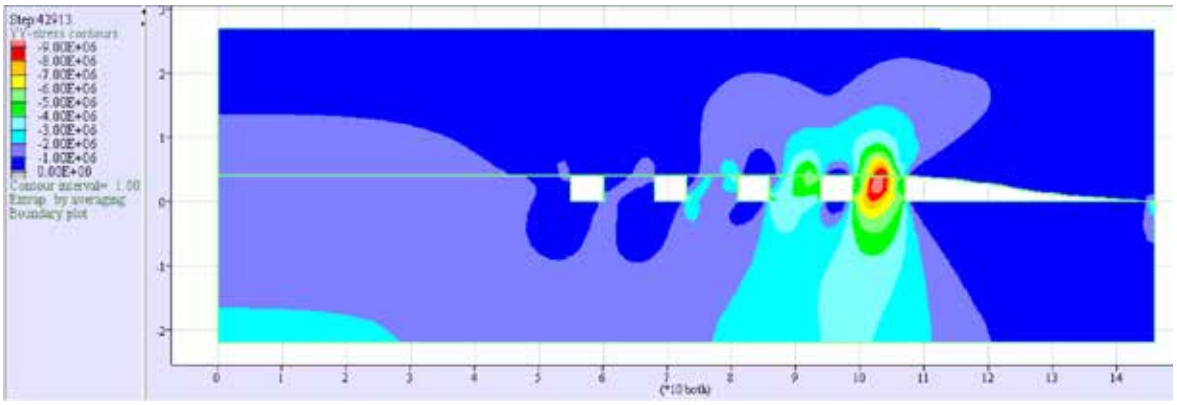

Figure 12 – Stress distribution in a coal pillar (a) in compression state and (b) in decompression state.

While the pillar collapse advance forward to the entrance of the section, the compression and decompression zones move together with the advance of the coal pillar collapse limit. In other words, the pillars was first subjected to decompression state, followed by compression state

CONCLUSIONS

This study showed the mechanism of the arc-effect, which is caused by pillar collapse and roof of high stiffness. Numerical modeling simulated the monitoring and behavior of the roof that was observed in-situ. The release of pressure on the pillar due to the separation of immediate roof decreases the confinement of pillar center and also the strength of pillar. When the pillar is subjected to high pressure and pillar strength is small, the domino effect will continue forward. The arc-effect was observed in another mine, which also had a very strong roof. Breaking (or cracking) the massive sandstone for stress relief should prevent violent pillar collapse as a consequence of the arc-effect.

Institucional Support:

Editorial Support:

Communication Agency:

Operations Management:

Executive Producer and Marketing:

Commercial Partner – India:

Commercial Partner – Canada/USA:

Promotion:

IBRAM
INSTITUTO BRASILEIRO DE MINERAÇÃO
Brazilian Mining Association
Cámara Minera de Brasil

24th World Mining Congress
MINING IN A WORLD OF INNOVATION

October 18-21, 2016
Rio de Janeiro /RJ • Brazil